

**Predictors of Treatment Benefit and Prognosis in Cutaneous
Malignant Melanoma**

Rosalyn Jewell

Submitted in accordance with the requirements for the degree of
Doctor of Philosophy

The University of Leeds
School of Medicine

August 2012

The candidate confirms that the work submitted is her own, except where work which has formed part of jointly-authored publications has been included. The contribution of the candidate and the other authors to this work has been explicitly indicated below. The candidate confirms that appropriate credit has been given within the thesis where reference has been made to the work of others.

Chapter 3 includes work from the publication: Conway, C.; Mitra, A.; Jewell, R.; Randerson-Moor, J.; Lobo, S.; Nsengimana, J.; Edward, S.; Sanders, D. S.; Cook, M.; Powell, B.; Boon, A.; Elliott, F.; de Kort, F.; Knowles, M. A.; Bishop, D. T.; Newton-Bishop, J., Gene expression profiling of paraffin-embedded primary melanoma using the DASL assay identifies increased osteopontin expression as predictive of reduced relapse-free survival. *Clin Cancer Res* 2009, 15 (22), 6939-46. I performed the statistical analysis presented in this publication, under the supervision of Jeremie Nsengimana and Faye Elliott, and contributed to the preparation of the manuscript. Tissue collection, sampling and RNA extraction were performed by Caroline Conway, Angana Mitra and Samira Lobo. Caroline Conway undertook the quantitative Real-time PCR (qRT-PCR) experiments to validate *SPP1* (osteopontin) expression. Pathway analysis was undertaken by Jeremie Nsengimana. Pathological review of samples was undertaken by Sara Edward, Andy Boon and Martin Cook. Gene expression microarrays were performed at Service XS, Leiden by Floor De Kort. Tissue samples were provided by Scott Sanders, Martin Cook and Barry Powell. The project was supervised by Tim Bishop and Julia Newton-Bishop, with additional advice provided by Margaret Knowles, who contributed to manuscript preparation.

Chapters 4 and 8 include work from the publication: Jewell, R.; Conway, C.; Mitra, A.; Randerson-Moor, J.; Lobo, S.; Nsengimana, J.; Harland, M.; Marples, M.; Edward, S.; Cook, M.; Powell, B.; Boon, A.; de Kort, F.; Parker, K. A.; Cree, I. A.; Barrett, J. H.; Knowles, M. A.; Bishop, D. T.; Newton-Bishop, J., Patterns of expression of DNA repair genes and relapse from melanoma. *Clin Cancer Res* 2010, 16 (21), 5211-21. I performed the statistical analysis used to identify prognostic and predictive genes from cDNA-mediated annealing, selection, extension and ligation (DASL) data and the analysis of qRT-PCR data provided by Katharine Parker and Ian Cree from the Translational Oncology Research Centre, Queen Alexandra Hospital, Portsmouth. I performed the qRT-PCR experiments, with the assistance of Mark Harland, used to validate expression of *RAD52*, *TOP2A* and *RAD54B* and contributed significantly to the preparation of the manuscript. Tissue collection, sampling and RNA extraction were performed by Caroline Conway, Angana Mitra and Samira Lobo. Caroline Conway undertook the qRT-PCR experiments to validate expression of *RAD51*. Pathway

analysis was undertaken by Jeremie Nsengimana. Pathological review of samples was undertaken by Sara Edward, Andy Boon and Martin Cook. Gene expression microarrays were performed at Service XS, Leiden by Floor De Kort. The project was supervised by Jenny Barrett, Tim Bishop and Julia Newton-Bishop, with additional advice provided by Margaret Knowles, who contributed to manuscript preparation.

Chapter 5 is based on work in the publication: Jewell, R.; Mitra, A.; Conway, C.; Iremonger, J.; Walker, C.; de Kort, F.; Cook, M.; Boon, A.; Speirs, V.; Newton-Bishop, J., Identification of differentially expressed genes in matched formalin-fixed paraffin-embedded primary and metastatic melanoma tumor pairs. *Pigment Cell Melanoma Res* 2012, 25 (2), 284-6. I performed the tissue sampling and RNA extraction of nodal samples, the data analysis and prepared the manuscript for publication. Samples were collected by Caroline Conway, Angana Mitra and Christy Walker. Sampling and RNA extraction of primary tumour samples was performed by Caroline Conway and Angana Mitra. Martin Cook provided a proportion of the tumours used for these analyses. Andy Boon supervised tissue sampling of nodal specimens. James Iremonger and Val Speirs assisted with tissue sampling. Gene expression microarrays were performed at Service XS, Leiden by Floor De Kort. The project was supervised by Julia Newton-Bishop who contributed to manuscript preparation.

This copy has been supplied on the understanding that it is copyright material and that no quotation from the thesis may be published without proper acknowledgement.

Acknowledgements

This research has been carried out by a team which has included Christy Walker, Sandra Tovey, Caroline Conway, Angana Mitra, Samira Lobo, Filomena Esteves, Jon Laye, Mark Harland, Juliette Randerson-Moor, Faye Elliott, Jeremie Nsengimana and May Chan from the Section of Epidemiology and Biostatistics. From outside of the Section, team members included Phil Chambers and Helen Snowden from the Genomics Facility, Binbin Liu and Lee Hazelwood from the Bioinformatics Group and James Iremonger and Val Speirs from the Section of Pathology and Tumour Biology all based in the Cancer Research UK Centre, Leeds Institute of Molecular Medicine. External collaborators were Katharine Parker and Ian Cree from the Translational Oncology Research Centre, Queen Alexandra Hospital, Portsmouth, Sarah Storr, Sabreena Safuan and Stewart Martin from the Academic Oncology group at the University of Nottingham, Andy Boon from the Leeds Teaching Hospitals NHS Trust, Martin Cook from the Royal Surrey County Hospital NHS Foundation Trust and Division of Medicine University of Surrey, Guildford and finally the service providers ServiceXS from Leiden, Netherlands and Gen-probe from Wythenshawe, Manchester.

My own contributions, fully and explicitly indicated in the thesis, have been:

- Sampling of tumour tissue from various studies and extraction of nucleic acids for work described in chapters 2, 5, 6, and 8.
- Performing quantitative Real-time PCR (qRT-PCR) experiments described in chapters 2, 4 and 8.
- Mutation screening of samples using the SNaPshot assay described in chapter 6.
- Planning and undertaking methodological studies to assess new technologies described in chapters 2, 4 and 8.
- Performing statistical analyses of gene expression microarray data (chapters 3-7), qRT-PCR data (chapters 2, 4 and 8), mutation data (chapter 6), immunohistochemical (chapter 7) and clinico-pathological data (chapters 3-8).
- Performing pathway analysis using DAVID (the database for annotation, visualisation and integrated discovery) software in chapters 4 and 7.
- Development of the “Predicting Benefit from Interferon Treatment” and “Predicting Response to Chemotherapy” studies described in chapters 2, 7 and 8.

The other members of the group and their contributions have been as follows:

- Christy Walker has project-managed the “Predicting Benefit from Interferon Treatment” and “Predicting Response to Chemotherapy” studies. He has traced tissue samples from patients recruited to these studies and the Retrospective Sentinel Node Biopsy study.
- Sandra Tovey has traced tissue samples for the Leeds Melanoma Cohort study.
- Caroline Conway, Angana Mitra and Samira Lobo sampled tumour specimens and extracted RNA used to generate gene expression microarray data described in this thesis.
- Filomena Esteves and Jon Laye have sectioned and sampled tumour tissues.
- Mark Harland and Juliette Randerson-Moor have provided advice regarding molecular biological methods. Mark also provided assistance with the DNA repair gene qRT-PCR experiments.
- Faye Elliott and Jeremie Nsengimana have provided statistical advice for the analyses presented in this thesis. Jeremie performed Ingenuity pathway analysis.
- May Chan has provided advice regarding database management for studies included in this thesis.
- Phil Chambers and Helen Snowden performed pyrosequencing analyses and assisted with Fluidigm experiments.
- Binbin Liu and Lee Hazelwood performed gene ontology analysis.
- James Iremonger and Val Speirs provided advice regarding laser capture microdissection techniques.
- Katharine Parker and Ian Cree undertook gene expression analysis of samples using the CGEA-1 array from patients treated with chemotherapy.
- Sarah Storr, Sabreena Safuan and Stewart Martin performed immunohistochemical experiments.
- Andy Boon and Martin Cook performed expert histological reviews of tumour samples. Martin Cook provided nodal tumour tissue for analysis of matched tumour pairs. Andy Boon supervised sampling of nodal samples.
- Floor de Kort from ServiceXS performed the gene expression microarray experiments and the qRT-PCR quality control assessment prior to the array.
- Gen-probe extracted nucleic acids from tumour cores from patients recruited to the “Predicting Response to Chemotherapy” study.

Without the assistance of the team members described above, the work presented in this thesis would not have been possible. I am hugely grateful for their hard work, support and sound advice.

I would like to thank my supervisors Professor Julia Newton-Bishop, Professor Tim Bishop and Professor Jenny Barrett for their support and guidance during my PhD and the opportunities they have provided me with.

During my research period I have been funded by a Bramall Fellowship and a Medical Research Training Fellowship (G0802123). Further support has been provided by Cancer Research UK programme and project grants.

Abstract

This thesis describes work designed to identify genomic prognostic and predictive markers for melanoma using nucleic acids extracted from formalin-fixed (FFPE) tumour samples and emerging technologies for gene expression profiling.

I report use of the cDNA-mediated annealing, selection, extension and ligation (DASL) assay using a 502-gene Human Cancer panel to identify prognostic markers. The study identified over-expression of *SPP1* and DNA repair genes in primary tumours as associated with reduced relapse-free survival time. These genes remained associated with survival in analyses adjusted for current prognostic markers. I also report use of the DASL assay to study gene expression of tiny metastatic specimens, allowing assessment of gene expression in matched primary and metastatic tumours.

I report studies of driver mutations in *BRAF* and *NRAS* as prognostic markers in which V600K *BRAF* mutations, were independently associated with survival in multivariate analysis. Gene expression profiling using the DASL assay identified a number of genes differentially expressed in *BRAF* and *NRAS* mutated tumours, for example *ETV1* and *TYRO3*, providing biological insight into these tumours.

Ulceration of a primary tumour is a poor prognostic sign, but paradoxically also predicts response to interferon- α adjuvant therapy. I report greater numbers of macrophages in ulcerated tumours and both over-expression of *interleukin-6* and deranged expression of genes in the interferon Jak-STAT signalling pathway. These factors may contribute to mechanisms of responsiveness to interferon- α in ulcerated tumours.

I report an investigation of predictive markers for dacarbazine therapy. The Fluidigm quantitative Real-time PCR system was used to identify over-expression of *MGMT* as independently associated with chemotherapy resistance and shorter survival after starting chemotherapy.

Following validation of these findings, prognostic and predictive markers were identified which could potentially be used clinically to provide additional information to patients with melanoma, allowing a more personalised approach to melanoma treatment.

Table of Contents

Acknowledgements	iv
Abstract	vii
Table of Contents	viii
List of Tables	xix
List of Figures	xxii
Abbreviations	xxv
1 Introduction	1
1.1 Major thesis aims	1
1.2 Aims of this chapter	2
1.3 Cutaneous malignant melanoma	2
1.3.1 Incidence	2
1.4 Melanoma development	2
1.4.1 Risk factors for melanoma development	2
1.4.2 Process of melanoma development	3
1.4.2.1 Mitogen-activated protein kinase (MAPK) pathway	3
1.4.2.2 p16 ^{INK4a} , cyclin dependent kinases 4/6 and retinoblastoma (RB) protein	6
1.4.2.3 p14 ^{ARF} and p53	6
1.4.2.4 PTEN and the phosphatidylinositol-3-kinase (PI3K) pathway	7
1.5 Melanoma tumour progression	7
1.5.1 Melanoma metastasis	7
1.5.2 Melanoma interactions with host immunity	8
1.6 Patient assessment and melanoma tissue processing	9
1.7 Prognosis in melanoma	11
1.7.1 Prognostic factors currently used in melanoma staging	11
1.7.1.1 Primary tumour features	11
1.7.1.1.1 Breslow thickness	11
1.7.1.1.2 Tumour ulceration	12
1.7.1.1.3 Mitotic rate	12
1.7.1.2 Nodal metastatic disease (stage III)	12
1.7.1.3 Systemic metastatic disease (stage IV)	13
1.7.2 Prognostic factors not part of current staging guidelines	16

1.7.2.1	Tumour factors	16
1.7.2.1.1	Vascular and lymphatic invasion	16
1.7.2.1.2	Perineural infiltration	16
1.7.2.1.3	Tumour regression.....	16
1.7.2.1.4	Tumour infiltrating lymphocytes (TILs)	17
1.7.2.1.5	Histological subtype	17
1.7.2.2	Host factors	18
1.7.3	Limitations of current melanoma staging.....	19
1.7.4	New prognostic biomarkers for melanoma	19
1.7.4.1	Biomarkers	19
1.7.4.2	Prognostic tumour biomarkers.....	20
1.7.4.2.1	Candidate biomarker studies	20
1.7.4.2.2	Identification of gene expression signatures.....	21
1.8	Treatment of melanoma	26
1.8.1	Adjuvant therapies	27
1.8.1.1	Interferon- α (IFN)	27
1.8.1.1.1	Action of endogenous type 1 interferons.....	27
1.8.1.1.2	Clinical trials of interferon- α in melanoma	28
1.8.2	Treatment of stage IV disease	30
1.8.2.1	Chemotherapy for stage IV disease.....	31
1.8.3	Personalized therapies for melanoma.....	32
1.8.4	Tumour factors that predict benefit from IFN therapy	32
1.8.5	Tumour factors that predict response from chemotherapy	33
1.9	Formalin-fixed paraffin embedded tissue (FFPE) for identification of prognostic and predictive biomarkers	34
1.10	Outline of thesis chapters	35
2	Methods	37
2.1	Aims	37
2.2	Patients and samples	37
2.2.1	Samples from patients recruited to studies	37
2.2.1.1	Leeds Melanoma Cohort Study	37
2.2.1.2	Retrospective Sentinel Node Biopsy Study.....	38
2.2.1.3	Predicting Benefit from Interferon Treatment: Personalised Therapy for Melanoma.....	38
2.2.1.4	Predicting Response to Chemotherapy in Malignant Melanoma: The role of DNA repair genes	39
2.2.2	Central review of tumour histology	39

2.2.3 Patient samples used in pilot work.....	40
2.3 Sampling of FFPE primary melanoma tumour blocks	40
2.3.1 Justification for sampling using a tissue microarray (TMA) needle.....	40
2.3.2 Sectioning of tumour blocks.....	42
2.3.3 Haematoxylin and eosin (H+E) staining	42
2.3.4 Slide review	42
2.3.5 Sampling using a tissue microarray (TMA) needle	43
2.4 Melanin score	44
2.5 Tumour sampling from small sentinel node biopsy samples	44
2.5.1 Laser capture microdissection (LCM).....	44
2.6 Extraction of nucleic acids from FFPE tissue cores	45
2.6.1 Extraction of RNA using the Roche High Pure RNA Paraffin Kit	45
2.6.1.1 De-paraffinisation of the tissue core and tissue homogenisation.....	46
2.6.1.2 Nucleic acid binding and washing.....	46
2.6.1.3 Elution of RNA.....	46
2.6.2 Extraction of DNA using the Qiagen QIAamp DNA FFPE kit.....	47
2.6.2.1 De-paraffinisation and tissue digestion	47
2.6.2.2 DNA binding, washing and elution	48
2.6.3 Extraction of RNA and DNA using the Qiagen AllPrep® RNA/DNA FFPE kit.....	48
2.6.3.1 Tissue de-paraffinisation and digestion.....	49
2.6.3.2 Extraction of RNA.....	49
2.6.3.3 Extraction of DNA.....	50
2.7 Extraction of RNA from microdissected sentinel node biopsy samples	51
2.8 cDNA synthesis from extracted RNA	51
2.8.1 cDNA generation using the Invitrogen Superscript™ First-strand synthesis system	51
2.8.1.1 cDNA synthesis for osteopontin qRT-PCR	51
2.8.1.2 cDNA synthesis for DNA repair gene qRT-PCR	52
2.8.2 cDNA generation using Applied Biosystems High Capacity cDNA Reverse Transcription kit	53
2.9 Cell line samples	53
2.9.1 Culture conditions.....	53
2.9.2 RNA extraction from cell line samples using the Qiagen RNeasy® Mini kit	54

2.9.3 DNA extraction from cell line samples using the Qiagen QIAamp DNA Mini kit.....	55
2.9.4 cDNA generation from RNA extracted from cell line samples.....	56
2.10 Quantification of nucleic acid concentrations using spectrophotometry	56
2.11 cDNA-mediated annealing, selection, extension and ligation (DASL) assay.....	56
2.11.1 The Sentrix Array Matrix (SAM) universal array	57
2.11.2 The HumanHT-12 v4 Expression Beadchip.....	58
2.11.3 The Illumina Human Cancer panel	59
2.11.4 The Illumina Whole-Genome DASL HT (WG-DASL HT) assay	59
2.11.5 Quality control measures before the DASL assay	59
2.11.6 Control and replicate samples	60
2.12 Normalisation of gene expression data.....	61
2.13 Assessment of the WG-DASL HT assay with FFPE melanoma samples.....	62
2.13.1 Background and methods	62
2.13.2 Results and discussion	62
2.14 Quantitative Real-time PCR (qRT-PCR) using Taqman® Gene Expression Assays	64
2.14.1 Standard TaqMan® gene expression protocol	65
2.14.2 Analysis of qRT-PCR data	66
2.15 Chemo-sensitivity Gene Expression Assay (CGEA-1)	67
2.16 Fluidigm Biomark HD qRT-PCR system	67
2.16.1 Integrated fluidic circuits (IFC).....	68
2.16.2 DELTAgene™ assays.....	68
2.16.3 Standard Fluidigm qRT-PCR protocol	69
2.16.3.1 Specific target amplification (STA) of samples.....	69
2.16.3.2 qRT-PCR reaction	70
2.17 Identification of mutations in FFPE primary melanoma tumours	71
2.17.1 BRAF and NRAS mutation screening using pyrosequencing	71
2.17.2 BRAF and NRAS mutation screening using Applied Biosystems PRISM® SNaPshot™ Multiplex system	74
2.17.3 Sequencing methods	79
2.18 Gene ontology and pathway analysis	79
2.18.1 Gene ontology analysis	80

2.18.2	DAVID (the database for annotation, visualisation and integrated discovery)	80
2.18.3	Ingenuity Pathway Analysis.....	81
2.19	Immunohistochemistry.....	81
2.19.1	Immunohistochemistry (IHC) methods	82
2.19.2	Assessment of microvessel density and macrophage count.....	85
2.19.3	Assessment of lymphatic density	85
2.19.4	Assessment of lymphatic vessel invasion and blood vessel invasion	85
2.20	Summary.....	86
3	Gene expression profiling of formalin-fixed paraffin-embedded primary melanoma using the cDNA-mediated annealing, selection, extension and ligation assay.....	87
3.1	Aims	87
3.2	Background	87
3.3	Detailed methodology.....	89
3.3.1	Patient samples and gene expression analysis.....	89
3.3.2	Target validation using quantitative Real-time PCR (qRT-PCR).....	90
3.3.3	Statistical methodology	91
3.3.3.1	Quality control analysis of gene expression data	91
3.3.3.2	Descriptive characteristics of the sample set	92
3.3.3.3	Identification of differentially expressed genes.....	92
3.3.3.4	Multiple testing and adjustment of analyses	92
3.3.4	Generation of gene networks using Ingenuity software	93
3.4	Results	93
3.4.1	RNA yields, quality control measures and performance of the DASL assay.....	93
3.4.2	Sample replicates	96
3.4.3	Descriptive statistics of samples sets.....	96
3.4.4	Genes most predictive of survival	97
3.4.5	Validation of <i>SPP1</i> expression using qRT-PCR	98
3.4.6	Co-expression of genes with <i>SPP1</i>	101
3.5	Discussion.....	105
3.5.1	Use of the Illumina DASL assay with FFPE melanoma tissue.....	105
3.5.2	Identification of <i>SPP1</i> as a prognostic biomarker in primary melanomas.....	108
4	Patterns of DNA repair gene expression in primary melanoma tumours ..	112
4.1	Aims	112

4.2	Background	112
4.3	Identification of genes associated with prognosis and histological features	117
4.3.1	Detailed methodology	117
4.3.1.1	Samples and generation of data set	117
4.3.1.2	Statistical methodology.....	117
4.3.1.2.1	Identification of differentially expressed genes	117
4.3.1.2.2	Multiple testing and adjustment of analyses	118
4.3.1.2.3	Gene ontology (GO) and pathway analysis of genes associated with survival.....	118
4.3.1.2.4	Principal components analysis and Ingenuity Pathway analysis.....	119
4.3.2	Results	119
4.3.2.1	Genes predictive of survival.....	119
4.3.2.1.1	Multivariate models including DNA repair genes associated with relapse, Breslow thickness and mitotic rate...	121
4.3.2.2	Gene expression in tumours with poor prognostic histopathological features.....	124
4.3.2.3	Correlations in expression levels between DNA repair genes.....	124
4.3.2.4	GO analysis and pathway analysis using DAVID.....	124
4.3.2.5	Principal components and Ingenuity Pathway Analysis (IPA).....	130
4.3.3	Summary of gene expression associated with prognosis and histological features of tumours	130
4.4	Validation of DASL results.....	133
4.4.1	Study to optimise methods for qRT-PCR using FFPE melanoma samples	133
4.4.1.1	Assessment of amplification efficiencies of Taqman® Gene Expression assays and choice of experimental design	133
4.4.1.1.1	Methods.....	133
4.4.1.1.2	Results and conclusions	134
4.4.1.2	Identification of suitable endogenous controls	135
4.4.1.2.1	Methods.....	135
4.4.1.2.2	Results and conclusions	136
4.4.2	Expression of <i>RAD52</i> , <i>RAD54B</i> and <i>TOP2A</i> in tumours from patients recruited to the Leeds Melanoma Cohort Study.....	139
4.4.2.1	Detailed methodology.....	139
4.4.2.2	Results	140
4.4.2.2.1	Validation of DASL results	140

4.4.2.2	Comparison of normalisation methods.....	145
4.4.3	Summary of qRT-PCR methodological work.....	145
4.5	Discussion.....	146
4.5.1	Development of methodology for qRT-PCR with FFPE melanoma tissue.....	146
4.5.2	Over-expression of DNA repair genes in melanoma tumours as a prognostic marker.....	147
5	Identification of differentially expressed genes in matched formalin-fixed paraffin-embedded primary and metastatic melanoma tumour pairs.....	152
5.1	Aims.....	152
5.2	Introduction.....	152
5.3	Further methodological details.....	154
5.3.1	Sampling of nodal and primary tumours.....	154
5.3.2	Gene expression profiling using the DASL assay.....	154
5.3.3	Statistical methodology.....	155
5.4	Results.....	156
5.4.1	Areas of nodal tumour sampled and RNA yields.....	156
5.4.2	Quality control measures, tissue characteristics and performance of samples with the DASL assay.....	158
5.4.3	Exclusion of samples.....	160
5.4.4	Reproducibility and detected genes across reference RNA samples.....	162
5.4.5	Genes detected across tissue types.....	162
5.4.6	Correlations between matched primary and nodal samples.....	162
5.4.7	Genes differentially expressed in matched primary and nodal pairs.....	163
5.4.8	Patient and primary tumour characteristics.....	166
5.5	Discussion.....	167
5.5.1	Use of the DASL assay with small sentinel node biopsy samples.....	167
5.5.2	Genes differentially expressed in matched primary and SNB samples.....	168
6	Identification of associations between somatic mutations in <i>BRAF</i> and <i>NRAS</i> in formalin-fixed melanoma tumours, clinico-pathological factors and gene expression profiles.....	171
6.1	Aims.....	171
6.2	Background.....	171
6.3	Identification of <i>BRAF</i> and <i>NRAS</i> mutations in FFPE primary melanoma tumours.....	183

6.3.1	Detailed methodology	183
6.3.1.1	Patients and samples	183
6.3.1.2	<i>BRAF</i> and <i>NRAS</i> mutation detection	183
6.3.1.3	Identification of patient and tumour factors associated with mutation status	184
6.3.1.4	Identification of gene expression profiles associated with mutation status	184
6.3.2	Results	185
6.3.2.1	Use of cDNA for mutation detection.....	185
6.3.2.1.1	Pyrosequencing of cell line DNA and cDNA.....	186
6.3.2.1.2	Pyrosequencing of FFPE melanoma metastasis DNA and cDNA.....	186
6.3.2.1.3	Pyrosequencing of cDNA from tumour samples....	186
6.3.2.1.4	Mutation screening of cDNA and DNA samples using the Applied Biosystems PRISM® SNaPshot™ Multiplex system for samples identified as having both <i>BRAF</i> and <i>NRAS</i> mutations in cDNA using pyrosequencing	188
6.3.2.2	<i>BRAF</i> and <i>NRAS</i> mutation results from FFPE primary melanoma specimens using DNA	190
6.3.2.2.1	Samples.....	190
6.3.2.2.2	Mutations identified	190
6.3.2.2.3	Correlations between results derived from pyrosequencing of matched cDNA and DNA samples.....	191
6.3.2.2.4	Associations with clinico-pathological features.....	192
6.3.2.2.5	Associations with survival	196
6.3.2.2.6	Gene expression patterns associated with mutation status.....	204
6.4	Discussion.....	204
6.4.1	Use of cDNA specimens for mutation detection	204
6.4.2	Associations between mutation status and clinico-pathological features and survival.....	207
6.4.3	Gene expression patterns associated with mutation status.....	209
6.4.4	Summary and conclusions.....	214
7	Primary melanoma tumour ulceration: relationship with gene expression profiles, tumour features and patient characteristics.....	216
7.1	Aims	216
7.2	Background	216
7.3	Methods	220
7.3.1	Patients and primary melanoma samples	220
7.3.2	Immunohistochemistry (IHC) methods	221

7.3.3	Gene expression data.....	222
7.3.4	Statistical analysis	222
7.3.5	Pathway analysis.....	223
7.4	Results	223
7.4.1	Patients and tumour samples.....	223
7.4.2	Effect of central histology review on ulceration status	223
7.4.3	Univariate analyses of clinico-pathological factors and ulceration ...	224
7.4.4	Factors independently associated with ulceration	228
7.4.5	Associations between IHC data and ulceration status.....	233
7.4.6	Gene expression profiles associated with tumour ulceration	236
7.5	Discussion.....	237
7.5.1	Relationship between ulceration and clinico-pathological factors	237
7.5.2	Ulceration status and immunohistochemical pathological factors	241
7.5.3	Gene expression and ulceration status	245
7.5.4	Summary	251
8	DNA repair gene expression and response to chemotherapy in stage IV melanoma.....	253
8.1	Aims	253
8.2	Background	253
8.3	Identification of genes associated with response to chemotherapy using the DASL assay	258
8.3.1	Further methodological details	258
8.3.1.1	Statistical methodology.....	258
8.3.2	Results	259
8.4	Validation of DASL results and further assessment of genes associated with chemotherapy response.....	259
8.4.1	Rationale	259
8.4.2	Further methodological details	260
8.4.2.1	The Chemo-sensitivity Gene Expression Assay (CGEA-1).....	260
8.4.3	Results	260
8.5	The “Predicting Response to Chemotherapy in Malignant Melanoma: The role of DNA repair genes” study	262
8.5.1	Study design and aims.....	262
8.5.2	Participants and samples.....	263
8.5.3	Clinical data.....	264
8.5.4	Power calculations.....	265

8.5.5	Regulatory approvals.....	265
8.6	Assessment of DNA repair gene expression in FFPE melanoma tumours using the Fluidigm qRT-PCR platform.....	266
8.6.1	Selection of genes for assessment	266
8.6.2	Pilot study	267
8.6.2.1	Samples	267
8.6.2.2	Methodological details	267
8.6.2.2.1	Specific target amplification (STA) of samples	267
8.6.2.2.2	Standard curve analysis.....	271
8.6.2.2.3	qRT-PCR reaction.....	271
8.6.2.2.4	Analysis of qRT-PCR data	271
8.6.2.3	Results	271
8.6.2.3.1	Amplification efficiencies of DELTAgene assays... ..	271
8.7	Assessment of DNA repair gene expression in tumours from patients recruited to the Chemotherapy study.....	274
8.7.1	Further methodological details	274
8.7.1.1	Samples	274
8.7.1.2	Fluidigm qRT-PCR	274
8.7.1.3	Data analysis.....	275
8.7.1.4	Statistical analysis	275
8.7.2	Results	276
8.7.2.1	Performance of the Fluidigm system	276
8.7.2.1.1	Reproducibility of replicate samples.....	276
8.7.2.1.2	Control samples.....	277
8.7.2.2	Gene expression analysis.....	278
8.7.2.2.1	Samples.....	278
8.7.2.2.2	Summary characteristics of patients and tumours assessed.....	279
8.7.2.2.3	Genes associated with response to chemotherapy.....	280
8.7.2.2.4	Genes with expression associated with survival after starting chemotherapy.....	282
8.8	Discussion.....	287
8.8.1	Gene expression profiling in FFPE primary melanoma tumours.....	287
8.8.2	DNA repair gene expression and response to chemotherapy	288
9	Final discussion.....	293
9.1	Prognostic biomarkers.....	293
9.2	Predictive biomarkers.....	295
9.3	Methodological assessments.....	296

9.4	Limitations and future study	296
10	Appendix I: Genes on the Human Cancer panel	298
11	References.....	300

List of Tables

Table 1-1: Survival rates for melanoma based on the American Joint Committee on Cancer staging system for cutaneous melanoma (7 th edition).....	15
Table 1-2: Studies using microarray technology to identify genes associated with prognosis or progression in melanoma tissue samples.	25
Table 2-1: PCR and pyrosequencing primer sequences for amplification and analysis of <i>NRAS</i> codons 12 and 13, <i>NRAS</i> codon 61 and <i>BRAF</i> codon 600.	72
Table 2-2: Primers used for PCR amplification of template cDNA and DNA prior to the SNaPshot assay.	75
Table 2-3: Probes used in the SNaPshot assay.....	76
Table 2-4: Primary antibodies used for IHC staining.....	83
Table 3-1: Taqman® Gene Expression Assay probes used for qRT-PCR of <i>SPP1</i>	90
Table 3-2 (following page): Associations between quality control procedures, tumour characteristics and performance with the DASL assay.....	94
Table 3-3: Comparison of technical and biological replicate samples assessed in each study.	96
Table 3-4: Descriptive statistics of the two samples sets.....	97
Table 3-5: Top 20 genes with expression associated with relapse-free survival from the Cohort study (unadjusted analysis).	99
Table 3-6: The association of <i>SPP1</i> expression with relapse-free survival in the Cohort and SNB studies.....	100
Table 3-7: Gene expression correlations for <i>SPP1</i>	102
Table 3-8: Correlations and differences in gene expression for genes identified in the Ingenuity network as being linked to <i>SPP1</i>	103
Table 4-1: Top 25 genes associated with relapse-free survival (analysis adjusted for study and SNB status).....	120
Table 4-2: The association of genes involved in DNA repair with relapse free survival in multivariate models.	122
Table 4-3: DNA repair genes differentially expressed in relation to Breslow thickness and mitotic rate.....	125
Table 4-4: Gene expression correlations for DNA repair genes adjusted for study and relapse status.	126
Table 4-5: Gene ontology terms associated with genes that influence relapse-free survival.	127

Table 4-6: KEGG (Kyoto Encyclopedia of Genes and Genomes) pathways associated with genes that influence relapse-free survival.....	129
Table 4-7 (following page): Remaining genes from the Human Cancer panel most correlated with principal component 1.	130
Table 4-8: Details of Taqman® Gene Expression assays for DNA repair gene qRT-PCR experiments.....	134
Table 4-9: Taqman® Gene Expression assay probe efficiencies in cDNA generated from RNA extracted from an FFPE metastatic melanoma sample.	134
Table 4-10: Mean cycle threshold values and intraclass correlation coefficients for sample replicates for each qRT-PCR assay.....	141
Table 4-11: Fold changes in mean gene expression of <i>RAD52</i> , <i>RAD54B</i> and <i>TOP2A</i> in tumours of patients who relapse compared to non-relapsers as determined using qRT-PCR.....	142
Table 4-12: Correlations between DNA repair gene expression data derived from qRT-PCR and DASL.	144
Table 5-1: Characteristics of nodal samples and extracted RNA.....	159
Table 5-2: Characteristics of sections used for tissue sampling.	160
Table 5-3: Genes most differentially expressed across matched primary and sentinel node biopsy samples.	164
Table 5-4: Clinical characteristics of patients and key primary tumour histological features of the samples assessed in analysis of matched primary and sentinel node biopsy specimens.....	166
Table 6-1: Patient and tumour characteristics associated with <i>BRAF</i> or <i>NRAS</i> mutations in melanoma tumours.....	177
Table 6-2: Summary of studies assessing gene expression profiles in tumours with <i>BRAF</i> or <i>NRAS</i> mutations.	181
Table 6-3: Summary of <i>BRAF</i> and <i>NRAS</i> mutation screening results from cDNA synthesised from RNA extracted from 160 primary melanoma samples.	187
Table 6-4: Summary of <i>BRAF</i> and <i>NRAS</i> pyrosequencing results for DNA extracted from 279 primary melanoma tumours.....	191
Table 6-5: Associations between tumour <i>BRAF</i> and <i>NRAS</i> mutation status and clinico-pathological features.	195
Table 6-6: Associations between tumour V600E and V600K <i>BRAF</i> mutations and clinico-pathological features.	198
Table 6-7: Associations between tumour mutation status and relapse-free survival in multivariate analysis.	203
Table 6-8: The top 10 most differentially expressed genes between wild-type tumours, tumours with <i>BRAF</i> mutations and <i>NRAS</i> mutations.	205
Table 7-1: Associations between clinico-pathological features and ulceration in univariate analysis.....	227

Table 7-2: Results of univariate and multivariate logistic regression analyses in the larger dataset identifying clinico-pathological factors associated with ulceration status.	230
Table 7-3: Results of univariate and multivariate logistic regression analyses with the significantly smaller data set subjected to central review of histology: clinico-pathological factors associated with ulceration status.	232
Table 7-4: Results of univariate and multivariate analyses identifying associations between lymphovascular parameters and macrophage count (determined using immunohistochemistry), and ulceration status in primary melanoma tumours.....	235
Table 7-5: Top 20 genes differentially expressed in ulcerated tumours.....	236
Table 7-6: Top 5 KEGG (Kyoto Encyclopedia of Genes and Genomes) pathways containing differentially expressed genes in ulcerated tumours.	238
Table 8-1: Genes on the Chemo-sensitivity Gene Expression Array (CGEA-1).	257
Table 8-2: Genes differentially expressed in tumours unresponsive to chemotherapy using the Chemo-sensitivity Gene Expression Array (CGEA-1).....	261
Table 8-3: Number of patients recruited to the Chemotherapy study.....	264
Table 8-4 (following 3 pages): Details of genes assessed using the Fluidigm qRT-PCR platform with DELTAgene assays in samples from the Chemotherapy study.	267
Table 8-5: Intraclass correlation coefficients with eighteen and twenty-two pre-amplification cycles.	273
Table 8-6: Summary of samples from the Chemotherapy study assessed using qRT-PCR of DNA repair genes.....	278
Table 8-7: Summary tumour and patient characteristics for samples used in the primary analysis for the Chemotherapy study.	279
Table 8-8: Top 10 genes associated with chemotherapy response in the whole dataset and then primary tumours, metastases and patients treated with dacarbazine or temozolomide monotherapy only.....	281
Table 8-9: Top 10 genes associated with survival after starting chemotherapy in the whole dataset and then primary tumours, metastases and patients treated with dacarbazine or temozolomide monotherapy only.....	285
Table 8-10: Results of multivariate survival analysis assessing the relationship between <i>MGMT</i> gene expression and survival after starting chemotherapy in the whole dataset and then primary tumours, metastases and tumours from patients who received DTIC/TMZ monotherapy only.	286

List of Figures

Figure 1-1: Melanoma development – a hypothetical model.	4
Figure 1-2: Deregulated pathways during melanoma progression.	5
Figure 1-3: Summary of surgical treatments and investigations used in the diagnosis and staging of melanoma.	10
Figure 1-4: Activation of the classical JAK-STAT pathway by type 1 IFN.	29
Figure 1-5: Production and action of endogenous type 1 interferons.	30
Figure 2-1: A haematoxylin and eosin slide marked for tumour sampling.	43
Figure 2-2: Using a tissue microarray needle to take a tissue core from a tumour block.	43
Figure 2-3: The DASL assay.	58
Figure 2-4: Scatter plot demonstrating correlation between probe signal intensities for replicate FFPE melanoma samples on the WG-DASL HT assay.	63
Figure 2-5: Action of Taqman® Gene Expression Assays.	65
Figure 2-6: The Fluidigm 96:96 Dynamic Array™ integrated fluidic circuit (IFC).	69
Figure 2-7: Pyrograms for <i>BRAF</i> codon 600.	73
Figure 2-8: A section of exon 15 of the <i>BRAF</i> gene to demonstrate the position of SNaPshot probes in relation to common <i>BRAF</i> mutations.	76
Figure 2-9: Examples of mutations detected using SNaPshot in cDNA and DNA.	78
Figure 2-10: Consecutive stains of melanoma sections with haematoxylin and eosin (H+E) (A), anti-D2-40 (B), anti-CD34 (C) and anti-CD68 (D) (20x magnification).	84
Figure 3-1: Gene network involving <i>SPP1</i> from Ingenuity Pathway Analysis in pooled data (showing only direct interactions except those involving <i>SPP1</i>).	104
Figure 4-1: Kaplan Meier survival function estimates for <i>RAD52</i> and <i>TOP2A</i> gene expression.	123
Figure 4-2: Hierarchical display of biological process GO terms associated with genes with expression fold change >1 between relapsers and non-relapsers.	128
Figure 4-3: Gene network significantly correlated with principal component 1 from Ingenuity Pathway Analysis: cancer, cell cycle and cell death.	132
Figure 4-4: Dot-plot of cycle threshold values for cDNA samples generated from RNA extracted from four metastatic melanoma samples and one intra-dermal naevus (calibrator sample).	137

Figure 4-5: Average gene stability values (M values) of control genes during stepwise exclusion of least stable control genes.....	138
Figure 4-6: DNA repair mechanisms.	149
Figure 5-1: Representative nodal sample before laser capture microdissection (A) and following laser capture microdissection (B).	157
Figure 5-2: Cumulative distribution of number of detected genes in nodal and primary samples.	161
Figure 5-3: Association between gene expression levels for 502 genes from the Human Cancer panel for a matched primary and nodal sample from the same patient.....	163
Figure 5-4: Genes most differentially expressed across matched primary and sentinel node biopsy samples.	165
Figure 6-1: The mitogen-activated protein kinase (MAPK) and phosphatidylinositol-3-kinase (PI3K) pathways.	172
Figure 6-2: Distribution of A allele levels for V600E <i>BRAF</i> mutations in cDNA samples with and without <i>NRAS</i> mutation.	188
Figure 6-3: Scatter plots showing percentage mutation levels for V600E <i>BRAF</i> (A) and <i>NRAS</i> (B) levels from matched cDNA and DNA samples using pyrosequencing.....	193
Figure 6-4: Kaplan-Meier plots and results of survival analyses used to identify associations between relapse-free (A), overall (B) and melanoma-specific survival (C) and tumour genotype.	200
Figure 6-5: Kaplan-Meier plots and results of survival analyses used to identify associations between relapse-free (A), overall (B) and melanoma-specific survival (C) and tumour genotype where V600E and V600K <i>BRAF</i> mutations were analysed separately.	202
Figure 7-1: Assessment of tumour samples for tissue sampling for gene expression and immunohistochemical studies.	221
Figure 7-2: Changes in reported ulceration status of melanoma primary tumours following central histological review.....	224
Figure 7-3: The KEGG (Kyoto Encyclopedia of Genes and Genomes) 'Jak-STAT signalling pathway' adapted to demonstrate fold changes in gene expression between ulcerated and non-ulcerated tumours.	239
Figure 7-4: The prognostic and predictive implications of greater macrophage infiltration and microvessel density in ulcerated tumours. ..	245
Figure 7-5 (following page): Loss of molecules involved in cell adhesion leading to epidermal loss and ulceration of primary melanoma tumours.	247
Figure 8-1: Mechanism of action of dacarbazine.....	255
Figure 8-2: Scatter plot demonstrating the association between sample reproducibility and mean cycle threshold (Ct) value for the assay.....	273
Figure 8-3: Scatter plot showing correlation between two replicate samples assessed on two separate Fluidigm qRT-PCR arrays.	277

Figure 8-4: Box-plots showing <i>MGMT</i> gene expression in tumours responding differently to chemotherapy.....	282
Figure 8-5: Overall survival following start of chemotherapy according to response to chemotherapy treatment.	283

Abbreviations

AJCC	American Joint Committee on Cancer
bp (suffix)	Base pair
BRAFi	BRAF inhibitor
cDNA	Complementary DNA
°C (suffix)	Degrees Celsius
CGEA-1	Chemo-sensitivity Gene Expression Assay
CI	Confidence interval
Ct	Cycle threshold value
CT	Computed tomography
DAB	3,3' diaminobenzidine
DASL	cDNA-mediated annealing, selection, extension and ligation
DC	Dendritic cell
ddNTPs	Dideoxynucleoside triphosphates
DEPC	Diethylpyrocarbonate
DMEM	Dulbecco's Modification of Eagles high glucose Medium
DMFS	Distant metastasis-free survival
DNA	Deoxyribonucleic acid
dNTPs	Deoxyribonucleotide triphosphates
DTIC	Dacarbazine
DTT	Dithiothreitol
EDTA	Ethylenediaminetetraacetic acid
EORTC	European Organisation for Research and Treatment of Cancer
FCS	Foetal calf serum
FFPE	Formalin-fixed paraffin-embedded
g (suffix)	Gram
g (suffix)	Force of gravity
H+E	Haematoxylin and eosin
HR	Hazard ratio
ICC	Intraclass correlation coefficient
IFC	Integrated fluidic circuit
IFN	Interferon- α
IHC	Immunohistochemistry
l (suffix)	Litre
IL	Interleukin

LCM	Laser capture microdissection
LDH	Lactate dehydrogenase
LVD	Lymphatic vascular density
LVI	Lymphatic vascular invasion
µg	Microgram
µl	Microlitres
µM	Micromolar
mM	Millimolar
MAPK	Mitogen-activated protein kinase
mg	Milligram
ml	Millilitre
mm	Millimetres
MM	Metastatic melanoma
mRNA	Messenger ribonucleic acid
MMS	Melanoma-specific survival
MREC	Multicentre Research Ethics Committee
MVD	Microvessel density
M	Molar
ng	Nanogram
nm	Nanometre
NM	Nodular melanoma
oligo(dT)	Oligodeoxythymidylic acid residues
OR	Odds ratio
OS	Overall survival
PBS	Phosphate-buffered saline
PCR	Polymerase chain reaction
pH	Measure of acidity or alkalinity
PIAG	Patient Information Advisory Group
PI3K	Phosphatidylinositol-3-kinase
qRT-PCR	Quantitative Real-time PCR
RECIST	Response Evaluation Criteria in Solid Tumours
REMARK	REporting Recommendations for Tumour MARKer
RFS	Relapse-free survival
RIN	RNA integrity number
RNA	Ribonucleic acid
SAM	Sentrix Array Matrix
SAMic	Significance analysis of microarrays
SDS	Sodium dodecyl sulphate

SNB	Sentinel node biopsy
SNP	Single nucleotide polymorphism
SSM	Superficial spreading melanoma
STA	Specific target amplification
TBS	Tris-buffered saline
TILs	Tumour infiltrating lymphocytes
TMA	Tissue microarray
TMZ	Temozolomide
TNM	Tumour, node, metastasis
UK	United Kingdom
WG-DASL HT	HT Human Whole-Genome DASL assay

1 Introduction

Histological prognostic markers are used in malignant melanoma to provide information regarding risk of relapse following diagnosis, the American Joint Committee on Cancer (AJCC) staging system being most widely used. Current prognostic markers however explain only a proportion of the variance in survival between patients and are therefore inadequate for subsets of patients. This thesis describes work carried out to identify new genetic predictors of outcome which I postulated would also increase knowledge of the biology of melanoma.

There are some predictive biomarkers associated with treatment benefit currently used in melanoma, for example codon 600 *BRAF* mutations predict benefit from BRAF inhibitors (BRAFi). However, much better markers are required; as yet we have no marker which predicts resistance to BRAFi and we have no markers predicting response to older therapies such as dacarbazine (DTIC). In this thesis I also report results of work to evaluate putative predictive biomarkers for benefit from DTIC.

Identification of prognostic and predictive markers provides more information for patients and clinicians allowing a more personalised approach to treatment for melanoma.

1.1 Major thesis aims

The major aims of this thesis are:

- To develop methods for use of formalin-fixed paraffin-embedded (FFPE) melanoma tumour tissue for genomic analyses.
- To assess use of technologies for gene expression profiling in FFPE tissue.
- To identify novel prognostic factors in melanoma tumour tissue which provide additional prognostic information to that provided by current staging algorithms.
- To identify tumour factors predictive of responses to treatment in melanoma.
- To gain biological insight into mechanisms of melanoma progression.

1.2 Aims of this chapter

The aims of this chapter are:

- To describe what is known about malignant melanoma and common genetic alterations in melanoma tumours.
- To provide an overview of current prognostic factors and their limitations.
- To review prognostic markers identified in melanoma tumour tissue.
- To review current options for therapies in more advanced melanoma and their mechanism of action.
- To provide an overview of current predictive markers of treatment benefit and their limitations.
- To introduce further chapters of this thesis.

1.3 Cutaneous malignant melanoma

The skin is the largest organ of the body arranged into three layers: the superficial epidermis, dermis and hypodermis [1]. The epidermis is mostly made up of keratinocytes, with five to ten percent of cells being of different cell types, mainly melanocytes, Merkel cells and Langerhans cells [1]. Melanocytes migrate from the neural crest to epidermis where they produce pigment called melanin [1]. Melanoma arises from melanocytes in response to environmental and genetic factors [2].

1.3.1 Incidence

Malignant melanoma is the sixth most common cancer in the UK with an age-standardised incidence rate of 16 new cases per 100,000 population in 2009 [3]. Incidence is rising faster than any other common cancer in the UK [3].

1.4 Melanoma development

1.4.1 Risk factors for melanoma development

There is clearly a genetic contribution to melanoma susceptibility with a strong risk factor being family history [4-6]. Other risk factors associated with genetic predisposition are having a sun-sensitive skin phenotype and presence of multiple melanocytic naevi (moles) [4, 5, 7-9]. The importance of having sun-sensitive skin is

highlighted by genome-wide association studies which have identified polymorphisms in a number of genes associated with pigmentation, for example the gene encoding melanocortin-1 receptor (*MC1R*), as being associated with increased melanoma risk [5, 10, 11]. Emergence of naevi is also genetically determined with sun-exposure having a small effect on naevus number [12, 13]. Additional risk factors for melanoma development are having a previous melanoma, exposure to ultraviolet radiation and immunosuppression [4, 5, 7-9, 14, 15]. The contribution of genetic factors to melanoma development has been estimated to be 18-55% [16, 17]

1.4.2 Process of melanoma development

During melanoma development from a normal melanocyte, a series of genetic alterations occur (Figure 1-1). This model is a useful for the purposes of discussion but relates to only one developmental route where melanoma commonly develops from naevi. Melanoma can also develop from otherwise phenotypically normal melanocytes [18].

It is known that as tumours progress an increasing number of genetic changes develop within the cells. However, genetic (mutations, amplifications, deletions or translocations) and epigenetic changes (such as promoter hypermethylation) either drive the development of a melanoma, so-called driver events, or are passenger events that occur but have no effect on the cell [4, 18-22]. Some of the genetic changes involved in these processes can be inherited through families and predispose an individual to melanoma [2, 23, 24]. I will briefly describe some of the pathways commonly altered in melanoma tumours during their development.

1.4.2.1 Mitogen-activated protein kinase (MAPK) pathway

Activation of the mitogen-activated protein kinase (MAPK) pathway appears to occur early in melanoma development with oncogenic mutations driving this pathway commonly found in benign and dysplastic naevi [2, 18, 25]. A dysplastic naevus is clinically diagnosed and larger in diameter with irregular or variable shape and pigmentation. Such naevi are associated with melanoma risk and are more common in families with multiple melanoma cases [26, 27]. The MAPK pathway (Figure 1-2) regulates a number of processes within a cell including cell survival, growth and cell migration [28, 29]. *BRAF* is mutated in around 40% of melanoma tumours, with the majority of mutations due to a single base substitution (V600E) [30-32]. In tumours without *BRAF* mutations, there are usually mutations elsewhere in the MAPK pathway,

such in *NRAS* in cutaneous melanomas (18%) [30, 31], *KIT* in acral or mucosal melanomas [33] and *GNAQ* in uveal melanomas [34]. Identification of mutations in this pathway are the subject of Chapter 6 and will be discussed in further detail in this chapter.

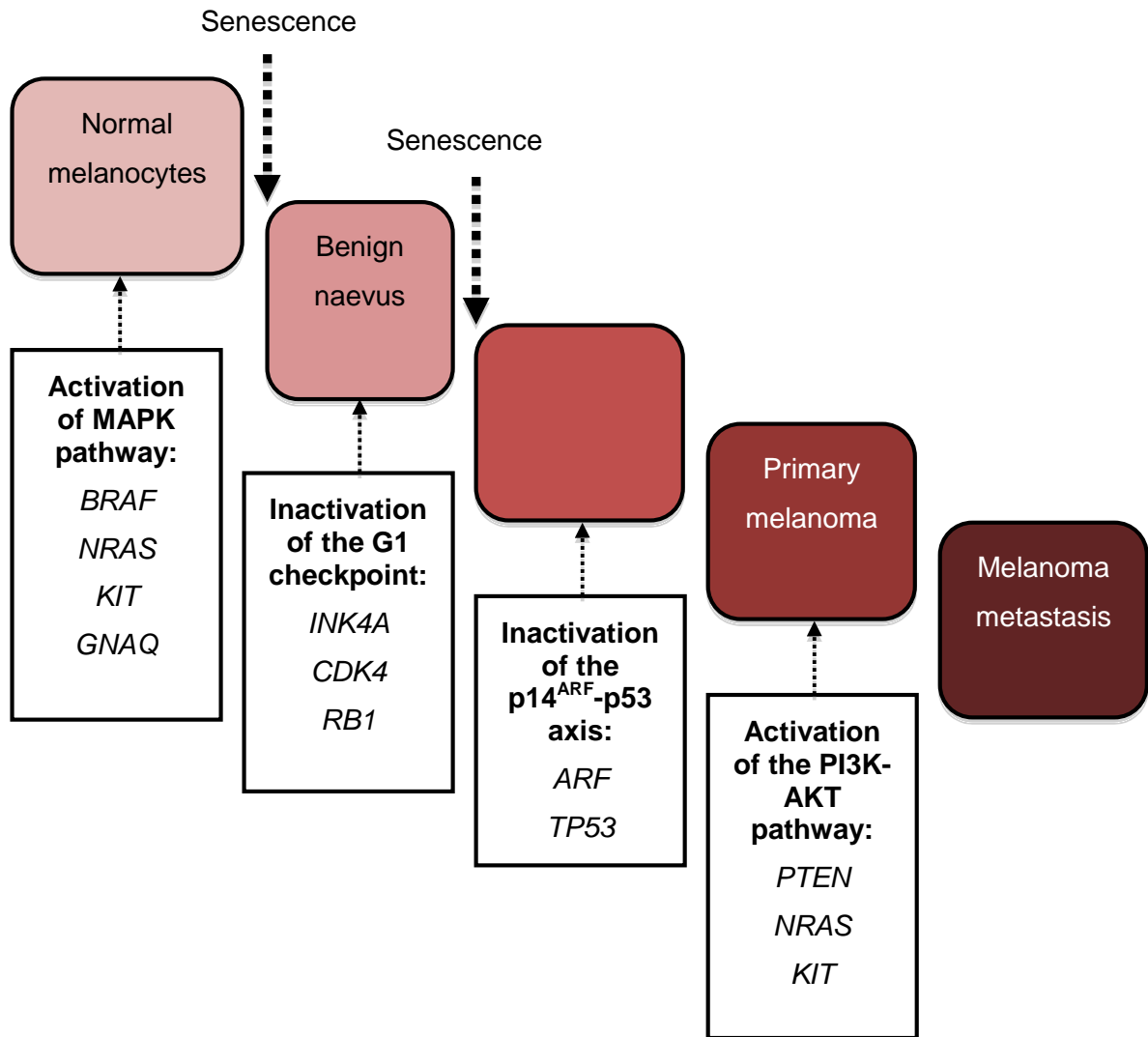


Figure 1-1: Melanoma development – a hypothetical model.

Genetic changes drive melanoma progression. Cells can only progress to the next step following changes in specific genes. See text for further details.

Adapted from [18, 22]. Abbreviations used: MAPK, mitogen-activated protein kinase; G1, gap 1 phase of the cell cycle; PI3K, phosphatidylinositol-3-kinase.

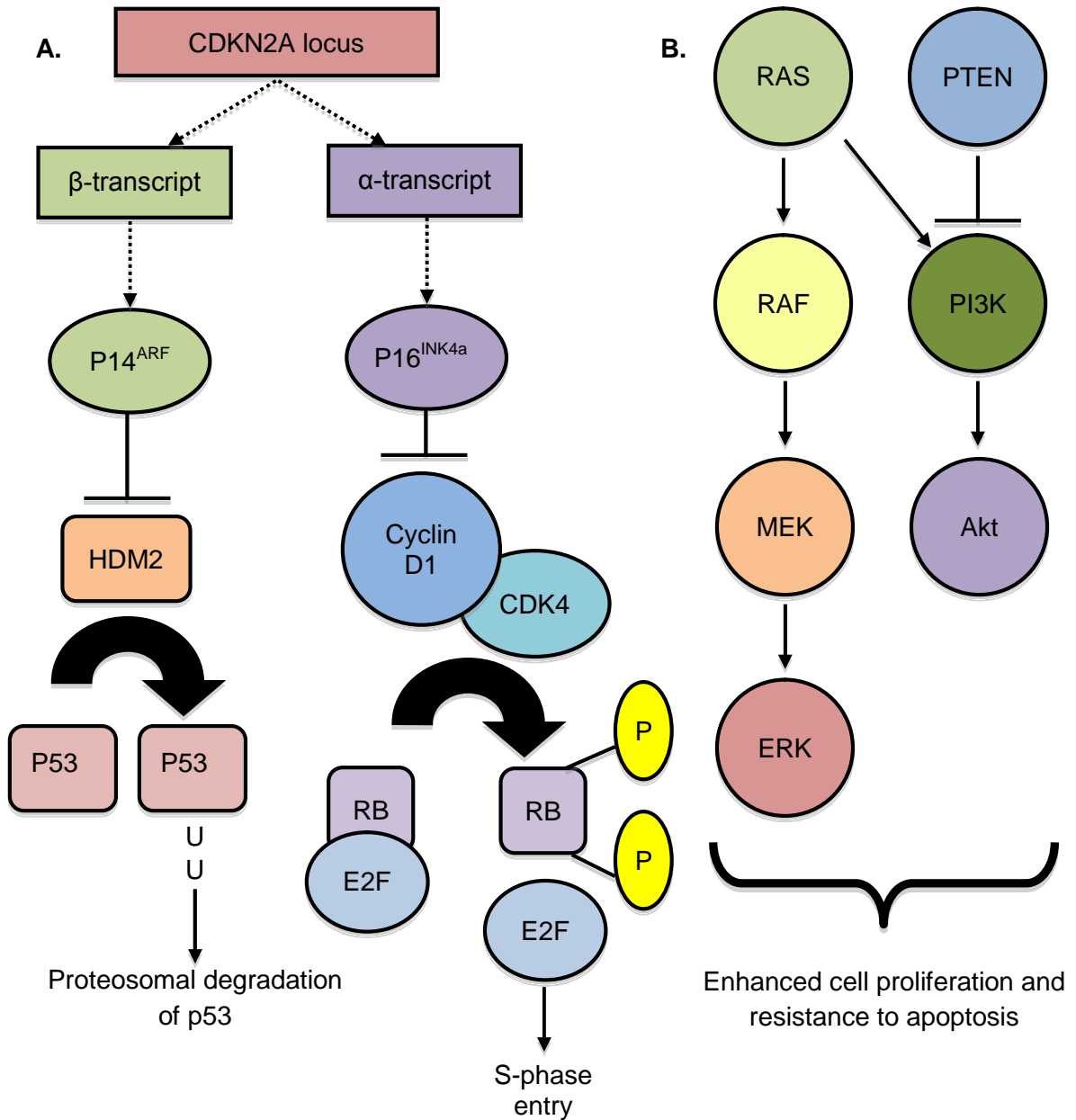


Figure 1-2: Deregulated pathways during melanoma progression.

A. The *CDKN2A* locus encodes p16^{INK4A} and p14^{ARF}, p16^{INK4A} inhibits the cyclin-D-dependent kinases CDK4 and CDK6. Loss of p16^{INK4A} leads to CDK-mediated phosphorylation of retinoblastoma protein (RB), leading to release of E2F transcription factors which stimulate entry into the cell cycle. HDM2 is inactivated by p14^{ARF} which activates the tumour suppressor p53. Inactivation of p14^{ARF} leads to HDM2-mediated inactivation of p53 via activation of HDM2, which targets p53 for degradation [18]. (Continued on following page)

(Figure 1-2 cont.) B. The mitogen-activated protein kinase (MAPK) pathway and phosphatidylinositol-3-kinase (PI3K) pathway. *NRAS* mutations activate both pathways. The MAPK pathway can also be activated by mutations in *BRAF*. *ERK* can also be constitutively active in absence of *NRAS* and *BRAF* mutations. The PI3K pathway may be activated by loss of the inhibitory function of *PTEN*, or by gene amplification of *AKT3* [35]. Figure adapted from reference [18].

1.4.2.2 p16^{INK4a}, cyclin dependent kinases 4/6 and retinoblastoma (RB) protein

Melanocytes that develop *BRAF* mutations usually do not evolve into a tumour as the cells enter senescence after a period of time as a result of induction of tumour suppressor proteins such as p16^{INK4A} or p15^{INK4b} [19, 36, 37]. When the p16^{INK4a} - cyclin dependent kinases 4/6 - RB senescence barrier is inactivated, continued development into a melanoma may occur [18, 19]. p16^{INK4A} is encoded by the *CDKN2A* locus [18, 19] and inhibits the cyclin-dependent kinases, CDK4 and CDK6, which maintains RB protein in an inactivated, hypophosphorylated state so preventing entry into the S-phase of the cell cycle (Figure 1-2) [18, 19]. p16^{INK4A} is usually inactivated in melanomas secondary to mutations, deletions or promoter hypermethylation of *CDKN2A* [19, 21]. Less frequently, genetic changes can affect other parts of this pathway, for example mutations in *CDK4* are found in up to 10% of melanomas [19, 21]. CDK4 mutant proteins cannot bind p16^{INK4A} and consequently RB protein remains phosphorylated and active [38]. Inactivating mutations in the gene that encodes RB protein (*RB1*) have been identified in melanoma cell lines, but have not been assessed further in melanoma tumours [38].

1.4.2.3 p14^{ARF} and p53

Melanocytic cells that lack p16^{INK4A} eventually undergo growth arrest in many cases [22] and up-regulate p53 [39] which is likely to be an alternative senescence barrier to that of the p16^{INK4A} - CDK4/6 - RB pathway. p14^{ARF} is a positive regulator of p53, therefore the p14^{ARF}-p53 senescence barrier may also need to be inactivated to allow melanoma development [18]. *TP53* mutations are found in 5-25% of melanoma tumours [19, 21]. However, p14^{ARF} is also encoded by the *CDKN2A* locus using an alternative reading frame to p16^{INK4a} and so is also lost when *CDKN2A* is mutated with p14^{ARF} loss having the same effect as p53 loss [18] (Figure 1-2). There is also evidence that inactivation of p14^{ARF} is common in melanomas and occurs independently of p16^{INK4A} inactivation [40].

1.4.2.4 PTEN and the phosphatidylinositol-3-kinase (PI3K) pathway

PTEN is a tumour suppressor which negatively regulates the PI3K signalling pathway; inactivation of *PTEN* by deletion or mutation activates this pathway, which stimulates cell growth and survival [18, 41] (Figure 1-2). The PI3K pathway is usually hyperactive in melanoma metastases, but *PTEN* inactivation accounts for less than 50% of cases, in the remaining cases mutations in other genes can activate the pathway, such as *NRAS* [30], *KIT* [33] and *PIK3CA* [42]. Inactivation of *PTEN* is usually associated with *BRAF* mutations, so *BRAF* mutated tumours have up-regulation of both MAPK and PI3K pathways [43, 44].

1.5 Melanoma tumour progression

1.5.1 Melanoma metastasis

A primary tumour is a heterogeneous mix of cells with a minority harbouring genetic alterations that allow them to spread and colonize distant organs [45-47]. Metastasis is the spread of primary tumour cells to distant organs that then grow and is the usual cause of death from cancer [46, 47]. It is dependent on characteristics of tumour cells as well as the response of the host [45-47]. Characteristics of primary tumour cells that predispose to metastasis formation are loss of cellular adhesion, greater motility and invasiveness, being able to enter and then survive in the circulation, leaving vessels into a new tissue and then colonization of a new site [46-48].

To expand further on the model presented in Figure 1-1, there are a number of histological changes that occur as normal melanocytes progress to a metastatic melanoma, which were originally described by Clark [49]. The Clark model describes five phases of progression from a melanocyte to melanoma, these being proliferation of melanocytes to form benign naevi where nested melanocytes lie along the basement membrane of the epidermis. Benign naevi transform into dysplastic naevi or dysplastic naevi can develop independently in a new location, the cells of these lesions are commonly more atypical. Melanoma cells then develop which progress through a radial growth phase where cells grow horizontally within the epidermis or the upper papillary dermis which then progress to a vertical growth phase where cells penetrate the basement membrane and invade the dermis. This primary melanoma then makes the transition into a metastatic melanoma, having sustained sufficient genetic aberrations to allow tumour cell growth throughout the body [4, 49]. In order for an established melanoma to progress through to the invasive vertical growth phases and then become metastatic, it develops some of the important characteristics of a metastatic tumour

described above. An example of this is that there is loss of adhesion between keratinocytes and melanoma cells in the epidermis, by down-regulation of E-cadherin expression, with up-regulation of N-cadherin allowing adhesion with dermal fibroblasts and vascular endothelium [50-52]. Metastases develop when cells leave the primary tumour, migrate into stroma and invade lymphatics and blood vessels to form tumour at a distant site [4, 53]. Typically, the first site for melanoma metastasis is the regional nodal basin, specifically a “sentinel-node”, which is the first tumour-draining node in the lymphatic chain [54, 55]. Following this, the tumour disseminates systemically [55]. This is the predominant pattern of metastasis in melanoma, but a minority develop systemic disease early, sometimes to a single organ, such as the lungs or the brain, but in some cases more widely to a number of visceral sites [56, 57]. The presence of nodal metastases is an important clinical predictor of outcome, which will be discussed further in section 1.7.1.2 [58, 59].

1.5.2 Melanoma interactions with host immunity

As discussed, melanoma spread is dependent on characteristics of tumour cells but it is clear that the response of the host to those cells is also critical [45-47]. Host/tumour interaction involves the immune system and the tumour microenvironment; these interactions are active and complicated. The reported efficacy of immunotherapies in melanoma in recent times however shows the potential for immunotherapies in the future [60, 61].

Immune responses to the tumour are usually categorised as either innate or adaptive, although both are intimately connected. Innate immune mechanisms are rapid compared to adaptive responses and are usually associated with inflammation [62]. Cells associated with innate responses are plasmacytoid dendritic cells and phagocytic neutrophils which are activated by pattern recognition receptors [62]. Natural killer cells recognise major histocompatibility complex (MHC) class 1 antigens on cells, and are regulated by balance in the function of activating and inhibitory receptors [63]. Myeloid dendritic cells, monocytes and macrophages are phagocytic and can present antigen to components of the adaptive immune response, such as T and B cells [62].

The immune system of the skin and lymphatics is essential for identifying and targeting destruction of melanoma cells by adaptive immune systems. Langerhans cells are dendritic cells present in the epidermis of skin, which migrate via dermal lymphatics to draining lymph nodes and present antigen to T cells [64]. Activated tumour antigen-specific T cells expressing the skin homing receptor cutaneous leucocyte antigen (CLA), migrate out of dermal blood vessels into the skin and mediate cellular immunity

[64]. Presence of cytokines either support or inhibit this process. Melanoma is a tumour that interacts with the immune system and expresses antigens that T cells recognise. T cells can destroy melanoma cells and regression of melanoma tumours indicating immune destruction of melanoma cells is well described [64]. The presence of a brisk T cell infiltrate in melanoma tumours is associated with longer survival [65, 66] as is the development of vitiligo due to autoimmune destruction of melanocytes [67-69] highlighting the prognostic importance of the immune response to tumour.

Although active immune responses to melanoma cells can be demonstrated, it is usually not effective in destroying the tumour and there are data to suggest that tumour cells inhibit these responses. Melanoma cells can inhibit antigen processing cell maturation preventing expression of co-stimulatory molecules required for T cell activation [70], tumour cells can also down-regulate MHC class 1 expression [71, 72] so becoming invisible to class 1 restricted cytotoxic T cells [70]. Factors secreted by the tumour microenvironment, such as immunosuppressive cytokines (IL10 and TGF β), can also render cytotoxic T cells inactive or enhance function of regulatory T cells which promote tolerance [73-75].

In summary, melanoma is an immunogenic tumour which interacts with the host immune system and adapts to evade detection and destruction. These interactions are relevant to both the prognosis of a patient with melanoma and to the response of the tumour to therapy, but much more needs to be understood about these interactions in order to optimise immunotherapies.

1.6 Patient assessment and melanoma tissue processing

I will briefly describe the assessment of a patient who presents with a suspicious skin lesion and focus on processing of melanoma tumour tissue following surgical removal because of the impact this has on tumour research. This process is summarized in Figure 1-3.

If a melanoma is suspected, it is excised completely ideally with a margin of 2mm of normal skin and a cuff of fat [76]. The specimen is then placed in 10% neutral buffered formalin which fixes the tissue by generating cross-links between proteins and nucleic acids [77]. The specimen is embedded in paraffin and sectioned. Sections are stained with haematoxylin and eosin (H+E) and reviewed by a pathologist. The Royal College of Pathologists has advised that a minimum dataset should be reported for all specimens which are tumour thickness, mitotic rate, histological subtype, margins of excision, growth phase, presence of ulceration, regression, tumour-infiltrating

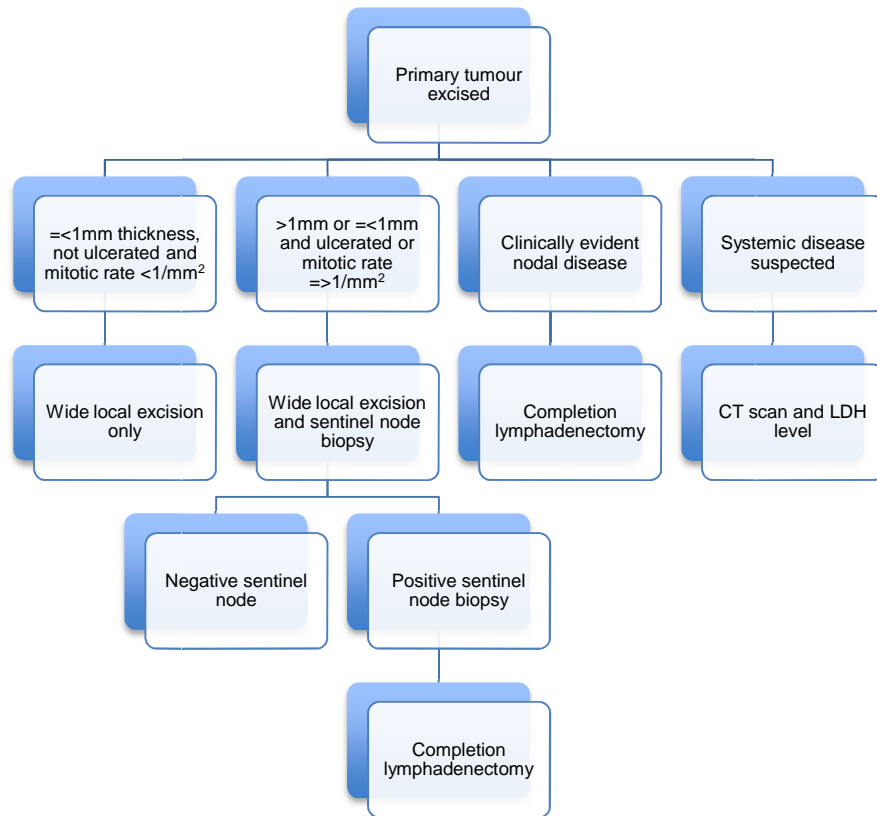


Figure 1-3: Summary of surgical treatments and investigations used in the diagnosis and staging of melanoma.

Further detail is provided in the text. This flow-chart presents guidelines in the UK [76]. Abbreviations used: CT, computed tomography; LDH, lactate dehydrogenase.

lymphocytes, lymphatic or vascular invasion, perineural invasion, microsatellites and pathological staging [76, 78]. Once the diagnosis of melanoma has been confirmed, patients usually undergo a wide local excision to the depth of the muscle fascia to ensure complete removal of the melanoma along with any micrometastases that may be present [76]. This specimen will also be formalin-fixed and examined pathologically to determine the margin of melanoma free tissue [76]. If a tumour is greater than 1mm in thickness or less than 1mm with ulceration or a mitotic rate equal to or greater than $1/\text{mm}^2$, a sentinel lymph node biopsy is usually offered to identify presence of metastatic deposits [79]. This procedure normally takes place simultaneously with the wide local excision procedure [76, 80]. It involves injecting blue dye and radioactive tracer into the skin where the melanoma is located and identifying the first draining node which is then removed [54, 80]. This “sentinel node” represents the node most likely to contain micrometastatic tumour cells. Assessment of the FFPE sentinel node involves bivalving the node and a minimum of six serial sections are taken [76, 81].

These sections are stained with H+E and immunohistochemical stains specific for melanoma cells, such as S100 or Melan A [76]. The depth of metastases from the node capsule is measured, as is the size of the largest deposit, and the site is categorized as either subcapsular or parenchymal [82, 83]. If a patient has a positive sentinel lymph node or palpable nodal disease at diagnosis, they will usually undergo a completion lymphadenectomy to remove regional nodes. The pathologist will examine sections stained with H+E and immunohistochemical stains from all the nodes from at least one level and count the number with metastatic deposits [76]. If there is any extracapsular spread or involvement of fat around the node this is also recorded [76]. If further systemic spread of disease is suspected, computed tomography (CT) scanning of the body is usually performed to identify sites of disease and lactate dehydrogenase (LDH) level measured [76]. The factors assessed are of importance prognostically and will be discussed further in section 1.7.1 below.

1.7 Prognosis in melanoma

Survival from melanoma has improved over the last 25 years in England and Wales [84, 85]. Prognosis for those with thin tumours ($\leq 1\text{mm}$) following surgery is excellent, however for those with thicker primary tumours ($\geq 2\text{mm}$) or with nodal or more extensive metastatic spread, survival rates at 5 and 10 years are much lower (Table 1-1)[58, 86].

Outcome from melanoma can be influenced by factors specific to the patient and to the tumour. Many of these factors have been identified by studying outcome in large cohorts of patients and are currently used to provide general prognostic estimates for patients with melanoma in the form of the American Joint Committee on Cancer (AJCC) Staging Guidelines (Table 1-1) [58]. I will review the current factors used for staging of melanoma tumours and then describe additional factors which influence prognosis, but are not currently included in staging criteria.

1.7.1 Prognostic factors currently used in melanoma staging

1.7.1.1 Primary tumour features

1.7.1.1.1 Breslow thickness

Tumour thickness was identified as an important prognostic factor in melanoma in 1953 [87] and was further developed by Breslow in 1970, who suggested that measurement of maximal tumour thickness can be used to calculate maximal cross-sectional area of

tumour which is proportional to tumour volume [88], which further correlates with prognosis [89, 90]. This was incorporated into the AJCC staging system and remains the most important single prognostic factor in localised melanoma today [58, 91]. It is now accepted that Breslow thickness is a more powerful prognostic factor than level of invasion as described by Clark *et al.* [92, 93]. Breslow thickness is also predictive of survival in patients with nodal metastases (stage III) disease [58, 59].

1.7.1.1.2 Tumour ulceration

Ulceration of a primary melanoma is defined as absence of intact epidermis, including stratum corneum and basement membrane [94]. Primary tumour ulceration is a powerful prognostic factor in both localised melanoma and stage III melanoma [58, 59]. Breslow thickness remains the strongest predictor of survival in localised disease, however presence of ulceration influences survival from tumours strongly, modifying survival to that of a non-ulcerated melanoma in the next thickness category [58]. Further discussion of the pathogenesis and prognostic influence of ulceration is presented in Chapter 7.

1.7.1.1.3 Mitotic rate

The mitotic rate (number of mitoses seen per mm² in the most mitotically active component of viable tumour sample) reflects proliferation and is a strong independent predictor of survival [58]. A number of studies have demonstrated that the presence and number of mitoses within a stage I or II tumour strongly correlates with prognosis second only to tumour thickness [95-98]. The 7th edition of AJCC staging criteria has replaced Clark level with mitotic rate ≥ 1 mitoses/mm² as a primary criteria (with ulceration) for defining a subcategory T1b [58].

1.7.1.2 Nodal metastatic disease (stage III)

Development of metastases is associated with poorer prognosis and is influenced by interaction between tumour characteristics, such as high proliferative rate and host factors, for example the immune system and physical barriers such as walls of lymphatic vessels. Development of metastases represents the tumour breaching host defences and biological features of the tumour indicating cellular ability to grow in disparate tissues.

The number of tumour bearing nodes and whether tumour deposits in involved nodes are microscopic, being diagnosed after a sentinel lymph node biopsy, or macroscopic, which are clinically detected, all determine prognosis with smaller burden associated with better outcome [58, 59]. Location of deposits in sentinel nodes is also of prognostic importance as deposits confined to the subcapsular sinus are less frequently associated with more extensive nodal spread, than deposits within the parenchyma of the node [99]. The size of sentinel node deposits also influences outcome, with small (<0.1mm) deposits associated with similar prognosis to patients with a negative sentinel node biopsy [100]. Location and size of sentinel nodal deposits are not currently integrated into staging criteria, however with more sentinel node biopsy procedures taking place and improved pathological reporting, this may change [58]. Primary tumour thickness and ulceration remain prognostic in stage III disease [58, 59]. In transit or satellite metastases are considered as intralymphatic metastases and consequently associated with poorer prognosis equivalent to that of stage III disease [101, 102].

1.7.1.3 Systemic metastatic disease (stage IV)

In stage IV disease, non-visceral metastases to skin, subcutaneous tissues and lymph nodes are associated with better survival than metastases at visceral sites [58, 91]. Furthermore, lung metastases are associated with better prognosis than other visceral sites [58, 103, 104]. These survival differences are likely related to biological differences between tumours able to grow in different tissues, but the determinants are as yet poorly understood.

Elevated serum levels of lactate dehydrogenase (LDH) correlate with poor prognosis in stage IV disease [58, 105-108]. This enzyme is widely distributed in cells of many lineages and levels are increased in the blood in the presence of cellular break down [108]. Levels of LDH in some cancer patients reflect tumour burden and rate of proliferation of cells [107, 108]. In the current AJCC guidelines, elevated LDH indicates a poorer prognosis in stage IV disease irrespective of the metastatic site [58].

Stage	TNM	Thickness (mm)	Ulceration and mitotic rate (per mm ²)	No. positive nodes	Nodal size	Distant metastasis	5-year survival %	10-year survival %	5 year UK survival %	10 year UK survival %
IA	T1a	≤1	No and mitosis <1	0	-	-	95.3	87.9	95	87-89
IB	T1b	≤1	Yes or mitosis ≥1	0	-	-	90.9	83.1	88-92	78-85
	T2a	1.01-2.0	No	0	-	-	89.0	79.2		
IIA	T2b	1.01-2.0	Yes	0	-	-	77.4	64.4	77-79	62-66
	T3a	2.01-4.0	No	0	-	-	78.7	63.8		
IIB	T3b	2.01-4.0	Yes	0	-	-	63.0	50.8	61-70	49-57
	T4a	>4.0	No	0	-	-	67.4	53.9		
IIC	T4b	>4.0	Yes	0	-	-	45.1	32.3	43-47	31-34
IIIA	N1a	Any	No	1	Micro	-	69.5	63.0	57-73	50-67
	N2a	Any	No	2-3	Micro	-	63.3	56.9		
IIIB	N1a	Any	Yes	1	Micro	-	52.8	37.8	41-57	29-53
	N2a	Any	Yes	2-3	Micro	-	49.6	35.9		
	N1b	Any	No	1	Macro	-	59.0	47.7		
	N2b	Any	No	2-3	Macro	-	46.3	39.2		
	N2c	Any	No	In transit metastases/satellites with no metastatic nodes	-	-	-	-		
IIIC	N1b	Any	Yes	1	Macro	-	29.0	24.4	20-34	11-29
	N2b	Any	Yes	2-3	Macro	-	24.0	15.0		
	N2c	Any	Yes	In transit metastases/satellites with no metastatic nodes	-	-	-	-		
	N2c	Any	Yes	In transit metastases/satellites with no metastatic nodes	-	-	-	-		

Stage	TNM	Thickness (mm)	Ulceration and mitotic rate (per mm ²)	No. positive nodes	Nodal size	Distant metastasis	5-year survival %	10-year survival %	5 year UK survival %	10 year UK survival %
IIIC cont.	N3	Any	Any	4 or more nodes, or matted nodes, or in transit metastases/satellites with metastatic nodes	Micro or macro	-	26.7	18.4		
IV	M1a	Any	Any	Any	Any	Distant skin, subcutaneous or nodal	18.8	15.7	5-22	
	M1b	Any	Any	Any	Any	Lung	6.7	2.5		
	M1c	Any	Any	Any	Any	Other visceral metastases or any distant metastasis with elevated LDH level	9.5	6.0		

Table 1-1: Survival rates for melanoma based on the American Joint Committee on Cancer staging system for cutaneous melanoma (7th edition).

Adapted from [58, 102]. Survival rates for pathological stage are for the UK taken from [109], with survival rates for individual TNM staging taken from [102] which used Clark (invasion) level to determine T1a and T1b stages and has now been replaced with mitotic rate.

Abbreviations used: TNM, tumour, node, metastasis; SEM, standard error mean; SC, subcutaneous; LDH, lactate dehydrogenase.

1.7.2 Prognostic factors not part of current staging guidelines

1.7.2.1 Tumour factors

1.7.2.1.1 Vascular and lymphatic invasion

As metastasis occurs via lymphatic and blood vessels, it is unsurprising that high tumour vascularity and presence of lymphovascular invasion in primary tumours has been associated with poorer prognosis in a number of studies [110-112]. Lymphatic invasion appears to predominate over vascular invasion in primary tumours [110, 113], however identification of lymphatic invasion using slides routinely stained using H+E alone can be difficult as invasion can be focal and it is difficult to distinguish vessel walls from other stromal tissues without special stains [114]. It has been shown that use of specific immunohistochemical staining for vessels can increase detection [110, 113]. These factors are not routinely reported on many primary melanoma histology reports and so have not been assessed in large sample sets, such as the AJCC staging database. Consequently, these factors do not form part of AJCC staging, but may represent a primary tumour factor which reflects propensity to metastasis. Use of immunohistochemical staining for these factors is discussed further in Chapter 7.

1.7.2.1.2 Perineural infiltration

Perineural invasion occurs when melanoma cells invade the nerve sheath and spread along the protective layer, the perineurium, that surrounds fascicles of nerve fibres [115]. This feature has been associated with increased incidence of local recurrences in desmoplastic melanomas which have a tendency to neurotropism [116]. Again, this feature is often not recorded on histology reports and so associations with prognosis in large cohorts of melanoma have not been assessed.

1.7.2.1.3 Tumour regression

Regression represents the result of interaction between tumour cells and the host immune system leading to replacement of tumour cells with non-malignant tissue [64, 117]. Regression can be focal or complete where no tumour cells are present [64]. Regression may lead to underestimation of Breslow thickness which may be related to greater metastatic potential in thin tumours where regression is seen [118]. It would be anticipated that an immune response leading to destruction of tumour cells would be beneficial, but if this process is limited, it has been postulated that cells that survive and escape immune recognition would be selected and progress [119]. The presence of regression and influence on prognosis is controversial with some studies suggesting

that presence of regression is a poor prognostic factor, especially in thin melanoma tumours [118, 120, 121] and others suggesting it does not influence survival [65, 122, 123]. This may be a consequence of lack of consensus on exact definition and measurement of regression [117, 118]. As the significance of the presence of regression on prognosis is unclear, it is not part of current AJCC staging guidelines [58].

1.7.2.1.4 Tumour infiltrating lymphocytes (TILs)

Tumour-infiltrating lymphocytes (TILs) are an important feature of the immune response to melanoma [124]. The infiltrate can be brisk (diffuse or involves the entire base of the tumour), non-brisk (focal infiltration) or absent (no lymphocytes mixed with melanoma cells) [125], however the reporting of this is highly subjective [65, 114, 117]. Presence of TILs indicates that the host immune system is responsive and that the melanoma cells can be recognised [126]. Generally presence of TILs has been reported to be associated with better prognosis [65, 66, 124, 127, 128], however the exact cellular composition of the infiltrate may have more prognostic and perhaps predictive value and needs to be assessed in large studies [129]. Currently, TILs are not part of AJCC staging [58], however presence of a brisk infiltrate appears to influence prognosis.

1.7.2.1.5 Histological subtype

Melanomas can be grouped by the histopathologist into superficial spreading (70%), nodular, lentigo maligna and acral lentiginous types, with various other rarer subtypes [92, 114, 130]. Nodular melanomas quickly spread downwards in the vertical growth phase, with superficial spreading tumours remaining in the radial growth phase for variable amounts of time before invading vertically [114]. Lentigo maligna tumours arise from a pigmented macule which may have been present for years prior to invasion developing [114]. The biological characteristics of these tumours are therefore very different and this is reflected in the poorer prognosis associated with nodular tumours compared to superficial spreading tumours, which in turn have a poorer prognosis than lentigo maligna tumours [114]. Acral tumours present on the palms, soles or nail matrix (subungual) are also associated with poorer prognosis which has been related to late diagnosis and the inherent aggressiveness of acral lentiginous tumours. This may be related to differing mutational profiles in acral tumours, with lower incidence of *BRAF* or *NRAS* mutations and higher incidence of *KIT* mutations

[33, 131, 132]. Again, histological subtype is not included in current AJCC staging guidelines [58], but is regularly reported on histology reports.

1.7.2.2 Host factors

In 2001, the American Joint Committee on Cancer (AJCC) staging guidelines were updated for the 6th edition and the committee reported the analysis of 17,600 melanoma patients from 13 cancer centres to identify prognostic factors in melanoma [91]. This assessment, amongst others, found that increasing age, male sex and tumours on the trunk, head, neck, palms, soles and under nails were associated with poorer prognosis [91, 132-134]. In the AJCC study, site of tumour and the age of the patient continued to influence survival for those with stage III disease [91]. This has been confirmed more recently in analysis of 2313 patients with stage III disease in the AJCC melanoma staging database, with age at diagnosis and site of tumour independently predicting survival in patients with micrometastases, and patient age remaining independently predictive when macrometastases are present [59].

The poorer prognosis associated with increasing age is especially evident for those over 60 years of age [135-138]. Older patients are more likely to have thicker or ulcerated tumours, both of which are important prognostic factors in melanoma, however the association between age and outcome remains significant when adjusted for these factors [135-138]. Delayed diagnosis or under-treatment of older patients may contribute, but melanoma presentation, outcome and pathology appear to be dependent on the age of the patient and it is unclear whether this is related to the tumour or the host response [139]. For example, older patients are less likely to develop regional metastases, but still have poorer survival [140, 141]. Immunological responses of elderly patients are lower and age-related changes to the lymphatic system, such as involution of lymph nodes or slower lymphatic flow, may also be contributing factors [139, 142, 143], however there is likely to be a biological explanation for this effect.

A recent pooled analysis of European Organisation for Research and Treatment of Cancer (EORTC) trials in patients with stage I or II disease has confirmed the superior prognosis for women with a relative survival advantage of 30% [144]. Tumours on the leg are more commonly found in women, with truncal tumours in men, however women have a survival advantage for tumours at both of these sites, indicating that primary location does not explain the difference [144]. Differences in behaviour between the sexes related to tumour detection and seeking treatment may contribute [145, 146], but gender is associated with survival independently of factors which may be related to

tumour detection, such as thickness or stage at diagnosis [146]. The more likely explanation is biological differences between men and women, perhaps related to sex hormones, immunological responses, oxidative stress or vitamin D metabolism [144, 147-150]. Understanding this gender effect may tell us something of fundamental importance about the biology of host/tumour interaction.

As discussed above, the site of a tumour has prognostic significance and is also related to the gender of the patient. The exception are tumours from the head and neck which have poorer prognosis, but are not related to gender [144]. These tumours more associated with chronic sun exposure and have lower rates of *BRAF* and *NRAS* mutations, with greater incidence of *KIT* mutations [33, 151, 152]. This is a similar genetic profile to that seen in the poorly prognostic tumours found on the palms, soles and subungual sites, suggesting that these tumours are inherently more aggressive [151]. It has been suggested that the poorer prognosis of truncal tumours may be related to drainage to multiple lymphatic basins [153, 154], but the far more likely explanation for differing prognosis in tumours according to site is related to biological differences in the tumours. These factors are not currently integrated into AJCC staging of melanoma [58], but remain as independent prognostic factors that need to be taken into account when making assessments of new prognostic indicators.

1.7.3 Limitations of current melanoma staging

Despite the intensive efforts that have been placed into identifying prognostic factors for patients with melanoma, within every stage of the disease there are still variations in survival which cannot be explained using current prognostic models [134] and there are a significant proportion of patients with 'low-risk' melanoma who go onto relapse [121]. There is increasing interest in identification of new prognostic biomarkers to further individualise risk of progression for patients with melanoma and enable early therapeutic intervention for those classified at high risk of relapse.

1.7.4 New prognostic biomarkers for melanoma

1.7.4.1 Biomarkers

A biomarker is measurable factor that can be used to indicate a biological process such as the presence of a disease [155, 156]. Prognostic biomarkers offer information about outcome from a disease, irrespective of treatment [157], and a number of prognostic biomarkers already exist for melanoma such as tumour Breslow thickness,

ulceration or nodal involvement. Additional biomarkers may provide further information to help further refine prognostic information.

This thesis focuses on identification of biomarkers in melanoma tumour tissue. A number of biomarkers have been identified in serum, for example LDH as previously discussed. There has also been interest in germline genetic variation that predicts outcome in melanoma, for example improved survival in patients with melanocortin 1 receptor gene (*MC1R*) variants [158], so far investigated predominantly of interest as a means of understanding host/tumour interaction better. The following section will review current progress in identification of biomarkers in tumour tissue.

1.7.4.2 Prognostic tumour biomarkers

A number of studies have sought to identify tumour markers that indicate disease progression or increased chance of recurrence. As discussed above, prognosis in melanoma is strongly linked to the histological features of the tumour, such as Breslow thickness, and the ability of the tumour to metastasise and spread. Consequently, many studies have assessed the relationship between biomarkers and poor prognostic histological features of the tumour.

1.7.4.2.1 Candidate biomarker studies

Techniques such as gene expression profiling, immunohistochemistry, mutation screening and comparative genomic hybridization have been used to identify tumour biomarkers that provide additional prognostic information to that already provided with histological staging [159]. For this review I have concentrated on studies which have sought to identify altered gene or protein expression. A number of studies have aimed to do this using melanoma cell lines, but the vast majority have used tissue samples and immunohistochemistry [155, 160, 161]. Many studies compared expression in benign tissues with that in primary or metastatic melanoma samples, or compared expression in primary melanomas with similar histological features from patients who do not relapse versus those that go onto relapse. Many reports are of relatively poor quality often because they were performed using small numbers of samples and were not validated in other sample/data sets. This was largely a function of the small size of melanomas and the consequent lack of cryopreserved tumour samples. The studies also often lacked multivariate analyses which provide vital information as to whether the biomarker identified adds anything additional to current staging [155, 160, 162]. Some of these markers however have been identified in more than one study, for example osteopontin [163, 164], E-cadherin [165] [166] and MMP2 [167-169], with

deranged expression of proteins involved in many biological processes, such as tissue invasion, cell adhesion, DNA repair and apoptosis. To be considered as a useful biomarker, these candidates require validation in large, prospective studies [155].

It has been suggested that the lack of consistency across studies is related to methodological differences, therefore the “REporting Recommendations for Tumour MARKer prognostic studies” (REMARK) guidelines were published, which recommend standardised reporting of study design, hypotheses, patients, specimens, assays and statistical analysis used in prognostic biomarker studies [162]. A recent systematic review and meta-analysis identified biomarker studies in melanoma which conformed to REMARK guidelines [161]. The authors specifically assessed reports which used primary cutaneous melanoma samples, reported clear methodological information regarding immunohistochemistry techniques used and statistical analysis using multivariate proportional hazards modelling adjusted for known prognostic factors in melanoma. They identified 51 eligible studies evaluating 80 proteins [160, 161]. Three studies assessed the combined effect of three or more proteins in multivariate analysis [170-172]. In meta-analysis, the use of multiple proteins most strongly predicted survival, these combinations being p16^{INK4a}, survivin and p53 [170], p16^{INK4a} and p21^{WAF1} [171] and RGS1, osteopontin (SPP1) and NCOA3 [172]. Individual proteins associated with survival were RGS1, nucleolin, HER3, ING4 and β -catenin [161]. Overall, proteins involved in the cell cycle (regulation of G₁-S transition) were most associated with progression [161]. Other pathways identified were those involved in immune responses, transcription, cell adhesion, cytoskeleton modelling, signal transduction, DNA damage, development, apoptosis and DNA damage [161].

The authors of this study extended their analyses to gene expression data from microarrays. Across the microarray studies assessed there was evidence at both the protein and expression level that PCNA and survivin were associated with outcome and so the authors highlighted these candidates for further assessment [161].

In view of the strength of multiple markers in predicting outcome, there have been high hopes that the development of gene expression arrays, allowing assessment of thousands of genes in a single sample, would identify single genes or profiles of genes associated with outcome and I will review the results of these studies now.

1.7.4.2.2 Identification of gene expression signatures

A number of studies have now been published using gene expression microarray technology to identify genes which are differentially expressed in melanoma tumours associated with prognosis, tumour progression or differing histological features. The

advantages of this technique are that novel genes can be identified which may serve to provide essential biological insight into the disease. Profiling of thousands of genes allows biological pathways to be assessed as a whole, again providing critical information about gene expression derangement. Some of the studies have used cell lines to identify genes differentially expressed in lines with differing characteristics [173-175]. Other studies have used frozen melanoma samples to identify gene signatures associated with relapse or progression and are summarised in Table 1-2. The main deficiencies of these studies to date are the small number of samples assessed and the limited number of studies using primary melanoma tissue. This is because frozen tissue is required to extract enough high quality RNA from tissues for use with traditional gene expression microarrays, and as melanoma tumours are small and require extensive pathological assessment to accurately stage a tumour, availability of frozen tissue is limited. I will discuss this further in Chapter 3 and section 1.9 as the microarray assay used to produce results for this thesis is designed for use with degraded RNA samples from well-annotated FFPE archival tissue with mature follow-up data.

Microarray studies have demonstrated that up-regulation of DNA repair and genes involved in the cell cycle or cell division are associated with progression of tumours and poorer outcome [175-180]. They have also shown that genes involved in cell adhesion and invasion are associated with progression [175, 176, 181-184], with over-expression of genes associated with the immune system associated with a better prognosis [179, 180, 183, 185]. An unpublished study of 79 frozen metastatic specimens has also found an association between immune response gene expression profiles and survival in stage III disease [186].

The meta-analysis of Schramm *et al.* (2011) identified only two microarray gene expression studies assessing gene expression in primary tumours reported to REMARK standards [161]. One of these studies is based on the data presented in Chapter 3 [187], the other by Winnepenninckx and colleagues [178]. Bioinformatic analysis of the Winnepenninckx microarray gene expression data in primary tumours revealed that expression of genes involved in the cell-cycle metaphase checkpoint was most deranged along with other cell cycle pathways [161]. Other pathways involved were apoptosis, immune responses and DNA damage [161]. When this analysis was extended to studies of metastatic tumour reported to REMARK standards, six studies were assessed [188]. Genes associated with immune response processes and the *NRAS*-regulation pathway were over-represented in these datasets [188]. Cross-validation of signatures between datasets predicted outcomes with low levels of

Samples	Number of samples	Methods	Outcome measure	Results	Reference
Frozen naevi and MM	6 naevi, 6 tumours	298 gene custom array, 9 genes validated with qRT-PCR	Progression	<i>THBD, FABP7, H2AFJ, RRAGD, MYADM, HR, CKS2, NCK2 and GDF15</i> associated with progression	[189]
Frozen naevi, primary and MM	9 naevi, 6 primary tumours, 19 MM. Independent 25 primary melanoma validation group	19,740 gene array, 2 genes validated with IHC in validation group	Progression	2602 gene signature that correlated with sample class including <i>MMP10</i> and <i>cadherin-3</i>	[182]
Frozen skin, benign and atypical naevi, early and MM	2 skin samples, 4 naevi, 6 early melanomas, 3 MM. Separate validation set of 2-4 tumours per stage of melanoma progression	14,500 array, 2 genes validated in separate samples. 1 gene validated with immunoblot in cell lines representing vertical growth phase and MM	Progression	Gene were found to be over-expressed (e.g. <i>osteopontin</i>) and under-expressed (e.g. <i>dermcidin</i>) in MM	[190]
Frozen skin, benign naevi and primary melanomas	7 skin samples, 18 naevi, 45 melanomas	14,500 array, 3 genes validated with qRT-PCR in 14 melanoma samples, 7 naevi and 5 skin samples (from same sample set as array data)	Progression	Genes differentially expressed between benign and melanoma samples, including <i>L1CAM</i> and <i>PLAB</i>	[184]
Frozen MM and normal melanocytes	10 tumours	1.2K human cancer array and human apoptosis array, 1 gene validated with qRT-PCR, 2 genes validated with Western blots	Progression	Hepatocyte growth factor receptor, <i>c-met</i> , <i>growth-factor receptor bound protein 10</i> , <i>BRAF</i> and several mitogen activated protein kinase genes were up-regulated	[191]
Frozen benign naevi and MM	4 naevi, 4 tumours	14,000 array, 1 gene validated with qRT-PCR in cell lines, 11 naevi and 4 MM tumours and with IHC in 35 naevi and 103 tumours	Progression	190 genes significantly over-expressed in tumours compared to naevi including <i>osteopontin</i> , which was validated using qRT-PCR and IHC	[192]

Samples	Number of samples	Methods	Outcome measure	Results	Reference
Frozen primary melanomas	83 primary melanomas, 58 patients with 4 years follow-up. 17 sample independent validation set. Further IHC validation independent set of 176 primary tumours	Whole human genome 41,000 microarray, 23 proteins confirmed with IHC. Gene signature validated in independent sample set. Five genes associated with survival in larger validation set with IHC	DMFS (OS in IHC validation set)	254 gene signature associated with DMFS: genes involved in activating DNA replication, e.g. minichromosome maintenance genes, <i>geminin</i>	[178]
Frozen MM	43 tumours samples from 38 patients	17,500 gene array, 2 genes validated with IHC. Survival prediction model cross-validated in dataset	OS	70 genes associated with survival. Immune cell genes in survival group, cell proliferation and invasion genes in poor survival group	[183]
Frozen primary and MM	19 primary melanomas, 22 MM. Independent validation set of 20 primary and 20 MM	14,500 gene array, 9 genes validated with immunoblots in a cell line. 4 genes validated in an independent set using IHC.	Progression	308 genes differentially expressed between primaries and MM. Associated with cell cycle, mitosis, cell communication and cell adhesion.	[176]
Frozen primary melanomas	34 tumours, independent validation set of 127 primary tumours	2,489 cancer gene cDNA array, 5 genes validated with IHC in separate cohort	Metastatic disease (DMFS in validation group)	243 genes with differential expression in tumour types. <i>N-cadherin</i> , <i>SPP1</i> and <i>SPARC/osteonectin</i> were associated with metastasis development in validation group	[164]
Frozen primary melanomas	Sample set as Winnepenninckx <i>et al.</i> (2006), 60 patients with 4 years follow-up	As above, then dataset analysed using "Searching for a biological interpretation of microarray experiments (SBIME)" with Gene Ontology annotations	DMFS	DNA repair and DNA replication pathways most significantly associated with metastasis	[177]
Frozen MM	29 patients, 2 independent validation sets of 10 and 14 MM	30,888 probe array, 21 genes validated with qRT-PCR. 2 predictive scores validated in independent sample sets	Progression to stage IV	2140 genes differentially expressed, including immunological signalling	[185]

Samples	Number of samples	Methods	Outcome measure	Results	Reference
Frozen primary cutaneous cancers (and primary melanomas) and MM	40 MM, 42 primary cutaneous cancers (16 melanomas)	14,500 gene array, 6 genes validated with qRT-PCR, 4 genes validated with Western blots	Progression	Gene signature identified when transition in expression from intermediate thickness tumour to thick tumour. Several oncogenes (<i>Osteopontin</i> , <i>MITF</i> etc.) and suppressor genes (<i>PITX-1</i> , <i>CST-6</i> etc.) change expression	[193]
Frozen MM	44 tumours from 38 patients	>47,000 transcript array, gene signature associated with survival validated in data from [185]	OS	266 genes identified as associated with survival. Good prognosis genes were associated with immune responses and poor prognosis with cell proliferation	[179]
Frozen MM	Tumours from 57 patients, independent validation sample set of 20 tumours	>47,000 transcript array, signatures validated in separate cohort and gene expression data from [179]	OS	Four distinct subtypes of tumour based on gene expression, with tumours of a proliferative subtype associated with poor prognosis and immune gene expression associated with better prognosis	[180]
Frozen MM	32 tumours validated in independent set of 89 MM	>47,000 transcript array, qRT-PCR and IHC used to assess expression of <i>TYRP1</i> in validation cohort	DMFS and OS	278 probes associated with survival with <i>TYRP1</i> most associated	[194]

Table 1-2: Studies using microarray technology to identify genes associated with prognosis or progression in melanoma tissue samples.

Abbreviations used: MM, metastatic melanoma; qRT-PCR, quantitative Real-time PCR; IHC, immunohistochemistry; DMFS, distant metastasis free survival; OS, overall survival.

misclassification, highlighting the importance of these pathways [188]. The authors of this review suggested that all new gene signatures should be assessed in a multivariate analysis with current prognostic clinico-pathological factors to identify whether gene expression adds to current prognostic algorithms [188]. Discussion of approaches for analysis of groups of genes using bioinformatics techniques is discussed further in Chapter 4.

As technology develops, it is likely that RNA-sequencing (RNA-seq), where cDNA synthesised from RNA is sequenced using next generation sequencing, will be increasingly used to identify genes with altered expression levels associated with melanoma prognosis [195, 196]. This method directly sequences the transcript which is mapped back to a reference genome, reads are then counted to assess the level of gene expression [197]. As the transcript is sequenced directly, this technology has many advantages, including detection of alternative splice variants and detection of transcripts from gene fusion events [198].

1.8 Treatment of melanoma

For patients with thin primary melanomas with no metastatic spread, treatment is surgical removal of the primary lesion and prognosis is excellent [58]. However for those with thick tumours or nodal spread (stages IIB-III) survival at 5 years is much less at 20-70% (Table 1-1) [109]. This group of patients are classified as having disease at high-risk of relapse and adjuvant treatments have been investigated in clinical trials to try to prevent recurrences in this high-risk group. For patients with stage IV disease, 5-year survival rates are 5-22% [109] and until relatively recently, chemotherapy and radiotherapy regimens were used only as palliation with very few long term survivors. More effective treatment options for stage IV disease are now found in the form of BRAFi [199] and immunotherapies [60, 61].

I will briefly review adjuvant therapies for melanoma and treatment options for stage IV disease and then concentrate on interferon- α (IFN) and chemotherapy with dacarbazine or temozolomide which are discussed further in this thesis. These are older approaches to treatment. They are of relevance here as these were the only options when I started my work and because they are likely to retain some value for the foreseeable future in patients without targetable oncogenic mutations. Furthermore both DTIC and IFN have a demonstrable therapeutic effect albeit in a small proportion of patients with melanoma and understanding the biological determinants of those effects is important.

1.8.1 Adjuvant therapies

Adjuvant treatments are used after tumour has been surgically removed to help reduce risk of recurrence. A range of adjuvant regimens have been tested in melanoma including chemotherapy, immunotherapy, radiotherapy, anti-angiogenic therapies and combination chemo-immunotherapy [200, 201]. Overall, studies assessing these agents have not demonstrated any survival benefit. The only promising results have come from use of IFN [200, 202-205] and ipilimumab [206].

Ipilimumab, is a monoclonal antibody that blocks the cytotoxic T-lymphocyte-associated antigen 4 (CTLA4). Expression of the CTLA4 protein causes inhibition of T cell activation and proliferation [207, 208]. In the adjuvant setting, a phase II trial of patients with high-risk resected stage IIIC or IV melanoma, was associated with improved survival outcome [209] and a phase III EORTC trial is on-going to assess this further in patients with stage III (with metastases >1mm) disease [206].

Part of this thesis focuses on identification of factors associated with benefit from IFN therapy, therefore I will discuss the evidence for use of IFN in further detail.

1.8.1.1 Interferon- α (IFN)

1.8.1.1.1 Action of endogenous type 1 interferons

Interferons are cytokines which have direct antiviral and anti-proliferative effects, but also enhance immune recognition of viruses and tumour cells [210]. IFN- α is a type 1 interferon as is IFN- β [211]. The major producers of type 1 interferons are plasmacytoid dendritic cells, which present antigen from tumour cells or viruses to T lymphocytes [212]. Type 1 interferons are also produced by T cells, monocytes, macrophages and natural killer cells [213]. Effects of type 1 interferons are predominantly mediated through the IFN $\alpha\beta$ receptor [214] which activates the JAK-STAT pathway (Figure 1-4). This signalling cascade induces expression of hundreds of IFN stimulated genes (ISGs) associated with a number of biological processes [211, 213, 214] (Figure 1-5).

IFN can have direct anti-proliferative effects on tumour cells by decreasing activity of cyclin dependent kinases (CDK) in the cell cycle via influences on function and expression of CDK2, cyclins, the transcription factor, E2F, retinoblastoma protein and CDK inhibitors, such as p15^{INK4b} [215-217]. The effects of IFN on host immunity have been reported to play a more central role in tumour response than direct antiproliferative effects [218]. These include increased anti-tumour responses by cytotoxic T cells and natural killer cells and reduction of regulatory T cells [219-221]. In view of the numerous actions of interferon, additional exogenous interferon therapy

would be expected to have a direct anti-proliferative effect on the tumour and aid the immune system in halting progression of any residual tumour that may be present following surgery or in-transit melanoma cells. However, clinical trials which have aimed to identify clear overall survival benefit with IFN therapy have yielded conflicting results. This may reflect tumour-induced immune suppression, for example defects in IFN signalling in lymphocytes, and tumour evasion of anti-tumour immune responses [70, 222-224].

1.8.1.1.2 Clinical trials of interferon- α in melanoma

There have been 14 randomised controlled trials to date comparing use of adjuvant IFN versus observation in patients with high risk melanoma with dosing regimens varying between trials [205, 225]. Results from these studies are conflicting. Some showed benefit in terms of prolonging relapse free survival (RFS) with little influence on overall survival (OS) [226-228] whereas others showed no benefit [229, 230]. However, in meta-analysis, it was clear that IFN does provide benefit in terms of RFS (hazard ratio from most recent analysis 0.82 (95% CI 0.77-0.87), $p < 0.001$), with a less clear benefit in terms of OS time (HR 0.89 (95% CI 0.83-0.96), $p = 0.002$) [203-205]. Dose and duration of IFN therapy did not appear to influence these effects [203-205]. In the most recent trial comparing pegylated IFN therapy (pegylation prolongs action of IFN so less injections are required) with observation, particular benefit was seen in RFS and OS for patients with microscopic nodal involvement compared with palpable nodal involvement and ulcerated primary tumours were more sensitive to IFN than non-ulcerated tumours [227]. The association between primary tumour ulceration and IFN benefit has been confirmed in recent meta-analysis of IFN trials [204, 227, 231]. This association will be explored in further detail in Chapter 7.

IFN therapy is associated with significant side effects, including most commonly fatigue, but also myalgia, arthralgia, anorexia, depression and liver toxicity [69, 229, 230]. The frequency of side effects is related to the dose of IFN received, with 15% of patients terminating treatment due to toxicity in lower dose regimens [230], increasing to 31% of patients in higher dose regimens [227]. For those patients who persevere with IFN therapy, treatment has been demonstrated to have a detrimental effect on their quality of life [232]. IFN causes release of a cascade of cytokines including tumour necrosis factor- α (TNF- α), interleukin-1 (IL1), IL2, IL6, IFN- γ and IFN inducible protein 10. These cytokines initiate cellular processes that produce many of the observed toxicities associated with IFN therapy [233]. The mechanism of hepatotoxicity associated with IFN is poorly understood [234, 235].

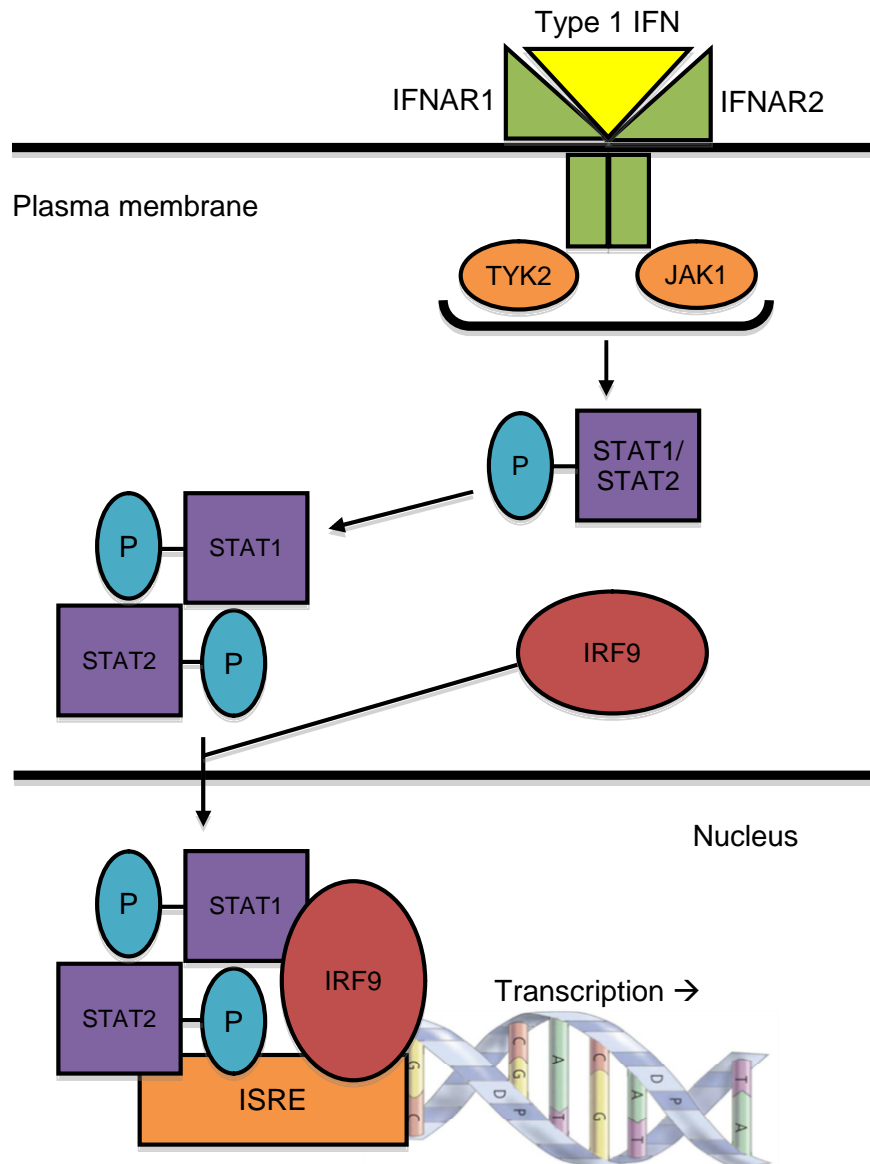


Figure 1-4: Activation of the classical JAK-STAT pathway by type 1 IFN.

The IFN receptor subunit, IFNAR1 is associated with TYK2 and IFNAR2 is associated with JAK1. Phosphorylation and activation of TYK2 and JAK1 result in tyrosine phosphorylation of STAT2 and STAT1, which leads to formation of STAT1-STAT2-IRF9 complexes, also known as ISGF3 complexes [236]. These complexes move to the nucleus and bind to ISREs in DNA and initiate transcription of ISGs. Figure adapted from [211, 214]. Abbreviations used: IFNAR1 and IFNAR2, IFN receptor subunits; TYK2, tyrosine kinase 2; JAK1, Janus activated kinase 1; STAT, signal transducer and activator of transcription; IRF9, IFN-regulatory factor 9; ISGF3, IFN-stimulated gene (ISG) factor 3; ISRE, IFN-stimulated response element; ISG, IFN stimulated genes.

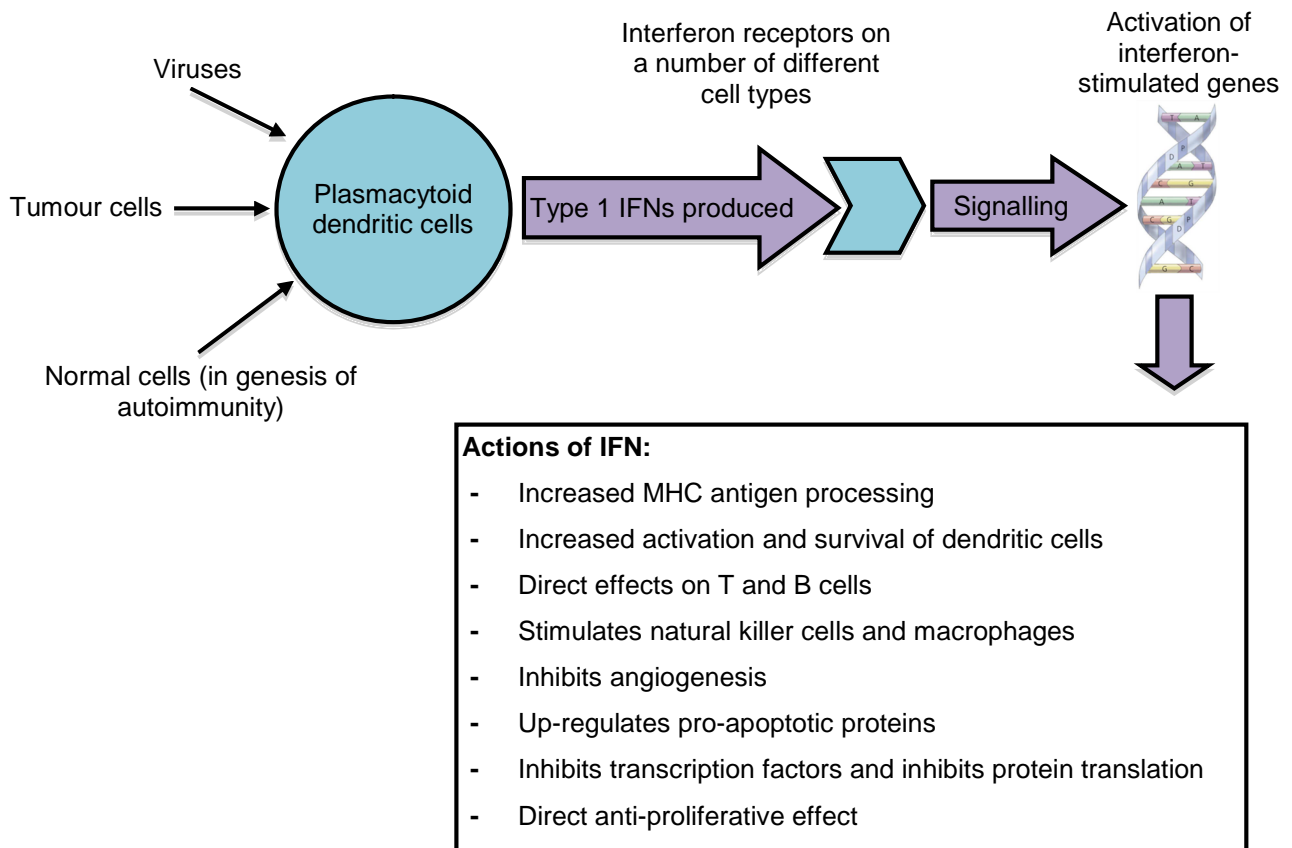


Figure 1-5: Production and action of endogenous type 1 interferons.

Reviewed by [211, 214, 220]. Abbreviations used: MHC, major histocompatibility complex.

IFN appears to provide benefit in terms of prolonging RFS time for patients with melanoma, but this benefit is limited by the toxicity associated with use of the drug. Currently clinicians cannot identify those patients who will obtain an overall benefit from IFN therapy so there is no standard systematic adjuvant therapy recommended in Europe for those with resected high risk melanoma [76, 200, 237].

1.8.2 Treatment of stage IV disease

Metastatic melanoma has a dismal prognosis and until recently, treatment was limited to chemotherapy with dacarbazine (DTIC) or temozolomide (TMZ). Recent advances have seen the development of immunotherapies and targeted therapies which are effective in stage IV disease. In phase III trials, the anti-CTLA4 antibody, ipilimumab, improves survival in unresectable stage III and stage IV disease compared to peptide vaccine or DTIC [60, 61]. As with IFN therapy, the use of ipilimumab is limited by the significant incidence of immune related side effects [60, 61, 206]. Investigation into new

immunoregulatory monoclonal antibodies with less toxicity continues. For example, antibodies against another molecules that regulate T-cell activation, such as the programmed death-1 protein (PD-1) and its ligand PD-L1 have shown promising results [238-241].

The BRAFi, vemurafenib, has been shown to prolong survival in a phase III trial with a relative reduction of 74% in risk of either death or disease progression and a 48% response rate in patients with metastatic melanoma with a *BRAF* V600E mutation compared to DTIC [199]. Despite the initial responses seen with vemurafenib, treatment is associated with side effects, such as development of cutaneous squamous cell carcinomas and keratoacanthomas [199, 206]. Of greater concern, is that resistance to vemurafenib invariably develops and understanding the mechanism by which a *BRAF* mutation modifies gene expression will greatly assist the intensive efforts underway investigating mechanisms of resistance [199, 206, 242].

Despite these significant advances in treatment of advanced disease, use of ipilimumab is limited by side-effects [60, 61, 206] and use of vemurafenib is limited to the approximately 40% of patients with tumours with mutated *BRAF* and resistance is an issue [31, 199, 206, 242]. Therefore, chemotherapy with DTIC and TMZ still has a role in treatment and is discussed in further detail.

1.8.2.1 Chemotherapy for stage IV disease

First line chemotherapy for advanced melanoma is DTIC, which achieves response rates of 7-13%, with a further 15-28% having stable disease, but few of these responses are long-lasting [243, 244]. Despite numerous trials to assess combination chemotherapies and chemotherapy in combination with IFN or interleukin-2 (IL2), none of these regimens prolong survival and any survival benefit is negated by toxicity and expense of the agents [245, 246]. Therefore, DTIC monotherapy is regularly used for patients with stage IV disease. DTIC is an alkylating agent which methylates DNA at the O⁶-position of guanine. During cell replication this causes mutations and following mismatch repair, double-stranded breaks in DNA which eventually lead to cell death by apoptosis [247]. Temozolomide (TMZ) is also an alkylating agent used in melanoma which undergoes spontaneous conversion to the active alkylating agent 5-(3-methyltriazene-1-yl)imidazole-4-carboximide (MTIC) which has similar actions to DTIC [248]. TMZ has the advantage that it can be administered orally and it crosses the blood-brain barrier making it suitable for treatment of brain metastases. TMZ has similar efficacy to DTIC [243, 249], and so is frequently used in melanoma.

In common with adjuvant IFN therapy, response to DTIC treatment cannot currently be predicted and predictive biomarkers of response would assist clinicians and patients in being able to decide whether DTIC treatment is worthwhile.

1.8.3 Personalized therapies for melanoma

Predictive biomarkers provide information about likely responses to treatment [157]. Host and tumour factors may influence how a patient and a tumour respond to treatments such as IFN or chemotherapy. Patient characteristics may influence toxicity derived from a therapy or efficacy by modifying metabolism of a drug. Tumour characteristics such as the presence of mutations or altered gene expression may influence how effective a treatment is if the therapy targets the pathway affected by the genetic alteration, for example *BRAF* mutations predict response to BRAFi [199].

As the focus of this thesis is on identification of biomarkers in tumour tissue, in the next section, I will review the tumour factors that have been associated with treatment benefit from IFN and DTIC chemotherapy.

1.8.4 Tumour factors that predict benefit from IFN therapy

As mentioned previously, patients with ulcerated tumours or those with microscopic nodal involvement appear to receive greater survival benefit with IFN therapy [204, 227, 231]. An EORTC trial is underway comparing adjuvant therapy with pegylated IFN or observation in patients with ulcerated melanoma and/or low lymph node burden to investigate this further. The biological significance of melanoma ulceration is furthermore unclear; because it is such a strong prognostic indicator and predictive factor, there is a need for better understanding of the biological processes in an ulcerated tumour and I will report an investigation of this in Chapter 7.

In melanoma cell lines, expression of a number of genes and proteins have been associated with IFN resistance or sensitivity. These genes have been identified using techniques such as gene expression microarrays and proteomic approaches. Many are associated with the classical IFN signalling pathway such as IFN-regulated transcription factors and genes with IFN responsive promoter regions [250-254]. Other markers identified include HLA antigens along with novel genes not previously known to be regulated by IFN [255]. Functional studies in cell lines have demonstrated that epigenetic mechanisms may also influence responses to IFN therapy [256-258]. These findings provide insight into the mechanisms of IFN resistance in cell lines, but require

confirmation in tumour samples before being considered as potential predictive biomarkers.

In a small study using 26 primary melanoma tumours which were methylthioadenosine phosphorylase (MTAP) positive using immunohistochemistry, patients who received IFN received significant benefit in terms of OS than those who did not receive IFN therapy. This observation was not seen in MTAP negative tumours [259]. MTAP catalyses phosphorylation of methylthioadenosine (MTA). MTA inhibits methyltransferase which reduces the level of methylated STAT1 in cells, methylated STAT1 is required for growth inhibition of cells by IFN so when MTAP is present in cells there are higher levels of methylated STAT1 which would correlate with the observation of better IFN response in MTAP positive tumours [260-262]. The association between STAT1 and STAT3, which down-regulates response to IFN, was further investigated in a small study of nodal tumour tissue from 21 patients. Phosphorylated STAT1 and STAT3 were identified using IHC and higher pSTAT1/pSTAT3 ratios before treatment were associated with longer OS after IFN therapy [263].

Again, studies using tumours to identify predictive markers of IFN benefit have been few and small. A well powered study to identify gene expression in tumours which correlates with IFN benefit would be likely to identify candidates which would provide insight into mechanisms of IFN resistance in melanoma cells and perhaps identify predictive markers of survival benefit or toxicity which could be used clinically. Currently tumour ulceration represents a predictive marker and further investigation into the biological processes of ulceration may provide insight into mechanisms of IFN responsiveness and is the subject of Chapter 7.

1.8.5 Tumour factors that predict response from chemotherapy

In view of the DNA damage caused by DTIC/TMZ therapy, over-expression of genes related to DNA repair in melanoma tumours has been postulated to be linked to the chemoresistance of melanoma [264]. The association between expression of candidate DNA repair genes and chemotherapy responses has been explored by a number of previous authors. Examples of genes and pathways investigated are O⁶-methylguanine-DNA-methyltransferase (MGMT), which removes alkyl groups from DNA [265-273], the mismatch repair pathway [248, 265, 274, 275] and the base excision repair pathway [265, 276-278]. The association between DNA repair gene expression and chemotherapy response is this subject of Chapter 8 and will be explored further in this chapter.

Bcl-2 is an antagonist of apoptosis and over-expression is common in melanoma, particularly in melanoma metastases that do not respond to chemotherapy [279, 280]. Studies have shown that use of *BCL2* antisense therapy and small-interfering RNAs sensitizes melanoma to apoptosis inducing therapies such as DTIC [279, 281], highlighting the importance of this protein in chemoresistance.

Isolated limb perfusion of chemotherapeutic drugs is occasionally used for treatment of metastatic melanoma. Melphalan is the chemotherapy typically used for these procedures and is also classified as an alkylating agent [282]. In a study of 30 patients treated with isolated limb perfusion with melphalan, high expression of the tumour suppressor p16^{INK4a} and absence of an activating *BRAF* mutation independently predict response to therapy [283].

Large-scale screens of cell lines from cancers which are either sensitive or resistant to chemotherapeutic regimens, other than DTIC or TMZ, have used genomic and gene expression analysis to identify biomarkers which predict chemotherapy sensitivity in validation datasets [284-287]. *In vitro* drug sensitivity assays of melanoma cells have been assessed as a means of identifying those patients with melanoma who will respond to non-standard chemotherapeutic regimens with some success [288]. These assays have also been used in other cancers [289]. Results from these approaches are promising and could be extended to DTIC or TMZ in melanoma treatment in the future.

In summary, there are a number of tumour biomarkers which have been linked with chemotherapy response. To assess these further, a well-powered study is required with robust response data, ideally to Response Evaluation Criteria in Solid Tumours (RECIST) standards [290]. I have developed such a study during my PhD, which is described in further detail in Chapter 8.

1.9 Formalin-fixed paraffin embedded tissue (FFPE) for identification of prognostic and predictive biomarkers

Identification of prognostic and predictive biomarkers in melanoma would be greatly enhanced by being able to use stocks of FFPE tissue from patients with long-term follow-up and information about current prognostic markers. Use of FFPE tissue has been limited in the past because of the severely degraded nature of RNA and DNA extracted from such tumour blocks, which has been unusable in many assays [291]. This thesis describes the analysis of FFPE melanoma tissue with new technologies, specifically designed for use with degraded nucleic acids, and more established

techniques, to identify prognostic and predictive biomarkers. I will briefly discuss some of the methodological issues faced when working with small melanoma tumours to identify genetic markers of prognosis and responses to therapy.

As previously discussed, histological examination of melanoma tumours is essential to accurately assess features that have prognostic value such as Breslow thickness or mitotic rate. Histological specimens are routinely fixed for histological diagnosis using formalin and then embedded in paraffin to allow sections to be taken for staining and histological review. Formalin is a cross-linking fixative which preserves tissue and cellular structure by cross-linking proteins and nucleic acids [77]. When nucleic acids are extracted, cross-links cause degradation. Furthermore addition of monomethylol groups to bases can interfere with down-stream reverse transcription and amplification reactions [292]. Despite modifications to RNA extraction protocols, RNA can be severely degraded being less than 300 base pairs in length, limiting the ability to examine variation in RNA [291]. Therefore, use of microarray technology has been limited with RNA extracted from FFPE tissue, restricting the use of this valuable tissue resource. This thesis describes use of the cDNA-mediated annealing, selection, extension and ligation (DASL) assay (Illumina, San Diego, CA) to assess gene expression in FFPE melanoma samples. DASL was specifically designed for use with degraded RNA, such as that extracted from FFPE tissue [293] and produces reproducible gene expression results from degraded RNA [293-297].

1.10 Outline of thesis chapters

To address the major aims of the thesis outlined in section 1.1, I will briefly outline the contents of the chapters of this thesis.

Chapter 2 describes the patients, samples and methods used throughout the thesis. It also presents methodological work assessing use of new technologies and discusses techniques for tumour sampling.

Chapter 3 presents results using the DASL assay to identify prognostic markers in FFPE primary melanoma tumours. It includes an assessment of quality control measures to predict assay performance and validates findings in an independent sample set.

Chapter 4 describes use of the DASL assay to identify a group of genes with prognostic significance in primary melanoma tumours. This chapter includes an assessment of gene ontology and pathway analyses with gene expression microarray

data. Development of methods for validation of DASL results using quantitative Real-time PCR with FFPE melanoma tissue are also presented.

Chapter 5 describes a pilot study to assess the performance of the DASL assay using very small sentinel node biopsy samples. Results from nodal specimens are compared with matched primary tumours to identify genes associated with metastatic progression. This chapter also includes an assessment of quality control methods for the DASL assay in different tissue types.

Chapter 6 reports identification of *BRAF* and *NRAS* mutations in primary melanoma tumours and identifies associations between mutation status, clinico-pathological factors and outcome. This chapter also presents gene expression profiles associated with mutation status.

Chapter 7 describes analyses to identify factors associated with primary tumour ulceration to gain insight into the prognostic and predictive significance of this tumour factor. Clinico-pathological factors independently associated with ulceration are identified in a large cohort of patients, with tumour gene expression profiles and immunohistochemical features assessed for a subset of patients.

Chapter 8 presents results of analyses using medium-throughput gene expression platforms assessing associations between DNA repair gene expression and response to DTIC or TMZ chemotherapy. This chapter includes a methodological assessment of the Fluidigm gene expression profiling system with FFPE melanoma tissue. It also describes the study design for the “Predicting Response to Chemotherapy” study, which I started during my PhD.

Finally, Chapter 9 will summarise the main findings of my thesis, discuss limitations and describe future work that will be required.

2 Methods

2.1 Aims

The aims of this chapter are:

- To describe the studies from which patient samples and clinical data have been derived for work presented in this thesis.
- To describe methodology used throughout the thesis.
- To justify use of tissue microarray needles to sample melanoma tumour tissue.
- To describe an assessment of the Illumina Whole-Genome cDNA-mediated annealing, selection, extension and ligation (DASL) HT assay with RNA extracted from formalin-fixed paraffin-embedded (FFPE) melanoma tissue.

2.2 Patients and samples

2.2.1 Samples from patients recruited to studies

Samples from patients recruited to the following studies have been used repeatedly in the work I will present in my thesis. Studies have received ethical approval for use of tissue samples. The Leeds Melanoma Cohort Study and Retrospective Sentinel Node Biopsy Study were underway when I started my PhD.

2.2.1.1 Leeds Melanoma Cohort Study

Patients diagnosed with melanoma in the Yorkshire and Northern region of the UK have been recruited to a population-based case-control/ cohort study since 2000. The aims of this study are to identify histological and molecular predictors of survival in primary melanomas, to investigate how hereditary variation in melanoma patients influences how a patient interacts with their tumour, how somatic changes in tumour may influence hereditary effects and to assess how environmental factors influence survival. A total of 2135 patients have been recruited and recruitment of patients ceased on 31st December 2011, except for those with melanomas of rare (sun-protected) sites. For each case, lifestyle indicators and lifetime environmental exposure data have been collected using questionnaires, and blood samples have been taken for DNA, lymphocytes, serum and plasma extraction. Patients have been followed-up

using annual questionnaires to identify melanoma relapses, and their general practitioners have been asked to complete updated surveys on their health/relapse status every two years. Further information relating to tumour relapse and overall survival has been obtained from hospital notes and the Office for National Statistics. Primary melanoma tumour samples are being traced for each case.

Between September 2000 and December 2001 and from July 2003 until December, patients with tumours of Breslow thickness less than 0.75mm were not recruited in order to increase the power of the study to identify predictors of relapse as tumours thinner than 0.75mm are usually cured by excision. Between January 2002 and June 2003 all patients diagnosed with invasive melanoma were recruited to the study for the purpose of the case-control component of the study. For this thesis, I will present data derived from the first 254 FFPE primary melanoma tissue blocks identified from patients with tumours greater than 0.75mm with the longest follow-up period. Approvals for the study have been granted by the Multicentre Research Ethics Committee (MREC) (1/3/057) and the Patient Information Advisory Group (PIAG) (3-09(d)/2003).

2.2.1.2 Retrospective Sentinel Node Biopsy Study

This study was carried out in order to identify the clinico-pathological predictors of positive sentinel node biopsy (micrometastases). Patients with tumours equal to, or greater than 0.75mm in thickness who underwent sentinel node biopsy to identify nodal metastatic spread of tumour between 1994 and 2006, were recruited from five centres to this retrospective study. Cases were patients who had had a positive sentinel node and controls were those with a negative sentinel node biopsy. Controls were randomly selected to be frequency matched with cases by year of sentinel node biopsy and centre where the biopsy was performed. Clinical and survival data relating to patients was obtained from hospital notes and the Office for National Statistics. The first 218 FFPE primary tumour blocks from participants with longest follow-up were used for work I will present. Ethical approval for the study was granted by Leeds (East) Research Ethics Committee (06/Q1206/149) and PIAG (3-06(b)/2006).

2.2.1.3 Predicting Benefit from Interferon Treatment: Personalised Therapy for Melanoma

Melanoma tumour samples are currently being collected for this study, which I developed and started during my PhD, and aims to identify genetic factors predictive of benefit from interferon- α . Although I set up the study the recruitment to it will continue beyond my PhD period, and in fact the direction of work that I pursued meant that I did

not need to use samples from this study as a major component of my work. A number of samples have been used for methodological work described in this chapter but I will not report any results from the study in this thesis. Ethical approval for this study has been granted by the North West Research Ethics Committee (08/H1010/61) and PIAG (3-06(d)/2008).

2.2.1.4 Predicting Response to Chemotherapy in Malignant Melanoma: The role of DNA repair genes

This is the second study I developed and ran, with management help from Mr Christy Walker, a Research Nurse within the research group, during my PhD and the study design and aims are described in detail in Chapter 8. Melanoma tumour samples are still being collected for this study to increase the statistical power to determine whether expression of DNA repair genes is associated with response to chemotherapy in advanced melanoma, but I have analysed sufficient to report in Chapter 8. A number of samples have been used for methodological work described in this current chapter. Ethical approval for this study has been granted by the Yorkshire and Humber Central Research Ethics Committee (10/H1313/72) and the National Information Governance Board for Health and Social Care (formerly PIAG) (ECC 8-02 (FT2)/2010).

2.2.2 Central review of tumour histology

For specimens from the Leeds Melanoma Cohort Study and the Retrospective Sentinel Node Biopsy Study used in gene expression work detailed in Chapters 3, 4, 6, 7 and 8 and immunohistochemical staining described in Chapter 7, diagnostic haematoxylin and eosin (H+E) slides of tumours were centrally reviewed by Dr Andrew Boon (Leeds Melanoma Cohort Study) or Professor Martin Cook (Retrospective Sentinel Node Biopsy Study). Both pathologists were blinded to the contents of the original histology report. There can be much variability in reporting of melanomas between pathologists [298, 299], therefore central review of the specimens was undertaken to ensure consistent reporting of histological features across tumours within each study. This process also allowed us to obtain a more complete dataset, for example by providing mitotic rate data which has only recently been added to the American Joint Committee on Cancer (AJCC) staging guidelines and has not been reported on histology reports for many of the older specimens used in this study [58]. For tumours from patients recruited to the Leeds Melanoma Cohort Study, the pathology review was limited to Breslow thickness, presence of ulceration, mitotic rate and histological subtype of tumour, whereas review of tumours from patients recruited to the Retrospective

Sentinel Node Biopsy Study was more detailed including assessment of vascular or perineural infiltration, presence of tumour infiltrating lymphocytes, regression, microsattelites and sentinel node biopsy status. For analyses described in Chapter 7, centrally reviewed data was used where available, if this was not available details from histology reports were used.

2.2.3 Patient samples used in pilot work

In view of the small size of melanoma primary tumours, pilot work has been undertaken using metastatic melanoma FFPE nodal samples which are much larger than primary tumours allowing multiple sampling without exhausting tissue blocks of tumour material. A total of 14 tissue blocks, from 10 patients were traced from the Pathology Department from Leeds Teaching Hospitals Trust which were archived between 2000-2005. Informed consent for use of these tissue samples has been obtained from all patients and tissue collection was approved by the Leeds Ethics Committee.

2.3 Sampling of FFPE primary melanoma tumour blocks

2.3.1 Justification for sampling using a tissue microarray (TMA) needle

In this work, sampling of tumour was carried out using a TMA needle inserted horizontally through the deepest part of the primary tumour containing the lowest proportion of stromal or inflammatory cells. The projects described here were intended to allow analysis of unselected, "population-ascertained" primary tumours thicker than 0.75mm. Therefore, this sample set is less biased than are normally available, especially when frozen samples were used. However most primaries are small and when selecting sampling procedure the priorities were to sample representative areas of the tumour without destroying the tissue block.

Loss of the block must be avoided in case it is needed by the patient again either for review of the histology if the diagnosis is contested, or if the tumour tissue is required for clinical genetic testing. Thus the need was to balance the clinical needs of the patient, which are paramount, with the scientific needs of the study. When the Leeds Melanoma Cohort study was instigated, the clinical need for mutation testing was a theoretical issue for the future, but became a clinical reality surprisingly quickly during the study.

The sampling options were using a TMA needle or taking tissue sections and using laser capture microdissection (LCM). The decision to use a TMA needle was made by the group after considering the following:

- Use of a TMA needle leaves the block physically intact so that the site of sampling can be reviewed subsequently. A section taken after sampling, compared with a clinical slide leaves a permanent image of the histological appearances of the tumour sampled.
- The shape of the melanocytic tumour and its relationship with the stroma is not then prejudiced if clinical re-review of the block is required.
- Sectioning wastes tissue as sections are discarded.
- LCM is too time consuming for large-scale studies.
- LCM is more likely to avoid stromal and inflammatory cells. However, work done by Dr Caroline Conway, as a previous PhD student, showed that when cores were horizontally sectioned, a minimum of tumour cells were present which is widely accepted as being required for accurate results when LCM cannot be performed [187] with percentages as low as 50% used for identification of prognostic gene expression profiles in breast cancer [300].
- Much of the work done by the group is directed towards the identification of biomarkers. Work done in breast cancer research has shown that signatures of good prognosis are often a result of the presence of inflammatory cells within the tumour [301, 302]. We judged that clinical tests are more likely to be feasible using TMA needles than using LCM, although evolving technology may prove this assumption to be wrong. The group therefore argues that TMA samples would be appropriate for biomarker work. Incidentally we have been consistent in sampling to choose the least inflamed component of the tumour but have not sampled tumours where the inflammatory component appeared to be dominant. For biomarker work there is an argument that all tumours should have been sampled but where sampling would have resulted in less than 70% of tumour cells this was avoided. There is some recognisable bias therefore in this approach.

To accurately sample an area of confluent tumour from a tissue block a section of tissue was taken for staining with H+E. Sectioning and staining of tissue was undertaken by Dr Filomena Esteves and Dr Jon Laye.

2.3.2 Sectioning of tumour blocks

Blocks were mounted onto a microtome and trimmed until a clean face was achieved. One five micron tissue section was taken from each primary tumour block and floated onto the surface of a microtome water bath at 45°C and then mounted onto a Superfrost glass slide (Solmedia, Romford, UK) labelled with study number. Sections were dried overnight in an oven at 36°C and then fixed to the slide by placing the slide tissue side up on a heating block at 60°C for 20 minutes.

2.3.3 Haematoxylin and eosin (H+E) staining

Slides were placed into a plastic slide rack with up to 24 slides being processed at once. Sections were dewaxed by immersing the slide in xylene for 5 minutes which was repeated 3 times using fresh xylene each time. The slides were drained on tissue paper and rehydrated by immersing in 100% ethanol for 2 minutes repeating 3 times using fresh ethanol each time followed by 90% ethanol for 2 minutes and 75% ethanol for 2 minutes. Slides were then placed under a fast flowing tap for 1 minute. Slides were stained in Mayer's haematoxylin for 2 minutes and then placed under a fast flowing tap for 1 minute before being immersed in Scott's Tap Water for 1 minute and then rinsed again in water for 1 minute. Slides were then placed in eosin stain for 3 minutes followed by rinsing in water for 1 minute. The slides were drained and then dehydrated by being immersed in 100% ethanol for 1 minute repeated twice using fresh ethanol each time. Slides were dried in air and immersed in xylene for 1 minute and then fresh xylene for another minute. Cover slips were mounted to the slides using one drop of Depex mounting medium (Solmedia, Romford, UK) and dried in a fume hood overnight.

2.3.4 Slide review

The stained slides were reviewed by Professor Newton Bishop to identify an area of tumour suitable for sampling. The optimum area was not necrotic and the deepest part of the tumour with the highest percentage of tumour cells and minimal stromal or lymphocyte contamination. This area was marked on the H+E slide using a fine-tipped permanent marker (Figure 2-1). If the tumour was large, and it was judged that more TMA cores could be taken without prejudicing the clinical sample, a maximum of two areas were marked for sampling on primary samples and a maximum of four areas on metastatic specimens. The number of cores which could be taken was stipulated in the protocol for each study.

As melanin interferes with polymerases [303], the function of which is essential for many of the molecular techniques described in this thesis, the least pigmented component of the dermal tumour was selected for sampling. Pigmentation of tumours reflects the biological nature of the cells [304, 305] and therefore avoiding these areas may limit our analyses. Furthermore, there are tumours which show marked heterogeneity having pigmented and non-pigmented areas. The group has planned studies to compare these areas in the future. For the studies described in this thesis, consistency of sampling was judged to be the priority.

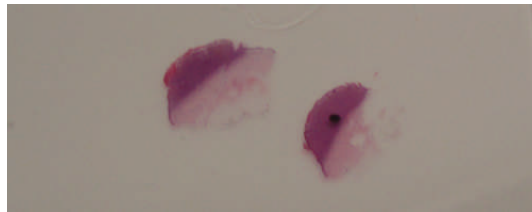


Figure 2-1: A haematoxylin and eosin slide marked for tumour sampling.

2.3.5 Sampling using a tissue microarray (TMA) needle

The marked slide was used to guide sampling from the tumour block. Tumour sampling was undertaken by a number of members of the Section of Epidemiology and Biostatistics, including myself. The tissue block was placed under the TMA needle, the H+E was placed on top of the block and the needle lined up above the mark on the slide. The slide was removed and the needle manually guided into the tissue block (Figure 2-2).

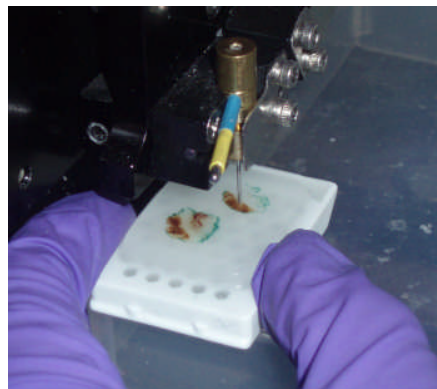


Figure 2-2: Using a tissue microarray needle to take a tissue core from a tumour block.

A 0.6mm x 2mm tissue core was taken from the block and placed into a labelled 1.5ml micro-centrifuge tube. The core was stored at 4°C prior to nucleic acid extraction. As the TMA needle is not disposable and cannot be cleaned using standard techniques, the TMA needle was effectively cleared of any residual tumour cells by two cores being taken from a blank, paraffin-only block.

Dr Caroline Conway has previously assessed the tumour content of tissue cores sampled using this technique. To do this, Dr Conway embedded representative cores horizontally in wax blocks and blocks were sectioned to obtain 5 micron sections throughout the tissue core. H+E sections were prepared from these sections and reviewed visually using light microscopy to determine the percentage tumour content of each core. The tumour content was estimated to be at least 70% tumour cells [187].

2.4 Melanin score

Melanin in melanoma tumours can lead to unreliable spectrophotometric quantification of nucleic acids [306] and can inhibit DNA polymerases [303]. To assess the association between dark, and therefore tumours with high melanin concentrations and performance in the cDNA-mediated annealing, selection, extension and ligation (DASL) assay, each tumour that was given a melanin score based on the visual melanin content of the TMA cores (0, no melanin to 3, black tumour).

2.5 Tumour sampling from small sentinel node biopsy samples

2.5.1 Laser capture microdissection (LCM)

In Chapter 5, tissue for RNA extraction was sampled from small sentinel node biopsy samples using LCM. There are two general types of microdissection; infrared laser capture systems and ultraviolet (UV) laser-cutting systems such as that used in this work [307, 308]. Laser-cutting systems use a narrow-beam UV-A laser to draw around and sample cells of interest. These cells are then catapulted using the laser into a collection tube or through contact with the collection cap [307]. Tissue sections for dissection using the PALM MicroBeam LCM microscope (Carl Zeiss, Jena, Germany) used in this work can be mounted onto polyethylene naphthalate (PEN) or polyethylene terephthalate (PET) coated slides which act to stabilise larger pieces of tissue so an entire piece of tissue can be drawn around and catapulted into the collection tube [309]. From normal glass slides sample material can be captured directly using the

“AutoLPC” function where pieces of tissue are catapulted into the collection tube using multiple laser pulses [309]. There are concerns that the UV laser can damage cells directly hit by the laser [310], however using the PALM MicroBeam system, dissection and catapulting of single live cells and subsequent culture appears to have no effect on proliferation rate suggests that any laser damage to cells is minimal [311].

In the study described in Chapter 5, tissue was sampled using LCM from either new tissue sections, unstained archival sections or diagnostic H+E slides with the coverslip removed. Coverslips were removed by soaking the slide in xylene until the coverslip floated off the specimen. Following coverslip removal, sections were dried and stored at -80°C prior to LCM. New and archival unstained sections were stained with H+E using diethylpyrocarbonate (DEPC) treated water as described in section 2.3.3 and dehydrated in ethanol before being stored at -80°C prior to sampling. LCM was performed using the PALM MicroBeam LCM microscope. As archival sections were stored on Superfrost slides, new sections were mounted onto Superfrost slides to allow a comparison between archival and new sections. Tissue was microdissected in “AutoLPC” mode under the supervision of a Consultant Histopathologist with expertise in melanoma (Dr Andrew Boon). Number of cells or area of tissue dissected, as calculated by microscope software, was recorded. Sample pieces were catapulted into 20µl 10% sodium dodecyl sulphate solution aliquoted into the cap of a 0.5µl micro-centrifuge tube. Tubes were immediately placed on dry ice prior to RNA extraction.

2.6 Extraction of nucleic acids from FFPE tissue cores

2.6.1 Extraction of RNA using the Roche High Pure RNA Paraffin Kit

RNA was extracted from cores of tissue using the High Pure RNA Paraffin Kit (Roche Diagnostics, Burgess Hill, UK) for the studies described in Chapters 3, 4, 6, 7 and 8. This kit uses a column containing two layers of glass fibre fleece in a filter. Nucleic acids are structurally altered and denatured when diluted in guanidine thiocyanate and in the presence of this high salt solution, they bind to glass fibres [312]. A series of washing steps removes cellular components. The column is optimized for RNA extraction, however a DNase I digestion step removes any contaminating DNA. Purified RNA is eluted from the filter in the presence of very low salt concentrations [313].

2.6.1.1 De-paraffinisation of the tissue core and tissue homogenisation

A single tissue core was de-paraffinised in a 1.5ml micro-centrifuge tube by adding 500µl xylene and mixing. Samples were heated to 45°C for 15 minutes on a heating block and then pulse vortexed for 10 seconds. The xylene was removed carefully using a pipette. Residual xylene was removed by adding 400µl of 100% ethanol to the tube, vortexing and careful removal using a pipette. This ethanol wash step was repeated and excess ethanol was evaporated by placing the open micro-centrifuge tube on a heating block at 55°C for 5 minutes.

The tissue was homogenised by adding 100µl tissue lysis buffer, 16µl 10% sodium dodecyl sulphate (SDS) solution and 40µl Proteinase K to the dried tissue pellet. This mixture was vortexed and incubated at 55°C until the tissue was fully digested (48-84 hours) with regular vortexing throughout the incubation period.

2.6.1.2 Nucleic acid binding and washing

Following complete tissue digestion, 325µl binding buffer, containing guanidine thiocyanate, and 325µl absolute ethanol was added to the lysate and mixed by gentle pipetting. This mixture was added to the upper reservoir of a High Filter tube inserted into a collection tube. The filter and collection tube were centrifuged at 8000g for 30 seconds. The flow-through liquid was discarded and the filter tube centrifuged again at 12,000g for 30 seconds to ensure the filter was dry.

The filter containing the bound nucleic acids was then washed. 500µl wash buffer 1 was added to the upper reservoir of the filter tube and centrifuged at 8000g for 15 seconds. The flow-through liquid was discarded and 500µl wash buffer 2 was added to the upper reservoir of the filter tube and centrifuged through the filter at 8000g for 15 seconds. The flow-through liquid was again discarded and a further 300µl wash buffer 2 was added to the upper reservoir and centrifuged through the filter at 8000g for 15 seconds. Following disposal of the flow-through liquid the filter was centrifuged at 12,000g for 2 minutes to ensure all residual wash buffer was removed.

2.6.1.3 Elution of RNA

The filter column was transferred into a sterile 1.5ml micro-centrifuge tube and 90µl elution buffer was added to the upper reservoir of the column. The column was centrifuged at 8000g for 1 minute and the filter column was discarded. Contaminating DNA was removed from the eluate by the addition of 10µl DNase incubation buffer and 1µl DNase I. The tube was mixed gently by inversion and incubated for 45 minutes at

37°C. A second incubation step with Proteinase K increases the purity of eluted RNA, so 20µl tissue lysis buffer, 18µl 10% SDS and 40µl Proteinase K was added to the eluate and the solution was incubated at 55°C for 1 hour. The binding and washing steps were then repeated as described in section 2.6.1.2. Following the final wash, the filter column was placed into a sterile 1.5ml microcentrifuge tube. The RNA was eluted by adding 26µl RNase-free deionized water to the upper reservoir of the filter column which was centrifuged through the filter at 8000g for 1 minute. The column was then discarded. In order to remove any contaminating residual glass fibres from the eluate, it was centrifuged at 12,000g for 2 minutes to pellet the fibres and the supernatant was carefully removed into a 0.2ml PCR tube. Extracted RNA was stored at -80°C.

2.6.2 Extraction of DNA using the Qiagen QIAamp DNA FFPE kit

DNA was extracted from tissue cores using the Qiagen QIAamp DNA FFPE kit (Qiagen, Crawley, UK) for the work described in Chapter 6. This kit uses a column containing a silica-gel membrane. Samples are de-paraffinised and lysed, DNA then binds to the membrane in a high salt, chaotropic environment, bound DNA is washed and finally eluted from the membrane in a low salt solution [314]. Following sample lysis, there is an incubation period at 90°C to partially remove formalin crosslinks [315, 316], which improves yield and performance of DNA in downstream reactions.

2.6.2.1 De-paraffinisation and tissue digestion

One tissue core was de-paraffinised in a 1.5ml micro-centrifuge tube by incubation at 37°C for 30 minutes in 1ml xylene with regular vortexing during the incubation period. The xylene was then carefully removed using a pipette and 1ml of absolute ethanol was added to the sample to remove residual xylene. The tube was then pulse vortexed and the ethanol carefully removed using a pipette, before 1ml of 70% ethanol was added. Again the tube was vortexed and ethanol removed using a pipette. The tubes were left open on a heat block at 37°C to allow any residual ethanol to evaporate.

The dry tissue core was resuspended in 180µl buffer ATL and 20µl Proteinase K was added. The tube was vortexed and incubated at 56°C, with agitation and regular vortexing, until the tissue pellet was fully digested (48-84 hours). The lysed sample was incubated at 90°C for 1 hour to partially reverse formalin cross-links then briefly centrifuged and incubated for 2 minutes at room temperature with 2µl RNase A (100mg/ml) to remove RNA.

2.6.2.2 DNA binding, washing and elution

Following this, 200µl buffer AL, which contains guanidine hydrochloride, was added to the sample. The tube was vortexed and 200µl of absolute ethanol was added followed by further mixing. The tube was briefly centrifuged and the entire lysate transferred to a QIAamp MinElute column, placed into a 2ml collection tube. The lid was closed and the column centrifuged at 6000g for 1 minute. The column was placed into a clean collection tube and the tube containing the flow-through liquid was discarded. Bound DNA was then washed by adding 500µl of wash buffer AW1 to the column and centrifuging at 6000g for 1 minute. The column was placed into a clean collection tube and a second wash was performed by adding 500µl of wash buffer AW2 to the column followed by centrifugation at 6000g for 1 minute. Again the column was transferred to a clean collection tube and centrifuged at 20,000g for 3 minutes to dry the silica-gel membrane. Finally, the column was placed into a labelled 1.5ml micro-centrifuge tube and 30µl of elution buffer ATE was applied to the centre of the membrane and incubated at room temperature for 5 minutes to maximise DNA yield. The column and micro-centrifuge tube were centrifuged at 16,000g for 1 minute to elute the DNA. Eluted DNA was stored at -20°C.

2.6.3 Extraction of RNA and DNA using the Qiagen AllPrep® RNA/DNA FFPE kit

Extraction of both RNA and DNA from one tissue core was achieved using the Qiagen AllPrep® RNA/DNA FFPE kit (Qiagen, Crawley, UK) for studies described in Chapters 6 and 8. This kit became available during my PhD. Methodological work, not presented here, has demonstrated that the yield and quality of DNA extracted using this kit is comparable to that from the Qiagen QIAamp DNA FFPE kit. However, the yield and quality of RNA is significantly better using the Qiagen AllPrep® RNA/DNA FFPE kit than when using the Roche High Pure RNA Paraffin Kit making it suitable for use in our studies, with the advantage that RNA and DNA can be derived from the same core, maximising the use of these precious tissue resources. The AllPrep® kit is designed to sequentially release RNA and DNA from the same sample. It integrates the QIAamp technology described in section 2.6.2 with well-established technology for RNA extraction. Optimized lysis conditions using different buffers allow differential release of DNA and RNA. Following de-paraffinisation, FFPE tissue is initially incubated in lysis buffer and Proteinase K optimised to allow RNA release into solution, while genomic DNA and other insoluble material is precipitated. The sample is then centrifuged to give a supernatant containing RNA and a DNA containing pellet. The supernatant is

incubated at 80°C to partially reverse formalin cross-links. Following mixing with ethanol and buffer containing guanidine thiocyanate, the sample is applied to an RNeasy MinElute spin column where RNA binds to the silica membrane. Bound RNA is treated with DNase to remove any residual DNA and washed to remove any further contaminants. Finally RNA is eluted into RNase-free water. The DNA containing pellet is lysed further using Proteinase K and incubated at 90°C to reverse formalin crosslinking. The sample is then mixed with buffer containing guanidine hydrochloride and ethanol to provide optimal DNA binding conditions and applied to a QIAamp MinElute spin column. Bound DNA is washed and finally eluted into a low salt buffer [317].

2.6.3.1 Tissue de-paraffinisation and digestion

Tissue cores were initially de-paraffinised using the methods described in section 2.6.2. The resulting pellet was resuspended in 150µl tissue lysis buffer PKD and 10µl Proteinase K was added, the mixture was then vortexed and incubated on a shaking heat block at 56°C overnight. Following this, the tube was placed on ice for 3 minutes and centrifuged for 15 minutes at 20,000g. The supernatant was carefully removed into a new 1.5ml micro-centrifuge tube, taking care not to disturb the DNA-containing pellet.

2.6.3.2 Extraction of RNA

The supernatant was incubated at 80°C for 15 minutes and following a brief centrifugation step, 320µl of buffer RLT, containing guanidine thiocyanate, was added. Following vortexing, 720µl absolute ethanol was added, the sample was thoroughly mixed and transferred to the RNeasy MinElute spin column in aliquots of up to 700µl. Following addition of each aliquot the lid of the spin column was closed gently and the column centrifuged at 8000g for 15 seconds. After each centrifugation step, the flow-through liquid was discarded and the bound RNA washed using 350µl buffer FRN, followed by centrifugation at 8000g for 15 seconds. To remove any contaminating DNA, 10µl of DNase I stock solution (1500 Kunitz units in 550µl RNase-free water) was mixed gently with 70µl buffer RDD, applied directly to the spin column membrane, and incubated at room temperature for 15 minutes. Once DNA digestion was complete, 500µl buffer FRN was added to the column which was centrifuged at 8000g for 15 seconds. As the flow-through contains RNA following the DNase I treatment, the column was placed into a new 2ml collection tube and the flow-through was applied to the column, followed by a further centrifugation step for 15 seconds at 8000g. The RNA on the column was washed twice using 500µl of buffer RPE, followed by centrifugation

for 15 seconds at 8000g. The flow-through liquid was discarded following each wash. The spin column was then placed into a new 2ml collection tube, the lid was opened and the column centrifuged at full speed (16,000g) for 5 minutes. This process dried the column membrane, as residual ethanol may interfere with downstream reactions. The column was finally placed into a 1.5ml micro-centrifuge tube and 26µl RNase-free water was applied to the membrane. Following incubation at room temperature for 1 minute, the column was centrifuged at 16,000g for 1 minute to elute RNA. The resulting RNA was stored at -80°C.

2.6.3.3 Extraction of DNA

The DNA containing pellet was resuspended in 180µl tissue lysis buffer ATL and 40µl Proteinase K was added. The mixture was vortexed and incubated on a shaking heat block at 56°C overnight. The lysate was then incubated at 90°C for two hours without agitation, briefly centrifuged and allowed to cool before 2µl of RNase A (100mg/ml) was added and incubated at room temperature for 2 minutes to remove any contaminating RNA. The tube was briefly centrifuged and 200µl buffer AL, which contains guanidine hydrochloride, was added and the sample vortexed. Once mixed, 200µl absolute ethanol was added and again the sample was thoroughly vortexed. The entire sample was transferred to a QIAamp MinElute spin column, the lid was closed gently and the column centrifuged for 1 minute at 8000g. The collection tube containing the flow-through liquid was discarded and the column was placed into a new 2ml collection tube. The bound DNA was then washed by addition of 700µl buffer AW1, followed by centrifugation at 8000g for 15 seconds, and 700µl buffer AW2, followed by further centrifugation for 15 seconds at 8000g. Following each centrifugation step, the flow-through liquid was discarded from the collection tube. As a final wash step, 700µl absolute ethanol was added to the column, which was centrifuged for 15 seconds at 8000g. To remove any residual ethanol, the column was then placed into a new collection tube, the lid of the column was opened and the column centrifuged at 16,000g for 5 minutes. Finally the column was placed into a 1.5ml micro-centrifuge tube, 30µl of elution buffer ATE was applied directly to the spin column, the lid was closed and the column was incubated at room temperature for 5 minutes to maximise DNA yield. The tube was centrifuged at 16,000g for 1 minute to elute DNA. DNA was stored at -20°C prior to use.

2.7 Extraction of RNA from microdissected sentinel node biopsy samples

For the gene expression study described in Chapter 5, RNA was extracted from small sentinel node biopsy samples sampled using LCM. Following tumour sampling, the micro-centrifuge tube cap contained tumour specimens in 10% sodium dodecyl sulphate solution. Tubes were briefly centrifuged and 100µl tissue lysis buffer and 40µl Proteinase K were added and then the contents digested at 55°C overnight. RNA was extracted using the High Pure Paraffin RNA kit (Roche Diagnostics Ltd, Burgess Hill, UK) as described in section 2.6.1 and eluted in 26µl nuclease free water. Extracted RNA was stored at -80°C prior to analysis.

2.8 cDNA synthesis from extracted RNA

2.8.1 cDNA generation using the Invitrogen Superscript™ First-strand synthesis system

The Invitrogen Superscript™ First-strand Synthesis System (Invitrogen, Paisley, UK) was used to generate cDNA from extracted tumour RNA from patients recruited to the Leeds Melanoma Cohort Study as described in Chapters 3 and 4. The standard protocol uses a mixture of oligo(dT)'s, to bind to mRNA 3`poly(A) tails, and random hexamers for priming to maximise the amount of cDNA generated from degraded RNA. First-strand cDNA synthesis is catalysed by Superscript™ II reverse transcriptase which has been engineered to reduce RNase H activity, which can degrade mRNA, and is not inhibited by ribosomal or transfer RNA so increasing the yield of cDNA from total RNA. RNase H is added at the end of the reaction to remove the RNA template and increase sensitivity of the following PCR reactions [318].

2.8.1.1 cDNA synthesis for osteopontin qRT-PCR

For work described in Chapter 3, 5µl of RNA of variable concentrations was used to generate cDNA using the manufacturers protocol.

An RNA and primer mix was prepared by combining 5µl RNA with 1µl of 10mM deoxyribonucleotide triphosphate (dNTP) mix (containing 10mM of deoxyadenosine triphosphate (dATP), deoxycytidine triphosphate (dCTP), deoxyguanosine triphosphate (dGTP) and deoxythymidine triphosphate (dTTP)), 100ng of random hexamers, 500ng of oligodeoxythymidylic acid residues (oligo(dT)₁₂₋₁₈) and diethylpyrocarbonate (DEPC)

treated water to a final volume of 10 μ l. The mixture was incubated at 65°C for 5 minutes and then placed on ice. In a separate micro-centrifuge tube a mix was prepared containing 2 μ l of 10x reverse transcriptase (RT) buffer (200mM Tris-HCl (pH 8.4), 500mM KCl), 4 μ l of 25mM magnesium chloride, 2 μ l 0.1M dithiothreitol (DTT) and 40 units of RNase OUT recombinant ribonuclease inhibitor in a final volume of 9 μ l. This mixture was added to the RNA and primer mix on ice, vortexed briefly and then incubated at 25°C for 10 minutes. 50 units of Superscript™ II reverse transcriptase were added to the mix and incubated at 25°C for 10 minutes, followed by 42°C for 50 minutes and finally 70°C for 15 minutes. Following first strand synthesis, the tube was placed on ice and 2 units of *E. Coli* RNase H were added. The mixture was incubated at 37°C for 20 minutes and cDNA was stored at 4°C until required.

2.8.1.2 cDNA synthesis for DNA repair gene qRT-PCR

For work described in Chapter 4, 200ng of input RNA measured using spectrophotometry was used in each reaction. This RNA quantity was selected as it did not exhaust stock of eluted RNA from precious samples and in qRT-PCR experiments, cDNA samples with 200ng of input RNA had lower cycle threshold (Ct) values with greater reproducibility between replicate samples, than cDNA samples generated using smaller amounts of RNA. In order to maximise the amount of cDNA generated in each reaction, the volume of reagents was increased from those stated in the manufacturers protocol. Methodological work, not presented here, has demonstrated that these modifications do not significantly alter gene expression results derived from samples.

In detail, reagents were used as described above. The RNA and primer mix was prepared in a 20 μ l final volume by combining 200ng of RNA with 3 μ l of 10mM deoxyribonucleotide triphosphate (dNTP) mix, 300ng random hexamers, 1.5 μ g of oligo(dT)₁₂₋₁₈ and DEPC treated water to a total volume of 20 μ l. The mixture was incubated at 65°C for 5 minutes and then placed on ice. In a separate micro-centrifuge tube, 6 μ l of 10x RT buffer, 12 μ l of 25mM magnesium chloride, 6 μ l 0.1M DTT and 120 units of RNase OUT recombinant ribonuclease inhibitor were mixed in a final volume of 27 μ l. This mixture was added to the RNA and primer mix on ice, vortexed briefly and then incubated at 25°C for 10 minutes. 150 units of Superscript™ II reverse transcriptase were added to the mix and incubated at 25°C for 10 minutes, followed by 42°C for 50 minutes and finally 70°C for 15 minutes. Following first strand synthesis, the tube was placed on ice and 6 units of *E. Coli* RNase H were added. The mixture was incubated at 37°C for 20 minutes and cDNA was stored at 4°C until required.

2.8.2 cDNA generation using Applied Biosystems High Capacity cDNA Reverse Transcription kit

For the Chemotherapy study (Chapter 8), cDNA was generated using the Applied Biosystems High Capacity cDNA Reverse Transcription kit (Warrington, UK) [319]. This kit became available during my PhD and uses a simplified protocol compared to the Invitrogen system. The kit uses random priming and MultiScribe™ reverse transcriptase to catalyse first strand synthesis [319]. Two further cDNA kits are marketed by Applied Biosystems, the High Capacity RNA-to-cDNA kit and the High Capacity RNA-to-cDNA master mix. These offer even simpler work-flows using a blend of random primers and oligo(dT)'s for priming [320]. When tested, the results of which are not presented here, the High Capacity cDNA Reverse Transcription kit using random priming produced superior cDNA from degraded melanoma RNA samples and so was used for cDNA generation for the Chemotherapy Study (Chapter 8).

For each sample a 2x RT master mix was prepared by mixing 2µl of 10x RT buffer with 0.8µl 25x dNTP mix (100mM), 2µl of 10x RT random primers, 50 units of MultiScribe™ reverse transcriptase, 1µl of RNase inhibitor and 3.2µl of nuclease-free water in a final volume of 10µl. This solution was mixed gently and pipetted into a well of a 96-well plate. 10µl of RNA (up to 1 microgram) was then added to the mixture, and pipetted gently to mix. The plate was sealed, briefly centrifuged and loaded into a thermal cycler for incubation at 25°C for 10 minutes, followed by 37°C for 2 hours, then 85°C for 5 minutes and finally cooled to 4°C. cDNA was stored at -20°C prior to use.

In all cDNA synthesis reactions, a positive control using supplied control RNA (50 ng/µl) and a reverse transcriptase negative control was included in each experiment. cDNA concentrations were measured using spectrophotometry as described in section 2.10.

2.9 Cell line samples

2.9.1 Culture conditions

To optimise assays used in this thesis described in Chapters 6 and 8, RNA and DNA were extracted from melanoma cell line samples to provide high quality RNA and DNA. MeWo, SkMel28, Mel Juso, Mel 624 and SkMel5 cell lines were routinely grown in Dulbecco's Modification of Eagles high glucose Medium (DMEM, Sigma-Aldrich, UK) supplemented with 10% foetal calf serum (FCS) and 2mM L-glutamine at 37°C in 5% carbon dioxide. Cells were harvested at 80-90% confluency, excess serum was

removed by rinsing cells in 10ml of phosphate-buffered saline (PBS) and then trypsin was added and incubated at 37°C to detach cells from the culture flask. Supplemented DMEM was added to the flask to neutralize the trypsin, the suspension was centrifuged at 400g for 5 minutes to pellet the cells and the pellet resuspended in fresh DMEM. Cells were counted using trypan blue exclusion and a haemocytometer. For MeWo and SkMel28 cells, the solution was split into two and centrifuged at 400g for 5 minutes to pellet the cells. One cell pellet was frozen at -80°C for RNA extraction, the other used immediately for DNA extraction. For other cells, the entire cell pellet was used for RNA extraction.

2.9.2 RNA extraction from cell line samples using the Qiagen RNeasy® Mini kit

The RNeasy® Mini kit (Qiagen, Crawley, UK) was used for RNA extraction from cell line samples according to the manufacturer's protocol for 'Purification of total RNA from animal cells using spin technology'. This kit uses technology similar to that described in section 2.6.3. Cells are homogenized and suspended in buffers containing guanidine thiocyanate, therefore when the lysate is centrifuged through the spin column, RNA binds to the membrane. Following DNase I treatment and wash steps, RNA is eluted into RNase-free water [321]. Depending on the cell line, varying numbers of cells were used for extraction but the number did not exceed 1×10^7 cells as recommended by the manufacturer.

Cell pellets were thawed and dislodged from the microcentrifuge tube. Cells were disrupted and homogenized by adding 600µl Buffer RLT, vortexing the suspension and transferring to a QIAshredder spin column. The column was centrifuged for 2 minutes at 16,000g and then 600µl 70% ethanol was added to the homogenized lysate. The sample was transferred in 700µl aliquots into an RNeasy spin column. Each aliquot was centrifuged for 15 seconds at 8000g and the flow through liquid was discarded. Once all the homogenized lysate had passed through the RNeasy column, 350µl of Buffer RW1 was added and centrifuged for 15 seconds at 8000g to wash the column membrane. Flow-through liquid was discarded and 10µl of DNase I stock solution (1500 Kunitz units dissolved in 550µl RNase-free water) was gently mixed with 70µl buffer RDD. The DNase I solution was applied directly to the spin column membrane and incubated at room temperature for 15 minutes to remove any DNA. A further 350µl Buffer RW1 was added to the column and centrifuged for 15 seconds at 8000g. Flow-through liquid was discarded and 500µl Buffer RPE was added to the column and centrifuged for 15 seconds at 8000g. Flow-through liquid was again discarded and a

further 500µl Buffer RPE was added followed by centrifugation for 2 minutes at 8000g to wash the spin membrane. The column was then placed into a new 2ml collection tube and centrifuged at 16,000g for 1 minute. Finally, the spin column was placed into a 1.5ml microcentrifuge tube, 30µl of RNase-free water was applied directly to the membrane and the column centrifuged at 8000g for 1 minute to elute RNA. RNA was stored at -80°C prior to use.

2.9.3 DNA extraction from cell line samples using the Qiagen

QIAamp DNA Mini kit

DNA was extracted from cultured cells using the QIAamp DNA Mini kit (Qiagen, Crawley, UK) according to the manufacturer's 'Protocol for cultured cells'. Different numbers of cells were used for extraction depending on the cell line, but this did not exceed 5×10^6 as recommended in the protocol. The kit uses Proteinase K to digest cells, followed by use of a spin column to bind DNA in optimal conditions. The protocol also contains an RNase A treatment step to remove any contaminating RNA [322].

Cell pellets were resuspended in 200µl PBS in a microcentrifuge tube and 20µl of Proteinase K was added. 4µl of RNase A (100mg/ml) (Qiagen) was then added and the mixture incubated for 2 minutes at room temperature. After removal of RNA 200µl Buffer AL was added, the sample was mixed and then incubated at 56°C for 10 minutes. Following digestion and brief centrifugation, 200µl 100% ethanol was added and the sample was vortexed again. The tube was briefly centrifuged and the mixture applied to the QIAamp Mini spin column. The column was centrifuged at 6000g for 1 minute and placed into a clean collection tube. To wash bound DNA, 500µl of Buffer AW1 was added, the column was centrifuged at 6000g for 1 minute and then placed into a new collection tube. The bound DNA was washed again by the application of 500µl Buffer AW2 followed by centrifugation at 16,000g for 3 minutes. The column was transferred into a fresh collection tube and centrifuged again at 16,000g to eliminate any wash buffer carryover. The column was then placed into a 1.5ml microcentrifuge tube and 200µl distilled water applied to the membrane. The column was incubated at room temperature for 5 minutes and centrifuged at 6000g for 1 minute to elute DNA. DNA samples were stored at -20°C prior to use.

2.9.4 cDNA generation from RNA extracted from cell line samples

cDNA was generated from extracted RNA using the standard method described in section 2.8.1 with the Invitrogen Superscript™ First-strand synthesis system. One microgram of RNA was used in each reaction and cDNA was stored at 4°C prior to use.

2.10 Quantification of nucleic acid concentrations using spectrophotometry

Concentration and quality of RNA and DNA extracted from FFPE melanomas was determined using the ND-8000 spectrophotometer (Nanodrop, Wilmington, DE, USA). Prior to nucleic acid quantification, the spectrophotometer pedestals were cleaned and the instrument was blanked using 1.5µl of molecular grade water. The sample (1.5µl) was placed on the pedestal for measurement. Between samples the pedestals were wiped dry using a clean tissue. Using UV spectrophotometry, nucleic acid concentration is measured. RNA, single stranded DNA and double stranded DNA absorb UV light at 260nm and the spectrophotometer also provides A_{260}/A_{280} and A_{260}/A_{230} nm ratios which give an indication of any contaminants in the sample that absorb UV light at 230nm (organic compounds) or 280nm (protein). An A_{260}/A_{280} ratio of around 1.8 is accepted to indicate pure DNA and 2.0 for pure RNA [312].

This method was also used to measure concentrations of cDNA generated from RNA samples.

2.11 cDNA-mediated annealing, selection, extension and ligation (DASL) assay

The DASL assay is a gene expression profiling platform which uses highly multiplexed Real-time PCR to allow analysis of thousands of genes at once [293]. This assay has been used to derive gene expression data from primary FFPE melanoma tumours described in Chapter 3 with gene expression data being used in Chapters 3 to 8. The assay is reported to have a dynamic range of 2.5-3 logs and can detect 1×10^4 molecules [323, 324]. It is specifically designed for use with degraded RNA typically extracted from FFPE tissue as it uses random priming in cDNA synthesis and a target sequence of only 50 nucleotides is required for probe groups to anneal [293]. Probe groups are composed of two oligonucleotides; the first oligonucleotide consists of a gene specific sequence and a universal PCR sequence at the 5' end, the second

consists of the gene specific sequence, a universal PCR sequence at the 3' end and, for the Human Cancer panel described in section 2.11.3, a short (approximately 22 nucleotides) unique address sequence and for the WG-DASL HT assay described in 2.11.4, 50 nucleotide sequences which allow hybridization to a universal array [293, 323, 324] (Figure 2-3).

For the work described in this thesis, the DASL assay was performed by Floor de Kort at the service provider, ServiceXS (Leiden, Netherlands). To start the assay, 200ng total RNA was converted into cDNA using biotinylated random nonamers, biotinylated oligo d(T)₁₈ and Illumina-supplied reagents. Pooled probe groups were annealed to sequence-specific targets [325]. Biotinylated cDNA was immobilized on streptavidin-conjugated paramagnetic beads and washed to remove unhybridized oligonucleotides [293]. Correctly annealed oligos were extended and ligated using Illumina supplied reagents and conditions to generate templates which were amplified using PCR. During PCR, templates were labelled with Cy3 or Cy5 fluorescent primers for the Human Cancer panel or Cy3-labelled primers only for the WG-DASL HT assay described in section 2.11.4 [326]. PCR products were denatured and then hybridized to a universal array [325] which was scanned using an automated BeadArray™ reader (Illumina Inc., San Diego, CA, USA) to generate fluorescence intensity data.

2.11.1 The Sentrix Array Matrix (SAM) universal array

There are two formats of universal array used with the DASL assay, the Sentrix Array Matrix (SAM) and the Beadchip platform. The SAM was used with the 502-gene Human Cancer panel described in 2.11.3 and uses nearly 50,000 individual light conducting fibre strands that are chemically etched to create a 3µm well at the end of each strand. Glass beads derivatised with one of 1536 address sequences are loaded into the bundles. These array bundles are approximately 1.4mm in diameter and are grouped together into a 96-array configuration allowing assessment of 96 samples at once [325]. For both SAM and the Beadchip platforms, each probe is represented by an average of 30 beads for each sample [324, 327]. Beads are positioned randomly, so require decoding to determine the position and identity of each bead on the array [293, 328, 329]. Isolated PCR products are hybridised at 45°C for 18 hours to the SAM array. After hybridization and scanning, fluorescence intensity data is analysed using BeadStudio software (Illumina, USA). BeadStudio summarizes the pixel intensities for each bead across the array and then averages across beads for each probe to generate intensity data which is used in downstream analysis [327].

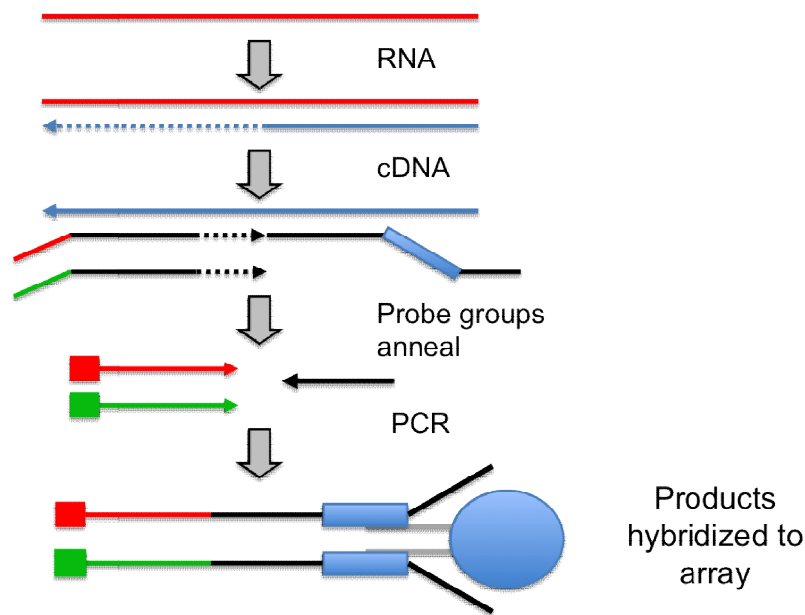


Figure 2-3: The DASL assay.

RNA is converted to cDNA using biotinylated primers. Pooled probe groups anneal to target sequences and biotinylated cDNA is immobilized on streptavidin-conjugated paramagnetic beads. Correctly annealed oligos are extended, ligated and amplified using PCR. During PCR, templates are labelled with Cy3 or Cy5 fluorescent primers. PCR products are then hybridized to a universal array and scanned to produce fluorescence intensity data. Short unique address sequences (blue sections on probes) are used to hybridize PCR products to the Sentrix Array Matrix (SAM) used with the Human Cancer panel. Longer, 50 nucleotide sequences, are used for hybridization to the HumanHT-12 v4 Expression Beadchip used with the WG-DASL HT assay. Figure adapted from [330].

2.11.2 The HumanHT-12 v4 Expression Beadchip

The HumanHT-12 v4 Expression Beadchip uses similar bead technology to SAM and is the array used with the whole-genome DASL HT (WG-DASL HT) assay described in section 2.11.4. Resultant PCR products from the WG-DASL HT assay are hybridized using 50 nucleotide sequences to the HumanHT-12 v4 Expression Beadchip for 16 hours at 58°C [324]. This array format allows processing of up to twelve samples and features content covering over 47,000 transcripts derived from the National Center for Biotechnology Information Reference Sequence (RefSeq) database (Release 38, November 2009) [330, 331]. The WG-DASL HT assay targets over 29,000 of those probes. After hybridization, HumanHT-12 v4 Beadchips are scanned using HiScan™ SQ, iScan or BeadArray™ readers and data are analysed using Illumina's GenomeStudio® software in a similar way to the SAM array format [330].

2.11.3 The Illumina Human Cancer panel

Gene expression profiling results presented in Chapters 3 to 8 were performed using the Illumina Human Cancer panel gene set (Illumina Inc.). The Cancer Panel includes 1536 unique sequence-specific probes which target 502 genes. Each gene is targeted in different locations by three probe pairs designed using a proprietary algorithm [293]. The genes on the Cancer Panel were derived from 10 publically available cancer gene lists and include oncogenes, tumour suppressor genes, cell cycle control genes and DNA repair genes among others (see Appendix I for full list).

2.11.4 The Illumina Whole-Genome DASL HT (WG-DASL HT) assay

The WG-DASL HT assay targets over 29,000 annotated transcripts and has been developed from the Human WG-DASL assay which previously targeted more than 24,000 transcripts and used the HumanRef-8 v3 Beadchip for hybridization. Targeted regions on the WG-DASL HT assay are 3' biased in common with HumanHT-12 v4 Expression Beadchip sequences unlike the Human Cancer panel where targeted regions are not restricted in position [323, 326]. In contrast to the Human Cancer panel, the WG-DASL HT assay has between one and eight probes representing each gene [324]. The original WG-DASL assay was found to provide reproducible results and has been used in a number of studies [332-335]. Illumina report that the WG-DASL HT assay provides highly reproducible gene expression profiles for replicate samples and that relative gene expression relationships are maintained in samples analysed using both the WG-DASL assay and the newer WG-DASL HT platform [326, 330]. An assessment of the performance of the WG-DASL HT assay with FFPE melanoma tissue is included below in section 2.13.

2.11.5 Quality control measures before the DASL assay

RNA sent for analysis using the DASL assay went through a number of quality control measures as recommended by Illumina and previous authors. A commonly used quality control measure is quantitative Real-time PCR (qRT-PCR) of the housekeeping gene, *RPL13a*. Cycle threshold (Ct) values of ≤ 29 cycles [296, 297] or ≤ 28 cycles [293, 294, 296] have been used to indicate adequate quality of RNA samples in previous studies. Others have used spectrophotometry to measure RNA concentration and A_{260}/A_{280} ratios. RNA concentrations of $< 20\text{ng}/\mu\text{L}$, $< 25\text{ng}/\mu\text{L}$ or total RNA input $< 50\text{ng}$ and A_{260}/A_{280} ratios < 1.5 or < 1.8 have been reported to indicate an inadequate sample

[293, 294, 296]. The Agilent 2100 Bioanalyzer has also been used to assess sample quality and generates an RNA integrity number (RIN) for each RNA sample derived from the electropherogram [336]. To generate a RIN, a number of features are assessed including total RNA ratio, measured as the fraction of the area in the region of the 18S and 28S peaks compared to the total area under the electropherogram curve, and the height of the 28S peak [336]. A score of 1 indicates totally degraded RNA and a score of 10 represents intact RNA [336]. It has been suggested that samples with an RIN number >2.0 or ≤ 2.0 with a RNA fragment size >200 nucleotides are suitable for use in the assay [294], however others have reported that RIN values do not correlate with performance of RNA samples in the DASL assay [296].

For samples sent for DASL analysis for my analyses, concentrations of extracted RNA were determined using the ND-1000 spectrophotometer (NanoDrop, Wilmington, DE, USA) as described in section 2.10. A selection of samples, detailed in Chapter 3, were analysed on the Agilent 2100 Bioanalyser using an RNA 6000 nano-chip and standard manufacturer's protocols to determine the average fragment length of the RNA. The RNA fragment length traces were visually evaluated by Dr Caroline Conway and a fragment analysis trace score of 1-3 was created where 1 = peak visible and labelled with fragment size marker, 2 = peak visible but not labelled with fragment size marker and 3 = little or no peak visible.

The final quality control measure performed on extracted RNA samples was a quantitative Real-time PCR (qRT-PCR) experiment to assess amplification of a 90bp fragment of the control gene *RPL13a*. The service provider, ServiceXS, performed these experiments. Samples were assessed in duplicate using SYBR Green and the ABI 7500 Real-time PCR System (Applied Biosystems) with standard protocols and PCR conditions. Primer sequences were, forward: GTACGCTGTGAAGGCATCAA and reverse: GTTGGTGTTTCATCCGCTTG. Mean cycle threshold values were determined for all samples and those samples with a Ct values ≤ 29 cycles were used in the assay.

An assessment of the usefulness of these quality control measures in FFPE melanoma samples is included in Chapter 3.

2.11.6 Control and replicate samples

To monitor intra-assay variation, each DASL assay experiment plate included 6-12 technical replicates (RNA samples from the same extraction) and biological replicates (RNA samples from different tissue cores removed from the same tumour) within and across plates. An assessment of equality and correlation across these replicate samples is included in Chapter 3.

To further monitor variation across plates and runs of the DASL assay, replicate Stratagene Universal Human Reference RNAs (Agilent Technologies, Edinburgh, UK) were assessed across DASL plates. Analysis of results from these reference RNAs is described in detail in Chapter 5.

2.12 Normalisation of gene expression data

The fluorescence intensity file generated following scanning of the array was sent to us by our service provider. This data was uploaded into Illumina BeadStudio software (Illumina Inc., CA, USA) for analysis of the 502-gene Human Cancer panel data and GenomeStudio (Illumina Inc.) for the WG-DASL HT data. The number of genes detected in each sample represents the genes for which target sequence signal is distinguishable from negative controls on the array with $p < 0.05$. Data were normalized within BeadStudio Gene Expression Module v3.4 (Illumina Inc.) for the Human Cancer Panel data and GenomeStudio v2010.3 Gene Expression Module 1.8.0 for the WG-DASL HT data. Normalization of gene expression data is required to remove any non-biological variation that may be present. This may be due to red-green bias due to differences in labelling efficiencies of the Cy5 and Cy3 dyes, differences in dye scanning properties with position on the array, artefacts on the array, variations in scanning across the array or because of non-uniform hybridization [337].

Fluorescence intensities from Cy3 and Cy5 dyes were averaged for each probe and the expression level for each gene was calculated as the mean of the average intensities from the three probes on the Human Cancer panel. PCR products from the WG-DASL HT assay were labelled with Cy3 only, the mean fluorescent intensities for the available probes for each gene were calculated as the gene expression level [326]. Background correction and cubic B-spline smoothing methods were used to normalise data. For samples assessed using SAM, sample scaling across plates removed variation between arrays assessing 96 samples from a 96-well plate.

Background correction removes gene expression from non-specific hybridization, the level of which is identified by the average expression for negative control genes, which is present on the array. The cubic spline method is a non-linear method of normalization in which a reference sample is generated using the average gene expression of all samples. This is then split into 15 quantiles which are used to fit smoothing B-splines. The splines are then used to normalize the signals of the sample in a given quantile by scaling signals to match intensities in the reference sample [338]. This method assumes that all transcripts have the same abundance and it is well suited

to remove the effects that might cause non-linear transformation such as saturation [337, 338]. Sample scaling is based on the presence of technical replicates across plates which are used to calculate a scaling factor that is applied to other samples to create equal average intensity for each probe across all plates. The quality of the normalisation was assessed by testing the equality and the correlation between gene expression levels across sample replicates.

2.13 Assessment of the WG-DASL HT assay with FFPE melanoma samples

2.13.1 Background and methods

The ability to perform unbiased whole-genome expression profiling using FFPE tissue would greatly enhance our ability to detect alterations in gene expression associated with prognosis and responses to treatment in malignant melanoma.

To assess the WG-DASL HT assay, 5 FFPE melanoma samples from patients recruited to the “Predicting Response to Chemotherapy in Malignant Melanoma” study, were sampled as described in section 2.3.5 and RNA was extracted using the Qiagen AllPrep® RNA/DNA FFPE kit as described in section 2.6.3. RNA samples were sent in duplicate for analysis using the WG-DASL HT assay at ServiceXS (Leiden, Netherlands) by Floor de Kort. All samples passed quality control procedures as described in section 2.11.5.

2.13.2 Results and discussion

Previous authors have used the number of genes detected in each sample using the DASL assay, defined as a probe signal significantly greater than average signal from negative controls with $p < 0.05$, as a measure of the quality of results [294]. An argument for not using this measure to determine result quality is presented in Chapter 5, however for the purposes of this assessment, number of detected genes was assessed. Generally the samples performed well with the mean number of genes detected ($p < 0.01$) being 11943 (range 6346-14287). One of the five samples performed less well with the number of detected genes being 6346 and 8050 in the replicate samples. For the samples with a high number of detected genes, reproducibility between replicate samples was good with probe signal intensity Pearson's correlation coefficients ranging from 0.96-1.00 (Figure 2-4). For the sample with lower numbers of detected genes, the Pearson's correlation coefficient was 0.89.

The assay appears to generate reproducible gene expression results in FFPE melanoma samples, therefore further assessment of the WG-DASL HT assay is underway using larger sample sets. In this pilot study, I was unable to identify the poorly performing sample using quality control measures described in section 2.11.5., therefore efforts will be directed to identifying further quality control measures to determine sample performance.

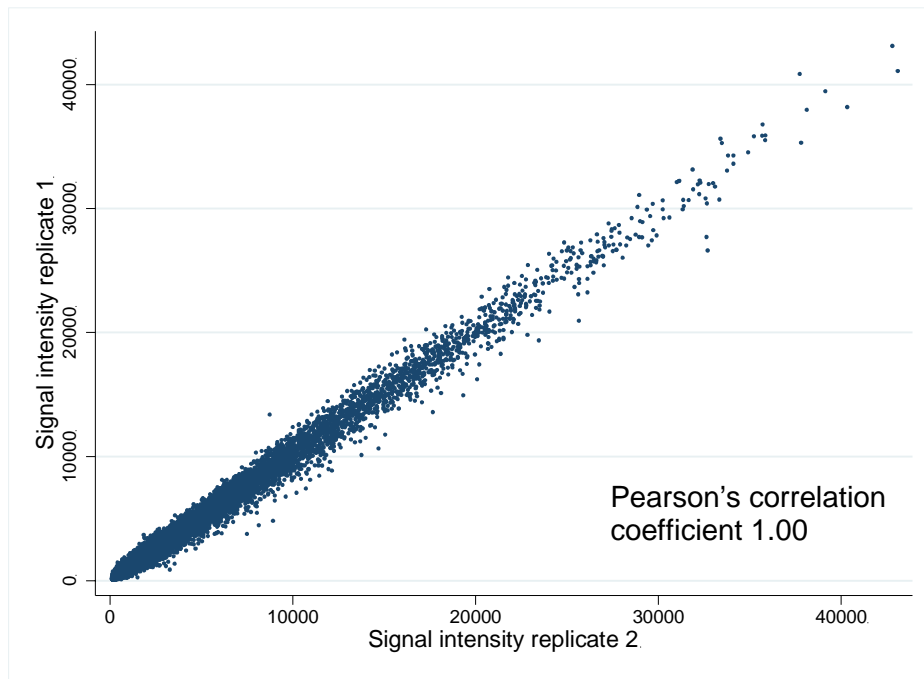


Figure 2-4: Scatter plot demonstrating correlation between probe signal intensities for replicate FFPE melanoma samples on the WG-DASL HT assay.

The Pearson's correlation coefficient is reported.

These results are the final in a number of test experiments using the WG-DASL HT assay. Previous assessments showed poor reproducibility between sample replicates and an analysis problem where a grid, which is superimposed onto the array to identify the position of beads, could not be placed by the scanning software. On enquiry, issues with sample reproducibility were also noted by other groups world-wide, however the grid registration problem was identified by our group and brought to the attention of Illumina. These issues were discussed in detail with Illumina and following investigation were attributed to the short shelf-life of the reagent used for cDNA synthesis. This led to withdrawal of the assay from the market and development of a new reagent. The new product was released in May 2012 and the results presented above indicate that

the assay now produces reproducible results, although some problems with grid placement remain and further investigation into this issue is on-going. Once these issues are resolved, a further test set of samples will be analysed and then a larger set of RNA samples extracted from primary melanoma tumours which will be published but which will not be available in sufficient time for this thesis.

2.14 Quantitative Real-time PCR (qRT-PCR) using Taqman® Gene Expression Assays

qRT-PCR experiments using Taqman® Gene Expression Assays have been used in Chapters 3 and 4 to validate gene expression findings from the DASL array. Taqman® Gene Expression Assays consist of a target specific oligonucleotide which has a reporter dye, such as 6-fluorescein amidite (FAM™), linked to the 5' end of the probe and a non-fluorescent quencher at the 3' end of the probe which suppresses the reporter fluorescence. During PCR the probe specifically anneals to the target of interest and the 5' nuclease activity of DNA polymerase then cleaves the probe. This separates the reporter and quencher dyes, resulting in fluorescence of the reporter. Polymerization of the strand continues and increasing amounts of PCR products are detected by directly monitoring the increase in fluorescence of reporter dye (Figure 2-5) [339].

Fluorescent intensity of the reporter dye is normalised to the fluorescence of a passive ROX dye which corrects for differences in fluorescent intensity due to different concentrations or volumes in the sample mix. The threshold of a PCR reaction is set when there is a significant increase in fluorescence for the reporter dye which occurs during the exponential phase of the PCR reaction. From this threshold, for each sample a cycle threshold (Ct) value is derived which is the number of PCR cycles at which the fluorescence of a sample crosses the threshold [339].

For qRT-PCR experiments reported in this thesis, the following section describes the standard protocol. Any deviation from this is described in the relevant chapter.

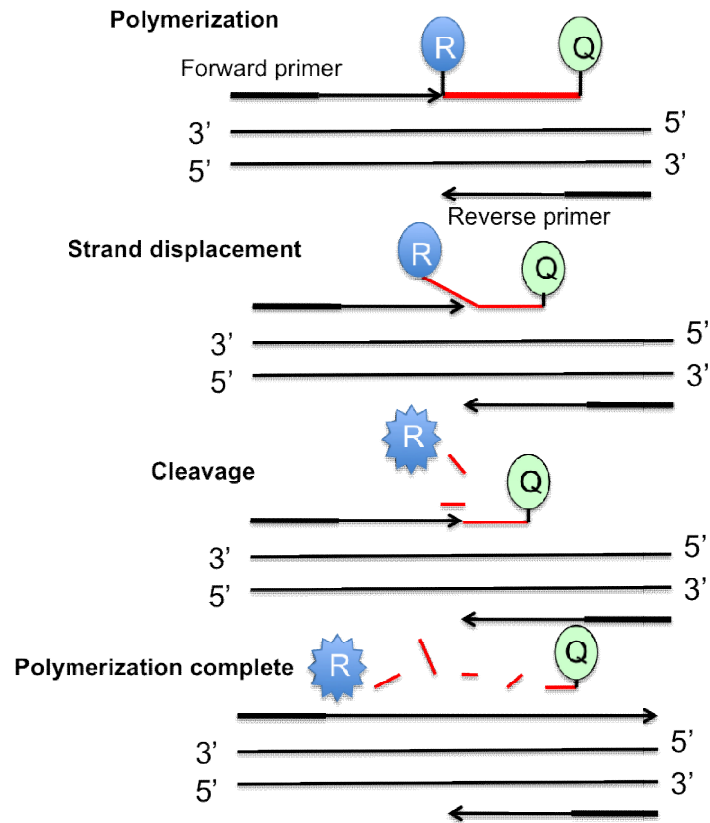


Figure 2-5: Action of Taqman® Gene Expression Assays.

During PCR, the Taqman® probe is cleaved by the 5' nuclease activity of AmpliTaq Gold® DNA Polymerase Ultra Pure. Diagram adapted from reference [339].

2.14.1 Standard TaqMan® gene expression protocol

Assays were performed in triplicate using 1 microgram of cDNA in each reaction. PCRs were performed using Gene Expression Master Mix (Applied Biosystems, Warrington, UK) which contains AmpliTaq Gold® DNA Polymerase Ultra Pure, Uracil-DNA Glycosylase (UDG), deoxyribonucleotide triphosphates (dNTPs), ROX™ Passive Reference and buffer components [339]. Reactions were performed in a 10µl final volume made up using 5µl Master Mix, 0.5µl Taqman® Assay, 3.5µl DNase-free water and 1µl cDNA sample. PCRs were performed using the ABI 7500 Fast Real-time PCR System (Applied Biosystems) using the following cycling conditions: UDG activation at 50°C for 2 minutes, AmpliTaq Gold® DNA Polymerase activation at 95°C for 10 minutes, then 50 cycles of 95°C for 15 seconds and 60°C for 1 minute. The number of cycles was increased to 50 to ensure that amplification of every sample was identified. Automatic settings were used for baseline and threshold determination, Ct values were

exported to Excel for further analysis. Mean Ct values for each probe for each sample were generated from replicate samples.

2.14.2 Analysis of qRT-PCR data

qRT-PCR can be used for absolute quantitation of gene products, or relative quantitation [340]. In this thesis, relative quantitation has been used to assess differences in gene expression between samples, reported as a fold-change, or relative quantity, in expression relative to a calibrator or reference sample [341]. Two methods for relative quantitation exist, the relative standard curve method and the comparative Ct method [342]. A detailed assessment of methods for relative quantitation using Taqman® Gene Expression Assays and methods for qRT-PCR is included in Chapter 4 and will not be discussed in further detail here.

I will briefly describe a method commonly used for analysis of comparative Ct studies, which has been used in Chapters 3 and 4. The comparative Ct method quantifies gene transcript levels relative to those of a single control gene [342]. To use this method, it is essential that the PCR efficiencies of probes for test genes and control genes are similar [340, 342]. If this is the case, $\Delta\Delta Ct$ values can be calculated where $\Delta Ct = Ct$ value for gene of interest – Ct value for endogenous control and $\Delta\Delta Ct = \Delta Ct$ sample – ΔCt calibrator sample. Relative quantity (RQ) levels are then calculated using $(1 + \text{efficiency of target amplification})^{-\Delta\Delta Ct}$. Therefore when amplification efficiency is 100%, with doubling of PCR product during every PCR cycle, $RQ = 2^{-\Delta\Delta Ct}$ [340, 342]. This method will be described as the $2^{-\Delta\Delta Ct}$ method in this thesis.

To improve accuracy of qRT-PCR normalisation, multiple control genes have been used for data normalisation in this thesis (discussed further in Chapter 4) according to the methods described by Vandesompele *et al.* [343]. For this method, ΔCt values are calculated, where $\Delta Ct = \text{mean Ct gene of interest in sample} - \text{mean Ct gene of interest in calibrator sample}$ [340]. ΔCt values are converted to $2^{-\Delta Ct}$ to provide a non-normalized value for each gene of interest for each sample. For each sample, the geometric mean of the $2^{-\Delta Ct}$ value for the normalisation genes is calculated as a normalisation factor. The $2^{-\Delta Ct}$ value for the unknown genes is divided by the normalisation factor to provide a normalised quantity [343].

2.15 Chemo-sensitivity Gene Expression Assay (CGEA-1)

Chapter 8 describes use of a customized Taqman® Array microfluidic qRT-PCR card (Chemo-sensitivity Gene Expression Assay, CGEA-1, CanTech Ltd, Portsmouth, UK) for validation of DASL gene expression results. For this study, I collaborated with the Translational Oncology Research Centre, Queen Alexandra Hospital, Portsmouth where the experimental work was performed by Dr Katharine Parker. The CGEA-1 assay contained 92 genes known or hypothesized to be involved in cytotoxic resistance or sensitivity based on the current literature [289] which are listed in Chapter 8.

Taqman® array cards (Applied Biosystems, Warrington, UK) are 384-well microfluidic cards which allow 384 simultaneous PCR reactions using Taqman® gene expression assays which are described in more detail in section 2.14.1 [344]. The gene expression assays are preloaded into each well, so samples and master mix are simply added to the card, the array is centrifuged and then sealed prior to PCR [344].

Each sample was made up with Taqman Gene Expression Master Mix and mixed with an equal volume of cDNA to give a final concentration ranging from 240-300ng/μl suitable for the small volume dry PCR Taqman array wells. Samples were then each pipetted into two ports (100μl per port) of the 384 well card, for the 96 genes assessed. The loaded array was then placed into a balanced centrifuge and spun at 380g to fill the card and then re-spun to remove any air bubbles. The card was sealed using a Taqman array slide sealer and loading ports cut from the card before loading into an ABI 7900HT thermal cycler (Applied Biosystems). PCR was performed using the following conditions: 50°C for 2 minutes, 94.5°C for 10 minutes, then 40 cycles of 30 seconds at 97°C and 1 minute at 59.7°C. Automatic settings were used for baseline and threshold determination and Cycle threshold (Ct) values for each target were exported to Excel and sent to myself further analysis. Details of data analysis are included in Chapter 8.

2.16 Fluidigm Biomark HD qRT-PCR system

To identify differential gene expression of DNA repair genes in samples from patients recruited to the “Predicting Response to Chemotherapy in Malignant Melanoma” study described in Chapter 8, the Fluidigm Biomark HD qRT-PCR system (Fluidigm, San Francisco, CA) was used. The Fluidigm Biomark HD quantitative PCR chip uses microfluidic technology to allow assessment of up to 96 genes in 96 samples in a total of 9216 PCR reactions in a single experiment. Fluidigm microfluidic technology uses integrated fluidic circuits (IFC) containing valves and channels which allows assembly

of individual PCR reactions in a volume of 10nl [345-347]. The ability to use small amounts of RNA to assess expression in up to 96 genes simultaneously is clearly useful for validation of microarray results or assessment of a group of biologically related genes. A detailed assessment of the performance of this system with FFPE melanoma tissue is included in Chapter 8.

2.16.1 Integrated fluidic circuits (IFC)

The IFC is a network of fluid lines, NanoFlex™ valves, which flex under pressure, and chambers [347] (Figure 2-6). Valves are used to regulate flow of liquid in the IFC. Before samples are loaded into the IFC, the chip is primed by pressurizing control lines which close interface valves. Gene expression assays are pipetted into the detector inlets and samples into sample inlets. The IFC is then loaded by pressure being applied to sample and detector inlets, samples are pushed into individual wells, but as the interface valves are shut assays cannot enter the wells. Containment valves are then closed, interface valves are opened which allows assays to enter the wells and mixing of sample and assay. Once mixed, the interface valves are shut and the IFC is ready for cycling [347]. In common with other qRT-PCR platforms, the chip is imaged following each PCR cycle to generate amplification curves for each gene for each sample [347]. Specific target amplification (STA) of cDNA samples for genes of interest increases the sensitivity of the technique [348].

2.16.2 DELTAgene™ assays

The Fluidigm systems can be used with Taqman® assays, but for the purposes of this study, we have used gene specific primers (DELTAgene™ assays, Fluidigm) in conjunction with the DNA-binding dye, EvaGreen. EvaGreen is a fluorophore, which when bound to double-stranded DNA emits a strong fluorescent signal, the intensity of which is directly proportional to the increase in the amount of double-stranded DNA during a PCR reaction [349, 350]. Use of EvaGreen significantly reduces the cost of the experiment, however the specificity of the reaction is reduced as only a primer pair are used for PCR, the additional probe present in Taqman® based assays being absent [349]. Primers were designed to target DNA repair genes in the study detailed in Chapter 8. A detailed assessment of the performance of DELTAgene™ assays in RNA extracted from FFPE melanoma tissues is included in Chapter 8.

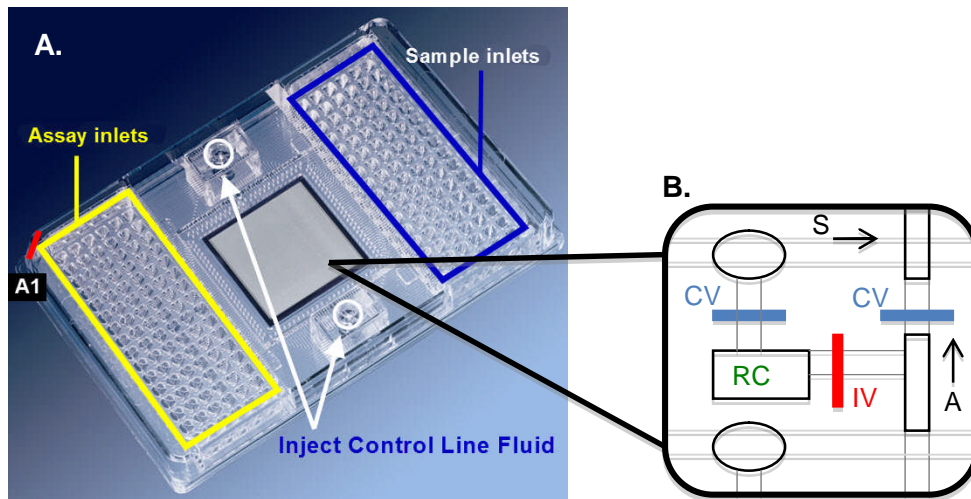


Figure 2-6: The Fluidigm 96:96 Dynamic Array™ integrated fluidic circuit (IFC).

(A) A photograph of the array showing assay and sample inlets. The IFC in the centre of the chip and is a network of fluid lines, Nanoflex™ valves and reaction chambers. (B) shows a close-up of the IFC with one of the reaction chambers (RC) and associated containment valves (CV) and interface valve (IV). Samples (S) and assays (A) are directed through the IFC using pressure and valves. Initially samples enter the RC as CVs are open. Assay is prevented from mixing with the sample by a closed IV. CVs are then closed and the IV opened to allow mixing of sample and assay prior to PCR. Figure adapted from [347, 351].

2.16.3 Standard Fluidigm qRT-PCR protocol

For experiments using the Fluidigm qRT-PCR system reported in Chapter 8, the following section describes the standard protocol. Any deviation from this is described in the relevant section in Chapter 8.

2.16.3.1 Specific target amplification (STA) of samples

Amplification of specific target assays is performed using pooled primers to increase the number of specific cDNA targets without introducing bias [348]. Each DELTAgene primer pair (100µM) was combined in equal volume and diluted in 1x DNA suspension buffer (10nM Tris, pH 8.0, 0.1mM EDTA) (TEKnova, Hollister, CA) so each primer is at a final concentration of 500nM. The primer mixture was vortexed and 0.5µl was combined with 2.5µl Taqman® Pre-amplification master mix (Applied Biosystems, Warrington, UK), 0.75µl of DNA suspension buffer and 1.25µl of cDNA in a 96-well plate. The plate was sealed and placed on a thermal cycler, cycling conditions were 95°C for 10 minutes, followed by 22 cycles of 95°C for 15 seconds and 60°C for 4

minutes, then finally the mixture was cooled to 4°C. Exonuclease I (New England Biolabs, Hitchin, UK) was used to remove unincorporated primers, 8 units were added to each STA reaction and heated to 37°C for 30 minutes, followed by 80°C for 15 minutes before being cooled to 4°C. The products were diluted 1:5 using DNA suspension buffer and stored at -20°C for use in the qRT-PCR reaction.

2.16.3.2 qRT-PCR reaction

To prepare the sample pre-mix solution for each sample, 3µl of 2x Taqman® gene expression master mix (Applied Biosystems) was mixed with 0.3µl 20x DNA binding dye sample loading reagent (Fluidigm, Amsterdam, Netherlands), 0.3µl EvaGreen DNA binding dye (Biotium, Cambridge, UK) and 2.4µl of the STA sample. The pre-mix solution was thoroughly vortexed and centrifuged. The assay mix was prepared by combining 3µl of 2x assay loading reagent (Fluidigm), with 2.46µl DNA suspension buffer and 0.54µl of each 100µM primer pair. This mix was thoroughly vortexed and centrifuged.

Control line fluid (Fluidigm) was injected into the two accumulators on the 96:96 Dynamic Array IFC (Fluidigm) (Figure 2-6). The chip was placed into the IFC Controller HX (Fluidigm) and primed with control line fluid. Five microliters of the samples and assays were loaded into the respective inlets on the chip (Figure 2-6), the chip was again placed into the IFC Controller HX and the chip was loaded with samples and assays. The chip was removed from the Controller and dust particles were removed from the chip surface using Scotch tape. The chip was placed into the Biomark HD Reader (Fluidigm) for the qRT-PCR reaction. Cycling conditions consisted of a thermal mix stage, consisting of 50°C for 2 minutes, followed by 70°C for 30 minutes and then 25°C for 10 minutes, uracil-N-glycosylase (UNG) was then activated at 50°C for 2 minutes followed by activation of polymerase at 95°C for 10 minutes and then 40 cycles of 95°C for 15 seconds, followed by 60°C for 1 minute. Finally a melt curve was generated by increasing the temperature from 60-90°C. Data from the Biomark Reader was imported into Fluidigm Real-time PCR Analysis software, the image view was assessed to confirm presence of ROX passive reference dye in each well of the IFC, if this was not present these wells were excluded from further analysis. The auto(global) method was used to determine thresholds for calculation of cycle threshold (Ct) values, linear baseline correction was used for baseline determination. Ct values were exported to Stata version 10 (StataCorp 2007, College Station, TX) for further analysis.

2.17 Identification of mutations in FFPE primary melanoma tumours

2.17.1 *BRAF* and *NRAS* mutation screening using pyrosequencing

Pyrosequencing was used to identify mutations in codon 600 of *BRAF* and codons 12, 13 and 61 of *NRAS* in FFPE melanoma tumour sample sets described in Chapter 6. Pyrosequencing is a DNA sequencing technique which uses primers to direct a polymerase extension reaction and then nucleotides are added sequentially to the reaction [352]. When a base is incorporated, pyrophosphate is released which is converted to ATP by ATP sulfurylase, which provides energy to luciferase to oxidise luciferin and generate light. The amount of light that is released is proportional to the number of nucleotides incorporated so allowing the DNA sequence to be determined. In liquid-phase pyrosequencing, the enzyme apyrase degrades the unbound nucleotides before the next nucleotide is added [352-355]. Previous authors have compared mutation detection results from codons 600 and 601 of *BRAF* in cell lines, fresh tissue and FFPE tissue using pyrosequencing and traditional sequencing. There was good concordance in mutation results between the methods and a mutant peak can be detected using pyrosequencing when 15-20% of mutated *BRAF* (V600E) melanoma cell line derived DNA is present [356]. Using traditional Sanger sequencing, at least 40% of DNA needs to be mutant to detect the mutation, suggesting that pyrosequencing is more sensitive than Sanger sequencing for detecting this mutation [356]. This study also compared pyrograms generated from paired frozen and FFPE tumours with V600E and V600K mutations; these pyrograms showed similar patterns and the authors concluded that pyrosequencing generated accurate results with FFPE tissue [356]. Another study compared mutation results generated using pyrosequencing, single-strand conformation polymorphism (SSCP) analysis and sequencing for *NRAS* codons 12, 13 and 61 in frozen melanoma tissue [353]. All mutation results were concordant across assays and the sensitivity of pyrosequencing was reported to be comparable to that of sequencing (15-30%), but less than SSCP analysis (10%) [353]. Therefore pyrosequencing produces accurate results for *BRAF* and *NRAS* mutation screening from FFPE tissue, it also requires small amounts of DNA and using automated systems, large numbers of samples can be processed quickly making it particularly suitable for mutation screening in my samples.

Pyrosequencing of cDNA and DNA samples was undertaken by Dr Philip Chambers in the Genomics Facility, Cancer Research UK Centre, Leeds Institute of Molecular Medicine with mutation detection based on NCBI RefSeq accession number

NM_004333 for *BRAF* and NM_002524 for *NRAS* [331]. Primers for amplification and pyrosequencing analysis of *NRAS* codons 12 and 13, *NRAS* codon 61 and *BRAF* codon 600 were designed using proprietary Pyrosequencing assay design software version 2.0.1.15 (Qiagen, Crawley, UK). *NRAS* codons 12 and 13 were amplified in one PCR reaction; *NRAS* codon 61 and *BRAF* codon 600 were amplified in separate PCR reactions (Table 2-1).

Region of interest	PCR primers (5' → 3')	Pyrosequencing primer (5' → 3')	Amplicon length (bp)
<i>NRAS</i> codons 12 and 13	Fwd: CTTGCTGGTGTGAAATGACTGAG Rev: biotin-TGGATTGTCAGTGCGCTTTTC	CTGGTGGTGGTTG GA	79
<i>NRAS</i> codon 61	Fwd: biotin-GAAACCTGTTTGTGGACATACTG Rev: TCGCCTGTCCTCATGTATTG	CTCTCATGGCACT GTACT	83
<i>BRAF</i> codon 600	Fwd: TGAAGACCTCACAGTAAAAATAGG Rev: biotin-TCCAGACAACCTGTTCAAACCTGAT	TGATTTTGGTCTAG CTACA	91

Table 2-1: PCR and pyrosequencing primer sequences for amplification and analysis of *NRAS* codons 12 and 13, *NRAS* codon 61 and *BRAF* codon 600.

PCR reactions contained 12.5µl of Qiagen HotStarTaq Master Mix (Qiagen, Crawley, UK), additional magnesium chloride to a final concentration of 2mM, 200nM each of forward and reverse primers, 20ng of genomic DNA or 2µl of undiluted cDNA and sufficient water to make a final volume of 25µl. Thermal cycling conditions were 94°C for 12 minutes followed by 40 cycles of 94°C for 10 seconds, 55°C for 20 seconds and 72°C for 20 seconds. Streptavidin-coated magnetic beads were used to capture biotinylated PCR product which were sequenced on a PyroMark ID system (Qiagen, Crawley, UK) following the manufacturer's protocols. Data were analysed by visual inspection of pyrograms and by analysis of peak height data. Examples of pyrograms from *BRAF* codon 600 are shown in Figure 2-7. Percentage mutation levels were calculated using peak height data. For example, for V600E A allele percentage levels, the calculation is (peak height of the A allele x 0.85)/(peak height of the A allele x 0.85 + peak height of the T allele [357]. Based on previous experience with the *BRAF* assay using other tumour types and other experimental data, Dr Phil Chambers has advised that the assay sensitivity is 5% with good quality data, where a peak can be

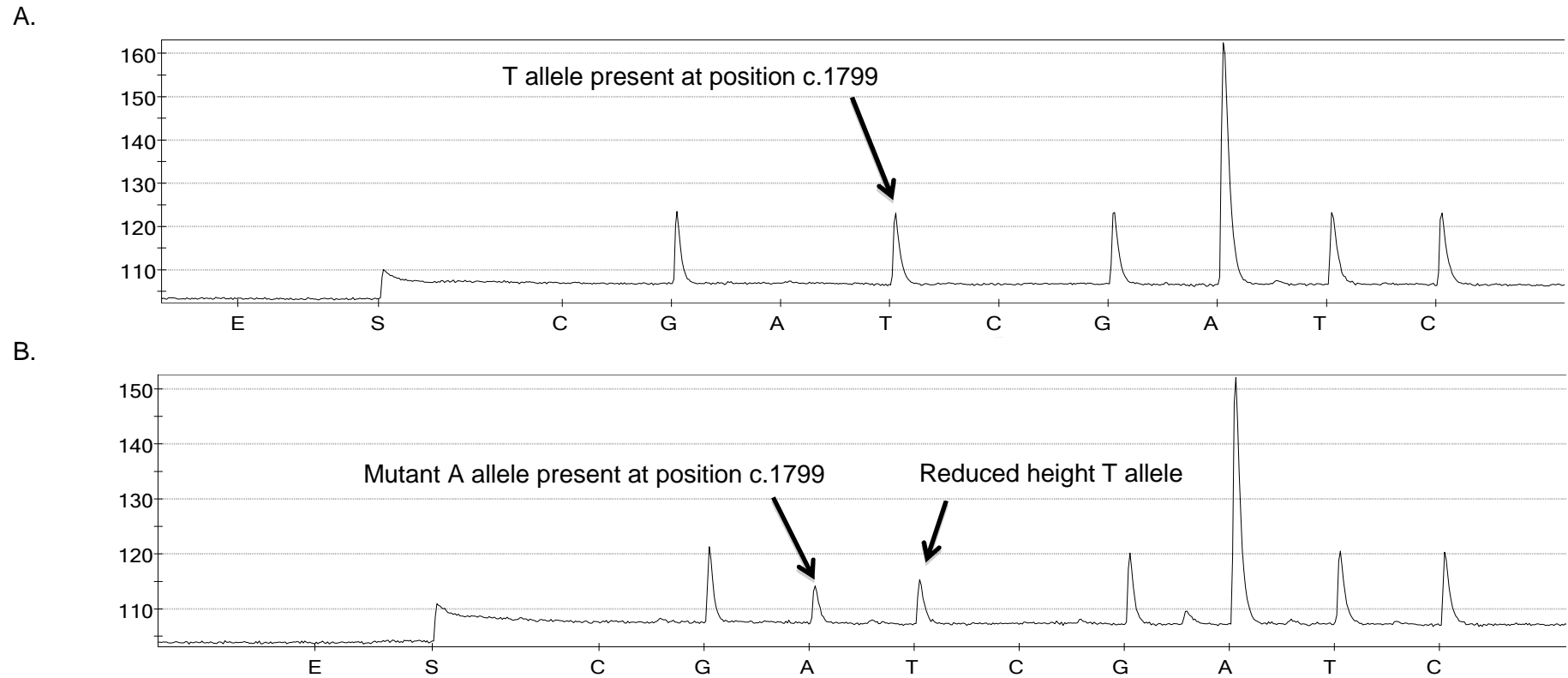


Figure 2-7: Pyrograms for *BRAF* codon 600.

A shows a pyrogram from a wild-type sample, B shows a pyrogram from a specimen with a V600E (c.1799T>A) mutation.

distinguished from background, and therefore samples with >5% A allele percentage were classified as having mutations. With poorer quality data, the sensitivity is less and for these runs, samples with >10% mutation levels for the *BRAF* assay were classified as mutated. As discussed further in Chapter 6, the term “mutation percentage” reflects the number of mutated alleles in cells assessed, but as tumours are heterogeneous it will also reflect the number of non-mutated tumour cells along with contaminating normal stromal cells. Pyrosequencing can detect low levels of mutation in FFPE melanoma samples and is more sensitive than Sanger sequencing based on the published literature described above. In some cases mutation results were confirmed using traditional sequencing using methods described in 2.17.3 by Dr Phil Chambers.

2.17.2 *BRAF* and *NRAS* mutation screening using Applied Biosystems PRISM® SNaPshot™ Multiplex system

The Applied Biosystems PRISM® SNaPshot™ Multiplex system (Applied Biosystems, Warrington, UK) was used to confirm mutations in *BRAF* and *NRAS* in FFPE tumour DNA or cDNA identified using pyrosequencing as described in Chapter 6. As discussed in Chapter 6, a limited spectrum of mutations has been found at specific hot-spots in *BRAF* and *NRAS* in melanoma tissues [30]. Most of these mutations involve either a single (e.g. V600E) or dinucleotide change (e.g. V600K), therefore the SNaPshot assay can be used to identify these mutations. The primer extension (SNaPshot) assay uses a reaction mix of four fluorescently labelled dideoxynucleoside triphosphates (ddNTPs) [358, 359]. Template DNA is amplified using PCR and a primer anneals to the sequence adjacent to the site of the altered base. Single-base extension occurs by the addition of the complementary dye-labelled ddNTP to the primer. The result is marker fragments for mutant and wild-type alleles that are the same length, but vary in colour. After electrophoresis and fluorescence detection, the alleles appear as different coloured peaks of roughly the same size in the electropherogram plot. The size of the different allele peaks will vary slightly due to differences in molecular weight of the fluorescent dyes [359]. Peaks are colour-coded by Genemapper® software (Applied Biosystems) according to the dye labelling of the incorporated ddNTP. The identification of a genotype is based on the peak colour and position of the peak relative to a size standard [358]. SNaPshot can be used to investigate up to ten sites simultaneously by using primers of different length [359].

In a previous study using the SNaPshot assay to detect *BRAF* V600E and various *NRAS* mutations in DNA extracted from FFPE tissues, assay sensitivity was determined using serially diluted positive control samples. Sensitivity to detect *BRAF*

mutations was 4.9% and for *NRAS* mutations 3.2-7.2% depending on the mutation [360]. These sensitivity levels were comparable to that of Sanger sequencing in this study [360] suggesting that this method is sensitive, but pyrosequencing is more sensitive for the V600E *BRAF* mutation as previously discussed [356].

To assess the mutation status of *BRAF* and *NRAS*, methods were optimised using cDNA and DNA from melanoma cell line material and metastases samples. PCR primers were selected as described in Table 2-2 to generate small exonic PCR fragments (70-80bp) suitable for use with DNA extracted from FFPE material and cDNA synthesized from degraded RNA. SNaPshot probes for detection of mutations in *NRAS* and *BRAF* as described in Table 2-3 were designed to anneal adjacent to the mutation site. Each probe was synthesised with a different length poly(dT) tail to allow separation of SNaPshot products during electrophoresis on the basis of size.

Gene	Exon (codons covered)	Forward sequence (5'→3')	Reverse sequence (5'→3')	Conc. in primer mix – cDNA (µM)	Conc. in primer mix – DNA (µM)
<i>NRAS</i>	2 (12/13)	GGTGTGAAATGAC TGAGTAC	GATTGTCAGTGCG CTTTCC	0.4	0.4
<i>NRAS</i>	3 (61)	TGGTGAAACCTGT TTGTTGG	TTGGTCTCTCATGG CACTGT	0.5	0.5
<i>BRAF</i>	15 (600/601)	TCTTCATGAAGAC CTCACAGT	CCAGACAACCTGTT CAAACCTGA	0.7	0.7

Table 2-2: Primers used for PCR amplification of template cDNA and DNA prior to the SNaPshot assay.

Primer concentrations in the final PCR mix for use with cDNA and DNA are also presented.

Two assays were performed separately on PCR products to assess the mutation status of the *BRAF* gene. The first assay used the V600E probe on the sense strand and K601E probe on the anti-sense strand, the second assay used the V600E/K probe on the anti-sense strand and the V600K probe on the sense strand to identify V600K mutations. This design was chosen because the V600K mutation is a dinucleotide change at c.1798_1799delinsAA, whereas the V600E mutation is a single base change at c.1799T>A [361]. Therefore, the V600E probe used in the first assay would not anneal in the presence of a V600K mutation, however the combination of the V600E/K probe on the antisense strand and V600K probe on the sense strand in the

second assay would allow identification of both V600E and V600K mutations (Figure 2-8). The K601E mutation is a single nucleotide change at c.1801A>G [361].

Probe (gene)	Sequence (5'→3')	Strand	Product Length (bp)	Conc. in SNaPshot probe mix (μM)
Position 182 (NRAS exon 3)	T ₃₃ GACATACTGGATACAGCTGGAC	Sense	55	0.6
Position 181 (NRAS exon 3)	T ₁₈ CTCATGGCACTGTACTCTTCTT	Anti-sense	40	0.1
Position 37 (NRAS exon 2)	T ₂₆ GGTGGTGGTTGGAGCAGGT	Sense	45	0.1
Position 35 (NRAS exon 2)	T ₇₁ CTGGTGGTGGTTGGAGCAG	Sense	90	0.3
V600E (BRAF)	T ₁₄ GGTGATTTTGGTCTAGCTACAG	Sense	36	0.2
V600E/K (BRAF)	T ₅₀ ACCCACTCCATCGAGATTTTC	Anti-sense	70	0.2
V600K (BRAF)	T ₄₀ GGTGATTTTGGTCTAGCTACA	Sense	62	0.1
K601E (BRAF)	T ₃₀ GGACCCACTCCATCGAGATT	Anti-sense	50	0.2

Table 2-3: Probes used in the SNaPshot assay.

The final working concentration of these probes in the SNaPshot reaction is also presented.

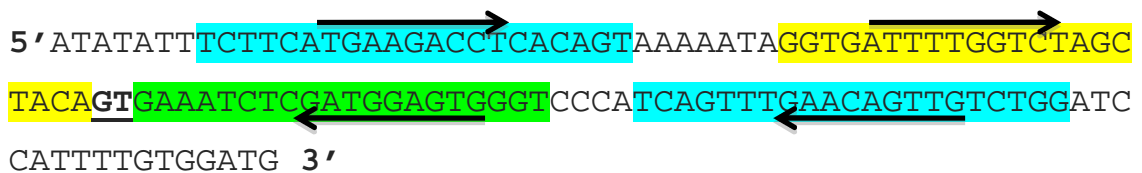


Figure 2-8: A section of exon 15 of the BRAF gene to demonstrate the position of SNaPshot probes in relation to common BRAF mutations.

The site of the V600K mutation is underlined and highlighted in bold. The position of the PCR primers are shown in blue, the site of the V600K probe is shown in yellow and the V600E/K probe on the anti-sense strand is shown in green.

Separate PCR mixes for *BRAF*, *NRAS* exon 3 and *NRAS* exon 2 contained 0.9x GeneAmp PCR Gold Buffer (Applied Biosystems), 0.5 units AmpliTaq Gold DNA polymerase (Applied Biosystems), 1.25 mM magnesium chloride solution, 0.2mM dNTPs (Applied Biosystems), 0.4-0.7 μM of each primer mix (listed in Table 2-2), 5% glycerol, 2 micrograms of cDNA or 20ng of DNA and nuclease-free water to a final

volume of 10 μ l. Thermal cycler conditions were 95°C for 5 minutes, 35 cycles of 95°C for 45 seconds, 55°C for 45 seconds and 72°C for 45 seconds followed by 72°C for 10 minutes. PCR products were treated with 2 units of shrimp alkaline phosphatase (USB, Affymetrix, High Wycombe, UK) and 1.3 units of exonuclease I (New England Biolabs, Hitchin, UK) and incubated at 37°C for 1 hour, followed by 72°C for 15 minutes, to remove excess dNTPs and primers, respectively.

SNaPshot analysis was performed using the Applied Biosystems PRISM® SNaPshot™ Multiplex kit. Two reaction mixes were prepared for analysis of *BRAF* as described above, and two reaction mixes were prepared for *NRAS* analysis, one containing the *NRAS* probes on exon 2, the other with probes for exon 3. Reactions contained 2.5 μ l SNaPshot Ready Multiplex Ready Reaction Mix, 1x BigDye sequencing buffer (Applied Biosystems), 0.1-0.6 μ M probe mix (Table 2-3), 1 μ l of the relevant PCR product and nuclease-free water to a final volume of 9 μ l. A control reaction without template was performed for each assay using the same reaction mix and 1 μ l nuclease-free water. Extension reactions were performed by incubating the mixture for 35 cycles at 96°C for 10 seconds to denature followed by 58.5°C for 40 seconds to anneal and extend. Products were treated with 1 unit of shrimp alkaline phosphatase, followed by incubation at 37°C for 60 minutes and then 72°C for 15 minutes. Products were diluted 1 in 5 using nuclease-free water. 1 μ l of the diluted extension product was mixed with 9.8 μ l HiDi™ formamide (Applied Biosystems) and 0.2 μ l of Genescan-120LIZ size standard (Applied Biosystems). Products were denatured at 100°C for 5 minutes and then separated using an Applied Biosystems PRISM 3130xl Genetic Analyzer with a 36cm length capillary and POP-7™ polymer. Analysis was performed using GeneMapper® 3.7 software. Some examples of the results obtained are presented in Figure 2-9. Significant peaks were not identified in traces from no template control reactions. Percentage mutation results were calculated based on peak heights using similar methods as for pyrosequencing data.

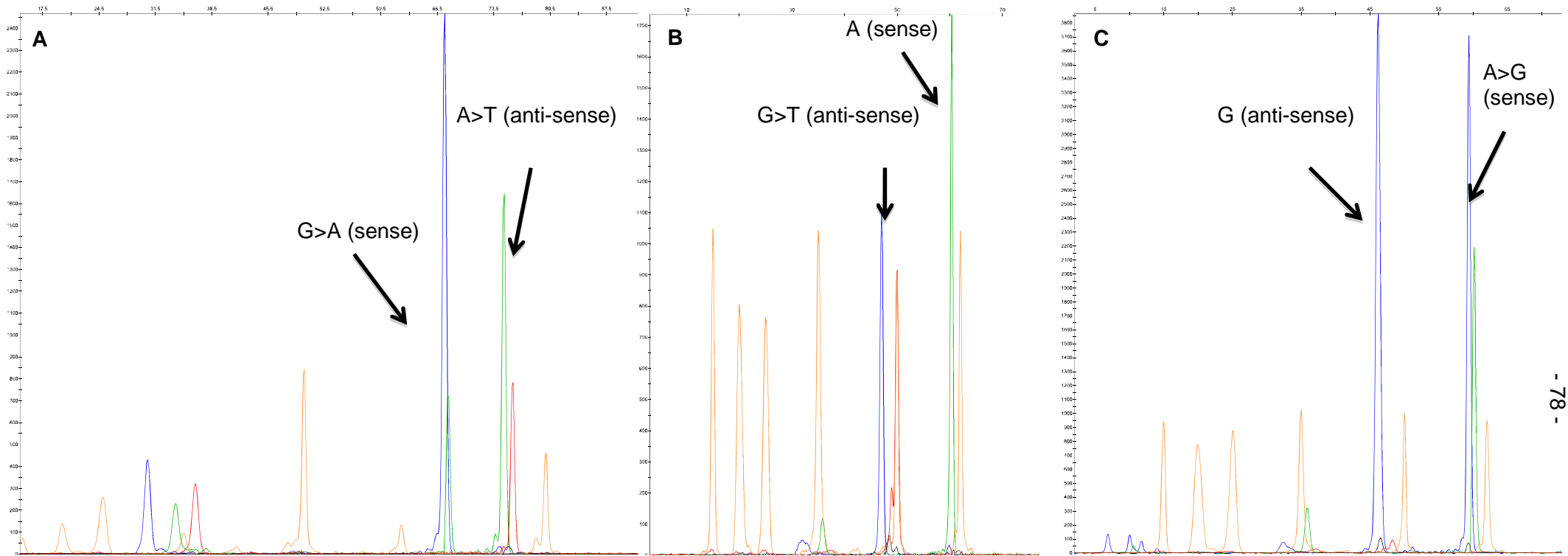


Figure 2-9: Examples of mutations detected using SNaPshot in cDNA and DNA.

Graph A demonstrates a V600K mutation in *BRAF*, the A>T change alone using the probe on the anti-sense strand would represent a V600E mutation. Graph B shows a c.181C>A mutation in exon 3 of *NRAS*. Graph C shows a c.182A>G mutation in exon 3 of *NRAS*. Orange peaks represent the internal Genescan-120LIZ size standards. Bases are represented by the following colours: A=green, C=black, G=blue and T=red. Small non-specific peaks are noted in graph A, which were seen in all *BRAF* assays.

2.17.3 Sequencing methods

To confirm mutations identified in *BRAF* and *NRAS* using pyrosequencing, traditional Sanger sequencing was performed on a selection of samples by Dr Phil Chambers. Pyrosequencing primers as described in Table 2-1 were used as sequencing primers in this analysis. Sequencing of both forward and reverse strands was performed.

To remove any unincorporated dNTPs and primers, 1µl of ExoSAP-IT (USB, Affymetrix, High Wycombe, UK) was added to 2.5µl of the PCR product, mixed and incubated at 37°C for 15 minutes, followed by 80°C for 15 minutes and finally cooled to 15°C. The sequencing reaction comprised of 1µl of 1.6µM primer, 1µl of purified PCR product, 4.25µl of distilled water, 3.5µl of ABI 5x Sequencing Buffer (Applied Biosystems, Warrington, UK) and 0.25µl of Ready Reaction Mix v1.1 (from Applied Biosystems BigDye® Terminator Cycle Sequencing kit v1.1). The mixture was incubated at 96°C for 1 minute, followed by 25 cycles of 96°C for 10 seconds, 50°C for 5 seconds and 60°C for 4 minutes, finally the mixture was cooled to 15°C.

Products were concentrated and purified using ethanol precipitation. To the sequencing product, 1µl of 3M sodium acetate and 25µl of 95% ethanol were added and the mixture incubated at room temperature for 15-30 minutes to precipitate the sequencing product. The samples were centrifuged at 2250g for 30 minutes to pellet the product, the 96-well plate was then inverted onto absorbent paper and centrifuged again at 180g for 1 minute. To the pelleted product, 70µl of 70% ethanol was added to wash away residual sodium acetate and the mixture centrifuged at 1650g at 4°C for 15 minutes. Again, the 96-well plate was inverted onto absorbent paper and centrifuged at 180g for 1 minute. The pellet of sequencing product was dried by heating to 95°C for 1 minute. Sequencing products were suspended in 20µl of Hi-Di™ formamide (Applied Biosystems) and heated to 95°C for 1 minute before being snap cooled on ice water immediately prior to electrophoresis. Products were separated using the Applied Biosystems PRISM 3130xl Genetic Analyzer with a 36cm length 16-capillary array and POP-7™ polymer. Sequence analysis was carried out using Sequencing Analysis 5.2 (Applied Biosystems) and Mutation Surveyor 3.2 (Soft Genetics, State College, PA).

2.18 Gene ontology and pathway analysis

Gene ontology and pathway analysis have been used in this thesis to further investigate lists of genes identified as differentially expressed in groups of interest. The function of these systems and an assessment of their usefulness is included in Chapter 4. I will briefly described the algorithms used by these analysis methods below.

2.18.1 Gene ontology analysis

Gene ontology analysis described in Chapter 4 was performed by Dr Binbin Liu and Dr Lee Hazelwood of the Bioinformatics Group in the Leeds Institute of Molecular Medicine. Cytoscape v2.8.1 [362, 363] and its plug-in, BiNGO v2.44 [364, 365] were used to search a custom built GO database with gene lists. Cytoscape provides a graphic interface for visualizing GO networks. BiNGO assesses the enrichment of a GO term in the test gene set using a hypergeometric approach and controls the false-positive rate by performing a multiple testing correction with either a Bonferroni [366] or Benjamini and Hochberg correction. The latter technique controls for the false discovery rate (FDR) which is the expected proportion of false positives among the positively identified tests [367]. For the analysis described in Chapter 4 a customized gene reference and annotation databank were built, as gene expression data were based on the 502-gene Human Cancer panel rather than a genome-wide platform. Therefore, the databank used contained GO terms associated with the 502 genes only.

2.18.2 DAVID (the database for annotation, visualisation and integrated discovery)

DAVID [368], maps a gene list to the associated biological annotation (e.g. GO terms) and then highlights the most overrepresented annotation [369-371]. This publically available software was used in Chapters 4 and 7, by myself, to identify pathways containing genes identified as differentially expressed in my analyses. The DAVID functional annotation tool uses a list of genes inputted by the user and iteratively tests the enrichment of each annotation term [369, 371, 372]. The individual annotation terms passing the enrichment P-value threshold are reported. In DAVID, these tests are performed using a Fisher's exact test (modified as EASE score using Expression Analysis Systematic Explorer (EASE) software) [371, 373]. Annotation terms can be combined into clusters which have an overall enrichment score which is the geometric mean of all the enrichment EASE scores [369]. EASE can calculate a number of probability corrections, including Bonferroni corrections and methods which correct for the FDR [373]. DAVID incorporates further network discovery algorithms by assessing relationships between enriched terms using a wide range of resources including pathway databases (KEGG (Kyoto Encyclopedia of Genes and Genomes), Biological Biochemical Image Database (BBID), Reactome Pathway, EC number, Biocarter and Panther Pathway) [371].

For the purposes of enrichment analysis described in this thesis, a background population of genes from the Human Cancer panel has been used for comparison with the annotation composition of the inputted gene lists [368].

2.18.3 Ingenuity Pathway Analysis

Ingenuity Pathway Analysis (IPA) (Ingenuity Systems, Redwood City, California, www.ingenuity.com) was used in Chapter 4 by Dr Jeremie Nsengimana and transforms gene lists into networks using the Ingenuity Pathways Knowledge Base (IPKB) [374, 375]. The IPKB contains annotations based on biological interactions and function created by modelling relationships based on literature between proteins, genes, isoforms, complexes, cells, tissues, drugs and diseases [376]. IPA users can specify cut-offs based on gene expression data, which select a subset of important focus genes. The IPA application maps each gene identifier to its corresponding gene object in the IPKB. Focus genes are then overlaid onto a global molecular network developed from information in the IPKB. Focus genes are sorted in order of interconnectedness. Genes connected with the largest number of other genes are ranked highest and this gene is labelled the seed gene. The next focus gene most connected to the seed gene is added to the growing network. This gene is identified by calculating the 'specific connectivity' metric which is a measure of how much a new gene's neighbourhood (new gene plus all genes related to the new gene) overlaps the current network. Connected genes are added until the maximum network size of 35 genes is reached. Smaller gene networks are combined to make larger networks where possible and for networks which still have less than 35 genes, additional genes are added to the periphery of the network to provide additional biological context to the focus genes. Each IPA network is assigned a significance score (p-score) derived from p-values representing the likelihood that the focus genes in the network are found by random chance. The p-value is the probability of finding one or more focus genes in a set of genes randomly selected from the global molecular network calculated using Fisher's exact test. The p-score is equal to the negative exponent of the respective significance value (p-score = $-\log_{10}(\text{p-value})$) [375-378].

2.19 Immunohistochemistry

Immunohistochemical staining of tissue sections was performed by Sarah Storr and Sabreena Safuan at the Department of Academic Oncology at the University of Nottingham on a subset of tumours described in Chapter 7. This collaboration was

designed to study associations between ulceration and tumour vascularity, blood and lymphatic vascular invasion, vessel density and presence of tumour-associated macrophages [113].

Sections of tumour were stained with the lymphatic-specific antibody D2-40, the endothelial marker, CD34, and a CD68 antibody to detect macrophages [113]. Immunohistochemistry (IHC) allows direct visualisation of specific antigens within a tissue using monoclonal antibodies [379, 380]. Following specific binding of an unlabelled primary antibody, the indirect method use a biotinylated IgG antibody against the species that the primary antibody was generated from and binds to the constant fragment (Fc) of the primary antibody. Streptavidin conjugated enzymes then bind to biotin on the secondary antibody which generate an insoluble substrate product which can be visualised [379-381].

Use of specific antibodies for lymphatic vessels increases detection rates versus H+E slides alone [382-385]. D2-40 is a monoclonal antibody against the 40-kD sialoglycoprotein, M2A, and is a specific marker for lymphatic endothelial cells [386-389]. CD34 is an endothelial marker in both lymphatic and blood vessels, but is more weakly expressed in lymphatic vessels [110, 389, 390]. It is not specific to endothelium in skin however, as CD34 is also expressed on dermal dendritic cells and perifollicular cells as well as endothelial cells in normal skin [391]. CD68 is widely used to stain for macrophages, but does have cross-reactivity with organelles in other cell types, so is not entirely macrophage specific [392-394]. Despite this, it has been used either alone or in combination with other antibodies to identify macrophages in melanoma tumours [393, 395-397].

2.19.1 Immunohistochemistry (IHC) methods

Samples used for IHC staining are described in Chapter 7. IHC staining and measurement of vessels and macrophages in consecutive tissue sections was performed at the University of Nottingham. To visualise vessels and macrophages, three consecutive tumour slides were stained with antibodies as described in Table 2-4.

Staining methods have been previously described [113, 398, 399]. Briefly, sections were deparaffinised in histolene and then rehydrated in a series of ethanol baths (100%, 90%, 70%, 50% and 30%) and finally immersed in water. For CD34 and CD68 antibodies, antigen retrieval was performed by immersing slides in 0.01mol/l sodium citrate buffer (pH6) which was heated in a microwave at 750W for 10 minutes, followed

by 400W for 10 minutes. Endogenous peroxidase activity was blocked by incubating tissue with 0.01% hydrogen peroxide in methanol for 10 minutes.

Antibody target	Target location	Manufacturer	Dilution
CD34	Endothelial cells (predominantly blood vessels)	AbD Serotec, Kidlington, UK	1:500
D2-40	Endothelial cells (lymphatic vessels)	Covance SIGNET, NJ, USA	1:100
CD68	Macrophages	Abcam, Cambridge, UK	1:100

Table 2-4: Primary antibodies used for IHC staining.

Antibody targets are presented with manufacturers details and dilutions used for IHC staining. All antibodies were diluted in blocking buffer.

To reduce non-specific binding, potential reactive sites were blocked by incubating sections with normal swine serum (Dako, Glostrup, Denmark) diluted 1:5 using Tris-buffered saline (TBS) for 10 minutes. Diluted primary antibodies (Table 2-4) were incubated with tissue for 1 hour and then a biotinylated secondary antibody (1:100 dilution in blocking buffer) was added for 30 minutes, followed by streptavidin-coupled horseradish peroxidase (1:100 dilution in blocking buffer) for 1 hour according to the manufacturer's instructions (StreptABComplex/HRP Duet, Dako, Ely, UK). In the case of CD34 and D2-40 reactions, coupled streptavidin-horseradish peroxidase reacted with 3,3' diaminobenzidine (DAB) to generate brown staining. For CD68 a permanent red substrate (Dako) was used to help distinguish macrophages from brown melanocytes. Sections were counterstained with Gill's formula haematoxylin (Vector Laboratories, Peterborough, UK), dehydrated and fixed in histolene. CD34 and D2-40 sections were mounted with Depex mounting medium (Solmedia, Romford, UK), Glycergel mounting medium (Dako) was used for CD68 stained sections. Sections of tonsil and placental tissue were used as controls, primary antibody was omitted for negative controls. The final tumour section was stained with H+E as described in section 2.3.3.

Examples of stained sections are presented in Figure 2-10.

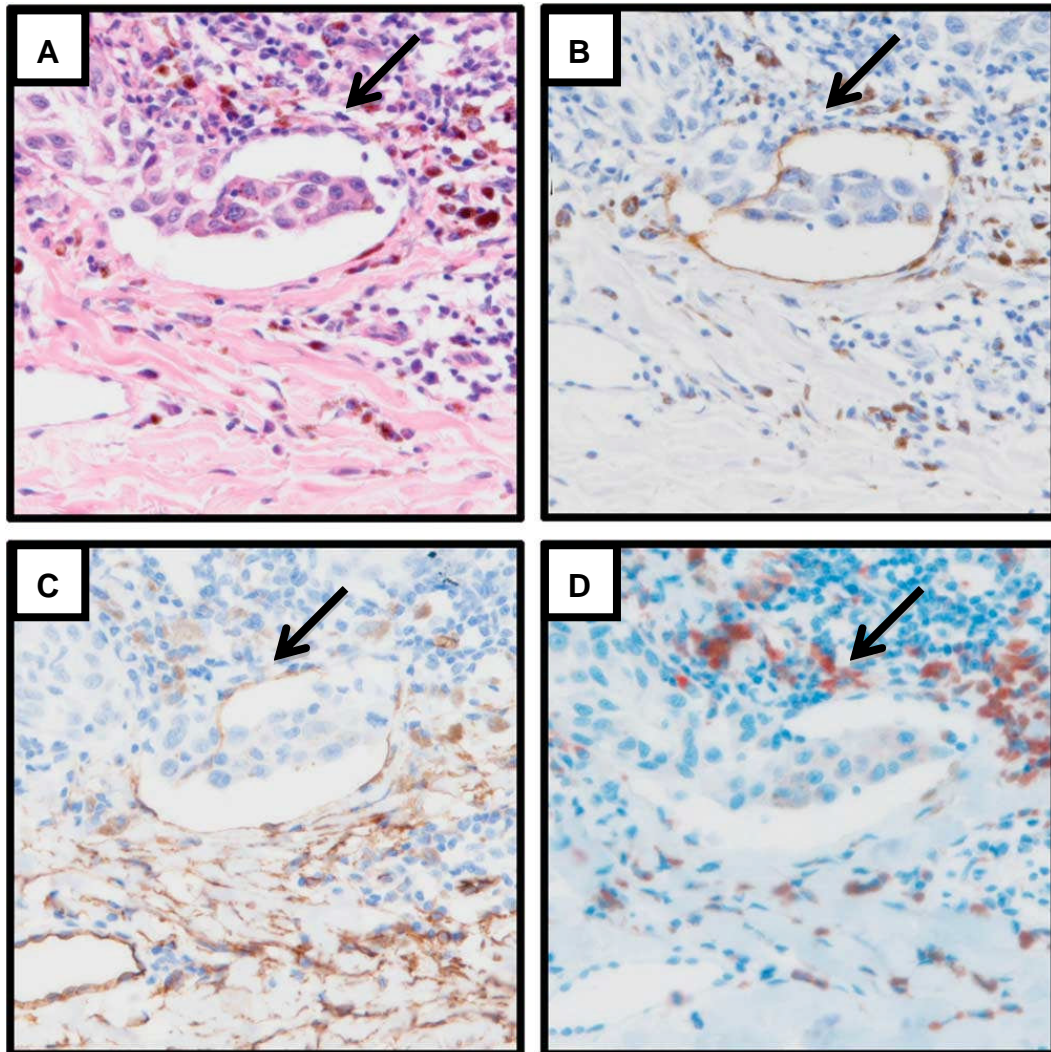


Figure 2-10: Consecutive stains of melanoma sections with haematoxylin and eosin (H+E) (A), anti-D2-40 (B), anti-CD34 (C) and anti-CD68 (D) (20x magnification).

A vessel is visible on the H+E slide (arrow) showing invasion by melanoma tumour cells. Invasion can also be seen in anti-D2-40 stained lymphatic vessels and anti-CD34-stained blood vessels. Anti-CD68 stained macrophages can be seen around the vessel invasion. Figure courtesy of Sarah Storr, University of Nottingham [113].

2.19.2 Assessment of microvessel density and macrophage count

Microvessel density and the number of macrophages were measured using the 'hotspot' Chalkley 25-point method in three areas on each section as previously described [398, 399]. To identify 'hotspots' of high blood vessel density or macrophages, sections were reviewed at 10x magnification. Areas with high vascular concentration or macrophage infiltration were viewed at 20x magnification and a 25-point Chalkley eyepiece graticule was applied and adjusted so there was maximum overlap between vessels or macrophages and the graticule points. A Chalkley count for each tumour was taken as the average of three counts. Twenty percent of the slides were reviewed by two independent assessors who were blinded to each other's scores and clinico-pathological data.

2.19.3 Assessment of lymphatic density

Lymphatic vessel density was determined by counting all positively stained lymphatic vessels across a whole tissue section as previously described [400]. Sections were divided into the intratumoural, inner two thirds of a tumour, and peritumoural areas which represents all normal tissue surrounding the tumour [400]. Stained vessels were counted across the two areas at 10x magnification, the size of each area was determined in mm² by counting the number of fields of view with each field of view having a surface area of 154mm². Lymphatic vessel density (vessels/mm²) was calculated by dividing the number of lymphatic vessels identified in an area by the total surface area. Total LVD for each section was the sum of intratumoural and peritumoural lymphatic vessel densities. In these cases, 30% of slides were examined by two independent assessors.

2.19.4 Assessment of lymphatic vessel invasion and blood vessel invasion

H+E sections were initially reviewed to determine whether a tumour was vascular invasion positive, possible or negative. Using IHC stained sections, lymphatic and blood vessel invasion was determined as presence of tumour cells within a D2-40 stained vessel or a CD34 stained vessel that was negative for D2-40, respectively. These sections were defined as vascular invasion positive. Lymphatic vessel invasion was assessed within intratumoural and peritumoural areas. Total vascular invasion was classified as positive if sections were either lymphatic or blood vessel invasion positive.

All slides were assessed by two independent assessors. In addition, any positive or probable cases were reviewed by pathologists, Professor Martin Cook or Professor Ian Ellis to confirm or refute. Following review, any 'possible' invasions, were grouped with positive cases for analysis.

2.20 Summary

This chapter presents methodology used in this thesis. It also reports an assessment of the WG-DASL HT assay with FFPE melanoma specimens. During my PhD new nucleic acid extraction and cDNA synthesis kits have been developed and assessed. Results from these newer products have been good, highlighting the importance of assessing new technologies to maximise use of precious tissue resources and improve results.

3 Gene expression profiling of formalin-fixed paraffin-embedded primary melanoma using the cDNA-mediated annealing, selection, extension and ligation assay

3.1 Aims

The main aim of this work was to identify genes which are differentially expressed in primary melanoma tumours in association with relapse or mortality and then validate these findings in an independent sample set.

Further aims were:

- To assess the utility of the cDNA-mediated annealing, selection, extension and ligation (DASL) assay to identify gene expression signatures in formalin-fixed paraffin-embedded (FFPE) primary melanoma tumours.
- To identify factors that influence performance of melanoma samples with the DASL assay.

3.2 Background

The established predictors of outcome for melanoma patients relate to the histological characteristics of the primary tumour (Breslow thickness, the presence of ulceration, mitotic rate), tumour site, sex and age [58, 91]. Histological characteristics are used to estimate prognosis as part of the AJCC staging system [58] and in various algorithms, to give a more personalized estimate [133, 401], but much of the variance in survival remains unexplained. In order to identify prognostic and predictive biomarkers, and increase the understanding of key biological pathways, molecular studies of primary melanomas are necessary.

Primary melanomas are small and as the histological characteristics conveying prognostic information are often focal within the primary tumour, pathologists are reluctant to cryopreserve tissue. Therefore, until recently genomic expression studies in primary melanoma tumours have been relatively few in number, limited in size and focusing on single genes [402, 403]. An increasing body of work has now been published using gene expression microarrays with cryopreserved melanoma tumours as presented in Chapter 1, including a number of studies conducted to REporting recommendations for tumour MARKer prognostic studies (REMARK) standards [161,

162]. In primary tumours, the only study of reasonable size was undertaken by Winnepeninckx *et al.* who used tumours from 58 patients to identify a 254-gene signature predictive of survival which included mini-chromosome maintenance genes. This signature was tested in an independent sample set in which 11 out of 17 cases were correctly classified [178]. Kauffman *et al.* used bioinformatics analysis of gene expression data from 60 samples, 58 from the Winnepeninckx study, and found that DNA repair genes were overrepresented [177]. As reviewed in the Chapter 1, a larger number of studies have been performed in metastatic tumours specimens [179, 180, 185, 186, 194], which have highlighted the importance of immune response processes and *NRAS*-regulation pathways for prognosis [188].

Whilst these studies represent major developments in the field, analysis of FFPE tumours would enable studies using large numbers of samples, including primary melanomas, with mature follow-up data. Potentially, studies of this kind would be less biased as tumours would not be selected based on whether they are deemed suitable for cryopreservation. Formalin is a fixative which preserves tissue and cellular structure by cross-linking proteins and nucleic acids [77]. Cross-links cause nucleic acid degradation during extraction procedures and addition of monomethylol groups to bases can interfere with downstream reverse transcription and amplification reactions [292]. Increasing amounts of degradation of nucleic acids have been associated with longer formalin fixation [404] and higher temperatures during paraffin embedding of samples [405]. In addition, RNA continues to degrade over time especially when stored at room temperature, compromising the quality of nucleic acids from older tissue blocks [291, 316]. Methodological studies have demonstrated that use of an overnight Proteinase K digestion step to degrade proteins cross-linked with RNA, a high temperature incubation step (50-55°C [292] or 60-70°C [315, 316]) to remove part of methylol groups and an on-column DNase digestion step to remove DNA, improves the quantity and quality of RNA extracted from FFPE tissues and performance in downstream assays [315, 316, 406]. Despite these modifications to RNA extraction protocols, RNA can be severely degraded being less than 300 base pairs in length [291]. Therefore, use of microarray technology has been limited using RNA extracted from FFPE tissue, restricting the use of this valuable tissue resource.

Illumina's DASL (cDNA mediated annealing, selection, extension and ligation) assay is specifically designed for use with degraded RNA, such as that extracted from FFPE tissue as it uses random priming in cDNA synthesis and a target sequence of only 50 nucleotides is required for probe groups to anneal [293]. Further details of the assay are included in Chapter 2. Previous studies have demonstrated that the DASL assay produces reproducible gene expression results from degraded RNA such as that

extracted from FFPE tissues [293-297]. Gene expression profiles generated from the assay correlate well with profiles derived for intact RNA extracted from frozen tissue or cell lines [293-295] and biologically useful results have been obtained from use of this technology [295, 297].

This chapter describes use of the DASL assay to investigate prognostic biomarkers in stored primary melanomas. Performance of the assay is highly dependent on the quality of RNA used and so samples go through a number of quality control procedures to assess suitability for use in the assay as described in Chapter 2. An assessment of these investigations as predictive of assay performance is included in this chapter.

A further issue with primary melanomas is melanin, which co-purifies with DNA and RNA. Melanin absorbs UV light which can lead to unreliable spectrophotometric quantification of nucleic acids [306] and more importantly, it can inhibit DNA polymerases leading to failure of downstream PCR reactions [303]. Therefore, assay performance has also been correlated with melanin content of melanoma tumours.

This chapter reports an evaluation of the DASL assay and confirmation of the significance of increased *SPP1* expression in a large study of FFPE primary melanoma tumours.

3.3 Detailed methodology

3.3.1 Patient samples and gene expression analysis

As described in Chapter 2, FFPE primary melanoma tumour blocks were identified from two study sets; the Leeds Melanoma Cohort Study henceforth referred to as the Cohort study and the Retrospective Sentinel Node Biopsy Study referred to as the SNB study. In the Cohort study, the first 254 blocks identified from participants within the cohort with tumours thicker than 0.75mm having the longest follow-up comprised the test set. In the SNB study (the validation set), the first 218 blocks identified from participants with the longest follow-up in a study designed to identify predictors of sentinel node positivity and relapse were sampled. To allow evaluation of the effect of melanin on gene expression analysis of melanoma samples, cores were graded using the melanin score. RNA was extracted using the Roche High Pure RNA Paraffin Kit and quantity and quality of RNA was determined using spectrophotometry. Further methodological details are in Chapter 2. Sample selection, melanin scoring, tissue sampling and RNA extraction were performed by Dr Caroline Conway (Cohort study), Dr Angana Mitra (SNB study) and Samira Lobo.

The Illumina DASL Human Cancer panel was used for gene expression profiling by Floor de Kort at the service provider, ServiceXS (Leiden, Netherlands) as described in Chapter 2.

3.3.2 Target validation using quantitative Real-time PCR (qRT-PCR)

SPP1 expression was identified as significantly associated with relapse and overall survival (section 3.4.4), and was therefore further investigated by qRT-PCR on samples from the Cohort study by Dr Caroline Conway. Small fragments of *SPP1* and the endogenous control gene, *GAPDH*, were amplified using Taqman® Gene Expression Assay probes (Applied Biosystems, Warrington, UK) as presented in Table 3-1.

	Gene	Exons targeted	Amplicon length	NCBI Reference Sequence	Assay Reference
<i>Gene for relative quantification</i>	<i>SPP1</i>	1/2	63bp	NM_000582.2	Hs00960942_m1
		5/6	84bp	NM_000582.2	Hs00959010_m1
<i>Endogenous control gene</i>	<i>GAPDH</i>	3	122bp	NM_002046.3	Hs99999905_m1

Table 3-1: Taqman® Gene Expression Assay probes used for qRT-PCR of *SPP1*.

Abbreviations used: NCBI, National Center for Biotechnology Information.

PCRs were performed in duplicate using cDNA previously synthesised from RNA samples sent for DASL analysis. cDNA was generated using the Invitrogen Superscript™ First-strand Synthesis System according to the manufacturers protocol as detailed in Chapter 2. cDNA was diluted 1:1 with nuclease free water and 1µl was used for each qRT-PCR assay. PCRs were performed with Gene Expression Master Mix (Applied Biosystems) in a 20µl final volume on the ABI 7900 Real-time PCR system (Applied Biosystems). Cycling conditions used were 50°C for 2 minutes, 95°C for 10 minutes and 40 cycles of 95°C for 15 seconds and 60°C for 1 minute. Automatic settings were used for baseline and threshold determination and cycle threshold (Ct) values for each target were exported to Excel for further analysis. Mean Ct values from replicate samples were calculated and ΔCt values were determined using the comparative Ct (or ΔCt) method [342], where $\Delta Ct = Ct \text{ gene of interest} - Ct \text{ endogenous control}$. ΔCt values were then converted to $2^{-\Delta Ct}$ for the calculation of fold

change between relapsers and non-relapsers where fold change = $2^{-\Delta Ct}$ relapsers \div $2^{-\Delta Ct}$ non-relapsers. A more detailed assessment of qRT-PCR methods in FFPE melanoma tumours has been undertaken in Chapter 4.

3.3.3 Statistical methodology

3.3.3.1 Quality control analysis of gene expression data

I performed the statistical analysis reported in this chapter. As reliability of the array data is critical and there are reasons to expect poorer quality data when generated from FFPE tissues I looked at age of the tumour block, degree of pigmentation of the paraffin-embedded tumour and RNA quality as determinants of the array data quality. I also report consistency between technical and biological replicates.

Previous authors have used the number of genes detected in each sample using the DASL assay (probe signal significantly greater than average signal from negative controls with $p < 0.05$) as a measure of the quality of results [294]. Use of number of detected genes may not be the best measure of result quality as discussed in Chapter 5. However, for the purposes of this assessment, the influence of age of tissue block and melanin level of the tumour on number of genes detected was investigated using Spearman's rank correlation and Kruskal-Wallis tests respectively.

Methods used to measure the quality and quantity of RNA prior to use in the DASL assay were assessed by correlating the number of genes detected in samples with the quality measures data using either Spearman's rank correlation or the Kruskal-Wallis test. Samples with less than 250 detected genes were classified as 'failed' as suggested by previous authors [294] and excluded from further analysis.

A number of RNA samples from the same extraction were analysed twice using the DASL assay (technical replicates). Biological replicates were also included which were RNA samples extracted from tissue cores sampled from adjacent parts of the same tumour. Equality and correlation between gene expression levels in replicates was assessed using paired t-tests and Pearson's correlation coefficients. Mean gene expression was used for replicate samples in further analysis.

To further monitor variation across plates and runs of the DASL assay, replicate Stratagene Universal Human Reference RNAs (Agilent Technologies, Edinburgh, UK) were assessed across DASL plates. Analysis of results from these reference RNAs is described in detail in Chapter 5.

3.3.3.2 Descriptive characteristics of the sample set

Patient factors and histological characteristics of the primary tumour were compared between the two studies using two-sample t-tests, Pearson's chi squared tests and Mann-Whitney U tests.

3.3.3.3 Identification of differentially expressed genes

Differential gene expression and survival analyses were performed using data which had been log-transformed (log2). As some of the raw gene expression levels were negative values, 1000 was added to all values prior to log-transformation. Survival analysis was performed using the Cox proportional hazards model to calculate hazard ratios and 95% confidence intervals for each gene. Significance values were ranked to identify genes most differentially expressed. Relapse-free survival (RFS) was defined as the period between diagnosis and date of first relapse at any site. The analysis was performed on the 11th February 2010 and survival data were censored on this date. Analyses were performed unadjusted and adjusted for demographic (patient gender, site of tumour and age of patient at diagnosis) and histological factors of prognostic importance in melanoma (Breslow thickness, mitotic rate of tumour and ulceration status). Analyses were also adjusted for whether the patient had undergone a sentinel node biopsy and the effect of the biopsy result (SNB status) as the use of SNB results in delay of the date of first relapse in melanoma patients as the usual site of first recurrence (nodal) is removed.

Correlations between gene expression patterns were identified using linear regression, adjusting for the study from which patients were recruited to, using the merged dataset from both studies which was generated as described in Chapter 4.

3.3.3.4 Multiple testing and adjustment of analyses

In view of the number of statistical tests in this analysis (502), a number of significant findings would be expected to occur by chance. Therefore, to correct for this issue of multiple testing, the Bonferroni method was used [366] and the significance level was set at 0.0001 for analyses identifying genes associated with survival. For survival analyses adjusted for known prognostic factors assessing the expression of a single gene in each test, the significance level for highlighting results of interest was set as 0.05. All statistical analyses were undertaken using Stata version 10 (StataCorp 2007, College Station, TX).

3.3.4 Generation of gene networks using Ingenuity software

Ingenuity Pathway Analysis was performed by Dr Jeremie Nsengimana in the Section of Epidemiology and Biostatistics. Using the combined data from the studies, fold changes and significance levels of genes differentially expressed in tumours from patients with reduced relapse-free survival time were analysed using Ingenuity Pathway Analysis software (Ingenuity Systems, Redwood City, California, www.ingenuity.com). The algorithms used by Ingenuity Pathway Analysis software are described in more detail in Chapter 2. Genes >1.2 times over- or under-expressed with significance levels <0.05 were interrogated by Ingenuity to find genes most related to each other and a network of these relationships was generated.

3.4 Results

3.4.1 RNA yields, quality control measures and performance of the DASL assay

Of the 472 tumours blocks identified from the two studies, 378 (80%) were sampled. Blocks were not sampled if there was too little residual tumour after sectioning carried out for diagnostic purposes or other research projects, or if the tumour was necrotic or too admixed with a large number of lymphocytes or stromal cells. In 17/378 (4.5%) a tissue core was taken and RNA extracted, but inadequate quantities were extracted (<20ng/µl) as measured by spectrophotometry. Overall, “adequate” amounts of RNA were therefore obtained from 361 (76%) tissue blocks.

A total of 423 RNA samples including replicate samples was sent to the service provider (ServiceXS) for DASL analysis (359 unique samples and 64 replicate samples). Six (1.4%) samples failed the assay, defined as less than 250 genes being detected. The failure rate was 2.1% in the Cohort Study and 0.9% in the SNB study. As discussed previously, age of tissue block and melanin content of tumours can have an influence on quality of RNA extracted and performance in PCR reactions. Table 3-2 summarizes the association between quality control measures, age of tissue block and melanin content of tumour and the number of genes detected in the DASL assay. Increased block age was negatively correlated with number of genes detected in the SNB study ($p=0.0002$), but not the Cohort study, which may be because the range of block age was much greater in the SNB study (SNB study: 2.23-15.16 years, Cohort study: 1.48-7.84 years). Melanin score was assessed for all tumours sampled in the SNB study, but only 102 samples in the Cohort study as the score was not recorded for

a proportion of samples. Higher melanin score was associated with fewer genes detected in the Cohort study ($p=0.04$) but not in the SNB study ($p=0.26$).

Samples were assessed with quality control measures as described in Chapter 2. RNA concentrations for all samples were measured using the ND-8000 spectrophotometer (Nanodrop, Wilmington, DE, USA) before being sent to the service provider. Samples in the Cohort study were also assessed using the Agilent 2100 Bioanalyzer using a RNA 6000 nano-chip and standard manufacturer's protocols by the service provider, however no data from this analysis was made available to us apart from electropherogram traces which when assessed subjectively as described in Chapter 2 did not correlate with number of genes detected in the DASL assay (Spearman's rho - 0.07, $p=0.37$). Twenty-seven samples from the SNB study were assessed with the Bioanalyzer. For these cases RNA concentration as determined by the Bioanalyzer and RNA integrity number (RIN) score [336] was provided for 21 samples. RIN scores are described in further detail in Chapter 2. qRT-PCR of the housekeeping gene *RPL13a*, described in further detail in Chapter 2, was undertaken for all samples but unfortunately failed for samples from the Cohort study. The quality control procedures that best predicted number of genes detected in the SNB study were RNA concentration as determined by spectrophotometry and the Bioanalyser, RIN number and Ct values determined using qRT-PCR of *RPL13a*.

Table 3-2 (following page): Associations between quality control procedures, tumour characteristics and performance with the DASL assay.

Performance with the assay was determined by the number of detected genes. Columns that present statistical association present the test performed, the test statistic and the significance value. Significant results are highlighted in bold. Abbreviations used: n, number; Ct, cycle threshold value; RIN, RNA integrity number.

	Cohort Study (188 samples)	Association between measure and number of detected genes	SNB study (235 samples)	Association between measure and number of detected genes
Number failed samples, n (%) (<250 genes)	4 (2.1)		2 (0.9)	
Number detected genes overall, mean (range)	434 (33-472)		457 (180-493)	
Age of block, years, mean (range)	4.63 (1.48-7.84)		6.26 (2.23-15.16)	
Number genes detected, mean (range):		Spearman's rho 0.11, p=0.13		Spearman's rho -0.24, p=0.0002
Block <5 years old	436 (33-468)		466 (371-491)	
Block 5-10 years old	442 (317-472)		456 (180-493)	
Block >10 years old	None		441 (376-477)	
Melanin score, n (%):	In 102 samples:	Kruskal-Wallis χ^2 8.44, p=0.04		Kruskal-Wallis χ^2 4.02, p=0.26
0	5 (4.9)		4 (1.7)	
1	30 (29.4)		58 (24.9)	
2	42 (41.2)		63 (27.0)	
3	25 (24.5)		108 (46.4)	
Nanodrop RNA concentration, ng/ μ L, mean (range)	44.6 (0-87)	Spearman's rho 0.09, p=0.23	53.7 (0.4-209.9)	Spearman's rho 0.13, p=0.05
Bioanalyser RNA concentration, ng/ μ L, mean (range)	Not assessed		In 27 samples: 24.6 (0-56)	Spearman's rho 0.59, p=0.001
Bioanalyser RIN number, median (range)	Not assessed		In 21 samples: 1.5 (1.0 -2.3)	Kruskal-Wallis χ^2 6.90, p=0.03
Ct values, mean (range)	Failed		24.3 (19.9-27.3)	Spearman's rho - 0.20, p=0.003

3.4.2 Sample replicates

Table 3-3 summarises results from replicate samples in each study. Correlation coefficients across technical replicates are good, however the mean correlation coefficient for biological replicates from the SNB study is lower. I have interpreted this as representing biological variation across tumours which has been well described and would explain differences in gene expression profiles in different tissue cores resulting from true tumour heterogeneity or variation in admixture of inflammatory or stromal cells [407].

Study	No. of replicate samples (biological replicates)	No. pairs with failed samples	Mean of correlation coefficients across technical replicates (range)	Mean of correlation coefficients across biological replicates (range)	Pairs with significantly different mean gene expression (t-test - p <0.05)
Cohort study	27 (2)	3	0.96 (0.59 - 0.99)	0.96 (only one pair without failed samples)	0
SNB study	37 (12)	1	0.95 (0.68 - 0.99)	0.88 (0.41 - 0.97)	0

Table 3-3: Comparison of technical and biological replicate samples assessed in each study.

Failed samples were classified as samples in which <250 genes were detected using the DASL assay. Pearson's correlation coefficients were calculated for each pair of replicates (failed samples were removed from this analysis) and mean gene expression was compared between the replicates using paired t-tests.

3.4.3 Descriptive statistics of samples sets

Table 3-4 presents a summary of the characteristics of the two sample sets. They are similar, the differences being that participants in the SNB study were slightly younger, had a significantly higher mitotic rate (p=0.001) and unsurprisingly had been more likely to have a sentinel node biopsy (p<0.0001) as this was the key recruitment characteristic. Patients recruited to the Cohort study had a significantly longer period of follow up than patients recruited to the SNB study (median 60.7 months and 38.4 months respectively, p<0.00001).

Variable	Cohort study	SNB study	Test statistic and significance value
Number of patients	156	198	
Age at diagnosis or at SNB, years, mean (range)	54.9 (19.9-78.5)	52.0 (14.4-88.0)	t value 1.87 p=0.06
Sex – female, n (%)	81 (51.9)	95 (48.0)	χ^2 0.54, p=0.46
Sex – male, n (%)	75 (48.1)	103 (52.0)	
Site of tumour, n (%)			
Arm	31 (19.9)	44 (22.2)	
Head-neck	24 (15.4)	17 (8.6)	χ^2 4.13, p=0.25
Leg	50 (32.0)	69 (34.9)	
Trunk	49 (31.4)	68 (34.3)	
Not recorded	2 (1.3)	0 (0.0)	
Breslow thickness, mm, median (range)	1.9 (0.9-12.0)	2.1 (0.4-19.0)	Mann-Whitney Z -0.58 p=0.56
Mitotic rate, per mm ² , n (%)			
<1	27 (17.3)	21 (10.6)	χ^2 13.62 p=0.001
1-6	76 (48.7)	91 (46.0)	
>6	34 (21.8)	85 (42.9)	
Not recorded	19 (12.2)	1 (0.5)	
Ulcerated tumours, n (%)	40 (25.6)	52 (26.3)	χ^2 0.02 p=0.90
Sentinel node biopsy status, n (%)			
No SNB performed	106 (67.9)	0 (0)	χ^2 248.78 p<0.0001
Had SNB – negative	17 (10.9)	68 (34.3)	
Had SNB – positive	5 (3.2)	130 (65.7)	
Not recorded	28 (17.9)	0 (0)	
Relapsers, n (%)	50 (32.1)	63 (31.8)	χ^2 0.02 p=0.88
Deaths, n (%)	40 (25.6)	47 (23.7)	χ^2 0.13 p=0.72
Follow-up time, months, median (range)	60.7 (5.1-105.9)	38.4 (0.03-111.7)	Mann-Whitney Z 7.38 p<0.00001

Table 3-4: Descriptive statistics of the two samples sets.

Significant results are highlighted in bold. Abbreviations used: n, number; SNB, sentinel node biopsy.

3.4.4 Genes most predictive of survival

Genes with expression levels most strongly related to RFS in the Cohort study are presented in Table 3-5. The gene most predictive of RFS was *SPP1* which codes for osteopontin, with increased expression being associated with shorter relapse-free survival time. In the Cohort study, the hazard ratio (HR) for RFS associated with doubling of *SPP1* expression was 2.64 ($p=2.74 \times 10^{-6}$). This association persisted when

the analysis was repeated adjusted for host variables known to predict relapse (age, sex, tumour site and SNB status $p=0.001$), and when adjusted additionally for Breslow thickness, mitotic rate and the presence of tumour ulceration ($p=0.003$) (Table 3-6). Fold change of expression signal was 1.55 between relapsers and non-relapsers in unadjusted analysis. Increased *SPP1* expression was also predictive of overall survival (HR 2.74 (95% CI 1.71-4.37), $p=9.57 \times 10^{-6}$) with a fold change of 1.52 between tumours from patients who had died versus tumours from alive patients. This association remained significant after adjusting for age, sex and tumour site (HR 2.73 (95% CI 1.68-4.42), $p=0.00005$) and further for Breslow thickness, mitotic rate and presence of tumour ulceration (HR 2.23 (95% CI 1.24-4.02), $p=0.008$). Expression signals from all three *SPP1* probes on the array were comparably predictive of reduced RFS (HR range 1.95-2.40, significance value range 0.00001-0.0008).

In the SNB study, increased *SPP1* expression was also associated with reduced RFS at the $p=0.006$ level in unadjusted analyses, with a similar fold change of 1.32 (Table 3-6). When corrected for age, sex, tumour site and SNB status, the significance of the association was $p=0.07$, but when the analysis was adjusted further for histological factors the influence on relapse-free survival was lost. Increased *SPP1* expression furthermore was associated with poorer OS in the SNB study (HR 1.64 (95% CI 1.08-2.50), $p=0.02$) in unadjusted analysis. The fold change between survivors and non-survivors was 1.26. *SPP1* remained associated with OS after adjusting for age, sex and tumour site (HR 1.72 (95% CI 1.11-2.67), $p=0.02$), but is no longer associated with overall survival once the analysis is adjusted for the tumour Breslow thickness, mitotic rate or ulceration status (HR 1.26 (95% CI 0.79-1.99), $p=0.33$).

3.4.5 Validation of *SPP1* expression using qRT-PCR

qRT-PCR with probes to exons 1/2 and 5/6 showed increased expression of *SPP1* with fold changes of 1.74 and 1.67 respectively in patients who relapsed versus those that did not relapse in the Cohort study (compared with a fold change of 1.55 in the DASL analysis).

Gene	Expression fold difference between relapsers and non-relapsers	Hazard ratio	95% confidence interval	Significance value
<i>SPP1</i>	1.55	2.64	1.72-4.03	2.74 x 10 ⁻⁶
<i>DSP</i>	0.63	0.59	0.47-0.74	0.00002
<i>RAD54B</i>	1.33	5.89	2.48-13.97	0.00003
<i>GRB7</i>	0.64	0.51	0.38-0.70	0.00004
<i>ITGB4</i>	0.74	0.36	0.22-0.58	0.00005
<i>ING1</i>	1.14	11.34	3.30-38.95	0.00006
<i>HLF</i>	0.72	0.27	0.13-0.54	0.0001
<i>PTPRF</i>	0.76	0.41	0.27-0.64	0.0002
<i>FGFR2</i>	0.67	0.42	0.25-0.71	0.0005
<i>EGFR</i>	0.74	0.39	0.23-0.66	0.0005
<i>RECQL</i>	1.17	5.87	2.13-16.15	0.0005
<i>PML</i>	0.94	0.04	0.005-0.27	0.0009
<i>FGFR3</i>	0.73	0.53	0.36-0.76	0.0009
<i>CDKN2B</i>	0.79	0.43	0.27-0.69	0.0009
<i>HMMR</i>	1.31	2.79	1.50-5.19	0.001
<i>EPHA1</i>	0.74	0.35	0.19-0.67	0.001
<i>FHIT</i>	1.23	3.06	1.53-6.14	0.001
<i>DAB2</i>	1.08	11.88	2.55-55.42	0.001
<i>AR</i>	0.68	0.35	0.18-0.68	0.001
<i>TGFB1</i>	0.76	0.29	0.13-0.65	0.002

Table 3-5: Top 20 genes with expression associated with relapse-free survival from the Cohort study (unadjusted analysis).

Hazard ratios for reduced RFS are calculated for doubling of gene expression value. P-values are from the proportional hazards model.

	Cohort study unadjusted	Cohort study adjusted for age, sex, site of tumour and SNB status	Cohort study adjusted additionally for histological measures	SNB study unadjusted	SNB study adjusted for age, sex, site of tumour and SNB status	SNB study adjusted additionally for histological measures
Mean signal (SD) relapsers	5172 (2587)	4980 (2567)	4946 (2280)	5812 (2752)	4240 (2623)	3982 (2415)
Mean signal (SD) non-relapsers	3346 (2156)	3516 (2184)	3845 (1999)	4411 (2818)	3334 (2642)	3480 (2439)
Fold change	1.55	1.42	1.29	1.32	1.27	1.14
Hazard ratio (95% CI)	2.64 (1.72-4.03)	2.19 (1.40-3.41)	2.49 (1.37-4.54)	1.60 (1.13-2.27)	1.40 (0.97-2.03)	1.11 (0.75-1.70)
Significance value	2.74 x 10 ⁻⁶	0.001	0.003	0.006	0.07	0.55

Table 3-6: The association of *SPP1* expression with relapse-free survival in the Cohort and SNB studies.

The unadjusted analysis for the Cohort study is presented in column 1. The association was adjusted for sex, patient age, tumour site and SNB status in column 2 (mean signal values are presented for a 45 year old female with a tumour on her leg who has not had a sentinel node biopsy). In column 3, further adjustment is made for known histological predictors of outcome: Breslow thickness, mitotic rate and ulceration (mean signal values are presented for a 45 year old female patient with a non-ulcerated tumour on her leg which has a Breslow thickness of 2.5mm, a mitotic rate of 1-6/mm² and has not had a sentinel node biopsy). SNB study analyses are similarly presented, however mean signal values are presented for a patient who did receive a sentinel node biopsy with a negative result (as all patients in this study had received a sentinel node biopsy). Abbreviations used: SD, standard deviation; CI, confidence interval; SNB, sentinel node biopsy.

3.4.6 Co-expression of genes with *SPP1*

The following analyses were performed by Dr Jeremie Nsengimana in the Section of Epidemiology and Biostatistics. The expression of genes most closely correlated with *SPP1* expression was studied in the pooled data set for both studies (analysis adjusted for study) in order to better understand the biological pathways involved. Results are presented in Table 3-7. Thirty-two genes are listed with expression significantly correlated (either positively or negatively) with that of *SPP1* at the 1.0×10^{-5} significance level or less. These results are further related to relapse status. Genes up-regulated with *SPP1* and associated with reduced RFS were *BIRC5*, *IL-8*, *TK1*, *HMMR*, *TOP2A*, *CCNA2*, *CDC2*, *RAD51*, *NQO1*, *PTPRH* and *MAPK10*. I also present a gene network for *SPP1* derived using Ingenuity Pathway Analysis (Table 3-8 and Figure 3-1). The literature-derived Ingenuity knowledge base identified *SPP1* as involved in cell adhesion, cell proliferation and cell migration. The network demonstrates that *SPP1* is the terminal component of many pathways and therefore over-expression of *SPP1* may reflect combined activity in many of these pathways.

Gene	Correlation and p value for pooled data set	Fold change	P-value for RFS	Correlation and p value for the Cohort study	Correlation and p value for the SNB study
<i>PBX1</i>	-0.34 (3.1 x 10 ⁻¹¹)	0.88	0.02	-0.36 (2.9 x 10 ⁻⁶)	-0.32 (5.5 x 10 ⁻⁶)
<i>BIRC5</i>	0.33 (2.0 x 10 ⁻¹⁰)	1.21	0.008	0.40 (2.7 x 10 ⁻⁷)	0.25 (0.0004)
<i>HLF</i>	-0.32 (5.5 x 10 ⁻¹⁰)	0.72	0.0001	-0.35 (7.3 x 10 ⁻⁶)	-0.28 (0.00007)
<i>IL8</i>	0.31 (1.4 x 10 ⁻⁹)	1.34	0.03	0.41 (9.7 x 10 ⁻⁸)	0.22 (0.003)
<i>HMMR</i>	0.30 (5.8 x 10 ⁻⁹)	1.31	0.001	0.33 (0.00003)	0.27 (0.00009)
<i>TOP2A</i>	0.29 (1.7 x 10 ⁻⁸)	1.13	0.007	0.30 (0.0001)	0.28 (0.00007)
<i>TK1</i>	0.29 (2.0 x 10 ⁻⁸)	1.13	0.01	0.28 (0.0004)	0.30 (0.00002)
<i>CTSL</i>	0.29 (2.8 x 10 ⁻⁸)	1.08	0.004	0.34 (0.00001)	0.24 (0.0006)
<i>CCNA2</i>	0.28 (5.6 x 10 ⁻⁸)	1.19	0.01	0.33 (0.00003)	0.24 (0.0006)
<i>BCL6</i>	-0.28 (8.3 x 10 ⁻⁸)	0.93	0.02	-0.33 (0.00003)	-0.24 (0.0007)
<i>CDC2</i>	0.27 (2.2 x 10 ⁻⁷)	1.17	0.03	0.31 (0.00008)	0.24 (0.0008)
<i>RAD51</i>	0.27 (3.3 x 10 ⁻⁷)	1.25	0.004	0.29 (0.0002)	0.23 (0.001)
<i>ERCC5</i>	-0.26 (5.1 x 10 ⁻⁷)	0.97	0.13	-0.17 (0.03)	-0.31 (9.2 x 10 ⁻⁶)
<i>NQO1</i>	0.26 (5.8 x 10 ⁻⁷)	1.12	0.09	0.28 (0.0005)	0.26 (0.0002)
<i>CBFA2T1</i>	-0.26 (7.6 x 10 ⁻⁷)	0.95	0.53	-0.28 (0.0003)	-0.24 (0.0007)
<i>MMP1</i>	0.26 (1.1 x 10 ⁻⁶)	1.07	0.45	0.44 (1.2 x 10 ⁻⁸)	0.13 (0.06)
<i>PTPRH</i>	0.26 (1.1 x 10 ⁻⁶)	1.15	0.21	0.27 (0.0006)	0.24 (0.0006)
<i>FGFR2</i>	-0.25 (1.2 x 10 ⁻⁶)	0.67	0.0005	-0.33 (0.00002)	-0.17 (0.02)
<i>EGFR</i>	-0.25 (1.2 x 10 ⁻⁶)	0.74	0.0005	-0.27 (0.0007)	-0.23 (0.0009)
<i>TIMP1</i>	0.25 (1.5 x 10 ⁻⁶)	1.03	0.24	0.18 (0.02)	0.29 (0.00003)
<i>GAS1</i>	-0.25 (1.6 x 10 ⁻⁶)	0.93	0.03	-0.27 (0.0006)	-0.23 (0.001)
<i>FLT3</i>	-0.25 (1.8 x 10 ⁻⁶)	0.97	0.57	-0.24 (0.003)	-0.26 (0.0002)
<i>RBL2</i>	-0.25 (2.1 x 10 ⁻⁶)	1.00	0.59	-0.27 (0.0007)	-0.25 (0.0004)
<i>ETS2</i>	-0.25 (2.5 x 10 ⁻⁶)	0.87	0.003	-0.27 (0.0006)	-0.20 (0.005)
<i>NUMA1</i>	-0.25 (2.9 x 10 ⁻⁶)	0.97	0.17	-0.31 (0.00009)	-0.18 (0.01)
<i>EPHA1</i>	-0.24 (4.3 x 10 ⁻⁶)	0.74	0.001	-0.23 (0.003)	-0.21 (0.002)
<i>MAP3K8</i>	-0.24 (4.7 x 10 ⁻⁶)	0.95	0.23	-0.30 (0.0002)	-0.20 (0.005)
<i>VEGF</i>	0.24 (5.0 x 10 ⁻⁶)	1.02	0.73	0.31 (0.0001)	0.20 (0.004)
<i>CCND3</i>	-0.24 (7.5 x 10 ⁻⁶)	0.96	0.29	-0.27 (0.0006)	-0.21 (0.003)
<i>AR</i>	-0.23 (9.4 x 10 ⁻⁶)	0.68	0.001	-0.43 (2.7 x 10 ⁻⁸)	-0.15 (0.04)
<i>FGFR3</i>	-0.23 (0.00001)	0.73	0.0009	-0.24 (0.003)	-0.20 (0.006)
<i>MAPK10</i>	0.23 (0.00001)	1.48	0.005	0.19 (0.02)	0.29 (0.00003)

Table 3-7: Gene expression correlations for *SPP1*.

Analysis was undertaken in merged dataset from the two studies and adjusted for study. Fold differences in gene expression between relapsers and non-relapsers and significance values (from the proportional hazards model) for association with RFS are also presented. Abbreviations used: RFS, relapse-free survival.

Gene	Correlation and p value for pooled data set	Fold difference gene expression between relapsers and non-relapsers	Significance level for RFS	Correlation and p value for the Cohort study	Correlation and p value for the SNB study
<i>IL8</i>	0.31 (1.4 x 10 ⁻⁹)	1.26	0.04	0.41 (9.7 x 10 ⁻⁸)	0.22 (0.003)
<i>CDC25C</i>	0.21 (0.00009)	1.28	0.005	0.18 (0.03)	0.17 (0.02)
<i>TERT</i>	0.13 (0.02)	1.40	0.0005	0.19 (0.02)	0.09 (0.23)
<i>RARB</i>	0.11 (0.04)	1.12	0.80	0.07 (0.35)	0.09 (0.20)
<i>IL3</i>	0.06 (0.25)	1.39	0.009	-0.06 (0.42)	0.15 (0.04)
<i>IL6</i>	0.05 (0.37)	1.27	0.46	0.09 (0.26)	-0.01 (0.84)
<i>E2F5</i>	0.06 (0.25)	1.26	0.004	0.05 (0.50)	0.02 (0.77)
<i>MCF2</i>	0.02 (0.70)	1.45	0.03	-0.01 (0.86)	-0.02 (0.79)
<i>CDKN2B</i>	-0.00 (0.93)	0.86	0.004	-0.10 (0.21)	0.05 (0.52)

Table 3-8: Correlations and differences in gene expression for genes identified in the Ingenuity network as being linked to *SPP1*.

Fold differences in gene expression between relapsers and non-relapsers and significance values (from the proportional hazards model) for association with RFS are also presented. Abbreviations used: RFS, relapse-free survival.

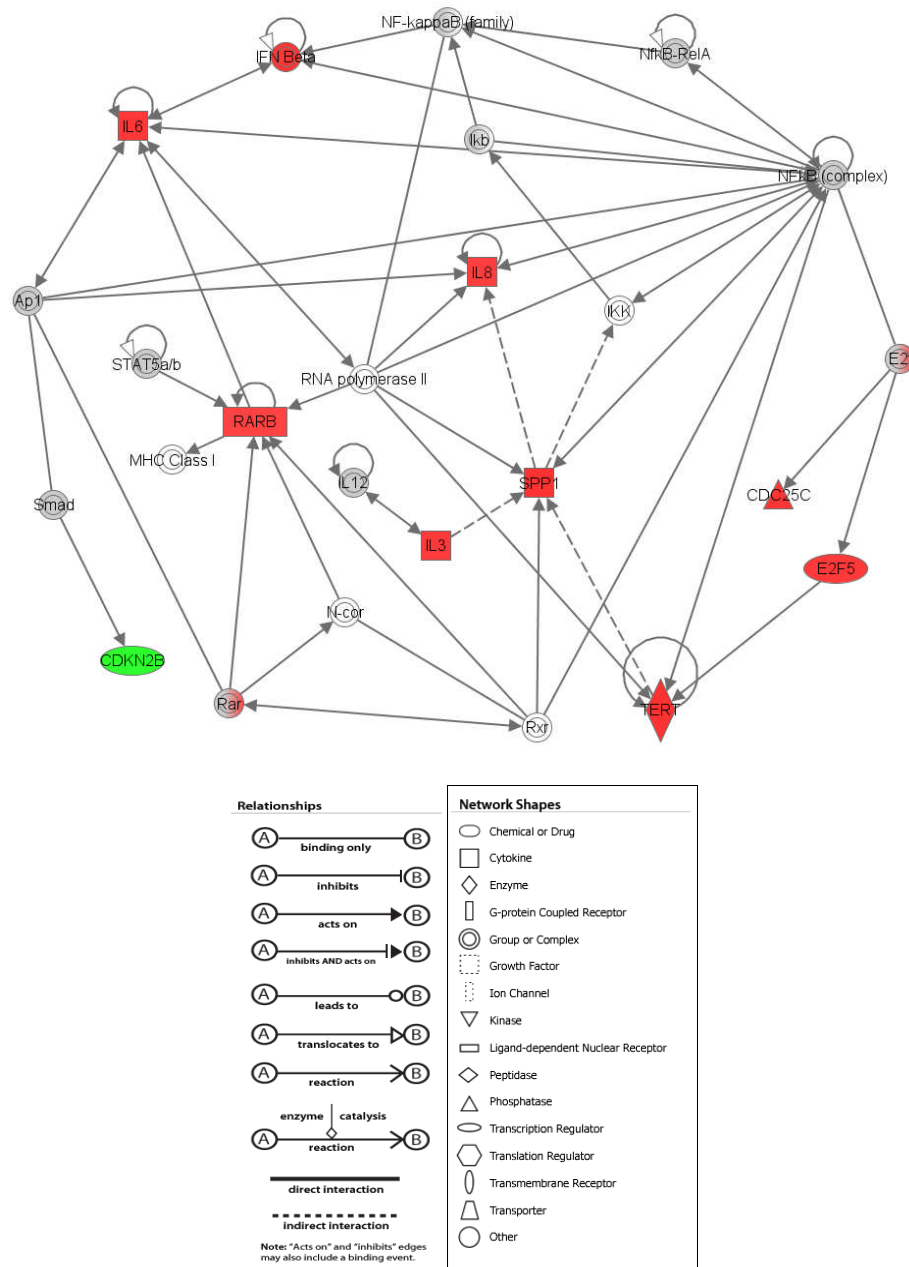


Figure 3-1: Gene network involving *SPP1* from Ingenuity Pathway Analysis in pooled data (showing only direct interactions except those involving *SPP1*).

Molecules are represented as nodes and the biological relationship between nodes is represented as a line (edge). Each edge is supported by at least one reference from the literature, from a textbook, or from canonical information stored in the Ingenuity Knowledge Base. The intensity of the node colour indicates the degree of up- (red) or down- (green) regulation.

3.5 Discussion

3.5.1 Use of the Illumina DASL assay with FFPE melanoma tissue

Gene expression studies in melanoma have hitherto been few in number and small in size. This is largely because platforms required good quality RNA which is rarely available for melanoma where primaries are very small and therefore pathologists are reluctant to cryopreserve tumours. This chapter describes my methodological assessments of a platform designed to allow gene expression from FFPE tissue thereby potentially giving access to large-scale sample sets with mature follow up data. I have also described the key findings of the study which identified up regulation of *SPP1* as poor prognostic biomarker.

As presented in Chapter 1 there have been a number of publications using cDNA microarray technology in cryopreserved tumours [177-180, 185, 194]. Many of these studies have been performed in metastatic samples from patients with advanced disease because of limited banks of cryopreserved primary tumours, therefore gene expression data has only been generated from a highly selected proportion of melanoma samples. There has been limited work identifying gene expression profiles with independent prognostic value in primary tumours [177, 178]. This study was designed to fill that gap and was started before many of the more recent studies using cDNA microarrays with cryopreserved tissues were published [187].

Concerns about the use of fixed tumours derive from the degradation of RNA. Increasingly however it has been suggested that technical modification of platforms, such as the Illumina DASL assay, can allow profiling of gene expression and micro-RNAs [408-411]. In this chapter, I report the generation of expression data from 74% of consecutive formalin-fixed melanomas, suggesting that future studies designed to identify predictive or prognostic biomarkers for melanoma would generate results from approximately 75% of samples depending on the age of the blocks, and the proportion that were deeply pigmented.

The Illumina DASL assay was originally described in 2004 [323]. The original assay permitted 1536 oligonucleotide pairs to be multiplexed in a single reaction, using a significantly smaller amount of template RNA than required for older cDNA microarray assays. An additional advantage was that the assay was suitable for use with degraded RNA because of short target gene sequences and random priming during cDNA generation [293, 323, 412]. This platform was developed into a 502-gene Human Cancer Panel targeting genes using three probes, using the Sentrix Array Matrix to allow processing of 96 arrays in one experiment [296, 413]. The assay has been further developed to combine the PCR and labelling steps from the DASL assay with

the whole-genome probe set of Illumina's Direct Hybridization Assay to allow profiling of over 29,000 transcripts using the HumanHT-12 Expression Beadchip (whole-genome DASL HT assay, further described in Chapter 2) [326, 414]. This chapter describes use of the 502-gene Human Cancer Panel, in work carried out to assess factors that may influence performance with the assay, such as age of tissue samples and melanin content of samples.

RNA is known to degrade over time especially when paraffin blocks are stored at room temperature [291, 316]. Melanin can lead to unreliable spectrophotometric quantification of nucleic acids [306] and can inhibit DNA polymerases in downstream PCR reactions [303]. In this study, gene expression data were derived from 98.6% of RNA samples extracted from FFPE melanoma tissue. Using the number of detected genes with the DASL assay as a quality control measure, increased block age (SNB study) and higher melanin score (Cohort study) were indeed negatively correlated with number of genes detected. Overall however the DASL platform performed well and age of block was not an issue, probably as 'failed' samples in this sample set (<250 genes detected) were less than 10 years old age. This is consistent with previous findings that RNA becomes increasingly degraded with storage time of tumour blocks as demonstrated by higher Ct values generated using qRT-PCR [293], but this does not appear to severely compromise the performance with the assay as one study has reported successful gene expression profiling using tumour blocks stored for over 24 years [295]. A number of 'failed' samples had high melanin scores in this analysis. To avoid melanin contamination, we could avoid sampling heavily pigmented tumours. In this study however, 24.5% of tumours from the Cohort study and 46.4% of tumours from the SNB study had a melanin score of 3, so being densely pigmented tumour. Exclusion of these samples would greatly reduce the number of tumours assessed and would seriously bias tumour sampling for the study. There are increasing data suggesting that pigmented tumours behave differently in terms of progression and even response to chemotherapy [304, 305, 415], therefore exclusion of these samples would compromise the quality of results. Melanin and DNA polymerase preferentially form a complex with decreased DNA polymerase activity [303]. Inhibition can be reduced by diluting these complexes or adding other proteins, such as bovine serum albumin which scavenge and inactivate inhibitors of polymerase [303, 416, 417]. As concentrations of eluted RNA are low from tissue cores, dilution is not an option, however addition of bovine serum albumin to eluted RNA may improve performance with the DASL assay and this will be tested in future experiments.

Prior to commencement of gene expression studies using DASL, in order to avoid use of RNA of insufficient quality, a number of quality control procedures were assessed to

identify measures that would predict sample performance with the assay. The measures that best predicted performance of the SNB study samples were RNA concentration as determined by the ND-8000 spectrophotometer, data generated using the Bioanalyser, (the Bioanalyser RIN number and RNA concentration) and Ct values generated by qRT-PCR of *RPL13a*. Unfortunately, spectrophotometry RNA concentration did not predict sample performance in the Cohort study and limited quality control assessment did not allow confirmation of Bioanalyser findings in the Cohort sample set. Many authors have suggested criteria that predict assay performance based on spectrophotometry, Bioanalyser results and qRT-PCR of *RPL13a* as discussed further in Chapter 2 [293, 294, 296, 297]. Illumina recommend these quality control measures are performed prior to using an RNA sample in the assay, however in this analysis the majority of samples with an RNA concentration over 20ng/µl as determined by spectrophotometry performed successfully with the assay irrespective of other quality control results. My conclusion was therefore that use of precious sample for quality control measures other than RNA concentration did not appear worthwhile based on these analyses.

A number of technical and biological replicate samples were assessed using the assay. Generally there was good correlation between gene expression for sample replicates as has been previously reported, with higher correlation coefficients for technical replicates than biological replicates. This was expected as biological replicate samples were derived from two extractions from different tissue cores from different parts of the tumour and so heterogeneity of the tumour would account for gene expression differences [407]. Good correlation between technical replicate samples demonstrates that the DASL assay provides reproducible results in FFPE melanoma tissue as previously demonstrated for other tumour types [293-297]. This chapter does not describe extensive comparisons between results from frozen or fresh and formalin fixed tumours as previous studies have addressed this in many tissues including melanoma [187, 293-295]. Both of these observations demonstrate that the DASL assay can be used to generate reproducible gene expression data from FFPE melanoma tissue.

The technical limitations of this study are related to the presence of a limited number of genes on the DASL Cancer Panel, and to sampling of tumours using tissue microarray (TMA) cores. Using a TMA core does not allow confirmation of the tumour content throughout the core and therefore there is potentially greater contamination with normal cells than in laser microdissected samples. Furthermore, by using this technique we were unable to sample very small tumours and so there is a bias towards sampling of larger tumours. The use of this method however, has allowed a far greater range of

tumours to be examined than in previous research based upon cryopreserved tumours. Using a TMA core results in extraction of both DNA and RNA yet preserves the architecture of the block for the clinical service which we viewed as crucial in this research programme. The use of microdissection would address some of these concerns but would be very much more time consuming for large-scale studies.

The work described in this chapter remains the largest assessment of gene expression in primary melanomas where a marker with independent prognostic value has been validated in an independent sample set of FFPE cutaneous primary melanoma tumours. It has demonstrated that gene expression studies using FFPE tumours are possible and a recent study has expanded on this work assessing expression in 223 FFPE primary melanoma tumours using the whole-genome DASL assay to assess whether expression signatures associated with outcome in metastatic tumours are also associated with survival in primary tumours [335]. The authors found that this was the case, with “high-grade” tumours, associated with poorer survival, expressing a proliferative/pigmentation signature and “low-grade” tumours with a high-immune/normal-like gene expression profile [335]. These findings were validated in two publically available gene expression datasets [178, 179, 335].

3.5.2 Identification of *SPP1* as a prognostic biomarker in primary melanomas

Fortunately, melanoma has a good prognosis in the majority of patients, but a proportion of patients with low risk disease go onto relapse with advanced disease being extremely difficult to treat. Therefore, identification of new prognostic biomarkers would assist in identification of patients likely to benefit from more aggressive treatment and allow clinicians to provide better prognostic information.

SPP1 was identified as the gene with increased expression most strongly associated with reduced RFS and overall survival. The validity of this finding was tested by comparison of test and validation sample sets. qRT-PCR detected similar fold changes associated with relapse in the test set. *SPP1* expression continued to be an independent predictor of relapse in the test set when analysis was adjusted for patient factors and histological factors of known prognostic value in melanoma. In the validation set, *SPP1* was less significantly associated with RFS and overall survival in unadjusted analyses ($p=0.006$ and $p=0.02$, respectively), however over-expression was associated with increased risk of relapse and death as in the test set. We did not go on to confirm the findings using immunohistochemistry because a large study

recently reported that osteopontin staining predicts sentinel node positivity and relapse in melanoma [163].

Osteopontin is a glycoposphoprotein cytokine with pleiotropic effects. There are two forms, secreted and intracellular, and post-translational modifications explain the large number of actions associated with this protein [418]. In normal tissues, osteopontin plays a role in inflammation, immune regulation, vascular and bone remodelling and wound repair [418]. In tumour cells, it has a role in cell adhesion, chemotaxis, prevention of apoptosis, invasion, migration and anchorage-independent growth [419, 420]. Osteopontin has a key role in the regulation of cell signalling which controls neoplastic and malignant transformation and has been identified as a possible drug target [421]. It is known to modulate several signalling pathways such as growth factor and receptor pathways via interactions with cell surface receptors such as CD44 and integrins [422, 423]. Osteopontin regulates $\alpha v\beta 3$ integrin mediated P13K/Akt/NF κ B dependent urokinase plasminogen activator and metalloproteinase expression, which is associated with tumour cell invasiveness [422, 424, 425]. This relationship between osteopontin and the NF κ B complex is pictured on the Ingenuity network (Figure 3-1). There is *in vitro* evidence that melanoma cells that secrete osteopontin are more aggressive [419, 426]. Transfection of KZ-28 melanoma cells with osteopontin siRNA leads to reduced cell proliferation, whereas stimulation of B16 melanoma cells with osteopontin from human milk enhances growth [424].

Osteopontin also increases epidermal growth factor receptor activation [427] and is thought to provide the molecular link between degradation of the extra-cellular matrix, tumour progression and vascularization [427]. In the data analysed in this chapter, there was commensurate increased expression of genes involved in the interaction between tumour cells, the extra-cellular matrix and angiogenesis such as *MMP1*, *IL8* and *VEGF*. In relation to the role of osteopontin in inhibition of apoptosis, increased expression of *SPP1* correlated with increased expression of *BIRC5* (survivin, $p=2.0 \times 10^{-10}$), which was also over-expressed in tumours from patients with poorer RFS. Survivin is recognized as a mediator of resistance to apoptosis, increased cell proliferation and invasiveness in melanoma [428, 429].

As presented in Figure 3-1, osteopontin is downstream of a number of pathways and therefore expression is influenced by a number of signalling cascades [430].

Osteopontin expression is regulated by the protein tyrosine kinase, Src, Wnt and T-cell factor 4 signalling, steroid hormones and receptors, such as oestrogen receptors and the vitamin D receptor, growth factors, for example platelet-derived growth factor and epidermal growth factor, p53, BRCA1, Ets and activator protein-1 (AP-1) transcription

factors [430-435]. A proportion of melanomas have *NRAS* mutations [436] and in these, *SPP1* transcription may be increased by a RAS-activated enhancer [437].

In the current analysis, increased *SPP1* expression was associated with increased expression of genes involved in cell cycling (*CCNA2*, *CDC2*); DNA replication and repair (*TOP2A*, *RAD51*); cell signalling (*PTPRH*, *MAPK10*); cell division and proliferation (*BIRC5*, *TK1*), observations that would be consistent with the known biological functions of osteopontin. *HMMR* expression was also positively correlated and is associated with cell motility and the cell cycle and expression levels have been shown to increase with melanoma progression [438]. Increased *SPP1* expression was associated with reduced expression of the tumour suppressor gene *GAS1*, which was also under-expressed in tumours from patients who relapsed. *GAS1* has been identified as a possible melanoma metastasis suppressor gene using a genome wide 'short hairpin' RNAi (shRNAi) screen, a finding which supports the observations in this dataset [439, 440].

Increased expression of osteopontin has been demonstrated in a number of different cancers and in some, secreted blood levels have prognostic value [422, 441, 442]. Osteopontin expression in plasma may also have prognostic utility in melanoma as osteopontin has been proposed as a marker of metastatic disease [443, 444].

The association between *SPP1* expression in human tumours and melanoma progression at both the transcriptomic and proteomic level has been observed previously. In a study using microarray analysis to assess 19,740 loci, *SPP1* was one of the most over-expressed genes in 6 cryopreserved primary melanomas in comparison with 9 benign naevi [182]. In a further study assessing expression of 14,000 genes, *SPP1* expression was found to be significantly higher in 4 cryopreserved metastatic melanomas versus 4 naevi [192]. This over-expression was confirmed in a further sample set using immunohistochemistry, where osteopontin expression was greater in primary and metastatic melanomas versus normal naevi, dysplastic naevi or melanoma *in situ* [192]. However, in this study there was no correlation between protein expression and Breslow thickness or patient survival, and there were also no significant differences in staining between primary or metastatic lesions [192]. A more recent study using 22,215 probe sets, found significantly higher levels of *SPP1* expression in 22 cryopreserved metastatic specimens in comparison with 19 primary tumours [176]. This was quickly followed by a large immunohistochemical study of 345 patients, in which increased osteopontin expression was associated with reduced relapse-free and overall survival and increased probability of sentinel node positivity [163]. Increased expression was also associated with greater tumour thickness, higher invasive (Clark) level and higher mitotic rate

[163]. Osteopontin protein expression has been incorporated into a multimarker assay including two further markers not present on the DASL Cancer panel (NCOA3 and RGS1), this assay was the most significant factor predicting disease specific survival in this study and this finding was validated in an independent cohort [161, 172].

The relationship between *SPP1* gene expression levels and sentinel node biopsy positivity has been further investigated in data from the SNB study described in this chapter. In this dataset, *SPP1* expression was the best predictor of SNB positivity, remaining significant in multivariate analyses adjusting for prognostic clinicopathological characteristics [445]. Given the role of osteopontin in degradation of extracellular matrix, cellular adhesion, invasion and tumour growth [419] increased expression of *SPP1* is likely to enhance propensity to lymphatic metastases, for example to sentinel lymph nodes, as has been noted in animal models of breast cancer and breast cancer tumours [446].

In summary, the work I have reported in this chapter provides strong corroborative evidence for *SPP1* expression as a prognostic biomarker in melanoma. The utility of pathway analysis in relation to *SPP1* expression has been limited, however it has provided a list of genes in the dataset with altered expression with evidence of association to *SPP1* based on the literature. It has also produced a network diagram which assists in understanding the relationship between *SPP1* and other genes. Use of pathway analysis is explored further for groups of genes in Chapter 4. This study is the largest in primary melanomas to date which identifies a biologically relevant biomarker validated in an independent test set. It also demonstrates that FFPE tissue can be used to identify prognostic markers in melanoma enabling further use of this invaluable tissue resource.

4 Patterns of DNA repair gene expression in primary melanoma tumours

4.1 Aims

The main aim of this work was to identify genes which are differentially expressed in primary melanoma tumours in relation to relapse in a large sample set generated by merging data from two smaller studies.

Additional aims were to:

- Assess use of gene ontology (GO) and pathway analysis with microarray gene expression data.
- Assess whether genes associated with survival were also differentially expressed in tumours with different histological features associated with a poor prognosis (increased Breslow thickness and higher mitotic rate).
- Develop a technique for validating cDNA-mediated annealing, selection, extension and ligation (DASL) assay findings using quantitative Real-time PCR (qRT-PCR) in formalin-fixed paraffin-embedded (FFPE) melanoma tumour tissue.

4.2 Background

A biomarker is a measurable factor that can be used to indicate a biological process such as the presence of a disease [155]. Prognostic biomarkers offer information about outcome from a disease, and a number of prognostic biomarkers already exist for melanoma, such as tumour Breslow thickness, mitotic rate, ulceration or nodal involvement [58]. Additional biomarkers may help further refine prognostic information. As reviewed in the introduction, a number of candidate prognostic biomarkers have been assessed in melanoma tumours using approaches such as immunohistochemistry and qRT-PCR. Use of microarray technology has greatly increased the number of genes assessed as potential prognostic biomarkers, and this chapter presents gene expression results from microarray analysis for a large number of FFPE primary melanoma tumours in relation to survival and prognostic tumour histological features. Generating gene expression data of this sort has led me to investigate methods for analysis of this data, for example, use of pathway software. I

also sought to confirm our findings using a different gene expression platform (qRT-PCR), which has led to an assessment of the use of this technology in FFPE melanoma samples as presented in this chapter.

Researchers have previously used cDNA microarray platforms to identify single genes and groups of genes with expression patterns associated with relapse and survival [161, 178, 180, 185]. Identification of differentially expressed genes can be performed in a 'supervised' fashion where characteristics of a sample or patient are known. Differences in gene expression can be based on simple identification of fold changes between two distinct groups, for example relapsers and non-relapsers or by using statistical tests, such as t-tests or modified tests, such as significance analysis of microarrays (SAMic) [447-450]. In Chapter 3 we have used survival analysis to generate a list of genes associated with relapse and so identified *SPP1* expression as an independent predictor of survival [187]. However, these techniques merely generate lists of genes, which require interrogation to identify the biological implications of genes differentially expressed. Identification of groups of genes with related biological functions can be more useful, especially in cases where hundreds to thousands of genes are differentially expressed [451]. Comparison of a gene list with Gene Ontology (GO) terms can be used to understand the function of genes that are over-represented [451]. GO terms were developed to describe the roles of genes in terms of associated biological processes, cellular components and molecular functions [451, 452]. Biological process terms refer to a series of events using one or more combinations of molecular functions; molecular function terms describe activities of genes, such as catalytic or binding activities, and cellular component terms describe the location of a gene product or a subcomponent of a larger cellular assembly [452]. To extend deeper into the biology of gene lists, options are to analyse at the molecular level using promoter and regulatory network analysis or use knowledge from the literature to perform pathway analysis [451]. Pathway analysis assesses interactions between genes, whereas GO terms represent gene function [453]. Pathway analysis also allows mapping of gene lists onto existing pathways, usually using databases of pathways generated from literature analysis [451].

In relation to cDNA microarray experiments with melanoma, many authors have utilised GO terms and pathway analysis to identify groups of genes with expression levels related to survival. Kauffmann *et al.* applied "searching for a biological interpretation of microarray experiments" (SBIME) with Gene Ontology (GO) annotations to a microarray dataset generated in an experiment to identify genes that differentiated between primary tumours that would or would not metastasise within 4 years [177, 178]. SBIME performs analysis of variance (ANOVA) on logarithmic gene expression

by metastasis status at 4 years. For each GO category, SBIME then compares the proportion of genes with an ANOVA P-value lower than 1.0×10^{-2} within that category with what would be expected if there was no relationship between the category and the genes [177]. Using this analysis, Kauffmann and colleagues showed that genes involved in DNA repair and genomic stability were over-represented among genes differentially expressed in primary melanomas that would metastasise and that over-expression of these genes was associated with metastasis [177]. In a study using lymph node metastases, gene expression profiles were compared between tumours from patients with “poor-prognosis” disease, progressing within 24 months of lymph node dissection, and patients with “good-prognosis” disease who did not progress within 24 months [185]. In this study, differentially expressed genes were grouped according to GO terms, and Mann-Whitney tests were performed to compare differentially expressed genes with existing GO-based gene lists to identify significant over-representation of GO terms [185]. Using this method, of the 2140 differentially expressed genes, genes involved in apoptosis, pathways associated with nuclear factor- κ B, Wnt/Frizzled signalling, immunologic signalling and developmental processes were over-represented [185].

An alternative approach to analysis of microarray data is ‘unsupervised’, where genes or samples are clustered based on expression patterns [449]. Jonsson and colleagues performed unsupervised hierarchical clustering of gene expression data from stage IV melanoma and identified four subgroups of tumours [180]. They then used SAMic to identify genes differentially expressed in each tumour subgroup and used DAVID (the database for annotation, visualisation and integrated discovery) to determine gene function [180, 369, 372]. DAVID, in common with many other publicly available tools, maps a gene list to the associated biological annotation (e.g. GO terms) and then highlights the most over-represented annotation [369-371]. In terms of the pathway analysis, DAVID provides links for searching a number of pathway databases [369]. A review of recent microarray studies used MetaCore (from GeneGo, St Joseph, MI) to compare gene lists from six studies to identify common subsets of genes followed by GO enrichment analysis [188, 454]. This highlighted immune response genes and the *NRAS*-pathway as significant biological processes across microarray studies in melanoma [188].

This chapter describes identification of a group of genes whose expression levels are associated with survival and adverse prognostic factors. In Chapter 3 we have described identification of a single gene (*SPP1*) with expression associated with survival and have used Ingenuity Pathway Analysis (IPA, Ingenuity Systems, Redwood City, California) to generate a network of genes associated with *SPP1*, based on the

expression dataset. In this chapter, DNA repair genes and genes associated with these processes, were easily identified as being associated with survival by simple review of the gene list; however GO and pathway analysis has been used to confirm these observations. Furthermore, IPA has been used in association with principal components analysis to identify a network of genes with expression correlated with DNA repair gene expression.

This chapter also describes an assessment of methods used for qRT-PCR with small FFPE melanoma specimens. This has been undertaken to ensure accuracy of results using precious samples, and I present experiments designed to identify the most suitable experimental design and endogenous control genes for use in this work. The two experimental designs for relative quantification of gene expression using qRT-PCR are the relative standard curve method and the comparative Ct method [342]. The relative standard curve method involves having a set of relative standards from which the unknown samples are quantified. This quantity is then reported as relative to a selected sample, which acts as a calibrator. Serial dilutions of cDNA, RNA or genomic DNA can be used to generate standard curves, which need to be accurately diluted, but do not need to be quantified. A standard curve is generated on each PCR plate for each probe (including endogenous controls), therefore more reagents and space are needed. However, this method is very accurate and requires the least amount of validation as the PCR efficiencies of probes for the endogenous controls and test genes do not need to be equal [341]. The comparative Ct ($2^{-\Delta\Delta C_t}$) method is described in Chapter 2 and does not require use of standard curves, so fewer reagents are used. However, it is essential that PCR efficiencies of probes for test genes and endogenous control genes are similar in order to use comparative Ct ($2^{-\Delta\Delta C_t}$) method [340, 455]. Taqman® Gene Expression assays used in the qRT-PCR work presented in this chapter have amplification efficiencies of 100% (+/-10%) when used in high quality RNA [456]; specifically there is doubling of PCR product during every PCR cycle [340, 457], although this is likely to be less in degraded RNA from melanoma FFPE tissue. Therefore, before deciding on an experimental design to use, an assessment of the amplification efficiencies of the assays was made.

The comparative Ct method requires quantification of an endogenous control gene, which will be used to normalise gene expression levels of unknown genes for the amount of mRNA used in each reaction. When choosing which gene to use as a control it is essential that the expression of this gene does not vary in response to an intervention or in certain biological states, that the amplification efficiency is similar to genes of interest and that the abundance of the reference gene is similar to that of the gene of interest [458]. A “housekeeping” gene is often used as an endogenous control,

however expression of these genes can vary considerably between different cell types and between identical cell types from different individuals [459-461]. Also, some genes used as endogenous control genes, for example *GAPDH* and beta-actin, have a number of pseudogenes (genomic sequences which often lack introns similar to transcribed mRNA sequences) which can amplify even when trace amounts of genomic DNA are present in a PCR mixture [462-464]. This has prompted authors to suggest that for experiments where internal control genes are used, these genes need to be assessed to ensure there is minimum variability of gene expression [465]. Extensive studies have suggested that for more reliable and accurate normalisation of data, multiple control genes are required from which a normalisation factor can be calculated [343, 466]. Software has been developed to select genes with most stable expression within the tissue of interest, such as geNorm [343] or Normfinder [467]. GeNorm calculates a gene stability measure based on the principle that the expression ratio of two ideal control genes is the same in all samples. For each control gene, the software determines the average pairwise variation with all other control genes as the standard deviation of the log-transformed expression ratios and defines an internal control gene-stability measure, M. Genes with the lowest M value have the most stable expression. GeNorm then excludes genes with the highest M value and recalculates new M values for the remaining genes, resulting in identification of the two endogenous control genes with the most stable expression in tested samples [343]. Vandesompele and colleagues suggested use of the geometric mean of control gene expression levels as a normalisation factor [343]. Most authors recommend that at least three genes are required for normalisation of data [343, 466], however a balance must be struck between practical considerations of analysing control genes and accuracy of data normalisation [343]. GeNorm can assist in identification of the number of genes required for normalisation. When additional genes are added to calculate the normalisation factor, GeNorm can calculate the pairwise variation between the original normalisation factor and the new normalisation factor (pairwise variation = $\frac{\text{normalisation factor using } n \text{ genes}}{\text{normalisation using } n+1 \text{ genes}}$) to identify whether addition of another gene significantly contributes to the normalisation factor [343]. If there is large difference between the normalisation factor calculated using the additional gene and the original normalisation factor, this suggests that the additional gene has a significant effect on the factor and should be included to calculate the most accurate normalisation factor [343]. Further genes can be added until there is little difference between normalisation factors indicating that additional genes do not contribute to calculation of an accurate normalisation factor. Vandesompele and colleagues suggest that a pairwise variation of <0.15 with addition of a further gene indicates that this control gene is not required for accurate normalisation [343]. In this

chapter, this software has been used to identify genes with the most stable expression in FFPE melanoma samples for use as endogenous control genes and the number of genes needed for accurate normalisation of qRT-PCR data.

In summary, this chapter describes use of the DASL assay to identify DNA repair genes and genes related to this process associated with relapse-free survival (RFS) and adverse histopathological tumour features. Pathway analysis was used to further investigate the data and DASL results were validated using qRT-PCR.

4.3 Identification of genes associated with prognosis and histological features

4.3.1 Detailed methodology

4.3.1.1 Samples and generation of data set

As described in Chapter 3, FFPE primary melanoma tumour blocks were identified from two study sets; the Leeds Melanoma Cohort Study (Cohort Study) and the Retrospective Sentinel Node Biopsy Study (SNB Study). Tissue blocks were sampled as described previously and RNA was extracted. Sample selection, tissue sampling and RNA extraction were performed by Dr Caroline Conway (Cohort study), Dr Angana Mitra (SNB study) and Samira Lobo. The Illumina DASL Human Cancer panel was used for gene expression profiling by Floor de Kort at the service provider, ServiceXS (Leiden, Netherlands). Data generated from the DASL array from the two sample sets were normalised separately as described in Chapter 2 before the two data sets were merged for analysis to identify differentially expressed genes. Gene expression data from 354 primary melanoma samples was used for analysis.

4.3.1.2 Statistical methodology

4.3.1.2.1 Identification of differentially expressed genes

Gene expression analyses were performed by myself using data which had been log-transformed (\log_2). As some of the normalised gene expression levels were negative, 1000 was added to all values prior to log-transformation. Within the sample sets, mean expression of each gene was compared between samples with differing Breslow thicknesses and mitotic rates using linear regression. For survival analysis, relapse-free survival (RFS) was defined as the period between diagnosis and date of first relapse at any site. Death from any cause was used for overall survival analyses.

Analysis was performed on the 11th February 2010, and survival data was censored at this date. Survival analysis was performed using the Cox proportional hazards model to calculate hazard ratios and 95% confidence intervals for each gene. Significance values were ranked to identify genes most differentially expressed between groups of interest.

Survival analysis identified a number of genes significantly associated with survival that were either DNA repair genes or genes linked to these processes. To identify which of the DNA repair genes independently predicted survival, a multivariate Cox proportional hazards model was generated using all DNA repair genes significantly ($p < 0.0001$) associated with Breslow thickness, mitotic rate or survival in the previous analyses. Fold changes for gene expression between groups of interest were calculated using normalised gene expression data which had not been log transformed. The associations between expression of different DNA repair genes were identified using Spearman's rank correlation.

4.3.1.2.2 Multiple testing and adjustment of analyses

To correct for multiple testing, the Bonferroni method was used [366] and the significance level was set at 0.0001. For survival analyses assessing the expression of single genes in each test, the significance level for highlighting results of interest was set as 0.05.

In view of non-biological variation that was present between the two DASL studies, all gene expression analyses were adjusted for the study from which the patients were recruited. Survival analyses were also adjusted for whether the patient had undergone a sentinel node biopsy and the effect of the biopsy result (SNB status), as the use of SNB results in delay of the date of first relapse in melanoma patients since the usual site of first recurrence (nodal) is removed. Analyses were further adjusted for demographic and histological factors of prognostic importance in melanoma. All statistical analyses were undertaken using Stata version 10 (StataCorp 2007, College Station, TX).

4.3.1.2.3 Gene ontology (GO) and pathway analysis of genes associated with survival

To further investigate differentially expressed genes, GO analysis was performed by Binbin Liu and Lee Hazelwood of the Bioinformatics Group in the Cancer Research UK Centre, Leeds Institute of Molecular Medicine. Cytoscape v2.8.1 [362, 363] and its plug-in, BiNGO v2.44 [364, 365] were used to search a custom built GO database with

gene lists generated from analyses described above. Further details of this software are included in Chapter 2. For this study a customized gene reference and annotation databank were built, as gene expression data was based on the 502-gene Human Cancer panel rather than a genome-wide platform. Therefore, the databank used contained GO terms associated with the 502 genes only.

DAVID [368] [369, 371, 372], was also used to identify over-represented gene functions and pathways in our gene lists. I performed this analysis myself. Further details of the algorithms used by DAVID are described in Chapter 2. For the purposes of enrichment analysis, a background population of genes from the Human Cancer panel has been inputted for comparison with the annotation composition of the inputted gene list [368].

Genes associated with survival in analyses described in section 4.3.1.2.1 were ranked in three ways according to hazard ratio, significance level and fold change in expression between relapsers and non-relapsers for input into the analysis software.

4.3.1.2.4 Principal components analysis and Ingenuity Pathway analysis

Principal components analysis and Ingenuity Pathway Analysis was performed by Jeremie Nsengimana in the Section of Epidemiology and Biostatistics. Ingenuity Pathway Analysis (IPA, Ingenuity Systems, Redwood City, California (www.ingenuity.com)) was used to identify the pathways and networks of genes co-regulated with the most significant DNA repair genes [468]. Principal components analysis was first applied to the dataset to summarize into one variable the expression of the DNA repair genes most strongly associated with RFS [468]. A Pearson's product-moment correlation coefficient was then calculated between the first principal component (summary variable) and each of the genes on the cancer panel. Finally IPA was interrogated using algorithms described in Chapter 2 to find pathways and networks involving genes significantly correlated with the principal component at a level of $p < 1 \times 10^{-10}$.

4.3.2 Results

4.3.2.1 Genes predictive of survival

Genes with expression levels most strongly related to RFS in the merged dataset from 354 primary melanoma samples are presented in Table 4-1 when analysis is adjusted for study type and SNB status only.

Gene	Mean fold difference between relapsers and non-relapsers	Hazard ratio	95% confidence interval	Significance value
<i>RAD51</i>	1.22	2.99	1.84-4.85	8.34 x 10 ⁻⁶
<i>TK1</i>	1.12	4.70	2.30-9.61	0.00002
<i>ING1</i>	1.11	5.86	2.58-13.31	0.00002
<i>RAD52</i>	1.16	4.49	2.23-9.01	0.00002
<i>TFAP2C</i>	0.83	0.49	0.35-0.69	0.00004
<i>CCNA2</i>	1.16	2.66	1.67-4.23	0.00004
<i>BIRC5</i>	1.19	2.75	1.67-4.52	0.00007
<i>TOP2A</i>	1.12	3.85	1.97-7.55	0.00008
<i>CDH13</i>	0.80	0.48	0.33-0.70	0.0002
<i>HLF</i>	0.78	0.45	0.30-0.69	0.0002
<i>SPP1</i>	1.41	1.67	1.26-2.21	0.0003
<i>ITGB4</i>	0.79	0.58	0.43-0.79	0.0004
<i>MLF1</i>	1.15	2.74	1.55-4.83	0.0005
<i>FLI1</i>	0.83	0.51	0.35-0.75	0.0005
<i>EPHB4</i>	0.89	0.41	0.25-0.69	0.0008
<i>VEGFB</i>	1.04	9.83	2.57-37.64	0.0009
<i>ELK3</i>	0.95	0.20	0.07-0.53	0.001
<i>RAD54B</i>	1.18	2.08	1.33-3.25	0.001
<i>E2F1</i>	1.10	2.79	1.47-5.27	0.002
<i>TERT</i>	1.29	1.80	1.25-2.59	0.002
<i>CDC2</i>	1.22	1.85	1.26-2.70	0.002
<i>CCNH</i>	1.08	3.39	1.58-7.26	0.002
<i>WNT2</i>	1.34	2.49	1.41-4.41	0.002
<i>IFNGR1</i>	0.89	0.47	0.29-0.76	0.002
<i>PML</i>	0.96	0.21	0.07-0.58	0.003

Table 4-1: Top 25 genes associated with relapse-free survival (analysis adjusted for study and SNB status).

Fold difference in gene expression between relapsers and non-relapsers is presented. Hazard ratios for reduced RFS are calculated for doubling of gene expression value, for example doubling of tumour *RAD51* levels is associated with a three times greater hazard of relapse. P-values are from the proportional hazards model. The significance level following a Bonferroni correction is indicated by a dashed line. DNA repair genes or those associated with this process are highlighted in dark green and genes involved in the cell cycle or cell proliferation are highlighted in light green.

A number of the genes which were differentially expressed in association with relapse in univariate analysis are DNA repair genes or involved in this process. Within this group, over-expression of *RAD51*, *RAD52* and *TOP2A* were most predictive of poor RFS (Table 4-2) with hazard ratios of 2.99 ($p=8.34 \times 10^{-6}$), 4.49 ($p=0.00002$) and 3.85 ($p=0.00008$) respectively for a doubling of expression levels. These genes continued to be predictive of RFS when the analysis was repeated and adjusted for factors of prognostic importance in melanoma (age of patient at diagnosis, sex of the patient and body site of tumour) and when adjusted further for tumour characteristics of prognostic importance (Breslow thickness, mitotic rate (number/mm²) and presence of tumour ulceration), confirming that these genes are independent predictors of relapse (Table 4-2, part (i)). Expression of *RAD51* was 1.22 times greater in tumours from patients who relapsed versus those that did not; the fold changes between tumours from relapsers and non-relapsers for *RAD52* and *TOP2A* were 1.16 and 1.12 respectively (Table 4-1). *RAD54B*, *RAD52*, *TOP2A* and *RAD51* were also over-expressed in tumours from patients who died versus surviving patients (fold changes of 1.15, 1.11, 1.09 and 1.10, respectively).

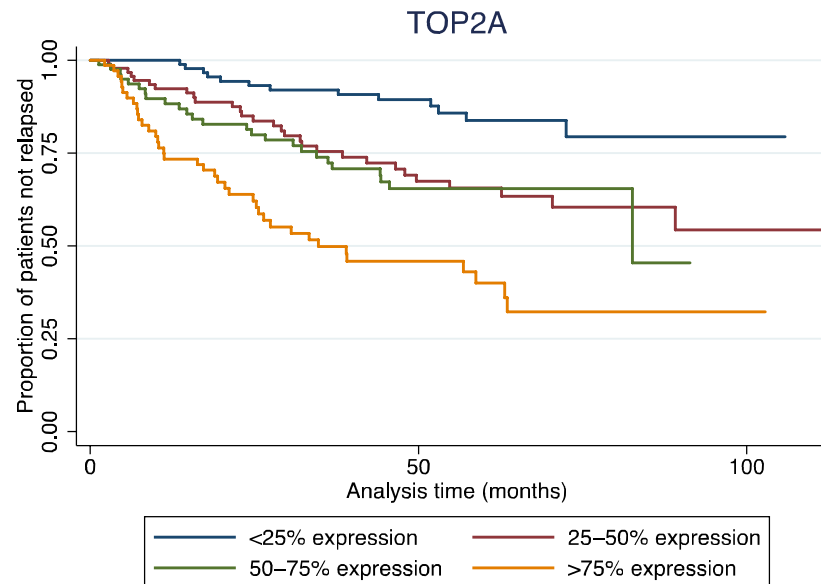
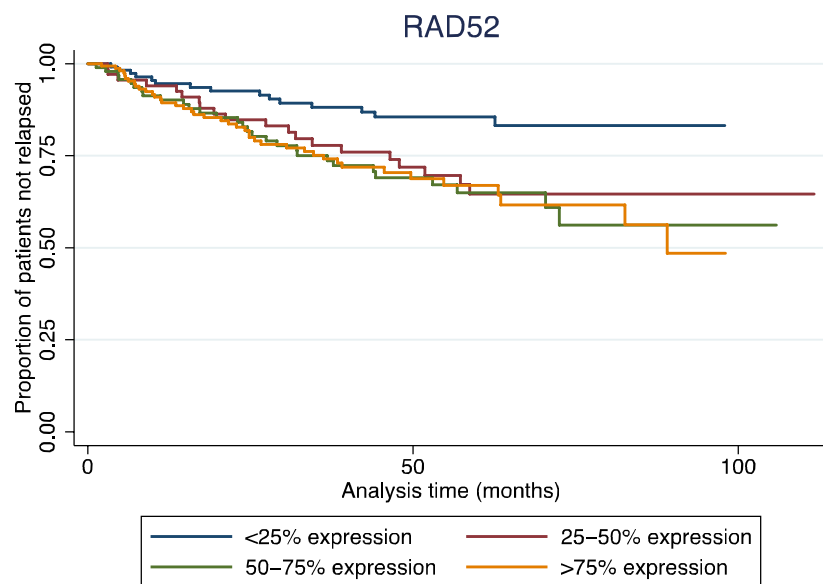
4.3.2.1.1 Multivariate models including DNA repair genes associated with relapse, Breslow thickness and mitotic rate

RAD52 and *TOP2A* continued to significantly influence survival in a Cox proportional hazards model when considered with all the other DNA repair genes identified as being significantly associated with Breslow thickness, mitotic rate or RFS (listed in Table 4-3) (multivariate model Table 4-2, part (ii) and Figure 4-1). In the multivariate model adjusted for study and SNB status only, hazard ratios (HR) for *RAD52* and *TOP2A* were 4.72 ($p=0.0004$) and 3.07 ($p=0.009$), respectively, for a doubling of levels. When analysed by quartiles of *RAD52* and *TOP2A* gene expression adjusted for study type and SNB status only, HRs generally increased for each quartile of gene expression (Figure 4-1). Both *RAD52* and *TOP2A* continued to have a significant independent predictive influence on RFS when analyses were adjusted for host variables (age, sex and tumour site) and histological factors (Breslow thickness, mitotic rate and ulceration) of prognostic importance (Table 4-2 part (ii)).

(i) Association between single gene expression and relapse free survival								(ii) Multivariable model with expression of all DNA repair genes predictive of RFS, Breslow thickness or mitotic rate					
Gene	1. Analysis adjusted for study and SNB status only (n=326)			2. Analysis further adjusted for age and sex of patient and site of tumour (n=325)		3. Analysis further adjusted for Breslow thickness, ulceration and mitotic rate of tumour (n=305)		1. Analysis adjusted for study and SNB status only (n=326)		2. Analysis further adjusted for age and sex of patient and site of tumour (n=325)		3. Analysis further adjusted for Breslow thickness, ulceration and mitotic rate of tumour (n=305)	
	Fold	HR (95% CI)	P-value	HR (95% CI)	P-value	HR (95% CI)	P-value	HR (95% CI)	P-value	HR (95% CI)	P-value	HR (95% CI)	P-value
<i>RAD51</i>	1.22	2.99 (1.84-4.85)	8.34x10 ⁻⁶	3.23 (1.96-5.33)	4.45x10 ⁻⁶	2.45 (1.41-4.24)	0.001	1.91 (0.98-3.72)	0.06	2.13 (1.09-4.19)	0.03	1.79 (0.88-3.67)	0.11
<i>RAD52</i>	1.16	4.49 (2.23-9.01)	0.00002	4.32 (2.12-8.80)	0.00006	2.50 (1.15-5.46)	0.02	4.72 (1.99-11.23)	0.0004	4.19 (1.77-9.92)	0.001	2.67 (1.08-6.61)	0.03
<i>TOP2A</i>	1.12	3.85 (1.97-7.55)	0.00008	3.87 (1.97-7.63)	0.00009	3.29 (1.58-6.85)	0.001	3.07 (1.33-7.08)	0.009	2.79 (1.20-6.47)	0.02	2.86 (1.16-7.06)	0.02

Table 4-2: The association of genes involved in DNA repair with relapse free survival in multivariate models.

Part (i) of the table shows the association between single gene expression and survival. Data adjusted for study and SNB status only are presented in column 1. The association was adjusted for sex, patient age and tumour site (as known predictors of outcome) in column 2. In column 3, further adjustment is made for known histological predictors of outcome: Breslow thickness, mitotic rate and ulceration. Part (ii) of the table presents results of a multivariate Cox proportional hazards model with expression of DNA repair genes identified as being predictive of RFS, Breslow thickness or mitotic rate (listed in Table 4-3). Significance values for genes that are independent predictors of survival within this model are highlighted in bold. Abbreviations used: RFS, relapse-free survival; HR, hazard ratio; CI, confidence interval; SNB, sentinel node biopsy.



Expression level	HR	95% CI	P-value	HR	95% CI	P-value
<25%	1			1		
25-50%	1.58	0.80-3.10	0.19	2.82	1.45-5.47	0.002
50-75%	1.79	0.95-3.37	0.07	2.67	1.34-5.29	0.005
>75%	2.90	1.57-5.36	0.001	3.59	1.78-7.25	<0.0001

Figure 4-1: Kaplan Meier survival function estimates for *RAD52* and *TOP2A* gene expression.

Survivor functions have been estimated for each quartile of gene expression. Hazard ratios compared with the lowest quartile increase for each successive quartile. Analysis is adjusted for study and SNB status. Abbreviations used: HR, hazard ratio; CI, confidence interval.

4.3.2.2 Gene expression in tumours with poor prognostic histopathological features

Genes involved in DNA repair were also over-expressed in tumours with greater Breslow thickness and mitotic rate, which are associated with a poorer prognosis in melanoma (Table 4-3). Generally, expression increased with each category of increasing Breslow thickness and mitotic rate. This association remains significant when the analysis was repeated and adjusted for host factors of prognostic importance (age of patient at diagnosis, sex of patient and site of tumour).

4.3.2.3 Correlations in expression levels between DNA repair genes

Expression of the majority of DNA repair genes identified as being associated with reduced survival or poor prognostic histological features correlated well with each other (Table 4-4). An exception was *RAD52*, with expression levels that did not correlate with the levels of *RAD54L*, *BRCA2* and *TOP2A*.

4.3.2.4 GO analysis and pathway analysis using DAVID

When the gene list was ranked in order of hazard ratio for association with RFS, 33 genes had significance values ≤ 0.01 and were used for GO analysis. Ten GO terms were significantly associated with expression of these genes (Table 4-5). Many of these terms describe cellular components, however eight genes are involved in the biological process of M-phase (mitosis) in the cell cycle (*CDC2*, *RAD54B*, *BIRC5*, *RAD52*, *CDC25C*, *CCNA2*, *CDK2* and *RAD51*).

Analysis based on ranking genes in order of fold change allowed input of 280 genes with fold changes greater than 1. In this analysis, genes were associated with four GO terms which described biological processes: DNA recombination (corrected p-value 0.005) and DNA replication (corrected p-value 0.007) which are subsets of DNA metabolic processes (corrected p-value 0.005), genes were also associated with M-phase (corrected p-value 0.02) (Figure 4-2). Sixty-two (22%) of the genes were associated with the term "DNA metabolic process". The limitation of these analyses is that only genes which increased risk of relapse or that were over-expressed in relapsers were assessed. Reduced relapse risk and under-expression of genes may also be of interest however as DNA repair genes were over-expressed, this analysis was most relevant. Analysis based on ranking of genes according to significance levels did not yield any significant results associations in GO analysis.

Gene	Breslow thickness					Mitotic rate			
	Fold difference in gene expression between indicated group and tumours ≤1mm thick (n=24)			Significance level (adjusted for study only)	Significance level – adjusted for age and sex of patient and site of tumour	Fold difference in gene expression between indicated group and tumours with mitotic rate <1/mm ² (n=48)		Significance level (adjusted for study only)	Significance level – adjusted for age and sex of patient and site of tumour
	>1-2mm (n=163)	>2-4 mm (n=118)	>4 mm (n=46)			1-6/mm ² (n=167)	>6/mm ² (n=119)		
<i>RAD52</i>	1.05	1.16	1.30	1.88 x 10 ⁻⁸	9.53 x 10 ⁻⁸	1.10	1.16	0.02	0.03
<i>MSH2</i>	1.03	1.20	1.36	2.18 x 10 ⁻⁸	2.24 x 10 ⁻⁷	1.20	1.29	0.0009	0.002
<i>RAD51</i>	1.06	1.30	1.48	5.53 x 10 ⁻⁸	2.16 x 10 ⁻⁷	1.26	1.59	4.61 x 10 ⁻¹⁰	3.67 x 10 ⁻⁹
<i>RAD54B</i>	1.20	1.45	1.66	6.30 x 10 ⁻⁸	7.61 x 10 ⁻⁷	1.19	1.50	5.94 x 10 ⁻⁶	0.00006
<i>CHEK1</i>	1.04	1.35	1.44	9.44 x 10 ⁻⁶	0.0001	1.17	1.38	0.0005	0.005
<i>BRCA1</i>	1.19	1.42	1.54	0.00002	0.00007	1.12	1.45	1.23 x 10 ⁻⁶	3.19 x 10 ⁻⁶
<i>TOP2A</i>	1.00	1.10	1.22	0.00003	0.00008	1.20	1.38	5.43 x 10 ⁻⁹	1.36 x 10 ⁻⁸
<i>RAD54L</i>	0.94	1.18	1.28	0.00005	0.0004	1.11	1.34	0.0007	0.004
<i>BRCA2</i>	1.13	1.27	1.41	0.00006	0.0004	1.06	1.24	0.0006	0.002
<i>MSH6</i>	0.94	1.01	1.03	0.001	0.002	1.08	1.16	0.00003	0.00003

Table 4-3: DNA repair genes differentially expressed in relation to Breslow thickness and mitotic rate.

Genes listed were identified as significantly differentially expressed (p<0.0001) in tumours with either greater Breslow thickness or mitotic rate using linear regression. Fold changes in gene expression are presented for each tumour thickness and mitotic rate group compared to baseline groups. Analyses are adjusted for study only and further adjusted for age of patient at diagnosis, site of tumour and sex of patient.

	<i>RAD51</i>	<i>RAD52</i>	<i>RAD54B</i>	<i>RAD54L</i>	<i>BRCA1</i>	<i>BRCA2</i>	<i>MSH2</i>	<i>MSH6</i>	<i>CHEK1</i>
<i>RAD52</i>	0.22 <0.0001								
<i>RAD54B</i>	0.39 <0.0001	0.25 <0.0001							
<i>RAD54L</i>	0.29 <0.0001	0.05 0.39	0.24 <0.0001						
<i>BRCA1</i>	0.40 <0.0001	0.29 <0.0001	0.46 <0.0001	0.25 <0.0001					
<i>BRCA2</i>	0.34 <0.0001	0.06 0.28	0.25 <0.0001	0.25 <0.0001	0.39 <0.0001				
<i>MSH2</i>	0.23 <0.0001	0.21 0.0001	0.43 <0.0001	0.27 <0.0001	0.41 <0.0001	0.36 <0.0001			
<i>MSH6</i>	0.33 <0.0001	0.26 <0.0001	0.31 <0.0001	0.21 0.0001	0.32 <0.0001	0.16 0.0029	0.33 <0.0001		
<i>CHEK1</i>	0.46 <0.0001	0.19 0.0005	0.29 <0.0001	0.32 <0.0001	0.39 <0.0001	0.29 <0.0001	0.37 <0.0001	0.27 <0.0001	
<i>TOP2A</i>	0.61 <0.0001	0.05 0.40	0.36 <0.0001	0.31 <0.0001	0.37 <0.0001	0.34 <0.0001	0.20 0.0002	0.25 <0.0001	0.30 <0.0001

Table 4-4: Gene expression correlations for DNA repair genes adjusted for study and relapse status.

Spearman's rho and significance value are presented.

GO-ID	Corrected significance value	Description
44428	0.013	nuclear part
5654	0.013	nucleoplasm
31981	0.013	nuclear lumen
43233	0.015	organelle lumen
31974	0.015	membrane-enclosed lumen
70013	0.015	intracellular organelle lumen
44446	0.016	intracellular organelle part
44422	0.017	organelle part
279	0.028	M phase
5634	0.031	nucleus

Table 4-5: Gene ontology terms associated with genes that influence relapse-free survival.

Many of these terms describe cellular components, terms which describe a biological process are highlighted in green. The P-value has been corrected using the Benjamini and Hochberg correction [367].

A list of 109 genes significantly associated with RFS ($p < 0.05$) were entered into DAVID software, 102 genes were recognised by the software and compared with a background of 479 recognised genes from the Human Cancer panel to identify enriched gene ontology terms or pathways in this dataset. Forty-six Kyoto Encyclopedia of Genes and Genomes (KEGG) pathways [469, 470] were identified which contained 66 of the input genes, the top 10 pathways are presented in Table 4-6.

Unsurprisingly, as a cancer panel was used for gene expression measurement, the majority of genes were involved in the cancer pathway. Genes were also significantly enriched in the cell cycle pathway (Table 4-6) and the homologous recombination pathway (17th most significant pathway) following adjustment of significance values using either the Bonferroni correction [366] or the Benjamini and Hochberg correction [367]. Genes were also present in the non-homologous end-joining pathway when the less stringent Benjamini and Hochberg correction was used (25th most significant pathway). The melanoma pathway contained four genes, but these genes were not significantly represented. This analysis suggests that genes involved in focal adhesion and cytokine-cytokine receptor interactions are also over-represented in this gene list. This result is useful as it may not have been appreciated on simple review of the gene list.

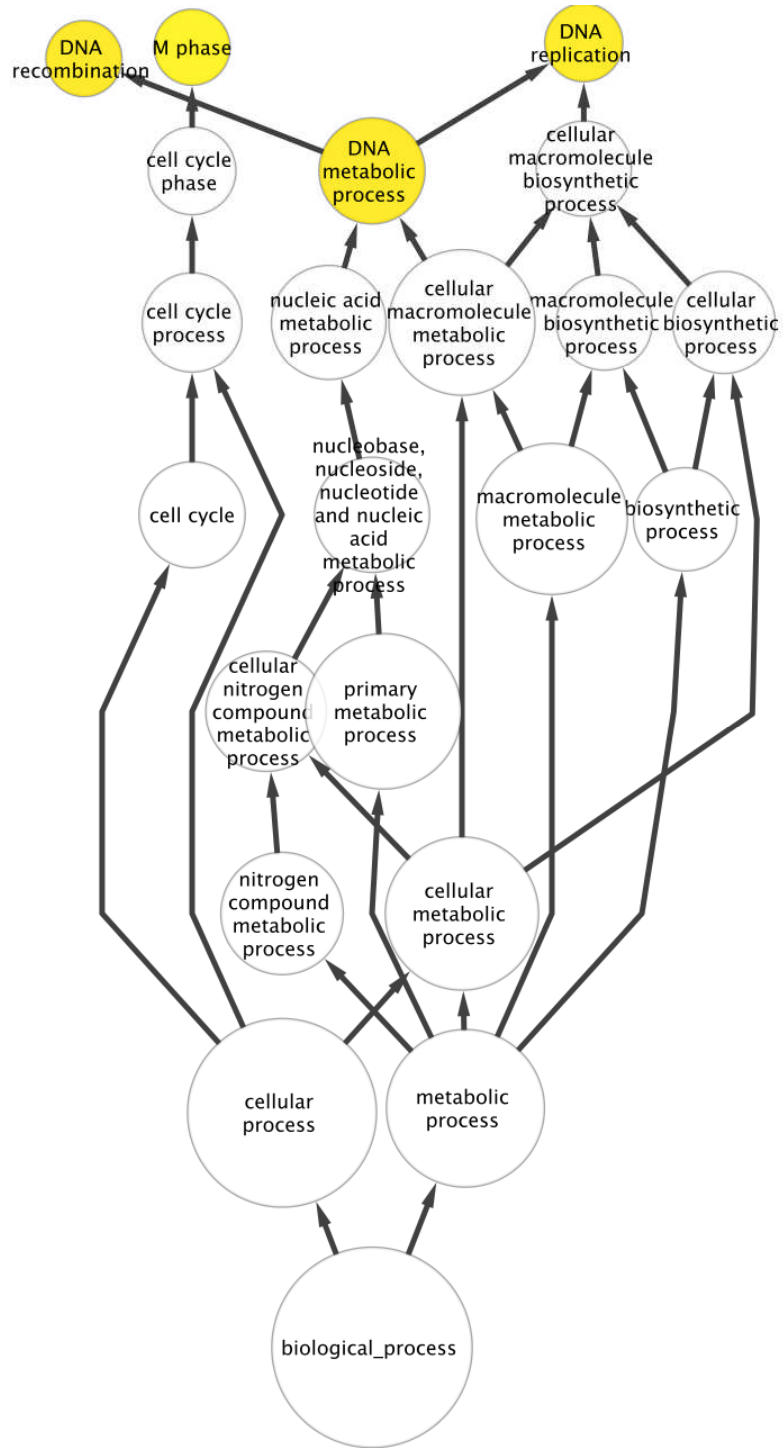


Figure 4-2: Hierarchical display of biological process GO terms associated with genes with expression fold change >1 between relapsers and non-relapsers.

GO terms associated with the gene list are highlighted in yellow.

Pathway	Number of genes in pathway	% of genes inputted	P-Value	Bonferroni corrected P-value	Benjamini corrected P-value	False discovery rate
hsa05200:Pathways in cancer	26	25.5	1.29×10^{-18}	1.03×10^{-16}	1.03×10^{-16}	1.37×10^{-15}
hsa04510:Focal adhesion	14	13.7	5.87×10^{-12}	4.70×10^{-10}	2.35×10^{-10}	6.24×10^{-09}
hsa04110:Cell cycle	12	11.8	8.71×10^{-11}	6.96×10^{-09}	2.32×10^{-09}	9.26×10^{-08}
hsa04060:Cytokine-cytokine receptor interaction	13	12.8	9.07×10^{-11}	7.25×10^{-09}	1.81×10^{-09}	9.64×10^{-08}
hsa05212:Pancreatic cancer	9	8.8	2.40×10^{-07}	1.92×10^{-05}	3.84×10^{-06}	2.55×10^{-04}
hsa05210:Colorectal cancer	8	7.8	4.63×10^{-06}	3.70×10^{-04}	6.17×10^{-05}	0.005
hsa04144:Endocytosis	7	6.9	8.14×10^{-06}	6.51×10^{-04}	9.30×10^{-05}	0.009
hsa05215:Prostate cancer	8	7.8	1.36×10^{-05}	0.001	1.36×10^{-04}	0.019
hsa04520:Adherens junction	6	5.9	1.84×10^{-05}	0.002	1.64×10^{-04}	0.02
hsa04810:Regulation of actin cytoskeleton	7	6.9	8.09×10^{-05}	0.007	6.47×10^{-04}	0.09

Table 4-6: KEGG (Kyoto Encyclopedia of Genes and Genomes) pathways associated with genes that influence relapse-free survival.

Significance values for representation of genes in the pathway without correction for multiple testing are presented, along with corrected significance values using the Bonferroni correction [366] and the Benjamini and Hochberg correction [367]. The false discovery rate is also presented.

4.3.2.5 Principal components and Ingenuity Pathway Analysis (IPA)

Principal components analysis of the top 10 significant DNA repair genes (listed in Table 4-3) identified one component which explained 40% of total variance in DNA repair gene expression whilst each of the other components explained 10% or less (analysis adjusted for study). Principal component 1 was also the only one that correlated with each of the 10 genes from which it was generated (Pearson's correlation coefficient ranging from 0.40 to 0.74). Table 4-7 presents the remaining genes from the cancer panel with expression that correlated with the first principal component at a level of $p < 1 \times 10^{-10}$. A large number of these genes are associated with cell cycle control or DNA repair (Table 4-7).

The 37 genes presented in Table 4-7 were used in IPA to infer cellular and molecular functions and to build gene networks. IPA built a gene network which contains 35 genes (Figure 4-3), among which 22 were correlated with the principal component of DNA repair genes at a significance level of $p < 1 \times 10^{-10}$. The major cellular and molecular functions making up this network were cell cycle and cell death, confirming the strong association between these processes and DNA repair.

4.3.3 Summary of gene expression associated with prognosis and histological features of tumours

Over-expression of DNA repair and related genes in 354 primary melanomas was prognostic and associated with shorter relapse-free survival time and poor histopathological features of the tumour. *RAD51*, *RAD52* and *TOP2A* are independent predictors of RFS in analyses adjusted for patient and tumour factors of prognostic importance. *RAD52* and *TOP2A* remained predictive of survival in multivariate analysis with other DNA repair genes. Expression of the majority of DNA repair genes was correlated and was also associated with expression of genes associated with cell cycle control and cell death.

Table 4-7 (following page): Remaining genes from the Human Cancer panel most correlated with principal component 1.

Correlation coefficients are adjusted for study. The National Center for Biotechnology Information Entrez Gene database was interrogated to identify gene function [471]. DNA repair genes or those associated with this process are highlighted in dark green and genes involved in the cell cycle or cell proliferation are highlighted in light green.

Gene	Correlation	P value	Role
<i>CDC2</i>	0.54	1.3x10 ⁻²⁷	Cell cycle
<i>TYMS</i>	0.51	8.4x10 ⁻²⁵	DNA repair and replication
<i>BIRC5</i>	0.50	1.2x10 ⁻²³	Inhibitor of apoptosis
<i>HMMR</i>	0.49	1.8x10 ⁻²²	Cell motility
<i>CCNA2</i>	0.48	9.0x10 ⁻²²	Cell cycle
<i>CDC25A</i>	0.48	1.1x10 ⁻²¹	Cell cycle
<i>TK1</i>	0.48	1.7x10 ⁻²¹	Cell cycle
<i>PCNA</i>	0.45	2.8x10 ⁻¹⁹	DNA repair and replication
<i>CDC25C</i>	0.45	5.6x10 ⁻¹⁹	Cell cycle
<i>DEK</i>	0.45	8.6x10 ⁻¹⁹	Chromatin organisation
<i>DCN</i>	-0.44	5.0x10 ⁻¹⁸	Role in connective tissue
<i>CDK4</i>	0.42	7.1x10 ⁻¹⁷	Cell cycle
<i>WEE1</i>	0.42	9.9x10 ⁻¹⁷	DNA replication and cell cycle
<i>ETS2</i>	-0.41	4.9x10 ⁻¹⁶	Transcription factor
<i>PDGFRA</i>	-0.41	8.9x10 ⁻¹⁶	Tyrosine kinase receptor
<i>BLM</i>	0.40	7.2x10 ⁻¹⁵	DNA repair and replication
<i>ITGB4</i>	-0.39	2.4x10 ⁻¹⁴	Cell adhesion
<i>CDKN2C</i>	0.39	2.4x10 ⁻¹⁴	Cell cycle
<i>E2F1</i>	0.38	1.5x10 ⁻¹³	DNA replication and cell cycle
<i>XRCC2</i>	0.38	2.4x10 ⁻¹³	DNA repair
<i>MYBL2</i>	0.37	3.8x10 ⁻¹³	Cell cycle
<i>FYN</i>	-0.37	5.7x10 ⁻¹³	Cell growth
<i>XRCC4</i>	0.37	1.2x10 ⁻¹²	DNA repair
<i>PDGFRB</i>	-0.37	1.3x10 ⁻¹²	Tyrosine kinase receptor
<i>BCL6</i>	-0.36	2.8x10 ⁻¹²	Transcriptional repressor
<i>CDH11</i>	-0.36	4.0x10 ⁻¹²	Cell adhesion
<i>FOSL2</i>	-0.36	4.4x10 ⁻¹²	Cell proliferation
<i>MAF</i>	-0.36	5.5x10 ⁻¹²	Transcriptional repressor/activator
<i>MLF1</i>	0.36	5.9x10 ⁻¹²	Haemopoietic cell development
<i>COL18A1</i>	-0.36	6.3x10 ⁻¹²	Collagen component
<i>PBX1</i>	-0.35	6.8x10 ⁻¹²	Osteogenesis and steroidogenesis
<i>JUNB</i>	-0.35	1.1x10 ⁻¹¹	Response to growth factors
<i>IFNGR1</i>	-0.35	2.2x10 ⁻¹¹	Interferon γ receptor
<i>AXL</i>	-0.34	3.5x10 ⁻¹¹	Tyrosine kinase receptor
<i>E2F3</i>	0.34	4.2x10 ⁻¹¹	DNA replication and cell cycle
<i>MCF2</i>	0.34	7.7x10 ⁻¹¹	Guanine nucleotide exchange factor
<i>RECQL</i>	0.34	9.0x10 ⁻¹¹	DNA repair

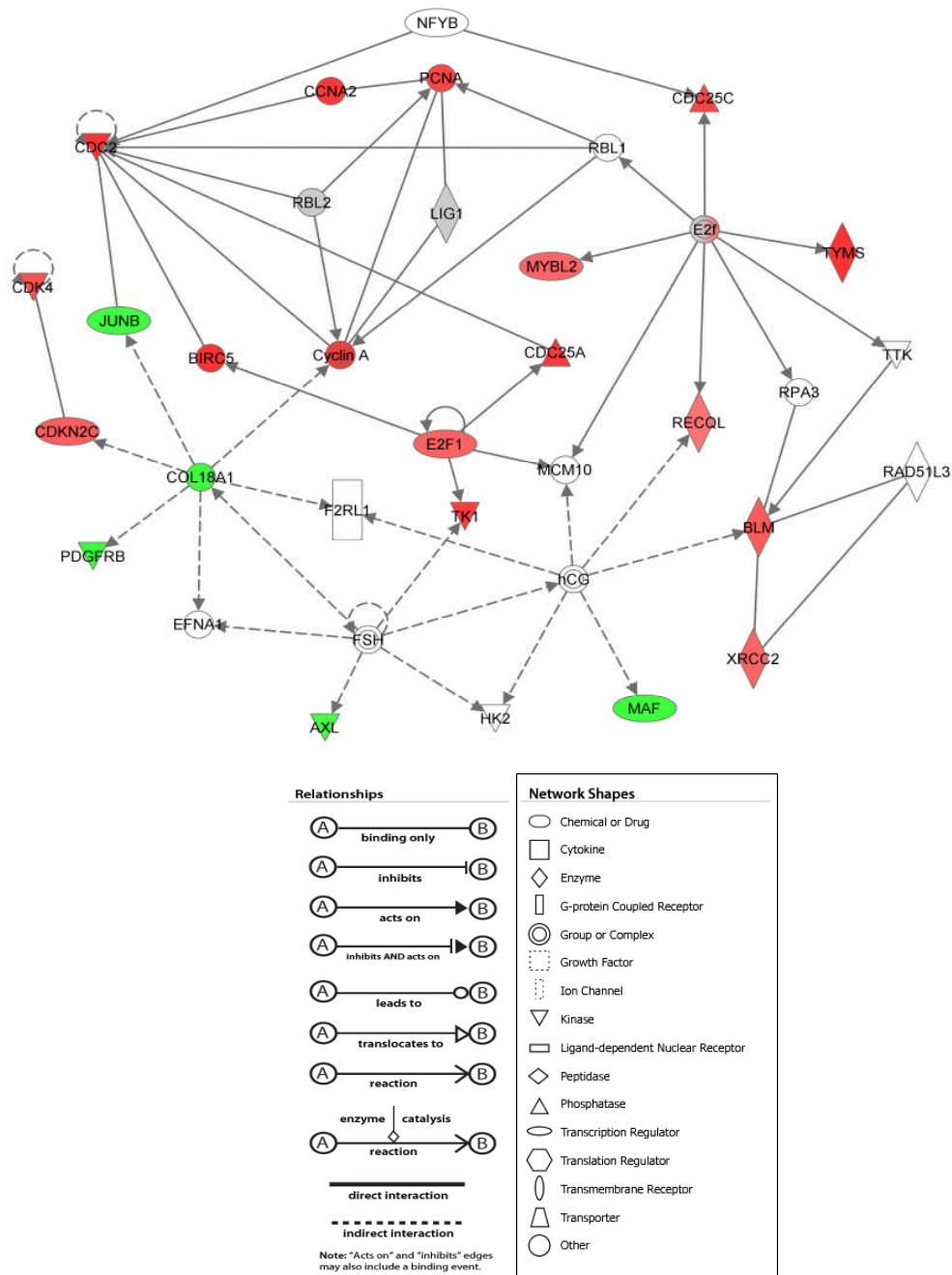


Figure 4-3: Gene network significantly correlated with principal component 1 from Ingenuity Pathway Analysis: cancer, cell cycle and cell death.

Molecules are represented as nodes and the biological relationship between nodes is represented as a line (edge). Each edge is supported by at least one reference from the literature, from a textbook or from canonical information stored in the Ingenuity Knowledge Base. The intensity of the node colour indicates the degree of positive (red) or negative (green) correlation with the principal component.

4.4 Validation of DASL results

Results generated from microarray analysis require validation to ensure that results are reproducible (and not platform specific) and warrant further investigation. To check the results using a different gene expression assay, a qRT-PCR experiment was performed to confirm expression levels of *RAD52*, *RAD54B* and *TOP2A* using samples from patients recruited to the Cohort Study.

To ensure that accurate results were being obtained from these precious samples, methodological work was undertaken to identify the best methods for qRT-PCR experiments with FFPE melanoma samples.

4.4.1 Study to optimise methods for qRT-PCR using FFPE melanoma samples

4.4.1.1 Assessment of amplification efficiencies of Taqman® Gene Expression assays and choice of experimental design

4.4.1.1.1 Methods

An assessment of the amplification efficiencies of Taqman® Gene Expression assays for unknown genes and endogenous control genes was performed to decide whether the comparative Ct method could be used with FFPE melanoma samples and Taqman® Gene Expression assays. cDNA was generated using the Invitrogen Superscript™ First-strand Synthesis System with a modified protocol, as described in Chapter 2, from RNA extracted from a FFPE metastatic melanoma sample as described in Chapter 2. cDNA concentration was measured using spectrophotometry and standard samples were prepared using a 1:2 dilution to generate standard curves for each assay assessed. Applied Biosystems (Warrington, UK) recommend that amplification efficiencies are assessed over a broad dilution (5-6 logs) [456], however previous experiments suggested that cDNA produced from RNA extracted from FFPE melanomas is too dilute to amplify in a concentration less than 100ng/μl so a 1:2 dilution was used to ensure enough results would be obtained to assess amplification efficiency.

Fragments of genes were amplified using Taqman® Gene Expression assays as detailed in Table 4-8.

	Gene	Exons targeted	Amplicon length	NCBI Reference Sequence	Assay Reference
Genes for relative quantification	<i>RAD52</i>	2/3	65bp	NM_134424.2	Hs00172536_m1
	<i>RAD54B</i>	1/2	64bp	NM_012415.2	Hs00610716_m1
	<i>TOP2A</i>	23/24	72bp	NM_001067.2	Hs03063307_m1
Endogenous control genes	<i>GAPDH</i>	3	122bp	NM_002046.3	Hs99999905_m1
	<i>IPO8</i>	20/21	71bp	NM_006390.2	Hs00183533_m1

Table 4-8: Details of Taqman® Gene Expression assays for DNA repair gene qRT-PCR experiments.

Abbreviations used: NCBI, National Center of Biotechnology.

PCRs were performed using standard methods described in Chapter 2. Automatic baseline and threshold levels were used to generate cycle threshold (Ct) values, and amplification efficiencies for each probe were calculated by the ABI 7500 Fast Real-time PCR System software (Applied Biosystems).

4.4.1.1.2 Results and conclusions

Ct values for replicate samples were plotted against sample cDNA amount. A line of best fit through the data points for each probe is applied by the software to generate standard curves from which probe efficiency can be calculated using the formula: efficiency = $10^{-(1/\text{slope})} - 1$ [456]. Probe efficiencies as calculated by the software are presented in Table 4-9.

	Assay	Slope of standard curve	Efficiency (%)
Genes for relative quantification	<i>RAD54B</i>	-4.92	59.7
	<i>RAD52</i>	-5.44	52.7
	<i>TOP2A</i>	-5.33	54.1
Endogenous control genes	<i>IPO8</i>	-5.60	50.9
	<i>GAPDH</i>	-4.68	63.5

Table 4-9: Taqman® Gene Expression assay probe efficiencies in cDNA generated from RNA extracted from an FFPE metastatic melanoma sample.

Applied Biosystems report that Taqman® Gene Expression assays are 100% (+/- 10%) in high quality RNA. This experiment showed that the assays were less efficient with degraded RNA extracted from FFPE tissue, but were comparable in efficiency with each test probe being within 10% of the efficiency of one of the endogenous control probes. Therefore I concluded that use of a comparative Ct method to assess the relative quantities of *RAD54B*, *RAD52* and *TOP2A* when using *GAPDH* and *IPO8* as endogenous control genes would be appropriate and this was used as the experimental design for validation of DASL results.

4.4.1.2 Identification of suitable endogenous controls

4.4.1.2.1 Methods

To identify endogenous control genes for use in qRT-PCR experiments using FFPE melanoma tissue, cDNA was generated using the Invitrogen Superscript™ First-strand Synthesis System using a modified protocol from RNA extracted from four FFPE melanoma metastases samples as described in Chapter 2. For a comparative experiment, a calibrator sample is also required to generate relative quantity values, and assessment of endogenous control gene expression in this sample was also made. For this work, a sample from an intradermal naevus was identified as a calibrator sample, RNA was extracted from 12 cores of tissue using the Roche High Pure RNA Paraffin Kit as described in Chapter 2 and cDNA was generated from calibrator RNA as described previously. Taqman® Express Endogenous Controls plates (Applied Biosystems, Warrington, UK) are 96-well MicroAmp® optical reaction plates with Taqman® Gene Expression Assays for 32 endogenous control genes dried into wells in triplicate (full list in Figure 4-4). One plate was used to assess each of the 5 samples. Each well was reconstituted to a final volume of 20µl with 10µl of Gene Expression Master Mix, 8µl DNase-free water and 2µl cDNA sample (total 1 microgram). PCRs were performed using the ABI 7500 Real-time PCR system (Applied Biosystems) using standard cycling conditions described in Chapter 2. Data from each of the 5 plates was imported into a single study and automatic settings were used for baseline and threshold determination across the samples. Ct values were exported to Excel for further analysis. Mean Ct values from replicate samples were used, and standard deviations were calculated for each gene across all samples. Data was uploaded into geNorm software (J. Vandesompele, Center for Medical Genetics, Ghent, Belgium) following conversion into non-normalised quantities. These quantities were calculated as follows: ΔCt values were calculated for each gene where $\Delta Ct =$

mean Ct value melanoma sample – mean value Ct calibrator sample, non-normalised values were calculated using $2^{-\Delta Ct}$ [340].

4.4.1.2.2 Results and conclusions

A number of gene expression assays failed to amplify with some of the samples, those being *HMBS*, *HPRT1* and *TBP*. Figure 4-4 shows the spread and mean Ct values for each gene across the five samples assessed. The genes with the lowest standard deviations were *HMBS* (for which a number of samples failed), *PPIA1*, *POP4*, *IPO8* and *CDKN1B*.

Figure 4-5 shows the average gene-stability measure (M values) of remaining control genes during stepwise exclusion of the least stable control gene using geNorm software [343]. The two genes with the lowest M value and hence the least average pairwise variation, have the most stable gene expression.

Based on these analyses *PPIA1*, *POP4*, *IPO8*, *CDKN1B*, *CASC3* and *PES1* would be candidates for endogenous control genes. In view of the limited amounts of RNA available to perform qRT-PCR validation work the lowest number of genes to allow accurate normalisation were identified. The calculated pairwise variation between a normalisation factor using 2 genes and 3 genes was only 0.097 (and therefore <0.15 [343]), indicating that normalisation using two genes would be adequate. *GAPDH* is commonly used as an endogenous control gene for normalisation. *GAPDH* had the 6th lowest standard deviation between samples of 0.61 and was the 6th most stably expressed gene as identified by geNorm, so was used as the first control gene. As discussed previously, an ideal control gene should be of similar abundance to the unknown genes. Figure 4-4 demonstrates that *GAPDH* is more abundant than many of our unknown genes with a lower Ct value, therefore it would be sensible to choose a gene of lower abundance as the second gene for normalisation. *IPO8* was identified as being the 3rd most stably expressed gene by geNorm and had low standard deviation between samples of 0.40. In this experiment, *IPO8* had a Ct value of 36.5 and *GAPDH* had a Ct value of 35.1, therefore *IPO8* was chosen as the second control gene for further qRT-PCR work to validate DASL results. As discussed previously, ideally three or more control genes are used and this represents a limitation of this work. However, in view of the small amounts of RNA available it cannot be justified to use more than two control genes to assess expression of three unknown genes.

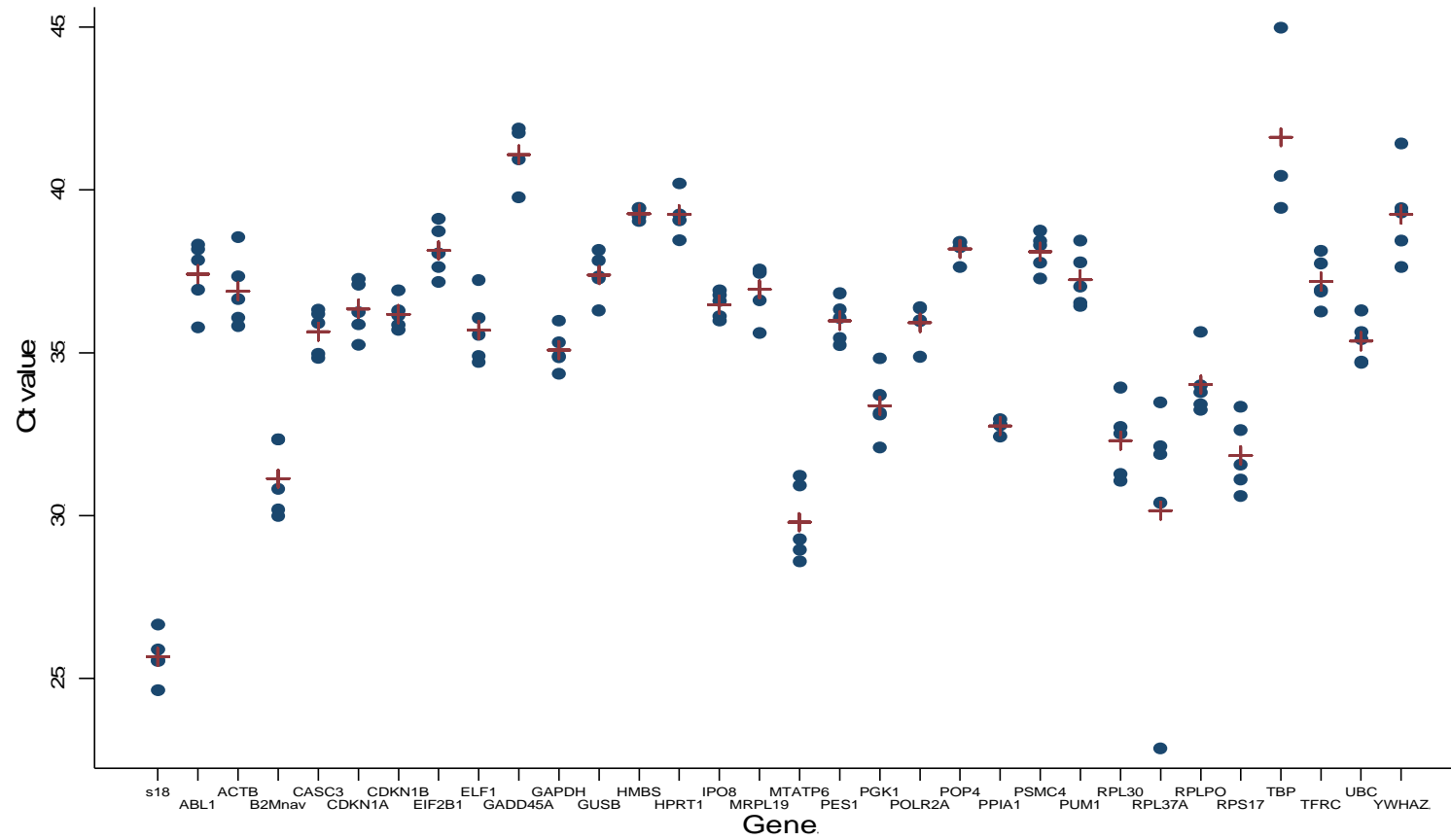


Figure 4-4: Dot-plot of cycle threshold values for cDNA samples generated from RNA extracted from four metastatic melanoma samples and one intradermal naevus (calibrator sample).

The mean is indicated by the plus sign. Abbreviation used: Ct, cycle threshold.

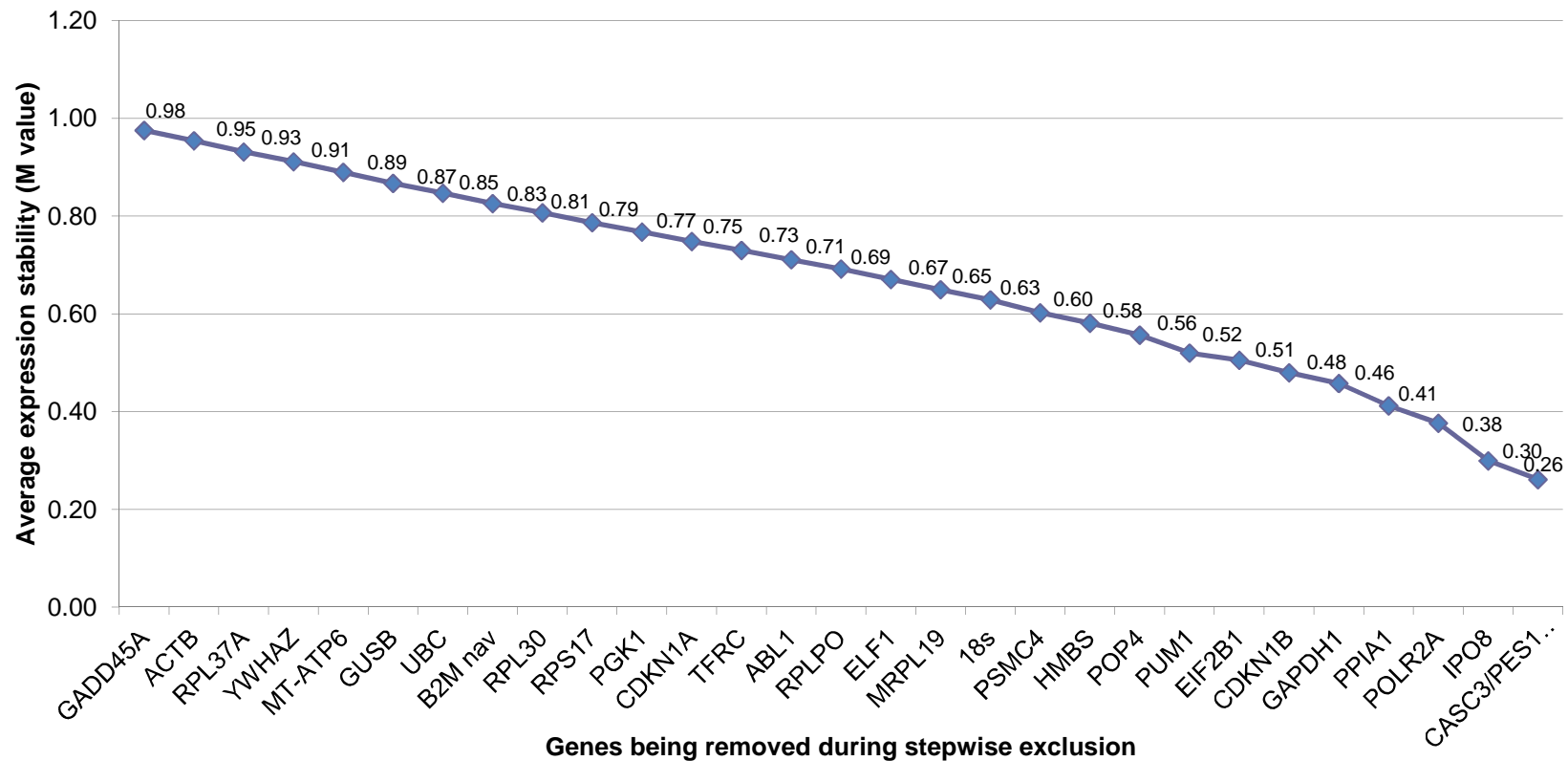


Figure 4-5: Average gene stability values (M values) of control genes during stepwise exclusion of least stable control genes.

CASC3 and *PES1* have the lowest M value and therefore have the most stable gene expression in four melanoma samples and one intradermal naevus sample .

4.4.2 Expression of *RAD52*, *RAD54B* and *TOP2A* in tumours from patients recruited to the Leeds Melanoma Cohort Study

4.4.2.1 Detailed methodology

cDNA was generated using the Invitrogen Superscript™ First-strand Synthesis System using a modified protocol as described in Chapter 2 from RNA extracted from 156 primary melanoma tumours from patients recruited to the Cohort Study and sent for DASL analysis. Thirteen samples from patients treated with chemotherapy were not included in the analysis as these samples were required for another study (Chapter 8). RNA was not available for two samples, one of which was from a patient treated with chemotherapy, leaving a total of 142 samples for analysis. Chemotherapy treated patients had all relapsed, leaving a total of 24 patients who had relapsed in the sample set assessed. cDNA was generated in two 96-well plates for all samples in the same reaction. cDNA generated from RNA extracted from an intradermal naevus sample, as described in section 4.4.1.2.1, was used as a calibrator sample.

Small fragments of *RAD52*, *RAD54B*, *TOP2A* and the endogenous control genes, *GAPDH* and *IPO8* were amplified using Taqman® Gene Expression Assay probes (Applied Biosystems, Warrington, UK) as listed in Table 4-8. PCRs were performed using standard conditions described in Chapter 2.

A total of 25 96-well plates were used for this experiment. The calibrator sample was amplified for all probes on 4 plates across the experiment to allow assessment of variability across the plate runs. Each 96-well plate was set up using the Corbett CAS4 robot (Qiagen Ltd, Crawley, UK) with the assistance of Dr Mark Harland, to minimise pipetting variation. Template negative controls for each assay and reverse transcriptase negative cDNA controls were rotated across the plates.

Following each run, results were assessed and any failed samples were omitted from the analysis. Groups of replicates with standard deviations greater than 0.5 cycles were reviewed to identify outliers. If a sample result was clearly erroneous when compared to other replicates (sample with Ct value >0.5 cycles different to other two samples), this sample was omitted from the analysis. When it was unclear which sample was the outlier (all Ct values within 0.5 cycles of each other) all samples were retained to generate a mean Ct value for replicates. All plates were imported into a single study, and automatic settings were used for baseline and threshold determination across all samples. Ct values were exported to Excel for further analysis. Reproducibility between sample replicates was calculated using intraclass correlation coefficients, which describe how strongly replicate samples within each group resemble each other. A value of 1 indicates perfect correlation, with lower values

representing more variation between samples within a group [472]. Mean Ct values were calculated for each sample for each gene from replicates and data were normalised using expression of *GAPDH* and *IPO8* according to the method of Vandesompele *et al.* [343], which is described in Chapter 2. Normalised gene expression quantities were used to calculate a fold change in expression between samples from patients that had relapsed and non-relapsers. The statistical significance of gene expression differences between the groups was assessed using the Mann-Whitney U test with the significance level being set at 0.05.

Non-normalised values for gene expression are given by the formula $(1+\text{efficiency of amplification})^{-\Delta\text{Ct}}$ [340]. For probes with 100% efficiency this equates to the formula $2^{-\Delta\text{Ct}}$, however as the efficiency of the assays in FFPE melanoma tissue was shown in Table 4-9 to be a mean value of 56%, the calculation was repeated using the formula $1.56^{-\Delta\text{Ct}}$ prior to normalisation. To compare gene expression results generated using different normalisation approaches, data was also normalised to *GAPDH* and *IPO8* separately using the $2^{-\Delta\Delta\text{Ct}}$ method as previously described in Chapter 2. Gene expression data from qRT-PCR was compared with that from the DASL assay using Spearman's rank correlation.

4.4.2.2 Results

4.4.2.2.1 Validation of DASL results

Nine samples failed to amplify with the probes for all genes assessed. Two further samples failed to amplify with the *RAD52* probe and three samples for the *RAD54B* probe. Negative controls failed to amplify as expected. Table 4-10 presents summary information about the assays used in this experiment. Mean Ct values for *RAD52* and *RAD54B* probes were higher than those for other genes and the intraclass correlation coefficients for replicate samples were lower. Mean Ct values were calculated from all calibrator samples for each probe for further analysis.

Table 4-11 presents the fold changes in mean gene expression between tumours from patients who relapsed (n=24) versus those that do not relapse (n=118). Table 4-11 also shows the different values obtained when analysis was normalised using the geometric mean of two control genes and each control gene separately, and the difference in values obtained when the lower efficiency of probes was taken into account when calculating relative quantities. The samples used for this analysis were from the Leeds Cohort study only, therefore Table 4-11 also presents the DASL results for the 142 samples used in this qRT-PCR validation for comparison with the merged dataset results in Table 4-1.

Gene	Mean Ct value for calibrator samples (n=4) (outliers removed)	Mean Ct value for test samples (n=133) (outliers removed)	Intraclass correlation coefficient for samples (outliers present)	Intraclass correlation coefficient for samples (outliers removed)
<i>GAPDH</i>	32.83	32.21	0.99	0.99
<i>IPO8</i>	35.36	35.26	0.94	0.97
<i>RAD52</i>	36.83	36.57	0.49	0.91
<i>RAD54B</i>	38.80	37.57	0.45	0.87
<i>TOP2A</i>	37.91	35.58	0.93	0.97

Table 4-10: Mean cycle threshold values and intraclass correlation coefficients for sample replicates for each qRT-PCR assay.

Mean Ct values for calibrator samples and test samples are presented following removal of outliers (156 values were classified as outliers from 2043 original Ct values). Intraclass correlation coefficients for replicate samples have been calculated before and after outliers have been removed.

Gene	Geometric mean normalisation, mean fold change (significance level)	Geometric mean normalisation - efficiency 0.56, mean fold change (significance level)	Normalised to GAPDH only $2^{-\Delta\Delta Ct}$, mean fold change (significance level)	Normalised to IPO8 only $2^{-\Delta\Delta Ct}$, mean fold change (significance level)	No. in DASL Cohort list of differentially expressed genes	Fold change in DASL cohort samples	Significance level in DASL cohort data
<i>RAD52</i>	0.72 (0.006)	0.81 (0.006)	0.56 (0.005)	0.80 (0.07)	125	1.09	0.08
<i>RAD54B</i>	1.08 (0.42)	1.07 (0.42)	0.80 (1.00)	1.38 (0.07)	4	1.35	0.00008
<i>TOP2A</i>	1.37 (0.01)	1.27 (0.009)	0.94 (0.26)	1.82 (0.0003)	29	1.16	0.004

Table 4-11: Fold changes in mean gene expression of *RAD52*, *RAD54B* and *TOP2A* in tumours of patients who relapse compared to non-relapsers as determined using qRT-PCR.

Column 1 presents results when normalised to the geometric mean of *GAPDH* and *IPO8* assuming the efficiency of the assays is 100%. Column 2 presents results when probe efficiency of 56% is used (as determined in FFPE melanoma tissues in section 4.4.1.1.2). Column 3 present results when normalised to the endogenous control gene, *GAPDH*, only using the $2^{-\Delta\Delta Ct}$ method. Column 4 presents results for data normalised to *IPO8* only (both columns assume probe efficiency of 100%). The Mann Whitney U test has been used to identify statistically significant differences between expression results between relapsers and non-relapsers and the significance value is presented. The final three columns show results from DASL analysis of 142 samples used in the qRT-PCR experiment, the first column shows the position of the gene on the list of most differentially expressed genes in relapsers versus non-relapsers, the second column show the fold change between relapsers and non-relapsers and the final column show the significance value from survival analysis using the proportional hazards model.

Expression of *RAD54B* and *TOP2A* was greater in tumours from relapsers versus non-relapsers using geometric mean normalisation and normalisation to *IPO8*. *TOP2A* was statistically significantly over-expressed, which is consistent with the DASL results, although over-expression of *RAD54B* did not reach statistical significance. *RAD52* was significantly under-expressed in tumours from relapsers versus non-relapsers, a result which therefore does not correlate with DASL results. Use of lower probe efficiencies to calculate relative quantities does not alter these results. To investigate the different results obtained for *RAD52* using these two methods, I looked at data from each of the three probes used in the DASL assay for *RAD52*. As presented in Table 4-12, expression results for *RAD52* from the DASL assay using the mean expression values from three probes do not correlate significantly with qRT-PCR results using Taqman assays (Spearman's rho 0.15, $p=0.08$). Two of the DASL probes are located on exon 12 of the *RAD52* gene and results from these probes correlated poorly with the qRT-PCR data (Spearman's rho -0.05 and 0.08, $p=0.59$ and 0.37, respectively). When a fold change in gene expression between relapsers and non-relapsers is calculated for these DASL probes, *RAD52* is over-expressed (fold change 1.05 and 1.08, respectively). The other *RAD52* probe is located on exon 4, closer to the Taqman assay which targets exons 2/3. DASL expression results correlate better with qRT-PCR results for this probe (Spearman's rho 0.26, $p=0.003$); however the fold change in gene expression for relapsers and non-relapsers for this DASL probe is smaller at 1.01. There may be a number of factors contributing to the lack of consistency across DASL results and qRT-PCR results. Results from the DASL or the qRT-PCR assay may be erroneous, which is supported by the lack of correlation between DASL expression results and qRT-PCR data for two of the three DASL assay probes. In addition, the fold change in gene expression between relapsers and non-relapsers was very small (1.01) for the probe which correlated with qRT-PCR results, decreasing the likelihood that this fold change would have been detected in the qRT-PCR experiment. Another factor that may also contribute to these results is the samples selected for qRT-PCR validation. As presented in Table 4-11, when DASL data for the 142 samples used in the qRT-PCR experiment is analysed, *RAD52* is the 125th gene most associated with RFS and expression is not significantly associated with RFS ($p=0.08$, fold change between relapsers and non-relapsers 1.09). In contrast, *RAD52* is the 4th gene most significantly associated with RFS in the merged dataset analysis ($p=0.00002$, fold change 1.16) (Table 4-1). Therefore, I could not validate DASL results for *RAD52* using qRT-PCR, likely due to lack of correlation between qRT-PCR results and DASL probes and lack of power within the dataset to identify gene expression differences between relapsers and non-relapsers.

	GAPDH and IPO8 geometric mean normalisation - efficiency 100%, Spearman's rho (p)			GAPDH and IPO8 geometric mean normalisation - efficiency 56%, Spearman's rho (p)			GAPDH only normalisation $2^{-\Delta\Delta CT}$, Spearman's rho (p)			IPO8 only normalisation $2^{-\Delta\Delta CT}$, Spearman's rho (p)		
	<i>RAD52</i>	<i>RAD54B</i>	<i>TOP2A</i>	<i>RAD52</i>	<i>RAD54B</i>	<i>TOP2A</i>	<i>RAD52</i>	<i>RAD54B</i>	<i>TOP2A</i>	<i>RAD52</i>	<i>RAD54B</i>	<i>TOP2A</i>
<i>RAD52</i>	0.15 (0.08)			0.15 (0.08)			0.06 (0.48)			0.16 (0.07)		
<i>RAD54B</i>		0.13 (0.13)			0.13 (0.13)			0.009 (0.92)			0.26 (0.003)	
<i>TOP2A</i>			0.55 (<0.0001)			0.52 (<0.0001)			0.34 (<0.0001)			0.72 (<0.0001)

Table 4-12: Correlations between DNA repair gene expression data derived from qRT-PCR and DASL.

Spearman's rho values and significance levels are presented for each gene. The first column compares gene expression results from qRT-PCR using the geometric mean of *GAPDH* and *IPO8* expression and assuming assay efficiency of 100%. The second column presents correlations between data when efficiency of assays is set at 56%. The third and fourth columns present correlations when qRT-PCR data has been normalised to *GAPDH* or *IPO8* respectively, using the $2^{-\Delta\Delta Ct}$ method and assuming a probe efficiency of 100%.

4.4.2.2.2 Comparison of normalisation methods

Table 4-12 presents the correlations between relative gene expression quantities calculated using qRT-PCR and gene expression values from DASL data. Irrespective of normalisation method or efficiency used to calculate relative quantities, expression of *TOP2A* using qRT-PCR correlated significantly with expression levels from DASL. Only when normalised to *IPO8* alone did expression of *RAD54B* correlate significantly between qRT-PCR and DASL. As discussed previously, expression of *RAD52* as determined by qRT-PCR is positively correlated with DASL expression data based on three probes, but not significantly. This is not altered by normalisation method and may contribute to the lack of correlation between fold changes in gene expression in relapsers and non-relapsers between the two methods. There are clearly differences in results depending on which normalisation method is used. Normalisation to *GAPDH* only decreases the differences between relapsers and non-relapsers with regards to *RAD54B* and *TOP2A* expression (Table 4-11), and decreases the correlation between qRT-PCR results and DASL results (Table 4-12). Normalisation to *IPO8* only increases the differences in gene expression of *RAD54B* and *TOP2A* and improves the correlation between DASL results and qRT-PCR results. This highlights the importance of correct normalisation. In view of these results it would be sensible to use genes which we have identified as being most stably expressed in melanoma samples in 4.4.1.2.2 (*CASC3* or *PES1*) instead of *GAPDH* in future work and undertake a similar assessment to compare results obtained with different normalisation techniques.

4.4.3 Summary of qRT-PCR methodological work

The work I have presented demonstrates that although the efficiencies of Taqman® Gene Expression assays are lower in RNA extracted from FFPE melanoma tissue, use of the comparative Ct method for gene quantification is valid. The importance of correct normalisation has been demonstrated and a number of suitable endogenous control genes (*PPIA1*, *POP4*, *IPO8*, *CDKN1B*, *CASC3* and *PES1*) for normalisation have been identified. DASL results for two genes have been validated using qRT-PCR (*TOP2A* and *RAD54B*), however results for *RAD52* could not be replicated.

4.5 Discussion

4.5.1 Development of methodology for qRT-PCR with FFPE melanoma tissue

The potential for reporting an erroneous result as a consequence of using a single gene expression platform, such as the DASL assay, is always a concern in gene expression work, thus it is important to confirm findings using another approach. I therefore attempted corroboration using qRT-PCR. This technique requires optimisation for use in different tissue types as amounts of starting material may vary, enzymatic efficiencies may differ and transcriptional activity can be highly variable [343]. “Housekeeping” genes, commonly used for normalisation, have expression which can vary considerably [459-461], leading authors to recommend that control genes are assessed for suitability in each experimental protocol [465]. In the case of FFPE melanoma tissue, optimisation is even more essential in view of the degraded RNA extracted from FFPE materials [291] and the presence of melanin which can interfere with PCR reactions [303].

This chapter therefore presents methodological work to investigate and optimise methods for qRT-PCR in FFPE melanoma tumours. The data described above show that there is not doubling of PCR product with every PCR cycle (100% efficiency) [340, 457] using Taqman® Gene Expression Assays in our degraded samples. However the efficiency of endogenous control genes is similar to those of test genes, and therefore a comparative Ct method is appropriate [340, 455]. This work has demonstrated that different normalisation strategies alter gene expression results. Using DASL gene expression data to compare qRT-PCR results using different normalisation strategies, use of *GAPDH* as a control gene decreases correlation between DASL and qRT-PCR results and fold changes in gene expression between relapsers and non-relapsers. This assessment is limited, as DASL results may themselves be subject to error; however in our assessment of candidate control genes, *GAPDH* was not as uniformly expressed as other genes, for example *CASC3* or *PES1*, making these genes more sensible choices for future gene expression work. Use of more than one control gene with uniform expression is more likely to yield accurate gene expression results so that many authors recommend use of at least three genes [343, 466]. This work represents a compromise using two genes, considering lack of available RNA and the number of genes quantified.

Despite efforts to optimise methods, validation of DASL results was only possible for two of the three genes assessed. This may be because of erroneous results from the DASL assay or the qRT-PCR assay; however it may also be because of a lack of

power to detect differences in gene expression level as a limited number of samples were used. This has not been assessed further as limited samples are available, but highlights the importance of a large sample set when attempting to identify small differences in gene expression levels.

4.5.2 Over-expression of DNA repair genes in melanoma tumours as a prognostic marker

Using the Illumina DASL assay, a group of genes has been identified with prognostic significance in melanoma. This technology has been used in a number of previous studies to identify prognostic markers using FFPE tissue using the Human Cancer panel [297, 473] and on a genome-wide scale [180, 474]. Genes of prognostic significance have been identified in uveal [475] and cutaneous melanoma (*SPP1*) (Chapter 3) [187].

The work described in this chapter represents the largest study to date using gene expression profiling to identify prognostic markers in melanoma, made possible by utilising FFPE primary melanoma tumours. A number of bioinformatics resources have been used to interrogate the data presented in this chapter. These systems are inherently biased as they are based on information currently available in the literature, however DNA repair genes and genes related to these processes were easily identified as a group of important genes by simple review of the list of genes significantly associated with survival. GO analysis confirmed the importance of these genes in DNA recombination, DNA replication and the M-phase of the cell cycle. Pathway analysis using DAVID highlighted that the data was derived from a cancer related gene panel, but also confirmed enrichment of genes involved in the cell cycle and DNA repair. Use of Ingenuity pathway analysis has identified correlations between genes associated with cell cycle control or DNA repair and the DNA repair genes identified in this analysis and has allowed generation of a network to visualise associations within the dataset. In summary, pathway analysis has helped to categorise and visualise the biological functions of genes within this dataset. The advantages of this are limited for gene expression data derived from a 502-gene cancer panel, but DAVID pathway analysis has highlighted the importance of focal adhesion and cytokines in our list of differentially expressed genes which may not have been identified by review of the list. Use of bioinformatics resources would be invaluable when using large, unbiased genome-wide data.

For this analysis we have assessed the data in a 'supervised' fashion to identify genes differentially expressed in tumours or patients with well documented characteristics,

such as relapse or Breslow thickness [448, 449]. This is the approach used in most previous microarray studies in melanoma tumours addressing gene expression associated with survival [177, 185], the exception being the recent report by Jonsson and colleagues which used unsupervised hierarchical clustering to identify groups of samples with similar gene expression profiles and then assessed prognosis between these groups [180]. With the detailed histological and survival data available in association with the samples analysed in this study, a supervised approach appears most sensible. Unsupervised analysis would also have been likely to identify groups of tumours within this dataset, however previous work indicates that most clustering performed in microarray datasets is not reproducible or reflective of patterns in a larger population [449, 476]. Identification of genes associated with survival can only be confirmed by validation in an independent sample set, an approach described in Chapter 3. Lack of validation of findings presented in this chapter represents a significant limitation of this work. We have been unable to identify a sample set of sufficient size to replicate these findings to date, however the development of microarray analysis in FFPE tissues will facilitate this in time.

There has been interest in the role of over-expression of DNA repair genes which has been associated with poorer prognosis in melanoma and metastasis in candidate gene [477, 478] and microarray studies [175, 177, 178]. These results are in agreement with those of Kauffman *et al.* who identified that over-expression of genes involved in recovery of stalled replication forks, especially genes involved in repair of double-stranded DNA breaks, were associated with melanoma metastasis in a study of 60 frozen melanoma tumours [177]. It has been suggested that in order for a melanoma cell to continue to divide and give rise to metastases, cells up-regulate genes associated with DNA repair processes to maintain genomic integrity [264]. This has been noted in other cancers such as bladder [479] and breast cancer [480, 481], however the proportion of DNA repair genes that are over-expressed in melanoma tumours that will metastasise is particularly high (90%) compared with bladder cancers (82%) and breast cancers (58-80%) [264]. Over-expression of DNA repair genes may help to explain why melanoma tumours are so especially resistant to chemotherapy and radiotherapy [264], a hypothesis which will be further investigated in Chapter 8.

The majority of genes identified in this work are involved in double-strand break (DSB) repair by homologous recombination (*RAD51*, *RAD52*, *RAD54B*, *RAD54L*, *BRCA1* and *BRCA2*) [264, 482]. (Figure 4-6). To repair DSBs, DNA is resected to expose single-stranded DNA (ssDNA) to which RAD51 binds, a process enhanced by direct interaction of RAD51, RAD52 [483-485] and the ssDNA binding protein replication protein A (RPA) [482]. RAD51 wraps around DNA to form a nucleoprotein filament in

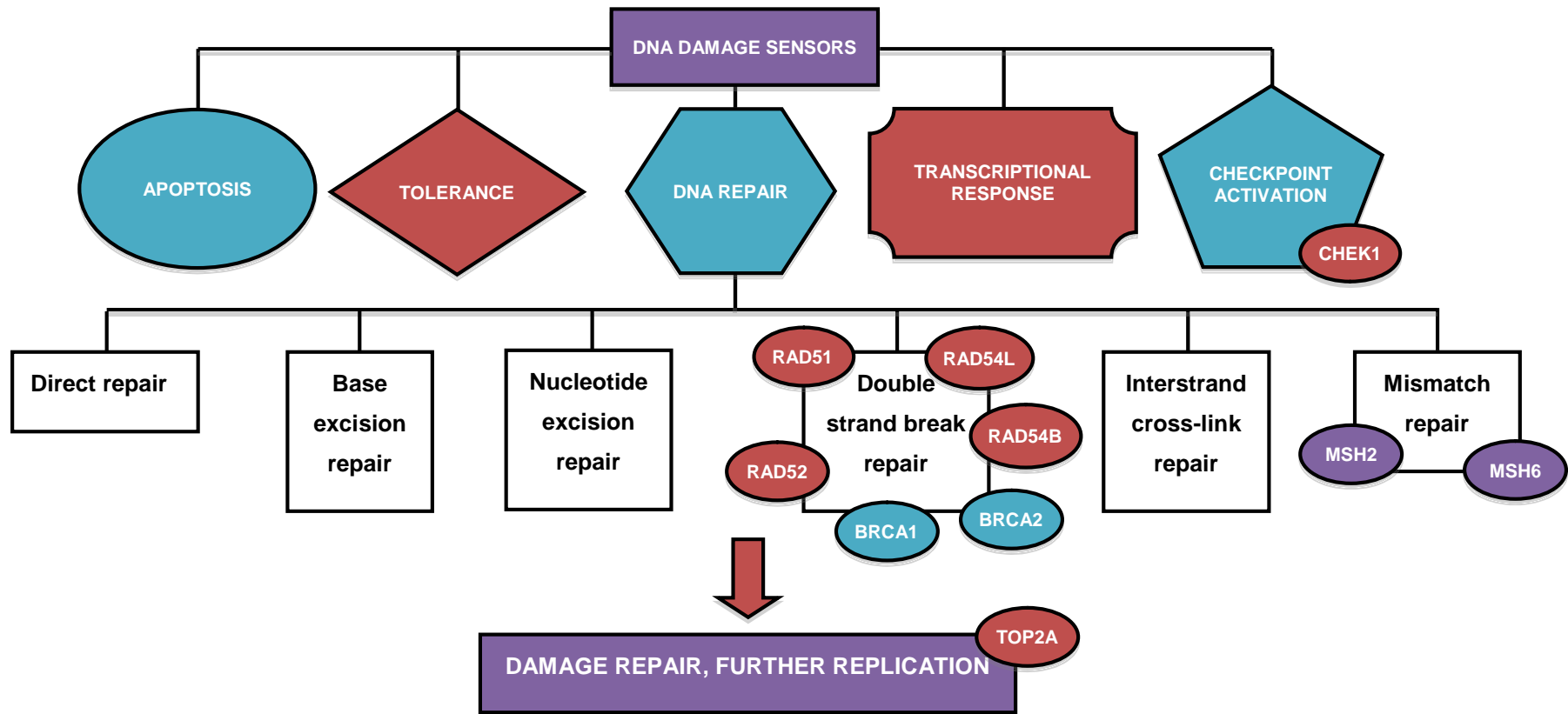


Figure 4-6: DNA repair mechanisms.

Adapted from reference [486]. DNA damage leads to a number of responses and repair mechanisms within a cell. The genes identified in this work are mostly related to double-stranded break repair and mismatch repair.

which DSB repair takes place [487], RAD52 is also involved in single strand annealing independently of RAD51 [488]. During DSB repair, ssDNA invades into double-stranded DNA (dsDNA) within the nucleoprotein filament, a process that requires binding of a cofactor such as ATP [489, 490]. Studies with yeast proteins have revealed that the efficiency of this binding is dependent on RAD54 [491]. The *RAD54* gene has significant homology with the human *RAD54B* gene [492]: RAD54L is also known as human RAD54 and has similar functions to those of RAD54 in yeast [493]. Once ssDNA has paired with dsDNA, strand exchange can occur. RAD51 and RAD52 promote capture of the other ssDNA tail, and DNA is synthesized using the two ssDNA ends as primers. Once DNA synthesis is complete, crossovers between DNA duplexes are resolved to allow repaired chromosomes to separate [482]. BRCA2 interacts with both RAD51 [494] and BRCA1. BRCA1 and BRCA2 are required for DSB repair by homologous recombination in cell lines, probably via RAD51-mediated DNA repair [482, 495, 496]. CHEK1 is part of the cell-cycle checkpoint pathway; it is a protein kinase activated by DNA damage such as DSBs and stalled DNA replication forks, which prevent progress from the G₂ to M phase of the cell cycle [177, 497]. *MSH2* and *MSH6* are not involved in DSB repair, but are mismatch repair genes that produce proteins which repair errors made in base-pairing by DNA polymerases during replication [177, 498]. *TOP2A* is another gene not involved in repair of DSBs, but induces transient DNA breaks to allow changes in DNA topology during DNA replication [499]. Expression of *TOP2A* closely reflects the proliferative activity of cells [499].

Formation of DSBs and DNA damage occurs during replication of cells, so it is unsurprising that DNA repair genes are over-expressed in more aggressive tumours with greater mitotic rate and Breslow thickness. As discussed above, it has been suggested that more aggressive tumours up-regulate DNA repair genes to allow more error-free cell division [264]. However an actively dividing tumour may well have higher levels of DNA repair gene expression secondary to DNA replication, an observation supported by the fact that *TOP2A* expression reflects the proliferative activity of non-malignant cells [499]. It is likely that a combination of these factors contributes to higher DNA repair gene expression. Using principal component analysis of genes associated with RFS, Breslow thickness and mitotic rate, we have shown that many of the genes with expression levels that correlate with the first principal component are involved in DNA repair processes and the cell cycle, indicating that over-expression of genes involved in these pathways is common in tumours with poorer prognosis, perhaps reflecting increased proliferation in these cells. *RAD52* is an exception, as expression levels were not correlated with expression of other genes involved in DSB

repair such as *RAD54L* and *BRCA2*. This may reflect the additional function of *RAD52* in repair by single strand DNA damage [488]. The correlation between genes involved in cell cycle control and genes identified in this analysis associated with prognosis is expected, given the importance of tumour mitotic rate as a prognostic marker [58].

RAD51 is the central protein involved in the DSB process and is over-expressed in many tumours [500]. Previous reports have identified the association between *TOP2A* expression and aggressive tumour features in prostate [501], hepatocellular carcinoma [502] and colorectal cancer [503]. More recent work has confirmed that high *TOP2A* gene expression is associated with shorter metastasis-free interval in breast cancer [504]. A recent study, published following the work described in this chapter [505], in 223 FFPE primary melanoma tumours has confirmed the association between poorer survival, prognostic tumour factors (Breslow thickness, ulceration and mitotic rate) and over-expression of *BRCA1* and DNA damage signalling genes [335].

In summary, in this large study of FFPE primary melanoma tumours, over-expression of DNA repair genes is associated with poorer survival and adverse histopathological features. The fact that over-expression of a number of the genes identified has already been published in the literature using gene expression profiles from frozen melanoma tumours [177] provides evidence that this finding is biologically relevant in melanoma and that the DASL assay is yielding results from FFPE tissue which corroborate with results using other microarray platforms with intact RNA. Expression of *RAD52* and *TOP2A* have independent prognostic value, even when analysis is adjusted for host factors known to be of prognostic importance in melanoma. A limited sample set was used to validate the over-expression of a number of genes in tumours from patients who relapse versus non-relapsers using qRT-PCR. *RAD52* was under-expressed in relapsers from qRT-PCR data, in contradiction with DASL data. However, over-expression of *TOP2A* was confirmed, and in view of the independent prognostic value of over-expression of *TOP2A*, this could be a candidate for a prognostic biomarker in melanoma requiring validation in an independent sample set.

Using FFPE tissue for gene expression analysis is challenging, however these efforts enable analysis of large numbers of samples with mature survival data and well-annotated tumour and patient characteristics. Studies of this kind will undoubtedly improve our understanding of the biological processes associated with melanoma progression and allow identification of prognostic biomarkers.

5 Identification of differentially expressed genes in matched formalin-fixed paraffin-embedded primary and metastatic melanoma tumour pairs

5.1 Aims

The main aim of this study was to assess the performance of the cDNA-mediated annealing, selection, extension and ligation (DASL) assay using very small formalin-fixed paraffin-embedded (FFPE) sentinel node biopsy (SNB) samples. Additional aims were:

- To identify tissue factors of small SNB samples which determine performance with the DASL assay.
- To clarify which quality control measures and sample characteristics determine performance on the array using small/ SNB samples.
- To assess use of number of detected genes as a quality control measure of sample performance with the DASL assay.
- To compare gene expression profiles between matched primary and SNB samples to identify differentially expressed genes.

These data have been published in part [506].

5.2 Introduction

Current predictors of outcome for melanoma fail to identify a proportion of patients with “low-risk” melanoma who go on to relapse [58, 121]. Therefore, there is a need to investigate the somatic genetic changes in the primary tumour which determine metastatic capacity. A number of studies have used naevi, primary melanomas and metastatic melanomas to assess alterations in gene expression profiles during melanoma progression [176, 182, 190, 193, 507, 508]. However, many of these studies have used limited numbers of samples because of lack of cryopreserved tissue for genomic work, and have often assessed gene expression in primary and metastatic tumours from different patients for the same reason [176, 190, 507]. Heterogeneity of primary melanoma tumours, germline genetic variation and epigenetic influences are postulated to modify gene expression profiles in melanoma tumours [509], therefore

assessment of gene expression profiles in matched primary and metastatic tumours from the same patient may yield more insight into the mechanisms of melanoma progression.

The sentinel lymph node is the usual site of initial metastasis in melanoma, with sentinel lymph node status being the single most important prognostic factor for patients without any other evidence of metastatic spread [58, 80]. The identification of gene expression differences between primary and nodal metastases is desirable in order to identify key pathways involved in this pattern of metastasis. Koh and colleagues compared whole-genome expression profiles in four matched FFPE primary and sentinel node biopsy samples, which were either macrodissected or sampled using laser capture microdissection, along with 11 unpaired specimens [510]. This study identified differential expression of 576 genes in unpaired samples, with most differences reflecting lower gene expression in metastatic samples compared to primary samples. This pattern was replicated in the matched specimens. Genes differentially expressed were typically associated with processes relevant to tumour metastasis, such as apoptosis, cell adhesion and the cell cycle [510].

This chapter reports a pilot study designed to assess the utility of the DASL assay to identify differentially expressed genes in extremely small FFPE SNB samples. In contrast to our sampling method for primary melanoma samples using a tissue microarray needle, laser capture microdissection (LCM) was used to sample these very small tissues. This technique has the advantage that single melanoma cells can be identified and sampled [511], although it is time consuming for large numbers of samples. LCM is discussed in further detail in Chapter 2.

Data from SNB samples have been compared with gene expression data from matched primary melanoma tumours where possible to explore the feasibility of using the DASL assay to identify genes differentially expressed between primary and early metastatic tumours which has the potential to give insight into early metastatic processes. In our previous work using primary melanomas, we have used the number of genes detected in each sample using the DASL assay (probe signal significantly greater than average signal from negative controls with $p < 0.05$) as a measure of the quality of results [294], indeed we have deemed a sample as “failed” with less than 250 (50%) genes expressed. This was a somewhat arbitrary cut off derived from previous reported studies [294]. My work with nodal biopsies has highlighted significant differences in the number of genes detected across different tissues and control RNA samples along with different patterns of “failed” probes, leading to a reappraisal of use of number of detected genes as a quality control measure.

5.3 Further methodological details

5.3.1 Sampling of nodal and primary tumours

FFPE SNB samples and primary tumours were identified from The Leeds Melanoma Cohort Study (Cohort study) and the Retrospective Sentinel Node Biopsy Study (SNB study) which are fully described in Chapter 2. From the Cohort study eight positive SNB samples were identified and from the SNB study, seventeen positive SNB samples were identified, from patients whose primary tumours had already been sampled for DASL studies as described in Chapters 3 and 4.

There was much variation in tissue availability between samples ranging from 8 cells (as detailed in the histopathology report) to large parenchymal deposits and we elected to test the sensitivity of DASL by attempting to extract RNA from all. For eight nodal samples, tumour was sampled using LCM from two new 5 micron sections cut from the nodal tumour block. For three samples no tumour remained on the nodal tumour block so a diagnostic haematoxylin and eosin (H+E) slide was used for tumour sampling following removal of the coverslip. For the remainder of the samples, archival unstained sections were available from Professor Martin Cook at the Royal Surrey County Hospitals NHS Foundation Trust. Details of coverslip removal, sectioning, section staining, LCM and RNA extraction are included in Chapter 2 and were undertaken by myself. LCM was performed under the supervision of Dr Andy Boon who is a dermatopathologist.

Primary tumour blocks were sampled using a tissue microarray (TMA) needle. Tissue cores were de-waxed and RNA extracted using the High Pure Paraffin RNA kit according to the manufacturer's protocol. Further methodological details are included in Chapter 2. Tissue sampling and RNA extraction of primary samples were performed by Dr Caroline Conway (Cohort study), Dr Angana Mitra (SNB study) and Samira Lobo. RNA concentration for nodal and primary samples was assessed using the ND-8000 spectrophotometer (NanoDrop, Wilmington, DE, USA).

5.3.2 Gene expression profiling using the DASL assay

The Illumina DASL Human Cancer panel was used for gene expression profiling as previously described in Chapter 2 by Floor de Kort at ServiceXS (Leiden, Netherlands). As a final quality control measure, quantitative Real-time PCR (qRT-PCR) of the housekeeping gene, *RPL13a*, was performed for each sample as described in Chapter 2 by Floor de Kort.

RNA samples derived from nodal specimens were sent for DASL analysis with RNA from primary specimens from the SNB study. Primary samples from the Cohort study were analysed in a separate DASL experiment. Data from the Cohort study and SNB study were normalised separately and merged for analysis as described in Chapter 4. Gene expression data from nodal samples were normalized with primary samples.

To monitor variation across plates and runs of the DASL assay, technical replicates were placed across plates within each run as described in Chapter 2 and a total of 10 replicate Stratagene Universal Human Reference RNAs (Agilent Technologies, Edinburgh, UK) were assessed across the two DASL experiments. These reference RNAs are composed of RNA from 10 human cell lines, including a melanoma cell line [512].

5.3.3 Statistical methodology

Associations between the area of tissue microdissected, reported size of tumour deposit and concentration of extracted RNA were investigated using Spearman's rank correlation.

In the DASL assay, the number of genes detected in each sample (probe signal significantly greater than average signal from negative controls with $p < 0.05$) was used as a measure of the quality of the results for our initial analysis. The influence of area of tissue microdissected, reported metastasis size, age of tissue block and age of the tissue slide on the number of genes detected was assessed using Spearman's rank correlation. The association between type of tissue section used for microdissection (new sections, diagnostic H+E slides or archival unstained sections) was assessed using the Kruskal-Wallis test. Quality control methods used to measure quality and quantity of RNA prior to use in the DASL assay were assessed by correlating the number of genes detected in samples with the quality measure data using Spearman's rank correlation. To assess reproducibility across the DASL runs, Spearman's rank correlation was used to assess gene expression across reference RNA samples.

The number of genes detected using the DASL assay in each sample has been traditionally used as a measure of the quality of the results with authors excluding samples with <50% genes detected [294]. To assess use of this measure in further detail in different tissue types, the mean number of genes detected in each tissue type (primary, nodal and reference RNA) was calculated and based on the cumulative distribution of number of detected genes, nodal samples with <166 genes detected and primary samples with <400 genes were excluded from further analyses. Genes which

failed across all samples of a particular tissue type (primary, nodal and reference RNA) were also identified.

Negative expression values for genes were removed for further analysis. Mean gene expression was used for any replicate samples. Correlation between gene expression levels in matched nodal and primary samples was assessed using Spearman's rank correlation. For each matched primary and nodal pair, the fold change in gene expression between nodal and primary sample was calculated for each gene. Genes were ranked in order of mean fold change in gene expression between primary and nodal samples across the matched pairs. Primary tumour details were derived from central pathology review as described in Chapter 2, SNB histology details were derived from histopathology reports. Patient details were available from study databases with survival variables assessed on 19th December 2011.

5.4 Results

5.4.1 Areas of nodal tumour sampled and RNA yields

Twenty-five nodal samples were selected for sampling (Figure 5-1). The size of deposits ranged from 8 cells seen within a section to 14mm in diameter. The majority of samples had both parenchymal and subcapsular deposits (55%), with smaller numbers having parenchymal (32%) or subcapsular deposits (9%) only (site of metastases was not recorded on the histopathology report for one sample). The area of tumour microdissected varied from 157 μm^2 to over $6 \times 10^6 \mu\text{m}^2$ which correlated well with the reported size of tumour deposit (Spearman's rho 0.76, $p=0.0001$). The mean concentration of RNA extracted was 32.5ng/ μl (range 0.4-73.1ng/ μl) but this measure did not correlate with area of tissue microdissected (Spearman's rho 0.08, $p=0.70$) or metastasis size as reported by the histopathologist (Spearman's rho 0.25, $p=0.31$).

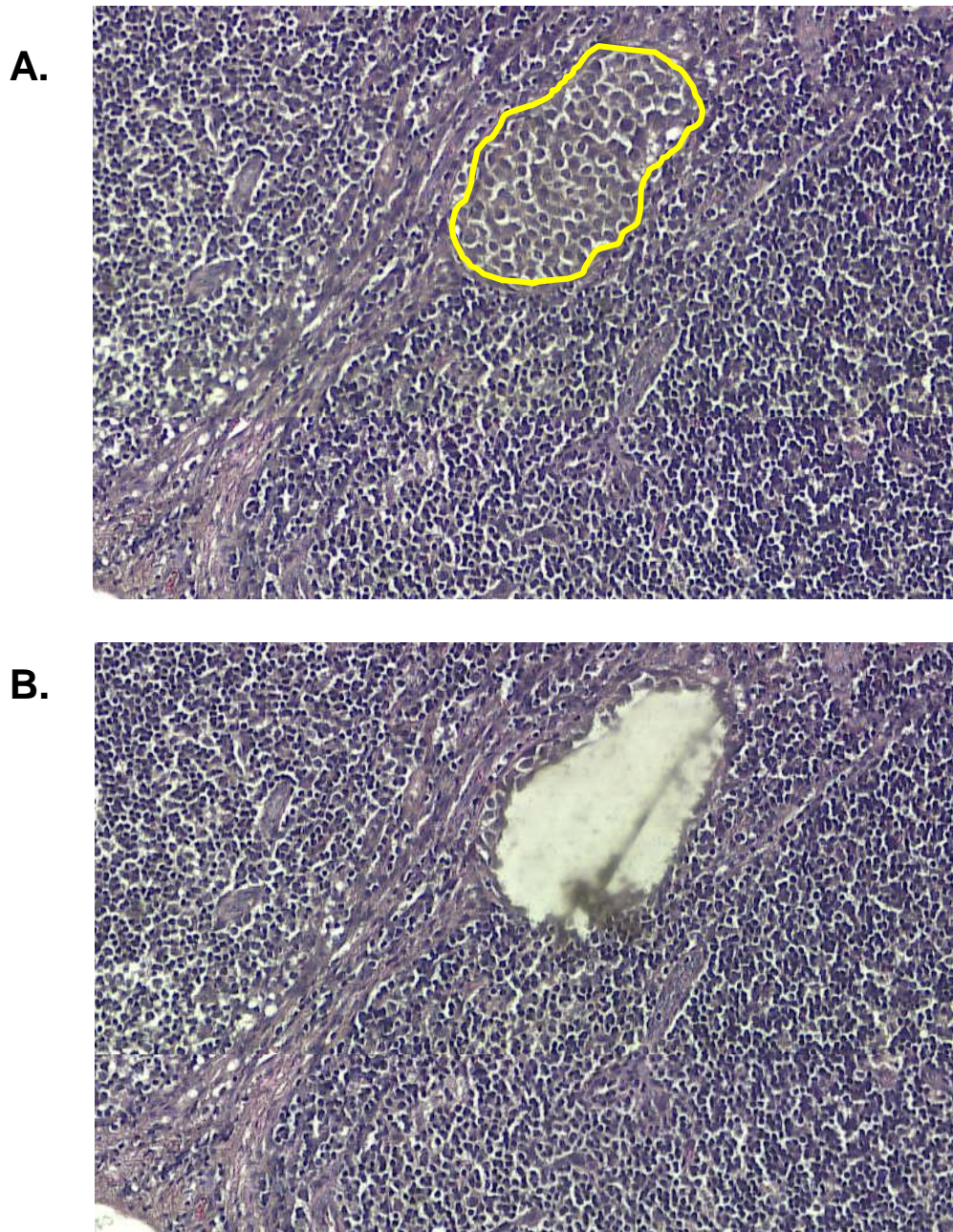


Figure 5-1: Representative nodal sample before laser capture microdissection (A) and following laser capture microdissection (B).

5.4.2 Quality control measures, tissue characteristics and performance of samples with the DASL assay

One nodal RNA sample, microdissected from a diagnostic H+E slide, was not sent for DASL analysis because of low RNA concentration (0.37 ng/μl), therefore a total of 26 nodal samples (including 2 replicate samples) were supplied to ServiceXS who performed the DASL assay. The mean number of genes detected from nodal samples (mean 242 (range 36-369)) was significantly less than number of genes detected from primary tumours (mean 434 and 457 from the Cohort and SNB studies, respectively), as reported in Chapter 3.

The characteristics of nodal samples and results of quality control measures are summarized in Table 5-1. Neither the area of tissue microdissected, RNA concentration as measured using spectrophotometry or cycle threshold (Ct) values generated from qRT-PCR of *RPL13a* correlated with number of genes detected in the DASL assay. However, the age of the FFPE tumour block (Spearman's rho -0.50, p=0.01) and the age of the tissue section prior to RNA extraction (Spearman's rho -0.51, p=0.01) both negatively correlated with number of genes detected (Table 5-1). The mean number of genes detected from the oldest tumours (>4.47 years) was 72 less than from the newer specimens (<2.29 years) (Table 5-1)

The type of section used for tumour sampling also influenced the number of genes detected (Table 5-2), with a lower proportion of samples failing the assay and a higher mean number of genes detected in newly cut sections (280 genes) or diagnostic H+E sections (301 genes) than from archival unstained sections (219 genes). The stored unstained sections were stored without a cover slip at room temperature.

	Nodal samples	Associations between sample factors and number of genes detected. Test statistic and significance value.
Area of tissue microdissected, median (range), μm^2	223124 (157-6051771)	
Number of genes detected for each quartile of area dissected, mean (range):		Spearman's rho -0.18, $p=0.41$
<25%	262 (182-365)	
25-50%	229 (167-275)	
50-75%	260 (209-314)	
>75%	237 (166-369)	
RNA concentrations, median (range), ng/ μl	30.3 (0.4-73.1)	Spearman's rho 0.18, $p=0.39$
Ct value, median (range)	24.1 (20.8-25.2)	Spearman's rho -0.05, $p=0.83$
Age of tissue block, median (range), years	3.8 (1.1-6.9)	
Number of genes detected for each quartile of block age, mean (range):		Spearman's rho -0.50, $p=0.01$
<2.29 years	299 (249-365)	
2.29-3.76 years	253 (193-369)	
3.77-4.36 years	217 (166-290)	
>4.47 years	227 (182-325)	
Age of tissue slide (before RNA extraction), median (range), months	41.5 (0.3-75.5)	Spearman's rho -0.51, $p=0.01$
Slide type, number (mean number of genes detected):		Kruskal-Wallis χ^2 8.79, $p=0.01$
New section	8 (280)	
Old unstained section	14 (219)	
Diagnostic H+E slide	3 (301)	
Number of genes detected, mean (range)	242 (36-369)	

Table 5-1: Characteristics of nodal samples and extracted RNA.

Associations between these factors and the number of genes detected in the DASL assay are presented. Significant results are highlighted in bold.

Abbreviations used: Ct, cycle threshold; H+E, haematoxylin and eosin.

Slide type	Number of samples	Number RNA successfully extracted and sent for analysis (%)	Number of genes detected, mean (range)	Number successful with DASL (≥ 240 genes detected) (% of samples assayed)	Area microdissected median (range), μm^2
Diagnostic H+E slide	3	2 (67)	301 (236-365)	1 (50)	138253 (13529-654932)
Archival unstained section	14	14 (100)	219 (166-325)	4 (29)	277555 (157-6051771)
New section	8	8 (100)	280 (227-369)	6 (75)	302413 (65346-2007508)

Table 5-2: Characteristics of sections used for tissue sampling.

The numbers of samples that yielded sufficient RNA for DASL analysis and were successful with the assay are presented in addition to the mean number of genes detected and area of tissue microdissected. Abbreviations used: H+E, haematoxylin and eosin.

5.4.3 Exclusion of samples

As discussed previously, in the DASL assay, the number of genes detected in each sample has been traditionally used as a measure of result quality with authors excluding samples with $<50\%$ genes detected [294]. The number of genes detected in nodal samples is much less than in primary samples (Figure 5-2) which from the literature was expected in a biological sense, but might also reflect poorer quality of gene expression data related to the smaller tissue sample. Based on the cumulative distribution of the number of genes detected (Figure 5-2), nodal samples with <166 genes detected and primary samples with <400 genes detected were excluded from further analyses. One nodal sample was excluded, however as this sample was a replicate, data from the other specimen could be used for analysis. No primary samples were excluded.

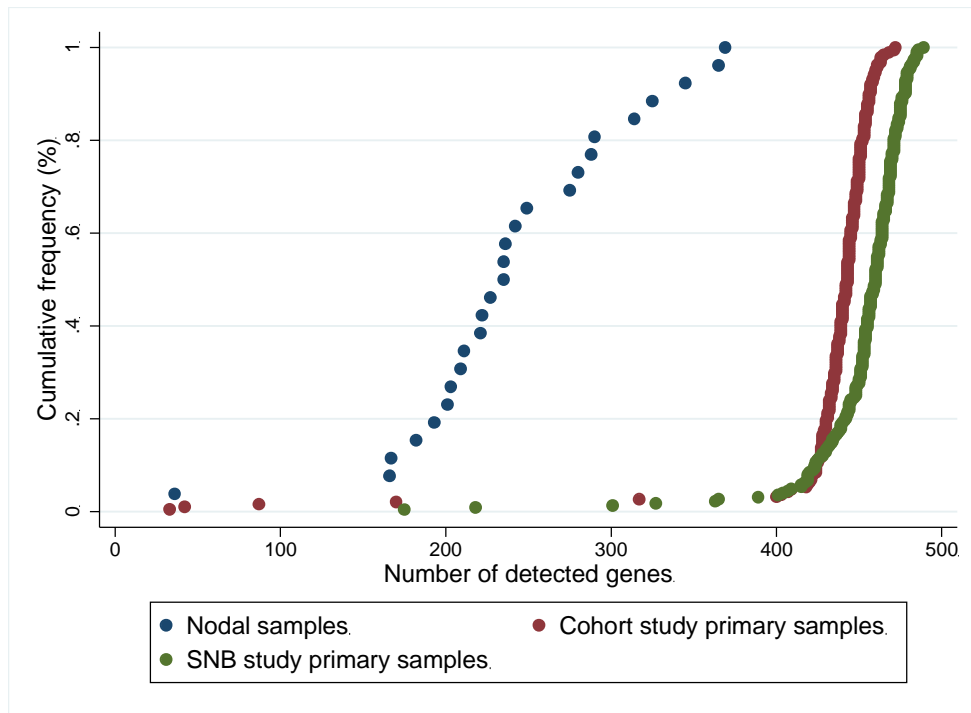


Figure 5-2: Cumulative distribution of number of detected genes in nodal and primary samples.

The cumulative distribution for primary samples is based on the larger sample sets previously assessed with the DASL assay as described in Chapter 3.

To assess whether our approach of excluding nodal samples with <166 genes detected was valid, we performed further analyses to identify genes differentially expressed between matched samples when the threshold for detection was higher. Samples were excluded when less than 240 genes were detected allowing assessment of 10 matched pairs and less than 200 genes allowing assessment of 18 matched pairs. Reassuringly, 12 of the most differentially expressed genes (presented in Figure 5-4) identified in these analyses matched those from the current analysis with *MMP2* remaining the gene most over-expressed in primary samples and *CSF3* the gene most over-expressed in nodal samples in all tumour pairs. This suggests that our results are representative of a larger sample set and that exclusion of nodal samples with <250 genes detected as suggested by previous authors [294] is an over-conservative approach to this particular analysis.

5.4.4 Reproducibility and detected genes across reference RNA samples

Across the two DASL runs, for the Cohort samples and the SNB primary and nodal samples, gene expression profiles across the ten reference RNAs were reproducible (Spearman's rho 0.90-0.99 ($p < 0.00001$)) and the mean number of genes detected in reference RNA samples was 479 (Cohort study) and 472 (SNB study).

5.4.5 Genes detected across tissue types

Eight genes were not detected across all 10 reference RNA samples including genes identified as being over-expressed in nodal samples in this analysis (*CSF3*, *FGF3*, *FGF6*, *FGF8* and *MOS*). I would argue this is because those genes were simply not expressed in the reference RNA samples chosen rather than because of a methodological issue. Only one gene (*MYCL2*) was not detected across all nodal samples assessed and there were no genes that were not detected across the primary samples assessed. The 502 genes on the Human Cancer panel were selected because of their importance in the cancer literature and therefore it is not perhaps surprising that some genes were not detected in the control RNAs but were seen in nodal and primary samples from a particular cancer type.

5.4.6 Correlations between matched primary and nodal samples

Of the samples successfully yielding gene expression data, 22 had matched primary samples for which gene expression data were available. Gene expression from 21 of the matched pairs was correlated to varying degrees (Spearman's rho 0.15-0.80, all significance values ≤ 0.001) (Figure 5-3).

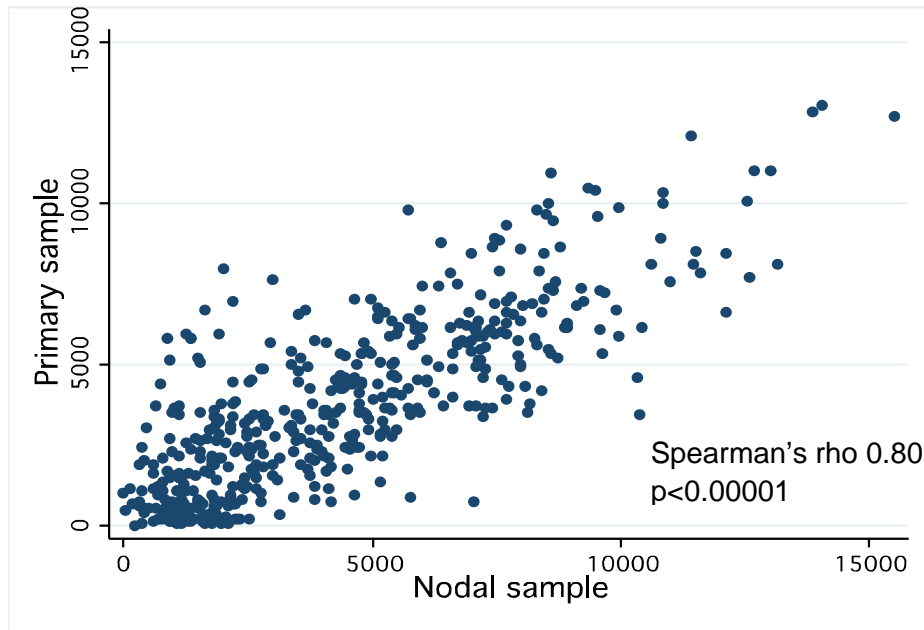


Figure 5-3: Association between gene expression levels for 502 genes from the Human Cancer panel for a matched primary and nodal sample from the same patient.

5.4.7 Genes differentially expressed in matched primary and nodal pairs

Table 5-3 and Figure 5-4 present genes most differentially expressed between nodal tumours and their matched primary tumours. For genes most over-expressed in nodal tumours, 9 out of 10 genes were over-expressed in all nodal samples from all matched pairs assessed (fold changes presented in Table 5-3). Gene expression data from nodal samples were normalized with primary samples. As the number of genes detected and pattern of gene expression differs between these tissue types, normalization procedures will have altered the magnitude of expression differences and absolute fold changes should be interpreted with caution.

A number of genes were differentially expressed in nodal metastases across all matched pairs including genes involved cellular proliferation and survival (*FGF3*, *FGF5*, *FGF6* and *FGF8*).

Higher gene expression	Gene	Mean fold difference (nodes/primaries)	Min fold change across matched pairs	Max fold change across matched pairs
Primaries	<i>MMP2</i>	0.40	0.12	1.04
	<i>ETV6</i>	0.41	0.17	1.17
	<i>PDGFRB</i>	0.44	0.15	1.28
	<i>KIT</i>	0.46	0.13	1.20
	<i>FYN</i>	0.47	0.18	1.02
	<i>EMS1</i>	0.47	0.10	1.42
	<i>PRCC</i>	0.47	0.16	1.19
	<i>CREBBP</i>	0.48	0.24	1.20
	<i>MXI1</i>	0.48	0.02	1.10
	<i>GAS7</i>	0.48	0.22	1.34
Nodes	<i>CSF3</i>	34.67	2.53	269.72
	<i>ERBB4</i>	29.53	1.99	169.66
	<i>FGF3</i>	26.22	2.96	160.62
	<i>PLG</i>	25.63	4.33	162.57
	<i>PLA2G2A</i>	15.90	1.65	196.99
	<i>MOS</i>	15.27	0.92	32.04
	<i>FGF8</i>	15.01	1.41	77.26
	<i>TFF1</i>	14.09	2.41	45.97
	<i>FGF6</i>	13.74	5.26	38.00
	<i>FGF5</i>	13.34	2.30	84.54

Table 5-3: Genes most differentially expressed across matched primary and sentinel node biopsy samples.

The mean fold difference in gene expression between nodal and primary samples and range of fold differences across 22 matched pairs is presented.

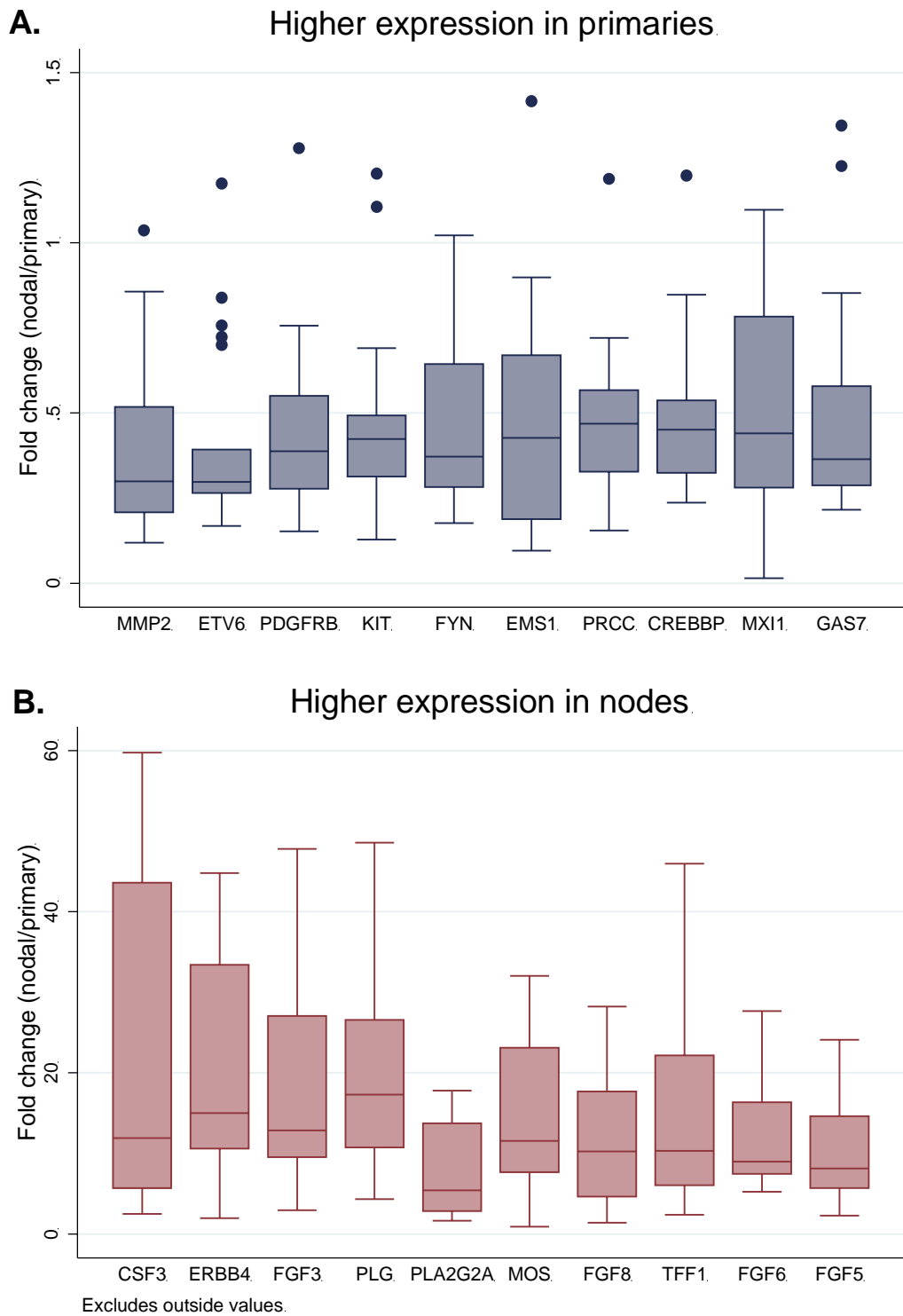


Figure 5-4: Genes most differentially expressed across matched primary and sentinel node biopsy samples.

Box-plots are presented for genes most over-expressed in primary (A) and nodal (B) samples. Outside values are excluded for clarity from graph B.

5.4.8 Patient and primary tumour characteristics

To provide some information regarding the final sample set analysed for this study, details of patients and key tumour characteristics are presented in Table 5-4.

Characteristic	
Breslow thickness, mm, median (range)	2.6 (0.9-6.0)
Mitotic rate, mm ² , median (range)	9 (1-39)
Ulceration, number (%):	
Absent	14 (63.6)
Present	7 (31.8)
Not recorded	1 (4.6)
Histological subtype, number (%):	
Superficial spreading	15 (68.2)
Nodular	2 (9.1)
Other	3 (13.6)
Not recorded	2 (9.1)
Tumour site, number (%):	
Trunk	9 (40.9)
Leg	8 (36.4)
Arm	1 (4.6)
Head or neck	3 (13.6)
Sun-protected site	1 (4.6)
Age at diagnosis, years, median (range):	56.8 (23.2-77.7)
Patient gender, number (%):	
Female	10 (45.5)
Male	12 (54.5)
Relapse status, number (%):	
Not relapsed	13 (59.1)
Relapsed	9 (40.9)
Relapse-free survival time, years, median (range)	2.7 (0.2-6.0)
Survival status, number (%):	
Alive	12 (54.6)
Died	10 (45.5)
Overall survival time, years, median (range)	3.4 (0.7-6.0)

Table 5-4: Clinical characteristics of patients and key primary tumour histological features of the samples assessed in analysis of matched primary and sentinel node biopsy specimens.

In primary samples used in this analysis, the median Breslow thickness (2.6mm), mitotic rate (9/mm²) and proportion of ulcerated tumours (32%) were greater than in the larger sample sets used for gene expression analysis in Chapter 3, reflecting the fact that these patients had higher risk disease associated with a positive sentinel node

biopsy. This is also reflected by the high proportion of patients who subsequently relapsed (41%) and died (46%). Most tumours were of the commonest superficial spreading subtype (68%) and from the trunk (41%) or leg (36%) in common with the larger gene expression sample set. There were more men than women in this sample set (55% and 45%, respectively).

5.5 Discussion

5.5.1 Use of the DASL assay with small sentinel node biopsy samples

This pilot study had a number of aims, the first of which was to identify the lower limits of volume of small tumour samples which can be used to generate gene expression data from the DASL assay. A deposit reported as being only 8 cells in size provided data, suggesting that very small FFPE tumour samples can be used to assess gene expression.

Quality control measures have been used to assess the relative performance in primary versus smaller nodal tumours. The traditional measure of performance is the total number of genes detected and in this respect, the assay did not perform as well with these samples as with RNA extracted from larger primary tissue cores. Other studies however provide some evidence to support the view that the number of genes expressed in metastases is smaller than in primaries, consistent perhaps with Fidler's hypothesis that metastases occur from sub clones of the primary [513, 514]. Previous gene expression studies in melanoma furthermore have demonstrated that the predominant change in advanced malignancy is decreased gene expression [176, 193]. Decreased expression has also been found in less advanced SNB metastases in comparison with primary tumours [510]. Therefore, number of genes detected may not be the best measure of assay performance and consequently we have included all nodal samples with a reasonable number of detected genes in this analysis.

Despite the problems using number of detected genes as a quality control measure, there are no other options for assessing the performance of a sample with the DASL assay. It is likely that a smaller number of genes would be detected in a poorly performing sample relative to other samples of the same tissue type, therefore we have used this measure to assess current RNA quality control measures. I found no relationship between the number of detected genes and RNA concentration by spectrophotometry or Ct values generated using qRT-PCR of *RPL13a*. We did find that

the age of the tissue sample and the age of tissue section used for sampling influenced the number of detected genes, suggesting that newer tissue blocks with freshly cut sections would be most likely to yield gene expression data. Previous published studies using the DASL assay have used a number of tissue sections with or without macrodissection or tissue cores for RNA extraction [296, 297, 474, 475], therefore it is likely that use of a larger number of freshly cut tissue sections for microdissection may have yielded better results. Previous evidence suggests that measures such as storing sections at 4°C or coating with paraffin preserves tissue antigenicity for use in immunohistochemistry [515, 516]. This work supports the hypothesis that similar measures may also preserve utility of stored cut sections for genomic work.

5.5.2 Genes differentially expressed in matched primary and SNB samples

Gene expression data derived from SNB samples were compared with those from matched primary tumour from the same patient. There was good correlation overall between gene expression profiles from matched primary and nodal samples as has been reported previously in a number of tumour types including melanoma [507, 508, 514, 517], which is reassuring methodologically. However, there were some interesting differences. Significant differences in gene expression profiles between primary tumours and matched metastases have been identified in melanoma [510], breast [518, 519] and colorectal cancer [520, 521] previously and in this current study a number of genes were differentially expressed in nodal metastases across all 10 matched pairs assessed. Genes coding for fibroblast growth factors were amongst these genes.

Fibroblast growth factors (FGFs) signal through FGF receptors (FGFRs) and regulate developmental pathways as well as wound repair and angiogenesis [522]. With broad mitogenic and angiogenic activities [523], FGFs are frequently overexpressed in a number of tumour types [524-526]. Furthermore, increased expression of FGF3 and FGF8 has been associated with higher grades of prostate cancer [527] and recurrence of hepatocellular carcinoma [528]. In melanoma, there has been interest in FGF2 as there is over-expression of FGF2 protein and *FGF2* transcripts in melanoma cell lines compared to melanocytes [529, 530] and in melanoma tumours [531]. Over-expression of FGF2 leads to transformation of melanocytes [532], with inhibition leading to regression of tumours in mice due to lack of angiogenesis in the tumour [533]. It has also been shown that *FGF5* transcripts and FGF5 protein are also over-expressed in cell lines compared to normal melanocytes [530]. There is little in the literature

investigating the function or expression levels of FGF3, FGF6 and FGF8 in melanoma cells, however this group of molecules is closely related to tumourigenesis and progression suggesting that over-expression of this family of genes may represent an important step in the early metastatic processes of malignant melanoma, which warrants further investigation in a larger sample set.

This study also identified lower expression of matrix metalloproteinase-2 (*MMP2*) in the majority of nodal samples compared to their matched primaries. Interestingly, Koh and colleagues also identified under-expression of another matrix metalloproteinase (*MMP1*) in SNB samples in their study of matched primary and SNB samples [510]. Matrix metalloproteinases degrade extracellular matrix causing release of growth factors and cytokines. Consequently, they are important in invasion and metastasis and regulate cell growth, survival, angiogenesis and inflammation [534, 535]. *MMP2* is a gelatinase, along with *MMP9* which can lyse numerous components of extracellular matrix [534]. A meta-analysis of studies aiming to identify protein markers of melanoma progression, found that over-expression of *MMP2* in primary tumours was associated with poorer prognosis [160, 169]. There is also evidence that *MMP2* expression increases as melanocytic tumours become more atypical [536]. There have been suggestions however that the predominant source of *MMP2* is not tumour, but stromal cells [537, 538]. In a syngenic *in vivo* mouse model which spontaneously develops metastases, *MMP2* was predominantly expressed by stromal cells at the border between tumour and stroma of subcutaneous tumours, however in spontaneous lymph node or lung metastases, tumour and stromal cells were largely negative for *MMP2* [538]. Therefore, the data reported in the literature suggest that increased expression detected in the primary tumours in my study relative to that in nodal metastases might in fact reflect overexpression by stromal cells in primaries destined to metastasise to nodes.

The gene most over-expressed in nodal tumours compared to primary tumours was *CSF3* which codes for granulocyte colony stimulating factor (GCSF). GCSF is predominantly produced by immune cells, but also endothelium, and stimulates bone marrow to produce granulocytes, such as neutrophils, and release them into the blood [539, 540]. This finding may reveal a potential problem when trying to sample tiny melanoma deposits from lymphoid tissue full of lymphocytes. The range of fold change in gene expression across the sample set in nodal samples compared to primary samples is very wide for *CSF3* (2.5-269.7) and the box-plot in Figure 5-4 shows the great range of fold changes. Very high levels of *CSF3* in some nodal samples may be related to sampling of immune cells from nodal tissue as well as tumour cells. It could be hypothesized that lymphocytes would up-regulate *CSF3* expression markedly in

response to tumour invading the lymph node. Sampling was carried out under the supervision of an expert dermatopathologist, however single tumour cells can reside amongst numerous lymphocytes making sampling difficult even when using fresh tissue sections on slides specifically designed for LCM. In this study, the majority of sections were archival sections on normal glass slides, therefore multiple laser pulses were used to remove tissue piece by piece reducing the accuracy of sampling further. Use of fresh tissue samples on slides designed to allow accurate sampling of intact tumour deposits would improve accuracy in future studies. In summary, greater expression of *CSF3* in the nodal samples may simply reflect contamination by inflammatory cells even in these laser microdissected samples.

It is important to acknowledge that the patient and primary tumour characteristics of this sample set were not representative of our larger cohort, reflecting the small numbers of samples assessed and the fact that all these patients had a positive SNB associated with poor prognostic factors. Therefore the applicability of these gene expression results to better prognosis tumours is limited.

This study is clearly also limited by the small number of samples assessed and the number of additional factors present in the study design that influence performance with the assay, such as age of tissue block, differences in tissue age between matched samples and sample availability for microdissection. Factors such as age of tissue blocks will continue to be a challenge for studies using FFPE tissue, but this work indicates that use of new sections yields superior results over archival unstained sections, and that storage of sections may be critical, storage under paraffin or a cover slip at 4°C would appear sensible.

In summary, this study demonstrates that very small, laser dissected, FFPE SNB samples can be used for RNA extraction for gene expression analysis, although with a higher fail rate than with larger samples, as defined by number of genes detected overall. The study produced interesting data on a possible role for FGFs in metastasis which should be explored in larger studies. The work also reflects the observation made by others that gene expression profiles may reflect expression by non-tumour cells [301, 302]. Further work will help clarify which sample characteristics will predict performance with the DASL assay and enable more extensive studies to assess alterations in gene expression profiles between primary and early metastatic tumours from the same patient.

6 Identification of associations between somatic mutations in *BRAF* and *NRAS* in formalin-fixed melanoma tumours, clinico-pathological factors and gene expression profiles

6.1 Aims

The aims of this chapter are:

- To identify mutations in *BRAF* and *NRAS* in a large number of formalin-fixed paraffin-embedded (FFPE) primary melanoma tumours.
- To identify tumour or patient characteristics associated with these mutations.
- To identify gene expression profiles associated with *BRAF* or *NRAS* mutation status.

The secondary aims were:

- To assess use of cDNA, generated in the course of gene expression studies in primary melanoma, rather than DNA as a substrate for mutation screening to maximise use of precious tumour material.

6.2 Background

The mitogen-activated protein kinase (MAPK) pathway (Figure 6-1) is a key signalling pathway activated in melanoma, which regulates a number of processes within cancer cells including cell survival, growth and migration [28, 29].

RAS is membrane bound and is activated by cytokines, growth factors and hormones [29]. RAS activates three closely related RAF proteins, ARAF, BRAF and CRAF, which when activated phosphorylate the MAP-kinases, Mek1 and Mek2, which then phosphorylate and activate Erk1 and Erk2 [30, 541] (Figure 6-1). Erk protein kinase activation regulates cellular proliferation, survival, invasion, differentiation and apoptosis [30, 541].

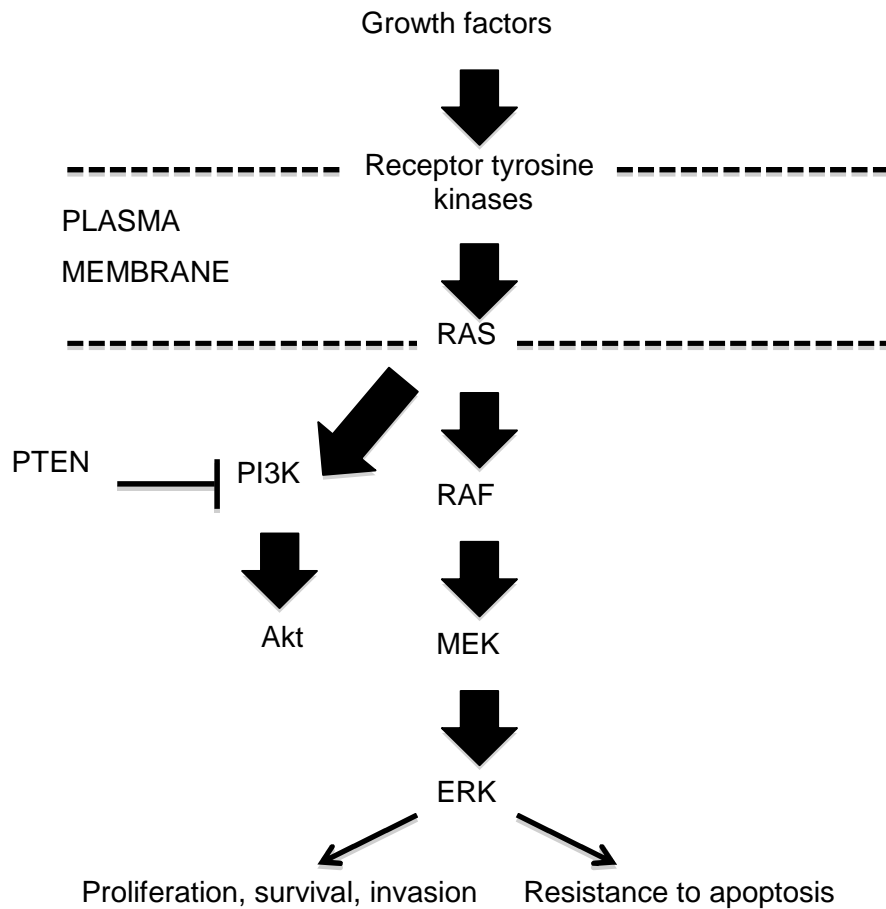


Figure 6-1: The mitogen-activated protein kinase (MAPK) and phosphatidylinositol-3-kinase (PI3K) pathways.

NRAS mutations activate both pathways. The MAPK pathway can also be activated by mutations in *BRAF*. In addition, *ERK* can be constitutively active in absence of *NRAS* and *BRAF* mutations. The PI3K-Akt pathway may be activated by loss of the inhibitory function of PTEN, or by gene amplification of *AKT3* [35]. Figure adapted from [541].

Mutations in genes within this pathway are frequently found in melanoma tumours and in this chapter, I will present my work identifying *BRAF* and *NRAS* mutations in FFPE tumours and an investigation of the clinico-pathological features and gene expression profiles associated with these mutations.

The reported frequency of *BRAF* mutations in melanoma tumours is variable ranging from 20-80%, however a recent meta-analysis of studies published between 1989 and

2010 found *BRAF* mutations in 41% of melanomas [30, 31]. A large proportion of mutations are due to a single substitution where adenine (A) replaces thymine (T) in codon 600 of exon 15 (V600E, c.1799T>A) leading to substitution of glutamic acid for valine [30, 32].

It is unclear why this site is so frequently mutated. *BRAF* mutations have been demonstrated in acquired melanocytic naevi (incidence of 21-82% in larger series) [25, 542] and naevus number is strongly associated with sunny holidays [15] so induction by sun exposure seems logical. However the T>A substitution is not characteristic of the cytosine (C)>T and CC>>TT pyrimidine dimer mutations more commonly found following UVB-damage [541, 543]. There have been suggestions that mutations may occur secondary to UVB-induced DNA photoproducts and subsequent errors in DNA synthesis which develop near to the V600 site [544]. There has also been some evidence that UVA, which is the predominant portion of sunlight, can trigger photosensitization reactions causing oxidative DNA damage, typical UV-induced DNA lesions and DNA cross-links [545, 546]. These lesions can lead to mutations, such as *BRAF* V600 mutations, in experimental systems [545]. Further support for the role of UVA is that V600E mutations are also common in colonic cancers in which oxidative stress is thought to play an aetiological role [32, 547, 548]. Despite these findings, the relationship between sunlight and development of *BRAF* mutations is still unclear.

Until relatively recently, V600E mutations were thought to account for over 90% of *BRAF* mutations, however studies have found that the V600K mutation (c.1798_1799delinsAA) can account for up to 30% of mutations in melanoma tumours [549-551]. The majority of *BRAF* mutations destabilize the structure of inactive *BRAF* kinase domains leading to activation and higher protein kinase activity causing activation of the MAPK pathway [32, 35, 552-555], along with insensitivity to negative feedback mechanisms [556]. V600E mutations can transform immortalized melanocytes [557] and cause growth and improved survival in melanoma cells *in vitro*, with inhibition of mutant *BRAF in vivo* leading to delay in tumour growth [558, 559]. Mutant *BRAF* also appears to have a role in angiogenesis, as blockade of mutant *BRAF* activity prevents further vascular development in established tumours via decreased secretion of vascular endothelial growth factor [560]. In mice, expression of *BRAF*^{V600E} in melanocytes at physiological levels, cause naevus development, which after a period of latency can develop into melanoma tumours [561]. However, when *PTEN* is lost in addition to *BRAF*^{V600E} expression, metastatic tumours develop quickly in all cases [562].

In humans, the fact that V600E *BRAF* mutations are commonly found in naevi is consistent with the view that those mutations drive proliferation. The majority of

melanocytes however subsequently senesce and there is evidence that in the normal cell, $BRAF^{V600E}$ induces tumour suppressor proteins such as $p16^{INK4a}$ which mediate the senescence of those melanocytes [36, 37]. Therefore, it appears that additional factors are required to act alongside mutated *BRAF* to cause progression to melanoma [563]. Animal data described above suggest that loss of *PTEN* is a potent means of inducing progression.

With regards to the morphological features of tumours, primary *BRAF* mutated tumours have been reported to have distinct appearances with larger, rounder and more pigmented tumour cells with increased upward scatter and nest formation of intraepithelial melanocytes [564]. The tumours are also associated with thickened epidermis and are more clearly circumscribed [564]. These features suggest that *BRAF* mutated tumours are biologically distinct which may prove to be reflected in gene expression profiles that differ to those of wild-type tumours.

Recently, the *BRAF* kinase inhibitor (BRAFi), vemurafenib, has been developed which has been shown to prolong progression-free and overall survival with a relative reduction of 74% in risk of either death or disease progression and a 48% response rate in patients with metastatic melanoma with a *BRAF* V600E mutation versus standard care with dacarbazine [199]. Vemurafenib also appears to produce clinical responses in patients with tumours harbouring the rarer V600K mutation [565]. Although relapse rapidly occurs in the majority of treated patients, this represents a major development in the treatment of advanced melanoma, where previous treatment achieved poor responses rates [243, 244] and highlights the importance of this pathway in melanoma development and progression. In tumours without *BRAF* mutations, there are usually mutations elsewhere in the MAPK pathway, such as *NRAS* in cutaneous melanomas (18%) [30, 31], *KIT* in acral or mucosal melanomas [33] and *GNAQ* in uveal melanomas [34].

The *NRAS* protein is encoded by one of the three *RAS* genes which encode four *RAS* proteins, *HRAS*, *KRAS4A*, *KRAS4B* and *NRAS* [566]. The *NRAS* gene is also frequently mutated in melanoma tumours with mutations most commonly occurring in codon 61 of exon 3 [30]. Again these mutations are not characteristic of UV-induced changes, but codon 61 preferentially forms pyrimidine dimer mutations following exposure to UV radiation and following transfection into a non-tumourigenic rat fibroblast cell line, Q61R and Q61R mutations develop, similar to those found in melanoma samples [567, 568]. Other sites which rarely form these dimers are codons 12 and 13, where again *NRAS* mutations are found [568]. *NRAS* mutations cause constitutive activation of the MAPK pathway [31] and in addition to signalling via *RAF* proteins, mutant *NRAS* can increase signalling via the phosphatidylinositol-3-kinase

(PI3K) pathway, the Ral guanine exchange factors (RalGEFs) and other signal transduction pathways [569-571]. Mutant RAS has transforming ability in a variety of cell types [572]. Many studies of RAS in melanoma models have used transgenic expression of *HRAS*, but have shown that *RAS* mutations alone are insufficient to cause melanomas in mice [573, 574]. However in a melanoma mouse model null for the tumour suppressor, p16^{INK4a}, expression of mutant *HRAS* in melanocytes leads to melanoma development [574]. In this model, subsequent loss of activated *HRAS* in established tumours leads to tumour shrinkage, suggesting that *HRAS* is required for tumour maintenance [575].

That *BRAF* mutations are commonly found in benign or dysplastic naevi and *NRAS* or *BRAF* mutations are generally maintained in paired primary and metastatic samples [2, 25, 576] has led to the suggestion that these mutations occur early in melanoma development [18]. Despite the early appearance of mutations, there is evidence however to suggest that the proportion of mutated cells increases as a melanoma becomes increasing invasive, for example in tumours moving from the radial to vertical growth phase or when they metastasise [577-579].

Generally, *BRAF* and *NRAS* mutations are not found in the same tumour [32, 541]. However, infrequent double mutations have been identified in naevi [25], melanoma cell lines [580, 581], melanomas from patients with germline *CDKN2A* mutations [582] and in small numbers of primary and metastatic melanomas [550, 577, 583]. Recent studies have demonstrated that primary melanomas, naevi and circulating tumour cells display heterogeneity, with some cells harbouring mutant *BRAF* and others wild-type *BRAF* [357, 579, 584-586]. Therefore, as the presence of both an *NRAS* and *BRAF* mutation does not confer any advantage in a single cell and has not been identified [580], detection of double mutations within a tumour may represent heterogeneity, with some cell clones containing mutant *NRAS* and others mutant *BRAF* [25].

A numbers of studies have attempted to identify relationships between tumour features, patient characteristics and mutation status. These findings are summarised in Table 6-1. It is clear in a large meta-analysis of studies involving tumours from 4493 patients that tumours with *BRAF* mutations are more commonly of the superficial spreading subtype in sun-protected sites, with *NRAS* mutations being more commonly found in tumours of the nodular subtype in sun-exposed sites [30, 31]. There is also strong evidence that patients with *BRAF* mutated tumours are diagnosed at a younger age than patients with wild-type tumours [549, 587, 588].

Tumour or patient characteristic	Association with <i>BRAF</i> mutations	Association with <i>NRAS</i> mutations	Strength of evidence	References
Histological subtype	Commoner in superficial spreading melanomas	Commoner in nodular melanomas	Meta-analysis of data from primary melanomas from 4493 patients (studies from 1989-2010)	[31]
Tumour site	Commoner on intermittently sun-exposed skin, e.g. trunk	Commoner on sun-exposed sites e.g. head or neck, extremities	Meta-analysis of data from primary melanomas from 4493 patients (studies from 1989-2010)	[31]
Patient age at diagnosis	Younger age at diagnosis than patients with wild-type tumours	No associations identified	<i>BRAF</i> mutations identified in FFPE metastatic tumours from 197 patients with unresectable stage IIIC or IV melanoma	[549]
			<i>BRAF</i> mutations identified in primary melanoma tumours from 544 patients	[587]
			<i>NRAS</i> and <i>BRAF</i> mutations identified in 365 primary melanoma tumours	[588]
Primary tumour mitoses	More common in primary tumour when <i>BRAF</i> mutation found in metastatic tumour	Higher mitotic rate compared to <i>BRAF</i> mutated or wild-type tumours	<i>BRAF</i> mutations identified in FFPE metastatic tumours from 197 patients with unresectable stage IIIC or IV melanoma	[549]
			<i>NRAS</i> and <i>BRAF</i> mutations identified in primary melanoma tumours from 249 patients	[589]

Tumour or patient characteristic	Association with <i>BRAF</i> mutations	Association with <i>NRAS</i> mutations	Strength of evidence	References
Primary tumour Breslow thickness	Greater than in wild-type tumours	Greater than in <i>BRAF</i> mutated or wild-type tumours	<i>NRAS</i> and <i>BRAF</i> mutations identified in primary melanoma tumours from 249 patients	[589]
			<i>NRAS</i> and <i>BRAF</i> mutations identified in 223 primary melanoma tumours	[583]
Primary tumour ulceration	Increased incidence compared to <i>NRAS</i> mutated or wild-type tumours	No associations identified	<i>NRAS</i> and <i>BRAF</i> mutations identified in 223 primary melanoma tumours	[583]
Stage at diagnosis	More likely to present with stage III (nodal metastases) disease than wild-type tumours	More likely to present with stage III disease (nodal metastases) than wild-type tumours	<i>NRAS</i> and <i>BRAF</i> mutations identified in 223 primary melanoma tumours	[583]

Table 6-1: Patient and tumour characteristics associated with *BRAF* or *NRAS* mutations in melanoma tumours.

Associations between mutation status and tumour or patient characteristics are presented with details of the studies describing these relationships. Where data from meta-analyses is available, this has been referenced in preference to single studies.

It is generally accepted that there is no relationship between *BRAF* or *NRAS* mutation status in primary tumours and either relapse-free survival or overall survival in melanoma patients [436, 555, 576, 583, 588, 590, 591]. An exception to this is in metastatic melanoma (stage III and IV), where there does appear to be some association with mutation status and survival. This was initially noted by Houben and colleagues where mutations were identified in 86 metastatic lesions and the presence of a *BRAF* or *NRAS* mutation was associated with shorter survival, whereas mutations in 114 primary melanoma tumours did not impact on progression-free or overall survival [555]. This has been subsequently confirmed in other studies [186, 549, 550, 592].

In summary, there is evidence that presence of a *BRAF* or *NRAS* mutation is associated with tumour histological subtype, tumour site and age at diagnosis. Presence of mutations in metastatic tumour negatively impacts survival, with no association between survival when a mutation is identified in the primary tumour.

There has been increasing interest in the biological relevance of non-V600E *BRAF* mutations. Menzies and colleagues obtained *BRAF* mutation status preferentially from FFPE metastatic melanoma tissue for 308 patients [593]. Mutations were identified in tumours from 46% of patients, with 73% being V600E mutations and 10% V600K mutations. The authors determined the prevalence of *BRAF* mutations according to each decade of diagnosis. In common with findings in primary melanoma, presence of a *BRAF* mutation was associated with a significantly younger age at diagnosis of metastatic disease, however the proportion of mutations which were not V600E, including V600K mutations, increased with each age-decade of diagnosis. There was no difference in the age of diagnosis between patients with wild-type tumours or V600K mutated tumours. The study also found increased evidence of cumulative sun damage, as determined by degree of solar elastosis, in skin from patients with V600K mutated tumours, but not V600E mutations which correlated with their finding that V600K mutant tumours were found more commonly on the head and neck, typically a sun-exposed site, with V600E tumours on the limbs. The distant metastasis disease-free period from diagnosis of the primary tumour was shorter for patients with a V600K mutation versus a V600E mutation, but there was no difference in overall survival. The number of V600K mutations identified in this study was 27, therefore these analyses were based on limited numbers, however these findings suggest that V600K mutations may have a different aetiology and behaviour to V600E mutations [593]. In a study where 229 tumour specimens were genotyped from patients with advanced cancer, 168 of which had melanoma, 13 V600K mutations were detected, one in a patient with colorectal cancer and the rest in melanoma tumours. Presence of a V600K mutation

was associated with more brain and lung metastases, earlier metastasis and shorter overall survival following diagnosis [594]. These data albeit in relatively small studies suggest that the V600K mutant may be biologically more deleterious than the V600E mutation. In common with V600E mutations, V600K mutations cause elevated kinase activity and ERK activation, but there is evidence that the kinase activity associated with V600K mutations is lower than that of V600E mutations [554]. Reduced survival associated with V600K mutations maybe related to modified kinase activity along with other, as yet unidentified, factors.

It is important to consider both the pathogenesis of melanomas driven by different oncogenes and the impact on biological pathways. The importance of fully understanding how *BRAF* and *NRAS* mutations alter downstream biological pathways is particularly important with the development of BRAFi which offer the first major targeted treatment option for advanced melanoma. Despite the initial responses seen with vemurafenib, treatment is associated with side effects, such as development of cutaneous squamous cell carcinomas and keratoacanthomas [199, 206]. Of greater concern, is that resistance to vemurafenib almost invariably develops and understanding the mechanism by which a *BRAF* mutation modifies gene expression will greatly assist the intensive efforts currently underway investigating mechanisms of resistance [199, 206, 242].

A number of studies have attempted to identify gene expression signatures related to mutation status using melanoma cell lines and frozen tumour specimens as summarised in Table 6-2. Another approach has been to study gene expression in melanocytes where activated $BRAF^{V600E}$ has been introduced, this work has identified over-expression of genes involved in cell growth and motility, inflammation and apoptosis including matrix metalloproteinase-1 (*MMP1*) [595]. As technologies have developed, cDNA sequencing (RNA-seq) has been used to compare gene expression in normal human melanocytes with and without $BRAF^{V600E}$ expression and two V600E *BRAF* mutated tumours to identify genes more specifically altered in cancer tissues [196]. $BRAF^{V600E}$ was associated with differential expression of 1027 protein-coding transcripts along with other unannotated transcripts, which were thought to represent new unidentified long non-coding RNAs (lncRNA) and specifically highlighted *BANCR* as a lncRNA which potentially regulated melanoma cell migration [196].

Study design and sample type	Number and type of samples	Comparisons made	Analysis method	Significant results	References
Cell lines genotyped for <i>BRAF</i> and <i>NRAS</i> and gene expression assessed with 18,107 microarray.	61 cell lines.	<i>BRAF</i> mutant versus wild-type and <i>NRAS</i> mutant versus wild-type cell lines.	Mann-Whitney U test to compare groups and support vector machines to develop a classifier to predict presence of <i>BRAF</i> mutations.	135 differentially expressed clones in <i>BRAF</i> mutant samples, 48 in <i>NRAS</i> mutant samples with 19 clones overlapping. Differential expression of genes encoding enzymes which regulate signal transduction pathways, e.g. protein tyrosine phosphatase receptor type A (<i>PTPRA</i>).	[596]
Cell lines genotyped for <i>BRAF</i> and <i>NRAS</i> and gene expression assessed with microarray targeting 22,277 transcripts (Affymetrix HG-U133A 2.0).	10 cell lines.	<i>BRAF</i> mutant versus <i>NRAS</i> mutant versus wild-type cell lines.	Pairwise comparisons, SAMic and marker analysis to identify genes correlated with a genotype.	61 differentially expressed genes in <i>BRAF</i> mutated samples and 109 in <i>NRAS</i> mutant samples with 56 overlapping. Genes which encode regulators of the MAPK pathway and genes involved in metastasis or invasion were differentially expressed.	[597]
Cells genotyped for <i>BRAF</i> and <i>NRAS</i> and gene expression assessed with Affymetrix microarrays (various HG-U133 arrays).	86 melanoma cell lines.	<i>BRAF</i> mutant versus <i>NRAS</i> mutant versus wild-type cell lines.	ANOVA with correction for multiple testing, hierarchical clustering.	No differentially expressed genes. Data from study of Pavey and colleagues was reanalysed using correction for multiple testing and only one gene differentially expressed (identity not reported).	[598]
Mutations in <i>BRAF</i> identified and whole-genome Affymetrix microarray (HG-U133 plus 2.0).	63 melanoma cell lines.	<i>BRAF</i> mutant versus wild-type.	Support vector machines to develop a classifier to identify <i>BRAF</i> mutations and SAMic.	Classifier identified in two thirds of samples and validated in the other third. Classifier predicted <i>BRAF</i> mutation status in a subset of the dataset from Hoek and colleagues. Overexpressed genes included T box 3 (<i>TBX3</i>), SPRY domain containing 5 (<i>SPRYD5</i>) and v-erb-b2 erythroblastic leukaemia viral oncogene homolog 3 (<i>ERBB3</i>).	[599]

Study design and sample type	Number and type of samples	Comparisons made	Analysis method	Significant results	References
<i>BRAF</i> and <i>NRAS</i> mutations identified and whole-genome Agilent array was used for gene expression profiling.	69 frozen primary melanomas.	<i>BRAF</i> mutant versus wild-type.	Two-sample t-test with control of the false discovery rate.	34 genes overexpressed in <i>BRAF</i> mutated tumours, including genes involved in immune responses and cell motility. These genes were not differentially expressed in <i>NRAS</i> mutated tumours.	[591]
<i>BRAF</i> and <i>NRAS</i> mutations identified and expression profiling using the Affymetrix HG-U133 plus 2.0 (main study aim to determine if a single metastatic lesion has a similar expression profile to other lesions to allow use of a single lesion to determine responsiveness to chemotherapy).	55 frozen in-transit metastatic melanomas from 29 patients.	<i>BRAF</i> mutant versus <i>NRAS</i> mutant versus wild-type tumours.	Unsupervised hierarchical clustering, ANOVA and regression.	Unsupervised hierarchical clustering revealed two groups with one group containing <i>BRAF</i> mutated tumours and the other <i>NRAS</i> mutated tumours or wild type <i>BRAF</i> genes. 2168 genes correlated with mutation status including under-expression of microphthalmia-associated transcription factor (<i>MITF</i>) and a member of the transient receptor potential cation channel family (<i>TRPM1</i>) in mutant tumours. Top 200 differentially expressed genes similarly expressed in <i>BRAF</i> mutant and <i>NRAS</i> mutant tumours.	[508]

Table 6-2: Summary of studies assessing gene expression profiles in tumours with *BRAF* or *NRAS* mutations.

Abbreviations used: SAMic, significance analysis of microarrays; MAPK, mitogen-activated protein kinase; ANOVA, analysis of variance.

To summarise gene expression studies, there has been much variation in reported gene profiles in mutant tumours which is likely to reflect tumour heterogeneity in association with different analysis methods and small numbers of samples assessed. The identification of gene expression profiles associated with *NRAS* mutated tumours has been particularly limited because of the lower frequency of mutations in melanoma cell lines and tumours. Where differentially expressed genes have been identified in mutant tumours, genes fall into common themes such as those involved in cell growth and motility [196, 591, 595, 597, 599] and regulators of the MAPK pathway [597, 599]. There has been some overlap in differentially expressed genes in *BRAF* and *NRAS* mutated tumours, perhaps reflecting similar alterations in biological pathways [508, 596, 597]. The exception to this statement is the study by Kannengiesser and colleagues which found no overlap in gene expression profiles of *BRAF* and *NRAS* mutated genes in the largest study of primary melanomas to date [591]. Use of FFPE tissue, as in the current study, will allow assessment of a larger number of tumours to identify gene expression signatures associated with *BRAF* and *NRAS* mutation status.

This chapter presents *BRAF* and *NRAS* mutation results from FFPE primary melanoma sample sets previously used for gene expression work in Chapters 3 and 4. I report the identification of *BRAF* and *NRAS* mutation status of primary melanomas and subsequent studies performed in order to identify patient and tumour factors which are associated with these mutations. Furthermore, mutation associated gene expression profiles were identified in the largest study of primary melanoma tumours to date and the only study using FFPE tissue.

The main method used for *BRAF* and *NRAS* mutation testing described in this chapter was pyrosequencing. This method is described in detail in Chapter 2, but briefly the technique uses primers to direct a polymerase extension reaction where nucleotides are added sequentially to the reaction and incorporation of a nucleotide causes light to be released which is detected to determine the DNA sequence [352-355]. This technique has been shown to be more sensitive than Sanger sequencing for detecting the V600E *BRAF* mutation [356] and has been previously used by a number of groups to identify *BRAF* and *NRAS* mutations in FFPE and frozen melanoma tissues [353, 356, 436, 600]. In order to preserve precious stocks of tumour DNA, mutation screening of *NRAS* and *BRAF* has been attempted using cDNA produced as part of concurrent gene expression studies and these results are also presented.

6.3 Identification of *BRAF* and *NRAS* mutations in FFPE primary melanoma tumours

6.3.1 Detailed methodology

6.3.1.1 Patients and samples

FFPE melanoma metastases and cell line samples were used for initial methodological testing; these sample sets are described further in Chapter 2. From metastatic samples, RNA was extracted from a single tissue core using the Roche High Pure RNA Paraffin Kit, cDNA was generated using 200ng of RNA using the Invitrogen Superscript™ First-strand synthesis system using a modified protocol. DNA was extracted from a single tissue core from the same tumour block used for RNA extraction using the Qiagen QIAamp DNA FFPE kit. RNA was extracted from pelleted cells of SkMel28 and MeWo melanoma cell lines using the Qiagen RNeasy® Mini kit. cDNA was generated using the standard protocol and one microgram of RNA using the Invitrogen Superscript™ First-strand synthesis system. DNA was extracted from pelleted cells of cell lines from the same flask used for RNA extraction using the Qiagen QIAamp DNA Mini kit. Details of extraction and cDNA synthesis methods used are included in Chapter 2.

Samples for the larger study were from patient study sets described in Chapter 3. cDNA had been synthesised from tumour RNA for use in gene expression studies from patients recruited to the Leeds Melanoma Cohort Study (Cohort Study) and a small number of samples from patients recruited to the Retrospective Sentinel Node Biopsy Study (SNB study) using the Invitrogen Superscript™ First-strand cDNA system using a modified protocol as described in Chapter 2. This stored cDNA was used to test the feasibility of using cDNA for mutation screening. DNA was extracted from available tumour tissue cores from patients recruited to both the Cohort and SNB study using either the Qiagen QIAamp DNA FFPE kit or the Qiagen AllPrep® RNA/DNA FFPE kit using methods described in Chapter 2 for mutation testing using DNA.

6.3.1.2 *BRAF* and *NRAS* mutation detection

Using methods described in Chapter 2, pyrosequencing was initially used to identify common *BRAF* and *NRAS* mutations in cDNA from melanoma metastases, cell line samples and the larger cohort of primary tumour samples. All pyrosequencing analyses were performed by Dr Phil Chambers in the Genomics Facility, Cancer Research UK Centre, Leeds Institute of Molecular Medicine. The “mutation percentage” calculated from pyrosequencing data reflects the number of mutated alleles in cells assessed, but

as tumour is heterogeneous it will also reflect the number of non-mutated tumour cells along with contaminating normal stromal cells. Pyrosequencing analysis was repeated using DNA from metastases samples and cell lines. For the larger study, cDNA and DNA from a proportion of samples were screened for *BRAF* and *NRAS* mutations using the Applied Biosystems PRISM® SNaPshot™ Multiplex system using methods described in Chapter 2 to confirm results from pyrosequencing. SNaPshot analysis was performed by myself. Finally, the *BRAF* and *NRAS* mutation status of DNA from samples in the larger cohort were assessed using pyrosequencing.

Correlations between percentage mutation results between cDNA and matched DNA samples were assessed using Spearman's rank correlation.

6.3.1.3 Identification of patient and tumour factors associated with mutation status

Patient factors and histological characteristics of the primary tumour were compared between samples with differing mutation status using Pearson's Chi squared (χ^2) tests or Fisher's exact test (where the frequency of observations in a subgroup was less than 5) for categorical variables and Kruskal-Wallis tests for continuous variables. For survival analysis, relapse-free survival (RFS) was defined as the period between diagnosis and date of first relapse at any site. Death from any cause was used for overall survival analyses with death from melanoma only used for melanoma-specific survival. Analysis was performed on the 19th December 2011 and survival data were censored at this date. Associations between mutation status and survival were assessed using plots of Kaplan-Meier estimates of survival function. Furthermore, survival analysis was performed using the Cox proportional hazards model to calculate hazard ratios and 95% confidence intervals for each group of patients with tumours of a particular genotype. Analysis was performed unadjusted and adjusted for factors of prognostic importance in melanoma. A significance level of 0.05 was set for these analyses.

6.3.1.4 Identification of gene expression profiles associated with mutation status

Gene expression data were generated using the Illumina DASL Human Cancer panel and the merged dataset from the Cohort and SNB studies as described in Chapter 4. Differential gene expression analysis was performed using data which had been log-transformed (\log_2). As some of the raw gene expression levels were negative values,

1000 was added to all values prior to log-transformation. Within the sample sets, mean expression of each gene was compared between samples with differing mutation status using linear regression. Significance values were ranked to identify genes most differentially expressed between groups of interest. In view of non-biological variation that was judged to be present between the two DASL studies, all gene expression analyses were adjusted for study from which the patients were recruited. To correct for multiple testing, the Bonferroni method was used [366] and the significance level was set at 0.0001. Fold changes in mean gene expression between tumours with different genotype were calculated using data that had not been log-transformed. Statistical analyses were undertaken using Stata version 10 (StataCorp 2007, College Station, TX).

To allow comparison of gene lists generated using different analysis methods for gene expression data, analysis was also performed using two-group significance of microarray analyses (SAMic) [450] (Stanford University, Stanford, CA) using a Δ threshold to keep the false discovery rate at zero. Data used from this analysis had been \log_2 transformed without addition of the constant value and then residuals from a linear regression model adjusting for study from which the patients were recruited were used for further analysis. Any missing values following log-transformation were imputed by SAMic using a K-Nearest Neighbor algorithm [601]. SAMic identifies statistically differentially expressed genes using a set of gene-specific t-tests, where a small constant is added to the denominator during calculation of the T-statistic to reduce the influence of genes with a small variance [450, 599]. Each gene is given a score based on its change in gene expression relative to the standard deviation of repeated measurements for that gene. Genes with a score greater than a particular threshold (Δ), set by the user, are significantly differentially expressed. The false discovery rate is estimated by analysing permutations of the measurements, in this case 5000, which will identify false positive results [450]. This analysis generates a q -value, which is the lowest false-discovery rate at which a gene is significant [602].

6.3.2 Results

6.3.2.1 Use of cDNA for mutation detection

When this work began, extraction of either DNA or RNA from tumour samples required use of a tissue core. A single tissue core can represent all, or a large proportion, of the tumour available for research. To avoid having to extract DNA from precious stored tumour material, experiments were performed to assess whether stored cDNA produced in the course of gene expression studies could be used for *BRAF* and *NRAS*

mutation screening. Initial experiments assessed use of high-quality nucleic acids from cell lines followed by assessment of nucleic acids from FFPE melanoma samples.

6.3.2.1.1 Pyrosequencing of cell line DNA and cDNA

To compare results generated using pyrosequencing with cDNA and DNA to screen for *BRAF* and *NRAS* mutations in high quality nucleic acids, pyrosequencing was used to screen DNA and cDNA from SkMel28 cells, which have a homozygous V600E *BRAF* mutation, and MeWo cells which do not have a *BRAF* or *NRAS* mutation as recorded by the Catalogue of Somatic Mutations in Cancer (COSMIC) [361]. Results were similar from DNA and cDNA, however an unexpected V600E *BRAF* mutation was identified in the MeWo cells in both cDNA and DNA. The A allele (mutant allele) percentage was higher when cDNA was analysed. For MeWo cells the A allele percentage was 72% for DNA and 76% for cDNA, and for SkMel28 cells, 95% for DNA and 98% for cDNA. No *NRAS* mutations were identified in these samples. DNA and cDNA from the cell line samples was also sequenced by Dr Phil Chambers using methods described in Chapter 2 and these results were confirmed.

6.3.2.1.2 Pyrosequencing of FFPE melanoma metastasis DNA and cDNA

To compare results from cDNA and DNA in degraded nucleic acids using pyrosequencing, a panel of five melanoma metastases samples were selected and results for *BRAF* and *NRAS* mutation screening using DNA and cDNA were compared. Two samples had V600E *BRAF* mutations identified in both cDNA and DNA. For samples with a mutation, the percentage A allele was higher when assessed with cDNA than DNA. One sample had an *NRAS* mutation (c.182A>G (p.Q61R)) which was found using both cDNA and DNA. DNA samples were sequenced by Dr Phil Chambers using methods described in Chapter 2 and these results were confirmed, however confirmatory sequencing of the cDNA samples failed.

6.3.2.1.3 Pyrosequencing of cDNA from tumour samples

As these initial results from cDNA and DNA were comparable, a larger number of cDNA samples were screened for mutations using pyrosequencing. cDNA samples had previously been generated from RNA extracted from FFPE primary tumours of patients recruited to the Cohort Study for use in quantitative Real-Time PCR (qRT-PCR) analysis as described in Chapter 4. A total of 154 cDNA specimens were available,

cDNA was also generated from 20 tumour RNA samples from patients recruited to the SNB study who were treated with chemotherapy (see Chapter 8), 6 of these samples were also sent for pyrosequencing with samples from the Cohort study. Therefore a total of 160 cDNA samples were screened for *BRAF* and *NRAS* mutations using pyrosequencing. A summary of results is presented in Table 6-3.

Sample status		Number of samples (%)
Total with <i>BRAF</i> mutation (A allele $\geq 10\%$)		105 (65.6)
<i>BRAF</i> V600E	0% A allele	28 (17.5)
	>0% and <5% A allele	12 (7.5)
	$\geq 5\%$ and <10% A allele	8 (5.0)
	$\geq 10\%$ and <20% A allele	19 (11.9)
	$\geq 20\%$ A allele	86 (53.8)
	No data	7 (4.4)
<i>NRAS</i>	Total with <i>NRAS</i> mutation	47 (29.4)
<i>NRAS</i> Codon 61	Mutation	44 (93.6)
	No data	11 (6.9)
<i>NRAS</i> Codon 12/13	Mutation	3 (6.4)
	No data	7 (4.4)
Double mutations (<i>BRAF</i> A allele $\geq 10\%$)		25 (15.6)

Table 6-3: Summary of *BRAF* and *NRAS* mutation screening results from cDNA synthesised from RNA extracted from 160 primary melanoma samples.

The percentage values for *BRAF* and *NRAS* mutations overall, percentage A allele, missing data and double mutations were calculated as a percentage of the total number of samples assessed. For mutations in separate *NRAS* codons, the percentage value was calculated as a proportion of the number of samples with an *NRAS* mutation.

Overall, 65.6% of samples had a V600E *BRAF* mutation with a percentage A allele level over 10%. All *BRAF* mutations identified were V600E. A total of 29.4% of samples had a mutation in *NRAS*, with the majority of mutations being p.Q61R (40.4%) and p.Q61K (40.4%). Both of these results are consistent with published results, however 15.6% of samples had mutations both in *BRAF* and in *NRAS* which is uncommon and inconsistent with previous reports [30].

On review of the data in more detail, samples with double mutations appeared to have lower A allele percentage levels than samples without an *NRAS* mutation (Figure 6-2).

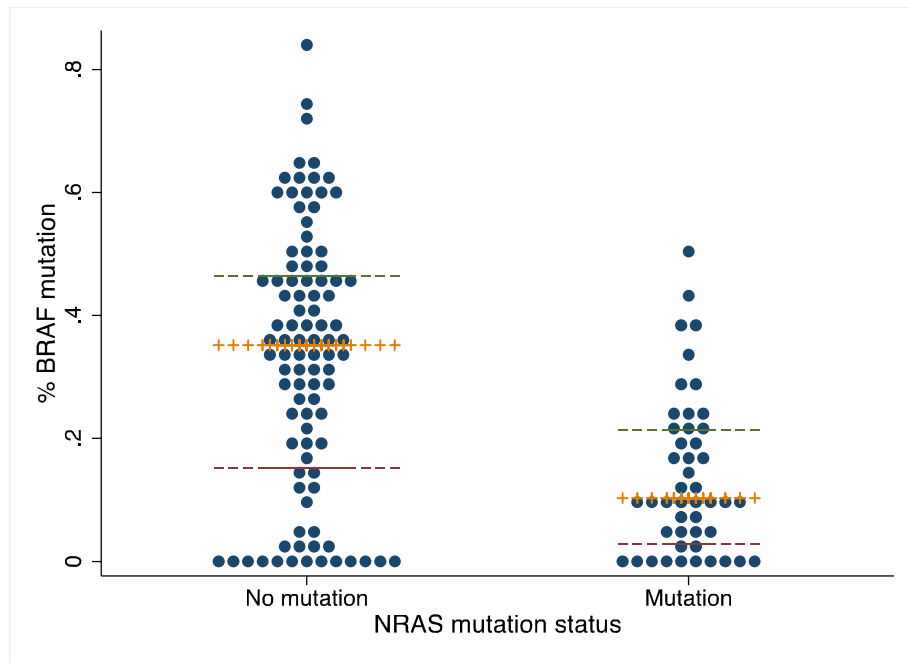


Figure 6-2: Distribution of A allele levels for V600E *BRAF* mutations in cDNA samples with and without *NRAS* mutation.

A single dot represents each sample. % *BRAF* mutation refers to A allele percentage levels. An orange line of pluses represents the median for the two groups; dashed lines indicate the upper and lower quartiles.

In order to confirm whether the results identified in cDNA samples were correct, pyrosequencing was repeated and similar results were obtained. A selection of samples were selected with different percentage A allele mutation results for sequencing to confirm the presence of these mutations, however the samples failed in this analysis. Therefore in order to confirm or refute these results, an Applied Biosystems PRISM® SNaPshot™ Multiplex system assay was developed to screen for *BRAF* and *NRAS* mutations in cDNA samples using methods described in Chapter 2.

6.3.2.1.4 Mutation screening of cDNA and DNA samples using the Applied Biosystems PRISM® SNaPshot™ Multiplex system for samples identified as having both *BRAF* and *NRAS* mutations in cDNA using pyrosequencing

cDNA samples identified as having double mutations using pyrosequencing were reassessed using the SNaPshot system. A further six samples with low levels of *BRAF* A allele levels (<10%) along with *NRAS* mutations were also assessed, therefore a total of 31 samples were analysed. Where there were further tissue cores available, DNA was extracted using the Qiagen QIAamp DNA FFPE kit from a matched core for

comparison of results using the SNaPshot system and pyrosequencing. A total of 25 samples had matched DNA samples available.

When cDNA was assessed using the SNaPshot system, four samples failed the *BRAF* assay. In the remainder, V600E *BRAF* mutations were detected in samples where the percentage A allele level using pyrosequencing was greater than 23%. Generally, in samples with lower percentage mutations, mutations were not detected, although for one sample, a V600E mutation was detected using the SNaPshot system when the mutation percentage was only 19% in the pyrosequencing assay. No V600K or K601 mutations were identified in these samples. No samples failed the *NRAS* assay and there was better concordance across the SNaPshot system and pyrosequencing for *NRAS* mutation results using cDNA, with mutation results being the same across the two assays for the majority of samples. The exception was that a c.182A>G mutation (Q61R) in codon 61 was identified in one sample using the SNaPshot system, whereas a c.181C>A mutation (Q61K) had been detected using pyrosequencing. Therefore, pyrosequencing appeared to be detecting low levels of V600E *BRAF* mutations in cDNA samples which could not generally be replicated using a different method of mutation detection, albeit a less sensitive detection method.

In order to investigate further, DNA was available for 25 samples for which we had previously tested the cDNA and this was assessed using both pyrosequencing and the SNaPshot system. Only one sample failed the *BRAF* and *NRAS* assay in pyrosequencing. There was excellent concordance between results across the two assays when DNA was used with all mutation results matching. Only one sample had a V600E *BRAF* mutation, which was the same sample identified as having a mutation in cDNA using the SNaPshot system and pyrosequencing where the A allele level was 19%. This sample was wild-type for *NRAS* when DNA was used for analysis, whereas a mutation was found in cDNA. No V600K or K601 mutations were identified in these samples. *NRAS* mutations were detected in all the samples assessed, except for the sample discussed previously, and the mutation spectrum was the same as results from cDNA. The sample with a different mutation identified using the SNaPshot system and pyrosequencing using cDNA was found to have a c.182A>G mutation (Q61R) in DNA using the SNaPshot system, however it failed in the pyrosequencing assay.

To summarise, using DNA from FFPE tumour specimens, samples previously identified as harbouring both *NRAS* and *BRAF* mutations when cDNA was assessed using pyrosequencing, were found to have only one mutation which is much more consistent with the published literature. Results for *NRAS* mutation screening were more concordant across cDNA and DNA, however using cDNA for *BRAF* mutation screening yielded inaccurate results, specifically low levels of mutation are identified in samples

where no mutation can be detected in matched DNA samples. Therefore to ensure accuracy of results, DNA was used for subsequent mutation screening.

6.3.2.2 *BRAF* and *NRAS* mutation results from FFPE primary melanoma specimens using DNA

6.3.2.2.1 Samples

Following completion of work using cDNA samples, the Qiagen AllPrep® RNA/DNA FFPE kit became available for use allowing us to extract DNA and RNA from a single core, thereby removing the necessity to consider mutation screening in cDNA. DNA was subsequently extracted using this kit by myself from 88 available primary tissue cores from patients recruited to the Cohort Study and 166 cores from patients recruited to the SNB study. DNA was used to identify *BRAF* and *NRAS* mutations using pyrosequencing as described previously. Results from this analysis were added to results for 25 tumours assessed in previous methodological work, therefore a total of 279 tumours were genotyped.

6.3.2.2.2 Mutations identified

Table 6-4 summarises the results of the pyrosequencing analysis. A total of 50.5% of the samples assessed had a *BRAF* mutation, the majority (83.7%) V600E mutations, which is consistent with levels quoted in the literature. A total of 27.2% of tumours had an *NRAS* mutation, most of which were in codon 61 as previously described. We were unable to obtain results for 3.2% of the samples assessed because of repeated PCR failure. No samples had both a *NRAS* and *BRAF* mutation.

The percentage mutation levels for V600E and *NRAS* mutations remained high in DNA samples analysed with pyrosequencing. Forty-one (15%) of tumours with V600E mutation had a percentage mutation levels over 50% and in the 75 tumours with *NRAS* mutations where mutation percentage could be calculated (p.G12N due to c.34_35delinsAA excluded), 38 (51%) of tumours had mutation percentage levels over 50%.

Gene	Mutation	Number of samples (%)
<i>BRAF</i>	All	141 (50.5)
	V600E	118 (83.7)
	V600K	18 (12.8)
	V600D	4 (2.8)
	K601E	1 (0.7)
<i>NRAS</i>	All	76 (27.2)
	p.Q61R	37 (48.7)
	p.Q61K	22 (29.0)
	p.Q61L	8 (10.5)
	p.Q61H	2 (2.6)
	p.G13R	5 (6.6)
	p.G12V	1 (1.3)
	p.G12N	1 (1.3)
Samples with double mutations		0
No mutation		53 (19.0)
Data not available		9 (3.2)

Table 6-4: Summary of *BRAF* and *NRAS* pyrosequencing results for DNA extracted from 279 primary melanoma tumours.

For each gene, the percentage number of samples is calculated for the whole sample set tested. For each separate mutation, the percentage number of samples is calculated as a proportion of samples with a mutation in the gene.

6.3.2.2.3 Correlations between results derived from pyrosequencing of matched cDNA and DNA samples

As discussed previously, there were discordant mutation results obtained from cDNA and matched DNA samples using pyrosequencing in the small sample set assessed in section 6.3.2.1.4. Whilst this discordance was thought likely to result from erroneous results from pyrosequencing, I investigated the relationship between cDNA and DNA results further to assess whether pyrosequencing was detecting small numbers of mutant *BRAF* cells in *NRAS* mutant tumours. Therefore, a comparison was made between results derived using pyrosequencing from matched cDNA and DNA samples in the larger sample set. All *BRAF* mutations detected in cDNA were V600E, however V600K mutations were detected in six DNA samples where V600E mutations have been previously identified in cDNA. In addition, a V600K mutation was identified in DNA where no mutation had been detected in the matched cDNA sample previously. Generally there was good concordance in the mutation spectrum detected in matched cDNA and DNA samples for *NRAS*, but mutations were detected in DNA, but not cDNA

for 4 samples, with mutations detected in cDNA and not DNA for 2 samples. Percentage mutation levels for V600E *BRAF* mutations and *NRAS* mutations were also compared between matched cDNA and DNA samples in the larger sample set. Results are presented in Figure 6-3.

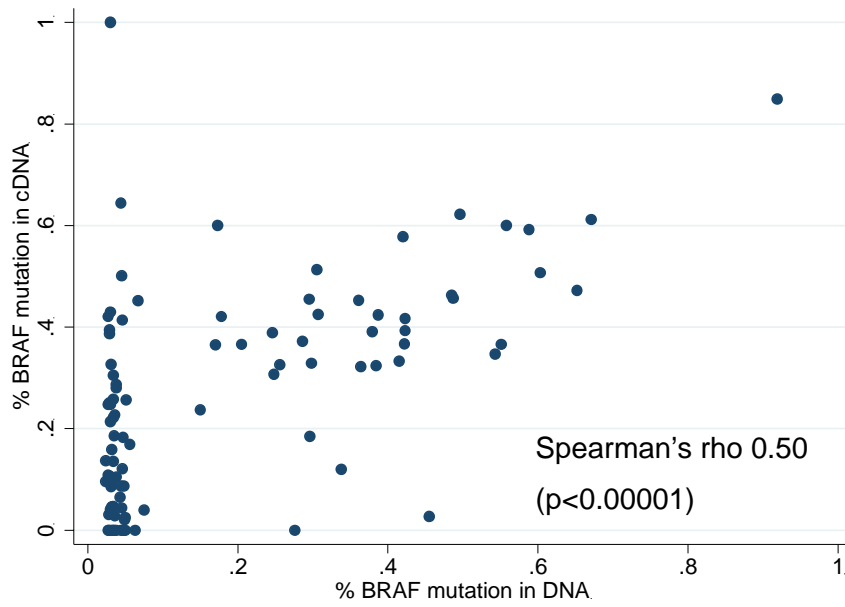
There were significant correlations between the level of mutation detected in matched cDNA and DNA samples for V600E *BRAF* (Spearman's rho 0.50) and *NRAS* (Spearman's rho 0.71) mutations, however it is clear from Figure 6-3 that for *BRAF*, high levels of mutant allele were detected in cDNA samples which are not replicated in DNA samples. The association between *NRAS* mutation levels was better between matched cDNA and DNA samples. Discordant results between cDNA and DNA samples demonstrate that cDNA cannot be used for accurate detection of mutations in *BRAF* and *NRAS* and this analysis confirms that DNA should be used for mutation screening in melanoma samples. I was unable to generate any data which explained this discordance.

6.3.2.2.4 Associations with clinico-pathological features

Table 6-5 presents results of analyses carried out to identify associations between mutation status and tumour histological features or patient characteristics.

There were a greater proportion of tumours with *BRAF* mutations in the SNB study, and *NRAS* mutations in the Cohort study. A higher proportion of superficial spreading melanomas were *BRAF* mutated, with a marginally greater proportion of nodular tumours being *NRAS* mutated. A higher proportion of truncal tumours had *BRAF* mutations, with *NRAS* mutations being more predominantly found in head and neck tumours or tumours on the limbs. A higher proportion of tumours on sun-protected sites were wild-type, however mutations were identified in four acral tumours (three *BRAF* and one *NRAS* mutation). The median age at diagnosis of patients with *NRAS* mutated tumours was significantly higher (61 years) than for patients with wild-type tumours (53 years) which was greater than for patients *BRAF* mutated tumours (51 years). This analysis found that patients with a positive SNB were more likely to have a *BRAF* mutated primary tumour, but these data are difficult to interpret given the observation that *BRAF* mutations were more common in people who elected to have a SNB rather than to decline it.

A.



B.

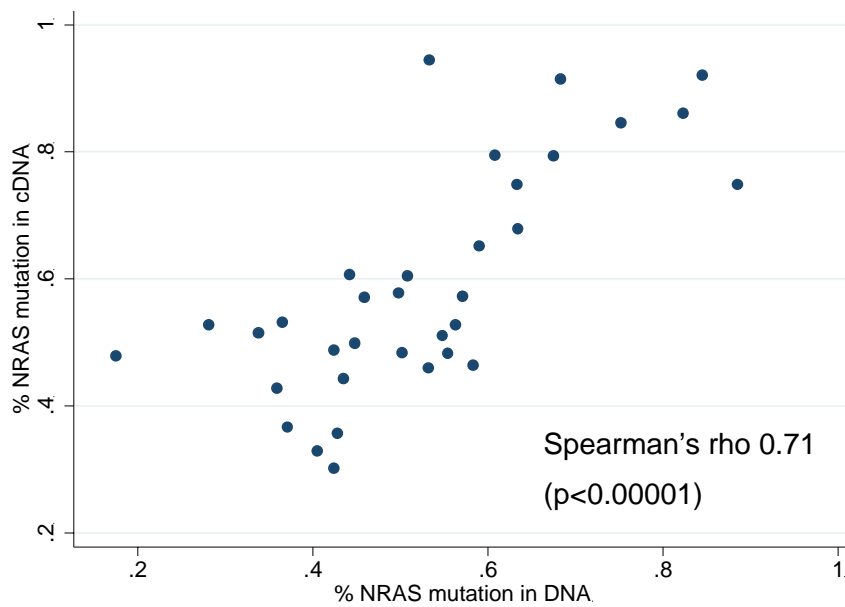


Figure 6-3: Scatter plots showing percentage mutation levels for V600E *BRAF* (A) and *NRAS* (B) levels from matched cDNA and DNA samples using pyrosequencing.

BRAF mutations are detected in cDNA samples, where none were found in DNA samples.

Factor	No mutation (n=53)	<i>BRAF</i> mutation (n=141)	<i>NRAS</i> mutation (n=76)	Test statistic and significance value
Study type, n (%):				
Cohort study	23 (21.7)	45 (42.5)	38 (35.9)	χ^2 (2) 7.3, p=0.03
SNB study	30 (18.3)	96 (58.5)	38 (23.2)	
Breslow thickness, mm, median (range)	2.1 (0.7-11.0)	2.0 (0.8-13.0)	2.5 (0.8-19.0)	Kruskal-Wallis χ^2 (2) 2.9, p=0.24
Mitotic rate per mm ² , median (range)	4 (0-37)	5 (0-40)	4 (0-32)	Kruskal-Wallis χ^2 (2) 0.8, p=0.67
Ulceration, n (%):				
None	38 (73.1)	103 (73.6)	50 (67.6)	χ^2 (2) 0.9, p=0.63
Present	14 (26.9)	37 (26.4)	24 (32.4)	
Tumour infiltrating lymphocytes, n (%):				
None	15 (29.4)	20 (15.5)	17 (25.0)	χ^2 (2) 5.2, p=0.08
Present	36 (70.6)	109 (84.5)	51 (75.0)	
Vascular or lymphatic invasion, n (%):				
None	44 (89.8)	121 (90.3)	67 (90.5)	χ^2 (2) 0.02, p=0.99
Present	5 (10.2)	13 (9.7)	7 (9.5)	
Perineural infiltration, n (%):				
None	28 (90.3)	93 (98.9)	41 (97.6)	Fisher's exact p=0.05
Present	3 (9.7)	1 (1.1)	1 (2.4)	
Regression, n (%):				
No	38 (80.9)	105 (84.0)	64 (91.4)	χ^2 (2) 3.0, p=0.22
Yes	9 (19.2)	20 (16.0)	6 (8.6)	
Microsatellites, n (%)				
None	40 (83.3)	110 (90.2)	60 (90.9)	χ^2 (2) 2.0, p=0.37
Present	8 (16.7)	12 (9.8)	6 (9.1)	
Histological subtype, n (%):				
SSM	28 (53.9)	104 (76.5)	40 (54.1)	χ^2 (4) 15.5, p=0.004
NM	17 (32.7)	25 (18.4)	27 (36.5)	
Other	7 (13.5)	7 (5.2)	7 (9.5)	

Factor	No mutation (n=53)	<i>BRAF</i> mutation (n=141)	<i>NRAS</i> mutation (n=76)	Test statistic and significance value
Age at diagnosis or SNB, median (range)	52.6 (19.9-79.0)	51.2 (14.4-80.2)	60.8 (26.7-88.0)	Kruskal-Wallis χ^2 (2) 17.6, p=0.0002
Patient gender, n (%)				
Female	31 (58.5)	68 (48.2)	36 (47.4)	χ^2 (2) 1.9, p=0.38
Male	22 (41.5)	73 (51.8)	40 (52.6)	
Site of tumour, n (%):				
Trunk	12 (22.6)	61 (43.3)	18 (23.7)	Fisher's exact, p<0.0001
Limbs	28 (52.8)	65 (46.1)	48 (63.2)	
Head/neck	5 (9.4)	12 (8.5)	9 (11.8)	
Sun protected	8 (15.1)	3 (2.1)	1 (1.3)	
SNB status, n (%)				
No SNB	19 (37.3)	36 (25.5)	29 (38.7)	χ^2 (4) 10.2, p=0.04
SNB performed – negative	15 (29.4)	31 (22.0)	21 (28.0)	
SNB performed – positive	17 (33.3)	74 (52.5)	25 (33.3)	
Relapse status, n (%)				
Not relapse	34 (64.2)	88 (64.2)	49 (64.5)	χ^2 (2) 0.002, p=1.00
Relapsed	19 (35.9)	49 (35.8)	27 (35.5)	
Overall survival, n (%)				
Alive	36 (67.9)	88 (62.4)	49 (64.5)	χ^2 (2) 0.52, p=0.77
Died	17 (32.1)	53 (37.6)	27 (35.5)	

Table 6-5: Associations between tumour *BRAF* and *NRAS* mutation status and clinico-pathological features.

Significance values quoted for Fisher's exact tests are 2-sided. Percentage values for study type are reported as the proportion within each study, with other percentage levels being the proportion of tumours with each mutation. Significant results are highlighted in bold.

Abbreviations used: SNB, sentinel node biopsy; n, number.

In view of the increasing interest in the biological significance of V600K *BRAF* mutations, in Table 6-6 I compared the clinico-pathological features associated with V600E mutated tumours and V600K mutated tumours.

V600K mutations were more commonly found in tumours from older and male patients. There were also a higher proportion of patients with V600K mutated tumours who had died, which was investigated further using survival analysis in section 6.3.2.2.5.

A comparison was also made between clinico-pathological features of tumours with the two commonest *NRAS* mutations (p.Q61R and p.Q61K), but there were no significant differences in features between these two groups.

6.3.2.2.5 Associations with survival

The influence of mutation status on survival was investigated further using survival analysis. Figure 6-4 presents Kaplan-Meier plots for relapse-free survival (RFS), overall survival (OS) and melanoma-specific survival (MSS) for patients with tumours of differing mutational status. Hazard ratios and 95% confidence intervals generated using the Cox proportional hazards model are also presented. Use of sentinel node biopsy results in delay of the date of first relapse in melanoma patients since the usual site of first recurrence (nodal) is removed, therefore analysis of RFS was adjusted for whether the patient had undergone a sentinel node biopsy and the effect of the biopsy result (SNB status). This analysis shows that mutation status did not modify RFS, OS or MSS in this sample set.

Survival analysis was also performed to identify associations between type of *BRAF* mutation (V600E or V600K) and RFS, OS or MSS. Patients with rare *BRAF* mutations (V600D in 4 patients and K601E in 1 patient) were excluded from this analysis. Figure 6-5 presents Kaplan-Meier plots for these analyses and results of survival analyses using the Cox proportional hazards model.

This analysis demonstrated that patients with a V600K positive tumour had a shorter RFS than patients with a wild-type tumour (HR 2.64, $p=0.02$, median RFS V600E 3.3 years, V600K 2.4 years) when the analysis was adjusted for sentinel node biopsy status. There was also some evidence that V600K mutations shorten OS (HR 2.03, $p=0.07$) and MSS (HR 1.97, $p=0.09$).

To investigate the association between mutation status and RFS further, the Cox proportional hazards model was adjusted in multivariate analysis for demographic and histological factors of prognostic value in melanoma, the results of which are presented in Table 6-7.

Factor	V600E mutation (n=118)	V600K mutation (n=18)	Test statistic and significance value
Study type, n (%):			
Cohort study	36 (81.8)	8 (18.2)	χ^2 (1) 1.4, p=0.24
SNB study	82 (89.1)	10 (10.9)	
Breslow thickness, mm, median (range)	2.0 (0.8-12.0)	2.2 (0.9-5.2)	Mann-Whitney z -0.87, p=0.38
Mitotic rate per mm ² , median (range)	4 (0-40)	6.5 (1-28)	Mann-Whitney z -1.79, p=0.07
Ulceration, n (%):			
None	86 (72.9)	13 (76.5)	Fisher's exact, p=1.00
Present	32 (27.1)	4 (23.5)	
Tumour infiltrating lymphocytes, n (%):			
None	17 (15.7)	2 (12.5)	Fisher's exact, p=1.00
Present	91 (84.3)	14 (87.5)	
Vascular or lymphatic invasion, n (%):			
None	101 (89.4)	15 (93.8)	Fisher's exact, p=1.00
Present	12 (10.6)	1 (6.3)	
Perineural infiltration, n (%):			
None	80 (98.8)	9 (100.0)	Fisher's exact, p=1.00
Present	1 (1.2)	0	
Regression, n (%):			
No	87 (83.7)	14 (82.4)	Fisher's exact, p=1.00
Yes	17 (16.4)	3 (17.7)	
Microsatellites, n (%)			
None	93 (90.3)	13 (92.7)	Fisher's exact, p=1.00
Present	10 (9.7)	1 (7.1)	
Histological subtype, n (%):			
SSM	88 (77.2)	13 (76.5)	Fisher's exact, p=0.54
NM	19 (16.7)	4 (23.5)	
Other	7 (6.1)	0	

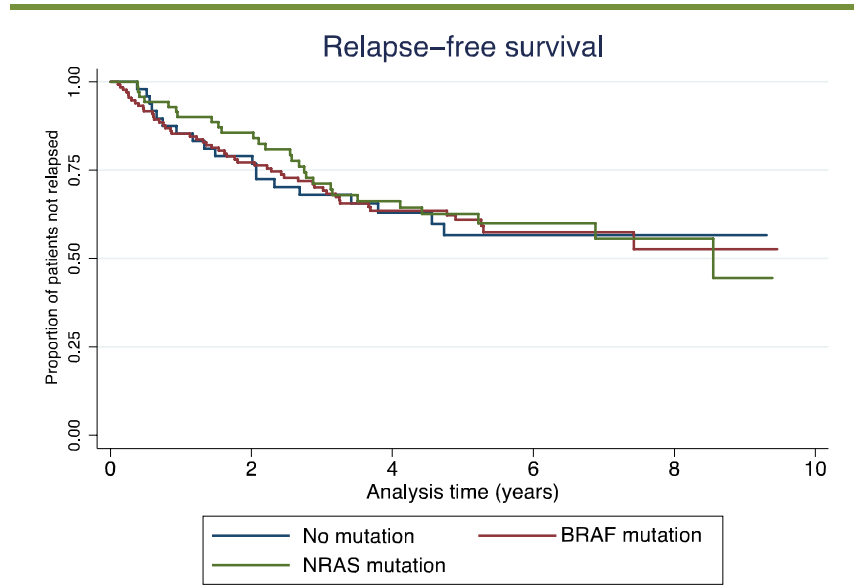
Factor	V600E mutation (n=118)	V600K mutation (n=18)	Test statistic and significance value
Age at diagnosis or SNB, median (range)	50.5 (14.4-80.2)	60.7 (32.8-79.1)	Mann-Whitney z -2.8, p=0.005
Patient gender, n (%)			
Female	63 (53.4)	4 (22.2)	Fisher's exact, p=0.02
Male	55 (46.6)	14 (77.8)	
Site of tumour, n (%):			
Trunk	48 (40.7)	11 (61.1)	Fisher's exact, p=0.47
Limbs	56 (47.5)	6 (33.3)	
Head/neck	11 (9.3)	1 (5.6)	
Sun protected	3 (2.5)	0	
SNB status, n (%)			
No SNB	31 (26.3)	4 (22.2)	Fisher's exact, p=0.08
SNB performed – negative	23 (19.5)	8 (44.4)	
SNB performed – positive	64 (54.2)	6 (33.3)	
Relapse status, n (%)			
Not relapse	77 (67.5)	8 (44.4)	χ^2 (1) 3.6, p=0.06
Relapsed	37 (32.5)	10 (55.6)	
Overall survival, n (%)			
Alive	78 (66.1)	7 (38.9)	χ^2 (1) 4.9, p=0.03
Died	40 (33.9)	11 (61.1)	

Table 6-6: Associations between tumour V600E and V600K *BRAF* mutations and clinico-pathological features.

Significance values quoted for Fisher's exact tests are 2-sided. Percentage values for study type are reported as the proportion within each study, with other percentage levels being the proportion of tumours with each mutation. Significant results are highlighted in bold.

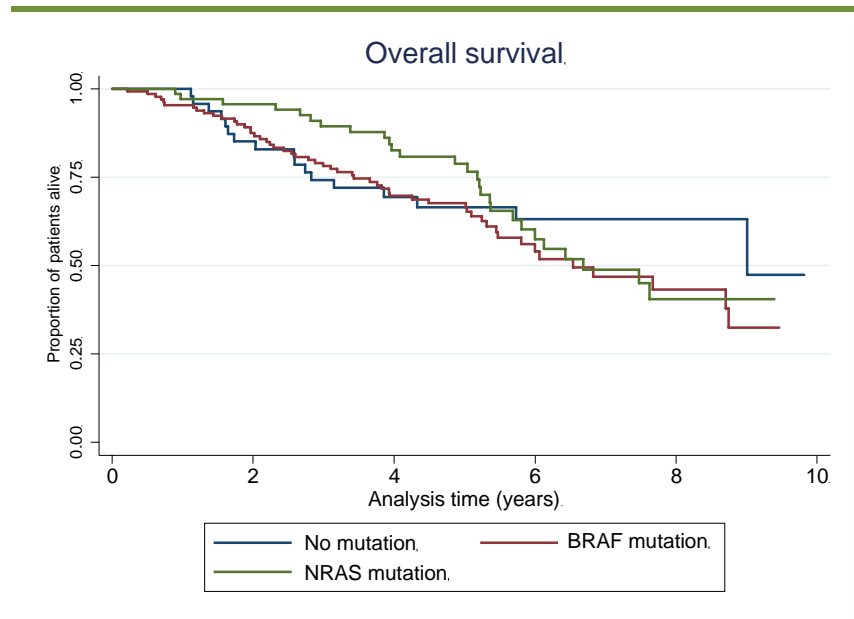
Abbreviations used: SNB, sentinel node biopsy; n, number.

A.



Genotype (analysis adjusted for SNB status)	HR	95% CI	P-value
No mutation	1		
<i>BRAF</i> mutation	0.94	0.54-1.62	0.81
<i>NRAS</i> mutation	0.89	0.49-1.62	0.70

B.



Genotype	HR	95% CI	P-value
No mutation	1		
<i>BRAF</i> mutation	1.29	0.74-2.23	0.37
<i>NRAS</i> mutation	1.01	0.55-1.86	0.97

C.

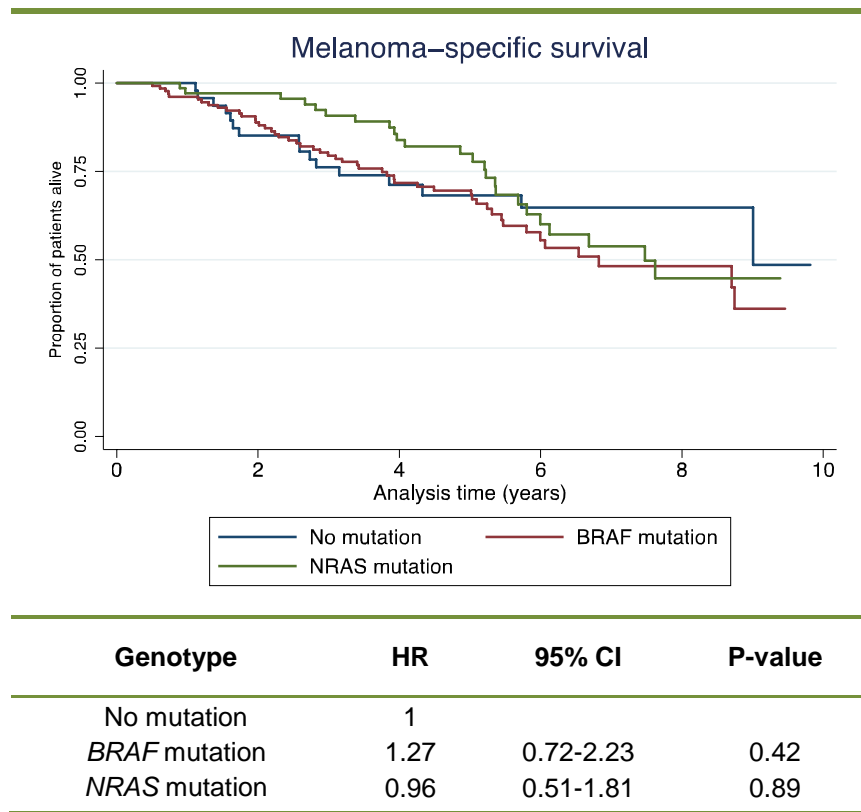
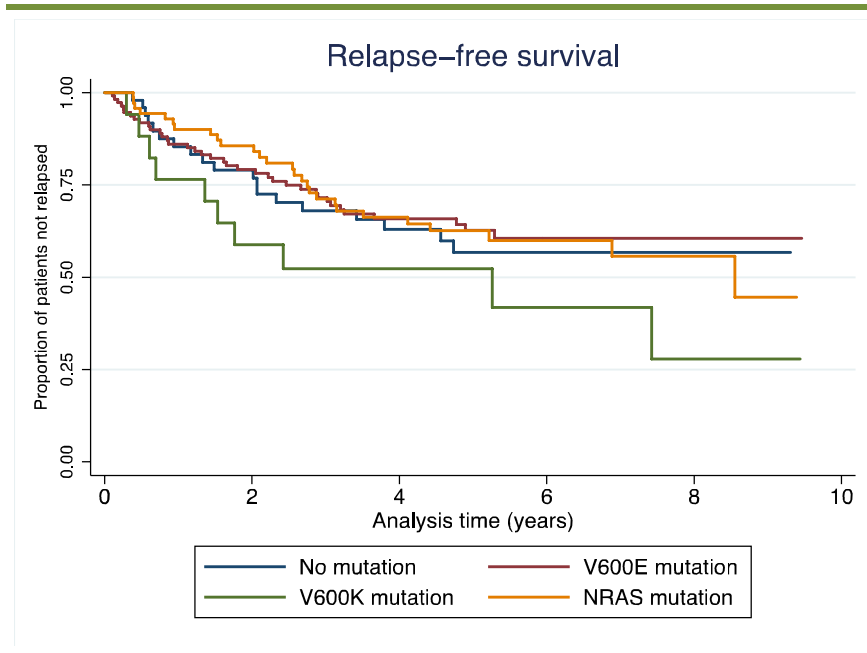


Figure 6-4: Kaplan-Meier plots and results of survival analyses used to identify associations between relapse-free (A), overall (B) and melanoma-specific survival (C) and tumour genotype.

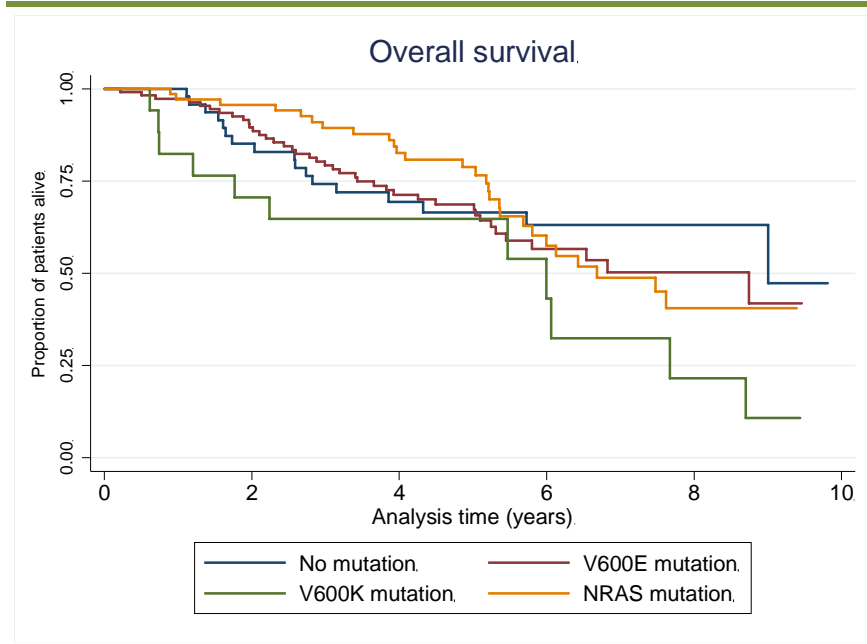
Hazard ratios and 95% confidence intervals generated using a Cox proportional hazards model are presented. For relapse-free survival, the analysis is adjusted for influence of sentinel-node biopsy status. Abbreviations used: HR, hazard ratio; CI, confidence interval; SNB, sentinel node biopsy.

A.



Genotype (analysis adjusted for SNB status)	HR	95% CI	P-value
No mutation	1		
V600E mutation	0.80	0.45-1.42	0.45
V600K mutation	2.64	1.20-5.80	0.02
NRAS mutation	0.89	0.49-1.62	0.69

B.



Genotype	HR	95% CI	P-value
No mutation	1		
V600E mutation	1.17	0.66-2.06	0.60
V600K mutation	2.03	0.95-4.33	0.07
NRAS mutation	1.02	0.55-1.86	0.96

C.

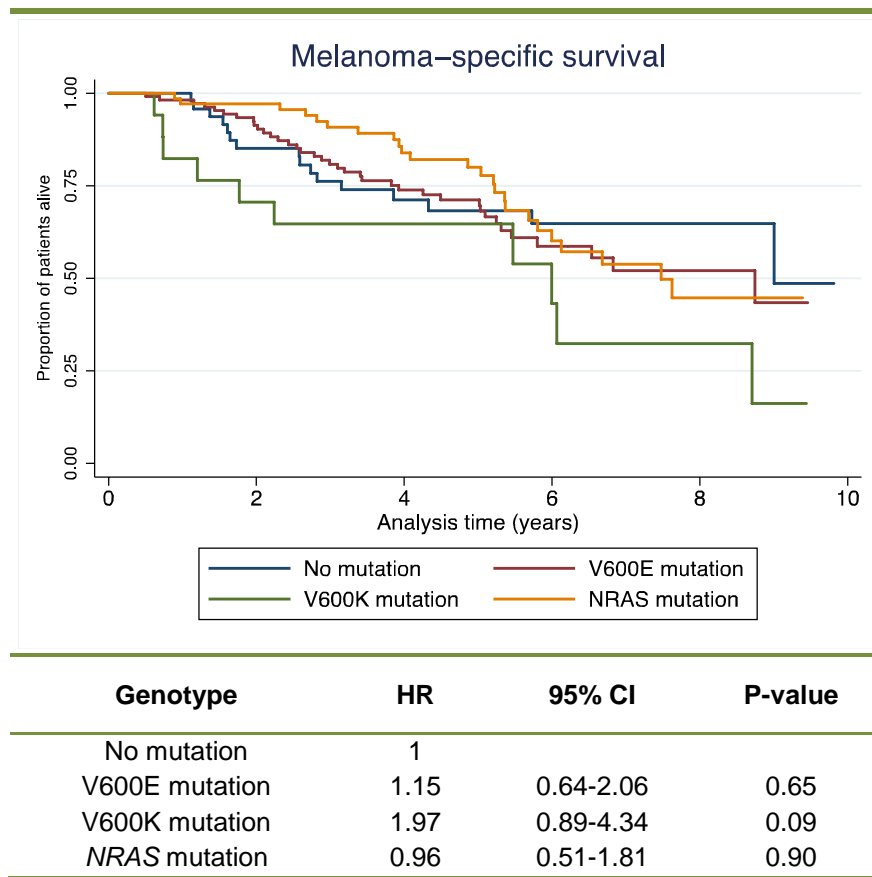


Figure 6-5: Kaplan-Meier plots and results of survival analyses used to identify associations between relapse-free (A), overall (B) and melanoma-specific survival (C) and tumour genotype where V600E and V600K *BRAF* mutations were analysed separately.

Hazard ratios and 95% confidence intervals generated using a Cox proportional hazards model are presented. For relapse-free survival, the analysis is adjusted for influence of sentinel-node biopsy status. Significant results are highlighted in bold. Abbreviations used: HR, hazard ratio; CI, confidence interval; SNB, sentinel node biopsy.

Mutation status	Analysis adjusted SNB status only (n=258)		Analysis further adjusted for age and sex of patient and site of tumour (n=258)		Analysis further adjusted for Breslow thickness, ulceration and mitotic rate of tumour (n=245)	
	HR (95% CI)	P-value	HR (95% CI)	P-value	HR (95% CI)	P-value
No mutation	1.00		1.00		1.00	
V600E <i>BRAF</i> mutation	0.80 (0.45-1.42)	0.45	0.89 (0.49-1.63)	0.71	1.04 (0.54-2.01)	0.90
V600K <i>BRAF</i> mutation	2.64 (1.20-5.80)	0.02	2.25 (0.97-5.19)	0.06	2.58 (1.03-6.48)	0.04
<i>NRAS</i> mutation	0.89 (0.49-1.62)	0.69	0.80 (0.42-1.52)	0.50	0.82 (0.41-1.65)	0.58

Table 6-7: Associations between tumour mutation status and relapse-free survival in multivariate analysis.

The first model is adjusted for sentinel node biopsy status only; the second further adjusted for demographic variables of prognostic importance (patient gender, age at diagnosis and site of tumour) in melanoma and finally the model is further adjusted for histological prognostic factors (Breslow thickness, mitotic rate and ulceration status). Presence of a V600K mutation was significantly associated with reduced relapse free survival time in the first model and the model fully adjusted for other prognostic factors. Significant results are highlighted in bold. Abbreviations used: HR, hazard ratio; CI, confidence interval; SNB, sentinel node biopsy.

In the multivariable analysis presented, the presence of a V600K mutation was significantly associated with reduced RFS time even when adjusted for prognostic factors in melanoma, indicating that presence of a V600K mutation was independently associated with RFS. As only 18 tumours had a V600K mutation, this study is limited in power to identify relationships with survival, however I have identified an association with RFS suggesting that this effect is significant and warrants further investigation in a larger sample set. Presence of a V600E mutation did not influence RFS, suggesting that V600K mutations may induce different biological properties in a tumour.

6.3.2.2.6 Gene expression patterns associated with mutation status

Genes differentially expressed between groups of tumours based on genotype were identified using linear regression adjusted for the study from which patients were recruited. This analysis was also performed using significance analysis of microarrays (SAMic) analysis, to allow comparison of gene lists, but the results were very similar, therefore the results of analysis based on linear regression are presented in Table 6-8.

6.4 Discussion

6.4.1 Use of cDNA specimens for mutation detection

In this chapter I have described experiments to assess whether cDNA could be used as an alternative to DNA for mutation screening from small volume FFPE melanoma specimens. This investigation was initiated to try and limit the amount of precious tumour material required for mutation screening by using available cDNA that had been previously generated for use in gene expression experiments. Despite promising initial results, further investigation demonstrated that different results are generated when cDNA and DNA are used for mutation detection of *BRAF* and *NRAS* using pyrosequencing. The spectrum of *BRAF* mutations identified and the percentage mutation levels differed in cDNA and DNA. There was better concordance for *NRAS*, however differences do exist and without accurate *BRAF* mutation screening, further analysis is limited.

<i>BRAF</i> mutated tumours compared to tumours with no mutation (fold difference in gene expression for <i>BRAF</i> mutated tumours/wild-type tumours)			<i>NRAS</i> mutated tumours compared to tumours with no mutation (fold difference in gene expression for <i>NRAS</i> mutated tumours/wild-type tumours)			<i>NRAS</i> mutated tumours compared to <i>BRAF</i> mutated tumours (fold difference in gene expression for <i>NRAS</i> mutated tumours/ <i>BRAF</i> mutated tumours)			V600K <i>BRAF</i> mutated tumours compared to V600E <i>BRAF</i> mutated tumours (fold change in gene expression for V600K mutations/V600E mutations)		
Gene	Mean fold difference	P-value	Gene	Mean fold difference	P-value	Gene	Mean fold difference	P-value	Gene	Mean fold difference	P-value
<i>ETV1</i>	1.34	9.75x10 ⁻⁷	<i>TYRO3</i>	1.44	1.90x10 ⁻⁷	<i>NRAS</i>	1.16	1.04x10 ⁻⁷	<i>TFAP2C</i>	0.54	0.00001
<i>ERBB3</i>	1.20	1.63x10 ⁻⁶	<i>CTNNB1</i>	1.08	3.27x10 ⁻⁷	<i>THBS2</i>	0.69	1.50x10 ⁻⁷	<i>BRAF</i>	1.11	0.0001
<i>CDK6</i>	1.22	2.29x10 ⁻⁶	<i>NRAS</i>	1.17	6.10x10 ⁻⁶	<i>VHL</i>	1.09	2.15x10 ⁻⁷	<i>CDK2</i>	1.21	0.0002
<i>PTPRG</i>	1.30	2.60x10 ⁻⁶	<i>PTPRG</i>	1.30	7.58x10 ⁻⁶	<i>WNT5A</i>	0.67	2.08x10 ⁻⁶	<i>DVL3</i>	1.12	0.002
<i>TYRO3</i>	1.33	5.90x10 ⁻⁶	<i>CDK6</i>	1.23	7.70x10 ⁻⁶	<i>RAP2A</i>	1.09	0.00001	<i>TRAF3</i>	1.25	0.002
<i>CD59</i>	1.13	0.00003	<i>ETV1</i>	1.37	0.00001	<i>PTEN</i>	1.06	0.00003	<i>EVI2A</i>	0.77	0.002
<i>CEACAM1</i>	1.54	0.00004	<i>TGFBR1</i>	1.13	0.00002	<i>CTNNB1</i>	1.03	0.00003	<i>JUN</i>	1.10	0.003
<i>MAP3K8</i>	1.54	0.00004	<i>ERBB3</i>	1.23	0.00003	<i>QARS</i>	1.08	0.00004	<i>EXT1</i>	1.07	0.003
<i>CAV1</i>	1.12	0.0001	<i>TRAF4</i>	1.19	0.00004	<i>BIRC2</i>	1.08	0.00007	<i>PDGFA</i>	0.80	0.004
<i>NFKB2</i>	0.83	0.0001	<i>TNFRSF5</i>	0.80	0.00005	<i>ERCC6</i>	1.13	0.0001	<i>MSF</i>	1.12	0.004

Table 6-8: The top 10 most differentially expressed genes between wild-type tumours, tumours with *BRAF* mutations and *NRAS* mutations.

The top ten most differentially expressed genes are listed for each comparison. Significance values are from linear regression analyses adjusting for study from which patients were recruited to. Genes highlighted in bold appear on more than one list. Cells highlighted in green shading contain genes which are part of the mitogen-activated protein kinase (MAPK) or phosphatidylinositol-3-kinase (PI3K) signalling pathway.

cDNA has been previously used for mutation screening in frozen tumour samples to allow detection of small numbers of mutant *BRAF* and *NRAS* alleles in heterogeneous tissues where both wild-type and mutant genes are present [603, 604]. The methods used cDNA amplified using PCR primers designed to introduce new site-directed restriction sites into the PCR amplicon when a mutation is present. Restriction enzymes then cut the cDNA and fragments are identified [603, 604]. These analyses identified mutations at a comparable frequency to other methods, with no double mutations identified [603, 604]. This technique has been used to screen for mutations in DNA extracted from small numbers of FFPE melanoma specimens, but not cDNA synthesised from mRNA extracted from FFPE materials [604]. A similar method which utilises a series of PCR amplifications and the presence of a restriction site to preferentially digest wild-type *BRAF* sequences in cDNA has been used for mutation detection in circulating tumour cells from peripheral blood, frozen and FFPE tumour specimens [605, 606]. Seventy melanoma tumour biopsies from frozen and FFPE tissue have been assessed previously with varying degrees of V600E *BRAF* mutation positivity identified. The authors report that this method using mRNA as template in association with PCR amplification, increases sensitivity compared to DNA based assays, especially in melanoma cells with high levels of V600E *BRAF* mRNA expression, however *NRAS* mutation status was not determined in this study to allow further comparison with our results [605].

cDNA synthesized from mRNA reflects the transcribed genes within the cell. RNA extracted from FFPE materials is degraded, leading to short cDNA sequences. This, in combination with the PCR amplification step used in pyrosequencing, has the potential to introduce errors, which may be detected as mutations in the highly sensitive pyrosequencing assay. The other possibility is that there is increased expression of *BRAF* transcripts in melanoma cells harbouring *BRAF* mutations. If these mutations are present in a small proportion of cells, this may not be detected using DNA based analysis, however if expression is increased in mutant cells, mutant transcripts may be detected in cDNA. There is evidence that there is copy number gain in association with *BRAF* activating mutations in short-term melanoma cultures, established cell lines and tumour samples with both gain across the entirety of chromosome 7 and in the specific 7q34 region which harbours the *BRAF* locus [44, 356, 607-611]. There also appears to be preferential amplification of mutant *BRAF* alleles [356, 609, 612]. As pyrosequencing is quantitative, the higher levels of mutation detected in cDNA samples may reflect greater transcription of mutant alleles, with detection of both *NRAS* and *BRAF* mutations in cDNA from a single tumour resulting from tumour heterogeneity. A number of factors argue against this hypothesis: low level *BRAF* mutations identified

using pyrosequencing in cDNA were not detected using the SNaPshot system, although this method is less sensitive than pyrosequencing [360]; we did not see differential expression of *BRAF* transcripts in *BRAF* mutated tumours compared with *NRAS* mutated or wild-type tumours and in *NRAS* mutated tumours with high levels of mutation detected in DNA and over-expression of *NRAS* (discussed in section 6.4.3), results from cDNA and DNA were more comparable. Therefore, it is likely that poor quality cDNA used in a highly sensitive assay has produced erroneous results.

6.4.2 Associations between mutation status and clinicopathological features and survival

In this study, 50.5% of tumours had a *BRAF* mutation and 27.2% had an *NRAS* mutation. These frequencies are higher than those quoted in a recent meta-analysis of studies using various mutation detection methods (*BRAF* 41% and *NRAS* 18%) [31], but are comparable to studies that have used more sensitive pyrosequencing for mutation detection (*BRAF* 53%, *NRAS* 29%) [436] (*NRAS* 32%) [353].

This study has identified associations between mutation status and a number of clinicopathological features, the majority of which have been previously described in the literature [30, 31, 549, 587, 588]. *BRAF* mutations were found more frequently in tumours of the superficial spreading subtype, with *NRAS* mutations more commonly in nodular tumours. Truncal tumours, on intermittently sun-exposed skin, were most likely to have a *BRAF* mutation, with *NRAS* mutations found more commonly on head and neck tumours or tumours of the limbs of chronically sun-exposed skin. These data are consistent with other studies and Whiteman's two route theory of carcinogenesis where intermittent excessive sun exposure is postulated to be associated with melanoma risk on the trunk in individuals with a tendency to develop naevi [152]. Tumours on sun-protected sites were less likely to harbour a *BRAF* or *NRAS* mutation, although mutations were identified in four acral tumours. In this study, *BRAF* mutations were more likely to be found in patients who were younger at diagnosis, with *NRAS* mutations in older patients.

I did not find any associations between tumour Breslow thickness, mitotic rate or ulceration and mutation status as has been described in other studies [549, 583, 589]. I report some evidence that patients with a positive SNB were more likely to have a *BRAF* mutated primary tumour. A recent study found that patients with a *NRAS* or *BRAF* mutated tumour were more likely to present with stage III disease, the association being strongest for palpable nodal disease [583]. My study indicates there may also be an association between presence of a *BRAF* mutation and

micrometastases identified using sentinel node biopsy, although a smaller proportion of patients with *BRAF* positive tumours appeared to have elected not to have a SNB (26% compared with 37% for patients with wild-type tumours and 39% for patients with *NRAS* mutated tumours) so these data are difficult to interpret.

There appeared to be differences in the clinical characteristics of patients with V600K *BRAF* positive tumours. Albeit, in a small sample, I found that V600K mutations are more commonly found in primary tumours from patients diagnosed at a later age (median 60.7 years versus 50.5 years with V600E mutations, $p=0.005$) and in male patients (77.8% tumours with V600K mutation were in male patients). As discussed in the background to this chapter, the association between age at diagnosis of metastatic disease and mutation status has been previously identified in a study of metastatic melanoma [593]. This study also found an association between V600K mutations and sun-induced damage, as determined by degree of solar elastosis, and V600K tumours were more commonly found in tumours on the head or neck, a sun-exposed site, with V600E tumours more commonly on the limbs [593]. In the current study, a higher proportion of V600K mutations were found in tumours on the trunk with V600E mutations more commonly on the limbs. This was a non-significant finding and I was unable to investigate the association between sun-damage and presence of V600K mutation based on the data available currently (pending central pathology review). The relationship between sun exposure and development of V600E mutations is not clear, however the evidence presented by Menzies and colleagues suggests that chronic sun exposure may be related to the pathogenesis of V600K mutations [593]. This is further supported by the higher incidence of V600K mutations in geographical locations with higher UV exposure [436, 550, 593]. Again, the V600K mutation is not characteristic of UVB DNA damage [541, 543], however there are suggestions that UVA and UVB radiation may cause mutations at the *BRAF* V600 site [544, 545]. Menzies and colleagues suggested that a number of factors are likely to contribute to V600K mutations, including sun-exposure on the background of genetic alterations related to the age of the patient [593]. Also, V600E mutations are predominantly found in young patients, suggesting that these mutations may be more likely have a specific aetiology, whether that is environmental or genetic, compared to V600K mutations [593]. My findings that V600K mutations are commoner in primary melanoma in older patients supports the hypothesis that chronic sun exposure may be important, however I found no further evidence to support this in my data. Menzies and colleagues did not report a difference in prevalence of V600K mutations in males and females [593]. My study suggests that V600K mutated tumours are commoner in male patients, however this requires confirmation in a larger sample set. This may be related to the higher

proportion of truncal tumours with V600K mutations in this dataset, with tumours on the trunk more commonly diagnosed in men [3]. However, the presence of these mutations may be contributing to the poor prognosis in male patients [85, 91, 613], which despite intensive investigation is thought to be due to biological differences between men and women, remains largely unexplained [144].

With regards to survival, consistent with previous reports, this study found no association between presence of a *BRAF* or *NRAS* mutation and RFS, OS or MSS [436, 555, 576, 583, 588, 590, 591]. However, there was a significant reduction in RFS for patients with a V600K positive tumour (HR 2.64 (95% CI 1.20-5.80), $p=0.02$), which remains significantly associated in multivariable analysis adjusted for prognostic factors in melanoma (HR 2.58 (95% CI 1.03-6.48), $p=0.04$). In metastatic melanoma, presence of a V600K mutation has been associated with shorter distant metastasis-free survival time and OS [593, 594]. My study is the first to assess this relationship in primary melanoma specimens, and therefore the identification of an independent association with RFS is clearly a significant finding. Differences in patient characteristics and RFS in patients with V600K mutated primary tumours supports the hypothesis that there may be different aetiology and biological behaviour of V600K mutated tumours compared with commoner V600E mutated tumours [593].

6.4.3 Gene expression patterns associated with mutation status

As discussed in the introduction to this chapter, identification of expression signatures in tumours associated with *NRAS* mutations has been particularly limited with more focus on the identification of signatures associated with *BRAF* mutated tumours [508, 591, 596-599]. The strength of this study is that we have been able to look at expression profiles in a large number of primary melanoma samples with differing mutations.

My study has shown that a number of genes are over-expressed in tumours with either a *BRAF* or *NRAS* mutation compared with wild-type tumours. Differentially expressed genes are ets variant 1 (*ETV1*), TYRO3 protein tyrosine kinase (*TYRO3*), v-erb-b2 erythroblastic leukaemia viral oncogene homolog 3 (*ERBB3* or *HER3*), cyclin-dependent kinase 6 (*CDK6*) and protein tyrosine phosphatase, receptor type G (*PTPRG*). As discussed in previous chapters, in order to confirm these results, validation of gene expression results is required within this sample set and in an independent validation study. However, a number of the genes are biologically interesting and I shall discuss them in further detail.

ETV1 and *TYRO3* are the most differentially expressed genes in *BRAF* and *NRAS* mutated tumours, respectively. *ETV1* is an ETS transcription factor and has been recently identified as an oncogene in melanoma [614]. *ETV1* is situated on 7p21 and is frequently amplified in primary and metastatic tumours [614]. In immortalized melanocytes and mouse models, over-expression of *ETV1* in combination with over-expression of *NRAS*^{G12D} or *BRAF*^{V600E} oncoproteins stimulated cell growth and tumourigenesis, an effect which was not seen when *ETV1*, *NRAS*^{G12D} or *BRAF*^{V600E} were over-expressed alone [614, 615]. Therefore, on the background of MAPK pathway activation by *BRAF* or *NRAS* mutations, *ETV1* over-expression can transform immortalized melanocytes [614]. The authors of the study also found that over-expression of *ETV1* in melanocytes over-expressing *NRAS*^{G12D} increased expression of the microphthalmia-associated transcription factor gene (*MITF*) and *MITF* protein and this increased level of *MITF* was required for cell growth [614]. *MITF* is a transcription factor required for melanocyte development which activates multiple downstream factors important for normal melanocyte physiology and survival, cell cycle regulation, and cellular growth [616]. Germline *MITF* mutations have been associated with melanoma development [617, 618] and *MITF* is amplified in around 20% of melanomas, where it can act as an oncogene [615]. *MITF* can also contribute to melanoma progression when not highly expressed by having tumour promoting actions, stimulating cell cycle progression but also inhibitory actions, by pushing the cell towards terminal differentiation or apoptosis, depending on protein levels within the cell [619, 620]. Multiple signalling pathways regulate *MITF* expression, for example the MAPK pathway, melanocyte-stimulating hormone acting via the melanocortin 1 receptor (MC1R) and KIT [616, 621]. Ectopic *MITF* expression in melanocytes expressing *BRAF*^{V600E} causes transformation [615], however in melanoma cells *MITF* expression is carefully controlled by mutated *BRAF* to allow survival and proliferation, as low *MITF* levels lead to apoptosis and high levels to terminal differentiation [622]. Previous studies suggest that ETS factors are activated by MAPK pathway mediated phosphorylation [623] and *ETV1* is a target of ERK signalling via MAPK activation [556]. Inhibition of MEK, which is downstream of *NRAS* and *BRAF* or inhibition of mutant *BRAF*, in V600E-mutated melanoma cell lines leads to down-regulation of gene expression in members of the ETS family, including *ETV1* [556, 563]. In cells where the MAPK pathway is driven by receptor tyrosine kinases without mutant *BRAF*, MEK inhibition does not cause altered gene expression [556]. These observations suggest that over-expression of *ETV1* enhances an oncogenic signal which functions, and is also enhanced, by MAPK activation [614]. It also appears that *MITF* activation participates in this pathway [614]. I have identified significant over-expression of *ETV1* in *NRAS* or *BRAF* mutated tumours compared with wild-type tumours which supports

the hypothesis that mutated tumours drive expression of *ETV1* which enhances the oncogenic effect of *NRAS* or *BRAF* mutations. MITF was not present on the Human Cancer panel used for gene expression profiling, so this association could not be assessed in my sample set. This study would suggest that *ETV1* is a strong driving force for oncogenesis in mutated tumours, indicating that this may be a candidate for therapeutic targeting.

TYRO3 was significantly over-expressed in *BRAF* and *NRAS* mutated tumours compared with wild-type tumours. *TYRO3* is a member of the TAM (*TYRO3*, *AXL* and *MER*) receptor tyrosine kinase family which have been shown to have effects on cellular migration and invasion, angiogenesis, cell survival and tumour growth in cancer [624]. In melanoma cell lines, *TYRO3* has been shown to be a positive regulator of the *MITF-M* isoform [625] and is over-expressed in primary tumour samples compared to normal tissues [625]. Over-expression of *TYRO3* in primary melanocytes overcomes *BRAF*^{V600E} induced senescence and knockdown in melanoma cells inhibits proliferation *in vitro* and reduces tumorigenic potential in mice [625]. Therefore, my study has identified another gene which is differentially expressed in *NRAS* and *BRAF* mutated tumours which has been shown to have a role in oncogenesis of *BRAF* mutated tumours and is also a regulator of *MITF* expression. Direct therapeutic targeting of MITF or *ETV1* may be difficult as they are transcription factors and difficult to target using small molecules [626], however *TYRO3* may represent a molecule more amenable to targeted therapies [616, 625].

ERBB3 is a transmembrane receptor which binds to molecules, such as transforming growth factor- α and epidermal growth factors leading to intracellular signalling causing cellular proliferation, organ development and repair [627, 628]. It lacks innate kinase function, but can dimerise with other *ERBB* receptors and is important in activation of the MAPK pathway [628, 629] and the PI3K-Akt pathway [627]. In melanoma, *ERBB3* signalling can inhibit expression of differentiation genes and increase expression of proliferation genes in melanocytes and melanoma cells, leading to proliferation and invasion [630]. I did not identify any differential expression of other members of the *ERBB* family, specifically *ERBB2*, which is the usual binding partner for *ERBB3* [627, 629]. As dimerisation of receptors is required for action this is perhaps surprising, however over-expression of *ERBB3* in mutated tumours, which is closely related to activation of MAPK and PI3K-Akt signalling is clearly of interest.

When our results are compared against other gene expression profiles identified in previous gene expression studies, it is reassuring to see that there is overlap between genes identified. I have confirmed the finding of Johansson and colleagues in tumour samples, that *ERBB3* was over-expressed in *BRAF* mutated cell lines versus wild-type

cell lines [599]. *ETV1* was found to be highly differentially expressed in *BRAF* mutated tumours in the EORTC study using frozen primary melanoma tumours. This has been confirmed in this dataset and I have also found that *ETV1* is differentially expressed in *NRAS* mutated tumours [591].

There is significant overlap between genes differentially expressed in *BRAF* and *NRAS* mutated tumours compared to wild-type tumours which is not unexpected, indicating that similar genes are dysregulated in cells harbouring a *NRAS* or a *BRAF* mutation. Studies identifying gene expression profiles in tumour tissue have been performed in small numbers of samples, with some studies showing overlap in gene expression profiles [508] and others no concordance in gene expression between *NRAS* and *BRAF* mutated tumours [591]. My study represents the largest study to date using primary melanoma tumours and indicates significant overlap in cancer-related genes differentially expressed in *NRAS* or *BRAF* mutated tumours compared to wild-type tumours. I have then gone on to compare gene expression between *NRAS* and *BRAF* mutated tumours, the results of which I will discuss now.

As this comparison in gene expression in *NRAS* mutated tumours with wild-type and *BRAF* mutated tumours has been limited to small numbers of tumour and cell lines, the results I present here are novel and will require extensive validation. One of the most interesting findings is that *NRAS* expression was significantly greater in *NRAS* mutated tumours compared with *BRAF* mutated tumours. *NRAS* is also highly expressed in *NRAS* mutated tumours when compared with wild-type tumours. *NRAS* mutations in melanoma are activating and these results indicate that expression is also increased. Changes in gene expression can be due to mutation, alteration in genomic organisation such as translocations, changes in DNA copy number or epigenetic alterations [631]. In common with *BRAF* mutations there is evidence of copy number gain at the *NRAS* locus associated with activating mutations in short-term melanoma cultures, but this is less well documented than in *BRAF* mutated tumours [607, 608, 610]. Therefore mutation in combination with copy number alteration may cause altered expression in *NRAS* mutated tumours. The pyrosequencing assay used for mutation screening in my study was quantitative with mutation levels in *NRAS* mutated tumours being greater than 50% in over half of the tumours. These results indicate an abundance of the mutated gene in these tumours, which could be due to a number of mechanisms such as homozygosity, preferential copy gain of the chromosome with the mutant gene or because of amplification of the mutant allele [609]. This hypothesis makes many assumptions about the accuracy of mutation levels detected using pyrosequencing and DASL gene expression results making it highly speculative;

further intensive investigation is needed to clarify the number of *NRAS* alleles in the samples and the expression levels.

PTEN was also over-expressed in *NRAS* mutated tumours compared with *BRAF* mutated tumours. *PTEN* is inhibitory to the PI3K pathway and resides in a commonly deleted area in melanoma on chromosome 10q [151]. *PTEN* is inactivated by mutation in approximately 10% of melanoma tumours [21, 632, 633]. *NRAS* and *PTEN* mutations rarely occur in the same tumour, but *PTEN* mutations are commonly found associated with *BRAF* mutations as are lower *PTEN* copy numbers [43, 44, 151]. Therefore, the over-expression of *PTEN* in *NRAS* mutated tumours may reflect normal levels when compared to lower levels of *PTEN* that may be found in *BRAF* mutated tumours. We have not assessed the copy number or mutation status of *PTEN* in these tumours, but this knowledge would help confirm or refute this hypothesis. It is also likely that *PTEN* expression would be elevated in an *NRAS* mutated tumour in an attempt to reduce signalling via the PI3K pathway.

The final comparison I have made is between gene expression in V600K *BRAF* mutated tumours versus V600E tumours. As the numbers involved in this analysis are small, there is limited power to detect differential gene expression but I will briefly discuss some observations. Once a correction had been made for multiple testing, only two genes were differentially expressed, *TFAP2C* was significantly under-expressed in V600K tumours and *BRAF* significantly over-expressed. Both V600K and V600E mutations cause high *BRAF* kinase activity, but this is greater in association with the V600E mutation [554]. In view of the differences in the prognostic influence of these mutation types, age-distribution and association with sun-damaged skin, there appear to be biological differences in tumours with these differing mutations [593]. The similarity in gene expression profile may suggest otherwise, but this analysis is limited by the small numbers of tumours with V600K mutations. In a previous study which assessed gene expression profiles in melanoma cell lines with a V600E mutation following inhibition with *BRAF*^{V600E} or MEK inhibitors, *TFAP2C* was down-regulated after treatment indicating that this is a direct transcriptional target of the activated pathway [563]. *TFAP2C* encodes AP2 γ , which is a member of the activating protein family 2 (AP2) family of transcription factors. Loss of AP2 transcription factors, specifically AP2 α is associated with transition from radial growth phase melanomas to vertical growth phase, with re-expression in highly metastatic melanoma cells leading to tumour growth inhibition and reduction in metastatic potential [634-637]. *TFAP2C* is the only AP2 factor on the Human Cancer Panel, so we could not assess expression in other AP2 factors. *BRAF* expression was also greater in V600K mutated tumours, suggesting that the level of pathway activation would be greater than in V600E mutated

tumours. As *TFAP2C* is a direct transcriptional target of the activated pathway [563], levels of *TFAP2C* would be expected to be greater if activation of the pathway was increased by higher *BRAF* levels. This suggests that over-expressed *BRAF* in V600K cells may not act to increase signalling through the pathway or that the relationship between signalling and *TFAP2C* expression may be more complicated than previously thought. In view of the relationship between AP2 α loss and progression in melanoma tumours, under-expression of *TFAP2C* in V600K mutated tumours compared with V600E may contribute to the biological properties of the V600K mutated tumour.

I have already alluded to some of the limitations of this work, such as poor power to assess relationships between tumour features, patient characteristics, gene expression profiles and the rarer V600K *BRAF* mutation. Gene expression data in this study was also limited to 502 cancer-related genes; assessment of gene expression on a genome-wide scale would yield further biological information, and with successful trial runs using the WG-DASL HT assay (described in Chapter 2) the hope is that this will be possible using FFPE melanoma tissue in the near future. A final limitation is related to the issue of tumour heterogeneity as tumours can contain a population of wild-type and mutant cells [357, 579, 584, 585]. Separate tissue cores, usually taken in close proximity to each other, from the same tumour were used to generate gene expression data and screen for mutations in a proportion of samples. Therefore it is possible that gene expression may be related to a wild-type part of the tumour which was found to be *BRAF* mutated in a separate tissue core. To reduce these errors, ideally RNA and DNA would be extracted from the same tissue core, extraction kits allowing extraction of both nucleic acids from a single FFPE specimen have recently been developed and will be used for future work of this type (as discussed in Chapter 2).

6.4.4 Summary and conclusions

This work has shown that cDNA is not suitable for mutation screening.

Results using DNA samples confirmed the associations between mutation status and clinico-pathological features previously identified in the literature and identified an independent association between the presence of V600K *BRAF* mutations in primary tumours and shorter RFS.

A large number of genes were found to be differentially expressed in *BRAF* and *NRAS* mutated tumours compared to wild-type tumours, some of which have been identified in previous gene expression studies, with overlap between the two lists suggesting similar biological processes are active in the tumours with *BRAF* or *NRAS* mutations.

The two most differentially expressed (*ETV1* and *TYRO3*) both have roles in oncogenesis in association with MAPK pathway activation in and *MITF* expression.

Presence of an *NRAS* mutation was associated with significantly greater *NRAS* and *PTEN* expression, a finding that requires validation. There were also small differences in the gene expression profile of V600K and V600E mutated tumours. This analysis has been performed in small numbers of tumours requiring extensive further investigation, but there is a suggestion of higher *BRAF* expression in V600K tumours with lower expression of a direct transcriptional target of the MAPK pathway, *TFAP2C*. This, in association with differing clinical features and modified prognosis in patients with a V600K mutated tumour supports the suggestion that these tumours may be aetiologically and biologically distinct from V600E mutated tumours [593]. If this hypothesis is proven, this may have relevance to use of BRAFi.

7 Primary melanoma tumour ulceration: relationship with gene expression profiles, tumour features and patient characteristics

7.1 Aims

The aims of this chapter are to:

- Identify tumour histological features and patient characteristics associated with primary melanoma ulceration in a large patient cohort.
- To identify whether lymphovascular invasion, microvessel density or macrophage infiltration assessed using immunohistochemistry (IHC) are associated with ulceration in a subset of tumours.
- To identify tumour gene expression profiles associated with ulceration.

Results of these analyses will be related to both the prognostic and predictive influence of tumour ulceration status in melanoma.

7.2 Background

Ulceration of a primary melanoma is defined as absence of intact epidermis, including stratum corneum and basement membrane [94]. Traumatic loss of epidermis can occur, but this can be distinguished because of a number of additional features which can be seen in spontaneous cases of ulceration, namely thinning, reactive hyperplasia or effacement of surrounding epidermis and evidence of a host response, such as neutrophil infiltration [94, 638]. As discussed in Chapter 1, ulceration of a primary melanoma tumour is a poor prognostic factor and is integral to the American Joint Committee on Cancer (AJCC) staging guidelines [58]. The prognostic influence of ulceration is apparent even in stage III disease, highlighting its strong influence on patient outcome [58, 59].

More recently, somewhat paradoxically, primary tumour ulceration has been associated with improved benefit in terms of longer relapse-free survival (RFS), distant metastasis-free survival (DMFS) and overall survival (OS) following treatment with adjuvant interferon- α (IFN) [204, 231, 639]. The meta-analysis of interferon trials demonstrates that IFN does provide benefit in terms of RFS, with less clear benefit in terms of OS

[203, 204]. When individual patient data from IFN randomised controlled trials, not including the European Organisation for Research and Treatment of Cancer (EORTC) 18991 trial of pegylated IFN, are analysed separately for patients with ulcerated tumours and non-ulcerated tumours in meta-analysis the positive effect on RFS and OS is lost for patients with non-ulcerated tumours but is greater for those with ulcerated tumours (RFS, odds ratio (OR) 0.76; OS, OR 0.77) with evidence of interaction between IFN effect and ulceration status ($p=0.03$) [204]. A further meta-analysis of the two largest IFN adjuvant trials, EORTC 18952 and 18991, showed similar results with evidence of interaction between IFN therapy and ulceration status for RFS ($p=0.02$), DMFS ($p<0.001$) and OS ($p<0.001$) [231]. In this study, greatest survival benefit was seen in patients with ulcerated tumours and stage IIb or III disease with microscopic nodal metastases [231]. The overall HR for OS in ulcerated patients was 0.77 [204, 231, 638]. Therefore, ulceration is a poor prognostic factor, but appears to be a beneficial predictive factor for IFN therapy. To assess efficacy of IFN therapy in patients with ulcerated tumours, a randomized phase III trial is planned in patients with stage II ulcerated primaries (EORTC 18081) [638]. As discussed in the introduction, there are currently no other confirmed predictive biomarkers for IFN therapy, therefore the association between ulceration and IFN benefit is unique and warrants further investigation to unravel the association [638].

Despite the profound prognostic influence of ulceration, very little is known about how or why a tumour ulcerates and the biological explanation for its impact on prognosis [155, 640]. Ulceration may be a feature that represents some characteristic of the tumour such as greater proliferative activity or superior metastatic capacity [155, 640]. Other hypotheses are that ulceration is associated with adverse host/tumour interaction which might be determined by innate characteristics of the host or tumour [155, 640]. I will explore the evidence for these hypotheses below.

Ulceration may simply result from increased proliferative activity which erodes the epidermis during tumour expansion and makes the tumour more likely to metastasise. However mitotic rate and ulceration are independently associated with prognosis in stage I/II melanoma, suggesting that a distinct biological process, in addition to cell proliferation, is occurring in ulcerated tumours, which contributes to poorer prognosis [58, 96, 98, 155, 640, 641].

The presence of ulceration may indicate differences in the way that tumour cells modify the local tumour environment, thereby contributing to spread of the tumour [155, 640, 642]. Once melanoma cells pass across the epidermal-dermal junction in skin, their ability to metastasise is greatly increased [643]. Normal melanocytes are linked by cell-cell adhesion molecules, such as E-cadherin and desmoglein, and gap junctions to

keratinocytes in the epidermis which control melanocyte cell growth and dendricity via paracrine growth factors, intracellular and intercellular mechanisms [53, 643-646]. When uncoupled from keratinocytes and their control mechanisms, melanoma cells communicate with each other and fibroblasts via N-cadherin, cell adhesion molecules from the immunoglobulin gene superfamily, integrins and connexins [53, 642]. Melanoma cells thus down-regulate receptors which mediate interaction with keratinocytes, such as E-cadherin and desmoglein, and up-regulate molecules that mediate melanoma cell communication or interactions between melanoma cells and fibroblasts, such as N-cadherin [53, 644]. Deranged expression of integrins which bind to extracellular matrix can also contribute to loss of keratinocyte communication by allowing separation from the basement membrane [53]. Lack of intact epidermis in ulcerated tumours may represent a mechanism by which a tumour directly modifies the microenvironment to further evade keratinocyte control [642]. In addition, there is evidence that deranged expression of proteins which influence tumour and extracellular matrix interaction are associated with tumour progression such as osteopontin (as discussed in Chapter 3) and CCN3 (nephroblastoma overexpressed or NOV) [640, 647]. Invasion of melanoma tumours with deranged expression of matrix proteins is likely to be enhanced by the lack of keratinocyte control within an ulcerated tumour [642], however there is little evidence currently to support this theory.

It has been hypothesised that the presence of tumour ulceration may modify immune responses, as suggested in a study of 537 sentinel lymph nodes containing micro-metastatic deposits of tumour [648]. Nodes were stained for mature dendritic cells (DCs); lower DC densities were found in nodes in association with an ulcerated primary tumour [648]. DCs are vital for antigen presentation to T-cells thereby initiating specific adaptive immune responses, and immature plasmacytoid DCs are the largest producers of type I interferons, such as IFN α [212, 649]. Therefore, it was suggested that ulceration might be associated with a defect in stimulation of adaptive immunity, which is likely to contribute to its prognostic and perhaps predictive influence [155, 640]. Whether the biology of an ulcerated tumour causes less mature DCs in sentinel nodes or whether host factors modify this response requires investigation [155, 640]. A further observation related to immune responses is provided by gene expression profiling of primary melanoma tumours from 58 patients [178]. A very different gene expression pattern was found in ulcerated tumours versus non-ulcerated tumours, and the authors specifically highlighted that the gene encoding the pro-inflammatory cytokine interleukin-6 (*IL6*) was differentially expressed [178]. The relationship between inflammation and cancer development and metastasis is known to be important [650, 651]. These data suggest that ulceration may contribute to this inflammatory process in

primary melanoma tumours. In addition, higher serum levels of pro-inflammatory cytokines, such as IL6, IL1 α and IL1 β , detected prior to IFN treatment have been associated with longer RFS following therapy [652], with higher serum levels of IL6 being associated with poorer prognosis in advanced disease [653-655]. The prognostic and predictive influence of serum IL6 levels requires confirmation; however levels of this cytokine appear to have very similar prognostic and predictive associations to tumour ulceration.

A number of poor prognostic primary tumour histological features have been associated with ulceration. Greater Breslow thickness was associated with higher incidence of ulceration in the large study of 17,600 patients used to validate the 6th edition of AJCC staging [91], and from the same database, higher mitotic rate, recorded for 13,296 patients, was also associated with ulceration status [98]. Kashani-Sabet and colleagues studied 417 primary tumours and found increased tumour vascularity in ulcerated tumours [111]. Recently, lymphovascular invasion has also been associated with ulceration in a study of 2183 patients, 171 of whom had evidence of tumour lymphovascular invasion [656]. These studies have used routine haematoxylin and eosin (H+E) staining to assess lymphovascular invasion and vascular density; however use of specific antibodies for vessels increases detection rates versus H+E slides alone [110, 382-384]. Studies using immunohistochemical staining of D2-40 or LYVE-1, for lymphatic vessels, and CD34, to assess all vessels, in primary melanoma tumours have also found that lymphovascular invasion and lymphatic density is associated with ulceration [110, 657]. The association between lymphovascular invasion and ulceration suggests that there may be common biological processes, perhaps related to tissue hypoxia and host/tumour interaction, causing both ulceration and vascular invasion [110]. What is unclear is whether vascular invasion or ulceration contributes most to tumour invasion [110]. As discussed previously, ulceration remains prognostic in stage III disease, therefore it is unsurprising that in a study of 1526 patients primary tumour ulceration is independently associated with positive sentinel node biopsy in multivariate analyses with primary tumour histology [658]. In summary, ulceration is associated with poor prognostic features in the primary tumour and tumour deposits in sentinel lymph nodes.

In order to gain some further insight into the biological processes within ulcerated tumours and how this relates to prognosis and IFN action, this chapter presents results of analyses designed to identify primary tumour and patient characteristics associated with tumour ulceration in a large cohort of patients. Gene expression data were generated for 502 cancer-related genes from a subset of the primary tumours, allowing identification of genes differentially expressed in ulcerated tumours. Furthermore,

immunohistochemical staining was performed at the University of Nottingham on a further subset of tumours to identify blood and lymphatic vascular invasion (D2-40 and CD34), vessel density and presence of tumour-associated macrophages (CD68), to allow examination of associations between these factors and ulceration [113]. Analysis of patient information, tumour histology, immunohistochemical staining and tumour gene expression data has allowed an extensive and integrated investigation of factors associated with ulceration. It has allowed identification of factors independently associated with ulceration in multivariate analyses and has revealed insight into biological processes within ulcerated tumours that are directly related to the influence of ulceration on prognosis and treatment response.

7.3 Methods

7.3.1 Patients and primary melanoma samples

Samples and data from patients recruited to the Leeds Melanoma Cohort Study (Cohort study) and Retrospective Sentinel Node Biopsy Study (SNB study) were used for this work. These studies are described in further detail in Chapter 2. Histology data for the majority of cases were derived from histology reports. For a subset of tumours diagnostic H+E slides were reviewed by Dr Andy Boon (Cohort study) or Professor Martin Cook (SNB study), described in further detail in Chapter 2, to standardize reporting across the specimens. Gene expression data were derived from formalin-fixed paraffin-embedded (FFPE) primary melanoma tumours from a subset of patients recruited to each of the two studies.

From the SNB study, H+E slides from FFPE primary tumours blocks were reviewed by Dr Angana Mitra to assess whether they would be suitable for IHC staining, based upon the need to sample representative areas of the tumour without excessive damage to the clinical block. Where two tumour blocks were available with similar tumour features from the same patient, one block was used for tumour sampling for gene expression analysis as described in Chapter 2 and the other was used for IHC. If only one block was available, the block was cored first for gene expression analysis and then sections were taken for IHC staining. Some blocks were not sampled because of size. Tumour blocks containing only punch or curettage specimens were not used for IHC staining as these specimens were not representative of the larger tumour. From the selected specimens, four consecutive 4µm sections were cut from each tumour block by Filomena Esteves, using a microtome. This process is summarised in Figure

7-1. Adjacent sections were carefully retained so that the IHC staining was of contiguous tumour.

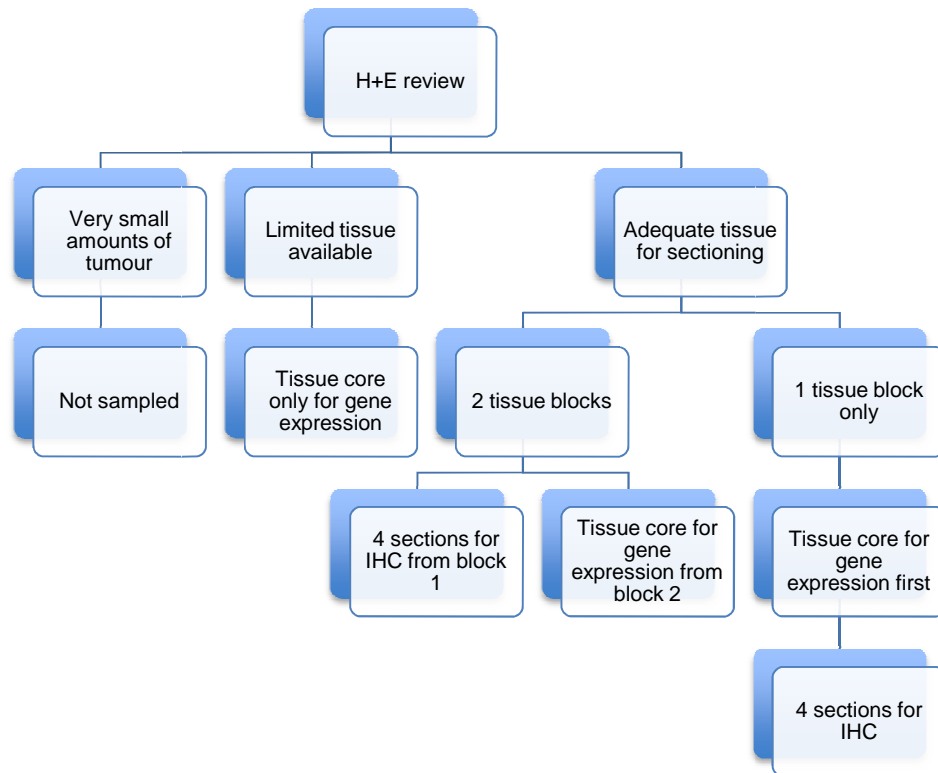


Figure 7-1: Assessment of tumour samples for tissue sampling for gene expression and immunohistochemical studies.

The process is described in further detail in the text. Abbreviations used: H+E, haematoxylin and eosin; IHC, immunohistochemistry.

7.3.2 Immunohistochemistry (IHC) methods

IHC staining and measurement of vessels and macrophages was performed by Sarah Storr and Sabreena Safuan at University of Nottingham by a Academic Oncology research group who perform studies primarily addressed to understanding the role of tumour vasculature in breast cancer progression. Sections were stained with D2-40, CD34, and a CD68 antibodies and microvessel density, macrophage count, lymphatic density and vascular invasion were assessed using methods described in Chapter 2. We were unable to assess subtypes of tumour-associated macrophages because of limited tissue availability.

7.3.3 Gene expression data

Gene expression data were generated for 502 cancer-related genes using the Human Cancer panel and the cDNA-mediated, annealing, selection, extension and ligation (DASL) assay as described in Chapter 2. The samples selected for gene expression analysis are described in Chapter 3 and processing of gene expression data to generate a merged dataset from the two studies is described in detail in Chapter 4.

7.3.4 Statistical analysis

To identify associations with ulceration status and histological (including IHC) or patient factors, Pearson's Chi-squared (χ^2) tests or Fisher's exact tests (where the frequency of observations in a subgroup was less than 5) were performed for categorical variables and Mann-Whitney U tests for continuous variables. For the subset of samples with H+E sections centrally reviewed by expert pathologists, analyses were repeated to confirm results found in the larger datasets. For IHC data, vessel density and macrophage counts were categorised into high and low groups around the median value. To identify factors independently associated with ulceration status, multiple logistic regression was performed using factors significantly associated with ulceration in univariate analysis. For these analyses, Breslow thickness and mitotic rate were analysed as categorical variables based on AJCC staging criteria, and results of a test for trend across the groups is presented. For Breslow thickness, categories were $\leq 1\text{mm}$, >1 to $\leq 2\text{mm}$, >2 to $\leq 4\text{mm}$ and $>4\text{mm}$. For mitotic rate, categories were <1 mitosis/ mm^2 , $1-6$ mitoses/ mm^2 and >6 mitoses/ mm^2 . To maximise the number of observations assessed in each analysis, multiple logistic regression was performed separately for clinico-pathological data and IHC data provided by the University of Nottingham. The significance level for these analyses was set at 0.05.

Gene expression analysis was performed using the dataset generated as described in Chapter 4. Differential gene expression analysis was performed using log-transformed (\log_2) data. As some of the raw gene expression levels were negative values, 1000 was added to all values prior to log-transformation. Associations between gene expression and ulceration status were identified using linear regression adjusting for the study type to which the patient was recruited. Fold changes in mean gene expression between ulcerated and non-ulcerated tumours were calculated using data that had not been log-transformed. A Bonferroni correction was used to adjust for multiple testing as described in Chapter 4, with significance level being set at 0.0001. All statistical analyses were undertaken using Stata version 10 (StataCorp 2007, College Station, TX).

7.3.5 Pathway analysis

Pathway analysis of gene expression data was performed using DAVID (the database for annotation, visualisation and integrated discovery) [368] to identify overrepresented pathways in the list of differentially expressed genes [369, 371, 372]. Further detail of algorithms used by DAVID software are described in Chapter 2. For this analysis, the 502-gene Human Cancer panel of genes was inputted as the background population of genes for comparison with the list of genes differentially expressed in ulcerated tumours. From the 502-gene background list, 479 genes were recognised by DAVID. A list of 109 differentially expressed genes (significance values <0.05) were inputted into DAVID, with 103 genes being recognised by the software for analysis. Enrichment analysis was performed to identify KEGG (Kyoto Encyclopedia of Genes and Genomes) [469, 470] pathways enriched in the gene list.

7.4 Results

7.4.1 Patients and tumour samples

A total of 1804 patients recruited to the Cohort study and SNB study had the ulceration status of primary tumour recorded, and these data were used for analysis of clinico-pathological features associated with ulceration status. Of these patients, 368 (20%) had centrally reviewed primary tumour histopathological data. Gene expression data was available for 348 primary tumours from this patient group, 339 (97%) of which had had central pathology review.

Out of the 218 tumour blocks received for the SNB study, 202 were suitable for sectioning for IHC staining. Of these 130 (64%) tumour blocks had also been cored for use in gene expression work described in Chapters 3 and 4. Of the 202 tumours stained, lymphovascular and macrophage measurements were successfully taken for the majority of samples, and 195 tumours had ulceration status recorded for use in the analyses described in this chapter. One hundred and eighty six (95%) of these tumours had had diagnostic H+E slides centrally reviewed.

7.4.2 Effect of central histology review on ulceration status

Figure 7-2 describes changes that were made to ulceration status following central histology review. This analysis demonstrates that a significant proportion of ulceration status in histopathology reports generated in clinical practice are changed following

review, highlighting the importance of central review and the variability that can be found in reporting between pathologists [298, 299]. This process has also increased the number of cases for which ulceration status is reported, increasing the power of the following analyses. Following this review, a total of 25% of tumours from the larger dataset were ulcerated.

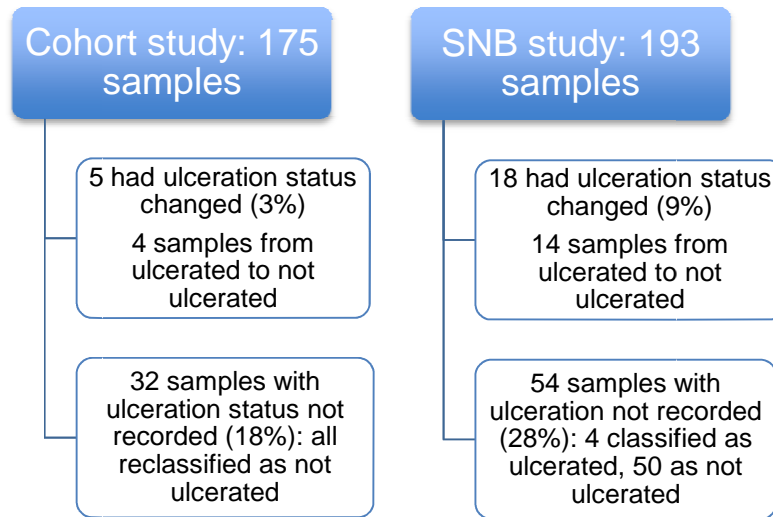


Figure 7-2: Changes in reported ulceration status of melanoma primary tumours following central histological review.

7.4.3 Univariate analyses of clinico-pathological factors and ulceration

Table 7-1 presents results of univariate analyses for the large dataset and the smaller centrally reviewed sample set. In the large dataset, greater Breslow thickness and mitotic rate were associated with ulceration ($p < 0.00001$). In addition, other prognostic tumour factors were associated with ulceration such as presence of vascular invasion ($p < 0.0001$), perineural infiltration ($p = 0.003$) and microsatellites ($p < 0.0001$). Nodular tumours and tumours on sun-protected sites are more likely to be ulcerated ($p < 0.0001$) and patients were more likely to be older ($p < 0.00001$) and male ($p = 0.001$) if the tumour was ulcerated. In view of the prognostic influence of ulceration, it is unsurprising that patients with ulcerated tumours were more likely to have positive sentinel node biopsies ($p < 0.0001$) and were more likely to relapse and die ($p < 0.0001$). The majority of these factors were also associated with ulceration in the smaller centrally reviewed dataset. Presence of perineural infiltration ($p = 0.61$), microsatellitosis ($p = 0.05$), patient gender ($p = 0.21$) and sentinel node biopsy status ($p = 0.20$) were no longer statistically significant in the smaller dataset, which likely reflects lower power, however the trends were similar to those in the larger dataset.

Factor	Whole dataset			Centrally reviewed dataset		
	Non-ulcerated (n=1357)	Ulcerated (n=447)	Test statistic and P-value	Non-ulcerated (n=276)	Ulcerated (n=92)	Test statistic and P-value
Study type, n (%):						
Cohort study	1008 (74.3)	311 (69.6)		131 (47.5)	44 (47.8)	
SNB study	349 (25.7)	136 (30.4)		145 (52.5)	48 (52.2)	
Breslow thickness, mm median (range)	1.4 (0.2-24.0)	3.0 (0.5-19.0)	Mann-Whitney z -19.1, p<0.00001	1.7 (0.4-12.0)	3.2 (1.0-19.0)	Mann-Whitney z -8.1, p<0.00001
Mitotic rate per mm ² median (range)	2 (0-52)	6 (0-84)	Mann-Whitney z -11.3, p<0.00001	3.0 (0-39)	7 (0-40)	Mann-Whitney z -5.1, p<0.00001
Tumour infiltrating lymphocytes, n (%):						
None	177 (15.7)	59 (15.6)	$\chi^2 (1) 0.002, p=0.97$	54 (21.9)	14 (16.1)	$\chi^2 (1) 1.3, p=0.25$
Present	951 (84.3)	319 (84.4)		193 (78.1)	73 (83.9)	
Vascular or lymphatic invasion, n (%):						
None	839 (95.5)	250 (82.8)	$\chi^2 (1) 50.2, p<0.0001$	253 (93.0)	75 (85.2)	$\chi^2 (1) 5.0, p=0.03$
Present	40 (4.6)	52 (17.2)		19 (7.0)	13 (14.8)	
Perineural infiltration, n (%):						
None	345 (98.0)	121 (92.4)	$\chi^2 (1) 9.0, p=0.003$	154 (97.5)	49 (96.1)	$\chi^2 (1) 0.3, p=0.61$
Present	7 (2.0)	10 (7.6)		4 (2.5)	2 (3.9)	
Regression, n (%):						
No	980 (83.3)	286 (82.2)	$\chi^2 (1) 0.2, p=0.64$	211 (86.8)	68 (80.0)	$\chi^2 (1) 2.3, p=0.13$
Yes	197 (16.7)	62 (17.8)		32 (13.2)	17 (20.0)	

Factor	Whole dataset			Centrally reviewed dataset		
	Non-ulcerated (n=1357)	Ulcerated (n=447)	Test statistic and P-value	Non-ulcerated (n=276)	Ulcerated (n=92)	Test statistic and P-value
Microsatellites, n (%)						
None	791 (96.6)	273 (90.7)	χ^2 (1) 16.0, p<0.0001	219 (92.4)	75 (85.2)	χ^2 (1) 3.8, p=0.05
Present	28 (3.4)	28 (9.3)		18 (7.6)	13 (14.8)	
Histological subtype, n (%):						
SSM	887 (68.3)	177 (41.8)	χ^2 (2) 111.8, p<0.0001	198 (72.8)	46 (50.0)	χ^2 (2) 16.8, p<0.0001
NM	234 (18.0)	175 (41.3)		52 (19.1)	35 (38.0)	
Other	177 (13.6)	72 (17.0)		22 (8.1)	11 (12.0)	
Age at diagnosis, median (range)	53.3 (14.4-87.0)	58.8 (18.1-88.5)	Mann-Whitney z -6.7, p<0.00001	52.6 (14.4-87.0)	57.2 (22.7-88.0)	Mann-Whitney z -2.5, p=0.01
Patient gender, n (%)						
Female	778 (57.3)	217 (48.6)	χ^2 (1) 10.5, p=0.001	144 (52.2)	41 (44.6)	χ^2 (1) 1.6, p=0.21
Male	579 (42.7)	230 (51.5)		132 (47.8)	51 (55.4)	
Site of tumour, n (%):						
Trunk	484 (35.7)	170 (38.0)	χ^2 (5) 74.9, p<0.0001	91 (33.0)	34 (37.0)	χ^2 (4) 10.4, p=0.04
Leg	440 (32.4)	112 (25.1)		94 (34.1)	21 (22.8)	
Arm	268 (19.8)	67 (15.0)		58 (21.0)	16 (17.4)	
Head/neck	133 (9.8)	46 (10.3)		26 (9.4)	14 (15.2)	
Sun protected	31 (2.3)	52 (11.6)		7 (2.5)	7 (7.6)	
Unknown	1 (0.07)	0		0	0	

Factor	Whole dataset			Centrally reviewed dataset		
	Non-ulcerated (n=1357)	Ulcerated (n=447)	Test statistic and P-value	Non-ulcerated (n=276)	Ulcerated (n=92)	Test statistic and P-value
SNB status, n (%)						
No SNB	725 (54.5)	203 (47.1)	χ^2 (2) 27.1, p<0.0001	98 (35.8)	34 (38.2)	χ^2 (2) 3.2, p=0.20
SNB performed – negative	386 (29.0)	108 (25.1)		78 (28.5)	17 (19.1)	
SNB performed – positive	219 (16.5)	120 (27.8)		98 (35.8)	38 (42.7)	
Relapse status, n (%)						
Not relapse	1138 (84.3)	263 (59.0)	χ^2 (1) 125.4, p<0.0001	204 (75.3)	42 (45.7)	χ^2 (1) 27.6, p<0.0001
Relapsed	212 (15.7)	183 (41.0)		67 (24.7)	50 (54.4)	
Overall survival, n (%)						
Alive	1147 (84.5)	275 (61.5)	χ^2 (1) 106.6, p<0.0001	200 (72.5)	47 (51.1)	χ^2 (1) 14.3, p<0.0001
Died	210 (15.5)	172 (38.5)		76 (27.5)	45 (48.9)	

Table 7-1: Associations between clinico-pathological features and ulceration in univariate analysis.

Results are presented for the larger dataset and the smaller centrally reviewed dataset. Statistical tests (degrees of freedom) and significance values are presented for association between the factor and ulceration status. Generally speaking analyses in the large and the much smaller centrally reviewed data sets produced similar results. Statistically significant results are highlighted in bold. Abbreviations used: SNB, sentinel node biopsy; n, number.

7.4.4 Factors independently associated with ulceration

Factors found to be associated with ulceration in the larger dataset in univariate analysis were analysed using multiple logistic regression to identify factors independently associated with ulceration. Perineural infiltration was omitted from the model because of small numbers of observations. The results for the larger dataset are presented in Table 7-2 with results for the smaller centrally reviewed dataset in Table 7-3.

Univariate logistic regression of the larger dataset confirmed that factors identified in Table 7-1 were associated with ulceration status. In multivariate analysis, greater Breslow thickness (test for trend across a categorical variable based on AJCC staging criteria, odds ratio (OR) 2.62 (95% CI 2.07-3.32) $p < 0.0001$), mitotic rate (test for trend, OR 1.53 (95% CI 1.12-2.09) $p = 0.008$) and tumours of sun-protected sites (OR 4.70 (95% CI 2.05-10.80) $p < 0.0001$) were independently associated with ulceration status. Overall, 63% of tumours from sun-protected sites were ulcerated, with the majority of tumours being from acral skin of the palms or soles of feet (60%) or subungual (21%). In the smaller centrally reviewed dataset, the only factor independently associated with ulceration status in multivariate analysis was greater Breslow thickness (test for trend, OR 2.93 (95% CI 1.94-4.45) $p < 0.0001$).

Factor	No. in non-ulcerated group	No. in ulcerated group	Univariate analysis		Multivariate analysis (n=892)	
			OR (95% CI)	P-value	OR (95% CI)	P-value
Breslow thickness, mm	1354	442	3.26 (2.84-3.74)	p<0.0001	2.62 (2.07-3.32)	p<0.0001
Mitotic rate per mm ²	831	291	3.01 (2.39-3.79)	p<0.0001	1.53 (1.12-2.09)	p=0.008
Tumour infiltrating lymphocytes:						
None	177	59	1.0	p=0.97		
Present	951	319	1.01 (0.73-1.39)			
Vascular or lymphatic invasion:						
None	839	250	1.0	p<0.0001	1.0	p=0.12
Present	40	52	4.36 (2.82-6.75)		1.60 (0.89-2.88)	
Perineural infiltration:					Not included because of low numbers of observations	
None	345	121	1.0	p=0.005		
Present	7	10	4.07 (1.52-10.94)			
Regression:						
No	980	286	1.0	p=0.64		
Yes	197	62	1.08 (0.79-1.48)			
Microsatellites:						
None	791	273	1.0	p<0.0001	1.0	p=0.63
Present	28	28	2.90 (1.69-4.98)		1.20 (0.57-2.54)	
Histological subtype:						
SSM	887	177	1.0		1.0	
NM	234	175	3.75 (2.91-4.83)	p<0.0001	1.14 (0.75-1.75)	p=0.54
Other	177	72	2.04 (1.48-2.80)	p<0.0001	1.06 (0.60-1.88)	p=0.84
Age at diagnosis, years	1357	447	1.03 (1.02-1.04)	p<0.0001	1.01 (1.00-1.02)	p=0.13

Factor	No. in non-ulcerated group	No. in ulcerated group	Univariate analysis		Multivariate analysis (n=892)	
			OR (95% CI)	P-value	OR (95% CI)	P-value
Patient gender						
Female	778	217	1.0	p=0.001	1.0	p=0.19
Male	579	230	1.42 (1.15-1.77)		1.28 (0.88-1.86)	
Site of tumour:						
Trunk	484	170	1.0		1.0	
Leg	440	112	0.73 (0.55-0.95)	p=0.02	1.13 (0.71-1.81)	p=0.60
Arm	268	67	0.71 (0.52-0.98)	p=0.04	1.02 (0.61-1.70)	p=0.96
Head/neck	133	46	0.99 (0.68-1.44)	p=0.94	0.90 (0.49-1.65)	p=0.73
Sun protected	31	52	4.78 (2.96-7.70)	p<0.0001	4.70 (2.05-10.80)	p<0.0001
SNB status:						
No SNB	725	203	1.0		1.0	
SNB performed – negative	386	108	1.00 (0.77-1.30)	p=1.00	1.14 (0.72-1.81)	p=0.57
SNB performed – positive	219	120	1.96 (1.49-2.57)	p<0.0001	0.78 (0.50-1.21)	p=0.27

Table 7-2: Results of univariate and multivariate logistic regression analyses in the larger dataset identifying clinico-pathological factors associated with ulceration status.

Breslow thickness, mitotic rate and origin in a sun-protected site were all independently associated with ulceration status. Odds ratios, 95% confidence intervals and significance values are presented for the associations between each factor and ulceration in the univariate setting and then significant factors were included in a multiple logistic regression model. Results for Breslow thickness and mitotic rate are from a test for trend across categorical variables based on American Joint Committee on Cancer staging criteria as described in 7.3.4. Statistically significant results are highlighted in bold. Abbreviations used: OR, odds ratio; CI, confidence interval; SNB, sentinel node biopsy.

Factor	No. in non-ulcerated group	No. in ulcerated group	Univariate analysis		Multivariate analysis (n=343)	
			OR (95% CI)	P-value	OR (95% CI)	P-value
Breslow thickness, mm	276	91	3.36 (2.39-4.73)	p<0.0001	2.93 (1.94-4.45)	p<0.0001
Mitotic rate per mm ²	268	87	2.17 (1.48-3.20)	p<0.0001	1.32 (0.85-2.07)	p=0.22
Tumour infiltrating lymphocytes:						
None	54	14	1.0	p=0.25		
Present	193	73	1.46 (0.76-2.79)			
Vascular or lymphatic invasion:						
None	253	75	1.0	p=0.03	1.0	p=0.96
Present	19	13	2.31 (1.09-4.89)		1.03 (0.43-2.47)	
Perineural infiltration:						
None	154	49	1.0	p=0.61		
Present	4	2	1.57 (0.28-8.84)			
Regression:						
No	211	68	1.0	p=0.13		
Yes	32	17	1.65 (0.86-3.15)			
Microsatellites:						
None	219	75	1.0	p=0.05		
Present	18	13	2.11 (0.99-4.51)			
Histological subtype:						
SSM	198	46	1.0		1.0	
NM	52	35	2.90 (1.70-4.95)	p<0.0001	1.37 (0.72-2.62)	p=0.34
Other	22	11	2.15 (0.98-4.75)	p=0.06	2.12 (0.82-5.46)	p=0.12
Age at diagnosis, years	276	92	1.02 (1.01-1.04)	p=0.01	1.02 (1.00-1.04)	p=0.09
Patient gender						
Female	144	41	1.0	p=0.21		
Male	132	51	1.35 (0.85-2.18)			

Factor	No. in non-ulcerated group	No. in ulcerated group	Univariate analysis		Multivariate analysis (n=343)	
			OR (95% CI)	P-value	OR (95% CI)	P-value
Site of tumour:						
Trunk	91	34	1.0			
Leg	94	21	0.60 (0.32-1.11)	p=0.10		
Arm	58	16	0.74 (0.37-1.46)	p=0.38		
Head/neck	26	14	1.44 (0.67-3.08)	p=0.35		
Sun protected	7	7	2.68 (0.87-8.20)	p=0.09		
SNB status:						
No SNB	98	34	1.0			
SNB performed – neg	78	17	0.63 (0.33-1.21)	p=0.16		
SNB performed – pos	98	38	1.12 (0.65-1.92)	p=0.69		

Table 7-3: Results of univariate and multivariate logistic regression analyses with the significantly smaller data set subjected to central review of histology: clinico-pathological factors associated with ulceration status.

The results were similar to those in the larger data set but were statistically less robust probably related to sample size. Odds ratios, 95% confidence intervals and significance values are present for the associations between each factor and ulceration in the univariate setting and then significant factors were included in a multiple logistic regression model. Results for Breslow thickness and mitotic rate are from a test for trend across categorical variables based on American Joint Committee on Cancer staging criteria as described in 7.3.4. Statistically significant results are highlighted in bold. Abbreviations used: OR, odds ratio; CI, confidence interval; SNB, sentinel node biopsy.

7.4.5 Associations between IHC data and ulceration status

A comparison between IHC and H+E staining methodologies and the relationship between vascular invasion and clinico-pathological data, including ulceration, using the data presented in this chapter has been previously published [113] and will not be described in further detail. Results presented here concentrate in more detail on the relationship between ulceration and tumour factors identified using IHC.

Results of univariate and multivariate analyses to identify associations between tumours factors determined by IHC and ulceration status are presented in Table 7-4. The variable “any vessel invasion” was not included in the multivariate model as it was generated from the “blood vessel invasion” and “lymphatic vessel invasion” variables. In addition, the variable “lymphatic invasion” was used in preference to “intratumoural lymphatic invasion” and “peritumoural lymphatic invasion” in the multivariate model as these variables were highly correlated with “lymphatic invasion” which was most associated with ulceration in univariate pairwise analysis. Univariate analyses showed that lymphatic invasion, both intratumourally (inner two thirds of the tumour) and peritumourally (all normal tissue surrounding tumour) was associated with tumour ulceration ($p < 0.0001$). Higher microvessel density and macrophage count were also associated with tumour ulceration ($p < 0.0001$). In the multivariate model, presence of lymphatic invasion (OR 3.59, 95% CI 1.64-7.87, $p = 0.001$), greater microvessel density (OR 2.59, 95% CI 1.16-5.80, $p = 0.02$) and macrophage count (OR 2.42, 95% CI 1.07-5.50, $p = 0.03$) remain independently associated with ulceration status.

Factor	Not ulcerated (n=145)	Ulcerated (n=50)	Test statistic and P-value	Univariate logistic regression		Multivariate logistic regression (n=169)	
				OR (95% CI)	P-value	OR (95% CI)	P-value
Invasion on H+E slide, n (%):							
No	129 (90.9)	48 (96.0)	Fisher's exact p=0.36	1.0	p=0.26		
Present/possible	13 (9.2)	2 (4.0)		0.41 (0.09-1.90)			
Blood vessel invasion (CD34), n (%):							
Negative	130 (97.0)	46 (93.9)	Fisher's exact p=0.39	1.0	p=0.34		
Positive	4 (3.0)	3 (6.1)		2.12 (0.46-9.83)			
Lymphatic invasion (D2-40), n (%):							
Negative	109 (82.6)	22 (46.8)	χ² (1) 22.6, p<0.0001	1.0	p<0.0001	1.0	p=0.001
Positive/possible	23 (17.4)	25 (53.2)		5.39 (2.60-11.16)		3.59 (1.64-7.87)	
Any vessel invasion using IHC, n (%):							
Both negative	103 (79.8)	22 (45.8)	χ² (1) 19.5, p<0.0001	1.0	p<0.0001		
Either positive/possible	26 (20.2)	26 (54.2)		4.68 (2.30-9.55)			
Intratumoural lymphatic invasion, n (%):							
Negative	121 (89.0)	31 (64.6)	χ² (1) 14.7, p<0.0001	1.0	p<0.0001		
Positive/possible	15 (11.0)	17 (35.4)		4.42 (1.99-9.83)			
Peritumoural lymphatic invasion, n (%):							
Negative	119 (91.5)	29 (65.9)	χ² (1) 17.0, p<0.0001	1.0	p<0.0001		
Positive/possible	11 (8.5)	15 (34.1)		5.60 (2.33-13.46)			
Lymphatic density, n (%):							
Low	69 (50.7)	23 (47.9)	χ ² (1) 0.1, p=0.74	1.0	p=0.74		
High	67 (49.3)	25 (52.1)		1.12 (0.58-2.16)			
Intratumoural lymphatic density, n (%):							
Low	69 (50.7)	21 (43.8)	χ ² (1) 0.7, p=0.41	1.0	p=0.41		
High	67 (49.3)	27 (56.3)		1.32 (0.68-2.57)			

Factor	Not ulcerated (n=145)	Ulcerated (n=50)	Test statistic and P-value	Univariate logistic regression		Multivariate logistic regression (n=169)	
				OR (95% CI)	P-value	OR (95% CI)	P-value
Peritumoural lymphatic density, n (%):							
Low	66 (50.8)	21 (47.7)	$\chi^2(1) 0.1,$ $p=0.73$	1.0	$p=0.73$		
High	64 (49.2)	23 (52.3)		1.13 (0.57-2.24)			
Microvessel density, n (%):							
Low	80 (59.7)	12 (24.5)	$\chi^2(1) 17.8,$ $p<0.0001$	1.0	$p<0.0001$	1.0	$p=0.02$
High	54 (40.3)	37 (75.5)		4.57 (2.19-9.55)		2.59 (1.16-5.80)	
Macrophage count, n (%):							
Low	79 (56.8)	14 (28.0)	$\chi^2(1) 12.2,$ $p<0.0001$	1.0	$p=0.001$	1.0	$p=0.03$
High	60 (43.2)	36 (72.0)		3.39 (1.68-6.84)		2.42 (1.07-5.50)	

Table 7-4: Results of univariate and multivariate analyses identifying associations between lymphovascular parameters and macrophage count (determined using immunohistochemistry), and ulceration status in primary melanoma tumours.

Statistical tests (degrees of freedom) and significance values are presented for association between the factor and ulceration status in pairwise tests. For logistic regression analyses, odds ratios, 95% confidence intervals and significance values are presented for the associations between each factor and ulceration in the univariate analysis and then significant factors were included in a multiple logistic regression model. Additional details of variables included in the multivariate model are included in the text. Vessel density and macrophage counts were categorised into high and low groups around the median value. Significance values quoted for Fisher's exact tests are 2-sided. Statistically significant results are highlighted in bold. Abbreviations used: H+E, haematoxylin and eosin; n, number.

7.4.6 Gene expression profiles associated with tumour ulceration

The top 20 genes differentially expressed in ulcerated tumours for the 348 tumours for which gene expression data were available are listed in Table 7-5.

Gene	Mean fold difference in gene expression (ulcerated/non-ulcerated)	Significance value
<i>HLF</i>	0.67	1.73x10 ⁻⁰⁸
<i>FGFR3</i>	0.73	3.96x10 ⁻⁰⁸
<i>DSP</i>	0.68	5.26x10 ⁻⁰⁸
<i>GRB7</i>	0.67	2.21x10 ⁻⁰⁷
<i>FGFR2</i>	0.59	4.17x10 ⁻⁰⁷
<i>MAF</i>	0.92	3.69x10 ⁻⁰⁶
<i>ITGB4</i>	0.78	6.39x10 ⁻⁰⁶
<i>IL6</i>	1.73	0.00001
<i>RAD52</i>	1.15	0.00001
<i>EPHA1</i>	0.74	0.00001
<i>FGF7</i>	1.35	0.00002
<i>SPP1</i>	1.34	0.00002
<i>CEBPA</i>	0.77	0.00002
<i>CDH1</i>	0.83	0.00003
<i>OSM</i>	1.80	0.00004
<i>MMP1</i>	1.52	0.00005
<i>EGFR</i>	0.74	0.0001
<i>PTGS1</i>	0.80	0.0001
<i>EPO</i>	0.81	0.0001

Table 7-5: Top 20 genes differentially expressed in ulcerated tumours.

Significance value is derived from linear regression adjusting for the study to which patients were recruited. Genes involved in cell adhesion are highlighted in dark green, fibroblast growth factors and their receptors are highlighted in medium green and the pro-inflammatory cytokine interleukin-6 is highlighted in light green.

This list shows that a number of genes involved in cell adhesion (*DSP*, *ITGB4* and *CDH1*) were down-regulated in ulcerated tumours. Fibroblast growth factor 7 (*FGF7*), otherwise known as keratinocyte growth factor, was up-regulated in ulcerated tumours, with fibroblast growth factors receptors (*FGFR2* and *FGFR3*) being down-regulated.

The pro-inflammatory cytokine gene interleukin-6 (*IL6*) was over-expressed in ulcerated tumours.

Pathway analysis was performed using DAVID software to identify enriched pathways in this dataset. Table 7-6 presents the top five most enriched KEGG (Kyoto Encyclopedia of Genes and Genomes) pathways out of a total of 52 pathways identified containing 70 of the inputted genes [469, 470]. The top five enriched KEGG pathways included 'Pathways in cancer', which is unsurprising as a cancer panel of genes was used for gene expression profiling, but also the 'Cytokine-cytokine receptor interaction' pathway, the 'Jak-STAT signalling pathway' and the 'Focal adhesion' pathway. Type 1 interferons act via Jak-STAT signalling [213, 220], therefore identification of deranged gene expression for components of this pathway in ulcerated tumours is of great interest. Genes involved with focal adhesion were identified by review of the gene list with pathway analysis confirming their importance. Figure 7-3 presents visually which genes are under- and over-expressed in ulcerated tumours in the Jak-STAT KEGG pathway.

7.5 Discussion

7.5.1 Relationship between ulceration and clinico-pathological factors

Tumour ulceration has a profound influence on the likelihood of survival for melanoma patients [58] and is reported to have a predictive influence on benefit received from IFN therapy [204, 231]. It is therefore important to understand the biology of this phenomenon.

In this study, analysis of clinico-pathological features associated with ulceration in a large sample set and the smaller centrally reviewed set has shown that a number of poor prognostic tumour features, such as Breslow thickness, mitotic rate and presence of lymphovascular invasion, were associated with the presence of ulceration. Ulcerated tumours were more likely to be of the nodular subtype, arising in a sun-protected site and found in older patients. The association with age was not independently significant, but the statistical power to detect a small effect was limited. As I discuss below chronic

KEGG Pathway	Number of genes	% of genes	P-Value	Bonferroni corrected P-value	Benjamini corrected P-value	False discovery rate
hsa05200: Pathways in cancer	31	30.10	5.78×10^{-24}	4.97×10^{-22}	4.97×10^{-22}	6.23×10^{-21}
hsa05219: Bladder cancer	11	10.68	4.04×10^{-11}	3.47×10^{-09}	1.74×10^{-09}	4.36×10^{-08}
hsa04060: Cytokine-cytokine receptor interaction	13	12.62	2.14×10^{-10}	1.84×10^{-08}	6.15×10^{-09}	2.31×10^{-07}
hsa04630: Jak-STAT signalling pathway	11	10.68	1.20×10^{-09}	1.03×10^{-07}	2.58×10^{-08}	1.29×10^{-06}
hsa04510: Focal adhesion	12	11.65	4.46×10^{-09}	3.84×10^{-07}	7.67×10^{-08}	4.81×10^{-06}

Table 7-6: Top 5 KEGG (Kyoto Encyclopedia of Genes and Genomes) pathways containing differentially expressed genes in ulcerated tumours.

The number and percentage of genes in the gene list associated with each term is presented. Significance values for representation of genes in the pathway without correction for multiple testing are presented with corrected significance values using the Bonferroni correction [366] and the Benjamini and Hochberg correction [367]. The false discovery rate (FDR) is also presented.

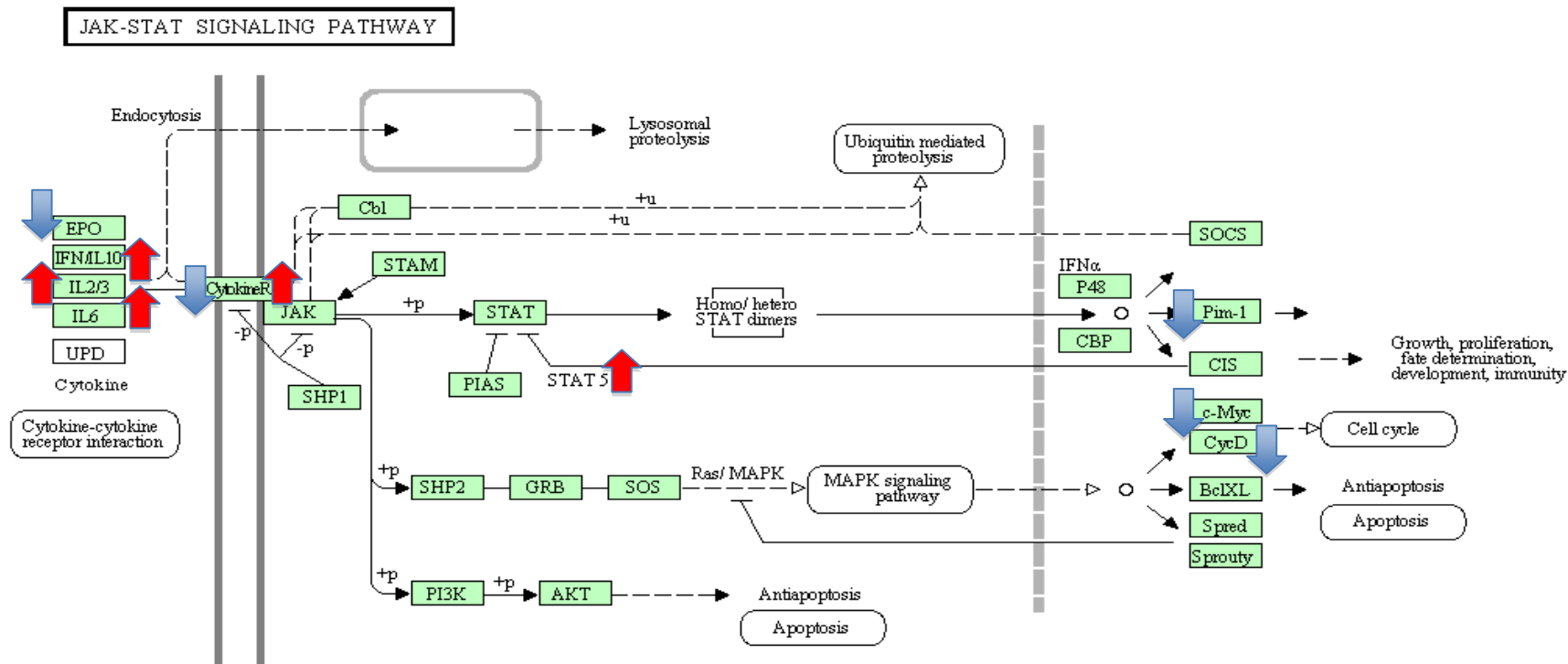


Figure 7-3: The KEGG (Kyoto Encyclopedia of Genes and Genomes) 'Jak-STAT signalling pathway' adapted to demonstrate fold changes in gene expression between ulcerated and non-ulcerated tumours.

Blue arrows indicate under-expression of genes in ulcerated tumours, with over-expression indicated by red arrows. The diagram has been adapted from the KEGG hsa04630: Jak-STAT signalling pathway diagram [469, 470, 659].

inflammation is postulated to be a mechanism involved in determining ulceration which is more frequent with age, which is perhaps of some interest [660, 661].

The factors which remained independently associated with ulceration in multivariate analysis of the large sample set were Breslow thickness, mitotic rate and tumour site, with ulceration being more frequently present in tumours arising in a sun-protected site, with only Breslow thickness remaining significant in the smaller centrally reviewed set. Breslow thickness and mitotic rate are the other two primary tumour features which contribute to current AJCC staging in stage I and II disease [58]. Therefore, it is perhaps unsurprising that these prognostic tumour features, representing an aggressive, proliferative tumour, are associated with the poorly prognostic tumour feature of ulceration. The association between thicker primary melanoma tumours and greater mitotic rate and presence of ulceration has been previously identified in large sample sets [91, 98]. However, no previous studies have attempted to identify tumour or patient features independently associated with ulceration. In this study, the independent association of ulceration with Breslow thickness and mitotic rate may contribute to the prognostic influence of ulceration status. Mitotic rate was not significantly associated in the smaller centrally-reviewed dataset, probably due to there being less power to detect this association.

I have found that tumours of sun-protected sites, such as acral, subungual and mucosal tumours were more likely to be ulcerated. In this study, 4.6% of tumours were from sun-protected sites and of these 63% were ulcerated compared with a proportion of 25% of ulcerated tumours overall. The majority of tumours (81%) in this group were subungual and from acral skin of the palms or soles of feet. In studies of acral and subungual tumours in Caucasian populations, the proportion of ulcerated tumours is greater at 30-33% [662, 663] than in cohorts including tumours from all sites, such as the AJCC staging dataset where approximately 27% of tumours were ulcerated [58]. Therefore, the literature provides support for my observation that the proportion of ulcerated tumours was higher in tumours from sun-protected sites. Further, my work demonstrates that the association with site is independent of Breslow thickness and mitotic rate, indicating that aggressiveness of the tumour or delay in diagnosis, which have been suggested as contributing factors to the poorer prognosis of acral tumours, does not fully explain the association with ulceration [131, 132].

It is possible that trauma to tumours on the sole of the foot or under the nail may have led to separation of the epidermis from the dermis and a failure of pathologists to distinguish this from true ulceration. To support this hypothesis the comparison I made between histopathology reports from routine clinical practice and review by expert dermatopathologists (Figure 7-2) showed that of the 23 tumours which had ulceration

status changed in review, 18 (78%) were reclassified as not being ulcerated. In the analysis of centrally reviewed data, the association of sun-protected tumour site and ulceration was less significant in pairwise analysis ($p=0.04$) and not significant in univariate logistic regression ($p=0.09$) suggesting that perhaps trauma-induced loss of epidermis being reported as ulceration may be a factor contributing to the association in the larger dataset. However, the more likely scenario is that the smaller dataset does not have the power to detect associations between tumour site and ulceration status.

My conclusions therefore are that:-

- Ulceration of melanoma primaries is associated with other poor prognostic factors.
- Ulceration was more common in older patients in the larger data set although this was not an independent predictor.
- Breslow thickness and mitotic rate were independent predictors of ulceration.
- Tumours in sun-protected sites were more frequently ulcerated than in other sites and there was support for this observation in the literature. It was not possible to exclude erroneous categorisation of traumatic damage, but I conclude that this is likely a real observation.

7.5.2 Ulceration status and immunohistochemical pathological factors

Analysis of IHC data identified associations between ulceration and presence of lymphatic invasion, greater microvessel density and macrophage infiltration in univariate and multivariate analyses. It must be acknowledged that multiple comparisons have been assessed in these analyses, which increases the chance of detecting false-positive results [367]. A significance level of 0.05 was chosen to highlight interesting findings and associations identified with clinico-pathological features in the large dataset were strongly significant, however the statistical significance of results from the smaller immunohistochemical dataset were less strong and would require validation in another sample set.

This study has found that presence of lymphatic invasion, when assessed using IHC, is independently associated with ulceration. Lymphatic invasion appears to predominate over vascular invasion in primary tumours [110, 113], and there was no evidence of an association between blood vessel invasion, assessed using IHC, and ulceration status in this sample set. There was also no association found between lymphatic vessel density and ulceration. Presence of lymphovascular invasion in primary tumours has been associated with poorer prognosis in a number of studies [110, 112], therefore this

association is likely to contribute to increased propensity to metastasis associated with ulcerated tumours. It has been suggested that there is likely to be a common biological process causing lymphovascular invasion and ulceration, which may be related to hypoxia [110]. The study also found that greater microvessel density was independently associated with tumour ulceration. This is a marker of tumour angiogenesis and may again be related to a hypoxic tumour environment. Normal skin is mildly hypoxic [664], and as a melanoma tumour grows, hypoxic regions appear which can promote tumour progression by supporting cell survival, enhancing metastatic spread as well as stimulating new blood vessel formation [665-667]. Under hypoxic conditions, there is induction of hypoxia-inducible factor 1 (HIF-1) and HIF-2 heterodimers [667]. HIF-1 is the predominant hypoxic factor produced in the majority of tissues and binds to hypoxia-response elements in the promoters of genes, such as vascular endothelial growth factor (*VEGF*), the expression of which is up-regulated in hypoxic conditions enhancing angiogenesis [667-669]. There are data in other cancers to support the hypothesis that hypoxic tumour microenvironments contribute to tumour invasiveness, by causing down-regulation of E-cadherin and disordered expression of genes involved in cell motility and invasion, such as metalloproteinase-2 (*MMP2*) and keratins [668-670]. To support this, expression of the α subunit of HIF-2 (HIF-2 α) assessed with IHC in melanoma tumours is a poor prognostic marker in association with high levels of VEGF and greater vascular density [671].

My study has shown that microvessel density is greater in ulcerated tumours. Higher microvessel density has been noted focally in breast tumours, where in some areas necrosis has occurred secondary to ischaemia, but in other areas there are regions of greater vascular density [672]. There is likely to be a similar process occurring in ulcerated tumours, where there is cell death as the tumour out-grows its blood supply, but there are focal areas with greater vascular density associated with less profound hypoxic conditions. In gene expression data analysed in this chapter, expression of *HIF1A*, which encodes the HIF-1 α subunit, was greater in ulcerated tumours, although not significantly following correction for multiple testing (fold change 1.06, $p=0.004$). This result supports the hypothesis that ulcerated tumours are more hypoxic than non-ulcerated tumours, which is likely to stimulate angiogenesis in areas where necrosis has not taken place. In breast tumours, tumour macrophage infiltration has been associated with greater microvessel density in necrotic tumours [672], and this association in melanoma will be further discussed below.

Microvessel density determined by review of H+E sections, has been identified as an independent predictor of overall survival [111]. There is controversy in the literature regarding the association between microvessel density and prognosis in melanoma

when IHC staining is used [396], with some authors reporting an association between higher microvessel density and poor prognosis or tumour progression [673-678], whereas others show no relationship or an association with better prognosis [679-681]. With regards to the association with ulceration status, studies using factor-VIII related antigen and anti-CD31 have found associations between higher microvessel density and tumour ulceration [673, 678]. A smaller study using anti-CD34 did not show any difference in microvessel density between ulcerated and non-ulcerated tumours [396]. My analyses are the first to identify microvessel density as a factor independently associated with ulceration in a multivariate model with other detailed tumour IHC data.

Macrophage count was independently associated with ulceration status. Macrophages are phagocytic cells which form part of the innate, non-specific, inflammatory immune response [651, 682]. They present antigen to components of the adaptive immune system and produce cytokines, such as interleukin-1, interleukin-6 and tumour-necrosis factor- α [682, 683]. There are two distinct macrophage phenotypes. Bacterial components and interferon- γ cause macrophages to become M1 macrophages which are associated with normoxic tissues, are antiangiogenic and are associated with tissue destruction, tumour cell killing and amplification of T helper type 1 (T_H1) immune responses [684-686]. M2 macrophages are polarized by tumour and T-cell derived cytokines and are usually found in association with tissue remodelling and hypoxic environments [684, 686, 687]. M2 macrophages are the subtype usually found in tumours [687-689] and release proangiogenic growth factors, support tumour growth, improve attachment of melanoma cells to extracellular matrix, suppress anti-tumour T-cell dependent adaptive immune responses and modify inflammatory responses, leading to chronic inflammation [651, 682, 684, 690-693]. The association between inflammatory processes and cancer has been well documented [651, 693]. Acute inflammation is rapid and usually self-limiting with later phases characterised by tissue remodelling and repair [693]. It is apparent that chronic inflammation contributes to the pathogenesis of many diseases associated with older age, including cancer, and M2 macrophages are key in development of chronic inflammation [651, 693]. M2 macrophages suppress adaptive immune responses via production of immunosuppressive indoleamine dioxygenase (IDO) metabolites [694], inhibition of dendritic cell maturation and stimulation of T regulatory cell infiltration into the tumour, which subsequently suppress effector T-cell activity and other inflammatory cells [695-697]. The presence of tumour-associated macrophages or a greater proportion of macrophages within tumour-infiltrating immune cells has been associated with poorer prognosis in a number of cancers, including uveal and metastatic cutaneous melanoma [684, 698-701]. In primary melanoma, these associations have been identified using

CD68 staining and when the more M2 macrophage specific CD163 antigen has been used [393, 394, 702-704]. With regards to ulceration, an earlier smaller study failed to find any association between CD68 stained macrophage levels in primary tumours and ulceration status [396]. In uveal melanoma, an association has also been identified between the presence of CD68-positive macrophages and greater microvessel density in tumours which is relevant to my findings [700].

In summary, ulcerated tumours, associated with tissue remodelling and hypoxia, were infiltrated by more macrophages, as detected using IHC in this current study. Although this could not be confirmed using the limited IHC performed, I postulate that these were M2 macrophages and that the pro-angiogenic effect of these macrophages may have contributed to the higher microvessel density in ulcerated tumours. The presence of M2 macrophages is likely to have profound effects on the tumour environment, enhancing tumour growth, angiogenesis, leading to a chronic inflammatory state and suppressing the adaptive immune system [393, 682, 684, 690-692]. Evidence exists that both higher microvessel density and macrophage count in melanoma tumours are associated with poorer prognosis; therefore the presence of these factors may contribute to prognostic significance of ulceration. Suppression of adaptive immune responses by M2 macrophages may also contribute to why ulcerated tumours are more amenable to the effects of exogenous IFN therapy (Figure 7-4).

In summary:

- Presence of lymphatic invasion and higher microvessel density, but not greater lymphatic density or blood vessel tumour invasion, are independently associated with ulceration. These factors may be secondary to the hypoxic tumour environment and macrophage infiltration. Higher microvessel density and presence of lymphatic invasion is associated with poor prognosis in melanoma, so contributing to the prognostic significance of ulceration.
- Higher macrophage count was independently associated with ulceration. Infiltration of M2 macrophages increases angiogenesis and leads to a chronic inflammatory state that suppresses adaptive immune mechanisms and is associated with poorer prognosis. I postulate that the presence of M2 macrophages may contribute to the prognostic and also predictive influence of ulceration on benefit from IFN therapy.

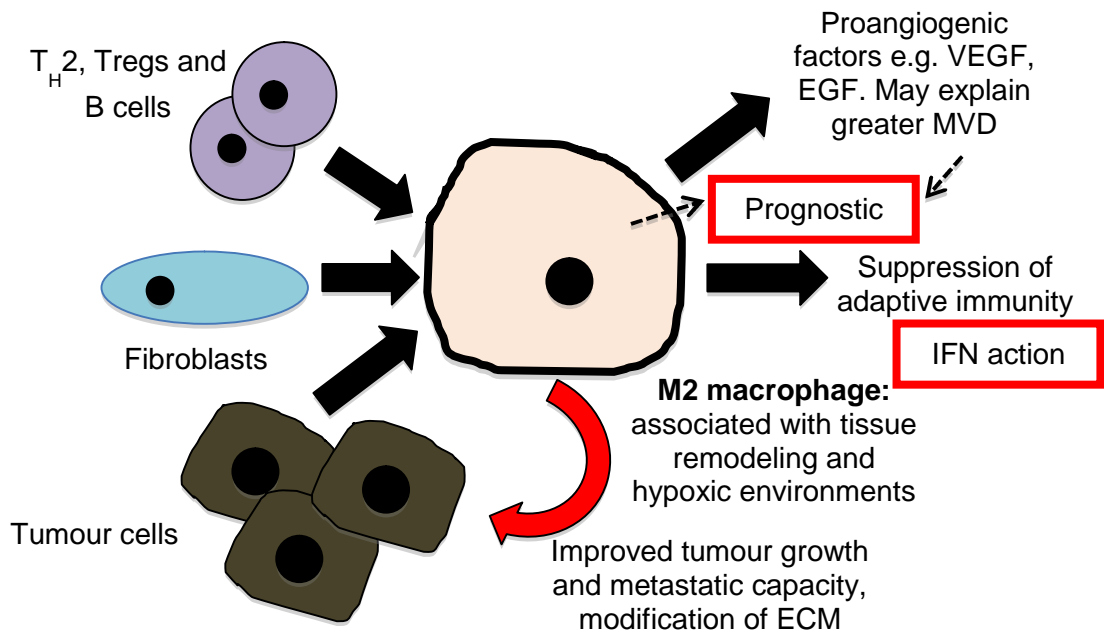


Figure 7-4: The prognostic and predictive implications of greater macrophage infiltration and microvessel density in ulcerated tumours.

I postulate that macrophages are polarized to the M2 phenotype in ulcerated tumours by release of cytokines and chemokines from immune cells (T_H2 cells, Treg cells and B cells), fibroblasts and tumour cells. M2 macrophages can enhance tumour growth and produce pro-angiogenic factors which may stimulate higher microvessel density in ulcerated tumours. They also suppress adaptive immune responses. Both tumour macrophage infiltration and microvessel density are associated with poorer prognosis in melanoma which may contribute to the prognostic influence of ulceration. Suppression of adaptive immunity may be modified by exogenous IFN therapy, explaining some of the predictive influence of ulceration. Figure adapted from [684, 705]. Abbreviations used: T_H2, T helper type 2 cells; Treg, T regulatory cells; ECM, extracellular matrix; VEGF, vascular endothelial growth factor; EGF, epidermal growth factor; MVD, microvessel density; IFN, interferon- α .

7.5.3 Gene expression and ulceration status

A number of genes shown in this study to be down-regulated in ulcerated tumours are known to be involved in cell adhesion, such as genes encoding desmoplakin (*DSP*), the integrin β 4 subunit (*ITGB4*) and E-cadherin (*CDH1*). *DSP* is part of intercellular

junctions called desmosomes, which are important in cellular adhesion, especially in the epidermis [706, 707]. In the skin, altered expression of parts of the desmosome can alter keratinocyte structure and function via modification of signalling pathways [708]. Another component of the desmosome, desmoglein 1, is down-regulated during melanoma progression, allowing melanoma cells to un-couple from keratinocyte mediated growth control [53, 709]. A study of gene expression of skin at the wound edge of venous ulcers found under-expression of DSP at the edge of non-healing ulcers versus healing ulcers [710]. However, there are no previous published reports which have identified under-expression of desmosome components in association with melanoma tumour ulceration. Down-regulation of *DSP* may cause breakdown of cellular adhesion and subsequent ulceration of the tumour. Melanoma cells are then released from keratinocyte control, enabling them to invade and progress.

It has been well established that the adherens junction protein, E-cadherin, is down-regulated in melanoma cells as the tumour progresses [53, 644]. Cadherin based junctions arrange microfilaments to maintain cell adhesion and integrate signalling within the cell and between cells [711, 712]. This study demonstrates that E-cadherin down-regulation occurs to a greater extent in ulcerated tumours. Ulceration of normal skin is believed to be due to cycles of hypoxia and then re-oxygenation leading to breakdown of skin integrity [713]. Previous studies assessing alterations in expression of cell adhesion molecules in models of skin ulceration have found that E-cadherin protein expression is dramatically down-regulated in response to hypoxia [713]. Interestingly, DSP expression is unaltered by exposure to hypoxic conditions [713]. Again, down-regulation of *CDH1* in ulcerated melanoma tumours has not been reported in the literature. However, cancer cells subjected to hypoxic conditions, especially those which up-regulate HIF-1 expression, have lower E-cadherin levels [714, 715], indicating that a more profoundly hypoxic, ulcerated tumour would have lower levels of E-cadherin expression than a more normoxic, non-ulcerated tumour. Lower levels of E-cadherin provide a further mechanism by which cells of ulcerated tumours evade keratinocyte control, contributing to tumour aggressiveness.

ITGB4 encodes the integrin $\beta 4$ subunit, which usually associates with the $\alpha 6$ subunit to mediate binding between keratinocytes and laminins in hemidesmosomes situated between the epidermal cells and dermis of normal skin [716, 717]. In mice models, where $\alpha 6\beta 4$ integrin is knocked-out, the epidermis separates from dermis, in a similar fashion to ulceration in primary melanoma tumours [716, 718]. Lack of the $\beta 4$ subunit also alters cell motility of keratinocytes, via modification of laminin organisation in extracellular matrix [719]. It has also been noted that $\alpha 6\beta 4$ integrin, along with other integrin subunits, is usually up-regulated during wound healing [716]. There is little in

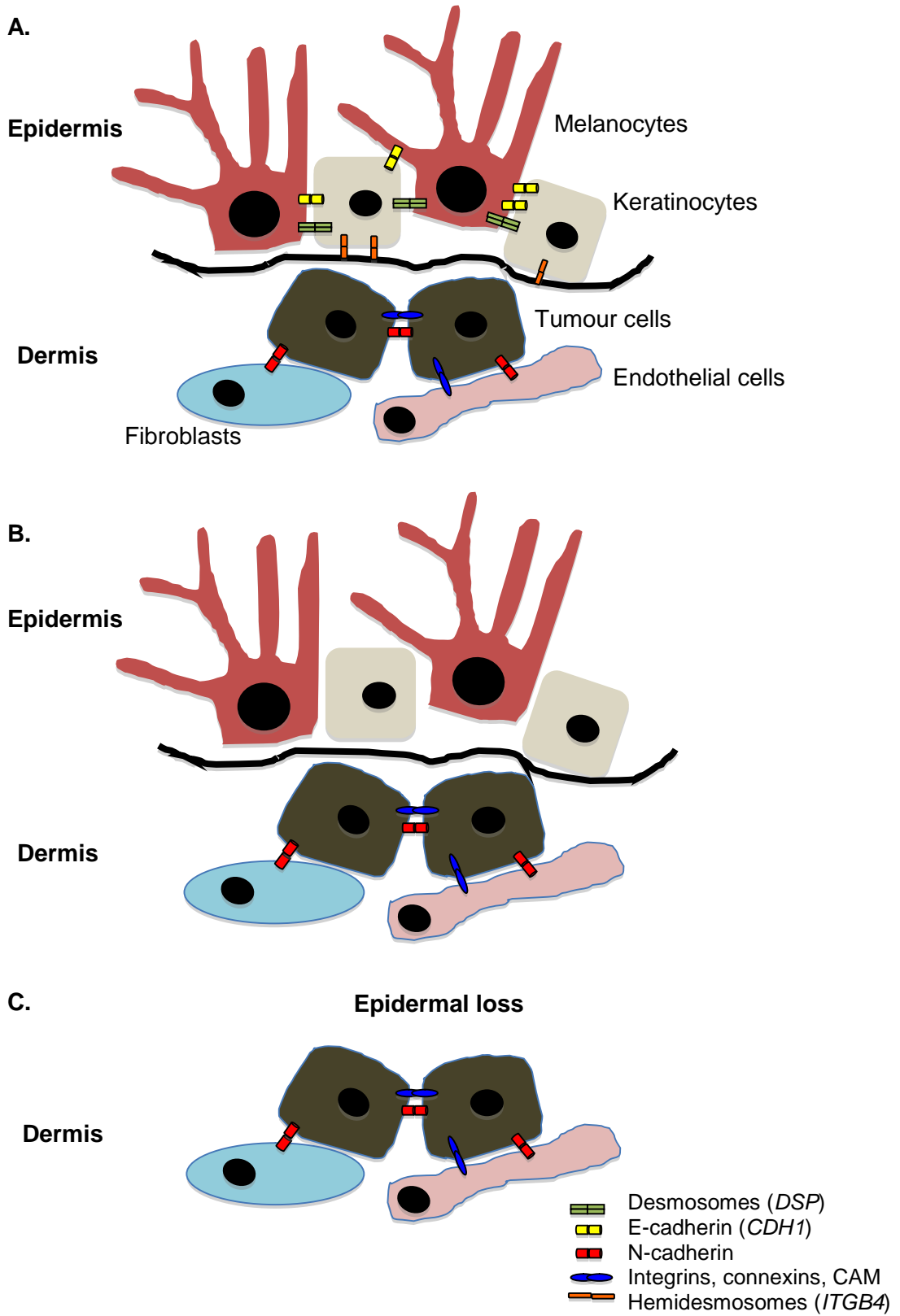
the literature investigating the role of the integrin $\beta 4$ subunit or the *ITGB4* gene in melanoma; however my study indicates that under-expression is associated with ulceration, a finding which correlates well with the known biological function of this integrin subunit in keratinocytes. We were unable to assess expression of the *ITGA6* gene as this gene was not on the 502-gene Human Cancer panel used for gene expression work. However it is likely that this would also be under-expressed in ulcerated tumours.

Figure 7-5 summarizes my hypothesis as to how down-regulation of genes involved in cell adhesion could lead to ulceration of primary melanoma tumours. Loss of cell adhesion and keratinocyte control mechanisms in ulcerated tumours is associated with increased motility of melanoma cells [53], which may be directly related to greater invasion of lymphatic vessels by tumour cells as detected using IHC.

DSP and the integrin $\beta 4$ subunit have roles in wound healing [716, 720, 721], and another gene involved in wound healing which is over-expressed in ulcerated tumours in my study is fibroblast growth factor 7 (*FGF7*), otherwise known as keratinocyte growth factor [722]. *FGF7* expression is up-regulated after tissue damage, and this growth factor acts through fibroblast growth factor 2b (FGFR2b), which is a splice variant of *FGFR2* found on epithelial cells [722, 723]. FGFs and FGFRs are proangiogenic and can stimulate cell proliferation and survival; they are often over-expressed or overactive in many cancers, secondary to a number of mechanisms, including gene amplification and mutations [522, 724, 725]. *FGF7* promotes proliferation of epidermal cells in association with improved survival and motility

Figure 7-5 (following page): Loss of molecules involved in cell adhesion leading to epidermal loss and ulceration of primary melanoma tumours.

(A) Keratinocytes and melanocytes are normally held together in the epidermis by desmosomes and E-cadherin (CDH-1). Adhesion of epidermal cells to the basement membrane is facilitated by hemidesmosomes which contain integrin subunits. As melanoma cells develop, E-cadherin is down-regulated along with components of the desmosome, such as desmoglein. Melanoma cells bind to each other by up-regulating N-cadherin and integrins, connexins and cell adhesion molecules (CAM). These molecules also allow binding to fibroblasts and endothelial cells. (B) In this study, there is down-regulation of *DSP*, which is a component of the desmosome, *CDH1* and the integrin subunit, *ITGB4* in ulcerated tumours. (C) Loss of these molecules would decrease cell adhesion in the epidermis leading to ulceration. Figure adapted from [53].



[726, 727] and is normally produced by mesenchymal cells, for example fibroblasts [728, 729]. There is evidence that normal and malignant melanocytes express *FGF7* transcripts; however it is unclear whether this has a role in epidermal cell proliferation and may be related to normal melanocyte development [730]. The current study has identified under-expression of *FGFR2*, which codes for the *FGF7* receptor, in ulcerated tumours. In contrast to many other gain of function *FGFR* mutations identified in cancer, loss of function mutations have been reported in *FGFR2* in melanoma cell lines, primary and metastatic tumours [731-733]. Decreased expression of *FGFR2* has been associated with progression of astrocytomas, prostate and bladder cancers, indicating that *FGFR2* can act as a tumour suppressor gene [734-736]. Over-expression of *FGF7* by ulcerated tumours in association with tissue damage may be expected to initiate wound healing. We have not assessed levels of *FGFR2* in keratinocytes, however in ulcerated tumours, *FGFR2* is markedly down-regulated, and *FGF7* would be unable to act via the *FGFR2b* receptor on melanoma cells in an ulcerated tumour. The role of *FGF7* in melanocytes and melanoma cells has not been elucidated [730], so further significance of these findings is unclear. In addition to higher *FGF7* expression secondary to tissue damage, pro-inflammatory cytokines, such as interleukin 6 (*IL6*), can stimulate *FGF7* production in dermal fibroblasts [737], therefore over-expression of *IL6* in ulcerated tumours may be contributing to the overexpression of *FGF7*. The current study has identified under-expression of *FGFR3* in ulcerated tumours. *FGFR3* binds to both basic and acidic fibroblast growth factors and is important in bone development [738]. *FGFR3* may be a tumour suppressor gene in melanoma [738, 739], so lower expression in ulcerated tumours would contribute to the prognostic significance of this tumour feature.

IL6 was over-expressed in ulcerated tumours in this study. A previous gene expression study using frozen tumour specimens has also reported differential expression of *IL6* [178]. *IL6* is a pro-inflammatory cytokine which can stimulate growth and survival of tumour cells and polarize immune cells, including macrophages, to aid tumour progression [740-742]. Melanoma tumours appear to produce *IL6* [652, 743-745] and as discussed previously, higher serum levels of *IL6* are related to poor survival and predictive of benefit from IFN therapy, which closely parallels the effects of tumour ulceration [652-655, 746]. This association indicates that production of this pro-inflammatory cytokine by ulcerated tumours may be an important factor determining disease progression and IFN action. Other proinflammatory cytokine genes, such as interleukin-1 α and interleukin-1 β , were also over-expressed in my analyses in ulcerated tumours (fold change ulcerated/non-ulcerated tumours 1.32 (p=0.03) and

1.74 ($p=0.0006$), respectively), although not significantly following a Bonferroni correction for multiple testing.

Pathway analysis has highlighted pathways containing genes differentially expressed in ulcerated tumours. Genes involved in focal adhesion and cytokine-cytokine receptor interaction pathways are clearly over-represented, as already discussed. However the over-representation of genes involved in Jak-STAT signalling is of great interest, as the anti-proliferative, immune, cytotoxic and anti-angiogenic effects of type 1 interferons are predominantly mediated by this pathway [213, 220]. Components of this pathway have been assessed in melanoma tumours in relation to benefit obtained from interferon therapy. As discussed in the introduction, binding of type 1 IFNs to receptors causes activation of STATs which then move to the nucleus activating gene expression [263]. STAT1 is thought to play a key role in promoting antiproliferative, proapoptotic and antiangiogenic effects on tumours by IFN therapy, and protein expression of phosphorylated STAT1 (pSTAT1) is increased by IFN therapy [747-749]. Defects within the Jak-STAT pathway are associated with resistance to IFN in melanoma cell lines [748, 750]. In this study, *STAT1* was not differentially expressed, but *STAT5B*, the gene which encodes one of the two highly related STAT5 proteins, was over-expressed in ulcerated tumours (fold change 1.08, $p=0.005$), although not significantly following a Bonferroni correction. Despite this non-significant result, the biological action of STAT5 is of interest and so will be further discussed. Studies investigating the role of STAT5 in melanoma cell lines have yielded conflicting results. STAT5 protein expression has been shown to be greater in IFN resistant melanoma cell lines with over-expression of STAT5 reducing the anti-proliferative ability of IFN in a normally IFN-sensitive cell line and depletion of STAT5 in resistant lines improving interferon responsiveness [751]. The authors of this study concluded that STAT5 inhibits STAT1 activation, with some inhibition occurring via involvement of suppressor of cytokine signalling (SOCS/CIS) factors [751]. A more recent study, again in melanoma cell lines, failed to find a relationship between phosphorylation of STAT1 following IFN treatment and the expression of STAT5 or levels of phosphorylated STAT5 [747]. The authors suggested that there are likely to be additional factors involved in regulation of STAT1 activation along with STAT5, following IFN exposure [747]. In the current study, non-statistically significant over-expression of *STAT5B* has been identified in the relatively IFN-sensitive group of ulcerated tumours, accompanied by down-regulation of factors downstream of STAT1 (Figure 7-3), such as *PIM1* (fold change 0.88, $p=0.02$), *MYC* (fold change 0.95, $p=0.008$) and *CCND3* (or cyclin D3, fold change 0.92, $p=0.01$). These findings indicate that STAT1 signalling is being suppressed in ulcerated tumours, and that STAT5 over-expression may be contributing to this; however other

factors are likely to be involved which may explain why these results appear contradictory to previous cell line data [751]. There is evidence that patients with melanoma have defects in IFN signalling in blood lymphocytes due to reduced phosphorylation of STAT1 following IFN stimulation [222, 223]. This defect can be improved by high-dose IFN therapy and the level of STAT1 activation in T-cells with IFN therapy correlates with the clinical outcome [223, 224]. A similar defect may be found in ulcerated tumours with deranged expression of components of the Jak-STAT signalling pathway, perhaps explaining the predictive nature of ulceration with IFN therapy. Exogenous IFN may enhance normal signalling through the pathway, leading to anti-tumour and immunomodulatory effects. Non-ulcerated tumours may have less deranged signalling via this pathway, which is not modified by IFN therapy, and hence little benefit is derived from the therapy. This hypothesis is speculative and may represent over-interpretation of my results. However it seems clear that deranged expression of components of this IFN signalling pathway must bear some relationship to why ulcerated tumours show greater benefit from IFN therapy and warrants further investigation.

To summarise, in ulcerated tumours:

- There is under-expression of genes involved in cell adhesion, which may be a primary event or secondary to other biological processes.
- Expression of fibroblast growth factors and receptors are deranged.
- Pro-inflammatory cytokine genes are over-expressed, which may contribute to the prognostic and predictive influence of tumour ulceration.
- There is evidence of deranged signalling via the Jak-STAT pathway, which is likely to modify responses to exogenous IFN therapy.

7.5.4 Summary

A number of poorly prognostic tumour features were shown to be independently associated with ulceration status, as was lymphatic invasion, higher microvessel density and macrophage count. I postulate therefore that tumour ulceration is associated with new blood vessel formation in the tumour, lymphatic invasion by tumour cells and polarization of macrophages to the M2 phenotype. I have been unable to confirm that the increased numbers of macrophages seen in ulcerated tumours were M2 rather than M1 and I would like to prove this in further experiments if I were able.

My study demonstrated under-expression of genes involved in cell adhesion in ulcerated tumours, which is an unsurprising finding; however we cannot prove whether

this is a primary process within the tumour, associated with a release from keratinocyte mediated growth control, or secondary to another biological characteristic of the tumour which predisposes it both to ulceration and subsequently improved metastatic capacity. Lack of cell adhesion and keratinocyte control will contribute to increased cell motility, explaining greater evidence of lymphatic invasion in ulcerated tumours.

My study revealed deranged expression of *FGF* and *FGFR* genes in ulcerated tumours and independent associations with macrophage infiltration, presence of lymphatic invasion, greater microvessel density, Breslow thickness and mitotic rate. These associations may explain some of the prognostic effects of tumour ulceration.

There is evidence in these analyses of altered immune mechanisms in ulcerated tumours. Macrophage infiltration was seen, and the literature would suggest that these are likely to be M2 cells capable of suppressing adaptive immunity. I also showed novel findings indicative of deranged expression of components of the Jak-STAT pathway and confirmed previously reported over-expression of pro-inflammatory genes such as *IL6* in melanomas.

Effects of the IFN used therapeutically are mediated by Jak-STAT signalling. Down-regulation of genes downstream to STAT1 suggests that signalling via this pathway is suppressed in ulcerated tumours, perhaps by increased STAT5 in association with other factors. I postulate that deranged signalling via this pathway may be modified by exogenous IFN therapy, enhancing antitumour effects of IFN and leading to prolonged survival following IFN therapy.

8 DNA repair gene expression and response to chemotherapy in stage IV melanoma

8.1 Aims

In a pilot study, gene expression data generated using the cDNA-mediated annealing, selection, extension and ligation (DASL) assay and the Human Cancer panel provided evidence that increased expression of a number of DNA repair genes was associated with resistance to treatment with alkylating agents, dacarbazine (DTIC) and temozolomide (TMZ) [505]. These findings were confirmed and the association between DNA repair gene expression and chemotherapy response was further explored using the Chemo-sensitivity Gene Expression Array (CGEA-1) [505]. These results were consistent with the published data related to this issue.

The primary aims of the of the work described in this chapter were:

- To explore the pilot data in a larger sample set in order to identify whether expression of DNA repair genes might prove to be a useful predictive biomarker of DTIC or TMZ response.
- To investigate the use of the Fluidigm quantitative Real-time PCR (qRT-PCR) system for the first time using formalin-fixed paraffin-embedded (FFPE) melanoma tumour to carry out multiple PCR reactions to measure gene expression.

To achieve these primary aims, this chapter also describes the:

- Concept, set-up and development of the “Predicting Response to Chemotherapy in Malignant Melanoma” study. These data (clinical and genomic) are nearing completion in July 2012 and here I report those data to which I currently have access.

8.2 Background

A number of effective treatments have been recently developed for advanced melanoma, however use of vemurafenib against mutant *BRAF* is limited to patients with a *BRAF* mutated tumours (40%) and resistance can develop [199]. Use of the second “revolutionary” agent, ipilimumab is also associated with improved survival but

only in a small number of patients and with considerable toxicity [60, 61]. Therefore, a proportion of patients still receive DTIC or TMZ chemotherapy for stage IV disease and are likely to be so treated in the future, especially if a predictive biomarker can be identified. Response rates are low at 7-13%, with a further 15-28% having stable disease during treatment, but few of these responses are long-lasting [243, 244]. DTIC is an alkylating agent which methylates DNA at the O⁶-position of guanine. O⁶-methylguanine often mispairs with thymine instead of cytosine during replication and this is recognised by the mismatch repair system which removes a section of DNA with the thymine molecule. Replication of this gapped structure leads to double-stranded breaks in DNA which eventually lead to cell death via apoptosis [247] (Figure 8-1).

TMZ is also an alkylating agent used in melanoma with similar efficacy to DTIC [243, 249]. TMZ undergoes spontaneous conversion to the active alkylating agent 5-(3-methyltriazene-1-yl)imidazole-4-carboximide (MTIC) which has similar actions to DTIC [248]. TMZ can be administered orally and has been used for the treatment of brain metastases as it crosses the blood-brain barrier [243, 249].

It has been suggested that over-expression of genes related to DNA repair is linked to the chemoresistance of melanoma [264, 752]. Increased activity of the DNA repair gene O⁶-methylguanine-DNA-methyltransferase (*MGMT*), which removes alkyl groups from DNA, is associated with resistance to alkylating agents in glioblastoma tumours [753, 754] and in melanoma cell lines [265, 755]. An inverse relationship between *MGMT* protein expression and gene expression with DTIC response in melanoma tumours has also been identified [267, 756] which supports the view that *MGMT* expression might be a predictive biomarker. Gene silencing by promoter methylation has also been associated with improved responses to TMZ therapy in metastatic tumours [757]. The relationship between melanoma response to alkylating agents and *MGMT* is not entirely clear however, as other studies have failed to show that *MGMT* activity [268, 269], protein expression [270], promoter methylation [271, 758] or *MGMT* polymorphisms [267] are associated with response to TMZ or DTIC. Disappointingly, clinical trials using extended dose TMZ to deplete *MGMT* levels and use of *MGMT* inactivators or pseudosubstrates did not enhance activity of TMZ in melanoma [271-273, 759].

The mismatch repair pathway is also important for the toxicity of alkylating agents. A deficiency in this pathway results in failure of cells to recognise and repair O⁶-methylguanine adducts produced by TMZ or DTIC and so double stranded breaks do not occur and DNA replication continues without apoptosis occurring [248, 274].

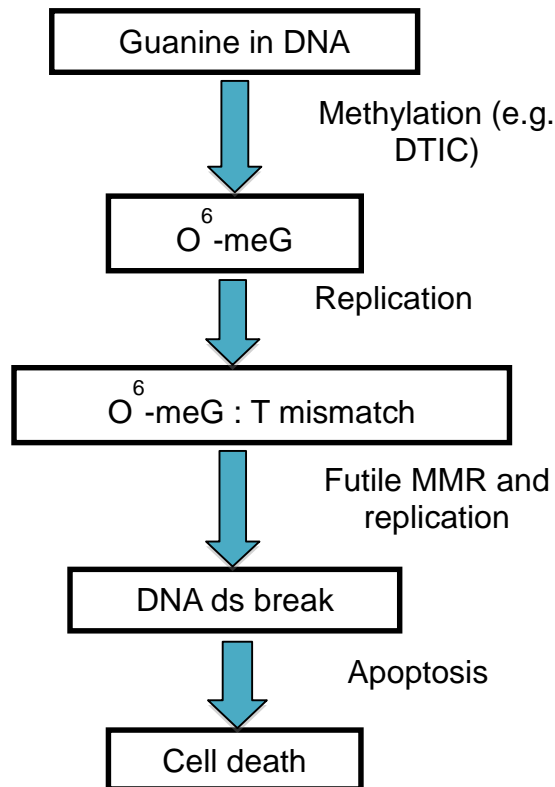


Figure 8-1: Mechanism of action of dacarbazine.

Further detail is provided in the text. Adapted from [247]. Abbreviations used: DTIC, dacarbazine; O⁶-meG, O⁶-methylguanine; T, thymine; MMR, mismatch repair; ds, doubled-stranded.

Studies using melanoma cell lines have demonstrated that the mismatch repair system in melanoma appears to be largely intact, so contributing little to TMZ resistance [265, 275].

The base excision repair (BER) pathway has also been reported to be related to resistance to TMZ and DTIC, as the DTIC-induced adducts, 3-methyladenine and N7-methylguanine can be processed and repaired by the BER pathway [760]. Inhibition of poly(ADP-ribose) polymerase (PARP) in cell lines has been reported to improve cytotoxicity of alkylating agents [276, 277, 761], but again this pathway appears to have minimal effect on TMZ resistance in melanoma cell lines [265]. A phase I study in advanced solid tumours, including melanoma, demonstrated that use of a PARP inhibitor (AG014699) with TMZ caused PARP inhibition with increased single-strand breaks and minimal toxicity suggesting that these agents could be used therapeutically alone or in combination with chemotherapy [278]. However, in another phase I trial using the PARP inhibitor Olaparib (AZD2281, KU0059436), the authors concluded

there was no clinical advantage over use of DTIC alone [762]. Haemotoxicity appeared to be an issue in phase II trials and further results are awaited [762]. Inhibitors of other DNA repair genes in the BER pathway, such as APE1 (or APEX-1), enhance alkylating agent toxicity in melanoma and glioma cell lines, again highlighting the potential importance of this pathway [763].

Development of *in vitro* assays that assess chemosensitivity will help isolate further candidates of chemotherapy resistance. When chemosensitivity of cutaneous melanomas has been assessed and correlated with quantitative gene expression of putative chemotherapy resistance genes, gene expression signatures associated with resistance to DTIC, treosulphan and cisplatin revealed that genes involved in DNA repair (*ERCC1*, *XPA*, *XRCC1*, *XRCC6*) were over-expressed [764].

In summary, DNA repair genes have been reported to be associated with poor response to alkylating agents in a number of studies, but the relationships are not clear and a more comprehensive assessment is required. Identification of biomarkers of treatment response will provide insight into tumour biology and in the long-term, may assist clinicians and patients in making informed decisions about treatment options.

This chapter describes the process by which I have explored the significance of expression of DNA repair genes as being associated with DTIC or TMZ chemotherapy response. Results from the DASL assay were validated using a different gene expression platform and then further explored in a larger separate sample set.

For the validation of DASL data, this chapter describes use of a customized Taqman® Array microfluidic qRT-PCR card (Chemo-sensitivity Gene Expression Array, CGEA-1, CanTech Ltd, Portsmouth, UK). This array contains 92 genes known or hypothesized to be involved in cytotoxic resistance or sensitivity based on the current literature [289] (Table 8-1). Mechanisms of resistance to chemotherapy include under-expression of target genes, altered drug metabolism, presence of membrane drug pumps, altered apoptotic sensitivity, deranged DNA repair and altered cellular growth or differentiation [289]. The CGEA-1 has been designed to assess gene expression of candidates within these pathways and was used in this chapter to validate microarray gene expression data. Taqman® array cards (Applied Biosystems, Warrington, UK) are 384-well microfluidic cards which allows 384 simultaneous PCR reactions using Taqman® gene expression assays which are described in more detail in Chapter 2 [344]. The ability to perform multiple reactions using one array reduces variability across plates so improving the reliability of results [344]. It also allows assessment of either multiple genes for a limited number of samples or assessment of a smaller number of genes for multiple samples [344].

Apoptosis	Pumps/Detox	DNA repair	Proliferation	Normalisation genes
<i>AKT</i>	<i>ATP7B</i>	<i>ATM</i>	<i>APC C-term</i>	<i>18S</i>
<i>APAF1</i>	<i>BCRP</i>	<i>BRCA1</i>	<i>APC N-term</i>	<i>HPRT</i>
<i>BAD</i>	<i>CES1</i>	<i>ERCC1</i>	<i>β-TUBULIN III</i>	<i>PBGD</i>
<i>BAX</i>	<i>CES2</i>	<i>ERCC2</i>	<i>COX2</i>	<i>SDHA</i>
<i>BCL2</i>	<i>cN II</i>	<i>GTF2H2</i>	<i>EGFR</i>	<i>TBP</i>
<i>BCL-x(L)</i>	<i>DPD</i>	<i>MGMT</i>	<i>HER2</i>	
<i>BID</i>	<i>FPGS</i>	<i>MLH1</i>	<i>HER3</i>	
<i>c-FLIP</i>	<i>γH2AX</i>	<i>MSH2</i>	<i>HER4</i>	
<i>FAS</i>	<i>GCLC</i>	<i>MSH6</i>	<i>HIF1A</i>	
<i>FASL</i>	<i>GCLM</i>	<i>RAD51</i>	<i>KI67</i>	
<i>HSP60</i>	<i>GSTπ</i>	<i>TOPO I</i>	<i>P16</i>	
<i>HSP70</i>	<i>hENT1</i>	<i>TOPO IIa</i>	<i>P21</i>	
<i>HSP90</i>	<i>hENT2</i>	<i>TOPO IIb</i>	<i>P27</i>	
<i>IAP2</i>	<i>MDR1</i>	<i>TS</i>	<i>P53</i>	
<i>IGF1</i>	<i>MRP1</i>	<i>XPA</i>	<i>VEGF</i>	
<i>IGF1R</i>	<i>MRP2</i>	<i>XRCC1</i>		
<i>IGF2</i>	<i>MRP3</i>	<i>XRCC5</i>		
<i>IGR2R</i>	<i>MRP4</i>	<i>XRCC6</i>		
<i>IGFBP1</i>	<i>MRP5</i>			
<i>IGFBP2</i>	<i>MRP6</i>			
<i>MCJ</i>	<i>MRP8</i>			
<i>MCL1</i>	<i>MTII</i>			
<i>mTOR</i>	<i>MVP</i>			
<i>NFκB</i>	<i>OPRT</i>			
<i>PIK3CA</i>	<i>RRM1</i>			
<i>PTEN</i>	<i>SOD1</i>			
<i>STAT3</i>	<i>TAP1</i>			
<i>SURVIVIN</i>	<i>TAP2</i>			
<i>XIAP</i>	<i>TAP4</i>			

Table 8-1: Genes on the Chemo-sensitivity Gene Expression Array (CGEA-1).

Genes are listed according to biological function. Table adapted from [289].

On a larger scale, the Fluidigm Biomark HD quantitative PCR chip (Fluidigm, San Francisco, CA) allows assessment of up to 96 genes in 96 samples in a total of 9216 PCR reactions in a single experiment. I used this technology to assess expression of 43 DNA repair genes (and 5 control genes) in a larger sample set from patients recruited to the “Predicting Response to Chemotherapy in Malignant Melanoma” study. This study will be further described in section 8.5. Fluidigm microfluidic technology uses integrated fluidic circuits (IFC) containing valves and channels which automatically assemble individual PCR reactions, enabling the simultaneous performance of PCR reactions in nanolitre volumes. Fluidigm technology is further

described in Chapter 2 [345, 346]. Each PCR reaction takes place in a volume of only 10nl versus the 10µl volume used for routine qRT-PCR reactions described elsewhere in this thesis [345-347]. Previous work has demonstrated that the Fluidigm system provides reproducible results for gene and micro-RNA expression when compared to traditional qRT-PCR experiments using Taqman® gene expression assays [346, 347] and results from micro-RNA analysis correlate well when fresh-frozen tissues or FFPE tissues are used for RNA extractions [346].

The Fluidigm systems can be used with Taqman® assays, but for the purposes of this study, we have used gene specific primers (DELTAgene™ assays, Fluidigm) in conjunction with the DNA-binding dye, EvaGreen. EvaGreen is a fluorophore, which when bound to double-stranded DNA emits a strong fluorescent signal, the intensity of which is directly proportional to the increase in the amount of double-stranded DNA during a PCR reaction [349, 350]. Use of EvaGreen significantly reduces the cost of the experiment, however the specificity of the reaction is reduced as only a primer pair are used for PCR, the additional probe present in Taqman® based assays (described in Chapter 2) being absent [349]. To our knowledge, this is the first experiment using cDNA derived from FFPE material for gene expression using the Fluidigm qRT-PCR system and so a thorough assessment of the quality of the assays has been made in FFPE melanoma tumour material. I have specifically assessed the efficiencies of the primers in a similar fashion to that described in Chapter 4 for Taqman® gene expression assays and the specificity of the amplicon using melt curve analysis.

8.3 Identification of genes associated with response to chemotherapy using the DASL assay

8.3.1 Further methodological details

8.3.1.1 Statistical methodology

Chemotherapy analysis was performed using the merged dataset generated from two sample sets (the Leeds Melanoma Cohort Study (Cohort study) and the Retrospective Sentinel Node Biopsy Study (SNB study)) described in further detail in Chapter 4. Log-transformed normalised data (log₂) were used for analysis, expression of genes of interest was compared between responders and non-responders to chemotherapy using linear regression. Response to chemotherapy was defined as those with stable disease, a mixed response, partial response or regression of disease determined using computed tomography (CT) scanning following 2 or 3 cycles of chemotherapy. In some

instances, response data was recorded according to Response Evaluation Criteria in Solid Tumours (RECIST) version 1.1 criteria by the reporting radiologist [290], in others response data was provided by review of the radiology assessed formally at the melanoma multidisciplinary team meeting. As expression of single genes were assessed, the significance level for highlighting results of interest was set at 0.05. In view of non-biological variations that were present between the Cohort and SNB studies, analyses were adjusted for the study to which patients were recruited. All analyses were undertaken using Stata version 10 (StataCorp 2007, College Station, TX).

8.3.2 Results

Forty-three patients, 23 from the SNB study and 20 from the Cohort study had received chemotherapy (11.9%). Of these patients, tumour response following chemotherapy had been recorded for 36 patients. The majority of patients received DTIC with three patients receiving treosulphan as first line chemotherapy. Six patients (17%) responded to DTIC chemotherapy as defined above. *RAD51* and *TOP2A* were significantly over-expressed in tumours from non-responders compared to responders (*RAD51* fold change 1.66, $p=0.01$; *TOP2A* fold change 1.43, $p=0.03$). *BRCA1* was also over-expressed in tumours from non-responders (fold change 1.36), but this difference was of borderline significance ($p=0.05$). In order to validate these findings and explore expression of other genes associated with chemotherapy response using a different platform, the CGEA-1 array was used as described below.

8.4 Validation of DASL results and further assessment of genes associated with chemotherapy response

8.4.1 Rationale

In order to validate DASL results and assess gene expression of other genes postulated to be associated with response to chemotherapy, a sample of tumour RNAs from patients treated with chemotherapy were also analysed using the CGEA-1 array in collaboration with the Translational Oncology Research Centre, Queen Alexandra Hospital, Portsmouth. The experimental work was performed by Dr Katharine Parker.

8.4.2 Further methodological details

8.4.2.1 The Chemo-sensitivity Gene Expression Assay (CGEA-1)

Table 8-1 lists the genes present on the array. Of the 36 patients from whom chemotherapy response data were available, 33 received DTIC and samples from these patients were selected for assessment with the CGEA-1 array. cDNA was generated from RNA using the Invitrogen Superscript™ First-strand Synthesis System with increased reagent volumes as described in Chapter 2. Two cDNA samples were unavailable as they were used in other studies. Therefore a total of 31 samples from patients treated with chemotherapy (5 from responders) were sent for qRT-PCR analysis using the CGEA-1 array in Portsmouth. The CGEA-1 was run according to manufacturer's instructions as previously reported [289] and described in further detail in Chapter 2. Cycle threshold (Ct) values from the experiment were sent to myself for further analysis. A calibrator sample was chosen with the lowest Ct value for a highly expressed gene, *18s*, to allow relative quantification of gene expression. This sample was selected to reduce the number of missing values for analysis. Five endogenous control genes were present on the array for normalisation of data. Expression levels of *18s* were much higher than unknown genes and as the abundance of a reference gene should be similar to that of the gene of interest [458], *18s* was not used for normalisation. A large number of samples did not amplify using the *HPRT* assay and so *PBGD*, *SDHA* and *TBP* were used as reference genes for normalisation according to the method described by Vandesompele *et al.* [343] and described in further detail in Chapter 2. The normalised gene quantities were used to calculate a fold difference in mean gene expression between chemotherapy non-responders and responders. Statistical significance was determined using a Mann-Whitney U test, with a significance level of 0.05. Statistical analysis was undertaken using Stata version 10 (StataCorp 2007, College Station, TX).

8.4.3 Results

Genes from which there were less than 10 results overall were deemed to have failed and were removed from further analyses (n=13). To allow a meaningful comparison between gene expression in responders and non-responders, genes for which there were less than 2 results for responders were also excluded from further analyses (n=2). All of the 17 genes involved in DNA repair on the array were over-expressed in tumours from patients who did not respond to chemotherapy (Table 8-2). These genes

	Gene	Number of non-responders/ number of responders	Mean fold difference in expression between non-responders and responders	Test statistic and significance value
DNA repair genes	<i>MSH6</i>	17/4	4.61	Z 1.4, p=0.15
	<i>TOPO1</i>	21/4	3.15	Z 0.2, p=0.82
	<i>MSH2</i>	16/4	3.06	Z 1.9, p=0.06
	<i>XRCC1</i>	13/4	2.95	Z 1.4, p=0.17
	<i>XRCC5</i>	22/5	2.87	Z 0.0, p=1.00
	<i>TOP2A</i>	17/3	2.53	Z 0.9, p=0.37
	<i>XRCC6</i>	22/5	2.47	Z 1.4, p=0.17
	<i>MGMT</i>	9/2	2.21	Z 0.9, p=0.35
	<i>RAD51</i>	17/3	2.13	Z 0.6, p=0.56
	<i>ERCC1</i>	22/5	2.07	Z 1.1, p=0.29
	<i>TOP2B</i>	22/4	1.96	Z 0.0, p=1.00
	<i>XPA</i>	20/5	1.87	Z 0.9, p=0.34
	<i>ATM</i>	18/3	1.81	Z 0.1, p=0.92
	<i>BRCA1</i>	17/3	1.77	Z -0.3, p=0.79
	<i>ERCC2</i>	18/4	1.73	Z -0.1, p=0.93
	<i>GTF2H2</i>	21/4	1.51	Z -0.9, p=0.37
<i>MLH1</i>	16/2	1.21	Z 0.1, p=0.89	
Genes most over-expressed in non-responding tumours	<i>TAP4</i>	15/2	24.63	Z 1.3, p=0.18
	<i>TS</i>	21/3	24.53	Z 1.6, p=0.11
	<i>KI67</i>	9/2	12.06	Z -0.2, p=0.81
	<i>MTII</i>	22/5	8.06	Z 1.5, p=0.13
	<i>mTOR</i>	21/4	7.33	Z 0.9, p=0.37
	<i>cN II</i>	19/5	6.62	Z -0.04, p=0.97
	<i>PIK3CA</i>	21/4	5.02	Z 1.2, p=0.24
	<i>MSH6</i>	17/4	4.61	Z 1.4, p=0.15
	<i>HSP90</i>	22/5	4.51	Z 1.4, p=0.17
<i>SOD 1</i>	22/5	4.40	Z 1.7, p=0.09	
Genes most under-expressed in non-responding tumours	<i>MCL1</i>	21/4	0.38	Z -0.07, p=0.94
	<i>FAS</i>	16/4	0.45	Z 0.4, p=0.71
	<i>FPGS</i>	12/2	0.71	Z -0.6, p=0.58
	<i>BAX</i>	21/5	0.86	Z -0.9, p=0.35
	<i>p53</i>	19/5	0.92	Z -0.1, p=0.92

Table 8-2: Genes differentially expressed in tumours unresponsive to chemotherapy using the Chemo-sensitivity Gene Expression Array (CGEA-1).

DNA repair genes on the array are listed followed by genes most over-expressed and under-expressed in unresponsive tumours. The number of samples from non-responders and responders is presented with fold difference in gene expression between non-responders and responders. Significance values are derived from the Mann-Whitney U test.

included *RAD51* (fold change 2.13), *TOP2A* (fold change 2.53) and *BRCA1* (fold change 1.77) as well as genes involved in nucleotide excision repair (e.g. *ERCC1*, *XPA*), base excision repair (e.g. *XRCC1*), removal of damaged DNA bases (*MGMT*), mismatch repair (e.g. *MLH1*, *MSH2*) and DNA non-homologous end joining (e.g. *XRCC5*, *XRCC6*) [289, 497]. Within the groups of genes encoding proteins associated with apoptosis, cellular proliferation and membrane transport molecules, some genes were under- and others over-expressed in tumours which did not respond to chemotherapy [289, 765]. As a result of the small numbers of samples included in these analyses, the power was too low to achieve statistical significance but this was essentially a validation step using different technology and was deemed confirmatory.

8.5 The “Predicting Response to Chemotherapy in Malignant Melanoma: The role of DNA repair genes” study

In view of the small number of samples available from patients treated with DTIC or TMZ in the previous analyses described, a larger sample set was required to confirm the association between DNA repair gene expression and chemotherapy response. A sample set of sufficient size was not available in the Section of Epidemiology and Biostatistics, so the “Predicting Response to Chemotherapy in Malignant Melanoma” study (Chemotherapy study), was developed. The study was started by myself with assistance from my supervisors and members of the Section, specifically Mr Christy Walker, who has project-managed the study and coordinated sample collection and Dr Jon Laye, who has processed and sampled tumours for the study. This study has permitted collection of a large number of tumours from patients with response and survival data allowing confirmation of previous findings.

8.5.1 Study design and aims

This retrospective study utilises FFPE primary and metastatic melanoma tumour samples from patients previously treated with DTIC or TMZ chemotherapy recruited to clinical trials, well annotated epidemiological studies or as part of routine clinical care in the UK. RNA has been extracted from tumour samples to assess expression of DNA repair genes. These data have been linked with chemotherapy response and survival data to determine gene expression profiles associated with chemotherapy response and survival after starting chemotherapy. This chapter describes use of tissue for gene expression analysis for DNA repair genes, however the intention will be to use tissue

for other techniques, such as whole-genome expression profiling, mutation screening, immunohistochemistry, micro-RNA expression, methylation analysis and assessment of copy number variation in the future in order to understand genetic associations with patterns of metastasis and response to treatment. Given the low response rate to DTIC and therefore the limited power within any one centre, to maximise the number of samples for analysis, this is a collaborative study with the European Organisation for Research and Treatment of Cancer (EORTC) Melanoma group and a European Union-funded consortium called Chemores. These groups have provided additional tumour samples and clinical data for analysis with samples collected in the UK. The study is managed in Leeds. It was hoped that a successful output from this study might encourage further similar biomarker studies for other cancers using archived FFPE tumour samples which had previously been supposed to be unsuitable for genomic studies.

8.5.2 Participants and samples

Patients that were eligible for inclusion in this study were:

- Patients recruited to the “EORTC 18032: Extended schedule, escalated dose TMZ versus DTIC in stage IV metastatic melanoma: a randomised phase III study” [249]. This study randomised 859 patients to receive oral TMZ or intravenous DTIC. The study concluded that use of TMZ did not improve overall survival or progression-free survival when compared to DTIC [249]. Potential participants were identified from European centres and the Nottingham University Hospitals NHS Trust. Samples and follow-up data were sent to Leeds for analysis. The use of material from patients recruited to clinical trials will help to ensure a more accurate assessment of response to treatment.
- From the Chemores group (www.chemores.org), which is collecting tissue samples from melanoma patients treated with DTIC and TMZ for identification of biomarkers of response to chemotherapy. Samples and follow-up data collected by this group have been sent to us in Leeds for analysis and pooled with other data.
- Patients recruited to cohort studies or case-control studies of melanoma such as the Leeds Melanoma Cohort Study were also eligible if treated with chemotherapy.
- Patients treated with DTIC or TMZ as part of routine clinical care in Leeds.

A number of patients were excluded following review where tissue was not available for tumour sampling or where the patient had not received chemotherapy treatment with DTIC or TMZ. Table 8-3 summarises the number of recruited patients in May 2012.

Primary and metastatic FFPE melanoma tumour blocks have been traced for eligible participants. Tumour tissue has been sampled and RNA and DNA extracted from tumour tissue cores using the Qiagen AllPrep® RNA/DNA FFPE kit as described in Chapter 2. Gene expression analysis of DNA repair genes has been undertaken using the Fluidigm qRT-PCR system which will be described in further detail below.

Recruiting centre	Total number of patients from each centre	Number recruited to the EORTC 18032 trial
Leeds	260	6
Nottingham	12	12
Leuvan (EORTC/Chemores)	87	0
Essen (EORTC/Chemores)	135	21
Excluded cases	(22)	(2)
Total	472	37

Table 8-3: Number of patients recruited to the Chemotherapy study.

The total number of cases is reported with the number recruited to the EORTC 18032 trial. Twenty-two cases were excluded as no tumour tissue was available or they did not received DTIC or TMZ chemotherapy. Abbreviation used: EORTC, European Organisation for Research and Treatment of Cancer.

8.5.3 Clinical data

Clinical data have been provided from treating clinicians, with negotiations currently underway to access trial databases for patients treated as part of clinical trials. For patients recruited to epidemiological studies in Leeds, data have been extracted from current study databases. The clinical data recorded include patient demographic details (age, gender, date and cause of death or last follow-up date), details of the primary melanoma (date of diagnosis, site of tumour, stage at diagnosis, tumour histological features), information regarding stage IV diagnosis (date of diagnosis, sites of disease), details of chemotherapy received (chemotherapy used and regimen, dates of chemotherapy, dose reductions, severe haemotoxicities) and lactate dehydrogenase (LDH) levels before, during and after treatment.

For the current study, chemotherapy response data are of paramount importance. For patients recruited to the EORTC 18032 trial, I hope to access objective response data based on the original version of RECIST criteria [766] determined using a CT scan after 3 cycles of treatment and then after 6 cycles if chemotherapy is continued. Overall response has been defined as complete response, partial response, stable disease or

progressive disease [766]. As this trial data is currently not available, response data for patients treated as part of the 18032 trial, other clinical trials or routine clinical care, have been provided by treating clinicians based on clinical and radiological tumour response. For example, for patients recruited in Leeds, where possible objective response has been determined using CT scan after 3 or 6 cycles of therapy. Where target lesions have been measured, updated RECIST version 1.1 criteria have been used to determine response to chemotherapy [290]. Where target lesions have not been measured, response has been determined by the reporting radiologist on CT scan, the treating clinician if a clinical determination has been made or the multidisciplinary team based on review of imaging and clinical factors. Where a response has been recorded by the multidisciplinary team, this has been deemed the most accurate data and used for analysis. When trial data are available, the source of response data is recorded to allow separate assessment of the subset of patients recruited to trials with RECIST criteria response data. In all cases, the best response whilst on treatment or the scan after the final chemotherapy cycle was recorded as the response to chemotherapy treatment and used for further analysis.

8.5.4 Power calculations

Power calculations are based on a range of DNA repair genes with varying mean gene expression levels and standard deviations identified as differentially expressed in tumours from non-responders to chemotherapy from the DASL gene expression data. Assumptions made were that 15% of patients respond (complete response, partial response or stable disease) to chemotherapy. With 450 eligible patients we have 99-100% power, depending on the differential expression of the gene, to detect a difference in gene expression level at a 0.001 significance level.

8.5.5 Regulatory approvals

Ethical approval for the study was granted by Yorkshire and Humber Central Research Ethics Committee on the 23rd August 2010 (10/H1313/72) and support under section 251 of the NHS Act 2006 was granted by the Ethics and Confidentiality Committee by the National Information Governance Board for Health and Social Care on the 4th October 2010 (ECC 8-02 (FT2)/2010).

8.6 Assessment of DNA repair gene expression in FFPE melanoma tumours using the Fluidigm qRT-PCR platform

Expression of DNA repair genes was assessed in primary and metastatic FFPE melanoma samples from patients recruited to the Chemotherapy study. Before the larger sample set was analysed a pilot study was performed to assess the Fluidigm system and DELTAgene assays when using FFPE melanoma tissue.

8.6.1 Selection of genes for assessment

The aim of this study was to assess gene expression of a larger panel of DNA repair genes. The Fluidigm IFC arrays allow assessment of 96 genes for 96 samples in a single reaction, therefore I decided to assess expression of 48 genes (43 test genes and 5 control genes) in duplicate on each array. DELTAgene assays were used for this work which were produced by Fluidigm based on RefSeq IDs using standard design procedures [331]. Table 8-4 lists the genes assessed and details of the DELTAgene assays. These genes were selected either because they were previously identified as associated with response to treatment using the DASL assay, were present on the CGEA-1 array or there was evidence in the literature that these genes were associated with chemotherapy response in melanoma or other cancers as referred to in Table 8-4. Five control genes (Table 8-4) were selected based on previous work using Taqman® gene expression assays as described in Chapter 4, however following the results of these analyses, *GAPDH* was not used for normalisation of data.

As these assays had not been used before in an experiment using FFPE melanoma tissue, a pilot Fluidigm plate was assessed using RNA extracted from melanoma cell line samples and FFPE metastases samples. This allowed assessment of performance of the assays, assay specificity and sample reproducibility. As discussed in Chapter 4, PCR efficiency of endogenous control gene and test genes needs to be comparable to allow use of the comparative Ct method for relative quantification [340, 455]. To assess PCR efficiencies of DELTAgene assays in FFPE melanoma samples, standard curves were generated using serially diluted samples.

8.6.2 Pilot study

8.6.2.1 Samples

The following experimental work was performed by myself. As a source of high-quality template RNA, RNA was extracted from 3 melanoma cell lines (SkMel5, Mel Juso and Mel 624) using the Qiagen RNeasy® Mini kit. RNA was extracted using a single tissue core from five FFPE melanoma metastasis samples using the Qiagen AllPrep® RNA/DNA FFPE kit. RNA was also extracted from an FFPE intradermal naevus sample, which was selected to act as a calibrator sample. The Roche High Pure RNA Paraffin Kit was used for RNA extraction from this sample. From cell line and FFPE samples, 400ng and 200ng of RNA, respectively, was used for cDNA synthesis using the Applied Biosystems High Capacity cDNA reverse transcription kit. Further methodological details are described in Chapter 2.

8.6.2.2 Methodological details

8.6.2.2.1 Specific target amplification (STA) of samples

Amplification of specific target assays was performed using 18 cycles of pre-amplification and the standard Fluidigm qRT-PCR protocol as described in Chapter 2. As *GAPDH* is already highly expressed, this assay was not included in the primer mix, therefore the remaining 47 primer pairs were pooled and used for pre-amplification.

Table 8-4 (following 3 pages): Details of genes assessed using the Fluidigm qRT-PCR platform with DELTAgene assays in samples from the Chemotherapy study.

Genes are grouped according to biological function [482, 497, 499, 767, 768]. RefSeq ID used for primer design [331], exons targeted, length of amplicon and primer sequence of the DELTAgene assays are also presented. The references column indicates the sources that associate the gene with chemotherapy responses or reasons why the gene has been included in the panel. Abbreviation used: bp, base pair.

Biological function	Gene	RefSeq ID used for primer design	Targeted exons	Amplicon length (bp)	Forward primer	Reverse primer	References
Endogenous control genes	<i>GAPDH</i>	NM_002046.3	2-3	61	ACACCATGGGGAAGGTGAAG	GTGACCAGGCGCCCAATA	
	<i>IPO8</i>	NM_001190995.1	16-17	79	TTCAGTGCAAAGGAAGGGGAA	ACCCCTCGAGTTAATCTCTCCA	
	<i>PES1</i>	NM_014303.2	10-11	81	GCCTGAAGTTCTTCCTGAACC	AGGACACTTCCCCACCAAAA	
	<i>CASC3</i>	NM_007359.4	9-10	75	CCCCTCCAGTGCATATCAGTA	GGGTATAGATTGGTCCCTGGAA	
	<i>SDHA</i>	NM_004168.2	11-12	81	ACATCGGAACTGCGACTCA	TTCTTGCAACACGCTTCCC	
Nucleotide excision repair	<i>XPA</i>	NM_000380.3	4-5	76	ACATCATTCACAATGGGGTGATA	ACCCCAAACCTTCAAGAGACC	[289]
	<i>ERCC1</i>	NM_202001.2	5-6	89	GCCGACTGCACATTGATCC	TCCGCTGGTTTCTGCTCATA	[289, 486]
	<i>ERCC2 (XPD)</i>	NM_000400.3	2-3	82	TACCCCGAGCAGTTCTCCTA	TCCGCTGGTTTCTGCTCATA	[289, 486]
	<i>ERCC4 (XPF)</i>	NM_005236.2	5-6	77	CTTCTGGAATCTCTGAGAGCAA	GAGGTGCTGGAGTCAAGAAA	[289, 486]
	<i>GTF2H2</i>	NM_001515.3	13-14	81	CACAGTGTCGGGCAAAGTAC	CCAAGTGGGGAGCAGACA	[289]
	<i>LIG1</i>	NM_000234.1	19-20	81	TGGGAAGTACCCGGACATCA	GCTTCGGTGTCCAGGATGAA	[265]
	<i>RPA1</i>	NM_002945.3	16-17	80	AGTCAGGGTCAAAGTGGAGAC	TGTAGTCCACGGGCTTCAC	[769]
Base excision repair	<i>XRCC1</i>	NM_006297.2	14-15	83	GAGAACACGGACAGTGAGGAA	AAGTGCTTGCCCTGGAAGAA	[289, 486, 770]
	<i>PARP1 (ADPRT)</i>	NM_001618.3	12-13	77	TTCTGGAGGACGACAAGGAA	GTTGCTACCGATCACCGTAC	[265, 278, 486, 771]
	<i>APEX1 (APE1)</i>	NM_080649.1	3-4	67	GGGCTTCGAGCCTGGATTA	ACAGTATATCTGGGGCTTCTTCC	[265, 486, 770]

Biological function	Gene	RefSeq ID used for primer design	Targeted exons	Amplicon length (bp)	Forward primer	Reverse primer	References
Base excision repair (cont.)	<i>MPG</i>	NM_001015054.1	2-3	124	GCCCAAAGGGCCACCTTA	CCTCGGAGTTCTGTGCCATTA	[265, 772]
	<i>OGG1</i>	NM_016829.2	2-3	113	CGTGGACTCCCACTTCCAA	CGATGTTGTTGTTGGAGGAACA	[486, 773]
Homologous recombination	<i>BRCA1</i>	NR_027676.1	11-12	74	AAGACTGCTCAGGGCTATCC	CAGGTTATGTTGCATGGTATCCC	Previous DASL study, [289]
	<i>BRCA2</i>	NM_000059.3	21-22	130	ATGCAGCAGACCCAGCTTA	TCCATGGCCTTCCTAATTTCCA	[486]
	<i>RAD50</i>	NM_005732.3	2-3	82	TCCCTCCTGGAACCAAAGGAA	AGACGAATCTGGGCTCTCACA	[264]
	<i>RAD51</i>	NM_002875.4	5-6	86	GGGAAGACCCAGATCTGTCA	ATGTACATGGCCTTTCTTCAC	Previous DASL study, [289, 482]
	<i>RAD52</i>	NM_134424.2	11-12	85	GGATCTTGGGACCTCCAAACTTA	TCTTCATGTCCTGGCTCTTCC	Previous DASL study [482]
	<i>RAD54B</i>	NM_012415.2	12-13	108	GTGGTGTAGGACTTAACCTCA	GACCATCTCTCCATACTCTAGAC	Previous DASL study
	<i>RAD54L</i>	NM_001142548.1	16-17	73	AAGAAGCGAGCCAAGGTTGTA	TGCTGCTCAGCATGAAGACA	Previous DASL study
	<i>MRE11A</i>	NM_005590.3	8-9	83	AACCTGGAAGCTCAGTGGTTA	CCTCCCTTTAATACGCAGCAAA	[774]
	<i>NBN (NBS1)</i>	NM_002485.4	8-9	78	GTGATCCTCAGGGCCATCC	CAACTGACACGCCTTGTGAAA	[769]
Non-homologous end joining	<i>XRCC5 (Ku80)</i>	NM_021141.3	3-4	75	GCTGGAGGACATTGAAAGCA	ATGCTCACGATTAGTGCATCC	[289, 486]
	<i>XRCC6 (Ku70)</i>	NM_001469.3	11-12	80	GATTTGATGGAGCCGGAACAA	ACCAAGGAGCCCAGTCTTTTA	[289, 486]
	<i>PRKDC</i>	NM_006904.6	23-24	83	GCTTGGATCTCTAGGAGGACAA	AGGCCACATAGCTCTTCATCA	[486, 769, 775, 776]
Mismatch excision repair	<i>MLH1</i>	NM_000249.3	12-13	68	AGAGGACCTACTTCCAGCAA	TCTTCCACCATTTCCACATCA	[289, 486, 777]
	<i>MSH2</i>	NM_000251.1	15-16	77	CCAGCAGCAAAGAAGTGCTA	TCTTCCACCATTTCCACATCA	[289, 486, 777]
	<i>MSH6</i>	NM_000179.2	1-2	97	CCAAGGCGAAGAACCTCAAC	TTGGCCCAAACCAATCTCC	[264, 289, 486, 777]

Biological function	Gene	RefSeq ID used for primer design	Targeted exons	Amplicon length (bp)	Forward primer	Reverse primer	References
	<i>PMS2</i>	NM_000535.5	6-7	81	GCTCTGTGTTTGGGCAGAA	ACTCTTCACACACGGAGTCA	[265, 777]
Genes defective in diseases with sensitivity to DNA damaging agents	<i>ATM</i>	NM_000051.3	43-44	83	TACCAAGCAGCATGGAGGAA	GATTCATGGTAACTGGTTCCTTC TAC	[289, 486]
	<i>BLM</i>	NM_000057.2	6-7	91	TGTGGGAACGAACTGCTTCA	AGCCAAGAAGACTGGCATCA	[264, 769]
DNA polymerases	<i>POLB</i>	NM_002690.1	9-10	63	CTACAGTCTGTGGCAGTTTCA	TCAGGAGAACATCCATGTCAC	[265, 772]
	<i>POLH</i>	NM_006502.2	7-8	73	GTTCACTGAATCCCAGCTCCA	CCCTCGGCACATGGCATATA	[177]
	<i>PCNA</i>	NM_182649.1	1-2	94	TCTGAGGGCTTCGACACCTA	CATTGCCGGCGCATTTTAGTA	[769]
Direct reversal of DNA damage	<i>MGMT</i>	NM_002412.3	3-4	100	CGAGGCTATCGAAGAGTTCCC	CACAACCTTCAGCAGCTTCC	[289, 486]
DNA helicases	<i>RECQL</i>	NM_032941.2	5-6	82	TATGCCTACAGGAGGTGGAA	TGGGCAAATGACGAGTGTA	[769]
Endonucleases	<i>MUS81</i>	NM_025128.4	4-5	76	AGTGATACTGCTGGTGCTCTAC	CAGCAGCTCCTCCTTGGTTA	[482, 497]
Induction of transient DNA breaks	<i>TOP1</i>	NM_003286.2	17-18	87	ACGCTACAGCAGCAGCTAA	AGCTCGATTGGCACGGTTA	[289]
	<i>TOP2A</i>	NM_001067.3	21-22	81	GGCGTTTGATGGATGGAGAA	GAGCCAGTTCTTCAATAGTACCC	Previous DASL study, [289]
	<i>TOP2B</i>	NM_001068.2	20-21	79	GATGCTGCAAGCCCTCGTTA	GGTTGTCATCCACAGCAGGAA	[289]
Conserved DNA damage response genes	<i>CHEK1</i>	NM_001274.4	8-9	76	TGGTACAACAAACCCCTCAA	CACTGGGAGACTCTGACAC	[778]
	<i>CHEK2 (CHK2)</i>	NM_007194.3	5-6	102	TGACTGTAGATGATCAGTCAGTT TA	AAGCCAGCTTTACCTCTCC	[778]
	<i>ATR</i>	NM_001184.3	46-47	80	CATTCCAAAGCGCCACTGAA	CGCTGCTCAATGTCAAGAACA	[486, 779]
Histone	<i>H2AFX</i>	NM_002105.2	1	83	TGCGGAAGGGCCACTAC	CTCAGCGGTGAGGTACTCC	[177, 769]

8.6.2.2.2 Standard curve analysis

Following amplification, one of the FFPE melanoma metastases samples was serially diluted to allow assessment of standard curves, and therefore amplification efficiency, for each assay. Two standard curves were produced using six standards generated by a 1:2 and 1:10 serial dilution of the sample. The curve based on 1:10 dilution allowed assessment of PCR efficiency over a large range, however as many of these samples were very dilute, the 1:2 standards would allow some assessment of efficiency if 1:10 samples failed to amplify.

8.6.2.2.3 qRT-PCR reaction

Sample and assay pre-mix solutions were prepared using the standard Fluidigm qRT-PCR protocol as described in Chapter 2. Each sample was assessed in triplicate and a no template control (water used instead of STA sample) was included. Each assay was assessed in duplicate. The 96:96 Dynamic Array IFC was loaded and the qRT-PCR reaction and melt curve analysis was performed as described in the standard protocol with initial data processing described in Chapter 2. Ct values were exported to Stata version 10 (StataCorp 2007) for further analysis.

8.6.2.2.4 Analysis of qRT-PCR data

The Fluidigm Real-time PCR Analysis software generated standard curves for diluted samples based on the mean Ct values across replicate samples and calculated assay efficiencies using the formula: $\text{efficiency} = 10^{(-1/\text{slope})} - 1$ [456]. Melt curves were assessed for each assay to identify evidence of primer-dimer formation or production of non-specific PCR products. Reproducibility was assessed between sample replicates by calculation of the intraclass correlation coefficients (ICC) described further in Chapter 4.

8.6.2.3 Results

8.6.2.3.1 Amplification efficiencies of DELTAgene assays

No template control samples were assessed and no amplification was seen for any assay. A number of wells in the IFC had not loaded properly as indicated by absent ROX passive reference dye in the wells and were excluded from further analysis. Many of the 1:2 dilution standards had not loaded well meaning there were less data points for analysis, however the 1:10 diluted samples were more successful, with the first four

most concentrated standard samples performing well and allowing generation of a standard curve and calculation of amplification efficiency. *GAPDH* failed to amplify for the majority of standard samples, probably because it was not included in the STA primer mix, therefore a standard curve could not be generated for assessment of assay efficiency.

Amplification efficiencies for the four control genes assessed (*CASC3*, *PES1*, *IPO8* and *SDHA*) ranged from 0.88-1.12. For use of a comparative Ct method for relative quantification of gene expression, the efficiencies of the test genes needs to be comparable to that of the control genes. Assuming that +/-10% of the efficiency of control genes is acceptable, three test assays had efficiencies greater than those of the control genes (*MLH1*, *OGG1* and *RECQL*), of these only *RECQL* was much greater. Therefore expression of the majority of genes can be assessed using the comparative Ct method using the endogenous control genes assessed in this panel.

Melt curve analysis demonstrated that the majority of assays generated a specific PCR product. In some melt curves there was evidence of primer/dimer formation (*ERCC1*, *MPG* and *MSH6*) and the curve for *XRCC6* showed multiple products. We were unable to redesign primers before starting the larger experiment, however being aware of these factors will allow a more correct interpretation of results.

Reproducibility across sample replicates was assessed using ICCs. ICC values were variable across the assays, however there appeared to be a clear inverse relationship between ICC value and the mean Ct value for the assay across the samples assessed (Figure 8-2). Following discussion with technical support at Fluidigm, it was decided to increase the number of pre-amplification cycles to 22 to reduce the mean Ct value for each probe and improve reproducibility between replicate samples. We also planned to remove samples with Ct values over 28 from further analysis as there was a lack of reproducibility between replicate samples, and therefore questionable data accuracy, at these Ct values. This approach was used in a second pilot plate where the calibrator sample, a cell line sample and four metastases samples were re-assessed for a limited panel of assays following 22 cycles of pre-amplification. Table 8-5 summarises the results of this experiment for the FFPE samples, which confirmed that increasing the number of pre-amplification cycles, reduced the mean Ct value for the assays and improved reproducibility across replicate samples.

Following this pilot work, I concluded that the system and assays were working well, so the larger sample set from the Chemotherapy study was assessed using the Fluidigm system.

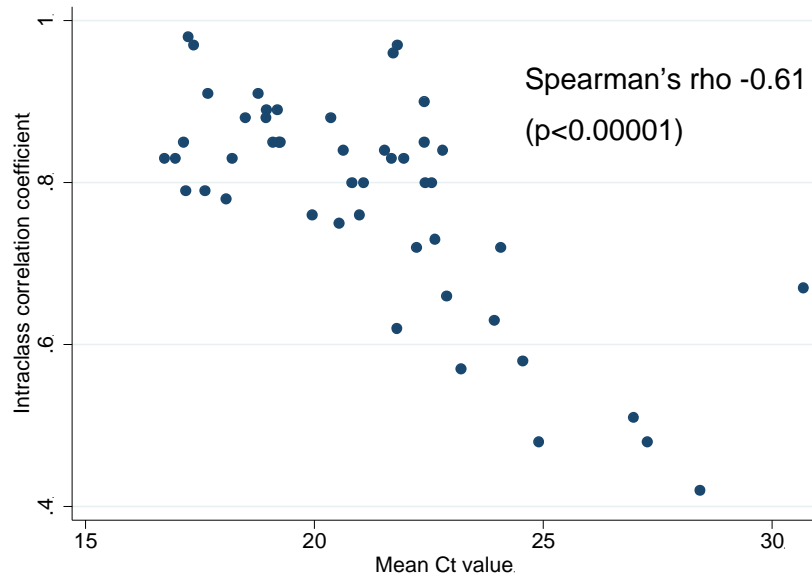


Figure 8-2: Scatter plot demonstrating the association between sample reproducibility and mean cycle threshold (Ct) value for the assay.

Reproducibility across replicate samples is reduced as the mean Ct value for the assay increases.

Probe	Mean Ct value 18 cycles	Mean Ct value 22 cycles	ICC 18 cycles	ICC 22 cycles
<i>APEX1</i>	13.53	8.86	0.92	1
<i>BRCA1</i>	17.01	13.24	0.99	1
<i>ERCC1</i>	15.48	10.77	0.73	1
<i>MGMT</i>	19.77	13.48	0.45	1
<i>MUS81</i>	18.61	13.09	0.85	1
<i>PARP1</i>	17.79	9.59	0.48	1
<i>POLB</i>	14.74	9.54	0.98	1
<i>RAD51</i>	19.15	14.50	0.71	1
<i>TOP2B</i>	13.42	8.99	0.86	1

Table 8-5: Intraclass correlation coefficients with eighteen and twenty-two pre-amplification cycles.

Mean Ct values and ICCs are listed for genes following 18 and 22 cycles of pre-amplification for a limited panel of genes. ICC values are greater with 22 cycles of pre-amplification indicating improved reproducibility between replicate samples. Abbreviations used: Ct, cycle threshold; ICC, intraclass correlation coefficients.

8.7 Assessment of DNA repair gene expression in tumours from patients recruited to the Chemotherapy study

8.7.1 Further methodological details

8.7.1.1 Samples

From the 450 patients eligible for the Chemotherapy study, samples from 222 patients were sent to us from European groups and other tissue samples were traced, focusing on patients who had responded to chemotherapy and completing sets of matched samples where more than one tumour sample was available. DNA repair gene expression from 416 tumour samples were assessed in this analysis.

8.7.1.2 Fluidigm qRT-PCR

Tissue cores were sent to us from European groups or tumour blocks were sampled using a tissue microarray needle and RNA extracted using the Qiagen AllPrep® RNA/DNA FFPE kit by a service provider, Gen-probe Life Sciences Ltd. (Wythenshawe, UK) using methods described in Chapter 2. Gen-probe normalised the RNA samples prior to cDNA synthesis. All RNA samples were used irrespective of RNA concentration measured using spectrophotometry. Tissue cores from Europe were much larger than the 0.6mm diameter tissue microarray cores sampled from tumours in Leeds. Therefore the RNA yield was much greater from European samples and 1 microgram of RNA was used in each cDNA reaction. For tissue cores sampled in Leeds with lower RNA yields, 200ng of RNA was used to make cDNA. If RNA yields were less than 100ng/µl for European samples, or less than 20ng/µl for Leeds tumour cores, 10µl of RNA was used to make cDNA. The rationale behind this approach was to use as much template RNA as possible, whilst maintaining consistency across the sample set. For European samples with greater RNA yields, excessive dilution of RNA to match samples from Leeds was impractical and use of larger amounts of RNA from Leeds samples would have exhausted RNA stocks from these cores. Accurate normalisation of gene expression data will correct for differences in template RNA concentration, therefore this approach was deemed acceptable for this large-scale study. cDNA was synthesised using the Applied Biosystems High Capacity cDNA Reverse Transcription kit in 96-well plates and STA of samples was performed using the standard protocol. Each sample and assay was assessed in duplicate on a 96:96 Dynamic Array IFC using the standard protocol. Further details of methods used are described in Chapter 2. The intradermal naevus sample used in the pilot study was to be used as a calibrator sample on each Fluidigm array, however a number of assays

failed for this sample on the first Fluidigm array so a well performing melanoma sample was used as calibrator sample on subsequent arrays. For each STA plate, a new aliquot of cDNA from the calibrator sample was amplified along with the samples for assessment and then used on the Fluidigm arrays. A number of negative control samples were rotated across the Fluidigm arrays, these being:

- cDNA control samples generated without reverse transcriptase (RT) and so no cDNA should be present (RT negative cDNA controls).
- Water used in the STA reaction instead of cDNA (no template samples that had undergone STA).
- Water used instead of STA product in the qRT-PCR reaction (no template controls).

A total of nine Fluidigm arrays were used for this experiment. Data were assessed using the methods described in Chapter 2, with baseline and threshold levels being calculated by Biomark HD Reader software (Fluidigm, San Francisco, CA) for each array. Ct values were exported to Stata version 10 (StataCorp 2007, College Station, TX) for further analysis.

8.7.1.3 Data analysis

Reproducibility between sample replicates was assessed using ICCs and any samples with Ct values over 28 were excluded from further analysis. Mean Ct values from sample replicates were calculated and data normalised to the expression of *CASC3*, *PES1*, *SDHA* and *IPO8* according to the method described by Vandesompele [343] as described in Chapter 2. Data from each Fluidigm array were normalised separately using the calibrator sample run on the array. Samples failing eight or more assays were removed from further analysis. Normalised data from the nine arrays were then merged for further analysis.

8.7.1.4 Statistical analysis

Reproducibility of Ct values generated from the calibrator samples across the arrays were compared using Spearman's rank correlation. For the primary analysis, gene expression data from the first available tumour sample was used. Fold differences in gene expression were calculated between progressing tumours and tumours showing any response to chemotherapy (stable disease, partial or complete response). The Cuzick test for trend [780] was used to identify genes differentially expressed in tumours from patients in each of the four response groups using un-transformed gene

expression data. Genes identified as being differentially expressed were assessed further in linear regression using gene expression data which was log-transformed (\log_2).

Survival analysis was performed to identify gene expression patterns associated with survival after starting chemotherapy. Survival analysis was performed on 25th April 2012 and data was censored on this date. The Cox proportional hazards model was used to calculate hazard ratios and 95% confidence intervals for each gene using log-transformed data (\log_2). Despite transformation, the distribution of data was not normal, therefore analysis was repeated using expression levels split into eight groups and survival analysis was repeated using this categorical variable. Significance values were ranked to identify genes most associated with survival.

Analyses were performed unadjusted and adjusted for prognostic factors in stage IV disease according to the AJCC staging guidelines [58]. Patients were classified based on sites of disease and LDH level at start of chemotherapy into M1a (distant skin, subcutaneous or nodal metastases), M1b (lung metastases) or M1c (all other visceral metastases or any distant metastasis with elevated LDH level) groups. Regression and survival analyses were adjusted by this variable (sub-stage) to identify genes independently associated with chemotherapy response or survival after starting chemotherapy. Furthermore, survival analysis was adjusted for chemotherapy response for genes of interest in multivariate analyses.

For these analyses, gene expression from the first available tumour sample was used, in some cases this was a primary tumour in others a metastatic specimen. As gene expression profiles are likely to differ between primary and metastatic tumours, analyses were repeated for primary tumours and metastatic tumours separately. A minority of patients received combination chemotherapy with an additional agent being given alongside DTIC or TMZ. Analysis was repeated for patients receiving DTIC or TMZ monotherapy only to assess differences in gene expression profiles specific to monotherapy. In view of the multiple testing involved in this study, a stringent significance value of 0.001 was set for the described analyses.

8.7.2 Results

8.7.2.1 Performance of the Fluidigm system

8.7.2.1.1 Reproducibility of replicate samples

As described above, the calibrator sample was RNA extracted from a melanoma sample. cDNA was synthesised from this sample and an aliquot of cDNA was used in

the STA reaction with test samples that were assessed with the calibrator sample on each Fluidigm array. The calibrator sample was used on all nine Fluidigm arrays and the Ct values for the 48 genes correlated very well across the arrays (Spearman's rho 0.97-1.00, all significance values <0.00001) (Figure 8-3).

These results show that reproducibility was excellent across the arrays even when samples were amplified separately.

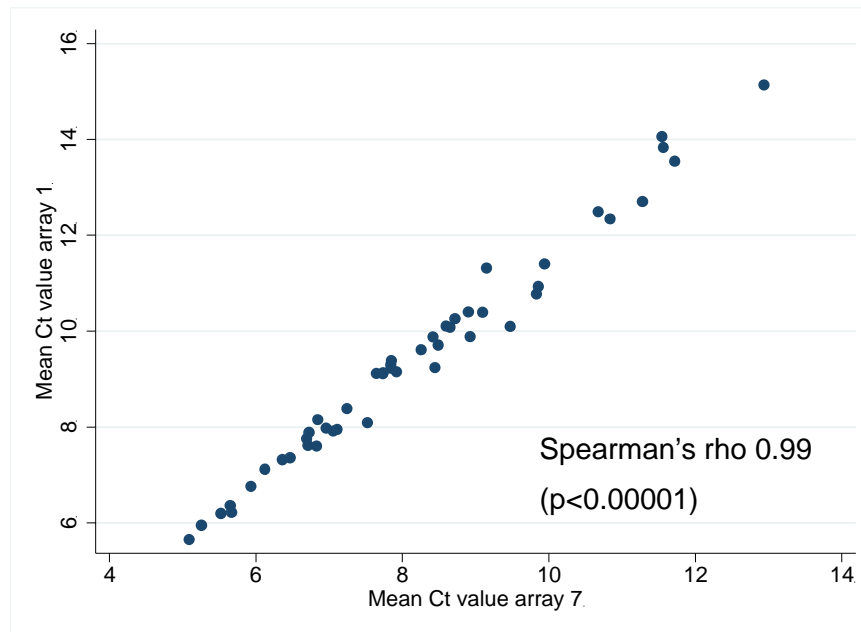


Figure 8-3: Scatter plot showing correlation between two replicate samples assessed on two separate Fluidigm qRT-PCR arrays.

Mean cycle threshold values from replicate samples are plotted for expression of each gene for the calibrator sample. Abbreviation used: Ct, cycle threshold.

8.7.2.1.2 Control samples

All the control samples where water was used instead of STA product in the qRT-PCR reaction failed to amplify for any assays as expected. However, some RT negative controls used in the STA reaction and no template samples that had undergone STA amplified for some of the genes assessed. These control samples were assessed across a number of arrays, and amplification was seen in a different spectrum of genes on each array with no amplification seen for many genes assessed. Across the arrays, the only two genes where amplification was repeatedly seen were for *GAPDH* and *TOP1*. For all genes, the Ct values generated for the control samples were much higher than those for the test samples: no template control mean Ct values were 12.9

cycles higher (range 2.7-22.1) and RT negative control mean Ct values were 5.3 cycles higher than test samples (range 2.8-12.9). Review of the melt curves from these control samples showed a product melting at a lower temperature than the test samples indicating the formation of primer-dimers. For test samples, no primer-dimer peaks were noted. The formation of primer-dimers only appeared to occur when control samples had been through the STA process and did not appear consistently for the majority of genes across the arrays, the exceptions being *GAPDH* and *TOP1*. This phenomenon may be reducing the accuracy of the qRT-PCR data and needs to be acknowledged. *GAPDH* was not used in further analysis, however *TOP1* is a gene of interest and therefore, results from this assay should be interpreted with caution.

8.7.2.2 Gene expression analysis

8.7.2.2.1 Samples

From the 416 tumour samples assessed using the Fluidigm system, 41 samples were not used in the analysis as they failed eight or more of the gene expression assays assessed. Therefore, 375 (90%) tumour samples yielded gene expression data. Three samples were removed from further analysis as they either represented a replicate sample or were samples from a metastasis removed on the same day as another metastasis. A further seven patients did not have stage IV disease when they received chemotherapy and two patients proved not to have received DTIC or TMZ. Thus gene expression data from a total of 363 tumours was analysed (summarised in Table 8-6).

Sample type	
Single sample per patient, number (% per total no. patients)	204 (76)
Patients with multiple samples, number (% per total no. patients):	66 (24)
2 samples, number (% of multiple samples)	50 (76)
3 samples, number (% of multiple samples)	10 (15)
4 samples, number (% of multiple samples)	4 (6)
5 samples, number (% of multiple samples)	1 (1.5)
8 samples, number (% of multiple samples)	1 (1.5)
Total number patients	270
Total number of samples	363

Table 8-6: Summary of samples from the Chemotherapy study assessed using qRT-PCR of DNA repair genes.

The number of patients from whom tumour samples were assessed is presented along with the number of samples. Multiple samples were from single patients as indicated in the table.

For the identification of genes associated with chemotherapy response and survival following start of chemotherapy, the first sample available from each patient was analysed so that some were primary tumours and others metastases (Table 8-7). A total of 270 patients were involved in this analysis.

Tumour or patient characteristic	Number or median (% or range)
Type of tumour used for primary analysis:	
Primary	89 (33.0)
Metastasis	181 (67.0)
Treatment received:	
Dacarbazine	133 (49.3)
Dacarbazine with other chemotherapy	61 (22.6)
Temozolomide	76 (28.1)
Response to chemotherapy:	
Progressive disease	143 (53.0)
Stable disease	46 (17.0)
Partial response	25 (9.3)
Complete response	11 (4.1)
No data available	45 (16.7)
AJCC staging IV subgroup:	
M1a	11 (4.1)
M1b	22 (8.2)
M1c	222 (82.2)
Missing data	15 (5.6)
Survival status:	
Alive	48 (17.8)
Died	222 (82.2)
Survival from start of chemotherapy, years	0.6 (0.003-7.1)

Table 8-7: Summary tumour and patient characteristics for samples used in the primary analysis for the Chemotherapy study.

See text for further description of AJCC subgroups for stage IV disease.

Abbreviation used: AJCC, American Joint Committee on Cancer.

8.7.2.2.2 Summary characteristics of patients and tumours assessed

Table 8-7 summarises the characteristics of the samples and patients in the primary analysis for this study. The majority of samples used for the primary analysis were metastatic samples (67%). The largest proportion of patients received DTIC alone (49%), however 23% of patients treated in Europe received DTIC in combination with other chemotherapies, these being the platinum containing agents, cisplatin or carboplatin. Response data were available for 83% of patients, with the majority

progressing despite chemotherapy treatment (53%). Response data were missing for 17% of patients, usually because the patients deteriorated clinically or died before an assessment of response was made. The majority of patients had stage M1c disease (82%) and 82% of patients had died at the time of analysis.

Gene expression profiles are likely to be different in primary and metastatic tumour specimens from the same patient (see Chapter 5)[510]. Therefore, assessment of gene expression in a mixture of primary and metastatic specimens reduces the power of the study to identify expression patterns specific to either primary or metastatic tumours alone. Based on the power calculations and assumptions described in section 8.5.4, for the 270 patients currently involved in this study, we have 93-100% power at a 0.001 significance level to detect a difference in gene expression level across a range of DNA repair genes. Calculations have been repeated assessing primary and metastatic tumours separately; for 89 primary samples there is only 28-80% power and for 181 metastatic specimens, this increases to 72-100%. As recruitment to this study continues, numbers of primary and metastatic samples available for analysis will increase, so increasing the power of these subgroup analyses.

8.7.2.2.3 Genes associated with response to chemotherapy

Table 8-8 presents the 10 genes most associated with response to chemotherapy in the whole dataset, primary tumours, metastatic tumours and patients treated with DTIC or TMZ monotherapy only. Of the 43 DNA repair genes assessed, the gene with expression most significantly associated with failure to respond in the whole dataset, metastatic samples and patients treated with DTIC/TMZ monotherapy only was *MGMT* (Cuzick test for trend in the whole dataset $z=-4.2$, $p=0.00003$). Figure 8-4 shows gene expression levels for *MGMT* across the response groups. Expression was greatest in tumours from patients who did not respond to therapy compared to those with stable disease, partial or complete responses. *MGMT* expression remained significantly associated with response to chemotherapy when analysis was adjusted for sub-stage at start of chemotherapy treatment in linear regression analysis (regression coefficient -0.75 (95% CI -1.08 - -0.42), $p=0.00001$).

When primary tumours were analysed alone, *MGMT* was less associated with response (Cuzick test for trend $z=-2.5$, $p=0.01$) with a smaller fold change between tumours from patients with progressive disease compared with patients who responded (fold change 1.16, compared to 1.46 for the whole dataset and 1.66 for metastases only). In this group, expression of *MLH1* was most associated with chemotherapy

All samples (n=225)			Primaries only (n=73)			Metastases only (n=152)			Monotherapy only (n=165)		
Gene	Fold difference	P-value	Gene	Fold difference	P-value	Gene	Fold difference	P-value	Gene	Fold difference	P-value
<i>MGMT</i>	1.46	0.00003	<i>MLH1</i>	1.25	0.002	<i>MGMT</i>	1.66	0.0008	<i>MGMT</i>	1.44	0.0003
<i>XPA</i>	1.32	0.02	<i>ERCC4</i>	1.36	0.003	<i>PCNA</i>	1.72	0.02	<i>XPA</i>	1.36	0.002
<i>PCNA</i>	1.39	0.07	<i>MGMT</i>	1.16	0.01	<i>BLM</i>	1.45	0.04	<i>ERCC4</i>	1.19	0.009
<i>XRCC5</i>	1.06	0.07	<i>LIG1</i>	0.82	0.02	<i>PARP1</i>	1.18	0.12	<i>MSH6</i>	0.78	0.05
<i>PRKDC</i>	1.02	0.08	<i>TOP1</i>	0.81	0.02	<i>PRKDC</i>	0.97	0.16	<i>MLH1</i>	1.19	0.05
<i>LIG1</i>	0.92	0.09	<i>XPA</i>	1.46	0.02	<i>NBN</i>	1.31	0.21	<i>POLB</i>	0.97	0.06
<i>PARP1</i>	1.13	0.14	<i>POLB</i>	0.81	0.06	<i>MUS81</i>	0.86	0.23	<i>PRKDC</i>	1.01	0.07
<i>NBN</i>	1.20	0.16	<i>BLM</i>	0.90	0.09	<i>XRCC5</i>	1.10	0.24	<i>CHEK1</i>	1.42	0.10
<i>POLB</i>	0.93	0.16	<i>RPA1</i>	1.21	0.09	<i>TOP2A</i>	1.45	0.25	<i>APEX1</i>	1.11	0.11
<i>CHEK1</i>	1.36	0.23	<i>TOP2B</i>	1.10	0.10	<i>XPA</i>	1.26	0.26	<i>XRCC5</i>	1.07	0.11

Table 8-8: Top 10 genes associated with chemotherapy response in the whole dataset and then primary tumours, metastases and patients treated with dacarbazine or temozolomide monotherapy only.

Significance values are from the Cuzick test for trend across four response groups (progressive disease, stable disease, partial and complete response). Fold differences are for gene expression in tumours from patients with progressive disease compared with those in which any response was reported. Abbreviations used: n, number.

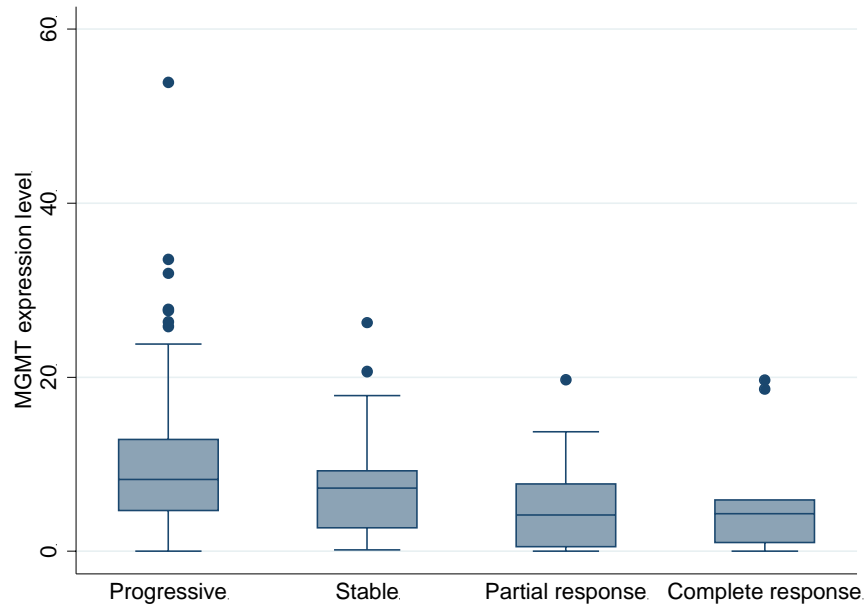


Figure 8-4: Box-plots showing *MGMT* gene expression in tumours responding differently to chemotherapy.

response (Cuzick test for trend $z=-3.1$, $p=0.002$) followed by *ERCC4* (Cuzick test for trend $z=-3.0$, $p=0.003$). The pilot study showed that the amplification efficiency of the *MLH1* assay was not comparable with the endogenous control genes assessed on the array, therefore it must be acknowledged that the accuracy of the results for this assay are questionable. There was no association between expression of *MLH1* and *ERCC4* with response in metastases (*MLH1* $p=0.68$, *ERCC4* $p=0.77$). In metastatic tumours, *PCNA* was differentially expressed in tumours from non-responders (Cuzick test for trend $z=-2.4$, $p=0.02$), but not in primary tumours ($p=0.85$). These findings suggest that patterns of gene expression associated with treatment response are different in primary and metastatic samples. This is not surprising but suggests that the value of predictive biomarkers will be stage specific.

Overall, the majority of the DNA repair genes assessed were over-expressed in tumours from patients who progressed compared to those who responded (Table 8-8). There are exceptions to this, for example *LIG1* was under-expressed in primary tumours from patients who progressed with chemotherapy treatment.

8.7.2.2.4 Genes with expression associated with survival after starting chemotherapy

Figure 8-5 presents a Kaplan-Meier plot for survival after starting chemotherapy for patients in the study, showing the association between response to chemotherapy and

survival time. As expected, patients with a complete response to chemotherapy survived longer (median survival time 2.2 years (range 0.6-4.0)) than those with a partial response (1.1 years (range 0.3-5.4)), stable disease (0.8 years (range 0.2-3.2)) or progressive disease (0.5 years (range 0.003-5.4)) (log-rank test $\chi^2(3)$ 31.7, $p < 0.00001$).

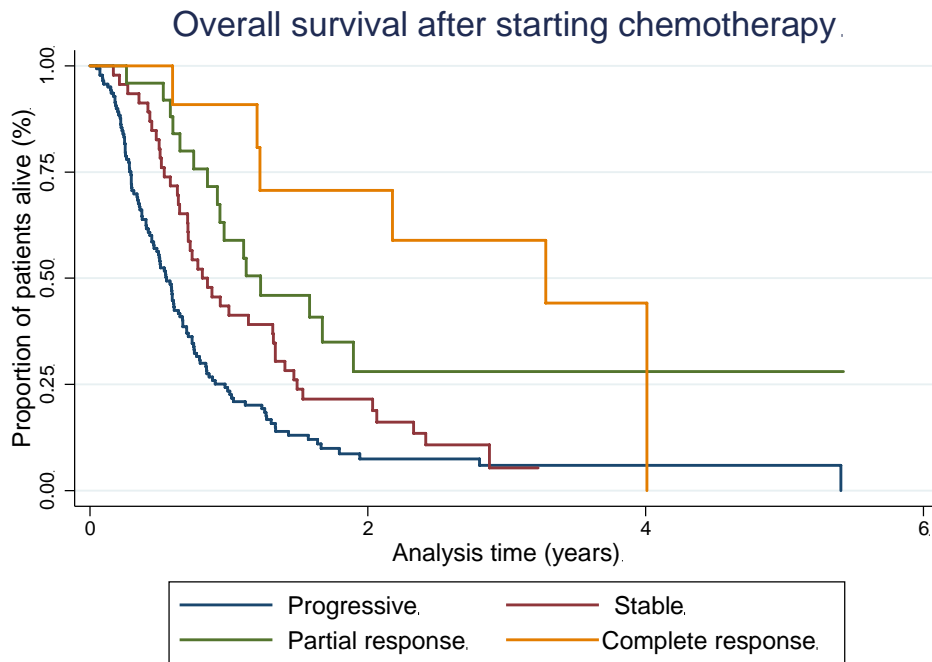


Figure 8-5: Overall survival following start of chemotherapy according to response to chemotherapy treatment.

Table 8-9 lists the genes with expression most associated with survival in analysis adjusted for the sub-stage of disease at start of chemotherapy treatment, being the strongest prognostic factor in stage IV disease. Results of survival analysis were compared using \log_2 transformed gene expression and data split into a categorical variable. The gene lists were similar and the results presented are from the analysis of \log_2 transformed gene expression data.

In view of the association between *MGMT* expression and chemotherapy response and survival, the gene was assessed in further detail. Multivariate survival analysis was performed further adjusting for the effect of chemotherapy response as this factor significantly influences survival as shown in Figure 8-5. Results of these analyses are presented in Table 8-10.

In the larger dataset, increased expression of *ATM* (hazard ratio (HR) for doubling of gene expression 1.30 (95% CI 1.10-1.52), $p=0.002$), *MGMT* (Table 8-10), *PRKDC* (HR 1.34 (95% CI 1.08-1.65), $p=0.007$) and *PARP1* (HR 1.33 (95% CI 1.08-1.64), $p=0.008$) were most associated with reduced overall survival time after starting chemotherapy. However, these genes were not significantly associated with survival ($p<0.001$) when correction is made for multiple testing. In multivariate analysis, *MGMT* expression remained associated with shorter survival when analysis was adjusted for prognostic factors relevant in stage IV disease (stage subset) and when adjusted further, for the influence of chemotherapy response (Table 8-10).

Again, there appeared to be a difference in the pattern of gene expression associated with survival in primary tumours compared to metastatic specimens, with *MGMT* over-expression associated with larger hazard ratios (HRs) in primary samples compared to metastatic specimens. Expression in primary tumours is more significantly associated with survival when adjusted for stage and response to chemotherapy (Table 8-10).

MSH2 and *PARP1* over-expression were associated with reduced survival in metastatic specimens (*MSH2* HR 1.44 (95% CI 1.18-1.77), $p=0.0004$; *PARP1* HR 1.37 (95% CI 1.08-1.75), $p=0.01$). However, there were no associations found between these genes and survival in primary tumours (*MSH2* HR 0.66 (95% CI 0.43-1.03), $p=0.07$; *PARP1* HR 1.16 (95% CI 0.77-1.76), $p=0.48$).

Over-expression of *ATM* appeared to influence survival in both primary (HR 1.40 (95% CI 1.02-1.91), $p=0.04$) and metastatic tumours (HR 1.25 (95% CI 1.03-1.51), $p=0.02$).

Analysis of patients receiving DTIC or TMZ monotherapy showed associations between expression of *PRKDC* (HR 1.35 (95% CI 1.09-1.67), $p=0.007$) and survival, with *MGMT* (Table 8-10) and *ATM* (HR 1.15 (95% CI 0.95-1.39), $p=0.15$) not associated with survival in this sample set.

The majority of DNA repair genes were over-expressed in tumours from patients who had died compared to those who remain alive. Exceptions to this are *POLH* and *POLB* which were under-expressed in tumours from patients who had died and greater expression of these genes was associated with longer overall survival time (all data *POLB* HR 0.81 (95% CI 0.69-0.96), $p=0.01$; primaries only *POLB* HR 0.67 (95% CI 0.48-0.95), $p=0.02$, *POLH* HR 0.72 (95% CI 0.54-0.95), $p=0.02$).

All samples (n=270)			Primaries only (n=89)			Metastases only (n=181)			Monotherapy only (n=209)		
Gene	Fold difference	P-value	Gene	Fold difference	P-value	Gene	Fold difference	P-value	Gene	Fold difference	P-value
<i>ATM</i>	1.40	0.002	<i>MGMT</i>	2.31	0.01	<i>MSH2</i>	1.34	0.0004	<i>PRKDC</i>	1.24	0.007
<i>MGMT</i>	1.51	0.006	<i>POLH</i>	0.79	0.02	<i>PARP1</i>	1.36	0.01	<i>ATR</i>	1.08	0.04
<i>PRKDC</i>	1.06	0.007	<i>POLB</i>	0.83	0.02	<i>PRKDC</i>	1.16	0.01	<i>PARP1</i>	1.24	0.05
<i>PARP1</i>	1.30	0.008	<i>ATM</i>	1.50	0.04	<i>RAD54L</i>	0.96	0.02	<i>PMS2</i>	1.01	0.07
<i>POLB</i>	0.81	0.01	<i>OGG1</i>	0.86	0.06	<i>ATM</i>	1.33	0.02	<i>TOP1</i>	0.83	0.08
<i>MSH2</i>	1.19	0.02	<i>ERCC4</i>	1.14	0.06	<i>ATR</i>	1.36	0.02	<i>BRCA2</i>	0.84	0.09
<i>RAD54L</i>	0.89	0.04	<i>MSH2</i>	0.94	0.07	<i>ERCC2</i>	0.97	0.06	<i>MGMT</i>	1.35	0.09
<i>ATR</i>	1.11	0.04	<i>TOP1</i>	0.74	0.09	<i>CHEK2</i>	1.55	0.07	<i>ERCC4</i>	1.13	0.09
<i>MLH1</i>	1.06	0.05	<i>ERCC1</i>	1.02	0.17	<i>POLB</i>	0.79	0.09	<i>MSH2</i>	1.17	0.10
<i>ERCC2</i>	0.89	0.08	<i>XRCC6</i>	1.37	0.19	<i>TOP2A</i>	1.19	0.09	<i>RAD54L</i>	1.30	0.12

Table 8-9: Top 10 genes associated with survival after starting chemotherapy in the whole dataset and then primary tumours, metastases and patients treated with dacarbazine or temozolomide monotherapy only.

Significance values were from a Cox proportional hazards model adjusting for sub-stage at start of therapy. Fold differences in expression are for tumours from patients who had died/alive patients. Abbreviations used: n, number.

	Unadjusted analysis		Adjusted for sub-stage at start of chemotherapy		Further adjusted for response to chemotherapy	
	Hazard ratio (95% CI)	Significance value	Hazard ratio (95% CI)	Significance value	Hazard ratio (95% CI)	Significance value
Whole dataset	1.10 (1.03-1.18)	0.007	1.12 (1.03-1.21)	0.006	1.10 (1.01-1.20)	0.03
Primaries only	1.13 (0.98-1.31)	0.08	1.24 (1.05-1.46)	0.01	1.27 (1.05-1.53)	0.01
Metastases only	1.09 (1.01-1.18)	0.03	1.07 (0.98-1.17)	0.11	1.06 (0.96-1.16)	0.25
Monotherapy only	1.05 (0.97-1.14)	0.24	1.08 (0.99-1.19)	0.09	1.05 (0.94-1.17)	0.42

Table 8-10: Results of multivariate survival analysis assessing the relationship between *MGMT* gene expression and survival after starting chemotherapy in the whole dataset and then primary tumours, metastases and tumours from patients who received DTIC/TMZ monotherapy only.

Hazard ratios and 95% confidence intervals are from the proportional hazards model and represent risk of death for doubling of *MGMT* gene expression. Analysis is presented without adjustment, adjusted for sub-stage at start of chemotherapy and further adjusted for response to chemotherapy. Significant results are highlighted in bold. Abbreviations used: CI, confidence interval.

8.8 Discussion

8.8.1 Gene expression profiling in FFPE primary melanoma tumours

This chapter has described use of a number of gene expression profiling platforms, namely the DASL assay, a customized Taqman Array microfluidic qRT-PCR card (the Chemo-sensitivity Gene Expression Array, CGEA-1) and the Fluidigm qRT-PCR system. The DASL assay is discussed in detail in Chapter 3, I will concentrate on the other gene expression profiling systems for this discussion.

The analysis of samples using the CGEA-1 array was performed at the Translational Oncology Research Centre, Queen Alexandra Hospital in Portsmouth. Therefore, my assessment of sample performance was limited, however Table 8-2 lists the variable and limited number of useable results from the total of 31 samples sent for analysis, indicating that FFPE melanoma samples did not perform well with this assay. For the Fluidigm platform, stringent criteria (failing 8 or more assays) were used to exclude samples from further analysis. This system, using a pre-amplification step, yielded useable gene expression data from 90% of tumours. There was also excellent reproducibility between gene expression results from replicate samples on each array and across arrays. Therefore, the Fluidigm system performed well, however it is possible that the CGEA-1 array would also have performed better if pre-amplification of samples had been performed [348].

Despite the good performance of the Fluidigm assay, there was amplification of control samples in which no cDNA was present and RT negative cDNA control samples that had been pre-amplified. The spectrum of genes where amplification was seen differed across the arrays with Ct values in control samples being greater than test samples. Review of control sample melt curves indicated the formation of primer-dimers which melt at a lower temperature compared to the specific gene product. Pre-amplification increases copies of target cDNA using pooled primers for use in the qRT-PCR experiment. It has been shown that this process does not introduce bias and decreases Ct values, so improving data quality [316, 348]. To improve reproducibility between sample replicates for this work, the number of pre-amplification cycles was increased to 22. This, in combination with a lack of template cDNA in control samples has led to formation of primer-dimers. As EvaGreen binds non-specifically to double-stranded DNA [350], it will not distinguish primer-dimers from the specific PCR product. However, formation of

primer-dimers is dependent on the cDNA concentration, so when no template is present, as in control samples, primer-dimers are formed, but when template is present at higher concentration, the specific product predominates [781, 782]. This is supported by there being no primer-dimer peaks in test samples. Formation of primer-dimers will reduce the accuracy of the PCR reaction as fluorescence from these products will be detected by data collection software and there will be competition for reaction components between the two products [781, 783, 784]. Amplification was repeatedly seen for *GAPDH* and *TOP1*, and ideally these assays need to be redesigned to remove this problem. Use of Taqman® based assays with the additional gene specific probe would also reduce amplification detected in association with primer-dimers [349, 783, 784]. The accuracy of this experiment does not appear to be severely compromised by this issue as the reproducibility in the Ct values from the calibrator sample, which was amplified in separate pre-amplification reactions, was excellent when assessed across different arrays (Spearman's rho 0.97-1.00, all significance values <0.00001).

Overall, the Fluidigm platform has worked well in an experiment where gene expression for a limited number of genes has been assessed in a large number of samples. The main advantage of this system is the speed with which samples can be processed, a total of 416 RNA samples have been assessed in a total of 82,944 PCR reactions. Over 850 96-well plates and significant amounts of time would be needed to perform this study using qRT-PCR methods described in Chapter 4, therefore we plan to use this system for further gene expression studies within our group, but refining the technique to reduce apparent amplification of control wells.

8.8.2 DNA repair gene expression and response to chemotherapy

Results from chemotherapy response data suggest that identification of predictive gene expression profiles is possible using FFPE primary melanoma tumours. In the small sample set assessed using the DASL assay, over-expression of *RAD51* and *TOP2A* were associated with poor response to chemotherapy. Using the CGEA-1 array, there was increased expression of genes involved in removal of direct DNA damage (*MGMT*), base-excision repair, nucleotide excision repair and DNA non-homologous end joining [497] in tumours unresponsive to chemotherapy, suggesting that DNA repair genes involved in other pathways are also relevant. In contrast, genes encoding proteins involved in apoptosis, cellular proliferation and membrane drug pumps exhibited both increased and decreased expression in non-responding tumours. Gene expression studies assessing multiple genes in

melanoma tumours have previously been small, and not designed to identify predictive markers, therefore the Chemotherapy study was designed to address this hypothesis in a larger sample set and allow more detailed analyses of the relationship between DNA repair genes and response.

In the larger study, over-expression of *MGMT* was most significantly associated with progression following chemotherapy treatment and associated with shorter survival after start of chemotherapy. The association between *MGMT* expression appeared however to be more complex than has been previously reported and this dataset has allowed some assessment of the relationship between expression in primary and metastatic tumour specimens and treatment response. Expression of *MGMT* appeared to be more closely related to chemotherapy response in metastatic specimens compared to primary tumours. This would be expected as DTIC is used to target metastatic disease which is likely to have undergone profound genetic alterations compared to the primary tumour in the path to metastasis and expression patterns in primary tumours are less likely to directly influence chemotherapy response in metastatic disease. In survival analysis from start of chemotherapy, the association between *MGMT* expression and shorter survival in the larger dataset appears to be driven more by expression in primary tumours. However, greater expression in metastatic tumours is associated with shorter survival and HRs for survival in the larger dataset, primary and metastatic tumours remain similar in multivariate analysis adjusting for sub-stage and chemotherapy response.

This study has used sensitive qRT-PCR gene expression analysis. Activity of *MGMT* can be measured to determine the number of active molecules and this level correlates with protein and mRNA levels [785]. However, *MGMT* activity assays have been reported by others to be inaccurate due to contamination by *MGMT* positive leucocytes or endothelial cells and immunohistochemistry can be highly subjective [786, 787]. Use of qRT-PCR to assess gene expression is more accurate, however it has been shown that there is variation in *MGMT* expression within melanoma tumours due to heterogeneity, with some areas expressing high levels and others none [788]. Therefore, using a tissue microarray needle, as in this study, to sample a specific area of tumour may not accurately reflect the overall expression.

MGMT expression is determined by activity of transcription factors, but also the methylation status of the *MGMT* promoter, with methylation decreasing expression, and methylation within the gene, leading to greater expression [756, 785, 789]. The

positive association between *MGMT* expression and TMZ treatment response has been previously noted in melanoma cell lines and the authors of this study found that this relationship is stronger than a gene expression signature generated using microarray analysis [265]. A study of frozen metastatic tumour specimens from 75 patients showed that lower expression of *MGMT* was associated with better response to DTIC and longer survival [756]. The authors also noted a association between metastatic tumour *MGMT* expression and the Breslow thickness of the primary tumour [756]. Similar results have been found with regards to protein expression, with lower expression of *MGMT* in metastatic specimens correlating with response to DTIC [270].

As reviewed in the introduction, there have been many studies showing no association between *MGMT* activity [268, 269], protein expression [270], gene silencing by promoter methylation [271, 758] and *MGMT* polymorphisms [267] and response to TMZ or DTIC in melanoma. It has been suggested that this lack of association is due to silenced apoptotic pathways, so despite formation of O⁶-methylguanine, which lead to double-stranded breaks in DNA, apoptosis does not occur [785, 790, 791]. The current study confirms that there is a significant association between *MGMT* expression levels and chemotherapy response in melanoma tumours.

In the current analysis, examples of other genes associated with chemotherapy response in primary tumours were *MLH1* and *ERCC4*. *PCNA* and *XPA* were differentially expressed in association with chemotherapy response in metastatic specimens, the larger dataset and those who received monotherapy with DTIC or TMZ only. What is notable is that over-expression of all of these genes are associated with poorer response to chemotherapy and that these genes are involved in many DNA repair pathways and processes, namely mismatch repair (*MLH1*), nucleotide excision repair (*ERCC4* and *XPA*) and *PCNA* is a DNA polymerase related gene [482, 497, 499, 767, 768]. This suggests that resistance to DTIC or TMZ reflects a general over-expression of DNA repair genes, which would be consistent with the data from the CGEA-1 array and the hypothesis that over-expression of DNA repair genes related to maintaining genomic integrity also causes resistance to chemotherapy [177, 264]. The situation is similar for genes with expression associated with survival. Examples of genes other than *MGMT* in the larger dataset are *ATM*, a gene defective in ataxia telangiectasia where DNA is sensitive to DNA damaging agents, *PRKDC* which is involved in non-homologous end joining and *PARP1* which is active in base excision repair [482, 497, 499, 767, 768]. *ATM* is particularly interesting as single nucleotide polymorphisms in this

gene have been associated with susceptibility to melanoma in genome-wide association studies [792]. Again, over-expression is associated with shorter survival and many pathways are involved, suggesting a generalised response of DNA repair mechanisms associated with resistance.

The differences between the genes identified as involved in chemotherapy response and those associated with survival suggests that survival is modified by other factors, not associated with chemotherapy response. The survival analysis presented adjusts for prognostic factors in stage IV disease (stage subset), however there are clearly other factors which will modify survival in this very poor prognosis group, including chemotherapy toxicity, co-morbidities, but also the prognostic influence of gene expression. The survival analysis presented includes all patients treated with chemotherapy, however the response analysis did not include 17% of patients for whom response data was not available. For the majority of patients this was because they deteriorated clinically or died before a formal assessment of response could be made, therefore survival analysis is reflecting expression of genes associated with early deaths which will not be associated with chemotherapy response. Twenty-three percent of patients involved in this analysis received DTIC or TMZ along with another chemotherapy, these being platinum-containing chemotherapies. In response analysis, the two genes associated with response in the larger dataset and the smaller set of patients treated with DTIC or TMZ monotherapy only were *MGMT* and *XPA*. This suggests that results in the larger dataset reflect genes associated with DTIC or TMZ response. Different genes were associated with survival compared to response data in the monotherapy group, again reflecting the different patients and end-points used in these analyses as discussed above.

This study represents the most comprehensive assessment of DNA repair gene expression in association with chemotherapy response for melanoma, the preliminary results of which are described in this chapter. Currently, there are a number of limitations to this study. I have assessed genes associated with response and also those associated with survival after starting chemotherapy. The different results from these analyses reflect that survival is also assessing the role of DNA repair genes as prognostic biomarkers, for which there is large amounts of evidence as described in Chapter 4 [177, 264, 335, 505]. Further analysis is required to unravel the prognostic and predictive nature of DNA repair gene expression and this will be explored. Other limitations are the use of both primary and metastatic specimens and patients who have received other chemotherapies in addition to DTIC or TMZ to identify chemotherapy response genes. This reduces

the power of the study to identify genes associated with chemotherapy response in these subgroups. Recruitment to the study continues and analysis will be repeated when further samples are available. A further significant limitation is the quality of response data available for this study. A small proportion of patients recruited were involved in clinical trials and trial data will be accessed to obtain response data according to RECIST criteria and analysis repeated for this subset of patients. However, for other patients, response data have come from a number of sources, across the UK and Europe. Where possible, response from imaging has been recorded to RECIST standards, however there is likely to be much variability in reporting across centres. Central radiological review of imaging would ensure consistency and this will be explored. Finally, there are likely to be biological determinants of DNA repair gene expression that have not been explored in melanoma. It will be important to fully characterise the tumours used in this study, for example by assessing *BRAF* and *NRAS* mutation status, to allow further assessment of DNA repair genes associated with chemotherapy response in different biological subgroups. The ability to perform these subgroup analyses is dependent on number of tumour samples available, therefore recruitment continues.

The results presented in this chapter are preliminary, however this chapter demonstrates the potential of this study to identify determinants of chemotherapy response. The collection of matched primary and metastatic tumour samples will allow further assessment of how gene expression changes as a tumour progresses. Despite these study limitations, it is clear that *MGMT* expression is important in chemotherapy response and survival. Clinical trials aiming to deplete or inactivate *MGMT* have not shown positive results [271-273, 759], however further investigation into use of *MGMT* expression levels as a biomarker are warranted based on my data. In particular further investigation into the different effects in primary and metastatic tumours would be of interest.

In summary, in this large scale assessment of gene expression profiles in FFPE primary melanomas I have identified over-expression of DNA repair genes in a variety of pathways as being associated with poorer responses to chemotherapy. In particular, over-expression of *MGMT* is associated with poorer responses to DTIC and TMZ and shorter survival after starting chemotherapy treatment. Although new therapeutic agents are effective for the treatment of melanoma, it is very likely that a role for DTIC will remain and the identification of predictive biomarkers will remain of crucial importance.

9 Final discussion

Current prognostic markers in the form of the American Joint Committee on Cancer (AJCC) staging criteria [58] are inadequate for a subset of patients with malignant melanoma [121, 134]. The work summarised in this thesis was designed to identify new prognostic markers in nucleic acids extracted from formalin-fixed paraffin-embedded (FFPE) melanoma tissue. An important aim of the work was to show that stored samples from mature studies might be used in a similar way in other cancer studies in the future.

The presence of *BRAF* mutations is predictive of response to the newer targeted therapies, inhibitors of mutant BRAF (BRAFi) but these need to be improved to predict resistance. There is also a need for predictive biomarkers in melanoma for older treatments such as chemotherapy with dacarbazine (DTIC) and identification of biomarkers and genes involved in treatment responses to these drugs has also been assessed in this thesis. To identify biomarkers and gain insight into tumour biology, I have used novel technologies to assess genetic alterations in FFPE tissues. This thesis presents an overview of my experience with these assays and detailed methodological assessments.

9.1 Prognostic biomarkers

Previous studies using microarray technology to assess gene expression have been limited by the small number of samples assessed [161]. This thesis reports the successful use of the cDNA-mediated annealing, selection, extension and ligation (DASL) assay to identify prognostic markers in a large number of primary FFPE melanoma tumours. This assay was developed especially for use on degraded RNA from FFPE tumours. Chapter 3 describes the identification and validation of *SPP1* using this technology as a gene whose expression was shown to be independently associated with relapse-free survival. *SPP1* codes for osteopontin. In multivariate analysis adjusting for current prognostic factors, doubling of *SPP1* gene expression was associated with a 2.5 times increased risk of relapse. Identification of this candidate has been previously reported to be associated with melanoma prognosis using immunohistochemistry [163, 176, 793], which increased confidence that the DASL assay was generating biologically relevant results and these data have been published [187].

I combined the test and validation datasets used this in work to produce more power and this led to the identification of over-expression of DNA repair genes, specifically those involved in repairing double-stranded DNA breaks, as being associated with shorter relapse-free survival time (Chapter 4). Expression of *RAD52* and *TOP2A* were independently prognostic in multivariate analysis. These data were consistent with those produced previously by others using frozen samples [177, 178], providing further support to the assay. Following publication of this work [505], a large study of primary tumours using the whole-genome DASL assay was reported which confirmed the prognostic importance of DNA repair gene expression [335]. I also assessed DNA repair gene expression associated with poor histological features, namely tumour thickness and mitotic rate in this chapter. This was further expanded in Chapter 7, where differentially expressed genes were identified in ulcerated tumours and discussed in reference to the prognostic and predictive influence of this tumour feature. Factors shown to be associated with ulceration included down-regulation of genes associated with cell adhesion, hypothesised to allow melanoma cells to dissociate from keratinocyte mediated growth control. Deranged expression of fibroblast growth factors and receptors, presence of lymphatic invasion, greater microvessel density and macrophages were also associated with ulceration, all factors which may contribute to the prognostic influence of this tumour feature.

I hypothesised that greater insight into the biological processes which determine nodal metastases would be achieved by analysis of gene expression profiles in matched primary and nodal specimens from the same patient. I report a pilot study designed to assess the utility of the DASL assay to perform such an experiment using small FFPE sentinel node biopsy samples was described in Chapter 5. In this limited analysis, again deranged expression of fibroblast growth factors was identified in nodal specimens compared to primary tumours, a finding that requires confirmation in a larger sample set.

A final prognostic marker was identified in Chapter 6, as the presence of a V600K *BRAF* mutation was shown to be associated with shorter relapse-free survival compared with the V600E *BRAF* mutated tumours, *NRAS* mutated tumours and wild-type specimens. This association in primary tumours remained independently associated with relapse-free survival in multivariate analysis adjusted for current prognostic factors, increasing risk of relapse 2.6 times. The importance of this finding has been highlighted by a recent publication of similar results in a cohort of metastatic tumour specimens [593].

To summarise, this thesis describes identification of statistically independent prognostic tumour markers which add additional prognostic information to current staging criteria.

Validation of these findings is at different stages, but previous reports associating *SPP1* and DNA repair gene expression to prognosis suggest that these are true findings. Osteopontin protein expression has already been reported to be associated with survival [163], and similarly investigation of protein expression of DNA repair genes would be useful to support my gene expression findings. Validation of factors association with ulceration and the prognostic effect of V600K *BRAF* mutations in independent sample sets is required. This will be achieved by collaborations with other groups and increasing the number of samples screened for mutations with transcriptomic analysis from patients recruited to studies running in Leeds.

9.2 Predictive biomarkers

The topic of predictive markers has been addressed in Chapter 8, in which I described studies in which over-expression of DNA repair genes, most significantly *MGMT*, was associated with response to DTIC or TMZ therapy and survival after starting chemotherapy. *MGMT* was confirmed to be associated with response and survival when adjusted for current prognostic markers in stage IV disease. This analysis is limited by the heterogeneous nature of the sample set and requires further investigation when more samples are available.

In Chapter 7, I report work done to understand the biological associations with ulceration status of the primary tumour as a predictive marker of response to interferon- α (IFN) therapy. A number of factors were identified as being associated with ulceration which may modify the response of a tumour to IFN therapy. Suppression of adaptive immune responses by infiltration of macrophages, likely from the M2 phenotype, over-expression of the pro-inflammatory gene, *IL6*, and deranged expression of genes involved in the type 1 IFN Jak-STAT signalling pathway were demonstrated which may all contribute to improved responses of ulcerated tumours to IFN.

Chapter 6 reports identified gene expression profiles associated with *BRAF* and *NRAS* mutations in primary tumours. Results from this analysis provide some further insight into the biological processes within mutated tumours, for example over-expression of *ETV1* was seen in *BRAF* mutated tumours. With regards to treatment with BRAFi, these results may offer insight into mechanisms of resistance and further targets for therapeutic intervention.

As discussed previously, validation of gene expression results associated with ulceration and mutation status is being sought in collaboration with other groups and samples in Leeds, which I hope will confirm the significance of these findings.

9.3 Methodological assessments

This thesis includes extensive methodological assessments of technologies for gene expression profiling and mutation detection in FFPE melanoma tumour samples (Chapters 2-6 and 8). Results from gene expression profiling using the DASL assay and the 502-gene Human Cancer panel have been used repeatedly in this thesis. Results are reproducible and appear to be biologically relevant and use of this technology has significantly enhanced progress in identification of prognostic gene expression markers in melanoma in our group and another at the University of Lund [187, 335, 445, 505]. Preliminary experiments with the whole-genome DASL HT assay when that became available suggested that this assay was not sufficiently robust. I identified a lack of reproducibility, highlighted the problem with the company and more recently have studied a revised product and these studies now suggest that the assay is reproducible (Chapter 2). The new product will be used for further gene expression studies in the near future. Use of Taqman® gene expression assays and the Fluidigm quantitative Real-time PCR (qRT-PCR) system have been assessed in detail using FFPE melanoma tissue (Chapters 4 and 8). Both systems generate reliable results, however I have shown that correct normalisation procedures are required to ensure the accuracy of qRT-PCR data (Chapter 4) and when using a DNA binding dye, such as EvaGreen, thorough assessment of melt curves and no template control samples will allow accurate interpretation of data.

9.4 Limitations and future study

The greatest limitation of the work presented in this thesis is that gene expression studies used a 502-gene Human Cancer panel for gene expression profiling rather than a whole genome array. The genes on this panel were derived from 10 publically available cancer gene lists. The limited number of genes assessed is biased which limits use of further bioinformatics analysis as discussed in Chapter 4. Whole-genome expression profiling allows a more agnostic approach, however it is likely that RNA-seq technology will supersede microarray gene expression profiling in the near future as it has many advantages, including detection of alternative splice variants and detection of transcripts from gene fusion events [197, 198]. Further limitations are the current lack of validation for many of my findings in independent sample sets. Other groups, for example, Goran Jonsson at Lund University, Sweden, have now generated gene expression data from large cohorts of well-annotated metastatic and primary melanoma tumour specimens [180, 335] allowing validation of our findings and have agreed to test

my findings in their data sets, this analysis is currently underway. In addition, a number of publically available gene expression datasets with accompanying clinico-pathological data are available, for example from Winnepeninckx and colleagues [178], which will allow further validation of gene expression profiles, for example those associated with ulceration. The samples assessed in this thesis are from a small proportion of patients recruited to the Leeds Melanoma Cohort study described in Chapter 2. Gene expression profiling and mutation screening will continue in samples from patients in this study, allowing assessment of gene expression profiles identified in this thesis in larger sample sets and validation in a further sample set.

The “Predicting Response to Chemotherapy in Malignant Melanoma” study continues to recruit patients, which will increase numbers of samples available for further evaluation of the use of expression changes in DNA repair genes as predictive biomarkers, These samples will also allow analysis of subgroups within this heterogeneous sample set. More extensive genomic characterisation, for example *BRAF* and *NRAS* mutation screening, will define biological subgroups further. Standardisation of reporting for imaging to assess chemotherapy response will also improve the data quality for this study and this will be addressed.

The focus of this thesis has very much been on gene expression, however to further explore biological function of alterations in gene expression, protein expression will also need to be assessed. This is also relevant to the clinical use of biomarkers, as currently use of qRT-PCR in a routine clinical setting with tissue samples is limited, with immunohistochemistry (IHC) techniques being more frequently available. Tissue sections are available from the samples in the Chemotherapy study and will be used for IHC studies once candidate genes have been confirmed. For other studies, further collaboration will be required to access tissue for IHC analyses.

This thesis has been successful in identifying prognostic tumour markers, which add more to current staging algorithms in melanoma. I have also identified potential predictive markers of response to DTIC or TMZ chemotherapy, with further data helping to define biological processes in melanoma tumours. Use of these prognostic and predictive markers could potentially assist clinicians and patients in making informed choices about their melanoma treatment.

10 Appendix I: Genes on the Human Cancer panel

Alphabetical Gene List					
ABCB1	BTK	CTSD	ERCC1	FOSL2	IL13
ABCC2	CASP10	CTSL	ERCC2	FRAP1	IL1A
ABCG2	CASP2	CUL2	ERCC3	FRZB	IL1B
ABL1	CASP3	CXCL9	ERCC4	FVT1	IL1RN
ADPRT	CASP8	CYP1A1	ERCC5	FYN	IL2
AHR	CAV1	CYP1B1	ERCC6	FZD7	IL3
AIM2	CBFA2T1	DAB2	ERG	G22P1	IL4
AKT1	CBL	DAP3	ESR1	GADD45A	IL6
AKT2	CBLB	DAPK1	ETS1	GAS1	IL8
ALK	CCNA2	DCC	ETS2	GAS7	ILK
ALOX12	CCNC	DCN	ETV1	GF11	ING1
APAF1	CCND1	DDB2	ETV6	GLI	INHA
APC	CCND2	DDIT3	EVI1	GLI2	IRF1
AR	CCND3	DDX6	EVI2A	GLI3	ITGB1
ARAF1	CCNE1	DEK	EXT1	GML	ITGB4
AREG	CCNH	DKC1	EXT2	GRB2	JAK2
ARHA	CD34	DLC1	FANCA	GRB7	JUN
ARHGDI B	CD44	DLEU1	FANCG	GRPR	JUNB
ARHH	CD59	DLG3	FAT	GSTP1	JUND
ARHI	CD9	DMBT1	FER	HCK	KAI1
ARNT	CDC2	DSP	FES	HDAC1	KDR
ATF1	CDC25A	DTR	FGF1	HDGF	KIT
ATM	CDC25B	DVL3	FGF12	HIF1A	KRAS2
AXL	CDC25C	E2F1	FGF2	HLF	L1CAM
BAD	CEBPA	E2F2	FGF3	HMMR	LAF4
BAG1	CHEK1	E2F3	FGF5	HOXA9	LAMB1
BAK1	COL18A1	E2F5	FGF6	HRAS	LCK
BARD1	COL1A1	EGF	FGF7	ICAM1	LCN2
BCL2	COL4A3	EGFR	FGF8	IFNG	LIF
BCL2A1	COMT	EGR1	FGF9	IFNGR1	LIG1
BCL2L1	COPEB	ELK1	FGFR1	IFNGR2	LIG3
BCL3	CREBBP	ELK3	FGFR2	IGF1	LIG4
BCL6	CRK	ELL	FGFR3	IGF1R	LMO1
BCR	CRKL	EMS1	FGFR4	IGF2	LMO2
BIRC2	CSF1R	ENC1	FGR	IGF2R	LTA
BIRC3	CSF2	EPHA1	FHIT	IGFBP1	LYN
BIRC5	CSF3	EPHB4	FLI1	IGFBP2	MAD
BLM	CSF3R	EPO	FLT1	IGFBP3	MADH2
BMI1	CSK	EPS15	FLT3	IGFBP5	MADH4
BMP4	CSPG2	EPS8	FLT4	IGFBP6	MAF
BRAF	CTGF	ERBB2	FOLR1	IL11	MALT1
BRCA1	CTNNA1	ERBB3	FOS	IL12A	MAP3K8
BRCA2	CTNNB1	ERBB4	FOSB	IL12B	MAPK10

Alphabetical Gene List continued

MAPK14	MXI1	PLA2G2A	RAP1GDS1	SYK	TOP1
MAS1	MYB	PLAG1	RAP2A	TAL1	TOP2A
MATK	MYBL2	PLAT	RARA	TCF7L2	TP53
MBD2	MYC	PLAUR	RARB	TDGF1	TP73
MCAM	MYCL1	PLG	RASA1	TEK	TPR
MCC	MYCL2	PML	RB1	TERT	TRAF3
MCF2	MYCN	PMS1	RBBP1	TFAP2C	TRAF4
MCL1	NAT2	PNUTL1	RBBP2	TFDP1	TSC1
MDM4	NBS1	PPARD	RBBP5	TFE3	TSC2
MDS1	NEO1	PPARG	RBBP6	TFF1	TSG101
MEL	NF1	PPP2R1B	RBL2	TFG	TYMS
MEN1	NFKB1	PRCC	RECQL	TFRC	TYRO3
MET	NFKB2	PRKAR1A	REL	TGFA	VAV1
MLF1	NFKBIA	PRKR	RELA	TGFB1	VAV2
MLF2	NGFR	PTCH	RET	TGFB2	VBP1
MLH1	NOS3	PTCH2	RIPK1	TGFB3	VEGF
MLL	NOTCH1	PTEN	RLF	TGFB1	VEGFB
MLLT3	NOTCH2	PTGS1	ROS1	TGFBR1	VHL
MLLT4	NOTCH4	PTGS2	RRAS	TGFBR2	VIL2
MLLT6	NQO1	PTHLH	S100A4	TGFBR3	WEE1
MMP1	NRAS	PTK2	SEMA3F	THBS2	WNT1
MMP10	NTRK1	PTK7	SERPINE1	THPO	WNT10B
MMP14	NTRK2	PTPRF	SH3BP2	TIAM1	WNT2
MMP2	NTRK3	PTPRG	SHH	TIMP1	WNT2B
MMP3	NUMA1	PTPRH	SIAH1	TIMP2	WNT5A
MMP7	OGG1	PURA	SKI	TIMP3	WNT8B
MMP9	OSM	PXN	SKIL	TK1	WRN
MOS	PBX1	QARS	SMARCA4	TNF	WT1
MPL	PCNA	RAD23A	SMARCB1	TNFAIP1	XPA
MRE11A	PCTK1	RAD50	SOD1	TNFRSF10A	XPC
MSF	PDGFA	RAD51	SPARC	TNFRSF10B	XRCC1
MSH2	PDGFB	RAD52	SPI1	TNFRSF1A	XRCC2
MSH3	PDGFRA	RAD54B	SPP1	TNFRSF1B	XRCC4
MSH6	PDGFRB	RAD54L	SRC	TNFRSF5	XRCC5
MST1R	PGF	RAF1	STAT1	TNFRSF6	YES1
MTA1	PGR	RALB	STAT3	TNFSF10	YY1
MTHFR	PIK3CA	RAN	STAT5B	TNFSF6	ZNF146
MUC1	PIM1	RAP1A	STK11	TNFSF8	ZNFN1A1

11 References

1. Kanitakis, J., *Anatomy, histology and immunohistochemistry of normal human skin*. Eur J Dermatol, 2002. **12**(4): p. 390-9; quiz 400-1.
2. Chin, L., *The genetics of malignant melanoma: lessons from mouse and man*. Nat Rev Cancer, 2003. **3**(8): p. 559-70.
3. Cancer Research UK Statistical Information Team. *UK Skin Cancer Incidence Statistics [online]*. 2009 [cited 2012 2nd July]; Available from: <http://info.cancerresearchuk.org/cancerstats/types/skin/incidence>.
4. Miller, A.J. and M.C. Mihm, Jr., *Melanoma*. N Engl J Med, 2006. **355**(1): p. 51-65.
5. Tucker, M.A., *Melanoma epidemiology*. Hematol Oncol Clin North Am, 2009. **23**(3): p. 383-95, vii.
6. Gandini, S., et al., *Meta-analysis of risk factors for cutaneous melanoma: III. Family history, actinic damage and phenotypic factors*. Eur J Cancer, 2005. **41**(14): p. 2040-59.
7. Chang, Y.M., et al., *A pooled analysis of melanocytic nevus phenotype and the risk of cutaneous melanoma at different latitudes*. Int J Cancer, 2009. **124**(2): p. 420-8.
8. Gandini, S., et al., *Meta-analysis of risk factors for cutaneous melanoma: I. Common and atypical naevi*. Eur J Cancer, 2005. **41**(1): p. 28-44.
9. Olsen, C.M., et al., *Nevus density and melanoma risk in women: a pooled analysis to test the divergent pathway hypothesis*. Int J Cancer, 2009. **124**(4): p. 937-44.
10. Chatzinasiou, F., et al., *Comprehensive field synopsis and systematic meta-analyses of genetic association studies in cutaneous melanoma*. J Natl Cancer Inst, 2011. **103**(16): p. 1227-35.
11. Bishop, D.T., et al., *Genome-wide association study identifies three loci associated with melanoma risk*. Nat Genet, 2009. **41**(8): p. 920-5.
12. Wachsmuth, R.C., et al., *Heritability and gene-environment interactions for melanocytic nevus density examined in a U.K. adolescent twin study*. J Invest Dermatol, 2001. **117**(2): p. 348-52.
13. Easton, D.F., et al., *Genetic susceptibility to naevi--a twin study*. Br J Cancer, 1991. **64**(6): p. 1164-7.
14. Gandini, S., et al., *Meta-analysis of risk factors for cutaneous melanoma: II. Sun exposure*. Eur J Cancer, 2005. **41**(1): p. 45-60.
15. Newton-Bishop, J.A., et al., *Relationship between sun exposure and melanoma risk for tumours in different body sites in a large case-control study in a temperate climate*. Eur J Cancer, 2011. **47**(5): p. 732-41.
16. Risch, N., *The genetic epidemiology of cancer: interpreting family and twin studies and their implications for molecular genetic approaches*. Cancer Epidemiol Biomarkers Prev, 2001. **10**(7): p. 733-41.
17. Shekar, S.N., et al., *A population-based study of Australian twins with melanoma suggests a strong genetic contribution to liability*. J Invest Dermatol, 2009. **129**(9): p. 2211-9.
18. Meyle, K.D. and P. Guldborg, *Genetic risk factors for melanoma*. Hum Genet, 2009. **126**(4): p. 499-510.

19. Bennett, D.C., *How to make a melanoma: what do we know of the primary clonal events?* Pigment Cell Melanoma Res, 2008. **21**(1): p. 27-38.
20. Chin, L., L.A. Garraway, and D.E. Fisher, *Malignant melanoma: genetics and therapeutics in the genomic era.* Genes Dev, 2006. **20**(16): p. 2149-82.
21. de Snoo, F.A. and N.K. Hayward, *Cutaneous melanoma susceptibility and progression genes.* Cancer Lett, 2005. **230**(2): p. 153-86.
22. Bennett, D.C., *Human melanocyte senescence and melanoma susceptibility genes.* Oncogene, 2003. **22**(20): p. 3063-9.
23. Goldstein, A.M., et al., *Features associated with germline CDKN2A mutations: a GenoMEL study of melanoma-prone families from three continents.* J Med Genet, 2007. **44**(2): p. 99-106.
24. Goldstein, A.M., et al., *High-risk melanoma susceptibility genes and pancreatic cancer, neural system tumors, and uveal melanoma across GenoMEL.* Cancer Res, 2006. **66**(20): p. 9818-28.
25. Pollock, P.M., et al., *High frequency of BRAF mutations in nevi.* Nat Genet, 2003. **33**(1): p. 19-20.
26. Greene, M.H., et al., *High risk of malignant melanoma in melanoma-prone families with dysplastic nevi.* Ann Intern Med, 1985. **102**(4): p. 458-65.
27. Tucker, M.A., et al., *A natural history of melanomas and dysplastic nevi: an atlas of lesions in melanoma-prone families.* Cancer, 2002. **94**(12): p. 3192-209.
28. Wellbrock, C., M. Karasarides, and R. Marais, *The RAF proteins take centre stage.* Nat Rev Mol Cell Biol, 2004. **5**(11): p. 875-85.
29. Robinson, M.J. and M.H. Cobb, *Mitogen-activated protein kinase pathways.* Curr Opin Cell Biol, 1997. **9**(2): p. 180-6.
30. Platz, A., et al., *Human cutaneous melanoma; a review of NRAS and BRAF mutation frequencies in relation to histogenetic subclass and body site.* Mol Oncol, 2008. **1**(4): p. 395-405.
31. Lee, J.H., J.W. Choi, and Y.S. Kim, *Frequencies of BRAF and NRAS mutations are different in histological types and sites of origin of cutaneous melanoma: a meta-analysis.* The British journal of dermatology, 2011. **164**(4): p. 776-84.
32. Davies, H., et al., *Mutations of the BRAF gene in human cancer.* Nature, 2002. **417**(6892): p. 949-54.
33. Curtin, J.A., et al., *Somatic activation of KIT in distinct subtypes of melanoma.* J Clin Oncol, 2006. **24**(26): p. 4340-6.
34. Van Raamsdonk, C.D., et al., *Frequent somatic mutations of GNAQ in uveal melanoma and blue naevi.* Nature, 2009. **457**(7229): p. 599-602.
35. Chudnovsky, Y., P.A. Khavari, and A.E. Adams, *Melanoma genetics and the development of rational therapeutics.* J Clin Invest, 2005. **115**(4): p. 813-24.
36. Gray-Schopfer, V.C., et al., *Cellular senescence in naevi and immortalisation in melanoma: a role for p16?* Br J Cancer, 2006. **95**(4): p. 496-505.
37. Michaloglou, C., et al., *BRAFE600-associated senescence-like cell cycle arrest of human naevi.* Nature, 2005. **436**(7051): p. 720-4.
38. Bartkova, J., et al., *The p16-cyclin D/Cdk4-pRb pathway as a functional unit frequently altered in melanoma pathogenesis.* Cancer Res, 1996. **56**(23): p. 5475-83.

39. Sviderskaya, E.V., et al., *p16/cyclin-dependent kinase inhibitor 2A deficiency in human melanocyte senescence, apoptosis, and immortalization: possible implications for melanoma progression*. J Natl Cancer Inst, 2003. **95**(10): p. 723-32.
40. Freedberg, D.E., et al., *Frequent p16-independent inactivation of p14ARF in human melanoma*. J Natl Cancer Inst, 2008. **100**(11): p. 784-95.
41. Cully, M., et al., *Beyond PTEN mutations: the PI3K pathway as an integrator of multiple inputs during tumorigenesis*. Nat Rev Cancer, 2006. **6**(3): p. 184-92.
42. Curtin, J.A., et al., *PI3-kinase subunits are infrequent somatic targets in melanoma*. J Invest Dermatol, 2006. **126**(7): p. 1660-3.
43. Tsao, H., et al., *Genetic interaction between NRAS and BRAF mutations and PTEN/MMAC1 inactivation in melanoma*. J Invest Dermatol, 2004. **122**(2): p. 337-41.
44. Jonsson, G., et al., *Genomic profiling of malignant melanoma using tiling-resolution arrayCGH*. Oncogene, 2007. **26**(32): p. 4738-48.
45. Chiang, A.C. and J. Massague, *Molecular basis of metastasis*. N Engl J Med, 2008. **359**(26): p. 2814-23.
46. Fidler, I.J., *The pathogenesis of cancer metastasis: the 'seed and soil' hypothesis revisited*. Nature reviews. Cancer, 2003. **3**(6): p. 453-8.
47. Gupta, G.P. and J. Massague, *Cancer metastasis: building a framework*. Cell, 2006. **127**(4): p. 679-95.
48. Folkman, J., *How is blood vessel growth regulated in normal and neoplastic tissue? G.H.A. Clowes memorial Award lecture*. Cancer Res, 1986. **46**(2): p. 467-73.
49. Clark, W.H., Jr., et al., *A study of tumor progression: the precursor lesions of superficial spreading and nodular melanoma*. Hum Pathol, 1984. **15**(12): p. 1147-65.
50. Danen, E.H., et al., *E-cadherin expression in human melanoma*. Melanoma Res, 1996. **6**(2): p. 127-31.
51. Hsu, M.Y., et al., *Shifts in cadherin profiles between human normal melanocytes and melanomas*. J Invest Dermatol Symp Proc, 1996. **1**(2): p. 188-94.
52. Hsu, M., et al., *Cadherin repertoire determines partner-specific gap junctional communication during melanoma progression*. J Cell Sci, 2000. **113** (Pt 9): p. 1535-42.
53. Haass, N.K., et al., *Adhesion, migration and communication in melanocytes and melanoma*. Pigment Cell Res, 2005. **18**(3): p. 150-9.
54. Morton, D.L., et al., *Technical details of intraoperative lymphatic mapping for early stage melanoma*. Arch Surg, 1992. **127**(4): p. 392-9.
55. Leong, S.P., et al., *Clinical patterns of metastasis*. Cancer Metastasis Rev, 2006. **25**(2): p. 221-32.
56. Reintgen, D., et al., *The orderly progression of melanoma nodal metastases*. Ann Surg, 1994. **220**(6): p. 759-67.
57. Patel, J.K., et al., *Metastatic pattern of malignant melanoma. A study of 216 autopsy cases*. American journal of surgery, 1978. **135**(6): p. 807-10.
58. Balch, C.M., et al., *Final version of 2009 AJCC melanoma staging and classification*. J Clin Oncol, 2009. **27**(36): p. 6199-206.
59. Balch, C.M., et al., *Multivariate analysis of prognostic factors among 2,313 patients with stage III melanoma: comparison of nodal*

- micrometastases versus macrometastases*. J Clin Oncol, 2010. **28**(14): p. 2452-9.
60. Robert, C., et al., *Ipilimumab plus dacarbazine for previously untreated metastatic melanoma*. N Engl J Med, 2011. **364**(26): p. 2517-26.
 61. Hodi, F.S., et al., *Improved Survival with Ipilimumab in Patients with Metastatic Melanoma*. N Engl J Med, 2010.
 62. Navarini-Meury, A.A. and C. Conrad, *Melanoma and innate immunity--aActive inflammation or just erroneous attraction? Melanoma as the source of leukocyte-attracting chemokines*. Semin Cancer Biol, 2009. **19**(2): p. 84-91.
 63. Orange, J.S. and Z.K. Ballas, *Natural killer cells in human health and disease*. Clin Immunol, 2006. **118**(1): p. 1-10.
 64. Halliday, G.M., *Skin immunity and melanoma development*, in *Textbook of Melanoma*, J.F. Thompson, D.L. Morton, and B.B.R. Kroon, Editors. 2004, Martin Dunitz: London. p. pp. 25-42.
 65. Clemente, C.G., et al., *Prognostic value of tumor infiltrating lymphocytes in the vertical growth phase of primary cutaneous melanoma*. Cancer, 1996. **77**(7): p. 1303-10.
 66. Mihm, M.C., Jr., C.G. Clemente, and N. Cascinelli, *Tumor infiltrating lymphocytes in lymph node melanoma metastases: a histopathologic prognostic indicator and an expression of local immune response*. Lab Invest, 1996. **74**(1): p. 43-7.
 67. Uchi, H., et al., *Unraveling the complex relationship between cancer immunity and autoimmunity: lessons from melanoma and vitiligo*. Adv Immunol, 2006. **90**: p. 215-41.
 68. Nordlund, J.J., et al., *Vitiligo in patients with metastatic melanoma: a good prognostic sign*. J Am Acad Dermatol, 1983. **9**(5): p. 689-96.
 69. Gogas, H., et al., *Prognostic significance of autoimmunity during treatment of melanoma with interferon*. N Engl J Med, 2006. **354**(7): p. 709-18.
 70. Kirkwood, J.M., et al., *Next generation of immunotherapy for melanoma*. J Clin Oncol, 2008. **26**(20): p. 3445-55.
 71. Chang, C.C., et al., *Defective human leukocyte antigen class I-associated antigen presentation caused by a novel beta2-microglobulin loss-of-function in melanoma cells*. J Biol Chem, 2006. **281**(27): p. 18763-73.
 72. Chang, C.C., et al., *Immune selection of hot-spot beta 2-microglobulin gene mutations, HLA-A2 allospecificity loss, and antigen-processing machinery component down-regulation in melanoma cells derived from recurrent metastases following immunotherapy*. J Immunol, 2005. **174**(3): p. 1462-71.
 73. Sharma, S., et al., *T cell-derived IL-10 promotes lung cancer growth by suppressing both T cell and APC function*. J Immunol, 1999. **163**(9): p. 5020-8.
 74. McKarns, S.C. and R.H. Schwartz, *Distinct effects of TGF-beta 1 on CD4+ and CD8+ T cell survival, division, and IL-2 production: a role for T cell intrinsic Smad3*. J Immunol, 2005. **174**(4): p. 2071-83.
 75. Mellman, I., G. Coukos, and G. Dranoff, *Cancer immunotherapy comes of age*. Nature, 2011. **480**(7378): p. 480-9.
 76. Marsden, J.R., et al., *Revised U.K. guidelines for the management of cutaneous melanoma 2010*. Br J Dermatol, 2010. **163**(2): p. 238-56.

77. Werner, M., et al., *Effect of formalin tissue fixation and processing on immunohistochemistry*. Am J Surg Pathol, 2000. **24**(7): p. 1016-9.
78. Association of Directors of Anatomic and Surgical Pathology, *Recommendations for the reporting of tissues removed as part of the surgical treatment of cutaneous melanoma*. Association of Directors of Anatomic and Surgical Pathology. Pathol Int, 1998. **48**(2): p. 168-70.
79. Leong, S.P., *Sentinel lymph node mapping and selective lymphadenectomy: the standard of care for melanoma*. Curr Treat Options Oncol, 2004. **5**(3): p. 185-94.
80. Morton, D.L., et al., *Sentinel-node biopsy or nodal observation in melanoma*. N Engl J Med, 2006. **355**(13): p. 1307-17.
81. Cook, M.G. and S. Di Palma, *Pathology of sentinel lymph nodes for melanoma*. Journal of clinical pathology, 2008. **61**(8): p. 897-902.
82. Dewar, D., et al., *The microanatomic location of metastatic melanoma in sentinel lymph nodes predicts nonsentinel lymph node involvement*. Journal of Clinical Oncology, 2004. **22**: p. 3345-3349.
83. Starz, H., et al., *A micromorphometry-based concept for routine classification of sentinel lymph node metastases and its clinical relevance for patients with melanoma*. Cancer, 2001. **91**(11): p. 2110-21.
84. Coleman, M.P., et al., *Trends and socioeconomic inequalities in cancer survival in England and Wales up to 2001*. Br J Cancer, 2004. **90**(7): p. 1367-73.
85. Cancer Research UK Statistical Information Team. *Skin cancer survival statistics [online]*. 2009 2nd April 2009 [cited 2012 3rd July]; Available from: <http://info.cancerresearchuk.org/cancerstats/types/skin/survival/>.
86. Gimotty, P.A., et al., *A population-based validation of the American Joint Committee on Cancer melanoma staging system*. J Clin Oncol, 2005. **23**(31): p. 8065-75.
87. Allen, A.C. and S. Spitz, *Malignant melanoma; a clinicopathological analysis of the criteria for diagnosis and prognosis*. Cancer, 1953. **6**(1): p. 1-45.
88. Breslow, A., *Thickness, cross-sectional areas and depth of invasion in the prognosis of cutaneous melanoma*. Ann Surg, 1970. **172**(5): p. 902-8.
89. Breslow, A., et al., *Stage I melanoma of the limbs: assessment of prognosis by levels of invasion and maximum thickness*. Tumori, 1978. **64**(3): p. 273-84.
90. Balch, C.M., et al., *A multifactorial analysis of melanoma: prognostic histopathological features comparing Clark's and Breslow's staging methods*. Ann Surg, 1978. **188**(6): p. 732-42.
91. Balch, C.M., et al., *Prognostic factors analysis of 17,600 melanoma patients: validation of the American Joint Committee on Cancer melanoma staging system*. J Clin Oncol, 2001. **19**(16): p. 3622-34.
92. Clark, W.H., Jr., et al., *The histogenesis and biologic behavior of primary human malignant melanomas of the skin*. Cancer Res, 1969. **29**(3): p. 705-27.
93. Gershenwald, J.E., M.I. Ross, and A.C. Buzaid, *Staging systems for cutaneous melanoma*, in *Textbook of melanoma*, J.F. Thompson, D.L. Morton, and B.B.R. Kroon, Editors. 2004, Martin Dunitz: London. p. pp. 164-180.
94. Spatz, A., et al., *Interobserver reproducibility of ulceration assessment in primary cutaneous melanomas*. Eur J Cancer, 2003. **39**(13): p. 1861-5.

95. Barnhill, R.L., et al., *The importance of mitotic rate as a prognostic factor for localized cutaneous melanoma*. J Cutan Pathol, 2005. **32**(4): p. 268-73.
96. Francken, A.B., et al., *The prognostic importance of tumor mitotic rate confirmed in 1317 patients with primary cutaneous melanoma and long follow-up*. Ann Surg Oncol, 2004. **11**(4): p. 426-33.
97. Nagore, E., et al., *Prognostic factors in localized invasive cutaneous melanoma: high value of mitotic rate, vascular invasion and microscopic satellitosis*. Melanoma Res, 2005. **15**(3): p. 169-77.
98. Thompson, J.F., et al., *Prognostic significance of mitotic rate in localized primary cutaneous melanoma: an analysis of patients in the multi-institutional American Joint Committee on Cancer melanoma staging database*. J Clin Oncol, 2011. **29**(16): p. 2199-205.
99. Dewar, D.J., et al., *The microanatomic location of metastatic melanoma in sentinel lymph nodes predicts nonsentinel lymph node involvement*. J Clin Oncol, 2004. **22**(16): p. 3345-9.
100. van Akkooi, A.C., et al., *Sentinel node tumor burden according to the Rotterdam criteria is the most important prognostic factor for survival in melanoma patients: a multicenter study in 388 patients with positive sentinel nodes*. Ann Surg, 2008. **248**(6): p. 949-55.
101. Buzaid, A.C., et al., *Critical analysis of the current American Joint Committee on Cancer staging system for cutaneous melanoma and proposal of a new staging system*. J Clin Oncol, 1997. **15**(3): p. 1039-51.
102. Balch, C.M., et al., *Final version of the American Joint Committee on Cancer staging system for cutaneous melanoma*. J Clin Oncol, 2001. **19**(16): p. 3635-48.
103. Manola, J., et al., *Prognostic factors in metastatic melanoma: a pooled analysis of Eastern Cooperative Oncology Group trials*. J Clin Oncol, 2000. **18**(22): p. 3782-93.
104. Barth, A., L.A. Wanek, and D.L. Morton, *Prognostic factors in 1,521 melanoma patients with distant metastases*. J Am Coll Surg, 1995. **181**(3): p. 193-201.
105. Sirott, M.N., et al., *Prognostic factors in patients with metastatic malignant melanoma. A multivariate analysis*. Cancer, 1993. **72**(10): p. 3091-8.
106. Eton, O., et al., *Prognostic factors for survival of patients treated systemically for disseminated melanoma*. J Clin Oncol, 1998. **16**(3): p. 1103-11.
107. Deichmann, M., et al., *S100-Beta, melanoma-inhibiting activity, and lactate dehydrogenase discriminate progressive from nonprogressive American Joint Committee on Cancer stage IV melanoma*. J Clin Oncol, 1999. **17**(6): p. 1891-6.
108. Agarwala, S.S., et al., *LDH correlation with survival in advanced melanoma from two large, randomised trials (Oblimersen GM301 and EORTC 18951)*. Eur J Cancer, 2009. **45**(10): p. 1807-14.
109. Cancer Research UK Statistical Information Team. *Melanoma statistics and outlook*. 2012 [cited 2012 3rd July]; Available from: <http://cancerhelp.cancerresearchuk.org/type/melanoma/treatment/melanoma-statistics-and-outlook>.
110. Rose, A.E., et al., *Clinical relevance of detection of lymphovascular invasion in primary melanoma using endothelial markers D2-40 and CD34*. Am J Surg Pathol, 2011. **35**(10): p. 1441-9.

111. Kashani-Sabet, M., et al., *Tumor vascularity in the prognostic assessment of primary cutaneous melanoma*. J Clin Oncol, 2002. **20**(7): p. 1826-31.
112. Xu, X., et al., *Lymphatic invasion is independently prognostic of metastasis in primary cutaneous melanoma*. Clin Cancer Res, 2012. **18**(1): p. 229-37.
113. Storr, S.J., et al., *Objective assessment of blood and lymphatic vessel invasion and association with macrophage infiltration in cutaneous melanoma*. Modern pathology : an official journal of the United States and Canadian Academy of Pathology, Inc, 2011.
114. Crowson, A.N., C.M. Magro, and M.C. Mihm, *Prognosticators of melanoma, the melanoma report, and the sentinel lymph node*. Mod Pathol, 2006. **19 Suppl 2**: p. S71-87.
115. Chan, M.M. and S.R. Tahan, *Low-affinity nerve growth factor receptor (P75 NGFR) as a marker of perineural invasion in malignant melanomas*. J Cutan Pathol, 2010. **37**(3): p. 336-43.
116. Quinn, M.J., et al., *Desmoplastic and desmoplastic neurotropic melanoma: experience with 280 patients*. Cancer, 1998. **83**(6): p. 1128-35.
117. Payette, M.J., M. Katz, 3rd, and J.M. Grant-Kels, *Melanoma prognostic factors found in the dermatopathology report*. Clin Dermatol, 2009. **27**(1): p. 53-74.
118. Guitart, J., et al., *Histological characteristics of metastasizing thin melanomas: a case-control study of 43 cases*. Arch Dermatol, 2002. **138**(5): p. 603-8.
119. Speeckaert, R., et al., *Immune reactions in benign and malignant melanocytic lesions: lessons for immunotherapy*. Pigment Cell Melanoma Res, 2011. **24**(2): p. 334-44.
120. Shaw, H.M., et al., *Cutaneous melanomas exhibiting unusual biologic behavior*. World J Surg, 1992. **16**(2): p. 196-202.
121. Slingluff, C.L., Jr., et al., *Lethal "thin" malignant melanoma. Identifying patients at risk*. Ann Surg, 1988. **208**(2): p. 150-61.
122. Brogelli, L., et al., *The prognostic significance of histologic regression in cutaneous melanoma*. Melanoma Res, 1992. **2**(2): p. 87-91.
123. Burton, A.L., et al., *Regression does not predict nodal metastasis or survival in patients with cutaneous melanoma*. Am Surg, 2011. **77**(8): p. 1009-13.
124. Taylor, R.C., et al., *Tumor-infiltrating lymphocytes predict sentinel lymph node positivity in patients with cutaneous melanoma*. J Clin Oncol, 2007. **25**(7): p. 869-75.
125. Clark, W.H., Jr., et al., *Model predicting survival in stage I melanoma based on tumor progression*. J Natl Cancer Inst, 1989. **81**(24): p. 1893-904.
126. Elder, D.E., *Prognostic models for melanoma*. J Cutan Pathol, 2010. **37 Suppl 1**: p. 68-75.
127. Tuthill, R.J., et al., *Risk assessment in localized primary cutaneous melanoma: a Southwest Oncology Group study evaluating nine factors and a test of the Clark logistic regression prediction model*. Am J Clin Pathol, 2002. **118**(4): p. 504-11.
128. Azimi, F., et al., *Tumor-Infiltrating Lymphocyte Grade Is an Independent Predictor of Sentinel Lymph Node Status and Survival in Patients With Cutaneous Melanoma*. J Clin Oncol, 2012.

129. Oble, D.A., et al., *Focus on TILs: prognostic significance of tumor infiltrating lymphocytes in human melanoma*. *Cancer Immun*, 2009. **9**: p. 3.
130. Cancer Research UK. *Types of melanoma*. 2012 26th March 2012 [cited 2012 10th July]; Available from: <http://cancerhelp.cancerresearchuk.org/type/melanoma/about/types-of-melanoma>.
131. Stalkup, J.R., I.F. Orengo, and R. Katta, *Controversies in acral lentiginous melanoma*. *Dermatol Surg*, 2002. **28**(11): p. 1051-9; discussion 1059.
132. Durbec, F., et al., *Melanoma of the hand and foot: epidemiological, prognostic and genetic features. A systematic review*. *Br J Dermatol*, 2012. **166**(4): p. 727-39.
133. Cochran, A.J., et al., *Individualized prognosis for melanoma patients*. *Hum Pathol*, 2000. **31**(3): p. 327-31.
134. Ross, M.I., *Early-stage melanoma: staging criteria and prognostic modeling*. *Clin Cancer Res*, 2006. **12**(7 Pt 2): p. 2312s-2319s.
135. Austin, P.F., et al., *Age as a prognostic factor in the malignant melanoma population*. *Ann Surg Oncol*, 1994. **1**(6): p. 487-94.
136. Balch, C.M., et al., *Long-term results of a multi-institutional randomized trial comparing prognostic factors and surgical results for intermediate thickness melanomas (1.0 to 4.0 mm)*. *Intergroup Melanoma Surgical Trial*. *Ann Surg Oncol*, 2000. **7**(2): p. 87-97.
137. Balch, C.M., et al., *Efficacy of an elective regional lymph node dissection of 1 to 4 mm thick melanomas for patients 60 years of age and younger*. *Ann Surg*, 1996. **224**(3): p. 255-63; discussion 263-6.
138. Sahin, S., et al., *Predicting ten-year survival of patients with primary cutaneous melanoma: corroboration of a prognostic model*. *Cancer*, 1997. **80**(8): p. 1426-31.
139. Tsai, S., C. Balch, and J. Lange, *Epidemiology and treatment of melanoma in elderly patients*. *Nat Rev Clin Oncol*, 2010. **7**(3): p. 148-52.
140. Stenius Muller, M.G., et al., *The sentinel lymph node status is an important factor for predicting clinical outcome in patients with Stage I or II cutaneous melanoma*. *Cancer*, 2001. **91**(12): p. 2401-8.
141. Gershenwald, J.E., et al., *Patterns of recurrence following a negative sentinel lymph node biopsy in 243 patients with stage I or II melanoma*. *J Clin Oncol*, 1998. **16**(6): p. 2253-60.
142. Pan, W.R., H. Suami, and G.I. Taylor, *Senile changes in human lymph nodes*. *Lymphat Res Biol*, 2008. **6**(2): p. 77-83.
143. Conway, W.C., et al., *Age-related lymphatic dysfunction in melanoma patients*. *Ann Surg Oncol*, 2009. **16**(6): p. 1548-52.
144. Joosse, A., et al., *Superior Outcome of Women With Stage I/II Cutaneous Melanoma: Pooled Analysis of Four European Organisation for Research and Treatment of Cancer Phase III Trials*. *J Clin Oncol*, 2012. **30**(18): p. 2240-7.
145. de Vries, E., et al., *Changing epidemiology of malignant cutaneous melanoma in Europe 1953-1997: rising trends in incidence and mortality but recent stabilizations in western Europe and decreases in Scandinavia*. *Int J Cancer*, 2003. **107**(1): p. 119-26.
146. Lasithiotakis, K., et al., *Age and gender are significant independent predictors of survival in primary cutaneous melanoma*. *Cancer*, 2008. **112**(8): p. 1795-804.

147. de Vries, E., et al., *Superior survival of females among 10,538 Dutch melanoma patients is independent of Breslow thickness, histologic type and tumor site.* Ann Oncol, 2008. **19**(3): p. 583-9.
148. Joosse, A., et al., *Reactive oxygen species and melanoma: an explanation for gender differences in survival?* Pigment Cell Melanoma Res, 2010. **23**(3): p. 352-64.
149. Correale, J., M.C. Ysraelit, and M.I. Gaitan, *Gender differences in 1,25 dihydroxyvitamin D3 immunomodulatory effects in multiple sclerosis patients and healthy subjects.* J Immunol, 2010. **185**(8): p. 4948-58.
150. Bouman, A., M.J. Heineman, and M.M. Faas, *Sex hormones and the immune response in humans.* Hum Reprod Update, 2005. **11**(4): p. 411-23.
151. Curtin, J.A., et al., *Distinct sets of genetic alterations in melanoma.* The New England journal of medicine, 2005. **353**(20): p. 2135-47.
152. Whiteman, D.C., et al., *Anatomic site, sun exposure, and risk of cutaneous melanoma.* J Clin Oncol, 2006. **24**(19): p. 3172-7.
153. Porter, G.A., et al., *Significance of multiple nodal basin drainage in truncal melanoma patients undergoing sentinel lymph node biopsy.* Ann Surg Oncol, 2000. **7**(4): p. 256-61.
154. McMasters, K.M., *Multiple nodal basin drainage in truncal melanomas.* Ann Surg Oncol, 2000. **7**(4): p. 249-50.
155. Gogas, H., et al., *Biomarkers in melanoma.* Ann Oncol, 2009. **20 Suppl 6**: p. vi8-13.
156. Biomarkers Definitions Working Group, *Biomarkers and surrogate endpoints: preferred definitions and conceptual framework.* Clin Pharmacol Ther, 2001. **69**(3): p. 89-95.
157. Buyse, M., et al., *Biomarkers and surrogate end points--the challenge of statistical validation.* Nat Rev Clin Oncol, 2010. **7**(6): p. 309-17.
158. Davies, J.R., et al., *Inherited variants in the MC1R gene and survival from cutaneous melanoma: a BioGenoMEL study.* Pigment cell & melanoma research, 2012.
159. Ugurel, S., J. Utikal, and J.C. Becker, *Tumor biomarkers in melanoma.* Cancer Control, 2009. **16**(3): p. 219-24.
160. Gould Rothberg, B.E., M.B. Bracken, and D.L. Rimm, *Tissue biomarkers for prognosis in cutaneous melanoma: a systematic review and meta-analysis.* J Natl Cancer Inst, 2009. **101**(7): p. 452-74.
161. Schramm, S.J. and G.J. Mann, *Melanoma Prognosis: A REMARK-Based Systematic Review and Bioinformatic Analysis of Immunohistochemical and Gene Microarray Studies.* Molecular cancer therapeutics, 2011.
162. McShane, L.M., et al., *REporting recommendations for tumor MARKer prognostic studies (REMARK).* Nat Clin Pract Oncol, 2005. **2**(8): p. 416-22.
163. Rangel, J., et al., *Osteopontin as a molecular prognostic marker for melanoma.* Cancer, 2008. **112**(1): p. 144-50.
164. Alonso, S.R., et al., *A high-throughput study in melanoma identifies epithelial-mesenchymal transition as a major determinant of metastasis.* Cancer Res, 2007. **67**(7): p. 3450-60.
165. Tucci, M.G., et al., *Involvement of E-cadherin, beta-catenin, Cdc42 and CXCR4 in the progression and prognosis of cutaneous melanoma.* Br J Dermatol, 2007. **157**(6): p. 1212-6.

166. Andersen, K., et al., *Expression of S100A4 combined with reduced E-cadherin expression predicts patient outcome in malignant melanoma*. Mod Pathol, 2004. **17**(8): p. 990-7.
167. Redondo, P., et al., *Expression and serum levels of MMP-2 and MMP-9 during human melanoma progression*. Clin Exp Dermatol, 2005. **30**(5): p. 541-5.
168. Vaisanen, A., et al., *Prognostic value of MMP-2 immunoreactive protein (72 kD type IV collagenase) in primary skin melanoma*. J Pathol, 1998. **186**(1): p. 51-8.
169. Vaisanen, A.H., M. Kallioinen, and T. Turpeenniemi-Hujanen, *Comparison of the prognostic value of matrix metalloproteinases 2 and 9 in cutaneous melanoma*. Hum Pathol, 2008. **39**(3): p. 377-85.
170. Piras, F., et al., *Combinations of apoptosis and cell-cycle control biomarkers predict the outcome of human melanoma*. Oncol Rep, 2008. **20**(2): p. 271-7.
171. Gould Rothberg, B.E., et al., *Melanoma prognostic model using tissue microarrays and genetic algorithms*. J Clin Oncol, 2009. **27**(34): p. 5772-80.
172. Kashani-Sabet, M., et al., *A multimarker prognostic assay for primary cutaneous melanoma*. Clin Cancer Res, 2009. **15**(22): p. 6987-92.
173. DeRisi, J., et al., *Use of a cDNA microarray to analyse gene expression patterns in human cancer*. Nat Genet, 1996. **14**(4): p. 457-60.
174. Hoek, K., et al., *Expression profiling reveals novel pathways in the transformation of melanocytes to melanomas*. Cancer Res, 2004. **64**(15): p. 5270-82.
175. Ryu, B., et al., *Comprehensive expression profiling of tumor cell lines identifies molecular signatures of melanoma progression*. PLoS One, 2007. **2**(7): p. e594.
176. Jaeger, J., et al., *Gene expression signatures for tumor progression, tumor subtype, and tumor thickness in laser-microdissected melanoma tissues*. Clin Cancer Res, 2007. **13**(3): p. 806-15.
177. Kauffmann, A., et al., *High expression of DNA repair pathways is associated with metastasis in melanoma patients*. Oncogene, 2008. **27**(5): p. 565-73.
178. Winnepeninckx, V., et al., *Gene expression profiling of primary cutaneous melanoma and clinical outcome*. J Natl Cancer Inst, 2006. **98**(7): p. 472-82.
179. Bogunovic, D., et al., *Immune profile and mitotic index of metastatic melanoma lesions enhance clinical staging in predicting patient survival*. Proc Natl Acad Sci U S A, 2009. **106**(48): p. 20429-34.
180. Jonsson, G.B., et al., *Gene Expression Profiling-Based Identification of Molecular Subtypes in Stage IV Melanomas with Different Clinical Outcome*. Clin Cancer Res, 2010.
181. Busam, K.J., et al., *Distinction of desmoplastic melanoma from non-desmoplastic melanoma by gene expression profiling*. J Invest Dermatol, 2005. **124**(2): p. 412-8.
182. Haqq, C., et al., *The gene expression signatures of melanoma progression*. Proc Natl Acad Sci U S A, 2005. **102**(17): p. 6092-7.
183. Mandruzzato, S., et al., *A gene expression signature associated with survival in metastatic melanoma*. J Transl Med, 2006. **4**: p. 50.

184. Talantov, D., et al., *Novel genes associated with malignant melanoma but not benign melanocytic lesions*. Clin Cancer Res, 2005. **11**(20): p. 7234-42.
185. John, T., et al., *Predicting clinical outcome through molecular profiling in stage III melanoma*. Clin Cancer Res, 2008. **14**(16): p. 5173-80.
186. Mann, G.J., et al. *BRAF mutation, NRAS mutation and absence of an immune-related expressed gene profile predict poor outcome in surgically resected stage III melanoma (abstract number 150)*. in Society of Melanoma Research. 2010. Sydney, Australia: Pigment Cell and Melanoma Res.
187. Conway, C., et al., *Gene expression profiling of paraffin-embedded primary melanoma using the DASL assay identifies increased osteopontin expression as predictive of reduced relapse-free survival*. Clin Cancer Res, 2009. **15**(22): p. 6939-46.
188. Schramm, S.J., et al., *Review and Cross-Validation of Gene Expression Signatures and Melanoma Prognosis*. The Journal of investigative dermatology, 2011.
189. de Wit, N.J., et al., *Analysis of differential gene expression in human melanocytic tumour lesions by custom made oligonucleotide arrays*. Br J Cancer, 2005. **92**(12): p. 2249-61.
190. Smith, A.P., K. Hoek, and D. Becker, *Whole-genome expression profiling of the melanoma progression pathway reveals marked molecular differences between nevi/melanoma in situ and advanced-stage melanomas*. Cancer Biol Ther, 2005. **4**(9): p. 1018-29.
191. Nambiar, S., et al., *Signaling networks in cutaneous melanoma metastasis identified by complementary DNA microarrays*. Arch Dermatol, 2005. **141**(2): p. 165-73.
192. Zhou, Y., et al., *Osteopontin expression correlates with melanoma invasion*. The Journal of investigative dermatology, 2005. **124**(5): p. 1044-52.
193. Riker, A.I., et al., *The gene expression profiles of primary and metastatic melanoma yields a transition point of tumor progression and metastasis*. BMC Med Genomics, 2008. **1**: p. 13.
194. Journe, F., et al., *TYRP1 mRNA expression in melanoma metastases correlates with clinical outcome*. British journal of cancer, 2011. **105**(11): p. 1726-32.
195. Berger, M.F., et al., *Integrative analysis of the melanoma transcriptome*. Genome Res, 2010. **20**(4): p. 413-27.
196. Flockhart, R.J., et al., *BRAFV600E remodels the melanocyte transcriptome and induces BANCR to regulate melanoma cell migration*. Genome Res, 2012. **22**(6): p. 1006-14.
197. Malone, J.H. and B. Oliver, *Microarrays, deep sequencing and the true measure of the transcriptome*. BMC Biol, 2011. **9**: p. 34.
198. Hawkins, R.D., G.C. Hon, and B. Ren, *Next-generation genomics: an integrative approach*. Nat Rev Genet, 2010. **11**(7): p. 476-486.
199. Chapman, P.B., et al., *Improved survival with vemurafenib in melanoma with BRAF V600E mutation*. N Engl J Med, 2011. **364**(26): p. 2507-16.
200. Molife, R. and B.W. Hancock, *Adjuvant therapy of malignant melanoma*. Crit Rev Oncol Hematol, 2002. **44**(1): p. 81-102.
201. Corrie, P.G., B. Basu, and K.A. Zaki, *Targeting angiogenesis in melanoma: prospects for the future*. Ther Adv Med Oncol, 2010. **2**(6): p. 367-80.

202. Eggermont, A.M., et al., *Utility of adjuvant systemic therapy in melanoma*. Ann Oncol, 2009. **20 Suppl 6**: p. vi30-4.
203. Wheatley, K., et al., *Does adjuvant interferon-alpha for high-risk melanoma provide a worthwhile benefit? A meta-analysis of the randomised trials*. Cancer Treat Rev, 2003. **29**(4): p. 241-52.
204. Wheatley, K., et al. *Interferon-alpha as adjuvant therapy for melanoma: An individual patient data meta-analysis of randomised trials*. in ASCO Annual Meeting Proceedings Part I. 2007. Journal of Clinical Oncology.
205. Mocellin, S., et al., *Interferon alpha adjuvant therapy in patients with high-risk melanoma: a systematic review and meta-analysis*. J Natl Cancer Inst, 2010. **102**(7): p. 493-501.
206. Eggermont, A.M. and C. Robert, *New drugs in melanoma: it's a whole new world*. Eur J Cancer, 2011. **47**(14): p. 2150-7.
207. O'Day, S.J., O. Hamid, and W.J. Urba, *Targeting cytotoxic T-lymphocyte antigen-4 (CTLA-4): a novel strategy for the treatment of melanoma and other malignancies*. Cancer, 2007. **110**(12): p. 2614-27.
208. Robert, C. and F. Ghiringhelli, *What is the role of cytotoxic T lymphocyte-associated antigen 4 blockade in patients with metastatic melanoma?* Oncologist, 2009. **14**(8): p. 848-61.
209. Sarnaik, A.A., et al., *Extended dose ipilimumab with a peptide vaccine: immune correlates associated with clinical benefit in patients with resected high-risk stage IIIc/IV melanoma*. Clin Cancer Res, 2011. **17**(4): p. 896-906.
210. Pfeffer, L.M., et al., *Biological properties of recombinant alpha-interferons: 40th anniversary of the discovery of interferons*. Cancer Res, 1998. **58**(12): p. 2489-99.
211. Plataniias, L.C., *Mechanisms of type-I- and type-II-interferon-mediated signalling*. Nat Rev Immunol, 2005. **5**(5): p. 375-86.
212. Siegal, F.P., et al., *The nature of the principal type 1 interferon-producing cells in human blood*. Science, 1999. **284**(5421): p. 1835-7.
213. Pestka, S., C.D. Krause, and M.R. Walter, *Interferons, interferon-like cytokines, and their receptors*. Immunol Rev, 2004. **202**: p. 8-32.
214. Moschos, S. and J.M. Kirkwood, *Present role and future potential of type I interferons in adjuvant therapy of high-risk operable melanoma*. Cytokine Growth Factor Rev, 2007. **18**(5-6): p. 451-8.
215. Kimchi, A., *Cytokine triggered molecular pathways that control cell cycle arrest*. J Cell Biochem, 1992. **50**(1): p. 1-9.
216. Sangfelt, O., S. Erickson, and D. Grander, *Mechanisms of interferon-induced cell cycle arrest*. Frontiers in bioscience : a journal and virtual library, 2000. **5**: p. D479-87.
217. Sangfelt, O., et al., *Molecular mechanisms underlying interferon-alpha-induced G0/G1 arrest: CKI-mediated regulation of G1 Cdk-complexes and activation of pocket proteins*. Oncogene, 1999. **18**(18): p. 2798-810.
218. Belardelli, F., et al., *Interferon-alpha in tumor immunity and immunotherapy*. Cytokine Growth Factor Rev, 2002. **13**(2): p. 119-34.
219. Hakansson, A., et al., *Tumour-infiltrating lymphocytes in metastatic malignant melanoma and response to interferon alpha treatment*. Br J Cancer, 1996. **74**(5): p. 670-6.
220. Bracarda, S., A.M. Eggermont, and J. Samuelsson, *Redefining the role of interferon in the treatment of malignant diseases*. Eur J Cancer, 2010. **46**(2): p. 284-97.

221. Ascierto, P.A. and J.M. Kirkwood, *Adjuvant therapy of melanoma with interferon: lessons of the past decade*. J Transl Med, 2008. **6**: p. 62.
222. Critchley-Thorne, R.J., et al., *Impaired interferon signaling is a common immune defect in human cancer*. Proc Natl Acad Sci U S A, 2009. **106**(22): p. 9010-5.
223. Critchley-Thorne, R.J., et al., *Down-regulation of the interferon signaling pathway in T lymphocytes from patients with metastatic melanoma*. PLoS Med, 2007. **4**(5): p. e176.
224. Simons, D.L., et al., *Interferon signaling patterns in peripheral blood lymphocytes may predict clinical outcome after high-dose interferon therapy in melanoma patients*. J Transl Med, 2011. **9**: p. 52.
225. Verma, S., et al., *Systematic review of systemic adjuvant therapy for patients at high risk for recurrent melanoma*. Cancer, 2006. **106**(7): p. 1431-42.
226. Kirkwood, J.M., et al., *Interferon alfa-2b adjuvant therapy of high-risk resected cutaneous melanoma: the Eastern Cooperative Oncology Group Trial EST 1684*. J Clin Oncol, 1996. **14**(1): p. 7-17.
227. Eggermont, A.M., et al., *Adjuvant therapy with pegylated interferon alfa-2b versus observation alone in resected stage III melanoma: final results of EORTC 18991, a randomised phase III trial*. Lancet, 2008. **372**(9633): p. 117-26.
228. Grob, J.J., et al., *Randomised trial of interferon alpha-2a as adjuvant therapy in resected primary melanoma thicker than 1.5 mm without clinically detectable node metastases. French Cooperative Group on Melanoma*. Lancet, 1998. **351**(9120): p. 1905-10.
229. Eggermont, A.M., et al., *Post-surgery adjuvant therapy with intermediate doses of interferon alfa 2b versus observation in patients with stage IIb/III melanoma (EORTC 18952): randomised controlled trial*. Lancet, 2005. **366**(9492): p. 1189-96.
230. Hancock, B.W., et al., *Adjuvant interferon in high-risk melanoma: the AIM HIGH Study--United Kingdom Coordinating Committee on Cancer Research randomized study of adjuvant low-dose extended-duration interferon Alfa-2a in high-risk resected malignant melanoma*. J Clin Oncol, 2004. **22**(1): p. 53-61.
231. Eggermont, A.M., et al., *Ulceration and stage are predictive of interferon efficacy in melanoma: results of the phase III adjuvant trials EORTC 18952 and EORTC 18991*. Eur J Cancer, 2012. **48**(2): p. 218-25.
232. Dixon, S., et al., *Quality of life and cost-effectiveness of interferon-alpha in malignant melanoma: results from randomised trial*. Br J Cancer, 2006. **94**(4): p. 492-8.
233. Kirkwood, J.M., et al., *Mechanisms and management of toxicities associated with high-dose interferon alfa-2b therapy*. J Clin Oncol, 2002. **20**(17): p. 3703-18.
234. Knickle, L.C., D.F. Spencer, and K.W. Renton, *The suppression of hepatic cytochrome P4504A mRNA mediated by the interferon inducer polyinosinic acid.polycytidylic acid*. Biochem Pharmacol, 1992. **44**(3): p. 604-8.
235. Islam, M., et al., *Differential effect of IFNalpha-2b on the cytochrome P450 enzyme system: a potential basis of IFN toxicity and its modulation by other drugs*. Clin Cancer Res, 2002. **8**(8): p. 2480-7.

236. Darnell, J.E., Jr., I.M. Kerr, and G.R. Stark, *Jak-STAT pathways and transcriptional activation in response to IFNs and other extracellular signaling proteins*. Science, 1994. **264**(5164): p. 1415-21.
237. Roberts, D.L., et al., *U.K. guidelines for the management of cutaneous melanoma*. Br J Dermatol, 2002. **146**(1): p. 7-17.
238. Butte, M.J., et al., *Programmed death-1 ligand 1 interacts specifically with the B7-1 costimulatory molecule to inhibit T cell responses*. Immunity, 2007. **27**(1): p. 111-22.
239. Brahmer, J.R., et al., *Phase I study of single-agent anti-programmed death-1 (MDX-1106) in refractory solid tumors: safety, clinical activity, pharmacodynamics, and immunologic correlates*. J Clin Oncol, 2010. **28**(19): p. 3167-75.
240. Topalian, S.L., et al., *Safety, activity, and immune correlates of anti-PD-1 antibody in cancer*. N Engl J Med, 2012. **366**(26): p. 2443-54.
241. Brahmer, J.R., et al., *Safety and activity of anti-PD-L1 antibody in patients with advanced cancer*. N Engl J Med, 2012. **366**(26): p. 2455-65.
242. Aplin, A.E., F.M. Kaplan, and Y. Shao, *Mechanisms of resistance to RAF inhibitors in melanoma*. J Invest Dermatol, 2011. **131**(9): p. 1817-20.
243. Middleton, M.R., et al., *Randomized phase III study of temozolomide versus dacarbazine in the treatment of patients with advanced metastatic malignant melanoma*. J Clin Oncol, 2000. **18**(1): p. 158-66.
244. Bedikian, A.Y., et al., *Bcl-2 antisense (oblimersen sodium) plus dacarbazine in patients with advanced melanoma: the Oblimersen Melanoma Study Group*. J Clin Oncol, 2006. **24**(29): p. 4738-45.
245. Lorigan, P., T. Eisen, and A. Hauschild, *Systemic therapy for metastatic malignant melanoma--from deeply disappointing to bright future?* Exp Dermatol, 2008. **17**(5): p. 383-94.
246. Brown, C.K. and J.M. Kirkwood, *Medical management of melanoma*. Surg Clin North Am, 2003. **83**(2): p. 283-322, viii.
247. Verbeek, B., et al., *O6-Methylguanine-DNA methyltransferase inactivation and chemotherapy*. Br Med Bull, 2008. **85**: p. 17-33.
248. Friedman, H.S., T. Kerby, and H. Calvert, *Temozolomide and treatment of malignant glioma*. Clin Cancer Res, 2000. **6**(7): p. 2585-97.
249. Patel, P.M., et al., *Extended schedule, escalated dose temozolomide versus dacarbazine in stage IV melanoma: final results of a randomised phase III study (EORTC 18032)*. Eur J Cancer, 2011. **47**(10): p. 1476-83.
250. Certa, U., et al., *Expression modes of interferon-alpha inducible genes in sensitive and resistant human melanoma cells stimulated with regular and pegylated interferon-alpha*. Gene, 2003. **315**: p. 79-86.
251. Craven, R.A., et al., *Identification of proteins regulated by interferon-alpha in resistant and sensitive malignant melanoma cell lines*. Proteomics, 2004. **4**(12): p. 3998-4009.
252. Certa, U., et al., *High density oligonucleotide array analysis of interferon-alpha2a sensitivity and transcriptional response in melanoma cells*. Br J Cancer, 2001. **85**(1): p. 107-14.
253. Certa, U., et al., *Interferon-a sensitivity in melanoma cells: detection of potential response marker genes*. Recent Results Cancer Res, 2002. **160**: p. 85-91.
254. Krepler, C., et al., *Pegylated and conventional interferon-alpha induce comparable transcriptional responses and inhibition of tumor growth in a*

- human melanoma SCID mouse xenotransplantation model*. J Invest Dermatol, 2004. **123**(4): p. 664-9.
255. Timar, J., et al., *Melanoma genomics reveals signatures of sensitivity to bio- and targeted therapies*. Cell Immunol, 2006. **244**(2): p. 154-7.
256. Reu, F.J., et al., *Overcoming resistance to interferon-induced apoptosis of renal carcinoma and melanoma cells by DNA demethylation*. J Clin Oncol, 2006. **24**(23): p. 3771-9.
257. Reu, F.J., et al., *Expression of RASSF1A, an epigenetically silenced tumor suppressor, overcomes resistance to apoptosis induction by interferons*. Cancer Res, 2006. **66**(5): p. 2785-93.
258. Borden, E.C., *Augmentation of effects of interferon-stimulated genes by reversal of epigenetic silencing: potential application to melanoma*. Cytokine Growth Factor Rev, 2007. **18**(5-6): p. 491-501.
259. Wild, P.J., et al., *Tissue microarray analysis of methylthioadenosine phosphorylase protein expression in melanocytic skin tumors*. Arch Dermatol, 2006. **142**(4): p. 471-6.
260. Wild, P.J., et al., *A potential predictive marker for response to interferon in malignant melanoma*. J Dtsch Dermatol Ges, 2007. **5**(6): p. 456-9.
261. Mowen, K.A., et al., *Arginine methylation of STAT1 modulates IFNalpha/beta-induced transcription*. Cell, 2001. **104**(5): p. 731-41.
262. Behrmann, I., et al., *Characterization of methylthioadenosin phosphorylase (MTAP) expression in malignant melanoma*. Am J Pathol, 2003. **163**(2): p. 683-90.
263. Wang, W., et al., *Modulation of signal transducers and activators of transcription 1 and 3 signaling in melanoma by high-dose IFNalpha2b*. Clin Cancer Res, 2007. **13**(5): p. 1523-31.
264. Sarasin, A. and A. Kauffmann, *Overexpression of DNA repair genes is associated with metastasis: a new hypothesis*. Mutat Res, 2008. **659**(1-2): p. 49-55.
265. Augustine, C.K., et al., *Genomic and molecular profiling predicts response to temozolomide in melanoma*. Clin Cancer Res, 2009. **15**(2): p. 502-10.
266. Passagne, I., et al., *O(6)-methylguanine DNA-methyltransferase (MGMT) overexpression in melanoma cells induces resistance to nitrosureas and temozolamide but sensitizes to mitocycin C*. Toxicology and Applied Pharmacology, 2006. **211**: p. 97-105.
267. Ma, S., et al., *O6-methylguanine-DNA-methyltransferase expression and gene polymorphisms in relation to chemotherapeutic response in metastatic melanoma*. Br J Cancer, 2003. **89**(8): p. 1517-23.
268. Middleton, M.R., et al., *O6-methylguanine-DNA methyltransferase in pretreatment tumour biopsies as a predictor of response to temozolomide in melanoma*. Br J Cancer, 1998. **78**(9): p. 1199-202.
269. Middleton, M.R., et al., *O6-methylguanine formation, repair protein depletion and clinical outcome with a 4 hr schedule of temozolomide in the treatment of advanced melanoma: results of a phase II study*. Int J Cancer, 2000. **88**(3): p. 469-73.
270. Ma, S., et al., *Analysis of O(6)-methylguanine-DNA methyltransferase in melanoma tumours in patients treated with dacarbazine-based chemotherapy*. Melanoma Res, 2002. **12**(4): p. 335-42.
271. Rietschel, P., et al., *Phase II study of extended-dose temozolomide in patients with melanoma*. J Clin Oncol, 2008. **26**(14): p. 2299-304.

272. Ranson, M., et al., *Randomized trial of the combination of lomeguatrib and temozolomide compared with temozolomide alone in chemotherapy naive patients with metastatic cutaneous melanoma*. J Clin Oncol, 2007. **25**(18): p. 2540-5.
273. Kefford, R.F., et al., *A phase I study of extended dosing with lomeguatrib with temozolomide in patients with advanced melanoma*. Br J Cancer, 2009. **100**(8): p. 1245-9.
274. Liu, L., S. Markowitz, and S.L. Gerson, *Mismatch repair mutations override alkyltransferase in conferring resistance to temozolomide but not to 1,3-bis(2-chloroethyl)nitrosourea*. Cancer Res, 1996. **56**(23): p. 5375-9.
275. Pepponi, R., et al., *The effect of O6-alkylguanine-DNA alkyltransferase and mismatch repair activities on the sensitivity of human melanoma cells to temozolomide, 1,3-bis(2-chloroethyl)1-nitrosourea, and cisplatin*. J Pharmacol Exp Ther, 2003. **304**(2): p. 661-8.
276. Boulton, S., et al., *Potentiation of temozolomide-induced cytotoxicity: a comparative study of the biological effects of poly(ADP-ribose) polymerase inhibitors*. Br J Cancer, 1995. **72**(4): p. 849-56.
277. Wu, Z., et al., *Expression of human O6-methylguanine-DNA methyltransferase in Chinese hamster ovary cells and restoration of cellular resistance to certain N-nitroso compounds*. Mol Carcinog, 1991. **4**(6): p. 482-8.
278. Plummer, R., et al., *Phase I study of the poly(ADP-ribose) polymerase inhibitor, AG014699, in combination with temozolomide in patients with advanced solid tumors*. Clin Cancer Res, 2008. **14**(23): p. 7917-23.
279. Jansen, B., et al., *Chemosensitisation of malignant melanoma by BCL2 antisense therapy*. Lancet, 2000. **356**(9243): p. 1728-33.
280. Hakansson, A., et al., *Bcl-2 expression in metastatic malignant melanoma. Importance for the therapeutic efficacy of biochemotherapy*. Cancer Immunol Immunother, 2003. **52**(4): p. 249-54.
281. Wacheck, V., et al., *Small interfering RNA targeting bcl-2 sensitizes malignant melanoma*. Oligonucleotides, 2003. **13**(5): p. 393-400.
282. Defty, C.L. and J.R. Marsden, *Melphalan in regional chemotherapy for locally recurrent metastatic melanoma*. Curr Top Med Chem, 2012. **12**(1): p. 53-60.
283. Gallagher, S.J., et al., *p16INK4a expression and absence of activated B-RAF are independent predictors of chemosensitivity in melanoma tumors*. Neoplasia, 2008. **10**(11): p. 1231-9.
284. Potti, A., et al., *Genomic signatures to guide the use of chemotherapeutics*. Nat Med, 2006. **12**(11): p. 1294-300.
285. Korrat, A., et al., *Gene signature-based prediction of tumor response to cyclophosphamide*. Cancer Genomics Proteomics, 2007. **4**(3): p. 187-95.
286. Garnett, M.J., et al., *Systematic identification of genomic markers of drug sensitivity in cancer cells*. Nature, 2012. **483**(7391): p. 570-5.
287. Barretina, J., et al., *The Cancer Cell Line Encyclopedia enables predictive modelling of anticancer drug sensitivity*. Nature, 2012. **483**(7391): p. 603-7.
288. Ugurel, S., et al., *In vitro drug sensitivity predicts response and survival after individualized sensitivity-directed chemotherapy in metastatic melanoma: a multicenter phase II trial of the Dermatologic Cooperative Oncology Group*. Clin Cancer Res, 2006. **12**(18): p. 5454-63.

289. Glaysher, S., et al., *Resistance gene expression determines the in vitro chemosensitivity of non-small cell lung cancer (NSCLC)*. BMC Cancer, 2009. **9**: p. 300.
290. Eisenhauer, E.A., et al., *New response evaluation criteria in solid tumours: revised RECIST guideline (version 1.1)*. Eur J Cancer, 2009. **45**(2): p. 228-47.
291. Cronin, M., et al., *Measurement of gene expression in archival paraffin-embedded tissues: development and performance of a 92-gene reverse transcriptase-polymerase chain reaction assay*. Am J Pathol, 2004. **164**(1): p. 35-42.
292. Masuda, N., et al., *Analysis of chemical modification of RNA from formalin-fixed samples and optimization of molecular biology applications for such samples*. Nucleic Acids Res, 1999. **27**(22): p. 4436-43.
293. Bibikova, M., et al., *Quantitative gene expression profiling in formalin-fixed, paraffin-embedded tissues using universal bead arrays*. Am J Pathol, 2004. **165**(5): p. 1799-807.
294. Ravo, M., et al., *Quantitative expression profiling of highly degraded RNA from formalin-fixed, paraffin-embedded breast tumor biopsies by oligonucleotide microarrays*. Lab Invest, 2008. **88**(4): p. 430-40.
295. Hoshida, Y., et al., *Gene expression in fixed tissues and outcome in hepatocellular carcinoma*. N Engl J Med, 2008. **359**(19): p. 1995-2004.
296. Abramovitz, M., et al., *Optimization of RNA extraction from FFPE tissues for expression profiling in the DASL assay*. Biotechniques, 2008. **44**(3): p. 417-23.
297. Bibikova, M., et al., *Expression signatures that correlated with Gleason score and relapse in prostate cancer*. Genomics, 2007. **89**(6): p. 666-72.
298. Calonje, E., *ACP best practice no 162. The histological reporting of melanoma*. Association of Clinical Pathologists. Journal of clinical pathology, 2000. **53**(8): p. 587-90.
299. Ivan, D. and V.G. Prieto, *An update on reporting histopathologic prognostic factors in melanoma*. Archives of pathology & laboratory medicine, 2011. **135**(7): p. 825-9.
300. Roepman, P., et al., *A gene expression profile for detection of sufficient tumour cells in breast tumour tissue: microarray diagnosis eligibility*. BMC Med Genomics, 2009. **2**: p. 52.
301. Kristensen, V.N., et al., *Integrated molecular profiles of invasive breast tumors and ductal carcinoma in situ (DCIS) reveal differential vascular and interleukin signaling*. Proc Natl Acad Sci U S A, 2012. **109**(8): p. 2802-7.
302. Finak, G., et al., *Stromal gene expression predicts clinical outcome in breast cancer*. Nat Med, 2008. **14**(5): p. 518-27.
303. Eckhart, L., et al., *Melanin binds reversibly to thermostable DNA polymerase and inhibits its activity*. Biochem Biophys Res Commun, 2000. **271**(3): p. 726-30.
304. Slominski, A., R. Paus, and M.C. Mihm, *Inhibition of melanogenesis as an adjuvant strategy in the treatment of melanotic melanomas: selective review and hypothesis*. Anticancer Res, 1998. **18**(5B): p. 3709-15.
305. Slominski, A., et al., *Melanin pigmentation in mammalian skin and its hormonal regulation*. Physiol Rev, 2004. **84**(4): p. 1155-228.
306. Dorrie, J., et al., *An improved method for RNA isolation and removal of melanin contamination from melanoma tissue: implications for tumor*

- antigen detection and amplification*. J Immunol Methods, 2006. **313**(1-2): p. 119-28.
307. Liu, A., *Laser capture microdissection in the tissue biorepository*. Journal of biomolecular techniques : JBT, 2010. **21**(3): p. 120-5.
308. Micke, P., et al., *Laser-assisted cell microdissection using the PALM system*. Methods in molecular biology, 2005. **293**: p. 151-66.
309. Burgemeister, R., *Nucleic acids extraction from laser microdissected FFPE tissue sections*. Methods in molecular biology, 2011. **724**: p. 117-29.
310. Espina, V., et al., *Laser-capture microdissection*. Nature protocols, 2006. **1**(2): p. 586-603.
311. Stich, M., et al., *Live cell catapulting and recultivation*. Pathology, research and practice, 2003. **199**(6): p. 405-9.
312. Farrell, R., *RNA Methodologies. A laboratory guide for isolation and characterization* 2005, Burlington: Elsevier. pp. 103-168.
313. Roche Diagnostics GmbH, *High Pure RNA Paraffin Kit*, 2008, Roche Diagnostics GmbH.
314. Qiagen, *QIAamp DNA FFPE Tissue Handbook*, 2007, Qiagen.
315. Specht, K., et al., *Quantitative gene expression analysis in microdissected archival formalin-fixed and paraffin-embedded tumor tissue*. Am J Pathol, 2001. **158**(2): p. 419-29.
316. Li, J., et al., *Improved RNA quality and TaqMan Pre-amplification method (PreAmp) to enhance expression analysis from formalin fixed paraffin embedded (FFPE) materials*. BMC Biotechnol, 2008. **8**: p. 10.
317. Qiagen, *AllPrep DNA/RNA FFPE Handbook*, 2010, Qiagen.
318. Invitrogen Life Technologies, *SuperScript First-Strand Synthesis System for RT-PCR*, 2003, Invitrogen Life Technologies.
319. Applied Biosystems. *High Capacity cDNA Reverse Transcription Kits*. 2010 [cited 2012 24th July]; Available from: http://tools.invitrogen.com/content/sfs/manuals/cms_042557.pdf.
320. Applied Biosystems. *Product Bulletin: High Capacity RNA-to-cDNA Master Mix*. 2008 February 2008 [cited 2012 15th February]; Available from: http://tools.invitrogen.com/content/sfs/brochures/cms_049862.pdf.
321. Qiagen, *RNeasy Mini Handbook*, 2006, Qiagen.
322. Qiagen, *QIAamp DNA Mini and Blood Mini Handbook*, 2007, Qiagen.
323. Fan, J.B., et al., *A versatile assay for high-throughput gene expression profiling on universal array matrices*. Genome Res, 2004. **14**(5): p. 878-85.
324. Reinholz, M.M., et al., *Expression profiling of formalin-fixed paraffin-embedded primary breast tumors using cancer-specific and whole genome gene panels on the DASL(R) platform*. BMC Med Genomics, 2010. **3**: p. 60.
325. Fan, J.B., et al., *Highly parallel SNP genotyping*. Cold Spring Harb Symp Quant Biol, 2003. **68**: p. 69-78.
326. April, C., et al., *Whole-genome gene expression profiling of formalin-fixed, paraffin-embedded tissue samples*. PLoS One, 2009. **4**(12): p. e8162.
327. Cairns, J.M., et al., *BASH: a tool for managing BeadArray spatial artefacts*. Bioinformatics, 2008. **24**(24): p. 2921-2.
328. Gunderson, K.L., et al., *Decoding randomly ordered DNA arrays*. Genome Res, 2004. **14**(5): p. 870-7.

329. Galinsky, V.L., *Automatic registration of microarray images. II. Hexagonal grid*. Bioinformatics, 2003. **19**(14): p. 1832-6.
330. Illumina Inc. *Data Sheet: RNA Analysis Whole-Genome DASL HT Assay for Expression Profiling in FFPE Samples*. 2010 14th October 2010 [cited 2012 16th February]; Available from: http://www.illumina.com/Documents/products/datasheets/datasheet_whole_genome_dasl.pdf.
331. National Center for Biotechnology Information. *RefSeq*. 2012 [cited 2012 16th February]; Available from: <http://www.ncbi.nlm.nih.gov/RefSeq/>.
332. April, C.S. and J.B. Fan, *Gene expression profiling in formalin-fixed, paraffin-embedded tissues using the whole-genome DASL assay*. Methods Mol Biol, 2011. **784**: p. 77-98.
333. Fountzilias, E., et al., *Identification and validation of gene expression models that predict clinical outcome in patients with early-stage laryngeal cancer*. Ann Oncol, 2012.
334. Sadi, A.M., et al., *Clinical relevance of DNA microarray analyses using archival formalin-fixed paraffin-embedded breast cancer specimens*. BMC Cancer, 2011. **11**: p. 253:1-13.
335. Harbst, K., et al., *Molecular Profiling Reveals Low- and High-Grade Forms of Primary Melanoma*. Clin Cancer Res, 2012.
336. Schroeder, A., et al., *The RIN: an RNA integrity number for assigning integrity values to RNA measurements*. BMC Mol Biol, 2006. **7**: p. 3.
337. Smyth, G.K., Y.H. Yang, and T. Speed, *Statistical issues in cDNA microarray data analysis*. Methods Mol Biol, 2003. **224**: p. 111-36.
338. Workman, C., et al., *A new non-linear normalization method for reducing variability in DNA microarray experiments*. Genome Biol, 2002. **3**(9): p. research0048.
339. Applied Biosystems. *Taqman Gene Expression Master Mix Protocol*. 2007 February 2007 [cited 2012 19th February]; Available from: http://www3.appliedbiosystems.com/cms/groups/mcb_support/documents/generalddocuments/cms_039284.pdf.
340. Livak, K.J. and T.D. Schmittgen, *Analysis of relative gene expression data using real-time quantitative PCR and the 2^{(-Delta Delta C(T))} Method*. Methods, 2001. **25**(4): p. 402-8.
341. Applied Biosystems. *Guide to Performing Relative Quantitation of Gene Expression Using Real-Time Quantitative PCR*. 2008 [cited 2012 15th February]; Available from: http://www3.appliedbiosystems.com/cms/groups/mcb_support/documents/generalddocuments/cms_042380.pdf.
342. Pfaffl, M.W., *A new mathematical model for relative quantification in real-time RT-PCR*. Nucleic Acids Res, 2001. **29**(9): p. e45.
343. Vandesompele, J., et al., *Accurate normalization of real-time quantitative RT-PCR data by geometric averaging of multiple internal control genes*. Genome Biol, 2002. **3**(7): p. RESEARCH0034.
344. Life Technologies. *Custom Taqman Array Cards*. 2012 [cited 2012 14th May]; Available from: http://www3.appliedbiosystems.com/cms/groups/mcb_marketing/documents/generalddocuments/cms_040127.pdf.
345. Melin, J. and S.R. Quake, *Microfluidic large-scale integration: the evolution of design rules for biological automation*. Annu Rev Biophys Biomol Struct, 2007. **36**: p. 213-31.

346. Jang, J.S., et al., *Quantitative miRNA expression analysis using fluidigm microfluidics dynamic arrays*. BMC Genomics, 2011. **12**: p. 144.
347. Spurgeon, S.L., R.C. Jones, and R. Ramakrishnan, *High throughput gene expression measurement with real time PCR in a microfluidic dynamic array*. PLoS One, 2008. **3**(2): p. e1662.
348. Applied Biosystems. *Taqman PreAmp Master Mix Kit*. 2010 [cited 2012 11th May]; Available from: http://tools.invitrogen.com/content/sfs/manuals/cms_039316.pdf.
349. Citri, A., et al., *Comprehensive qPCR profiling of gene expression in single neuronal cells*. Nat Protoc, 2012. **7**(1): p. 118-27.
350. Mao, F., W.Y. Leung, and X. Xin, *Characterization of EvaGreen and the implication of its physicochemical properties for qPCR applications*. BMC biotechnology, 2007. **7**: p. 76.
351. Fluidigm Corporation, *Fluidigm 96:96 Real-Time PCR Workflow Quick Reference*, Fluidigm Corporation.
352. Ronaghi, M., M. Uhlen, and P. Nyren, *A sequencing method based on real-time pyrophosphate*. Science, 1998. **281**(5375): p. 363, 365.
353. Sivertsson, A., et al., *Pyrosequencing as an alternative to single-strand conformation polymorphism analysis for detection of N-ras mutations in human melanoma metastases*. Clin Chem, 2002. **48**(12): p. 2164-70.
354. Garcia, C.A., et al., *Mutation detection by pyrosequencing: sequencing of exons 5-8 of the p53 tumor suppressor gene*. Gene, 2000. **253**(2): p. 249-57.
355. Ronaghi, M., *Pyrosequencing sheds light on DNA sequencing*. Genome Res, 2001. **11**(1): p. 3-11.
356. Spittle, C., et al., *Application of a BRAF pyrosequencing assay for mutation detection and copy number analysis in malignant melanoma*. J Mol Diagn, 2007. **9**(4): p. 464-71.
357. Yancovitz, M., et al., *Intra- and inter-tumor heterogeneity of BRAF(V600E) mutations in primary and metastatic melanoma*. PLoS One, 2012. **7**(1): p. e29336.
358. Hurst, C.D., et al., *A SNaPshot assay for the rapid and simple detection of four common hotspot codon mutations in the PIK3CA gene*. BMC research notes, 2009. **2**: p. 66.
359. Applied Biosystems. *SNaPshot Kit Analysis Getting Started Guide*. 2005 June 2006 [cited 2012 20th February]; Available from: http://tools.invitrogen.com/content/sfs/manuals/cms_042037.pdf.
360. Dias-Santagata, D., et al., *Rapid targeted mutational analysis of human tumours: a clinical platform to guide personalized cancer medicine*. EMBO Mol Med, 2010. **2**(5): p. 146-58.
361. Wellcome Trust Sanger Institute. *Catalogue of Somatic Mutations in Cancer*. 2012 18th January [cited 2012 21st February]; Available from: <http://www.sanger.ac.uk/genetics/CGP/cosmic/>.
362. Cytoscape Consortium. *Cytoscape*. 2010 [cited 2012 25th January]; Available from: <http://www.cytoscape.org/>.
363. Shannon, P., et al., *Cytoscape: a software environment for integrated models of biomolecular interaction networks*. Genome research, 2003. **13**(11): p. 2498-504.
364. Flanders Interuniversity Institute for Biotechnology (VIB). *BiNGO*. 2010 [cited 2012 25th January 2012]; Available from: <http://www.psb.ugent.be/cbd/papers/BiNGO/Home.html>.

365. Maere, S., K. Heymans, and M. Kuiper, *BiNGO: a Cytoscape plugin to assess overrepresentation of gene ontology categories in biological networks*. *Bioinformatics*, 2005. **21**(16): p. 3448-9.
366. Bland, J.M. and D.G. Altman, *Multiple significance tests: the Bonferroni method*. *BMJ*, 1995. **310**(6973): p. 170.
367. Benjamini, Y. and Y. Hochberg, *Controlling the False Discovery Rate: A practical and powerful approach to multiple testing*. *Journal of the Royal Statistical Society, Series B (Methodological)*, 1995. **57**(1): p. 289-300.
368. National Institute of Allergy and Infectious Diseases (NIAID), N. *DAVID Bioinformatics Resources 6.7*. 2012 [cited 2012 25th January]; Available from: <http://david.abcc.ncifcrf.gov/>.
369. Huang, D.W., B.T. Sherman, and R.A. Lempicki, *Systematic and integrative analysis of large gene lists using DAVID bioinformatics resources*. *Nat Protoc*, 2009. **4**(1): p. 44-57.
370. Khatri, P. and S. Draghici, *Ontological analysis of gene expression data: current tools, limitations, and open problems*. *Bioinformatics*, 2005. **21**(18): p. 3587-95.
371. Huang, D.W., B.T. Sherman, and R.A. Lempicki, *Bioinformatics enrichment tools: paths toward the comprehensive functional analysis of large gene lists*. *Nucleic acids research*, 2009. **37**(1): p. 1-13.
372. Dennis, G., Jr., et al., *DAVID: Database for Annotation, Visualization, and Integrated Discovery*. *Genome biology*, 2003. **4**(5): p. P3.
373. Hosack, D.A., et al., *Identifying biological themes within lists of genes with EASE*. *Genome biology*, 2003. **4**(10): p. R70.
374. Ficenec, D., et al., *Computational knowledge integration in biopharmaceutical research*. *Briefings in bioinformatics*, 2003. **4**(3): p. 260-78.
375. Calvano, S.E., et al., *A network-based analysis of systemic inflammation in humans*. *Nature*, 2005. **437**(7061): p. 1032-7.
376. Ingenuity Systems, I., *Datasheet: IPA*, in *Ingenuity Systems, Inc., I.* Ingenuity Systems, Editor 2011, Ingenuity Systems, Inc.: Redwood City.
377. Shanley, T.P., et al., *Genome-level longitudinal expression of signaling pathways and gene networks in pediatric septic shock*. *Molecular medicine*, 2007. **13**(9-10): p. 495-508.
378. Ingenuity Systems Proprietary and Confidential, *IPA Network Generation Algorithm*, 2005.
379. Nelson, P.N., J. Astley, and P. Warren, *Monoclonal antibodies: the generation and application of 'tools of the trade' within biomedical science*, in *Molecular Biology in Cellular Pathology*, J. Crocker and P.G. Murray, Editors. 2003, Wiley: Chichester, UK. p. pp. 329-349.
380. Ramos-Vara, J.A., *Technical aspects of immunohistochemistry*. *Vet Pathol*, 2005. **42**(4): p. 405-26.
381. Abbas, A.K., A.H. Lichtman, and S. Pillai, *Appendix III - Lab techniques commonly used in immunology*, in *Cellular and Molecular Immunology*, A.K. Abbas, A.H. Lichtman, and S. Pillai, Editors. 2007, Saunders Elsevier: Philadelphia. p. pp. 525-537.
382. Doeden, K., et al., *Lymphatic invasion in cutaneous melanoma is associated with sentinel lymph node metastasis*. *J Cutan Pathol*, 2009. **36**(7): p. 772-80.
383. Petersson, F., et al., *Immunohistochemical detection of lymphovascular invasion with D2-40 in melanoma correlates with sentinel lymph node*

- status, metastasis and survival.* J Cutan Pathol, 2009. **36**(11): p. 1157-63.
384. Niakosari, F., et al., *Lymphatic invasion identified by monoclonal antibody D2-40, younger age, and ulceration: predictors of sentinel lymph node involvement in primary cutaneous melanoma.* Arch Dermatol, 2008. **144**(4): p. 462-7.
385. Xu, X., et al., *Lymphatic invasion revealed by multispectral imaging is common in primary melanomas and associates with prognosis.* Hum Pathol, 2008. **39**(6): p. 901-9.
386. Niakosari, F., et al., *Detection of lymphatic invasion in primary melanoma with monoclonal antibody D2-40: a new selective immunohistochemical marker of lymphatic endothelium.* Arch Dermatol, 2005. **141**(4): p. 440-4.
387. Kahn, H.J., D. Bailey, and A. Marks, *Monoclonal antibody D2-40, a new marker of lymphatic endothelium, reacts with Kaposi's sarcoma and a subset of angiosarcomas.* Mod Pathol, 2002. **15**(4): p. 434-40.
388. Marks, A., et al., *Characterization and distribution of an oncofetal antigen (M2A antigen) expressed on testicular germ cell tumours.* Br J Cancer, 1999. **80**(3-4): p. 569-78.
389. Mohammed, R.A., et al., *Improved methods of detection of lymphovascular invasion demonstrate that it is the predominant method of vascular invasion in breast cancer and has important clinical consequences.* Am J Surg Pathol, 2007. **31**(12): p. 1825-33.
390. Mohammed, R.A., et al., *Vascular invasion in breast cancer; an overview of recent prognostic developments and molecular pathophysiological mechanisms.* Histopathology, 2009. **55**(1): p. 1-9.
391. Nickoloff, B.J., *The human progenitor cell antigen (CD34) is localized on endothelial cells, dermal dendritic cells, and perifollicular cells in formalin-fixed normal skin, and on proliferating endothelial cells and stromal spindle-shaped cells in Kaposi's sarcoma.* Arch Dermatol, 1991. **127**(4): p. 523-9.
392. Falini, B., et al., *PG-M1: a new monoclonal antibody directed against a fixative-resistant epitope on the macrophage-restricted form of the CD68 molecule.* Am J Pathol, 1993. **142**(5): p. 1359-72.
393. Jensen, T.O., et al., *Macrophage markers in serum and tumor have prognostic impact in American Joint Committee on Cancer stage I/II melanoma.* J Clin Oncol, 2009. **27**(20): p. 3330-7.
394. Lau, S.K., P.G. Chu, and L.M. Weiss, *CD163: a specific marker of macrophages in paraffin-embedded tissue samples.* Am J Clin Pathol, 2004. **122**(5): p. 794-801.
395. Shi, L., et al., *Clinicopathological implications of tumour-associated macrophages and vascularization in sinonasal melanoma.* J Int Med Res, 2010. **38**(4): p. 1276-86.
396. Kiss, J., et al., *Association of microvessel density with infiltrating cells in human cutaneous malignant melanoma.* Pathol Oncol Res, 2007. **13**(1): p. 21-31.
397. Piras, F., et al., *The predictive value of CD8, CD4, CD68, and human leukocyte antigen-D-related cells in the prognosis of cutaneous malignant melanoma with vertical growth phase.* Cancer, 2005. **104**(6): p. 1246-54.
398. Mohammed, R.A., et al., *Objective assessment of lymphatic and blood vascular invasion in lymph node-negative breast carcinoma: findings*

- from a large case series with long-term follow-up. *J Pathol*, 2011. **223**(3): p. 358-65.
399. Ammar, A., et al., *Lymphatic expression of CLEVER-1 in breast cancer and its relationship with lymph node metastasis*. *Anal Cell Pathol (Amst)*, 2011. **34**(1-2): p. 67-78.
400. Mohammed, R.A., et al., *Lymphatic and angiogenic characteristics in breast cancer: morphometric analysis and prognostic implications*. *Breast Cancer Res Treat*, 2009. **113**(2): p. 261-73.
401. Elder, D. and G. Murphy, *Malignant tumors (melanomas and related lesions)*. *Atlas of Tumor Pathology: Melanocytic Tumors of the Skin 2 (third series)*1991, Washington: Armed Forces Institute of Pathology.
402. Vuoristo, M., et al., *Increased gene expression levels of collagen receptor integrins are associated with decreased survival parameters in patients with advanced melanoma*. *Melanoma Res*, 2007. **17**(4): p. 215-23.
403. Udart, M., et al., *Chromosome 7 aneusomy. A marker for metastatic melanoma? Expression of the epidermal growth factor receptor gene and chromosome 7 aneusomy in nevi, primary malignant melanomas and metastases*. *Neoplasia*, 2001. **3**(3): p. 245-54.
404. Bresters, D., et al., *The duration of fixation influences the yield of HCV cDNA-PCR products from formalin-fixed, paraffin-embedded liver tissue*. *J Virol Methods*, 1994. **48**(2-3): p. 267-72.
405. Madabusi, L.V., G.J. Latham, and B.F. Andruss, *RNA extraction for arrays*. *Methods Enzymol*, 2006. **411**: p. 1-14.
406. Scicchitano, M.S., et al., *Preliminary comparison of quantity, quality, and microarray performance of RNA extracted from formalin-fixed, paraffin-embedded, and unfixed frozen tissue samples*. *J Histochem Cytochem*, 2006. **54**(11): p. 1229-37.
407. Laga, A.C. and G.F. Murphy, *Cellular heterogeneity in vertical growth phase melanoma*. *Archives of pathology & laboratory medicine*, 2010. **134**(12): p. 1750-7.
408. Hoefig, K.P., et al., *Unlocking pathology archives for microRNA-profiling*. *Anticancer research*, 2008. **28**(1A): p. 119-23.
409. Brizova, H., et al., *Quantitative measurement of cyclin D1 mRNA, a potent diagnostic tool to separate mantle cell lymphoma from other B-cell lymphoproliferative disorders*. *Diagnostic molecular pathology : the American journal of surgical pathology, part B*, 2008. **17**(1): p. 39-50.
410. Knudsen, B.S., et al., *Evaluation of the branched-chain DNA assay for measurement of RNA in formalin-fixed tissues*. *The Journal of molecular diagnostics : JMD*, 2008. **10**(2): p. 169-76.
411. Linton, K.M., et al., *Acquisition of biologically relevant gene expression data by Affymetrix microarray analysis of archival formalin-fixed paraffin-embedded tumours*. *British journal of cancer*, 2008. **98**(8): p. 1403-14.
412. Bibikova, M., et al., *Gene expression profiles in formalin-fixed, paraffin-embedded tissues obtained with a novel assay for microarray analysis*. *Clinical chemistry*, 2004. **50**(12): p. 2384-6.
413. Illumina, I., *RNA Profiling with the DASL Assay (Technical Bulletin)*, I. Illumina, Editor 2005: San Diego.
414. Illumina, I., *Array-Based Gene Expression Analysis (Data Sheet)*, I. Illumina, Editor 2011, Illumina, Inc: San Diego

415. Slominski, A., B. Zbytek, and R. Slominski, *Inhibitors of melanogenesis increase toxicity of cyclophosphamide and lymphocytes against melanoma cells*. *Int J Cancer*, 2009. **124**(6): p. 1470-7.
416. Kreader, C.A., *Relief of amplification inhibition in PCR with bovine serum albumin or T4 gene 32 protein*. *Applied and environmental microbiology*, 1996. **62**(3): p. 1102-6.
417. Giambernardi, T.A., U. Rodeck, and R.J. Klebe, *Bovine serum albumin reverses inhibition of RT-PCR by melanin*. *Biotechniques*, 1998. **25**(4): p. 564-6.
418. Buback, F., et al., *Osteopontin and the skin: multiple emerging roles in cutaneous biology and pathology*. *Experimental dermatology*, 2009. **18**(9): p. 750-9.
419. Bellahcene, A., et al., *Small integrin-binding ligand N-linked glycoproteins (SIBLINGs): multifunctional proteins in cancer*. *Nature reviews. Cancer*, 2008. **8**(3): p. 212-26.
420. Geissinger, E., et al., *Autocrine stimulation by osteopontin contributes to antiapoptotic signalling of melanocytes in dermal collagen*. *Cancer research*, 2002. **62**(16): p. 4820-8.
421. Johnston, N.I., et al., *Osteopontin as a target for cancer therapy*. *Frontiers in bioscience : a journal and virtual library*, 2008. **13**: p. 4361-72.
422. Tuck, A.B., A.F. Chambers, and A.L. Allan, *Osteopontin overexpression in breast cancer: knowledge gained and possible implications for clinical management*. *Journal of cellular biochemistry*, 2007. **102**(4): p. 859-68.
423. Rangaswami, H. and G.C. Kundu, *Osteopontin stimulates melanoma growth and lung metastasis through NIK/MEKK1-dependent MMP-9 activation pathways*. *Oncology reports*, 2007. **18**(4): p. 909-15.
424. Philip, S., A. Bulbule, and G.C. Kundu, *Osteopontin stimulates tumor growth and activation of promatrix metalloproteinase-2 through nuclear factor-kappa B-mediated induction of membrane type 1 matrix metalloproteinase in murine melanoma cells*. *The Journal of biological chemistry*, 2001. **276**(48): p. 44926-35.
425. Philip, S. and G.C. Kundu, *Osteopontin induces nuclear factor kappa B-mediated promatrix metalloproteinase-2 activation through I kappa B alpha /IKK signaling pathways, and curcumin (diferuloylmethane) down-regulates these pathways*. *The Journal of biological chemistry*, 2003. **278**(16): p. 14487-97.
426. El-Tanani, M.K., *Role of osteopontin in cellular signaling and metastatic phenotype*. *Frontiers in bioscience : a journal and virtual library*, 2008. **13**: p. 4276-84.
427. Rangaswami, H., A. Bulbule, and G.C. Kundu, *Osteopontin: role in cell signaling and cancer progression*. *Trends in cell biology*, 2006. **16**(2): p. 79-87.
428. Raj, D., et al., *Survivin repression by p53, Rb and E2F2 in normal human melanocytes*. *Carcinogenesis*, 2008. **29**(1): p. 194-201.
429. Grossman, D., et al., *Expression and targeting of the apoptosis inhibitor, survivin, in human melanoma*. *The Journal of investigative dermatology*, 1999. **113**(6): p. 1076-81.
430. El-Tanani, M.K., et al., *The regulation and role of osteopontin in malignant transformation and cancer*. *Cytokine Growth Factor Rev*, 2006. **17**(6): p. 463-74.

431. Levin, V.A., *Basis and importance of Src as a target in cancer*. Cancer Treat Res, 2004. **119**: p. 89-119.
432. El-Tanani, M., et al., *Ets gene PEA3 cooperates with beta-catenin-Lef-1 and c-Jun in regulation of osteopontin transcription*. J Biol Chem, 2004. **279**(20): p. 20794-806.
433. Chatterjee, M., *Vitamin D and genomic stability*. Mutat Res, 2001. **475**(1-2): p. 69-87.
434. Morimoto, I., et al., *Identification of the osteopontin gene as a direct target of TP53*. Genes Chromosomes Cancer, 2002. **33**(3): p. 270-8.
435. El-Tanani, M.K., et al., *BRCA1 suppresses osteopontin-mediated breast cancer*. J Biol Chem, 2006. **281**(36): p. 26587-601.
436. Edlundh-Rose, E., et al., *NRAS and BRAF mutations in melanoma tumours in relation to clinical characteristics: a study based on mutation screening by pyrosequencing*. Melanoma Res, 2006. **16**(6): p. 471-8.
437. Guo, X., et al., *Identification of a ras-activated enhancer in the mouse osteopontin promoter and its interaction with a putative ETS-related transcription factor whose activity correlates with the metastatic potential of the cell*. Molecular and cellular biology, 1995. **15**(1): p. 476-87.
438. Ahrens, T., et al., *CD44 is the principal mediator of hyaluronic-acid-induced melanoma cell proliferation*. The Journal of investigative dermatology, 2001. **116**(1): p. 93-101.
439. Gobeil, S., et al., *A genome-wide shRNA screen identifies GAS1 as a novel melanoma metastasis suppressor gene*. Genes Dev, 2008. **22**(21): p. 2932-40.
440. Linja, M. and L.A. Garraway, *Stepping on the GAS: a brake pedal for melanoma metastasis?* Pigment cell & melanoma research, 2009. **22**(1): p. 8-9.
441. Rittling, S.R. and A.F. Chambers, *Role of osteopontin in tumour progression*. British journal of cancer, 2004. **90**(10): p. 1877-81.
442. Rodrigues, L.R., et al., *The role of osteopontin in tumor progression and metastasis in breast cancer*. Cancer epidemiology, biomarkers & prevention : a publication of the American Association for Cancer Research, cosponsored by the American Society of Preventive Oncology, 2007. **16**(6): p. 1087-97.
443. Maier, T., et al., *Osteopontin expression in plasma of melanoma patients and in melanocytic tumours*. Journal of the European Academy of Dermatology and Venereology : JEADV, 2011.
444. Kluger, H.M., et al., *Plasma markers for identifying patients with metastatic melanoma*. Clinical cancer research : an official journal of the American Association for Cancer Research, 2011. **17**(8): p. 2417-25.
445. Mitra, A., et al., *Melanoma sentinel node biopsy and prediction models for relapse and overall survival*. Br J Cancer, 2010. **103**(8): p. 1229-36.
446. Allan, A.L., et al., *Role of the integrin-binding protein osteopontin in lymphatic metastasis of breast cancer*. Am J Pathol, 2006. **169**(1): p. 233-46.
447. Kim, S.Y., J.W. Lee, and I.S. Sohn, *Comparison of various statistical methods for identifying differential gene expression in replicated microarray data*. Stat Methods Med Res, 2006. **15**(1): p. 3-20.
448. Slonim, D.K., *From patterns to pathways: gene expression data analysis comes of age*. Nature genetics, 2002. **32 Suppl**: p. 502-8.

449. Allison, D.B., et al., *Microarray data analysis: from disarray to consolidation and consensus*. Nature reviews. Genetics, 2006. **7**(1): p. 55-65.
450. Tusher, V.G., R. Tibshirani, and G. Chu, *Significance analysis of microarrays applied to the ionizing radiation response*. Proceedings of the National Academy of Sciences of the United States of America, 2001. **98**(9): p. 5116-21.
451. Werner, T., *Bioinformatics applications for pathway analysis of microarray data*. Current opinion in biotechnology, 2008. **19**(1): p. 50-4.
452. Ashburner, M., et al., *Gene ontology: tool for the unification of biology*. The Gene Ontology Consortium. Nature genetics, 2000. **25**(1): p. 25-9.
453. Thomas, P.D., H. Mi, and S. Lewis, *Ontology annotation: mapping genomic regions to biological function*. Current opinion in chemical biology, 2007. **11**(1): p. 4-11.
454. Ekins, S., et al., *Pathway mapping tools for analysis of high content data*. Methods in molecular biology, 2007. **356**: p. 319-50.
455. Schmittgen, T.D. and K.J. Livak, *Analyzing real-time PCR data by the comparative C(T) method*. Nat Protoc, 2008. **3**(6): p. 1101-8.
456. Applied Biosystems, *Application Note: Amplification Efficiency of Taqman Gene Expression Assays*, A. Biosystems, Editor 2006, Applied Biosystems: Foster City.
457. Liu, W. and D.A. Saint, *A new quantitative method of real time reverse transcription polymerase chain reaction assay based on simulation of polymerase chain reaction kinetics*. Analytical biochemistry, 2002. **302**(1): p. 52-9.
458. Mahoney, D.J., et al., *Real-time RT-PCR analysis of housekeeping genes in human skeletal muscle following acute exercise*. Physiol Genomics, 2004. **18**(2): p. 226-31.
459. Giricz, O., J.L. Lauer-Fields, and G.B. Fields, *The normalization of gene expression data in melanoma: investigating the use of glyceraldehyde 3-phosphate dehydrogenase and 18S ribosomal RNA as internal reference genes for quantitative real-time PCR*. Anal Biochem, 2008. **380**(1): p. 137-9.
460. Bustin, S.A., *Absolute quantification of mRNA using real-time reverse transcription polymerase chain reaction assays*. J Mol Endocrinol, 2000. **25**(2): p. 169-93.
461. Thellin, O., et al., *Housekeeping genes as internal standards: use and limits*. J Biotechnol, 1999. **75**(2-3): p. 291-5.
462. Williams, T.K., C.J. Yeo, and J. Brody, *Does this band make sense? Limits to expression based cancer studies*. Cancer Lett, 2008. **271**(1): p. 81-4.
463. Garbay, B., E. Boue-Grabot, and M. Garret, *Processed pseudogenes interfere with reverse transcriptase-polymerase chain reaction controls*. Anal Biochem, 1996. **237**(1): p. 157-9.
464. Harper, L.V., A.C. Hilton, and A.F. Jones, *RT-PCR for the pseudogene-free amplification of the glyceraldehyde-3-phosphate dehydrogenase gene (gapd)*. Mol Cell Probes, 2003. **17**(5): p. 261-5.
465. Nolan, T., R.E. Hands, and S.A. Bustin, *Quantification of mRNA using real-time RT-PCR*. Nat Protoc, 2006. **1**(3): p. 1559-82.
466. Kwon, M.J., et al., *Identification of novel reference genes using multiplatform expression data and their validation for quantitative gene expression analysis*. PLoS One, 2009. **4**(7): p. e6162.

467. Andersen, C.L., J.L. Jensen, and T.F. Orntoft, *Normalization of real-time quantitative reverse transcription-PCR data: a model-based variance estimation approach to identify genes suited for normalization, applied to bladder and colon cancer data sets*. *Cancer Res*, 2004. **64**(15): p. 5245-50.
468. Ringner, M., *What is principal component analysis?* *Nature biotechnology*, 2008. **26**(3): p. 303-4.
469. Kanehisa, M., et al., *KEGG for integration and interpretation of large-scale molecular data sets*. *Nucleic Acids Res*, 2012. **40**(Database issue): p. D109-14.
470. Kanehisa, M. and S. Goto, *KEGG: kyoto encyclopedia of genes and genomes*. *Nucleic Acids Res*, 2000. **28**(1): p. 27-30.
471. National Center for Biotechnology Information. *Entrez Gene 2012* [cited 2012 18th January]; Available from: <http://www.ncbi.nlm.nih.gov/gene>.
472. Koch, G.G., *Intraclass correlation coefficient*, in *Encyclopedia of Statistical Sciences*, S. Kotz and N.L. Johnson, Editors. 1982, John Wiley & Sons: New York. p. pp. 213-217.
473. Hammoud, Z.T., et al., *Differential gene expression profiling of esophageal adenocarcinoma*. *J Thorac Cardiovasc Surg*, 2009. **137**(4): p. 829-34.
474. Chien, J., et al., *Analysis of gene expression in stage I serous tumors identifies critical pathways altered in ovarian cancer*. *Gynecol Oncol*, 2009. **114**(1): p. 3-11.
475. Di Cesare, S., et al., *Expression profiling of formalin-fixed paraffin embedded primary human uveal melanomas using DASL matrices*. *J Cancer Res Clin Oncol*, 2009.
476. Garge, N.R., et al., *Reproducible clusters from microarray research: whither?* *BMC Bioinformatics*, 2005. **6 Suppl 2**: p. S10.
477. Csete, B., et al., *Poly(adenosine diphosphate-ribose) polymerase-1 expression in cutaneous malignant melanomas as a new molecular marker of aggressive tumor*. *Pathol Oncol Res*, 2009. **15**(1): p. 47-53.
478. Niezabitowski, A., et al., *Prognostic evaluation of cutaneous malignant melanoma: a clinicopathologic and immunohistochemical study*. *J Surg Oncol*, 1999. **70**(3): p. 150-60.
479. Dyrskjot, L., et al., *Identifying distinct classes of bladder carcinoma using microarrays*. *Nat Genet*, 2003. **33**(1): p. 90-6.
480. van 't Veer, L.J., et al., *Gene expression profiling predicts clinical outcome of breast cancer*. *Nature*, 2002. **415**(6871): p. 530-6.
481. Wang, Y., et al., *Gene-expression profiles to predict distant metastasis of lymph-node-negative primary breast cancer*. *Lancet*, 2005. **365**(9460): p. 671-9.
482. West, S.C., *Molecular views of recombination proteins and their control*. *Nat Rev Mol Cell Biol*, 2003. **4**(6): p. 435-45.
483. New, J.H., et al., *Rad52 protein stimulates DNA strand exchange by Rad51 and replication protein A*. *Nature*, 1998. **391**(6665): p. 407-10.
484. Benson, F.E., P. Baumann, and S.C. West, *Synergistic actions of Rad51 and Rad52 in recombination and DNA repair*. *Nature*, 1998. **391**(6665): p. 401-4.
485. Shen, Z., et al., *Specific interactions between the human RAD51 and RAD52 proteins*. *J Biol Chem*, 1996. **271**(1): p. 148-52.

486. Madhusudan, S. and M.R. Middleton, *The emerging role of DNA repair proteins as predictive, prognostic and therapeutic targets in cancer*. *Cancer Treat Rev*, 2005. **31**(8): p. 603-17.
487. Ogawa, T., et al., *Similarity of the yeast RAD51 filament to the bacterial RecA filament*. *Science*, 1993. **259**(5103): p. 1896-9.
488. Mortensen, U.H., et al., *DNA strand annealing is promoted by the yeast Rad52 protein*. *Proc Natl Acad Sci U S A*, 1996. **93**(20): p. 10729-34.
489. Stark, J.M., et al., *ATP hydrolysis by mammalian RAD51 has a key role during homology-directed DNA repair*. *J Biol Chem*, 2002. **277**(23): p. 20185-94.
490. Morrison, C., et al., *The essential functions of human Rad51 are independent of ATP hydrolysis*. *Mol Cell Biol*, 1999. **19**(10): p. 6891-7.
491. Petukhova, G., S. Stratton, and P. Sung, *Catalysis of homologous DNA pairing by yeast Rad51 and Rad54 proteins*. *Nature*, 1998. **393**(6680): p. 91-4.
492. Hiramoto, T., et al., *Mutations of a novel human RAD54 homologue, RAD54B, in primary cancer*. *Oncogene*, 1999. **18**(22): p. 3422-6.
493. Sigurdsson, S., et al., *Homologous DNA pairing by human recombination factors Rad51 and Rad54*. *J Biol Chem*, 2002. **277**(45): p. 42790-4.
494. Wong, A.K., et al., *RAD51 interacts with the evolutionarily conserved BRC motifs in the human breast cancer susceptibility gene brca2*. *J Biol Chem*, 1997. **272**(51): p. 31941-4.
495. Xia, F., et al., *Deficiency of human BRCA2 leads to impaired homologous recombination but maintains normal nonhomologous end joining*. *Proc Natl Acad Sci U S A*, 2001. **98**(15): p. 8644-9.
496. Moynahan, M.E., A.J. Pierce, and M. Jasin, *BRCA2 is required for homology-directed repair of chromosomal breaks*. *Mol Cell*, 2001. **7**(2): p. 263-72.
497. Helleday, T., et al., *DNA repair pathways as targets for cancer therapy*. *Nat Rev Cancer*, 2008. **8**(3): p. 193-204.
498. Modrich, P. and R. Lahue, *Mismatch repair in replication fidelity, genetic recombination, and cancer biology*. *Annu Rev Biochem*, 1996. **65**: p. 101-33.
499. Nitiss, J.L., *DNA topoisomerase II and its growing repertoire of biological functions*. *Nat Rev Cancer*, 2009. **9**(5): p. 327-37.
500. Schild, D. and C. Wiese, *Overexpression of RAD51 suppresses recombination defects: a possible mechanism to reverse genomic instability*. *Nucleic Acids Res*, 2009.
501. Kosari, F., et al., *Identification of prognostic biomarkers for prostate cancer*. *Clin Cancer Res*, 2008. **14**(6): p. 1734-43.
502. Wong, N., et al., *TOP2A overexpression in hepatocellular carcinoma correlates with early age onset, shorter patients survival and chemoresistance*. *Int J Cancer*, 2009. **124**(3): p. 644-52.
503. Coss, A., et al., *Increased topoisomerase IIalpha expression in colorectal cancer is associated with advanced disease and chemotherapeutic resistance via inhibition of apoptosis*. *Cancer Lett*, 2009. **276**(2): p. 228-38.
504. Brase, J.C., et al., *ERBB2 and TOP2A in breast cancer: a comprehensive analysis of gene amplification, RNA levels, and protein expression and their influence on prognosis and prediction*. *Clin Cancer Res*, 2010. **16**(8): p. 2391-401.

505. Jewell, R., et al., *Patterns of expression of DNA repair genes and relapse from melanoma*. Clin Cancer Res, 2010. **16**(21): p. 5211-21.
506. Jewell, R., et al., *Identification of differentially expressed genes in matched formalin-fixed paraffin-embedded primary and metastatic melanoma tumor pairs*. Pigment Cell Melanoma Res, 2012. **25**(2): p. 284-6.
507. Harbst, K., et al., *Multiple metastases from cutaneous malignant melanoma patients may display heterogeneous genomic and epigenomic patterns*. Melanoma Res, 2010. **20**(5): p. 381-91.
508. Augustine, C.K., et al., *Gene expression signatures as a guide to treatment strategies for in-transit metastatic melanoma*. Mol Cancer Ther, 2010. **9**(4): p. 779-90.
509. Cookson, W., et al., *Mapping complex disease traits with global gene expression*. Nat Rev Genet, 2009. **10**(3): p. 184-94.
510. Koh, S.S., et al., *Differential gene expression profiling of primary cutaneous melanoma and sentinel lymph node metastases*. Mod Pathol, 2012. **25**(6): p. 828-37.
511. Emmert-Buck, M.R., et al., *Laser capture microdissection*. Science, 1996. **274**(5289): p. 998-1001.
512. Stratagene. *Universal Human Reference RNA Catalog 740000*. 2005 [cited 2012 2nd January]; Available from: <http://www.genomics.agilent.com/files/Manual/740000.pdf>.
513. Fidler, I.J. and M.L. Kripke, *Metastasis results from preexisting variant cells within a malignant tumor*. Science, 1977. **197**(4306): p. 893-5.
514. Weigelt, B., et al., *Gene expression profiles of primary breast tumors maintained in distant metastases*. Proc Natl Acad Sci U S A, 2003. **100**(26): p. 15901-5.
515. Jacobs, T.W., et al., *Loss of tumor marker-immunostaining intensity on stored paraffin slides of breast cancer*. J Natl Cancer Inst, 1996. **88**(15): p. 1054-9.
516. DiVito, K.A., et al., *Long-term preservation of antigenicity on tissue microarrays*. Lab Invest, 2004. **84**(8): p. 1071-8.
517. Roepman, P., et al., *Maintenance of head and neck tumor gene expression profiles upon lymph node metastasis*. Cancer Res, 2006. **66**(23): p. 11110-4.
518. Vecchi, M., et al., *Breast cancer metastases are molecularly distinct from their primary tumors*. Oncogene, 2008. **27**(15): p. 2148-58.
519. Feng, Y., et al., *Differentially expressed genes between primary cancer and paired lymph node metastases predict clinical outcome of node-positive breast cancer patients*. Breast Cancer Res Treat, 2007. **103**(3): p. 319-29.
520. Ki, D.H., et al., *Whole genome analysis for liver metastasis gene signatures in colorectal cancer*. Int J Cancer, 2007. **121**(9): p. 2005-12.
521. Stoecklein, N.H. and C.A. Klein, *Genetic disparity between primary tumours, disseminated tumour cells, and manifest metastasis*. Int J Cancer, 2009. **126**(3): p. 589-98.
522. Turner, N. and R. Grose, *Fibroblast growth factor signalling: from development to cancer*. Nature reviews. Cancer, 2010. **10**(2): p. 116-29.
523. Chaffer, C.L., et al., *Aberrant fibroblast growth factor receptor signaling in bladder and other cancers*. Differentiation, 2007. **75**(9): p. 831-42.

524. Tai, A.L., et al., *Co-overexpression of fibroblast growth factor 3 and epidermal growth factor receptor is correlated with the development of nonsmall cell lung carcinoma*. *Cancer*, 2006. **106**(1): p. 146-55.
525. Tanaka, A., et al., *High frequency of fibroblast growth factor (FGF) 8 expression in clinical prostate cancers and breast tissues, immunohistochemically demonstrated by a newly established neutralizing monoclonal antibody against FGF 8*. *Cancer Res*, 1998. **58**(10): p. 2053-6.
526. Ropiquet, F., et al., *Increased expression of fibroblast growth factor 6 in human prostatic intraepithelial neoplasia and prostate cancer*. *Cancer Res*, 2000. **60**(15): p. 4245-50.
527. Murphy, T., et al., *Evidence for distinct alterations in the FGF axis in prostate cancer progression to an aggressive clinical phenotype*. *J Pathol*, 2010. **220**(4): p. 452-60.
528. Hu, L., et al., *Up-regulation of fibroblast growth factor 3 is associated with tumor metastasis and recurrence in human hepatocellular carcinoma*. *Cancer Lett*, 2007. **252**(1): p. 36-42.
529. Halaban, R., et al., *bFGF as an autocrine growth factor for human melanomas*. *Oncogene Res*, 1988. **3**(2): p. 177-86.
530. Metzner, T., et al., *Fibroblast growth factor receptors as therapeutic targets in human melanoma: synergism with BRAF inhibition*. *J Invest Dermatol*, 2011. **131**(10): p. 2087-95.
531. Birck, A., et al., *Expression of basic fibroblast growth factor and vascular endothelial growth factor in primary and metastatic melanoma from the same patients*. *Melanoma Res*, 1999. **9**(4): p. 375-81.
532. Nesbit, M., et al., *Basic fibroblast growth factor induces a transformed phenotype in normal human melanocytes*. *Oncogene*, 1999. **18**(47): p. 6469-76.
533. Wang, Y. and D. Becker, *Antisense targeting of basic fibroblast growth factor and fibroblast growth factor receptor-1 in human melanomas blocks intratumoral angiogenesis and tumor growth*. *Nat Med*, 1997. **3**(8): p. 887-93.
534. Bauvois, B., *New facets of matrix metalloproteinases MMP-2 and MMP-9 as cell surface transducers: outside-in signaling and relationship to tumor progression*. *Biochim Biophys Acta*, 2012. **1825**(1): p. 29-36.
535. Roy, R., J. Yang, and M.A. Moses, *Matrix metalloproteinases as novel biomarkers and potential therapeutic targets in human cancer*. *J Clin Oncol*, 2009. **27**(31): p. 5287-97.
536. Vaisanen, A., et al., *Matrix metalloproteinase-2 (72 kD type IV collagenase) expression occurs in the early stage of human melanocytic tumour progression and may have prognostic value*. *J Pathol*, 1996. **180**(3): p. 283-9.
537. Hofmann, U.B., et al., *Stromal cells as the major source for matrix metalloproteinase-2 in cutaneous melanoma*. *Arch Dermatol Res*, 2005. **297**(4): p. 154-60.
538. Hofmann, U.B., et al., *Expression of matrix metalloproteinases in the microenvironment of spontaneous and experimental melanoma metastases reflects the requirements for tumor formation*. *Cancer research*, 2003. **63**(23): p. 8221-5.
539. Thomas, J., F. Liu, and D.C. Link, *Mechanisms of mobilization of hematopoietic progenitors with granulocyte colony-stimulating factor*. *Curr Opin Hematol*, 2002. **9**(3): p. 183-9.

540. Metcalf, D., *The granulocyte-macrophage colony-stimulating factors*. Science, 1985. **229**(4708): p. 16-22.
541. Garnett, M.J. and R. Marais, *Guilty as charged: B-RAF is a human oncogene*. Cancer Cell, 2004. **6**(4): p. 313-9.
542. Yazdi, A.S., et al., *Mutations of the BRAF gene in benign and malignant melanocytic lesions*. J Invest Dermatol, 2003. **121**(5): p. 1160-2.
543. Daya-Grosjean, L., N. Dumaz, and A. Sarasin, *The specificity of p53 mutation spectra in sunlight induced human cancers*. J Photochem Photobiol B, 1995. **28**(2): p. 115-24.
544. Thomas, N.E., M. Berwick, and M. Cordeiro-Stone, *Could BRAF mutations in melanocytic lesions arise from DNA damage induced by ultraviolet radiation?* J Invest Dermatol, 2006. **126**(8): p. 1693-6.
545. Besaratinia, A. and G.P. Pfeifer, *Sunlight ultraviolet irradiation and BRAF V600 mutagenesis in human melanoma*. Hum Mutat, 2008. **29**(8): p. 983-91.
546. Besaratinia, A., et al., *Riboflavin activated by ultraviolet A1 irradiation induces oxidative DNA damage-mediated mutations inhibited by vitamin C*. Proc Natl Acad Sci U S A, 2007. **104**(14): p. 5953-8.
547. Leufkens, A.M., et al., *Biomarkers of oxidative stress and risk of developing colorectal cancer: a cohort-nested case-control study in the European Prospective Investigation Into Cancer and Nutrition*. Am J Epidemiol, 2012. **175**(7): p. 653-63.
548. Rajagopalan, H., et al., *Tumorigenesis: RAF/RAS oncogenes and mismatch-repair status*. Nature, 2002. **418**(6901): p. 934.
549. Long, G.V., et al., *Prognostic and clinicopathologic associations of oncogenic BRAF in metastatic melanoma*. Journal of clinical oncology : official journal of the American Society of Clinical Oncology, 2011. **29**(10): p. 1239-46.
550. Jakob, J.A., et al., *NRAS mutation status is an independent prognostic factor in metastatic melanoma*. Cancer, 2011.
551. Amanuel, B., et al., *Incidence of BRAF p.Val600Glu and p.Val600Lys mutations in a consecutive series of 183 metastatic melanoma patients from a high incidence region*. Pathology, 2012. **44**(4): p. 357-9.
552. DeLuca, A.M., A. Srinivas, and R.M. Alani, *BRAF kinase in melanoma development and progression*. Expert Rev Mol Med, 2008. **10**: p. e6.
553. Garnett, M.J., et al., *Wild-type and mutant B-RAF activate C-RAF through distinct mechanisms involving heterodimerization*. Mol Cell, 2005. **20**(6): p. 963-9.
554. Wan, P.T., et al., *Mechanism of activation of the RAF-ERK signaling pathway by oncogenic mutations of B-RAF*. Cell, 2004. **116**(6): p. 855-67.
555. Houben, R., et al., *Constitutive activation of the Ras-Raf signaling pathway in metastatic melanoma is associated with poor prognosis*. J Carcinog, 2004. **3**(1): p. 6.
556. Pratilas, C.A., et al., *(V600E)BRAF is associated with disabled feedback inhibition of RAF-MEK signaling and elevated transcriptional output of the pathway*. Proc Natl Acad Sci U S A, 2009. **106**(11): p. 4519-24.
557. Wellbrock, C., et al., *V599E-BRAF is an oncogene in melanocytes*. Cancer Res, 2004. **64**(7): p. 2338-42.
558. Hingorani, S.R., et al., *Suppression of BRAF(V599E) in human melanoma abrogates transformation*. Cancer Res, 2003. **63**(17): p. 5198-202.

559. Karasarides, M., et al., *B-RAF is a therapeutic target in melanoma*. *Oncogene*, 2004. **23**(37): p. 6292-8.
560. Sharma, A., et al., *Mutant V599EB-Raf regulates growth and vascular development of malignant melanoma tumors*. *Cancer Res*, 2005. **65**(6): p. 2412-21.
561. Dhomen, N., et al., *Oncogenic Braf induces melanocyte senescence and melanoma in mice*. *Cancer Cell*, 2009. **15**(4): p. 294-303.
562. Dankort, D., et al., *Braf(V600E) cooperates with Pten loss to induce metastatic melanoma*. *Nat Genet*, 2009. **41**(5): p. 544-52.
563. Packer, L.M., et al., *Identification of direct transcriptional targets of (V600E)BRAF/MEK signalling in melanoma*. *Pigment Cell Melanoma Res*, 2009. **22**(6): p. 785-98.
564. Viros, A., et al., *Improving melanoma classification by integrating genetic and morphologic features*. *PLoS Med*, 2008. **5**(6): p. e120.
565. Woodman, S.E., et al., *New strategies in melanoma: molecular testing in advanced disease*. *Clin Cancer Res*, 2012. **18**(5): p. 1195-200.
566. Pylayeva-Gupta, Y., E. Grabocka, and D. Bar-Sagi, *RAS oncogenes: weaving a tumorigenic web*. *Nat Rev Cancer*, 2011. **11**(11): p. 761-74.
567. Van der Lubbe, J.L., et al., *Activation of N-ras induced by ultraviolet irradiation in vitro*. *Oncogene Res*, 1988. **3**(1): p. 9-20.
568. Tormanen, V.T. and G.P. Pfeifer, *Mapping of UV photoproducts within ras proto-oncogenes in UV-irradiated cells: correlation with mutations in human skin cancer*. *Oncogene*, 1992. **7**(9): p. 1729-36.
569. Repasky, G.A., E.J. Chenette, and C.J. Der, *Renewing the conspiracy theory debate: does Raf function alone to mediate Ras oncogenesis?* *Trends in cell biology*, 2004. **14**(11): p. 639-47.
570. Meier, F., et al., *The RAS/RAF/MEK/ERK and PI3K/AKT signaling pathways present molecular targets for the effective treatment of advanced melanoma*. *Frontiers in bioscience : a journal and virtual library*, 2005. **10**: p. 2986-3001.
571. Mishra, P.J., et al., *Dissection of RAS downstream pathways in melanomagenesis: a role for Ral in transformation*. *Oncogene*, 2010. **29**(16): p. 2449-56.
572. Campbell, P.M. and C.J. Der, *Oncogenic Ras and its role in tumor cell invasion and metastasis*. *Semin Cancer Biol*, 2004. **14**(2): p. 105-14.
573. Powell, M.B., et al., *Hyperpigmentation and melanocytic hyperplasia in transgenic mice expressing the human T24 Ha-ras gene regulated by a mouse tyrosinase promoter*. *Mol Carcinog*, 1995. **12**(2): p. 82-90.
574. Chin, L., et al., *Cooperative effects of INK4a and ras in melanoma susceptibility in vivo*. *Genes Dev*, 1997. **11**(21): p. 2822-34.
575. Chin, L., et al., *Essential role for oncogenic Ras in tumour maintenance*. *Nature*, 1999. **400**(6743): p. 468-72.
576. Omholt, K., et al., *NRAS and BRAF mutations arise early during melanoma pathogenesis and are preserved throughout tumor progression*. *Clin Cancer Res*, 2003. **9**(17): p. 6483-8.
577. Greene, V.R., et al., *Frequencies of NRAS and BRAF mutations increase from the radial to the vertical growth phase in cutaneous melanoma*. *J Invest Dermatol*, 2009. **129**(6): p. 1483-8.
578. Dong, J., et al., *BRAF oncogenic mutations correlate with progression rather than initiation of human melanoma*. *Cancer Res*, 2003. **63**(14): p. 3883-5.

579. Lin, J., et al., *Polyclonality of BRAF mutations in primary melanoma and the selection of mutant alleles during progression*. British journal of cancer, 2011. **104**(3): p. 464-8.
580. Sensi, M., et al., *Mutually exclusive NRASQ61R and BRAFV600E mutations at the single-cell level in the same human melanoma*. Oncogene, 2006. **25**(24): p. 3357-64.
581. Gorden, A., et al., *Analysis of BRAF and N-RAS mutations in metastatic melanoma tissues*. Cancer research, 2003. **63**(14): p. 3955-7.
582. Jovanovic, B., et al., *Coexisting NRAS and BRAF mutations in primary familial melanomas with specific CDKN2A germline alterations*. J Invest Dermatol, 2010. **130**(2): p. 618-20.
583. Ellerhorst, J.A., et al., *Clinical correlates of NRAS and BRAF mutations in primary human melanoma*. Clinical cancer research : an official journal of the American Association for Cancer Research, 2011. **17**(2): p. 229-35.
584. Lin, J., et al., *Polyclonality of BRAF mutations in acquired melanocytic nevi*. J Natl Cancer Inst, 2009. **101**(20): p. 1423-7.
585. Sakaizawa, K., et al., *Mutation analysis of BRAF and KIT in circulating melanoma cells at the single cell level*. Br J Cancer, 2012. **106**(5): p. 939-46.
586. Colombino, M., et al., *BRAF/NRAS Mutation Frequencies Among Primary Tumors and Metastases in Patients With Melanoma*. J Clin Oncol, 2012. **30**(20): p. 2522-9.
587. Bauer, J., et al., *BRAF mutations in cutaneous melanoma are independently associated with age, anatomic site of the primary tumor, and the degree of solar elastosis at the primary tumor site*. Pigment cell & melanoma research, 2011. **24**(2): p. 345-51.
588. Broekaert, S.M., et al., *Genetic and morphologic features for melanoma classification*. Pigment Cell Melanoma Res, 2010. **23**(6): p. 763-70.
589. Devitt, B., et al., *Clinical outcome and pathological features associated with NRAS mutation in cutaneous melanoma*. Pigment Cell Melanoma Res, 2011. **24**(4): p. 666-72.
590. Shinozaki, M., et al., *Incidence of BRAF oncogene mutation and clinical relevance for primary cutaneous melanomas*. Clin Cancer Res, 2004. **10**(5): p. 1753-7.
591. Kannengiesser, C., et al., *Gene expression signature associated with BRAF mutations in human primary cutaneous melanomas*. Mol Oncol, 2008. **1**(4): p. 425-30.
592. Moreau, S., et al., *Prognostic Value of BRAF (V600) Mutations in Melanoma Patients After Resection of Metastatic Lymph Nodes*. Ann Surg Oncol, 2012.
593. Menzies, A.M., et al., *Distinguishing Clinicopathologic Features of Patients with V600E and V600K BRAF-Mutant Metastatic Melanoma*. Clin Cancer Res, 2012.
594. El-Osta, H., et al., *BRAF mutations in advanced cancers: clinical characteristics and outcomes*. PLoS One, 2011. **6**(10): p. e25806.
595. Ryu, B., et al., *Global Analysis of BRAF(V600E) Target Genes in Human Melanocytes Identifies Matrix Metalloproteinase-1 as a Critical Mediator of Melanoma Growth*. The Journal of investigative dermatology, 2011.
596. Pavay, S., et al., *Microarray expression profiling in melanoma reveals a BRAF mutation signature*. Oncogene, 2004. **23**(23): p. 4060-7.

597. Bloethner, S., et al., *Effect of common B-RAF and N-RAS mutations on global gene expression in melanoma cell lines*. Carcinogenesis, 2005. **26**(7): p. 1224-32.
598. Hoek, K.S., et al., *Metastatic potential of melanomas defined by specific gene expression profiles with no BRAF signature*. Pigment Cell Res, 2006. **19**(4): p. 290-302.
599. Johansson, P., S. Pavey, and N. Hayward, *Confirmation of a BRAF mutation-associated gene expression signature in melanoma*. Pigment Cell Res, 2007. **20**(3): p. 216-21.
600. Venesio, T., et al., *In melanocytic lesions the fraction of BRAF V600E alleles is associated with sun exposure but unrelated to ERK phosphorylation*. Mod Pathol, 2008. **21**(6): p. 716-26.
601. Troyanskaya, O., et al., *Missing value estimation methods for DNA microarrays*. Bioinformatics, 2001. **17**(6): p. 520-5.
602. Storey, J.D., *A direct approach to false discovery rates*. J R Statist Soc B, 2002. **64**(3): p. 479-498.
603. Alsina, J., et al., *Detection of mutations in the mitogen-activated protein kinase pathway in human melanoma*. Clin Cancer Res, 2003. **9**(17): p. 6419-25.
604. Goydos, J.S., et al., *Detection of B-RAF and N-RAS mutations in human melanoma*. J Am Coll Surg, 2005. **200**(3): p. 362-70.
605. Panka, D.J., R.J. Sullivan, and J.W. Mier, *An inexpensive, specific and highly sensitive protocol to detect the BrafV600E mutation in melanoma tumor biopsies and blood*. Melanoma Res, 2010. **20**(5): p. 401-7.
606. Fusi, A., et al., *Enhanced detection of BRAF-mutants by pre-PCR cleavage of wild-type sequences revealed circulating melanoma cells heterogeneity*. Eur J Cancer, 2011. **47**(13): p. 1971-6.
607. Modrek, B., et al., *Oncogenic activating mutations are associated with local copy gain*. Molecular cancer research : MCR, 2009. **7**(8): p. 1244-52.
608. Gast, A., et al., *Somatic alterations in the melanoma genome: a high-resolution array-based comparative genomic hybridization study*. Genes Chromosomes Cancer, 2010. **49**(8): p. 733-45.
609. Willmore-Payne, C., et al., *BRAF and c-kit gene copy number in mutation-positive malignant melanoma*. Hum Pathol, 2006. **37**(5): p. 520-7.
610. Lin, W.M., et al., *Modeling genomic diversity and tumor dependency in malignant melanoma*. Cancer Res, 2008. **68**(3): p. 664-73.
611. Greshock, J., et al., *Distinct patterns of DNA copy number alterations associate with BRAF mutations in melanomas and melanoma-derived cell lines*. Genes Chromosomes Cancer, 2009. **48**(5): p. 419-28.
612. Maldonado, J.L., et al., *Determinants of BRAF mutations in primary melanomas*. J Natl Cancer Inst, 2003. **95**(24): p. 1878-90.
613. Roulin, D., et al., *Prognostic value of sentinel node biopsy in 327 prospective melanoma patients from a single institution*. European journal of surgical oncology : the journal of the European Society of Surgical Oncology and the British Association of Surgical Oncology, 2008. **34**(6): p. 673-9.
614. Jane-Valbuena, J., et al., *An oncogenic role for ETV1 in melanoma*. Cancer Res, 2010. **70**(5): p. 2075-84.

615. Garraway, L.A., et al., *Integrative genomic analyses identify MITF as a lineage survival oncogene amplified in malignant melanoma*. Nature, 2005. **436**(7047): p. 117-22.
616. Rudloff, U. and Y. Samuels, *TYRO3-mediated regulation of MITF: a novel target in melanoma?* Pigment Cell Melanoma Res, 2010. **23**(1): p. 9-11.
617. Yokoyama, S., et al., *A novel recurrent mutation in MITF predisposes to familial and sporadic melanoma*. Nature, 2011. **480**(7375): p. 99-103.
618. Bertolotto, C., et al., *A SUMOylation-defective MITF germline mutation predisposes to melanoma and renal carcinoma*. Nature, 2011. **480**(7375): p. 94-8.
619. Levy, C., M. Khaled, and D.E. Fisher, *MITF: master regulator of melanocyte development and melanoma oncogene*. Trends Mol Med, 2006. **12**(9): p. 406-14.
620. Steingrimsson, E., N.G. Copeland, and N.A. Jenkins, *Melanocytes and the microphthalmia transcription factor network*. Annu Rev Genet, 2004. **38**: p. 365-411.
621. Mitra, D. and D.E. Fisher, *Transcriptional regulation in melanoma*. Hematol Oncol Clin North Am, 2009. **23**(3): p. 447-65, viii.
622. Wellbrock, C., et al., *Oncogenic BRAF regulates melanoma proliferation through the lineage specific factor MITF*. PLoS One, 2008. **3**(7): p. e2734.
623. Oikawa, T. and T. Yamada, *Molecular biology of the Ets family of transcription factors*. Gene, 2003. **303**: p. 11-34.
624. Linger, R.M., et al., *TAM receptor tyrosine kinases: biologic functions, signaling, and potential therapeutic targeting in human cancer*. Adv Cancer Res, 2008. **100**: p. 35-83.
625. Zhu, S., et al., *A genomic screen identifies TYRO3 as a MITF regulator in melanoma*. Proc Natl Acad Sci U S A, 2009. **106**(40): p. 17025-30.
626. Yokoyama, S., et al., *Pharmacologic suppression of MITF expression via HDAC inhibitors in the melanocyte lineage*. Pigment Cell Melanoma Res, 2008. **21**(4): p. 457-63.
627. Hynes, N.E. and H.A. Lane, *ERBB receptors and cancer: the complexity of targeted inhibitors*. Nat Rev Cancer, 2005. **5**(5): p. 341-54.
628. Yarden, Y. and M.X. Sliwkowski, *Untangling the ErbB signalling network*. Nat Rev Mol Cell Biol, 2001. **2**(2): p. 127-37.
629. Baselga, J. and S.M. Swain, *Novel anticancer targets: revisiting ERBB2 and discovering ERBB3*. Nat Rev Cancer, 2009. **9**(7): p. 463-75.
630. Buac, K., et al., *NRG1 / ERBB3 signaling in melanocyte development and melanoma: inhibition of differentiation and promotion of proliferation*. Pigment Cell Melanoma Res, 2009. **22**(6): p. 773-84.
631. Chin, L. and J.W. Gray, *Translating insights from the cancer genome into clinical practice*. Nature, 2008. **452**(7187): p. 553-63.
632. Guldberg, P., et al., *Disruption of the MMAC1/PTEN gene by deletion or mutation is a frequent event in malignant melanoma*. Cancer Res, 1997. **57**(17): p. 3660-3.
633. Wu, H., V. Goel, and F.G. Haluska, *PTEN signaling pathways in melanoma*. Oncogene, 2003. **22**(20): p. 3113-22.
634. Bar-Eli, M., *Gene regulation in melanoma progression by the AP-2 transcription factor*. Pigment Cell Res, 2001. **14**(2): p. 78-85.
635. Tellez, C.S., et al., *Quantitative analysis of melanocytic tissue array reveals inverse correlation between activator protein-2alpha and*

- protease-activated receptor-1 expression during melanoma progression.* J Invest Dermatol, 2007. **127**(2): p. 387-93.
636. Huang, S., et al., *Loss of AP-2 results in downregulation of c-KIT and enhancement of melanoma tumorigenicity and metastasis.* EMBO J, 1998. **17**(15): p. 4358-69.
637. Braeuer, R.R., et al., *Transcriptional control of melanoma metastasis: the importance of the tumor microenvironment.* Semin Cancer Biol, 2011. **21**(2): p. 83-8.
638. Eggermont, A.M., et al., *Is ulceration in cutaneous melanoma just a prognostic and predictive factor or is ulcerated melanoma a distinct biologic entity?* Curr Opin Oncol, 2012. **24**(2): p. 137-40.
639. McMasters, K.M., et al., *Ulceration as a predictive marker for response to adjuvant interferon therapy in melanoma.* Ann Surg, 2010. **252**(3): p. 460-5; discussion 465-6.
640. Spatz, A., et al., *The biology of melanoma prognostic factors.* Discov Med, 2010. **10**(50): p. 87-93.
641. Azzola, M.F., et al., *Tumor mitotic rate is a more powerful prognostic indicator than ulceration in patients with primary cutaneous melanoma: an analysis of 3661 patients from a single center.* Cancer, 2003. **97**(6): p. 1488-98.
642. Spatz, A., G. Batist, and A.M. Eggermont, *The biology behind prognostic factors of cutaneous melanoma.* Curr Opin Oncol, 2010. **22**(3): p. 163-8.
643. McGary, E.C., D.C. Lev, and M. Bar-Eli, *Cellular adhesion pathways and metastatic potential of human melanoma.* Cancer Biol Ther, 2002. **1**(5): p. 459-65.
644. Hsu, M.Y., et al., *E-cadherin expression in melanoma cells restores keratinocyte-mediated growth control and down-regulates expression of invasion-related adhesion receptors.* Am J Pathol, 2000. **156**(5): p. 1515-25.
645. Daniel-Wojcik, A., et al., *Cell motility affects the intensity of gap junctional coupling in prostate carcinoma and melanoma cell populations.* Int J Oncol, 2008. **33**(2): p. 309-15.
646. Haass, N.K., K.S. Smalley, and M. Herlyn, *The role of altered cell-cell communication in melanoma progression.* J Mol Histol, 2004. **35**(3): p. 309-18.
647. Fukunaga-Kalabis, M., A. Santiago-Walker, and M. Herlyn, *Matricellular proteins produced by melanocytes and melanomas: in search for functions.* Cancer Microenviron, 2008. **1**(1): p. 93-102.
648. Elliott, B., et al., *Long-term protective effect of mature DC-LAMP+ dendritic cell accumulation in sentinel lymph nodes containing micrometastatic melanoma.* Clin Cancer Res, 2007. **13**(13): p. 3825-30.
649. Colonna, M., G. Trinchieri, and Y.J. Liu, *Plasmacytoid dendritic cells in immunity.* Nat Immunol, 2004. **5**(12): p. 1219-26.
650. Melnikova, V.O. and M. Bar-Eli, *Inflammation and melanoma metastasis.* Pigment Cell Melanoma Res, 2009. **22**(3): p. 257-67.
651. Mantovani, A., et al., *Cancer-related inflammation.* Nature, 2008. **454**(7203): p. 436-44.
652. Yurkovetsky, Z.R., et al., *Multiplex analysis of serum cytokines in melanoma patients treated with interferon-alpha2b.* Clin Cancer Res, 2007. **13**(8): p. 2422-8.
653. Tas, F., et al., *The value of serum levels of IL-6, TNF-alpha, and erythropoietin in metastatic malignant melanoma: serum IL-6 level is a*

- valuable prognostic factor at least as serum LDH in advanced melanoma. Medical oncology, 2005. 22(3): p. 241-6.*
654. Mouawad, R., et al., *An unexpected inverse correlation between soluble epidermal growth factor receptor and interleukin-6 in metastatic malignant melanoma patients. Melanoma Res, 2006. 16(4): p. 335-40.*
655. Hoejberg, L., et al., *Serum interleukin-6 as a prognostic biomarker in patients with metastatic melanoma. Melanoma Res, 2012. 22(4): p. 287-93.*
656. Egger, M.E., et al., *Lymphovascular invasion as a prognostic factor in melanoma. Am Surg, 2011. 77(8): p. 992-7.*
657. Sahni, D., et al., *The use of LYVE-1 antibody for detecting lymphatic involvement in patients with malignant melanoma of known sentinel node status. Journal of clinical pathology, 2005. 58(7): p. 715-21.*
658. White, R.L., Jr., et al., *Factors predictive of the status of sentinel lymph nodes in melanoma patients from a large multicenter database. Ann Surg Oncol, 2011. 18(13): p. 3593-600.*
659. Kanehisa Laboratories. *KEGG Pathway Database. 2012 26th March [cited 2012 4th April]; Available from: http://www.kegg.jp/kegg-bin/highlight_pathway?scale=1.0&map=map04630&keyword=jak-stat.*
660. Clendenen, T.V., et al., *Factors associated with inflammation markers, a cross-sectional analysis. Cytokine, 2011. 56(3): p. 769-78.*
661. Ahmad, A., et al., *Aging and inflammation: etiological culprits of cancer. Curr Aging Sci, 2009. 2(3): p. 174-86.*
662. Phan, A., et al., *Acral lentiginous melanoma: histopathological prognostic features of 121 cases. Br J Dermatol, 2007. 157(2): p. 311-8.*
663. Tan, K.B., et al., *Subungual melanoma: a study of 124 cases highlighting features of early lesions, potential pitfalls in diagnosis, and guidelines for histologic reporting. Am J Surg Pathol, 2007. 31(12): p. 1902-12.*
664. Stewart, F.A., J. Denekamp, and V.S. Randhawa, *Skin sensitization by misonidazole: a demonstration of uniform mild hypoxia. Br J Cancer, 1982. 45(6): p. 869-77.*
665. Pouyssegur, J., F. Dayan, and N.M. Mazure, *Hypoxia signalling in cancer and approaches to enforce tumour regression. Nature, 2006. 441(7092): p. 437-43.*
666. Lartigau, E., et al., *Intratumoral oxygen tension in metastatic melanoma. Melanoma Res, 1997. 7(5): p. 400-6.*
667. Bedogni, B. and M.B. Powell, *Hypoxia, melanocytes and melanoma - survival and tumor development in the permissive microenvironment of the skin. Pigment Cell Melanoma Res, 2009. 22(2): p. 166-74.*
668. Semenza, G.L., *Targeting HIF-1 for cancer therapy. Nat Rev Cancer, 2003. 3(10): p. 721-32.*
669. Lee, J.T. and M. Herlyn, *Microenvironmental influences in melanoma progression. J Cell Biochem, 2007. 101(4): p. 862-72.*
670. Vaupel, P. and A. Mayer, *Hypoxia in cancer: significance and impact on clinical outcome. Cancer Metastasis Rev, 2007. 26(2): p. 225-39.*
671. Giatromanolaki, A., et al., *Hypoxia-inducible factors 1alpha and 2alpha are related to vascular endothelial growth factor expression and a poorer prognosis in nodular malignant melanomas of the skin. Melanoma Res, 2003. 13(5): p. 493-501.*
672. Leek, R.D., et al., *Necrosis correlates with high vascular density and focal macrophage infiltration in invasive carcinoma of the breast. Br J Cancer, 1999. 79(5-6): p. 991-5.*

673. Depasquale, I. and W.D. Thompson, *Microvessel density for melanoma prognosis*. *Histopathology*, 2005. **47**(2): p. 186-94.
674. Marcoval, J., et al., *Angiogenesis and malignant melanoma. Angiogenesis is related to the development of vertical (tumorigenic) growth phase*. *J Cutan Pathol*, 1997. **24**(4): p. 212-8.
675. Straume, O. and L.A. Akslen, *Expression of vascular endothelial growth factor, its receptors (FLT-1, KDR) and TSP-1 related to microvessel density and patient outcome in vertical growth phase melanomas*. *Am J Pathol*, 2001. **159**(1): p. 223-35.
676. Neitzel, L.T., et al., *Angiogenesis correlates with metastasis in melanoma*. *Ann Surg Oncol*, 1999. **6**(1): p. 70-4.
677. Valencak, J., et al., *Selective immunohistochemical staining shows significant prognostic influence of lymphatic and blood vessels in patients with malignant melanoma*. *Eur J Cancer*, 2004. **40**(3): p. 358-64.
678. Straume, O., H.B. Salvesen, and L.A. Akslen, *Angiogenesis is prognostically important in vertical growth phase melanomas*. *Int J Oncol*, 1999. **15**(3): p. 595-9.
679. Carnochan, P., et al., *The vascularity of cutaneous melanoma: a quantitative histological study of lesions 0.85-1.25 mm in thickness*. *Br J Cancer*, 1991. **64**(1): p. 102-7.
680. Busam, K.J., et al., *Tumor vascularity is not a prognostic factor for malignant melanoma of the skin*. *Am J Pathol*, 1995. **147**(4): p. 1049-56.
681. Ilmonen, S., et al., *Prognostic value of tumour vascularity in primary melanoma*. *Melanoma Res*, 1999. **9**(3): p. 273-8.
682. Hussein, M.R., *Tumour-associated macrophages and melanoma tumorigenesis: integrating the complexity*. *Int J Exp Pathol*, 2006. **87**(3): p. 163-76.
683. Hussein, M.R., *Dendritic cells and melanoma tumorigenesis: an insight*. *Cancer Biol Ther*, 2005. **4**(5): p. 501-5.
684. Biswas, S.K. and A. Mantovani, *Macrophage plasticity and interaction with lymphocyte subsets: cancer as a paradigm*. *Nat Immunol*, 2010. **11**(10): p. 889-96.
685. Mantovani, A., et al., *The chemokine system in diverse forms of macrophage activation and polarization*. *Trends Immunol*, 2004. **25**(12): p. 677-86.
686. Movahedi, K., et al., *Different tumor microenvironments contain functionally distinct subsets of macrophages derived from Ly6C(high) monocytes*. *Cancer Res*, 2010. **70**(14): p. 5728-39.
687. Mantovani, A., et al., *Macrophage polarization: tumor-associated macrophages as a paradigm for polarized M2 mononuclear phagocytes*. *Trends Immunol*, 2002. **23**(11): p. 549-55.
688. Sica, A. and V. Bronte, *Altered macrophage differentiation and immune dysfunction in tumor development*. *J Clin Invest*, 2007. **117**(5): p. 1155-66.
689. Mills, C.D., et al., *M-1/M-2 macrophages and the Th1/Th2 paradigm*. *J Immunol*, 2000. **164**(12): p. 6166-73.
690. Schmidt, T. and P. Carmeliet, *Blood-vessel formation: Bridges that guide and unite*. *Nature*, 2010. **465**(7299): p. 697-9.
691. Fantin, A., et al., *Tissue macrophages act as cellular chaperones for vascular anastomosis downstream of VEGF-mediated endothelial tip cell induction*. *Blood*, 2010. **116**(5): p. 829-40.

692. Kuang, D.M., et al., *Activated monocytes in peritumoral stroma of hepatocellular carcinoma foster immune privilege and disease progression through PD-L1*. J Exp Med, 2009. **206**(6): p. 1327-37.
693. Balkwill, F., K.A. Charles, and A. Mantovani, *Smoldering and polarized inflammation in the initiation and promotion of malignant disease*. Cancer Cell, 2005. **7**(3): p. 211-7.
694. Bronte, V., et al., *L-arginine metabolism in myeloid cells controls T-lymphocyte functions*. Trends Immunol, 2003. **24**(6): p. 302-6.
695. Curiel, T.J., et al., *Specific recruitment of regulatory T cells in ovarian carcinoma fosters immune privilege and predicts reduced survival*. Nat Med, 2004. **10**(9): p. 942-9.
696. Hori, S., T. Nomura, and S. Sakaguchi, *Control of regulatory T cell development by the transcription factor Foxp3*. Science, 2003. **299**(5609): p. 1057-61.
697. Woo, E.Y., et al., *Cutting edge: Regulatory T cells from lung cancer patients directly inhibit autologous T cell proliferation*. J Immunol, 2002. **168**(9): p. 4272-6.
698. Herwig, M.C. and H.E. Grossniklaus, *Role of macrophages in uveal melanoma*. Expert Rev Ophthalmol, 2011. **6**(4): p. 405-407.
699. Erdag, G., et al., *Immunotype and immunohistologic characteristics of tumor-infiltrating immune cells are associated with clinical outcome in metastatic melanoma*. Cancer Res, 2012. **72**(5): p. 1070-80.
700. Makitie, T., et al., *Tumor-infiltrating macrophages (CD68+) cells) and prognosis in malignant uveal melanoma*. Investigative ophthalmology & visual science, 2001. **42**(7): p. 1414-21.
701. Bronkhorst, I.H., et al., *Detection of M2-macrophages in uveal melanoma and relation with survival*. Investigative ophthalmology & visual science, 2011. **52**(2): p. 643-50.
702. Weaver, L.K., et al., *Pivotal advance: activation of cell surface Toll-like receptors causes shedding of the hemoglobin scavenger receptor CD163*. Journal of leukocyte biology, 2006. **80**(1): p. 26-35.
703. Buechler, C., et al., *Regulation of scavenger receptor CD163 expression in human monocytes and macrophages by pro- and antiinflammatory stimuli*. Journal of leukocyte biology, 2000. **67**(1): p. 97-103.
704. Moestrup, S.K. and H.J. Moller, *CD163: a regulated hemoglobin scavenger receptor with a role in the anti-inflammatory response*. Ann Med, 2004. **36**(5): p. 347-54.
705. Mantovani, A., et al., *Cancer-promoting tumor-associated macrophages: new vistas and open questions*. Eur J Immunol, 2011. **41**(9): p. 2522-5.
706. Getsios, S., A.C. Huen, and K.J. Green, *Working out the strength and flexibility of desmosomes*. Nat Rev Mol Cell Biol, 2004. **5**(4): p. 271-81.
707. Holthofer, B., et al., *Structure and function of desmosomes*. Int Rev Cytol, 2007. **264**: p. 65-163.
708. Garrod, D. and M. Chidgey, *Desmosome structure, composition and function*. Biochim Biophys Acta, 2008. **1778**(3): p. 572-87.
709. Li, G., et al., *Downregulation of E-cadherin and Desmoglein 1 by autocrine hepatocyte growth factor during melanoma development*. Oncogene, 2001. **20**(56): p. 8125-35.
710. Charles, C.A., et al., *A gene signature of nonhealing venous ulcers: potential diagnostic markers*. J Am Acad Dermatol, 2008. **59**(5): p. 758-71.

711. Gumbiner, B.M., *Regulation of cadherin-mediated adhesion in morphogenesis*. Nat Rev Mol Cell Biol, 2005. **6**(8): p. 622-34.
712. Tian, X., et al., *E-cadherin/beta-catenin complex and the epithelial barrier*. J Biomed Biotechnol, 2011. **2011**: p. 567305.
713. Straseski, J.A., et al., *Oxygen deprivation inhibits basal keratinocyte proliferation in a model of human skin and induces regio-specific changes in the distribution of epidermal adherens junction proteins, aquaporin-3, and glycogen*. Wound Repair Regen, 2009. **17**(4): p. 606-16.
714. Esteban, M.A., et al., *Regulation of E-cadherin expression by VHL and hypoxia-inducible factor*. Cancer Res, 2006. **66**(7): p. 3567-75.
715. Imai, T., et al., *Hypoxia attenuates the expression of E-cadherin via up-regulation of SNAIL in ovarian carcinoma cells*. Am J Pathol, 2003. **163**(4): p. 1437-47.
716. Kligys, K.R., et al., *alpha6beta4 integrin: a master regulator of the expression of integrins in human keratinocytes*. J Biol Chem, 2012.
717. de Pereda, J.M., et al., *Advances and perspectives of the architecture of hemidesmosomes: lessons from structural biology*. Cell Adh Migr, 2009. **3**(4): p. 361-4.
718. Dowling, J., Q.C. Yu, and E. Fuchs, *Beta4 integrin is required for hemidesmosome formation, cell adhesion and cell survival*. J Cell Biol, 1996. **134**(2): p. 559-72.
719. Sehgal, B.U., et al., *Integrin beta4 regulates migratory behavior of keratinocytes by determining laminin-332 organization*. J Biol Chem, 2006. **281**(46): p. 35487-98.
720. Garrod, D.R., et al., *Hyper-adhesion in desmosomes: its regulation in wound healing and possible relationship to cadherin crystal structure*. J Cell Sci, 2005. **118**(Pt 24): p. 5743-54.
721. Wallis, S., et al., *The alpha isoform of protein kinase C is involved in signaling the response of desmosomes to wounding in cultured epithelial cells*. Mol Biol Cell, 2000. **11**(3): p. 1077-92.
722. Finch, P.W. and J.S. Rubin, *Keratinocyte growth factor/fibroblast growth factor 7, a homeostatic factor with therapeutic potential for epithelial protection and repair*. Adv Cancer Res, 2004. **91**: p. 69-136.
723. Katoh, M., *Cancer genomics and genetics of FGFR2 (Review)*. Int J Oncol, 2008. **33**(2): p. 233-7.
724. Steiling, H. and S. Werner, *Fibroblast growth factors: key players in epithelial morphogenesis, repair and cytoprotection*. Current opinion in biotechnology, 2003. **14**(5): p. 533-7.
725. Wesche, J., K. Haglund, and E.M. Haugsten, *Fibroblast growth factors and their receptors in cancer*. Biochem J, 2011. **437**(2): p. 199-213.
726. Marchese, C., et al., *Human keratinocyte growth factor activity on proliferation and differentiation of human keratinocytes: differentiation response distinguishes KGF from EGF family*. J Cell Physiol, 1990. **144**(2): p. 326-32.
727. auf dem Keller, U., et al., *Keratinocyte growth factor: effects on keratinocytes and mechanisms of action*. Eur J Cell Biol, 2004. **83**(11-12): p. 607-12.
728. Werner, S., *Keratinocyte growth factor: a unique player in epithelial repair processes*. Cytokine Growth Factor Rev, 1998. **9**(2): p. 153-65.
729. Boismenu, R. and W.L. Havran, *Modulation of epithelial cell growth by intraepithelial gamma delta T cells*. Science, 1994. **266**(5188): p. 1253-5.

730. Albino, A.P., B.M. Davis, and D.M. Nanus, *Induction of growth factor RNA expression in human malignant melanoma: markers of transformation*. *Cancer Res*, 1991. **51**(18): p. 4815-20.
731. Gartside, M.G., et al., *Loss-of-function fibroblast growth factor receptor-2 mutations in melanoma*. *Molecular cancer research : MCR*, 2009. **7**(1): p. 41-54.
732. Katoh, M., *FGFR2 abnormalities underlie a spectrum of bone, skin, and cancer pathologies*. *J Invest Dermatol*, 2009. **129**(8): p. 1861-7.
733. Greulich, H. and P.M. Pollock, *Targeting mutant fibroblast growth factor receptors in cancer*. *Trends Mol Med*, 2011. **17**(5): p. 283-92.
734. Yamaguchi, F., et al., *Differential expression of two fibroblast growth factor-receptor genes is associated with malignant progression in human astrocytomas*. *Proc Natl Acad Sci U S A*, 1994. **91**(2): p. 484-8.
735. Naimi, B., et al., *Down-regulation of (IIIb) and (IIIc) isoforms of fibroblast growth factor receptor 2 (FGFR2) is associated with malignant progression in human prostate*. *Prostate*, 2002. **52**(3): p. 245-52.
736. Diez de Medina, S., et al., *Decreased expression of keratinocyte growth factor receptor in a subset of human transitional cell bladder carcinomas*. *Oncogene*, 1997. **14**: p. 323-330.
737. Brauchle, M., et al., *Large induction of keratinocyte growth factor expression by serum growth factors and pro-inflammatory cytokines in cultured fibroblasts*. *Oncogene*, 1994. **9**(11): p. 3199-204.
738. Bloethner, S., et al., *Identification of ARHGEF17, DENND2D, FGFR3, and RB1 mutations in melanoma by inhibition of nonsense-mediated mRNA decay*. *Genes Chromosomes Cancer*, 2008. **47**(12): p. 1076-85.
739. Cheng, S.L., et al., *Toxicogenomics of kojic acid on gene expression profiling of a375 human malignant melanoma cells*. *Biol Pharm Bull*, 2006. **29**(4): p. 655-69.
740. Allavena, P., et al., *The inflammatory micro-environment in tumor progression: the role of tumor-associated macrophages*. *Crit Rev Oncol Hematol*, 2008. **66**(1): p. 1-9.
741. Duluc, D., et al., *Tumor-associated leukemia inhibitory factor and IL-6 skew monocyte differentiation into tumor-associated macrophage-like cells*. *Blood*, 2007. **110**(13): p. 4319-30.
742. Lazar-Molnar, E., et al., *Autocrine and paracrine regulation by cytokines and growth factors in melanoma*. *Cytokine*, 2000. **12**(6): p. 547-54.
743. Singh, R.K., M. Gutman, and R. Radinsky, *Heterogeneity of cytokine and growth factor gene expression in human melanoma cells with different metastatic potentials*. *J Interferon Cytokine Res*, 1995. **15**(1): p. 81-7.
744. Bennicelli, J.L. and D.t. Guerry, *Production of multiple cytokines by cultured human melanomas*. *Exp Dermatol*, 1993. **2**(4): p. 186-90.
745. Ciotti, P., et al., *Cytokine expression in human primary and metastatic melanoma cells: analysis in fresh bioptic specimens*. *Melanoma Res*, 1995. **5**(1): p. 41-7.
746. Tartour, E., et al., *Serum interleukin 6 and C-reactive protein levels correlate with resistance to IL-2 therapy and poor survival in melanoma patients*. *Br J Cancer*, 1994. **69**(5): p. 911-3.
747. Lesinski, G.B., et al., *Melanoma cells exhibit variable signal transducer and activator of transcription 1 phosphorylation and a reduced response to IFN-alpha compared with immune effector cells*. *Clin Cancer Res*, 2007. **13**(17): p. 5010-9.

748. Wong, L.H., et al., *Interferon-resistant human melanoma cells are deficient in ISGF3 components, STAT1, STAT2, and p48-ISGF3gamma*. J Biol Chem, 1997. **272**(45): p. 28779-85.
749. Wang, T., et al., *Regulation of the innate and adaptive immune responses by Stat-3 signaling in tumor cells*. Nat Med, 2004. **10**(1): p. 48-54.
750. Pansky, A., et al., *Defective Jak-STAT signal transduction pathway in melanoma cells resistant to growth inhibition by interferon-alpha*. Int J Cancer, 2000. **85**(5): p. 720-5.
751. Wellbrock, C., et al., *STAT5 contributes to interferon resistance of melanoma cells*. Curr Biol, 2005. **15**(18): p. 1629-39.
752. Sarasin, A. and P. Dessen, *DNA repair pathways and human metastatic malignant melanoma*. Current molecular medicine, 2010. **10**(4): p. 413-8.
753. Hegi, M.E., et al., *Clinical trial substantiates the predictive value of O-6-methylguanine-DNA methyltransferase promoter methylation in glioblastoma patients treated with temozolomide*. Clin Cancer Res, 2004. **10**(6): p. 1871-4.
754. Friedman, H.S., et al., *DNA mismatch repair and O6-alkylguanine-DNA alkyltransferase analysis and response to Temodal in newly diagnosed malignant glioma*. J Clin Oncol, 1998. **16**(12): p. 3851-7.
755. Passagne, I., et al., *O(6)-methylguanine DNA-methyltransferase (MGMT) overexpression in melanoma cells induces resistance to nitrosoureas and temozolomide but sensitizes to mitomycin C*. Toxicol Appl Pharmacol, 2006. **211**(2): p. 97-105.
756. Busch, C., et al., *MGMT expression levels predict disease stabilisation, progression-free and overall survival in patients with advanced melanomas treated with DTIC*. European journal of cancer, 2010. **46**(11): p. 2127-33.
757. Schraml, P., et al., *Predictive value of the MGMT promoter methylation status in metastatic melanoma patients receiving first-line temozolomide plus bevacizumab in the trial SAKK 50/07*. Oncol Rep, 2012. **28**(2): p. 654-8.
758. Hassel, J.C., et al., *MGMT gene promoter methylation correlates with tolerance of temozolomide treatment in melanoma but not with clinical outcome*. Br J Cancer, 2010. **103**(6): p. 820-6.
759. Tawbi, H.A., et al., *Inhibition of DNA repair with MGMT pseudosubstrates: phase I study of lomeguatrib in combination with dacarbazine in patients with advanced melanoma and other solid tumours*. British journal of cancer, 2011.
760. Fromme, J.C., A. Banerjee, and G.L. Verdine, *DNA glycosylase recognition and catalysis*. Current opinion in structural biology, 2004. **14**(1): p. 43-9.
761. Tentori, L., et al., *Pharmacological inhibition of poly(ADP-ribose) polymerase (PARP) activity in PARP-1 silenced tumour cells increases chemosensitivity to temozolomide and to a N3-adenine selective methylating agent*. Current cancer drug targets, 2010. **10**(4): p. 368-83.
762. Khan, O.A., et al., *A phase I study of the safety and tolerability of olaparib (AZD2281, KU0059436) and dacarbazine in patients with advanced solid tumours*. British journal of cancer, 2011. **104**(5): p. 750-5.
763. Mohammed, M.Z., et al., *Development and evaluation of human AP endonuclease inhibitors in melanoma and glioma cell lines*. British journal of cancer, 2011. **104**(4): p. 653-63.

764. Parker, K.A., et al., *The molecular basis of the chemosensitivity of metastatic cutaneous melanoma to chemotherapy*. Journal of clinical pathology, 2010. **63**(11): p. 1012-20.
765. Meric-Bernstam, F. and A.M. Gonzalez-Angulo, *Targeting the mTOR signaling network for cancer therapy*. J Clin Oncol, 2009. **27**(13): p. 2278-87.
766. Therasse, P., et al., *New guidelines to evaluate the response to treatment in solid tumors. European Organization for Research and Treatment of Cancer, National Cancer Institute of the United States, National Cancer Institute of Canada*. J Natl Cancer Inst, 2000. **92**(3): p. 205-16.
767. Wood, R.D., et al., *Human DNA repair genes*. Science, 2001. **291**(5507): p. 1284-9.
768. Wood, R.D., M. Mitchell, and T. Lindahl, *Human DNA repair genes, 2005*. Mutat Res, 2005. **577**(1-2): p. 275-83.
769. Branzei, D. and M. Foiani, *Regulation of DNA repair throughout the cell cycle*. Nat Rev Mol Cell Biol, 2008. **9**(4): p. 297-308.
770. Figl, A., et al., *Single nucleotide polymorphisms in DNA repair genes XRCC1 and APEX1 in progression and survival of primary cutaneous melanoma patients*. Mutation research, 2009. **661**(1-2): p. 78-84.
771. Tentori, L., et al., *Stable depletion of poly (ADP-ribose) polymerase-1 reduces in vivo melanoma growth and increases chemosensitivity*. Eur J Cancer, 2008. **44**(9): p. 1302-14.
772. Trivedi, R.N., et al., *The role of base excision repair in the sensitivity and resistance to temozolomide-mediated cell death*. Cancer research, 2005. **65**(14): p. 6394-400.
773. Goode, E.L., C.M. Ulrich, and J.D. Potter, *Polymorphisms in DNA repair genes and associations with cancer risk*. Cancer epidemiology, biomarkers & prevention : a publication of the American Association for Cancer Research, cosponsored by the American Society of Preventive Oncology, 2002. **11**(12): p. 1513-30.
774. Mirzoeva, O.K., T. Kawaguchi, and R.O. Pieper, *The Mre11/Rad50/Nbs1 complex interacts with the mismatch repair system and contributes to temozolomide-induced G2 arrest and cytotoxicity*. Mol Cancer Ther, 2006. **5**(11): p. 2757-66.
775. Collis, S.J., et al., *Enhanced radiation and chemotherapy-mediated cell killing of human cancer cells by small inhibitory RNA silencing of DNA repair factors*. Cancer Res, 2003. **63**(7): p. 1550-4.
776. Shinohara, E.T., et al., *DNA-dependent protein kinase is a molecular target for the development of noncytotoxic radiation-sensitizing drugs*. Cancer Res, 2005. **65**(12): p. 4987-92.
777. Francia, G., et al., *Down-regulation of DNA mismatch repair proteins in human and murine tumor spheroids: implications for multicellular resistance to alkylating agents*. Mol Cancer Ther, 2005. **4**(10): p. 1484-94.
778. Matthews, D.J., et al., *Pharmacological abrogation of S-phase checkpoint enhances the anti-tumor activity of gemcitabine in vivo*. Cell Cycle, 2007. **6**(1): p. 104-10.
779. Bartz, S.R., et al., *Small interfering RNA screens reveal enhanced cisplatin cytotoxicity in tumor cells having both BRCA network and TP53 disruptions*. Molecular and cellular biology, 2006. **26**(24): p. 9377-86.
780. Cuzick, J., *A Wilcoxon-type test for trend*. Stat Med, 1985. **4**(1): p. 87-90.

781. Brisson, M., et al., *Identification of nonspecific products using melt-curve analysis on the iCycle iQ Detection System (tech note 2684)*, I. Bio-Rad Laboratories, Editor 2012, Bio-Rad Laboratories, Inc.
782. Lind, K., et al., *Combining sequence-specific probes and DNA binding dyes in real-time PCR for specific nucleic acid quantification and melting curve analysis*. Biotechniques, 2006. **40**(3): p. 315-9.
783. Peters, I.R., et al., *Real-time RT-PCR: considerations for efficient and sensitive assay design*. J Immunol Methods, 2004. **286**(1-2): p. 203-17.
784. Yin, J.L., et al., *Real-time reverse transcriptase-polymerase chain reaction (RT-PCR) for measurement of cytokine and growth factor mRNA expression with fluorogenic probes or SYBR Green I*. Immunol Cell Biol, 2001. **79**(3): p. 213-21.
785. Christmann, M., et al., *O(6)-Methylguanine-DNA methyltransferase (MGMT) in normal tissues and tumors: Enzyme activity, promoter methylation and immunohistochemistry*. Biochimica et biophysica acta, 2011. **1816**(2): p. 179-190.
786. Preusser, M., et al., *Anti-O6-methylguanine-methyltransferase (MGMT) immunohistochemistry in glioblastoma multiforme: observer variability and lack of association with patient survival impede its use as clinical biomarker*. Brain Pathol, 2008. **18**(4): p. 520-32.
787. Sasai, K., et al., *Careful exclusion of non-neoplastic brain components is required for an appropriate evaluation of O6-methylguanine-DNA methyltransferase status in glioma: relationship between immunohistochemistry and methylation analysis*. Am J Surg Pathol, 2008. **32**(8): p. 1220-7.
788. Egyhazi, S., et al., *Immunohistochemical examination of the expression of O6-methylguanine-DNA methyltransferase in human melanoma metastases*. Eur J Cancer, 1997. **33**(1): p. 129-34.
789. Wang, Y., et al., *Correlation between DNA methylation and expression of O6-methylguanine-DNA methyltransferase gene in cultured human tumor cells*. Mutat Res, 1992. **273**(2): p. 221-30.
790. Naumann, S.C., et al., *Temozolomide- and fotemustine-induced apoptosis in human malignant melanoma cells: response related to MGMT, MMR, DSBs, and p53*. Br J Cancer, 2009. **100**(2): p. 322-33.
791. Roos, W.P., et al., *Intrinsic anticancer drug resistance of malignant melanoma cells is abrogated by interferon- γ and valproic acid*. Cancer research, 2011.
792. Barrett, J.H., et al., *Genome-wide association study identifies three new melanoma susceptibility loci*. Nature genetics, 2011.
793. Kashani-Sabet, M., et al., *A multi-marker assay to distinguish malignant melanomas from benign nevi*. Proc Natl Acad Sci U S A, 2009. **106**(15): p. 6268-72.